Quantitative prediction of stratigraphic architecture in fluvial overbank successions.

Catherine Elizabeth Burns

Submitted in accordance with the requirements for the degree of Doctor of Philosophy.

The University of Leeds

School of Earth and Environment

July 2017

The candidate confirms that the work submitted is her own, except where work has formed part of jointly-authored publications has been included. The contribution of the candidate and other authors to this work has been explicitly indicated below. The candidate confirms that appropriate credit has been given within the thesis where reference has been made to the work of others.

The thesis comprises two chapters that were prepared for publication and has been subsequently modified for inclusion in this thesis. The current status of these parts of the manuscript at the time of submission, is as follows:

Chapter 4:

Anatomy and dimensions of fluvial crevasse-splay deposits: examples from the Cretaceous Castlegate Sandstone and Neslen Formation, Utah, U.S.A. Sedimentary Geology. 2017.

Author Contributions:

Burns, C.E. – Main author. Responsible for data collection, processing, collation and interpretation, and writing of the manuscript.

Mountney, N.P. – In depth discussion and detailed review of the manuscript

Hodgson, D.M. – In depth discussion and detailed review of the manuscript

Colombera, L– In depth discussion and detailed review of the manuscript

Chapter 5:

Stratigraphic architecture and hierarchy of fluvial overbank crevasse-splay deposits. Journal of Geology Society. London. To be submitted summer 2017.

Author Contributions:

Burns, C.E. – Main author. Responsible for data collection, processing, collation and interpretation, and writing of the manuscript.

Mountney, N.P. – In depth discussion and detailed review of the manuscript

Hodgson, D.M. – In depth discussion and detailed review of the manuscript

Colombera, L– In depth discussion and detailed review of the manuscript

Acknowledgements

Firstly I would like to thank my supervisors, Nigel Mountney, David Hodgson and Luca Colombera for giving me the opportunity to do a PhD, supporting me throughout the whole endeavour and allowing me the freedom to work as I wished. Nige, thank you for being the first line of defence in the war against my poor English and the numerous first drafts you have had to deal with over the years. Dave, thank you for asking the hard questions I did not want to answer, but needed to think about. Luca, thank you for your almost frightening efficiency in returning manuscripts and your help with the database. I need to thank the sponsors of the Fluvial & Eolian Research Group: Areva, BHPBilliton, ConocoPhillips, Aker BP, Murphy Oil Corporation, Nexen, Saudi Aramco, Shell, Tullow Oil, Woodside, and YPF.

I would like to thank my field assistants Kate Melbourne and Joshua Khan who both took 2 months out of their lives to drive me around Utah and Colorado, your company, enthusiasm and tolerance were greatly appreciated. The members of FRG I spent time with in the field: Hollie Romain, Luca Colombera, Catherine Russell and particularly Michelle Shiers, thank you for that first introduction to the Book Cliffs and all the additional help over the years. I also would like to thank Amanda Owen for initial guidance and suggestions of field sites in the Morrison Formation. To the members of STRAT group for bringing me as a field assistant to South Africa (fantastic!), thank you Hannah Brooks, Colleen Kurcinka, Sarah Cobain, Luz Gomis-Cartesio, and Miquel Poyatos-Moré. Also, thank you to all the various people who came along on the Ireland fieldtrips over the years and particularly to Jeff Peakall and Paul Wignall, who, many years ago on my 6 week undergraduate mapping, first put the idea into my head that doing a PhD was a good idea!

Thank you to all the people in the office who have helped along the way: Janet Richardson, Luan Viet Ho, Yvonne Spychala, Menno Hofstra, Ricardo Teloni, Andrea Ortiz-Karpf and anybody I have forgotten.

Finally, I'd like to thank my parents and my friends from home, Marie, Lynsey, Alex, Josh and Kate, who have supported my throughout this PhD. And Dan for all the hard work and effort particularly in those last few weeks, my thanks.

Abstract

Most outcrop-based studies of fluvial successions predominantly focus on sand-prone channel complexes; less attention has been directed towards fluvial overbank successions. Crevasse-splay deposits represent an important component of the stratigraphic record of fluvial overbank systems and yield information about the size, form and behaviour of formative fluvial systems.

Quantitative facies and architectural-element analysis was undertaken on outcrop successions from the Morrison Formation (Upper Jurassic) and the Castlegate and Nelsen formations, Mesaverde Group (Upper Cretaceous), this was then supported by analysis of 10 modern fluvial systems to better constrain the planform variations in overbank areas,

Lithofacies arrangements are used to establish the following: (i) recognition criteria for splay elements; (ii) criteria for the differentiation between distal parts of splay bodies and flood plain fines; and (iii) empirical relationships with which to establish the extent (ca. 280-500 m long by 180-1000 m wide) and planform shape of splay bodies in the Morrison Formation (teardrop) and Castlegate and Neslen formations(semi-elliptical).

A nested, hierarchical stacking of the deposits of fluvial overbank successions are recognized and records accumulation of the following components: (i) lithofacies; (ii) individual event beds comprising an association of lithofacies; (iii) splay elements comprising genetically related beds that stack vertically and laterally and represent the deposits of individual flood events; (iv) splay complexes comprising one or more genetically related elements that have a common breakout point and represent the deposits of multiple flood events.

Splay accumulations occur as parts of larger successions in which floodplain-dominated intervals accumulate and become preserved in response to longer-term autogenic controls, such as rate of lateral migration and avulsion frequency of parent channels, and allogenic controls, such as changes in subsidence, climate, base-level and sediment supply. Sandy splays contribute ‘hidden’ volume to fluvial reservoirs and may form significant connectors that

link otherwise isolated primary channel bodies, thereby contributing to reservoir connectivity.

Table of Contents

List of figures

List of tables

Chapter 1 Introduction

This chapter sets out the rationale of the research programme, the aims and objectives of the thesis, and describes its structure. The research questions that are used to fulfil the overall aims of the work are introduced and the methods used to address these questions are also introduced. Brief summaries of the geological evolution of the site of main data collection, the Cordilleran foreland basin and the Western Interior Seaway of the Western United States and the outcrop expressions studied there— the Morrison Formation, Castlegate Sandstone and Neslen Formation are presented.

1.1 Project rationale

In fluvial systems, overbank river floods are common natural events. The deposits formed due to these floods can make up significant proportions of preserved successions (Wright and Marriott, 1993; Walling and He, 1998; Walling et al., 1998; Bristow et al., 1999; Anderson, 2005; Colombera et al., 2013). Therefore, understanding the pre-requisite conditions, processes, and products during sediment transfer from fluvial channels to floodplains is important to better understand this sedimentary archive, and can help to refine depositional models. The primary components of fluvial-overbank settings are crevasse-splays, crevasse-channels, levees, abandoned channels and floodplains (Coleman, 1969; Farrell, 1989; Smith et al., 1989, Miall, 1996), the corresponding deposits of which have been recognised for their importance as aquifers, placer deposits, and hydrocarbon reservoirs (Mjøs et al., 1993; Ambrose et al., 2008; Stuart et al., 2014; van Tooreneburg et al., 2016). The wide range and complexity of fluvial systems, including in overbank areas, results in a wide-range of preserved architectures that can make accurate prediction of facies distributions and connectivity in the subsurface challenging.

The majority of studies of the stratigraphic architecture of fluvial successions have focused on channel belts, with less attention historically given to overbank deposits despite their potential to archive past environmental variability (Cecil,

1990; Nanson and Croke, 1992; Mack and James, 1994; Kraus, 1999) and their ability to act as stratigraphic connectors between generally higher quality reservoir rocks (Bos and Stouthamer, 2011; Stuart et al., 2014; Sahoo et al., 2016; van Tooreneburg et al., 2016). Numerous studies make passing comment on overbank deposits, while focussing on major fluvial channel-fills (e.g. Friend et al., 1979; Allen, 1983; Miall, 1985, Alexander, 1992; Bridge et al., 1995, Hornung and Aigner, 1999, Holbrook, 2001, Donselaar et al., 2008; Ielpi and Ghinassi, 2014; Shiers et al., 2014; Hampson, 2016). However, there has been increasing interest in overbank deposits and the various roles they can play in fluvial reservoir models (Anderson and Carr, 2007; Boerboom et al., 2016; van Toorenenburg et al., 2016). However, research on overbank deposits in outcrop has generally remained qualitative in nature, with some exceptions (e.g. Mjøs et al., 1993; Anderson, 2005; van Toorenenburg et al., 2016; Gulliford et al., 2017), and with less research done on the sedimentological relationships and stacking style present in such successions (van Toorenenburg et al., 2016; Gulliford et al., 2017). Furthermore, past studies that have foccussed upon overbank deposits tend not have linked the stratigraphic architecture to the broad-scale allogenic controls and also to autogenic processes occurring at the time of sedimentation (Stuart, 2015).

The purpose of this study is to address these shortcomings through the detailed analysis of three fluvial successions: the Jurassic Morrison Formation and the Cretaceous Castlegate Sandstone and Neslen Formation. Each succession comprises significant amounts of overbank deposits that warrant study (Mullen and Freeman, 1957; Franczyk et al., 1990; Miall 1993; Hettinger and Kirschbaum, 2002; Turner and Peterson, 2004; Mclaurin and Steel, 2007; Robinson and McCabe, 2007; Shiers et al., 2014; Owen et al., 2015). The primary focus of this study on the fluvial overbank setting has been the analysis of crevasse-splay components partially due to increased preservation potential in the rock record and partially due to common occurrence in the studied successions. Crevasse splay deposits are the product of a exceeding or breakout at a levee of floodwaters during a river flood event (Coleman, 1969; Elliott, 1974 ;). Crevasse-splays are distinct from avulsion splays that are

inherently linked and precede avulsion of the main channel (Smith et al., 1989; Slingerland and Smith, 2004; Jones and Hajek, 2007), and terminal splays which are deposited at the terminus of distributive fluvial systems with no need for river flooding events or levee confinement (Fisher et al., 2007; Fisher et al., 2008). To achieve this goal, a set of detailed sedimentary graphic profiles and architectural-element analysis panels have been recorded in strategically located sites across each of the three studied formations. The interpretations of these sites will aid in understanding the spatial distribution of the overbank elements and their relationship to the fluvial channel elements. These data can then be compared to a series of case examples, with comparable allogenic controls, from the literature via the Fluvial Architecture and Knowledge Transfer (FAKTS) database, an in-house database containing an extensive catalogue of case studies from the scientific literature and on-site fieldwork compiled at the University of Leeds (Colombera et al., 2012, 2013). This allows the impacts of allogenic factors on fluvial overbank architectures to be better understood.

1.2 Aims and Objectives: Research questions

The aim of this study is to develop a series of depositional models with which to account for and understand the complexity and variability found in the preserved stratigraphic architecture from a variety of fluvial floodplain settings, including coal-bearing successions developed in humid settings and successions developed in semi-arid settings.

Specific objectives of this research are as follows:

(i) To document the lithofacies types and organisation of these lithofacies present within overbank successions;

(ii) To define a series of overbank elements based on Miall (1985, 2014), quantify the dimensions, geometries of these elements and to establish the stacking patterns of these elements within successions.

(iii) To assess the controls on the stacking and occurrence of these elements together within successions.

Specifically, this project seeks to address these aims through consideration of following research questions detailed in the next section.

1.2.1 Question 1: What is the detailed morphology, sedimentology and depositional architecture of overbank elements?

Rationale: Fluvial architectural elements schemes were first proposed by authors such as Friend (1983), Allen (1983), and Miall (1985). Elements that were deposited beyond the confines of the main channel were defined by these same authors at first using the terms extra-channel, also called overbank settings (Friend, 1983; Miall, 1985). Extra-channel or overbank elements are defined as crevasse-splay, crevasse-channel, levee, floodplain fines and abandoned channels (Miall, 1994). These terms have been used by many workers in the study of many different fluvial successions (e.g. Willis, 1993; Olsen et al., 1995; Corbeanu et al., 2001) and have been built upon by others (e.g. Colombera et al., 2013). However, past research on overbank elements in ancient successions has mostly been as part of studies on intra-channel deposits, albeit with some notable exceptions from individual systems (e.g. Mjøs et al., 1993; van Toorenburg et al., 2016; Gulliford et al., 2017). There remains a lack of quantification of overbank elements, particularly those interpreted to be from humid settings. There is far less research that considers overbank deposits in the Castlegate and Neslen formations than the intra-channel deposits (Miall, 1993; Adams and Bhattacharya, 2005; Hampson et al., 2005; Cole, 2008; Hampson, 2016). Similarly, in the Morrison Formation, the channel deposits have been the focus of attention of many authors (e.g. Cowan, 1992; Hartley et al., 2015; Owen et al., 2015), with overbank research focussed on palaeosol analysis (Demko et al., 2004).

Work on the morphology, sedimentology and depositional architecture of overbank elements can aid in development of better understanding of the stratigraphic architecture of extrachannel areas in fluvial successions and development of more accurate, quantitative models for fluvial successions as a whole. Work on morphology and sedimentology of such elements can provide information on floodplain dynamics at the time of deposition, and on the floods that have produced these deposits. Work on depositional architectures can also

aid in understanding the morphologies of the elements that produced such deposits and conditions on the floodplain at the time of deposition.

1.2.2 Question 2: What is the stratigraphic organisation of fluvial overbank successions?

Rationale: Fluvial overbank successions are composed of various components that are present at a variety of scales. How these different components— from facies-scale, to element-scale, to complex-scale— build together will have important implications for the models that decribe such successions as will the internal complexity of these different components.

Research on the organisation of overbank sediments within a stratigraphic succession tend have been the incorporated in studies of the stratigraphic organisation of fluvial successions in general (e.g. Miall, 1985; Hornung and Aigner, 1999; Holbrook, 2001), with a few studies focusing on overbank successions deposited under ephemeral settings (van Toorenenburg et al., 2016 and Gulliford et al., 2017) and related deltaic settings (Mjøs et al., 1993; Gugliotta et al., 2015). Some studies of the hierarchical organisation of fluvial successions also comment upon overbank deposits (e.g. Sprague et al., 2002; Ford and Pyles, 2014). However, there are no published studies entirely dedicated to an investigation of the hierarchical organisation of overbank successions.

The different stratigraphic architectures of overbank elements within a succession will have implications for the reservoir potential of that succession: if sand-prone overbank elements cluster together, such as sandstone-rich crevasse-splay or channel elements, this will result in a better reservoir quality part of the succession. However, if silt-prone overbank elements, such as siltstone-rich crevasse-splay elements, abandoned channels or floodplain elements, cluster this will result in a gross- part of the succession. Different planform morphologies of overbank elements will also have an impact on stratigraphic organisation and connectivity, on how sand-prone parts of overbank elements interact with other sand-prone or silt-prone parts of the overbank, and their relationships with sand-prone channel deposits (Stuart et

al., 2014; Sahoo et al., 2016). This has implications for reservoir quality and for connectivity in fluvial successions from an applied geology standpoint (Keogh et al., 2008; van Toorenburg et al., 2016).

1.2.3 Question 3: What are the spatial and temporal controls on splay deposition?

Rationale: Sedimentation in fluvial settings has long been ascribed to the interplay of allogenic controls, such as climate, tectonism and base-level changes (Allen and Posamentier, 1993; Ethridge et al., 1998; Blum and Törnqvist, 2000; Ambrose et al., 2009; Abels et al., 2013). Autogenic controls have also been highlighted (Goldhammer, 1978; Goodwin and Anderson, 1985; Muto et al.,2007; Hampson , 2016; Colombera et al.,2015, 2016; Shiers et al., 2017). However, less attention has been paid to how such controls affect the preserved stratigraphic architecture of fluvial overbank successions.

Climate variations are known to exert an influence on floodplain development (Fielding, 1986; Benedetti, 2003), particularly the occurrence of palaeosols and coals (Blum and Price, 1998; Abels et al., 2013; Shiers et al., 2017). However, the impact of climate variations on other elements of the overbank, such as crevasse-splays, are less known. Tectonism has a very important impact on sedimentation through uplift of the source area to generate sediment and control drainage basin configurations (Miall, 2014), and through generation of accommodation space through subsidence (Leeder, 1993). However, these controls on splay sedimentation are understudied. Changing base level and its effects on crevasse-splay deposition are relatively well documented (Bristow et al., 1999). Avulsion has been proposed as having a major role in bringing coarse-grained deposits onto the floodplain (Perez-Arlucea and Smith, 1999; Miall, 2014). Crevasse splays sometimes can act as initiation for full avulsion events (Perez-Arlucea and Smith, 1999; Morozova and Smith, 2000; Buehler et al., 2011; Weissmann et al., 2013). However, more work is needed to identify the role that splay deposition can play in inducing and shaping avulsion events. Duration of river flooding events will also influence splay deposits, i.e. evolution of a splay from simple to more complicated morphology and corresponding composite deposit will increase with time. Spatial controls, such as the lateral

juxtaposition of splays next to floodplain deposits, also have important implications for the prediction of stratigraphic complexity in fluvial overbank successions.

Many different factors will influence the type and rate of splay deposition occurring at a given time and location and that in turn results in different amounts of sand transported to the floodplain. This work endeavours to understand these controls in terms of how they influence splay deposition.

1.2.4 Question 4: How do splays and their deposits impact fluvial hydrocarbon reservoirs?

Rationale: Fluvial floodplain deposits have been characterised in a qualitative manner by various authors (e.g. Fisher et al., 2007; Hampton and Horton, 2007; Jones and Hajek, 2007; Nichols and Fisher, 2007; Keogh et al., 2007 ; Gulliford et al., 2014). In addition, heterogeneous fluvial intervals, which can include overbank deposits, have been quantified within reservoir-architecture studies (e.g. Keogh et al., 2007; Pranter et al., 2008; 2009; McKie, 2011; Ford and Pyles, 2014). Each of these studies have introduced the idea that crevasse-splay deposits can contribute to reservoir volumes, but a more direct assessment of the reservoir potential, in terms of addition to net sand volume or as connectors between sand-rich channels, is missing from the literature.

Work on the sedimentation of crevasse splays can aid in developing petroleum models for fluvial successions with a greater understanding of how such splay deposits will appear in core, whether splays can act as connectors to larger channel bodies, and how splays can be defined within 3D space.

1.3 Methodology

1.3.1 Dataset

Data were collected during 3 field seasons between 2013 and 2015, totalling 5 months of work in field. This fieldwork was undertaken in Eastern Utah (Fig. 1.1) and Western Colorado (Fig. 1.1), and focused on the Jurassic-age Morrison Formation and the Cretaceous-age Castlegate Sandstone and Neslen

Formation. Additional data were derived from literature using the Fluvial Architecture and Knowledge Transfer System (FAKTS) database an in-house database with an extensive catalogue of case studies from the scientific literature and on-site fieldwork at the University of Leeds (Colombera et al., 2012; 2013). These additional data complement the primary field data collected as an important part of this study.

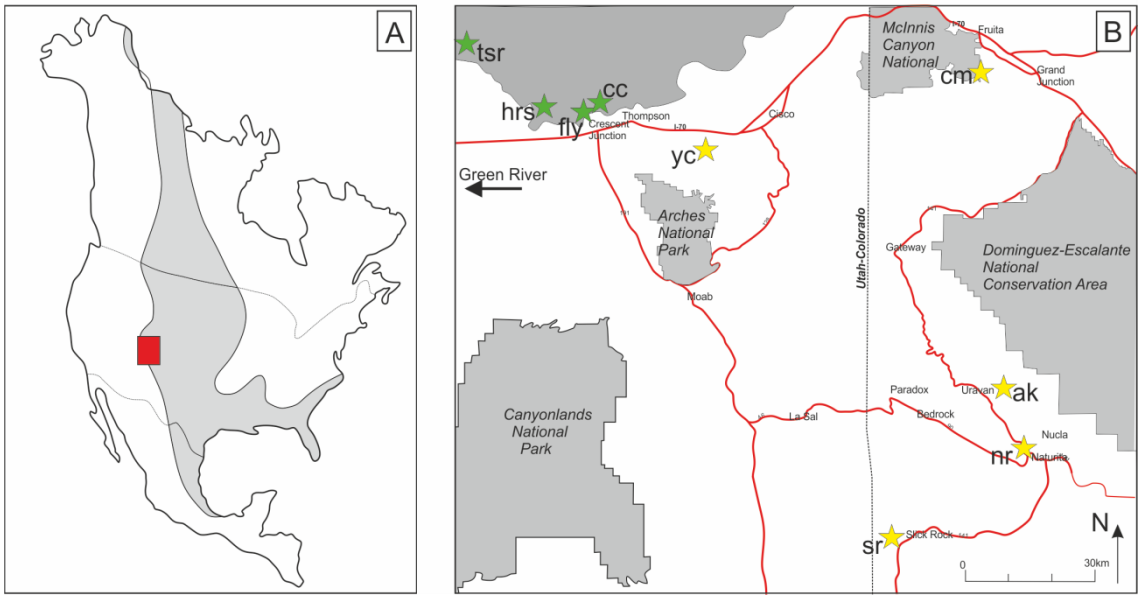

Figure 1.1: (A) Map showing location of study area in USA; (B) Map depicting the main sites of data collection in the Cretaceous Mesaverde Group, Utah, (green stars) and in the Jurassic Morrison Formation, Utah and Colorado (yellow stars), USA Abbreviations for each canyon or site are thus: Tuscher Canyon two sites (tsr); Horse Canyon (hrs); Floy Wash (fly); Crescent Canyon two sites (cc); Yellow Cat Canyon (yc); Slick Rock (sr); Atkinson Creek (ak); Naturita (nr); Colorado National Monument (cn).

1.3.2 Field techniques

Sedimentary graphic measured logs

In total, 114 vertical sections were measured recording 1241 m of sedimentary succession (Appendix A). Sixty-two logs were measured in the Book Cliffs, and Eastern Utah in the Castlegate Sandstone and Neslen Formation (Fig. 1.1, 1.2). Forty-two logs were measured across Western Colorado in the Morrison

Formation (Fig. 1.1, 1.2). The resolution of logging was dependant on size and detail required. Regional logs were measured to place each succession in context of the formation; detailed local logs were recorded to capture measured facies and their associations and successionswithin individual architectural elements and to record the stratigraphic arrangement of these elements.

Architectural diagrams

Architectural panels have been created from direct field measurement, supported by analysis of photographs and in-field sketches (Appendix B). These panels aid in determining the distribution of different architectural elements in each of the studied overbank successions in the studied formations. The panels were constructed by lateral tracing and subsequent correlation of key stratal surfaces. By in-field walking out of key surfaces, these observations are then supported by subsequent analysis of the high-resolution photopanels.

Palaeocurrent analysis

Palaeocurrent data have been collected to aid in determination of spatial trends of flow direction in overbank successions. One-thousand, one-hundred-and-eighteen palaeocurrent indicators were collected from the Book Cliffs study area encompassing the Castlegate Sandstone and the Neslen Formation. Nine-hundred palaeocurrent indicators were collected from Western Colorado from the Morrison Formation. These palaeocurrent data were collected from various sedimentary structures, including cross-bedding foresets, ripple cross-lamination, ripple-forms on bedding surfaces and low-angle-inclined accretion surfaces. The low degree of tectonic tilt negated the need to restore measurements.

1.3.3 Modern satellite imagery

Satellite imagery of modern systems was collected using G*oogleEarth* software. Data were collected from 9 modern rivers: the Helodrano Mahajambe, Madagascar; the Okavango River, Zimbabwe; the Lli River, Kazakhstan; the Paraguay River, Argentina; the Saskatchewan River, Saskatchewan; the

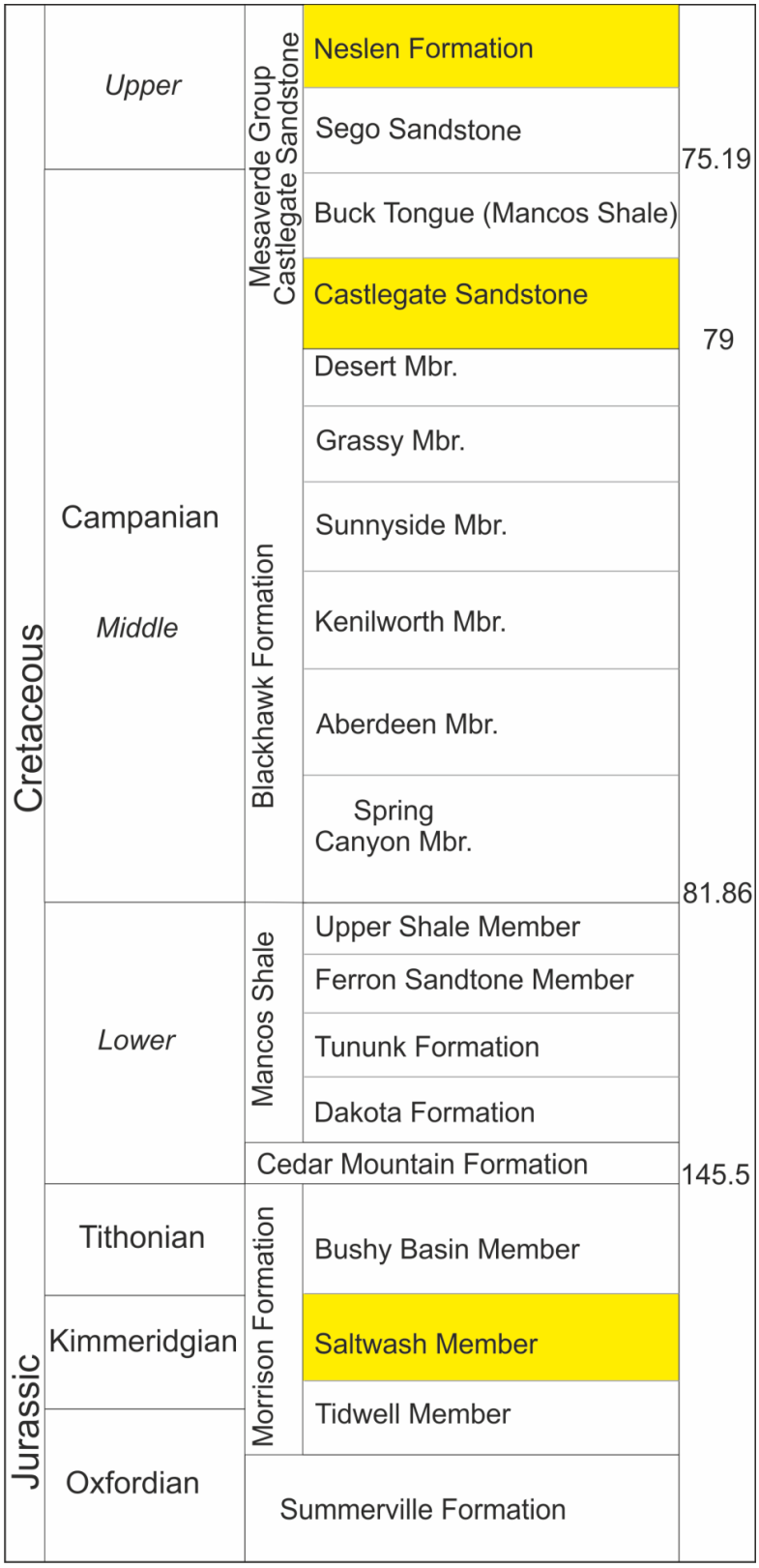

Figure 1.2: Stratigraphic column of units deposited across Western Interior of United Stares from Jurassic to Cretaceous. Units studied in this work are highlighted. Modified after Kirschbaum and Hettinger (2004), Aschoff and Steel (2011), Trudgill (2011).

Betsiboka River, Madagascar; the Peace River, Alberta; the Mississippi River, Mississippi; the Saloum River, Russia. Various data types were collected: (i) lengths perpendicular to flood breakout point and trunk channel; (ii) widths parallel to flood breakout point and trunk channel; and (iii) planform geometries of splays and their associated trunk channel sizes.

1.4 Brief overview of tectonic setting.

The North American Cordilleran foreland basin was a north-south trending basin (>3000 km long, 300-600 km wide) that spanned much of the length of North America; it developed from the Late Jurassic through to the Palaeocene (Beaumont, 1981; Jordan, 1981; DeCelles, 2004; Aschoff and Steel, 2011a) (Fig. 1.3). The basin was subject to mutiple transgressions and regressions of the Western Interior Seaway, which at times extended as far north as the Arctic Circle and as far south as the Gulf of Mexico (Fillmore, 2010).

The North American Cordilleran foreland basin developed in association with the Sevier thrust belt and associated shorterning caused by the subduction of the Farallon Plate at the western margin of North America (Aschoff and Steel, 2011a,b). The basin started to develop during the Late Jurrasic with collision of the Farralon Plate at a rate of ~8mm/year (DeCelles, 2004), but opinions are split as to whether the foreland basin was developed suffiently to receive sediment at this time (Turner and Peterson, 2004). If major thrusting and loading began during the Late Jurrasic, then deposition could have occurred in the foreland basin or in the back-buldge of the overfilled foreland basin (Decelles and Burden, 1991; Decelles and Currie, 1996; Currie, 1997, 1998), with the latter scenerio requiring a foredeep (Decelles, 2004). The presence of a foredeep is shown to be plausible by the development of a series of cross sections by Royse (1993). Subsidence and accomodation in this scenerio would have been driven by forebulge migration or flexural and regional dynamic subsidence (Currie, 1997, 1998; Decelles, 2004). If, however, significant

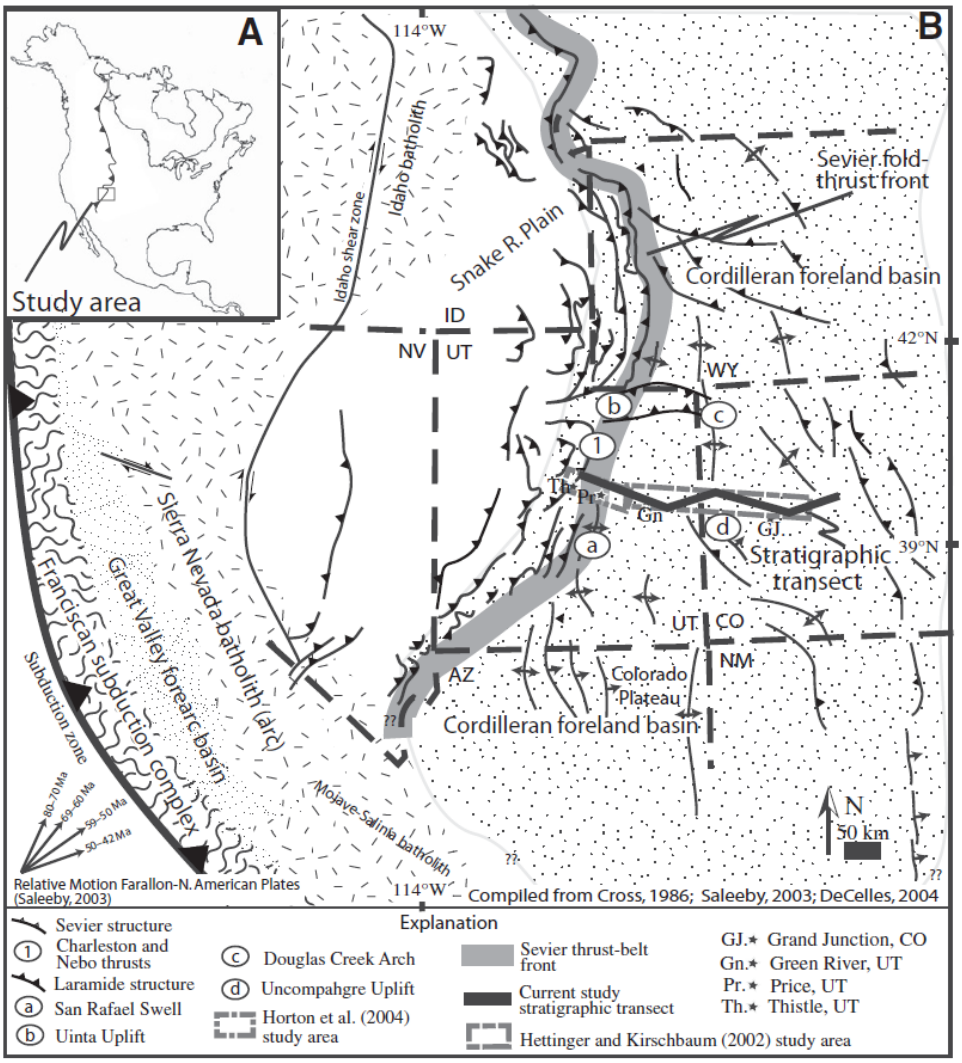

Figure 1.3: Overview map depicting the geometry and extent of the North Cordilleran Foreland Basin after Aschoff and Steel (2011).

thrusting did not occur until the Early Cretaceous (Heller et al., 1986; Lawton, 1994; Decelles et al., 1995), then the foreland basin would not have commenced full development until then, meaning accomodation must have been created in an alternative way. Regional tectonothermal subsidence, related to a Middle Jurrasic thermal metamorphic event or thursting to the west of the Sevier thrust sheet, could have created the accomodation space for the late Jurrassic deposits, the Morrison Formation (Heller et al., 1986). Alternatively, the subduction of the Farallon Plate at this time could have had a role in creating subsidence in the area (Dickinson and Lawton, 2001a,b).

These different scenerios for the timing of thrusting is less important in the Cretaceous, by which time most authors agree a full foreland basin had developed (Aschoff and Steel, 2011a,b). Rates of collison of the Farallon Plate, and consquently the development of the Sevier thrust belt, had increased to 150 mm/year by the Paleocene, with abrupt increases in early, mid- and late Cretecous times (Decelles, 2004). Sediment supply to the basin at this time was likely controlled by episodes of thrust faulting (Goldstand, 1994; Aschoff and Steel, 2011b).

1.4.1 Western Interior Seaway

The Western Interior Seaway was an eperic sea during the Late Jurassic with multiple transgressions and regression recorded in the stratigraphy of the Western Interior of North America (Blakey and Ranney, 2009). By the Late Jurassic the seaway had retreated geographically away from where the Morrison Formation was deposited (Fig 1.4) (Owen et al., 2015).

The Cretaceous was a period of eustatic sea-level variation with a number of transgressive-regressive episodes, with most authors agreeing on 2-4 major transgressions. Each cycle left a mark on the sedimentary record (Hancock and Kauffman, 1979; Sethi and Leithold, 1994). Much of North America was subject to these repeated transgression-regressive cycles by the Western Interior Seaway (Fillmore, 2010). During the Cretaceous, the North American Cordilleran foreland basin was occupied by the Western Interior Seaway, at which time the seaway was generally thought to have relatively shallow water depths along its length, and not usually exceeding 100 m (Plint et al., 1993; Longhitano and Steel, 2016). The seaway was present for 35 Myr, during the Campanian, across the Western Interior (Fig. 1.5) before it became fully terrestrial in the Maastrichtian (Roberts and Kirshbaum, 1995). The palaeo-shoreline is thought to have been orientated in a northwest-southeast to northeast-southwest direction (Aschoff and Steel, 2011b).

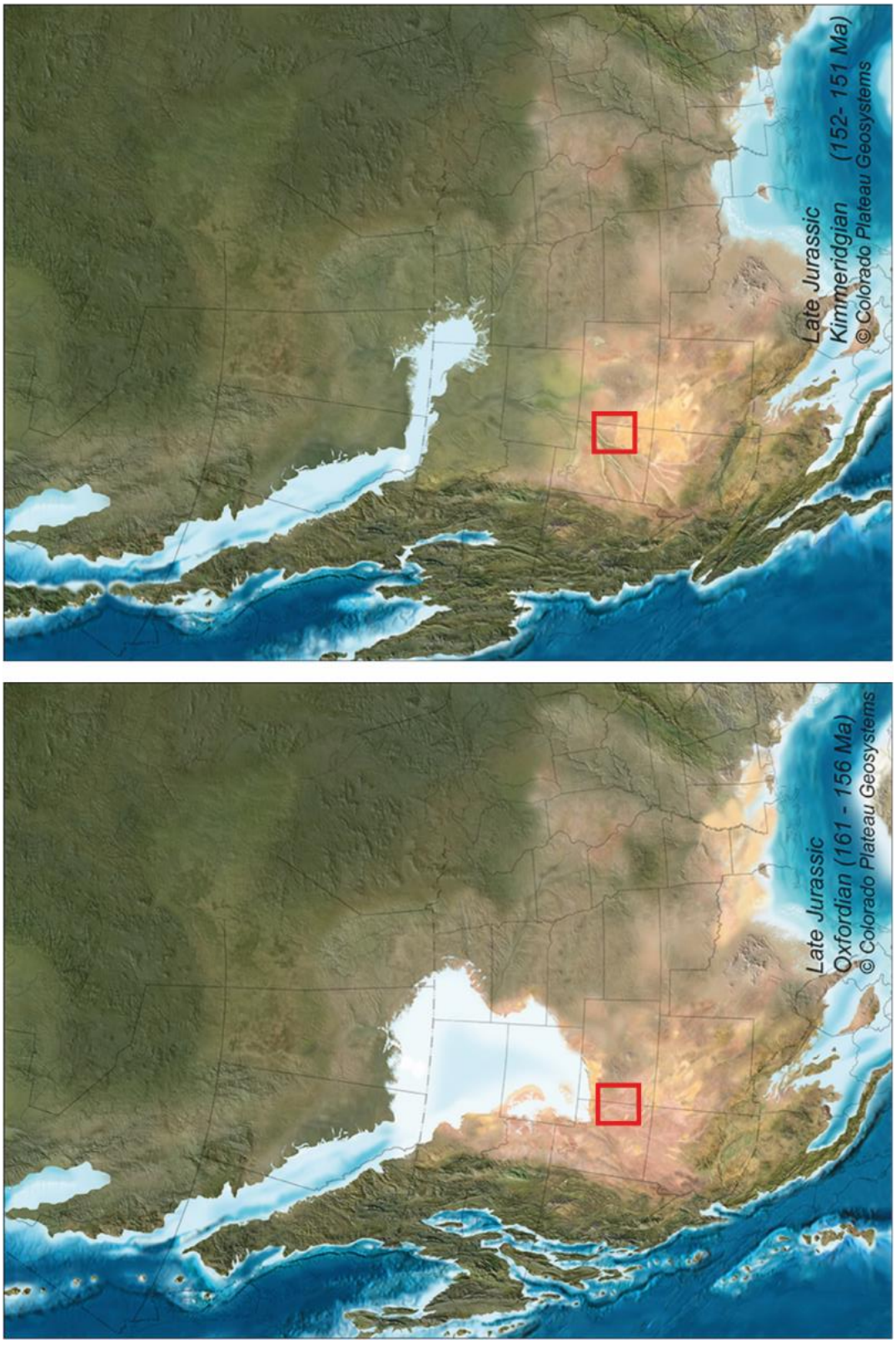

Figure 1.4: Palaeogeographic map of Western Interior. Middle and Late Jurassic times (161 Ma to 151 Ma). The Western Interior Seaway had advanced across American during the Oxfordian but retreated during the Kimmeridgian. After Blakey, 2016.

Figure 1.5: Palaeogeographic map of Western Interior. Middle and Late Campanian times (90 Ma- 72.1 Ma). Western Interior Seaway is extensive across the whole of the US and North America. After Blakey, 2016.

The sedimentary fill of the Western Interior Basin thickens overall towards the west, and has a maximum thickness of 2 km (van Wagoner, 1995). The basin fill consists mainly of Cretaceous sediments with some Jurassic and Triassic strata (Fig. 1.6) (Aschoff and Steel, 2011b). The sedimentary successions focussed on in this study are the Jurassic Morrison Formation, and the Cretaceous Castlegate Sandstone and Neslen Formation (Fig. 1.2, 1.6).

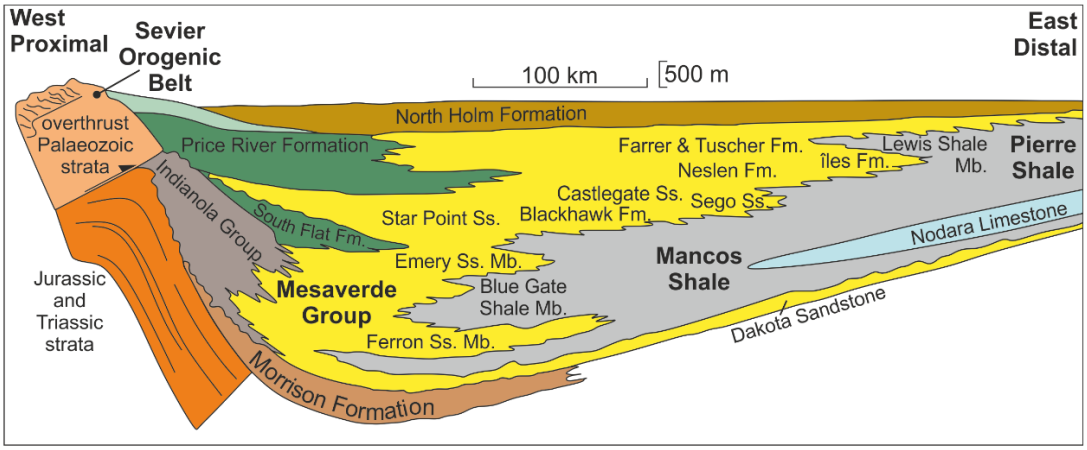

Figure 1.6: Cross-section of sedimentary infill of the foreland basin after Armstrong, 1968; Kauffman, 1997; Seymour and Fielding, 2013.

1.5 Outcrop expression of the Morrison Formation

The Morrison Formation is a 50 to 250 m thick succession (Anderson and Lucas, 1997) comprising three separate members: the Tidwell, Saltwash and Brushy Basin members (Anderson and Lucas, 1997; Robinson and McCabe, 1998; Owen et al., 2015) The Tidwell is the lowest Member of the Morrison Formation and consists of sandstones, limestones, siltstones and gypsum deposited onto a mud flat which had some fluvial and lacustrine sub-environments (Peterson, 1980, 1986; Robinson and McCabe, 1997, 1998). The Tidwell Member has within it parts that have a marine component (Turner and Peterson, 2004) and minor aeolian intervals occur towards its most southern extent (Peterson, 1980, 1986).

The Saltwash Member has a gradational contact with the underlying Tidwell Member (Robinson and McCabe, 1998) and consists of interbedded sandstones and siltstones deposited from fluvial channel and overbank settings (Mullen and Freeman, 1957; Peterson, 1980; Robinson and McCabe, 1997; Turner and Peterson, 2004). The Saltwash Member is the focus of this study. The fluvial planform morphology of the Salt Wash Member has commonly been interpreted to be braided due to high-sandstone to mud-rock ratios, coarse-grain size of many of the sandstones and sheet-like nature of sandstone (Robinson and McCabe, 1998). However, not all of the channel pattern is braided. Other workers have interpreted parts of it as a sandy-amalgamated meander belt due to point-bar forms identified in the stratigraphic record on satellite imagery (Hartley et al., 2015). The Saltwash Member can be subdivided in two ways, depending on regional location. In the Slick Rock, (Colorado) area, the member can be divided into three intervals: i) a sandstone-dominated interval at the base; ii) a interbedded interval in the middle; and iii) a sandstone-dominated upper interval (Tyler and Ethridge, 1983). By contrast, in the Henry Mountains regions, (Utah) the member can be subdivided into two intervals: i) a lower interval at the base of amalgamated sands; and ii) an upper interval made up of sandstone and thick mud packages (Robinson and McCabe, 1997).

The Brushy Basin Member is the uppermost Member of the Morrison Formation and has an enigmatic relationship with the underlying Saltwash Member (Peterson, 1988), with the contact placed at the last laterally extensive sandstone in the Saltwash Member (Peterson, 1980; Robinson and McCabe, 1998). The Member consists of siltstones, limestones, sandstones and conglomerates interpreted to have been deposited from fluvial channels, fluvial overbank, wetland and lacustrine settings (Craig et al., 1955; Turner and Peterson, 2004)

1.6 Outcrop expression of the Castlegate Sandstone

The Castlegate Sandstone passes laterally to the Lower Castlegate Sandstone, the Buck Tongue of the Mancos Shale and vertically to the Sego Sandstone

and the Neslen Formation east of Green River, Utah (Kirschbaum and Hettinger, 2004). This study does not go west of the town of Green River so reference to the Castlegate Sandstone here means the Lower Castlegate Sandstone. The Lower Castlegate Sandstone is a 60m thick (average) succession of cliff forming sheet sandstone bodies with sheet-like geometries (Van Wagoner, 1990; Hettinger and Kirschbaum, 2002; Adams and Bhattacharya, 2005, McLaurin and Steel, 2007). The unit consists of predominantly very fine-medium grained sandstone (Olsen et al., 1995, Hettinger and Kirschbaum, 2002), with sporadic and limited zones of continuous overbank fines (Mclaurin and Steel, 2007). The Lower Castlegate Sandstone in the Book Cliffs thins towards the south-east and then fines and passes laterally into the Mancos Shale close to the Colorado border (Hettinger and Kirschbaum, 2002). The Blackhawk Formation underlies the Lower Castlegate; the base of the Castlegate can be taken as a major sequence boundary (Van Wagoner, 1990; Olsen et al. 1995, Adams and Bhattacharya, 2005).

The Lower Castlegate Sandstone is generally considered to be deposited within low-sinuosity braided channel systems (Van Wagoner, 1990; Olsen et al., 1995: Hettinger and Kirschbaum, 2002) with some lateral variations with proximity to the palaeo-shoreline, closer to the shoreline the systems changes from a braided system to a shoreline-delta front in present-day outcrops towards Colorado (Miall 1993, Hettinger and Kirschbaum, 2002). At the time of Castlegate Sandstone deposition there was thought to be a low rate of base-level rise, hence the dominance of sand throughout the succession, with the gradual increase in the rate of base-level rise over time (Olsen et al., 1995).

1.7 Outcrop expression of the Neslen Formation

The Neslen Formation is a coal-bearing formation made up of very fine- to medium- grained sandstones, siltstones and mudstones (Hettinger and Kirschbaum, 2002). It is defined based on the first occurrence of coal-bearing strata above the Sego Sandstone (Fig 1.2; Fisher, 1936). The Neslen Formation is traditionally subdivided into four coal zones (Franczyk et al., 1990):

the Palisade, Ballard, Chesterfield and Cabonera zones. Within these zones, two laterally extensive sandstone marker beds, the Thompson Canyon Sandstone Bed (Shiers et al., 2014) and the Sulphur Canyon Bed (Hettinger and Kirschbaum, 2002) are prevalent and laterally extensive. The Neslen Formation is of variable thickness from 40 m at Tuscher Canyon (Fig. 1.1) to over 120 m at the Utah-Colorado border (Shiers, 2017), due to its gradational contact with the overlying Farrer Formation (Fisher, 1936; Franczyk et al., 1990). Laterally, the Neslen Formation merges west towards Green River with the Castlegate Sandstone, and merges east at the Colorado border with the Lower Mount Garfield Formation (Hettinger and Kirschbaum, 2002).

The Neslen Formation was deposited as part of a low-gradient, low-relief fluvial and coastal plain (Lawton, 1986; Pitman et al., 1987), but has also been interpreted as a delta plain (Karaman, 2012; O'Brien, 2015; Gates and Scheetz, 2015; Burton et al., 2016; Shiers et al., 2017), and as an estuarine complex (Willis 2000; Kirschbaum and Hettinger, 2004; Cole, 2008). Overall, there is a general coarsening upwards trend within the Neslen Formation, which can be linked to a change in palaeoenvironment from lower coastal plain, to upper coastal plain, to a lower alluvial-plain setting. Hence there is a dominance of coals and fine-grained sediment towards the base of the succession, and an increase in sand proportion toward the top (Franczyk et al., 1990; Hettinger and Kirschbaum, 2002). The Neslen Formation grades into the overlying fluvial Farrer Formation above (Franczyk et al., 1990; Hettinger and Kirschbaum, 2002).

The Neslen Formation can be divided into a "lower" and an "upper" part. The lower part of the formation accumulated in brackish water and fresh water environments within multiple sub-environments such as tidal flats, lagoons, bays, marshes and oyster reefs (Pitman et al., 1987; Chan and Pfaff, 1991; Shiers et al., 2014, 2017). The upper part was deposited within in a more alluvial-plain setting (Pitman et al., 1987; Shiers et al., 2014, 2017).

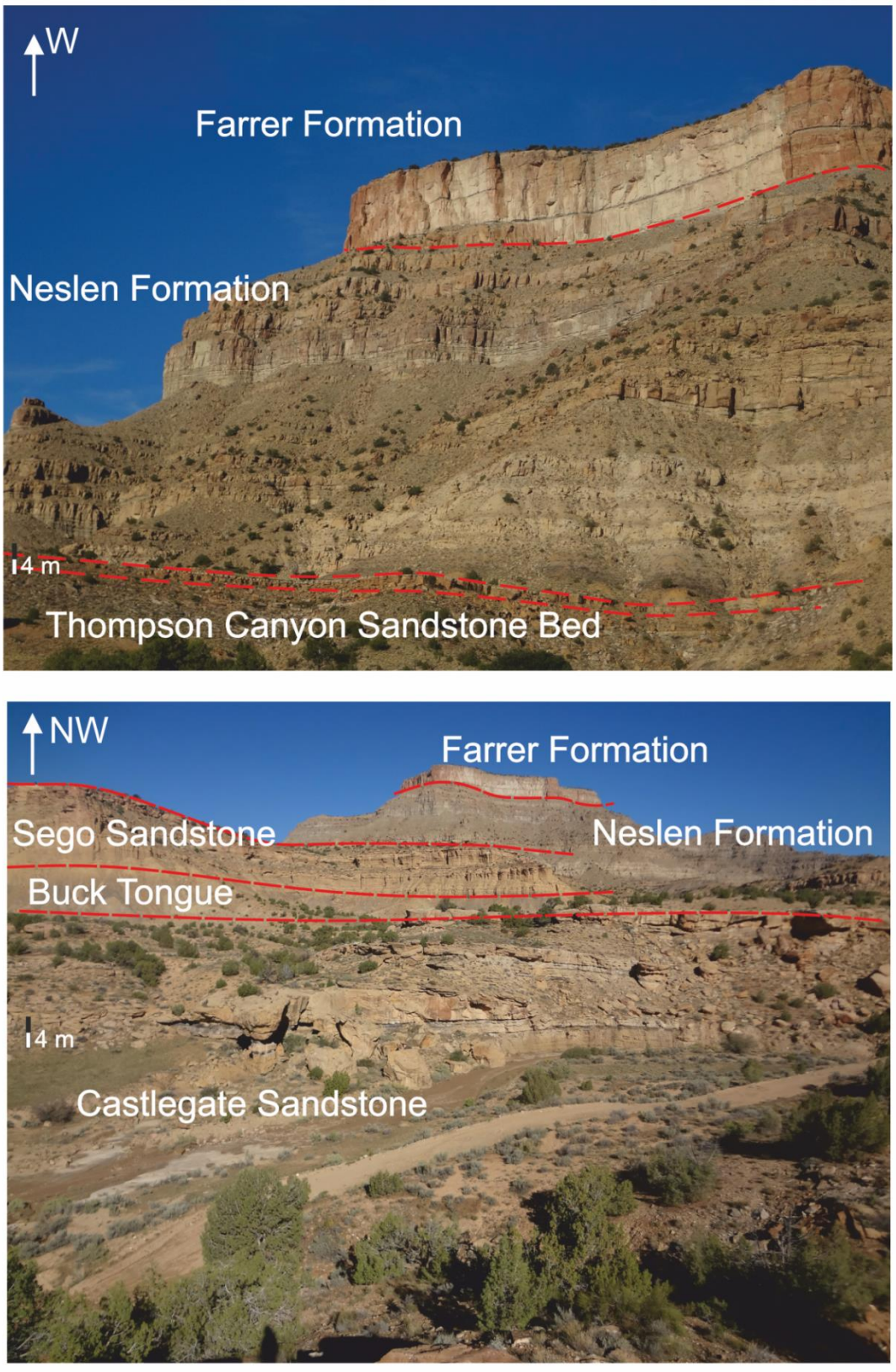

Figure 1.7: Outcrop expression of the Castlegate Sandstone and Neslen Formation at Crescent Canyon, Utah. Photograph looking West(Fig. 1.1)

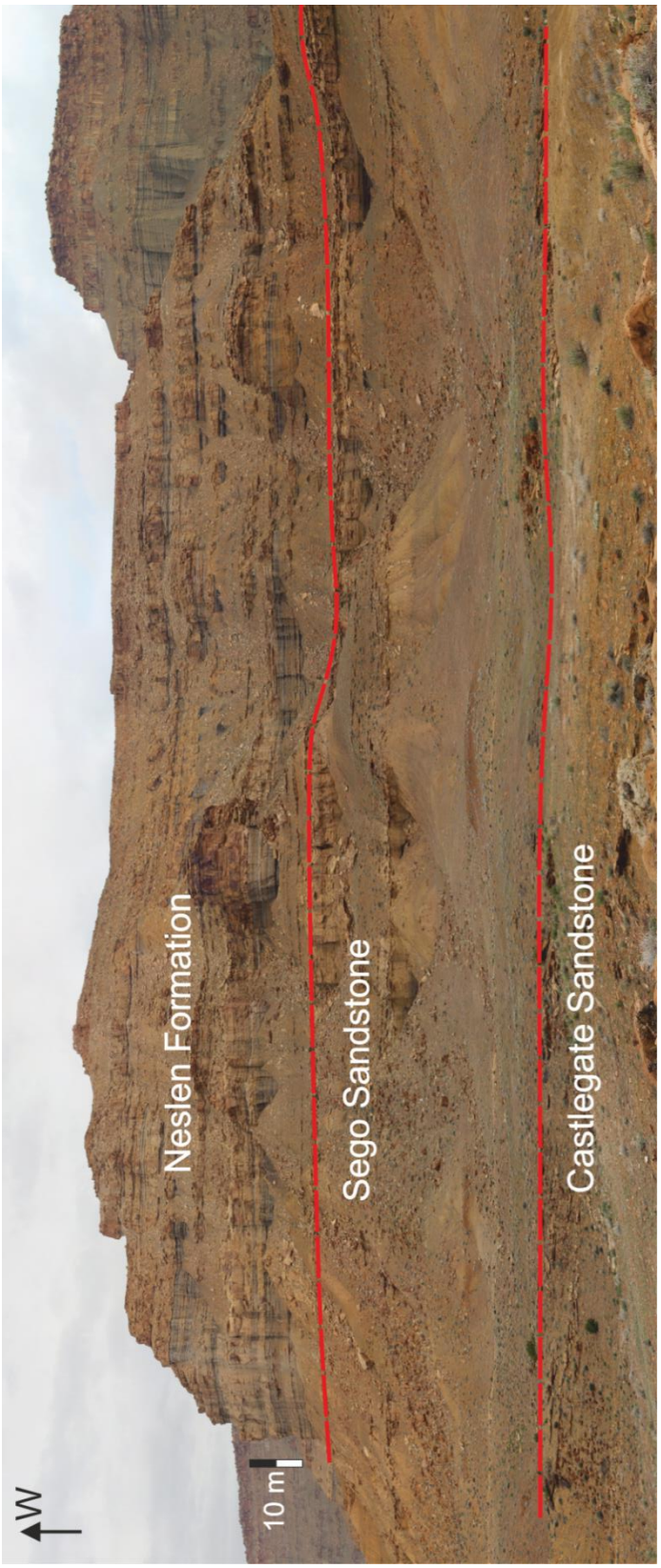

Figure 1.8: Outcrop expression of the Neslen Formation and Castlegate Sandstone at Tuscher Canyon, Utah (Fig. 1.1).

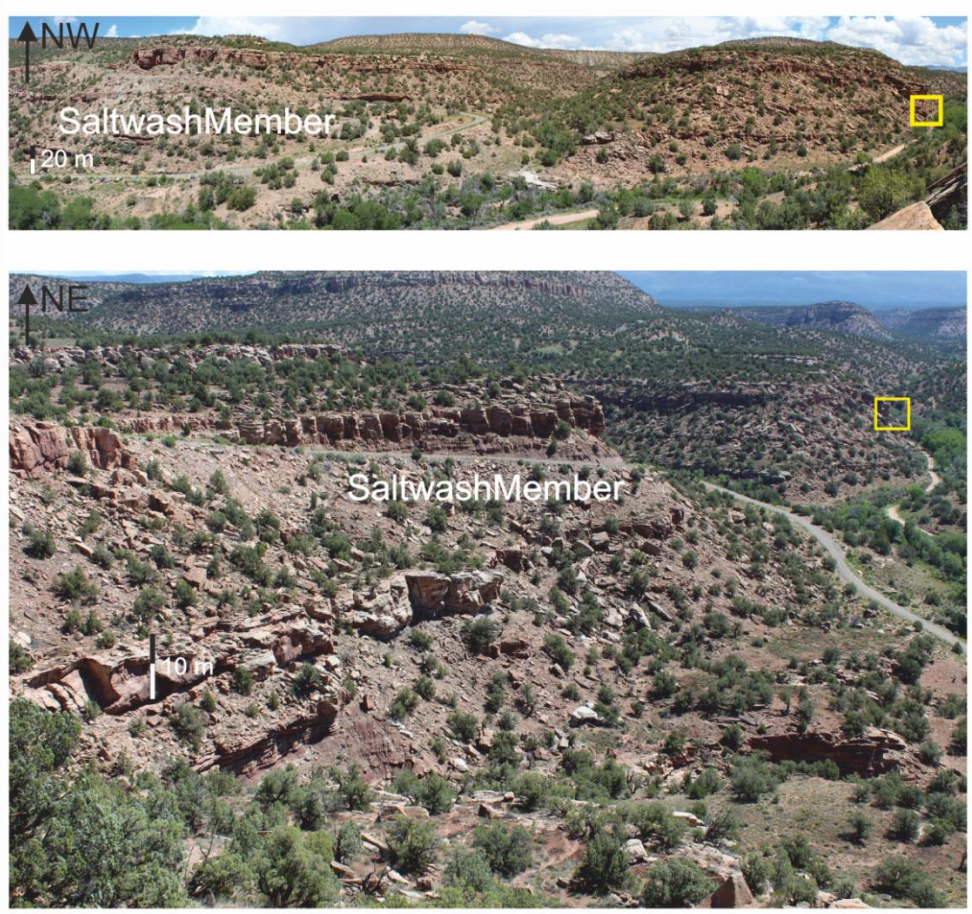

Figure 1.1.9: Outcrop expression of the Saltwash Member of the Morrison Formation, Atkinson Creek, Colorado (Fig. 1.1).

Figure 1.10: Outcrop expression of overbank deposits and the relationship with a channel body within the Saltwash Member of the Morrison Formation at Atkinson Creek, Colorado (Fig. 1.1).

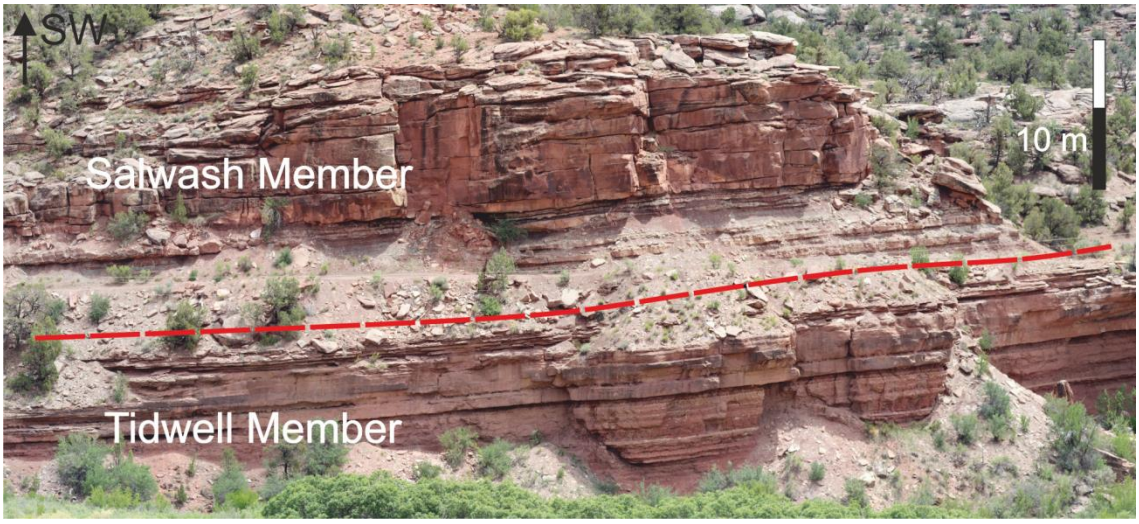

Figure 1.11: Outcrop expression of the Morrison Formation at the proximal-medial end of the system, Slick Rock, Colorado (Fig. 1.1).

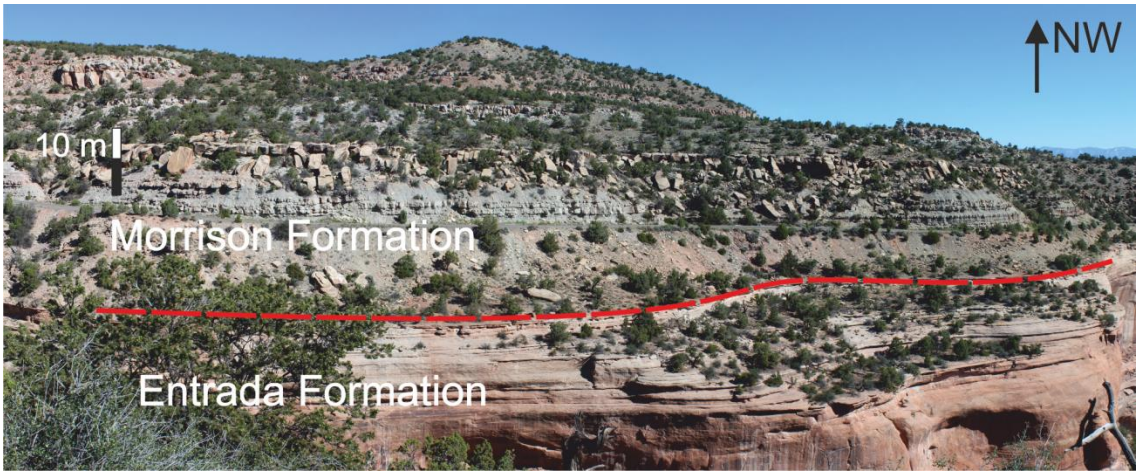

Figure 1.12: Outcrop expression of the Morrison Formation at the most distal-end of the system, Colorado National Monument, Colorado (Fig. 1.1).

1.8 Thesis structure

Within this thesis, chapters 1-3 constitute the introductory part of the work. These chapters include a review of background research to the topic, an outline of the study area and stratigraphy, and an introduction to the lithofacies identified in this study. The research questions are addressed in three separate chapters: 4, 5, and 6. The research questions are then discussed and answered directly in Chapter 7, and synthesised in the conclusion in Chapter 8. In each

data chapter (4, 5, and 6), there are modest restatements of key background information to frame the key observations and remind the reader of relevant points relating to background geology.

Chapter 1: Introduction

This chapter introduces the research rationale, aim, objectives and key research questions of the study, data collection methods are also introduced. This chapter also introduces the geological and stratigraphic settings of the Morrison Formation, Castlegate Sandstone and Neslen Formation.

Chapter 2: Literature review

This chapter provides a short review of pertinent published literature and definitions of the terminology used throughout this thesis.

Chapter 3: Lithofacies of the Morrison Formation, Castlegate Sandstone and Neslen Formation

This chapter introduces the lithofacies identified in each of the formations studied and provides possible interpretations for each.

Chapter 4: Anatomy and dimensions of crevasse-splay deposits in Mesaverde Group

This chapter quantifies lithofacies distributions and dimensions of exhumed crevasse-splay architectural elements in the Campanian lower Castlegate Sandstone and Neslen Formation, Mesaverde Group, Utah, USA. Lithofacies arrangements are used to establish the following: (i) recognition criteria for crevasse-splay elements; (ii) criteria for the differentiation between distal parts of crevasse-splay bodies and floodplain fines; and (iii) empirical relationships with which to establish the extent and overall planform shape of crevasse-splay bodies. These relationships have been established by high-resolution stratigraphic correlation and palaeocurrent analysis to identify outcrop orientation with respect to splay orientation. This permits lateral changes in crevasse-splay facies architecture to be resolved. Facies models describing the sedimentology and architecture of crevasse-splay deposits preserved in

floodplain successions serve as tools for determining both distance from, and direction to major trunk channel sandbodies.

(Paper 1: Catherine E. Burns, Nigel P. Mountney, David. M Hodgson and Luca Colombera (2017) Anatomy and dimensions of fluvial crevasse-splay deposits: Examples from the Cretaceous Castlegate Sandstone and Neslen Formation, Utah, USA. Sedimentary Geology, 351, 21-35. https://doi.org/10.1016/j.sedgeo.2017.02.003)

Chapter 5: Stratigraphic architecture ad hierarchy of fluvial overbank crevasse-splay deposits.

This chapter recognizes nested elements at a hierarchy of scales. These represent the following components: (i) lithofacies; (ii) individual event beds (~1 m thick) comprising an association of lithofacies and occurring proximal to major parent channels but thinning and fining laterally, and representing the deposits of parts of individual flood events; (iii) splay elements comprising genetically related beds that stack vertically and laterally and represent the deposits of individual flood events; (iv) splay complexes comprising one or more genetically related elements that have a common breakout point and represent the deposits of multiple flood events. Recognition criteria for splay complexes are discussed; emphasis is placed on identification of bounding surfaces, thinning and fining trends of splay elements and complexes, and variability of palaeoflow indicators. Stacking of bodies that comprise each tier of the hierarchy is influenced by: (i) the rate of local accommodation generation, which influences whether splay elements are laterally offset due to compensational stacking; (ii) floodplain gradients; (iii) erosive force of floodwaters; and (iv) confined or unconfined nature of the floodplain. Gaining an improved understanding of the geometry and distribution of sand-prone splay bodies has applied importance because such elements contribute volume to fluvial reservoirs and may form significant connectors that link otherwise isolated primary channel bodies, thereby enhancing to reservoir connectivity.

The content of this chapter to be submitted to Journal of Sedimentary Research in Summer 2017.

Chapter 6: Controls on the fluvial overbank successions in the humid Cretaceous Neslen Formation and semi-arid Jurassic Morrison Formation.

This chapter examines how allogenic controls, particularly climate, and autogenic controls, particularly floodplain conditions, influence the accumulation of sediment in fluvial overbank settings. Elements common to all the formations studied (Jurassic Morrison Formation and Cretaceous Neslen Formation) are defined and then compared. Facies type, thicknesses, lengths, widths, geometries and presence of bioturbation and rooting are all compared. The stratigraphic organisation and architecture of these elements are then demonstrated from five type successions; three from the Morrison Formation and two from the Neslen Formation. These data are then compared to similar case studies from the literature using the FAKTS (Fluvial and Architectural Knowledge Transfer System) database.

Models for the overbank stratigraphy found in the different parts of the two formations (Morrison and Neslen formations) are then proposed and two formation scale models to demonstrate the differences in architecture both within each formation and between the two formations.

Chapter 7: Discussion

This chapter summarise the answers to the questions posed in Chapter 1. The chapter integrates and summarises results of the preceding questions but also presents a wider discussion of fluvial overbank successions and the controls on such successions, and considers the reservoir implications of this work.

Chapter 8: Conclusions and future work

This chapter summarises the main findings of this thesis and topics for future work are also presented.

Chapter 2 Literature review

This chapter provides and overview of past and current concepts related to fluvial overbank sedimentation. The distributive fluvial system concept and the components of the fluvial overbank are introduced. The terminology used in this study is defined and justified, and the key concepts used for the later discussion are also introduced.

2.1 Fluvial depositional systems

Fluvial systems are the major transport routes for sediment from the hinterland to the coastline (Miall, 1994). However, in order to reach the shelf and deep-water areas, sediment may be subject to a range of different processes in fluvial and fluvio-deltaic systems.

The fundamental characteristics of fluvial systems are linked to discharge and sediment supply (Blum and Törnqvist, 2000). An increase in bedload transport leads to aggradation, whereas an increase in discharge causes degradation (Miall, 2014). When a system is degradational, it has limited-to zero preservation potential; instead the river will act as a conduit for sediment transport and deposition preferentially occurs at the river termination (e.g. at the coast or lake) (Davidson et al., 2013). Aggradational systems have a high preservation potential and are more likely to be transferred into the rock record (Hartley et al., 2010). However, tributary systems often typically in net-degradational settings. In contrast, present-day net-aggradational settings have sedimentation patterns that have been more commonly classified as distributive fluvial systems (Weissmann et al., 2010; Hartley et al., 2010; Hartley et al., 2015). Tributary river systems are one of the main conduits for sediment to be transported to either the coastline or an interior lake (Davidson et al., 2013). However recent studies have revealed that in, aggrading basins, distributive fluvial systems dominate basins (Weissmann et al. 2010) and form a significant part of the continental rock record (Owen et al., 2015).

Fluvial system channel planform geometries have been classified into four end-members: straight, braided, anastomosing and meandering (Fig. 2.1) (Allen,

1965; Schumm, 1972; Leopold et al., 1995). However, fluvial channel systems may have planform morphologies intermediate between these respective end-members and which can change both spatially and temporally.

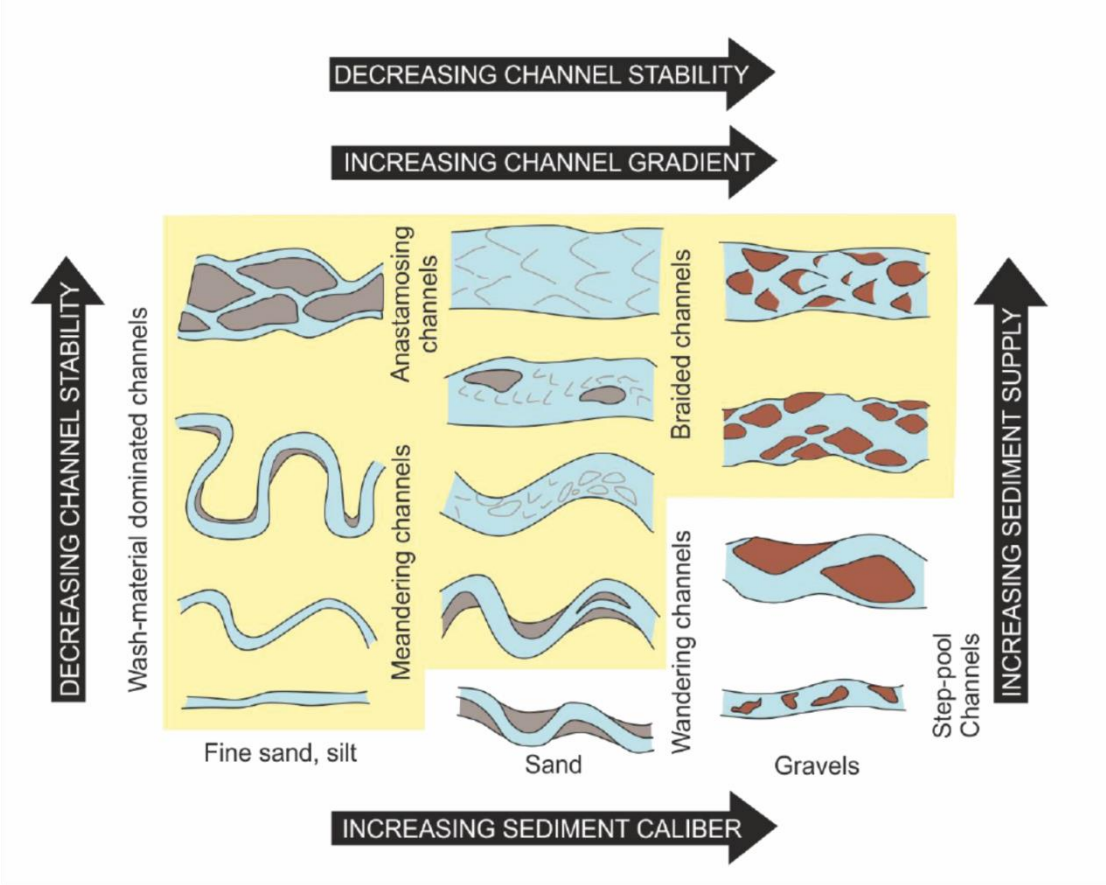

Figure 2.1: Plan-view geometrical classification of fluvial channel systems adapted after Church (2006).

Meandering channel patterns have higher sinuosity than those in braided systems (Fig. 2.1). Flows within meandering channels commonly contain a mixture of fine to coarse grained sediment (Church, 2006), and associated deposits accumulate in four different ways: (1) lateral and downstream accretion (Friend et al., 1979) (2) channel avulsion (see chapter 2.4.7); (3) meandering bend neck cut-off (Erskine et al., 1992); and (4) chute cut-off (Constantine et al., 2010). Extensive floodplain areas are commonly associated with meandering fluvial channels and are episodically inundated with sediment-

laden floodwaters when channel levees are overtopped and/or broken through (Shen et al., 2015). The Morrison Formation (Hartley et al., 2015) and the Nelsen Formation (Willis, 2000; Kirschbaum and Hettinger, 2004) are both interpreted to have accumulated in fluvial systems with predominately meandering channels.

Braided channels patterns are characterised by a lower sinuosity than meandering channels and braid bars where the flow divides and diverges (Fig. 2.1; Bridge, 1984). Components of the Morrison Formation have in the past thought to be accumulated in channels with a braided planform morphology (Craig et al., 1995; Robinson and McCabe, 1998), as too has the Castlegate Sandstone, which is partly time-equivalent to the Neslen Formation in the Western Book Cliffs (Fig.1.2; Olsen et al., 1995; Adams and Bhattacharya, 2005).

Development of fluvial facies models are the basis for understanding sedimentary processes of ancient fluvial systems (Allen, 1983; Miall, 1996). Facies models describing sedimentary relationships of ancient successions are primarily based on recognition of sedimentary structures and grain size variations and stratigraphic architecture. The first fluvial facies models were originally defined on the grain-size of the system and the sinuosity of that system (Bridge, 1993; Miall, 1996). Sediment within the channel is entrained when the velocity is great enough to overwhelm the force from gravity and friction that holds that particle in place (Hjulström, 1939); Leeder, 1983). Sediment deposition occurs when the flow energy decreases sufficiently for the range of grain sizes within the flow to come to rest. During sediment traction, bedform generation and the possible sedimentary structures formed depend on the grain size, flow velocity and water depth (Harms, 1975). In general, associated overbank sediment will have finer grain sizes than those in the parent channel. Consequently, overbank sediments are more likely to be characterised by formation of ripples, relatively small-scale 2D dunes and upper stage plane beds (Fig. 2.2).

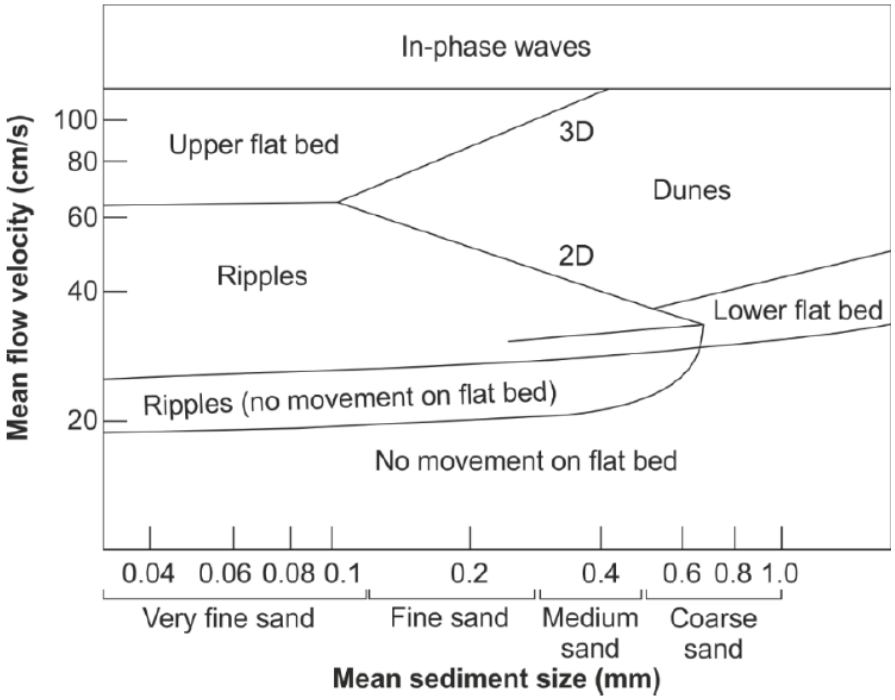

Figure 2.2.2: Bedform stability diagram, Harms (1975).

2.1.1 Distributive fluvial systems

A Distributive Fluvial System (DFS) is a fluvial channel and overbank pattern that radiates from the point at which a river enters a sedimentary basin, termed the apex (Fig. 2.3) (Weissman et al., 2010). The proportion of active channels within this network can be highly variable (North and Warwick, 2007) but some DFS might only have a small number of channels with active flow (Weissmann et al., 2010; Hatley et al., 2010; Weissmann et al., 2011). Distributive Fluvial Systems may terminate at the coastline, lakes or onto dry floodplains, whereas others may feed into axial systems (Fisher et al., 2007; Weissmann et al., 2010).

Distributive Fluvial Systems geometries vary according to basin type (compressional, extensional, strike-slip or cratonic basins) and may have meandering or braided river geometries (Weissmann et al., 2010; Hartley et al., 2015). Within a DFS, there are several possible sedimentary components (Fig. 2.3). These include sub-components with fan-shaped geometries on several possible spatial scale that are similar to the overall geometry of the DFS,

including alluvial, fluvial, terminal and mega fans (Weissmann et al., 2010; Hartley et al., 2010; Weissmann et al., 2011). The deposits formed from a DFS will generally but not exclusively have an overall fan-shaped plan-view morphology (Fig. 2.3; Hartley et al., 2010). Sedimentary models of DFS systems predict several downstream trends: (1) decreasing grain size; (2) decreasing channel size; and (3) increasing floodplain-to-channel ratios (Kelly and Olsen, 1993; Nichols and Fisher, 2007). These trends have been identified in outcrop investigations of interpreted ancient DFS (Owen et al., 2015).The Morrison Formation has been identified as a DFS (Owen et al., 2015).The Castlegate and the Neslen formations may also be classified as marine-terminating DFS systems with the apex of these systems in the Sevier Orogenic belt (Shiers et al., 2014).

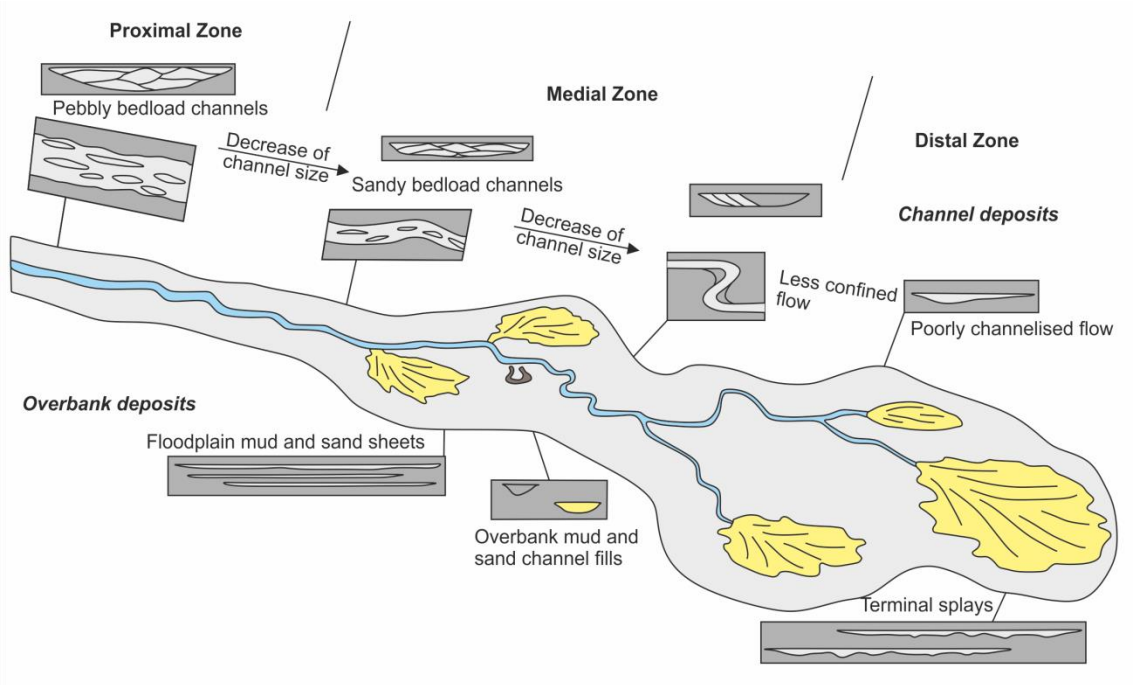

Figure 2.3: Overview diagram of a generalized DFS showing the idealised stratigraphy associated with the different planform geometrical components. Adapted after Nichols and Fisher (2008).

2.2 Components of fluvial overbank

The term fluvial overbank is a gross-scale element for any extra-channel setting (for example, in a DFS; Fig. 2.3). The overbank can be divided into several morphological components based on unit size, geometry and facies (Fig. 2.4, 2.5). A standard scheme for overbank elements recognises four separate morphological elements: (1) floodplains (including palaeosols); (2) crevasse splays ((including crevasse-channels); (3) fluvial levees; and (4) abandoned channels (Fig. 2.4). These components have different spatial dimensions (Fig. 2.5).

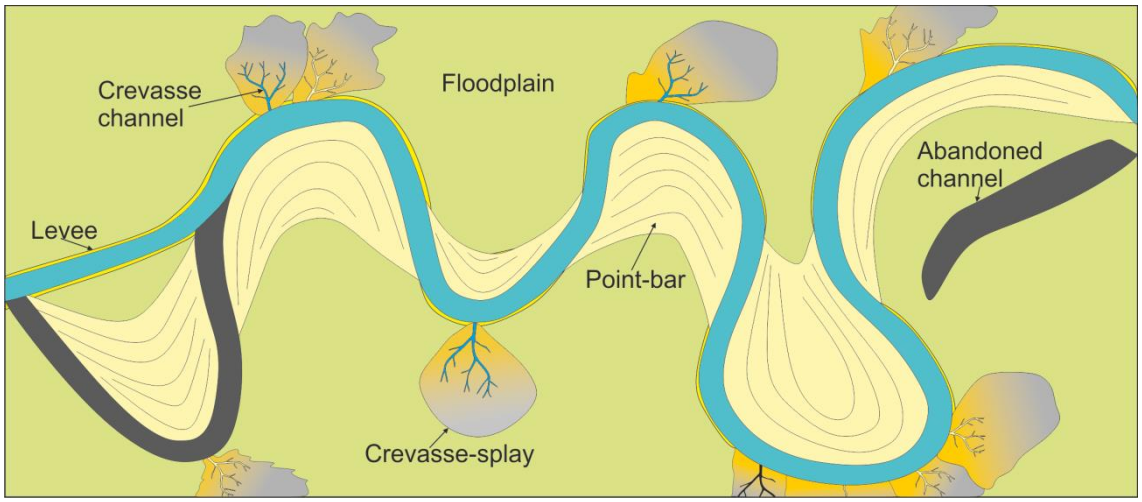

Figure 2.4: Conceptal diagram illustrating different elements in the overbank.

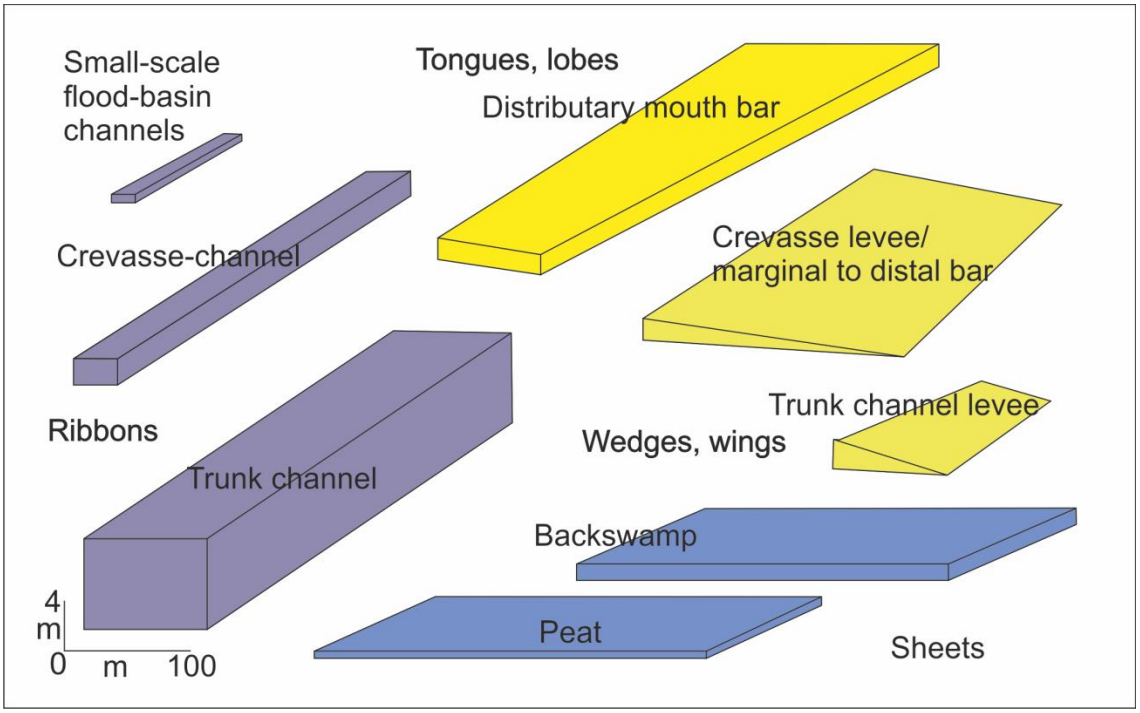

Figure 2.5: Geometries of overbank elements with approximate dimesions for a small-to-mid-size river after Farrell (2001).

2.2.1 Floodplain and deposits

A floodplain is defined as the area of land adjacent to a channel that is subject to episodic flooding (Nanson and Croke 1992; Bridge 2006). The floodplain is more prevalent in unconfined settings (Fig. 2.6; Jain et al., 2008) and acts as an important sediment storage sink for the finer grained fraction of sediment within a fluvial system (Walling and He, 1998; Wright and Mariott, 1993; Jain et al., 2008). Floodplain deposits develop in all alluvial valleys and fans regardless of the river system pattern (Bridge, 2006) and are commonly the product of lateral accretion of point bars and/or vertical accretion of floodplain fines during inundation periods (Wright and Marriott, 1993). Floodplains in the geographic sense begin when the river is no longer confined by the alluvial valley. At first the floodplain is discontinuous, and separated in plan-view by the main channel, but downstream it becomes continuous (Fig. 2.6)(Jain et al., 2008).

Floodplain fines can be defined as tabular sheets of the finest material of a succession that can be laterally extensive for hundreds of metres (Miall, 1985;

Colombera et al., 2013). Beds within floodplain strata tend to stack vertically and have flat bounding surfaces, indicative of an aggradational regime (Miall, 1985, 1996; Platt and Keller, 1992; Colombera et al., 2013).

Palaeosols are fossilised soils that form from physical, biological and chemical modification of exposed rocks or sediment (Kraus, 1999). Although palaeosols tend to develop in humid conditions on alluvial plains, the extent of development depends on proximity to the channel. Well-developed palaeosols generally develop in relatively distal locations with slow, gradual deposition, whereas relatively poorly-developed palaeosols are commonly found in closer proximity to the channel due to more frequent, episodic but rapid deposition (See Chapter 2.3.5) (Kraus, 1987,1999).

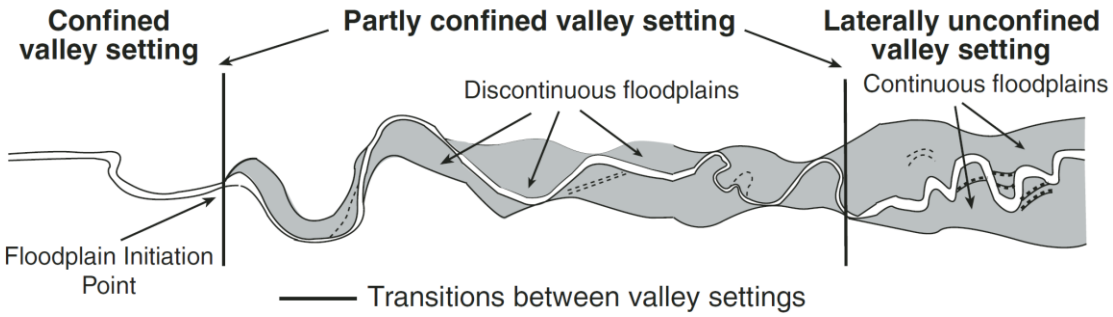

Figure 2.6: Conceptual image of downstream changes in river morphology and the effect on floodplain continuity, after Jain et al. (2008).

2.2.2 Crevasse splays, crevasse channels and deposits

Crevasse splays are defined as fan or wedge shaped features that form adjacent to the margins of main channels and build out onto the floodplain (Figs. 2.4, 2.7; Miall, 1996; Bridge, 2006; Miall, 2014). Splays commonly have smaller crevasse channels incising into them that split downslope into distributary networks (Bridge, 2006). Crevasse-splay morphology varies through time: splays are initially relatively simple but become more complex as the splay develops and becomes more stable over time (Smith et al., 1989). Splay deposits are typically coarser and thicker than contemporaneous levee

deposits, but in distal regions, splay deposits can resemble time-equivalent levee deposits (Bridge, 2006; Miall, 2014). Crevasse channels can have similar geometrical characteristics to the parent channel deposits but are smaller in scale (Fig. 2.4) and are generally relatively coarser grained than the surrounding, time-equivalent, crevasse splay deposits (Bridge, 2006).

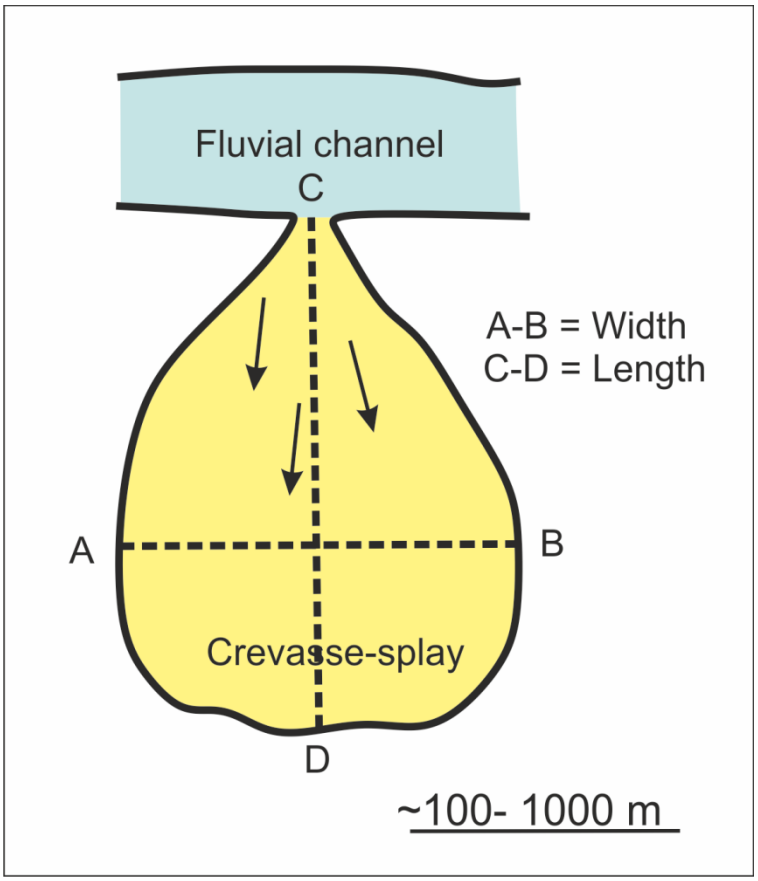

Figure 2.7: Diagram of an idealised, equidimensional crevasse splay in plan view after Mjøs et al. (1993).

2.2.3 Fluvial levees and deposits

Levees are defined as wedge-shaped, discontinuous aggradational features that are located on alluvial channel margins and which decrease in elevation towards the floodplain (Figs. 2.4. 2.5; Brierley et al., 1997; Cazanacli and Smith, 1998; Adams et al., 2004, Bridge 2006). Levees typically consist of coarsening

upward facies successions made up of beds of sand interbedded with silts (Miall, 2014). Levees significantly affect the distribution of water and sediment within river systems, especially floodwater and sediment transfer to overbank splays and floodplain (Brierley et al., 1997). The shape of a levee depends on the mechanism by which it forms, which is principally controlled by: (1) the amount, type of sediment in the system; (2) the degree of floodplain confinement; and (3) the hydrodynamic carrying capacity of the fluvial channel. In modern systems, levees are recognised by the following characteristics: (i) the close proximity of the levee to the channel margin; (ii) a prism or wedge- like cross-sectional shape of the body; (iii) the ribbon-like planform geometry, which is most commonly aligned parallel to the edge of the channel; and (iv) the elevation profile, which tends to be highest close to the channel margin and decreased gently towards the floodplain.

Defining levees based on these criteria in the ancient record is very difficult. As well the limitations of outcrop quality and preservation potential of levees, identification of levees is also limited by a lack of consistent scaling relationship between levee height and width, pattern of levee location in outcrop and the wide variation in the texture of the levee deposits, which can range from clay to coarse sand. The most common sedimentological trends and stratigraphic features recognised in modern and ancient levee deposits are: (1) coarsening upward facies successions comprising beds of sand interbedded with silts (Miall, 2014); (2) proximal to distal fining; and (3) shallow dipping of beds away from the channel (Brierley et al., 1997).

2.2.4 Abandoned channels and deposits

Abandoned channels are defined as floodplain depressions typically infilled with siltstone and claystone, which represents the previous position of an active channel (Smith et al., 1989; Toonen et al., 2012; Miall, 2014). Abandoned channels are formed by a combination of meander cut-off and channel avulsion across the floodplain (Toonen et al., 2012) and are similar in scale to the active channels (Fig. 2.5).

The mode of channel abandonment significantly impacts the type of deposits preserved: oxbow cut-offs produce relatively thick, laminated, clay-dominated abandoned channel-fills due to the dramatic decrease in river discharge in the disconnected oxbow lake; whereas abandoned channels formed due to avulsion are generally filled with coarser-grained deposits since the abandoned channel still maintains a level of connection with the relatively active river (Fig. 2.8; Toonen et al., 2012; Toonen et al., 2015). Whether the channel is at the early or later stages of abandonment will also affect the abandoned channel fill facies succesions. At the early stage of abandonment, the initial fill will be coarser-grained than the subsequent, later-stage deposits (Fig. 2.8; Toonen et al., 2012; Toonen et al., 2015).

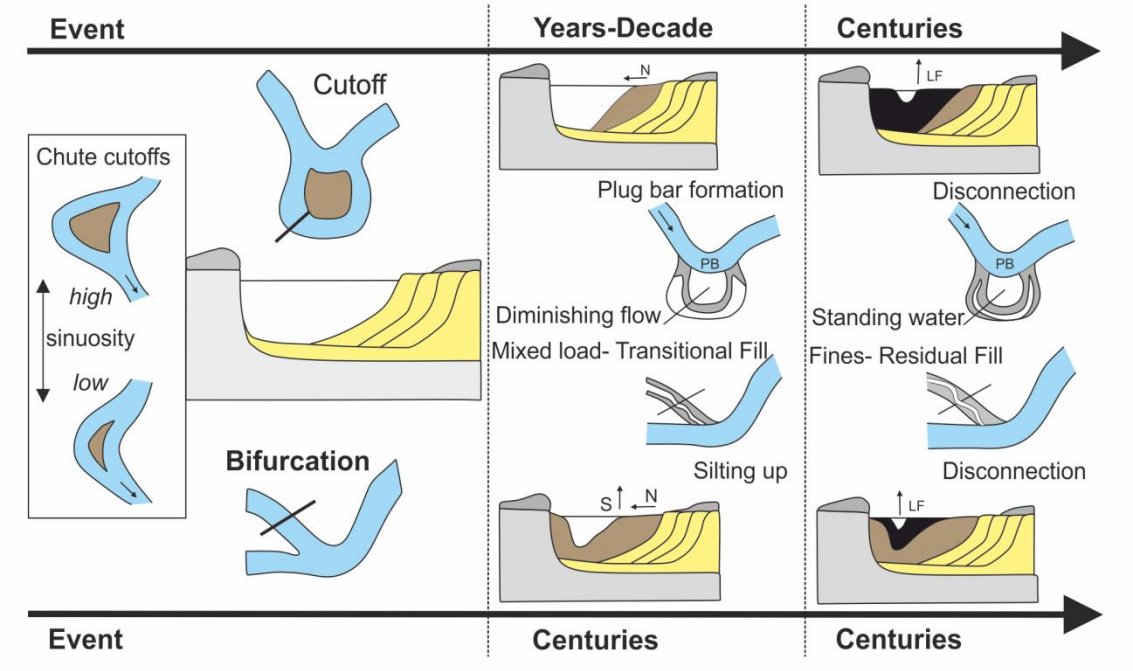

Figure 2.8: Cut-off styles, timescales and associated abandoned channel fills adapted from Toonen et al. (2012).

2.3 Key concepts

2.3.1 What are the internal complexities recognised in splay deposits?

Grain-size distributions in both modern and ancient splay deposits are variable in terms of both area and thickness (Fig. 2.9). The majority of splay deposits can be subdivided into more sand-prone parts and more silt-prone parts (Fig. 2.9; Farrell, 1987; Mjøs et al., 1993; Behrensmeyer et al., 1995; Bristow et al., 1999; Arnaud-fassetta, 2013; van Toorenenburg et al., 2016).

The majority of splay deposits studied in the rock record contain siltstone (Farrell, 1985). Several commonly recognised facies types, including: (i) trough or planar cross-bedded sandstones; (ii) cross-laminated sandstone; (iii) convoluted sandstone; (iv) structureless siltstones; and (v) laminated siltstones, which can be calcareous (Mjøs et al., 1993; Miall, 1994; Behrensmeyer et al., 1995; Anderson, 2005). In sand-rich fluvial systems, sandstone facies in splay deposits commonly dominate (e.g. Anderson, 2005). The sand-prone parts of splays are generally interpreted to relate to sediment transfer and deposition by crevasse channels, for example, the organisation of small “lobes” around the crevasse channel (Fig.2.10; Mjøs et al., 1993).

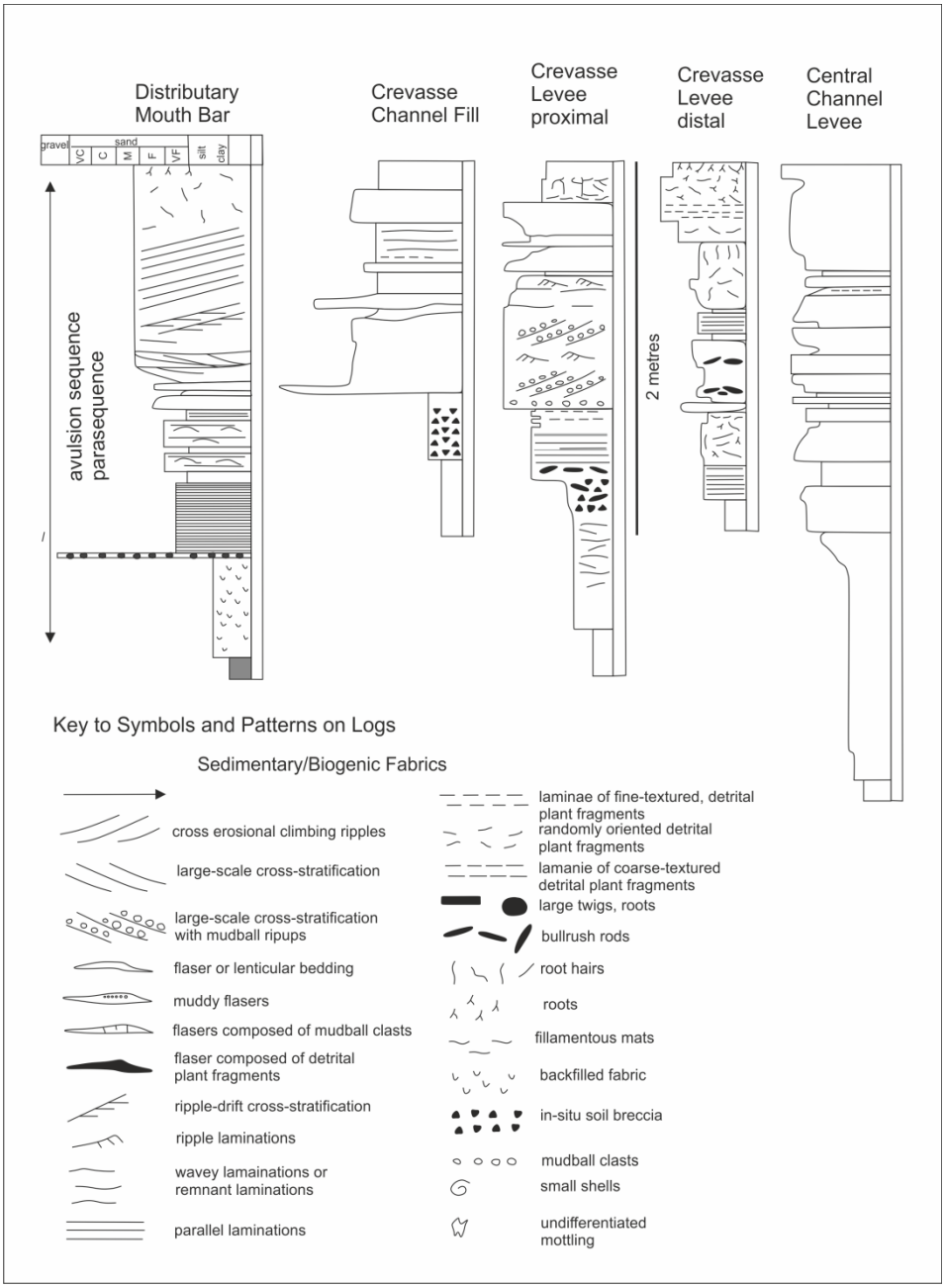

Figure 2.9: Summary logs of stratigraphic sections of different sub-environments in overbank areas of the Mississippi River, illustrating the lateral and vertical variations in sedimentary and stratigraphic characteristics between these subenvironments after Farrell (2001). "Crevasse-Levee proximal" is comparable to proximal splay in this study and "Crevasse-Levee distal" is comparable to distal splay in this study.

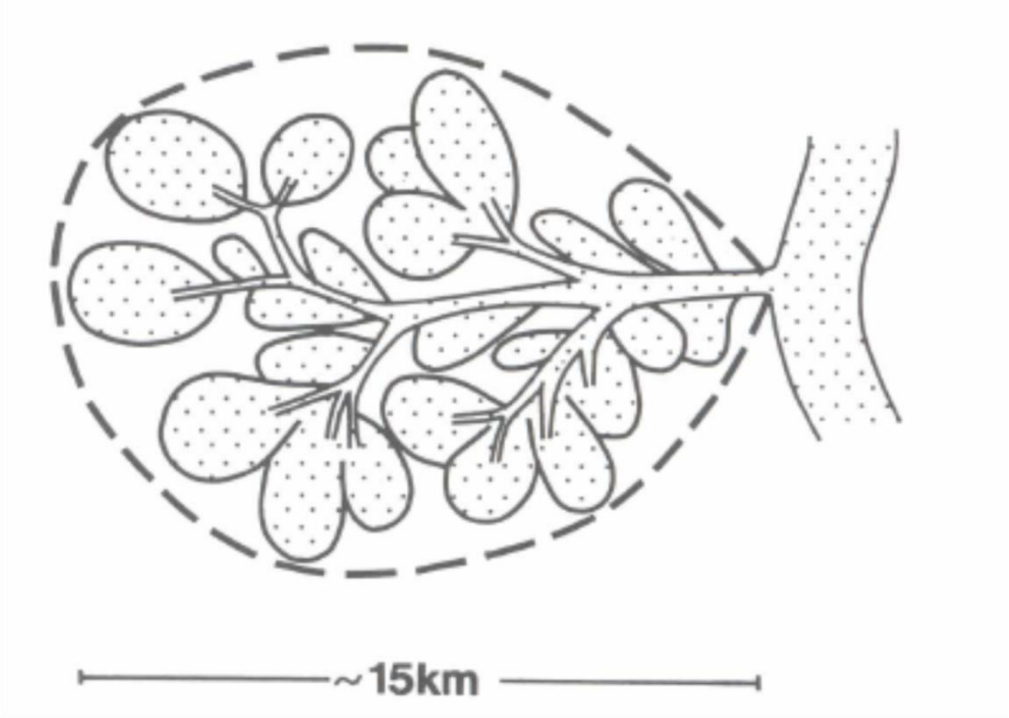

Figure 2.10: Schematic diagram of the possible internal complexities of a single complicated crevasse splay deposit in a fluvial-deltaic environment. The resulting stratigraphic architecutre would generally comprise erosional-based channelised sandstones in proximal areas, sharp-based sandstones in medial areas and single or mutiple coarsening upward lobes in distal areas. After Fielding (1984), Mjøs et al. (1993).

2.3.2 Crevasse splays and terminal splays

The definitions of crevasse splays and terminal splays are fundamentally distinct. However, there are few outcrop studies that have previously investigated the sedimentological and stratigraphic differences between ancient crevasse-splay and terminal-splay deposits (e.g. Donselaar et al., 2013).

A crevasse splay develops where the river breaks its banks and most likely destroys the levee at that point along the channel (Elliott, 1974). During this event, river water flows from this position onto the floodplain and may transport and deposit sediment (Fig. 2.11). Crevasse splays can occur at any point in the fluvial system (Fig. 2.6).

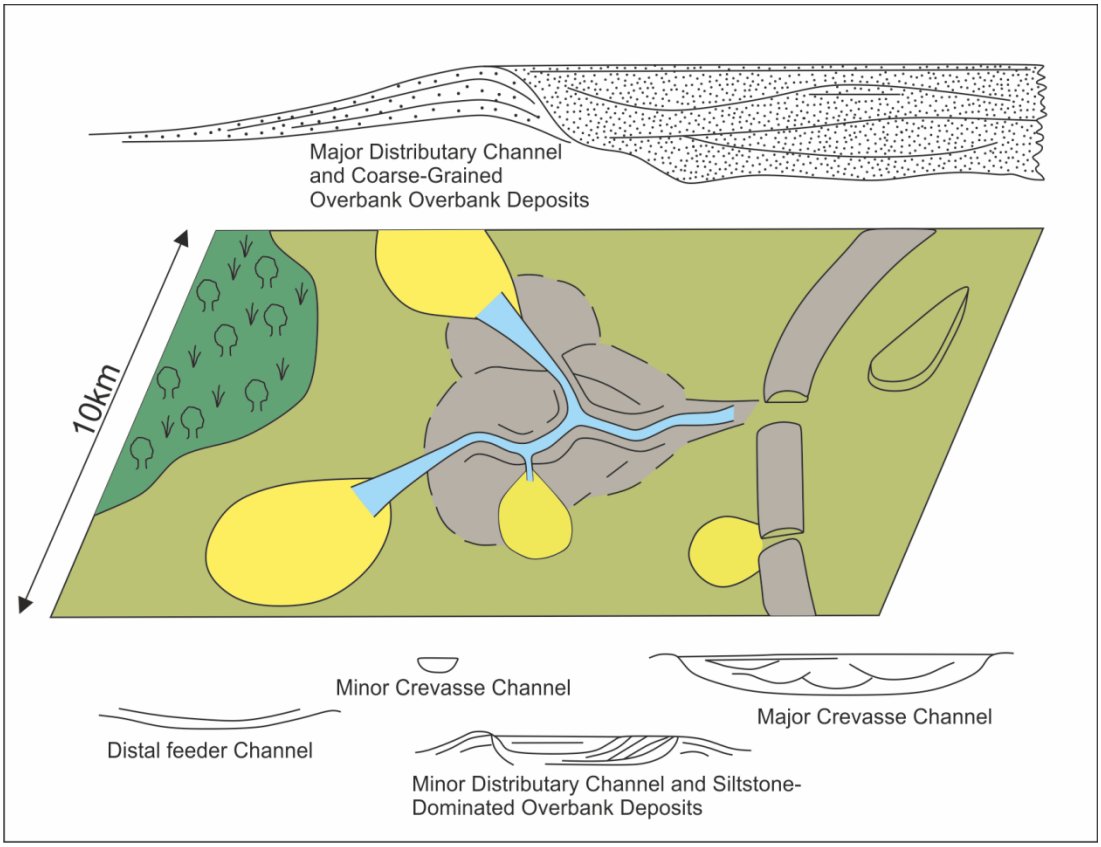

Figure 2.11: Environmental reconstruction of the Durham Coal Measures, showing the various channel types recorded within them and their relationshipto overbank areas. Diagramalso depicts several crevasse and terminal splays, after Fielding (1986).

A terminal splay is defined as a lobe-shaped deposit found at the terminus of river channel which has been deposited from an unconfined sheet-like flood that propagated over a dry floodplain (Lang et al., 2004; Fisher et al., 2008). Terminal-splay deposits also show a general proximal-to-distal decrease in grain size similar to crevasse-splay deposits; proximal areas are generally dominated by sand-prone facies, including planar cross-bedded or massive sandstones and current ripple cross-laminated sandstones, whereas relatively distal areas are generally dominated by finer grained facies (Fig. 2.12). In proximal area, bed thicknesses are typically less than 2 m and may be as low as 0.5 m, whereas bed thicknesses decrease to 0.1- 0.6 m in distal areas (Fisher et al., 2008). However, the internal complexity of terminal splays is

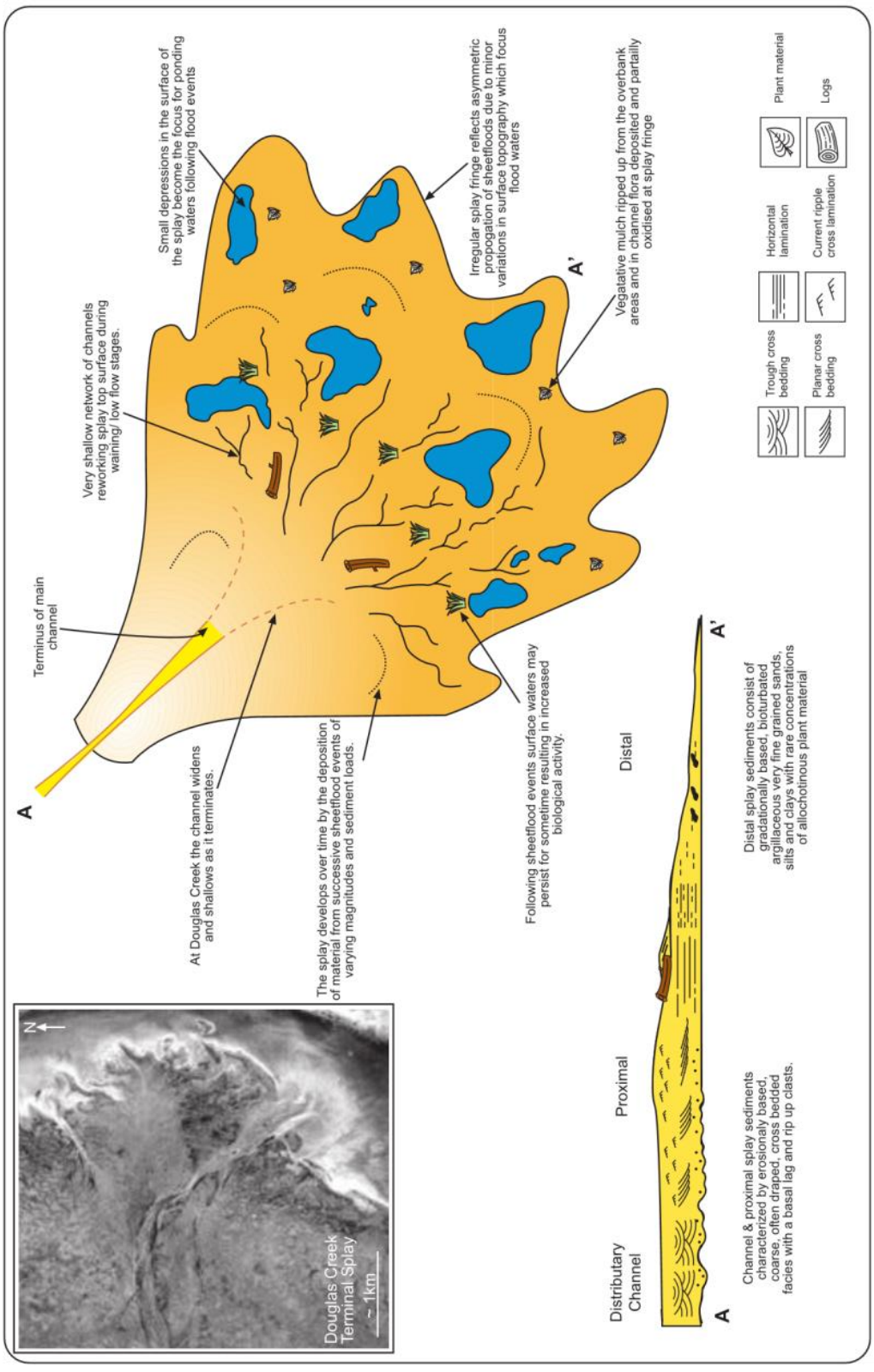

Figure 2.12: Depositional model and cross section through a terminalsplay at Douglas Creek, Australia from Fisher et al. (2008).

generally thought to be lower than that of crevasse splays because, at the terminus of channels, the associated flow energies are lower, which decreases the extent of crevasse-channel development (Fig. 2.12; Fisher et al., 2008). Terminal splays are generally located in the distal parts of dryland fluvial systems, where lower gradients favour diminished fluvial flow energy and termination of channels (Li et al., 2015). In contrast, crevasse-splays formation is associated with higher river flow energies that require steeper gradients and greater discharges, more typical of relatively proximal or medial reaches of a fluvial system (Li et al., 2015).

However, crevasse and terminal splays may be closely associated in modern systems. For example, terminal splays have been found to amalgamate with crevasse-splays along the downstream portions of river channels, resulting in a channel terminus consisting of a ‘crevasse-channel-like’ network with terminal splay sheets (Donselaar et al., 2013).

2.3.3 Crevasse-channel networks

A fundamental control on the internal stratigraphic architecture of splay deposits is the development of crevasses channel network. If the flow is predominantly unconfined and migrates freely across the top of the crevasse-splay body, for example if a crevasse channel network development is ephemeral or if channels have a low degree of flow confinement, then the resultant deposit will be a relatively simple sheet –like body with high lateral connectivity (Fig. 2.13A; Smith et al., 1989). In more-established (i.e. non-ephemeral) crevasse-channel networks, flow and sediment is more confined within the channels, resulting in a more channelised deposits with decreased lateral continuity (Fig. 2.13B, C; Smith et al., 1989). In splays with well-established crevasse channel networks, the planform and cross-sectional stratigraphic architecture is predominantly controlled by the size, density and type of channels within the splay element (Fig. 2.13B, C; Smith et al., 1989).

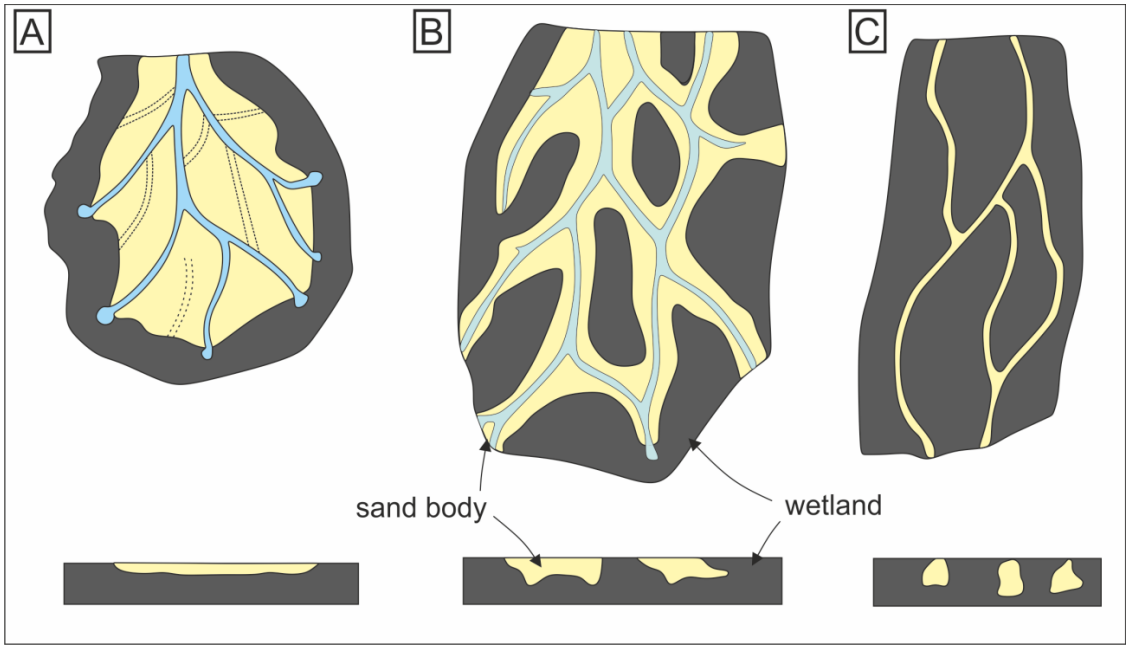

Figure 2.13: Conceptual diagram showing the relationships between crevasse-channel network development and planform geometry of the associated sediment body, schematically sand (yellow) versus mud (grey). (A) Relatively small and emphemeral crevasse-channel network results in a more even sand distribution over time and a more sheet-like deposit. (B) Well-developed, established crevasse-channel network with sand confined in or adjacent to channel, resulting in an increased heterogenisty in the distribution of sand. (C) Subsquent end and overfilling of crevasse-channel network but with high degree of sand confinement within the channels after Smith et al. (1989).

2.3.4 Importance of coal deposits

The Castlegate Sandstone and the Neslen Formation both contain significant amounts of coal deposits (Kirschbaum and Hettinger, 2002), which may be important for overbank deposition. Coals are produced in raised or low-lying mires from the accumulation of vegetation in environments close association to sites of clastic accumulation, such as floodplains and delta plain, but under relatively low clastic deposition rates (Gersib and McCabe, 1981). Coals from

raised mires are rain-fed and aggrade above the regional water table, which means the organic mineral content is low, typically below 10% (Clymo, 1987; Davies et al., 2005; Jerrett et al., 2011a). Coals from low-lying mires are groundwater-fed and generally form within topographic depressions that allow contact with the water table. This means that coals formed in peat-mires can accommodate higher input levels of clastic material before the coal accumulation is disrupted (Cohen et al., 1987; Petersen and Anjsberg, 1996; Jerett et al., 2011a, Jerett et al., 2011c).

The relationship between peat production and accommodation generation is a key control on coal formation (Cross, 1988). Other controls such as climate, tectonics and eustasy are important in modifying how coals are preserved and how peat turns into coal when buried (Shiers, 2017). Peat formation can exert a fundamental control on fluvial overbank sedimentation is by impacting the main channel position. For example, peat compaction may produce relatively localised subsidence and topographic depression in which channels may cluster (van Asselen, 2010).

2.3.5 Palaeosol types and implications for climate types

Palaeosols are soils of an ancient landscape preserved by lithification (Retallack, 2001). As well as coals, which are a type of palaseosol called a histosol (Fig. 2.14; Mack et al., 1993), other types of palaeosols are also common in the Morrison Formation (Demko et al., 2004). As for the formation of modern soils, palaeosols initially (pre-burial) form during periods of low or no clastic sediment input (Demko et al., 2004). The classification of palaeosols is based on a combination of composition, fabric and interpretation of pedogenic processes operating during formation (Fig.2.14; Mack et al., 1993). High organic matter content defines histosols, in low organic content palaeosols, poor horizonations defines a protosols and vertisols (Fig. 2.14; Mack et al., 1993). Good horizonation with low redox conditions defines gleysols. High redox conditions indicates either calcisols (if carbonate rich) or gypsisol (if sulphate rich). The addition of clays defines argillisols, the addition of iron spodosols and if the minerals are altered in situ this is indicative of oxisols (Fig.2.14; Mack et al., 1993).

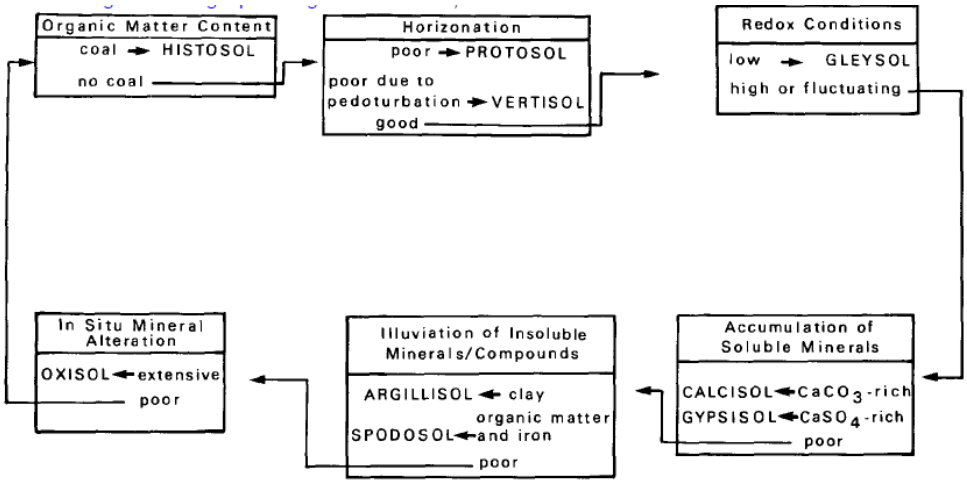

Figure 2.14: Classification procedure for palaeosols (from Mack et al., 1993).

Dry stable floodplain conditions favour the accumulation of mature red palaeosols (in particular calcisols), whereas less stable and wetter floodplain conditions favour the accumulation of gleysols (Fig. 2.15; Cecil, 1990). Highly weathered palaeosols (e.g. oxisols and argillisols; Fig. 2.14) are characteristic of a wet equatorial climate with little seasonal variations. Argillisols, spodosols and gleysols are more likely to form in humid environments (Mack and James, 1994; Kraus, 1999). Calcisols have been described and interpreted in the Morrison Formation (Owen et al., 2015) and are indicative of dry subtropical climates (Mack and James, 1994; Kraus, 1999).

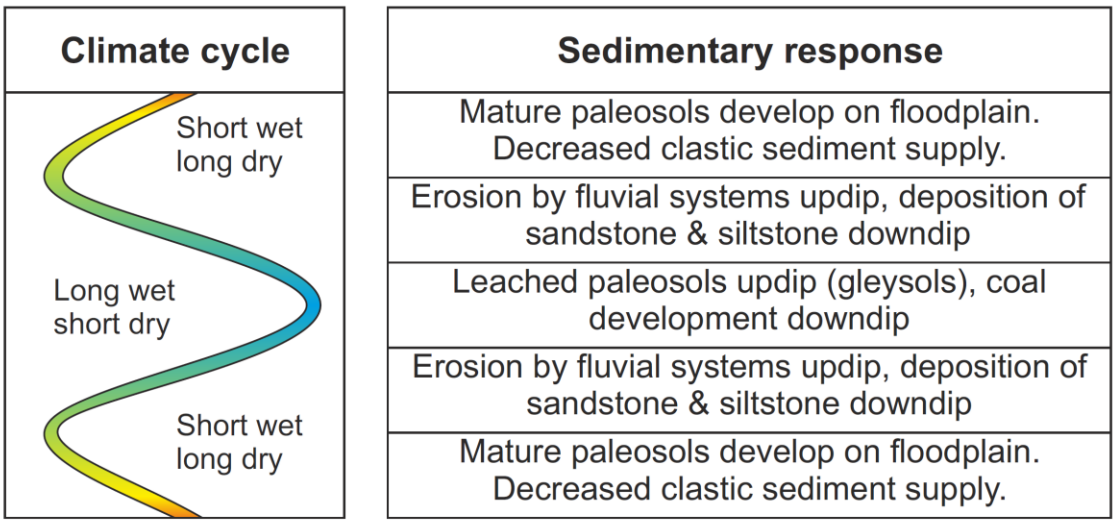

Figure 2.15: The sedimentary conditions favouring formation of different palaeosols. Short wet seasons lead to formation of mature palaeosols (particularly calcisols), whereas long wet seasons favour formation of gleysols and coals (histosols) from Stuart (2015) modified after Cecil (1990).

2.3.6 Stacking styles in sedimentary environments

A variety of stacking styles of sedimentary deposits are recognised and these are principally controlled by the relative rates of accommodation creation and sediment supply in the depositional setting (Muto and Steel, 1997). Compensational stacking forms where sediment preferentially infills topographic lows between preceding deposits (Mutti and Sonnino, 1981; Straub et al, 2009) and is commonly recognised in lobe-shaped deposits, including deep-water lobe settings (e.g. Deptuck et al., 2008; Prélat et al, 2013), delta lobe deposits (e.g. Frazier, 1967), and crevasse-splays deposits (Fig. 2.16; van Toorenburg et al., 2016; Gulliford et al., 2017). Aggradational stacking describes vertical build-up of sediments, for example, vertical accretion of lobes, and forms when the rate of accommodation creation and sediment supply are approximately equal (e.g. Emery and Myers, 1996). In channel-lobe systems, aggradational stacking occurs when channel migration and avulsion is limited due to high

levels of confinement and high levels of sediment input. Consequently sediments stack with no lateral offset; has been recognised in deep-water lobes

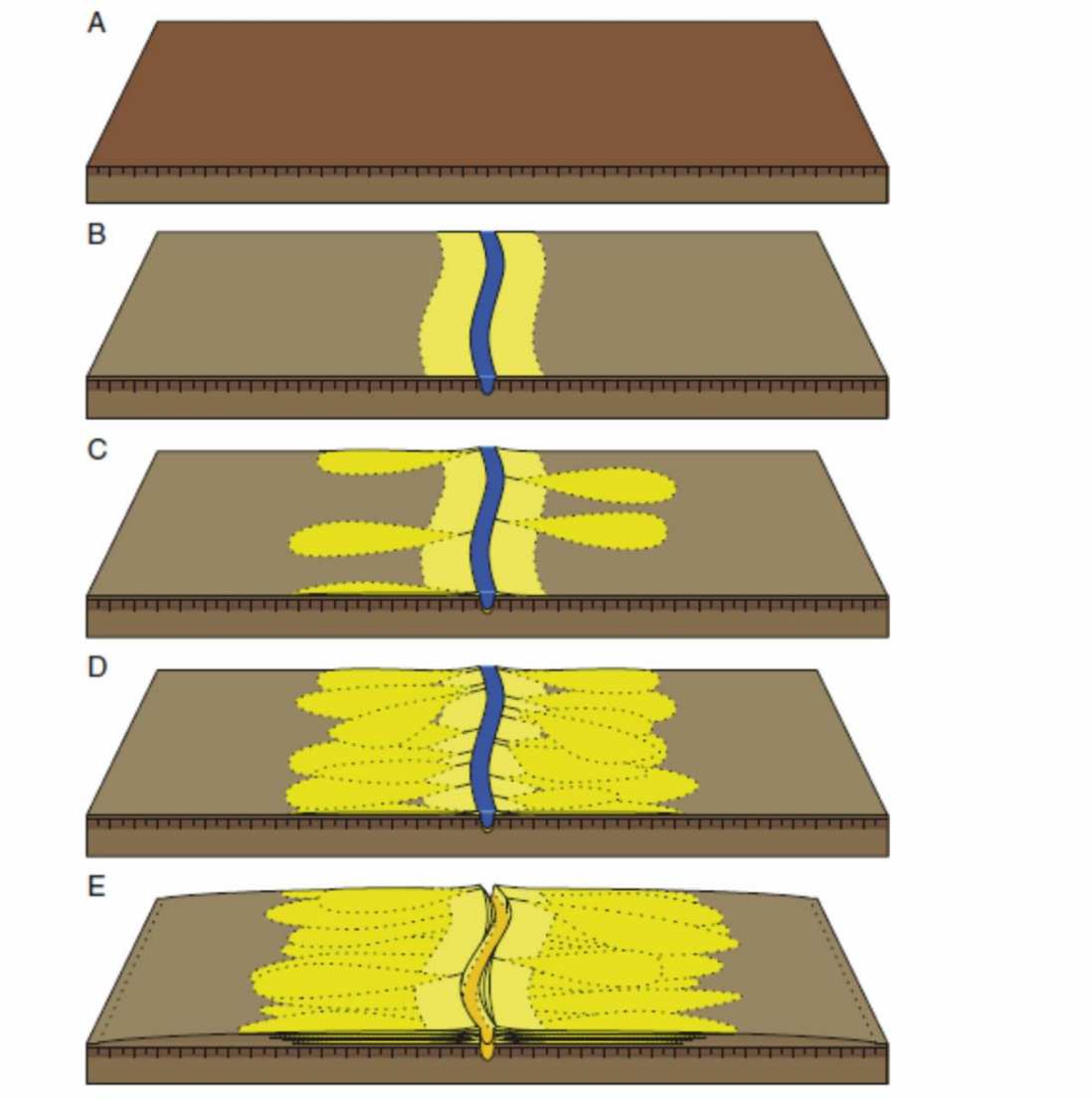

Figure 2.16: Schematic model showing the evolution of compensational stacking of crevasse-splay deposits from van Toorenenburg et al. (2016).

(e.g. Burgreen and Graham, 2014). However, there are no examples of aggradational stacking in fluvial crevasse splay deposits. In a progradational stacking pattern, successively younger stratigraphic units are deposited further in the direction of sediment transport, for example basinward (Emery and Myers, 1996) or further away from the channel and onto the floodplain in the

case of splays. Progradation stacking is formed when the rate of sediment supply exceeds the rate of accommodation space creation (Emery and Myers, 1996), or some level of confinement preventing lateral migration (Grundvag et al., 2014). Progradational stacking patterns have been recognised in deep-water lobe deposits (e.g. MacDonald et al., 2011; Prélat et al., 2009), extensively in delta lobe deposits (e.g. Van Wagoner et al., 1990) and only rarely in crevasse-splay deposits (e.g. van Toorenenburg et al., 2016). In a retrogradational stacking pattern, successively younger stratigraphic units are deposited farther upstream towards the sediment source and is formed when sediment supply rate is lower than the rate of accommodation space creation, or insufficient to infill the available accommodation space (Emery and Myers, 1996). Retrogradational stacking patterns have been observed in deep-water lobe deposits (e.g. Amy et al., 2007) and delta lobe deposits (e.g. Van Wagoner et al., 1990) but not in fluvial crevasse-splay deposits.

2.3.7 River avulsion, flood deposits and crevasse-splays

Splay evolution in modern systems has been categorized using a three-stage model based principally on observations from the Cumberland Marshes, Canada (Smith et al. 1989). Simple lobate splays are classified as Type I (Fig. 2.17A). A splay in which a crevasse-channel network has developed is classified as Type II (Fig. 2.17B), and which may affect sediment distribution (Fig. 2.17). Type III splays have extensive, well-developed, more complex and anastomosing crevasse-channel network that causes significant lateral variations in sediment characteristics (Fig. 2.17C).

Termination of splays may occur by two methods: (i) detachment (cut-off) from the main parent fluvial channel, resulting in abandonment and subsequent stabilisation by vegetation, chemically precipitated crusts and/or bio-chemical soils (Arnaud-Fassetta, 2013); or (ii) further development such that an active splay serves as the initial phase of a major avulsion of the parent channel (Fig. 2.18; Smith et al., 1989; Jones and Harper, 1998; Farrell, 2001; Buehler at al., 2011). Avulsion splays are splays that form the initiation phase of a channel avulsion (Smith et al., 1989; Slingerland and Smith, 2004; Jones and Hajek, 2007). Avulsion splays and the subsequent avulsion channel initially develop by

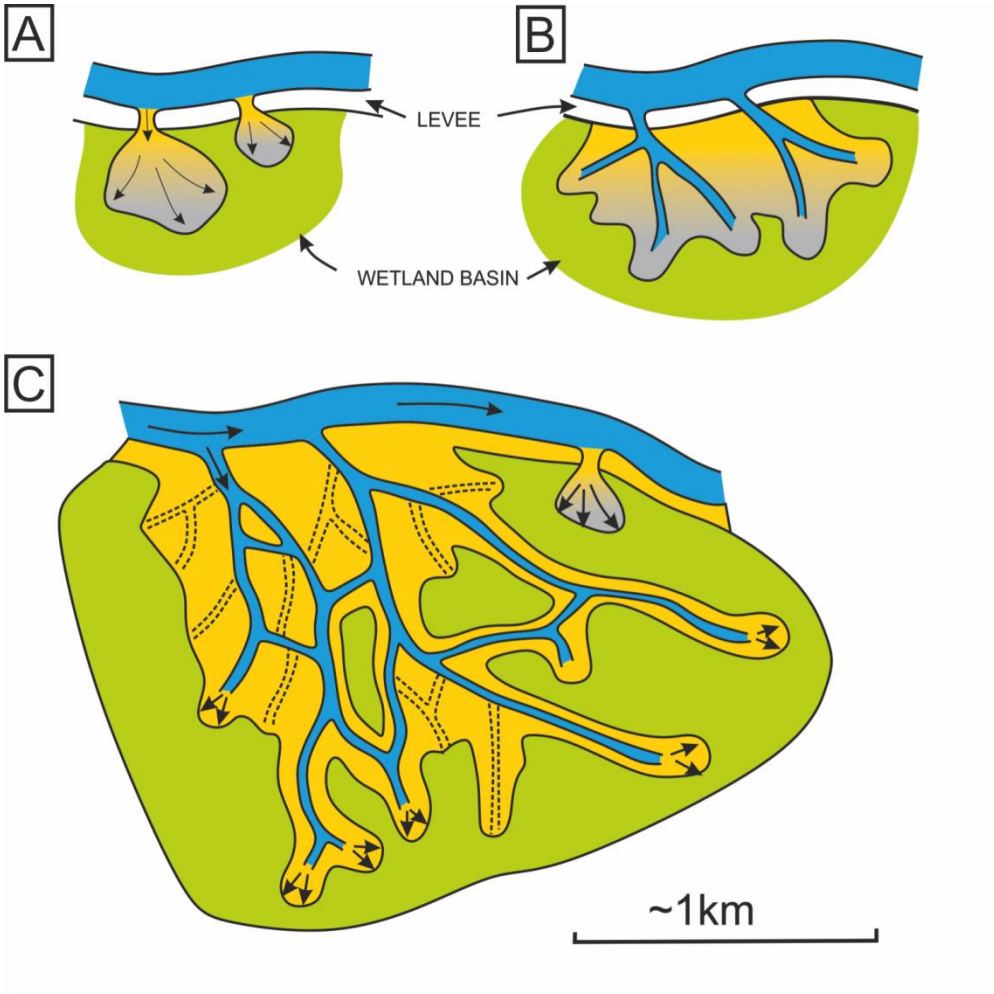

Figure 2.17: Classification of crevasse-splays based on the evolutionary development of crevasse-channel network adapted after Smith et al. (1989).

local erosion of the parent channel bank and formation of a crevasse channel through which sediment and water are diverted (Fig. 2.18). As the discharge of water and sediment through a crevasse channel increases, so the parent river eventually avulses into the course of the main crevasse channel (Fig. 2.18; Bristow et al., 1999; Mohrig et al., 2000; Miall, 2014). This has been documented in the development of an avulsion channel related to the central channel in Cumberland Marshes fluvial system, Canada (Fig. 2.19; Toonen et al., 2015). In the rock record, such evolution is manifest as a transitional

avulsion stratigraphy (Jones and Hajek, 2007). The resultant idealised stratigraphic succession comprises crevasse-splay deposits below the erosional surface and subsequent infill of the avulsion channel and both the splay and the succeeding channel bodies exhibit similar palaeocurrent trends (Bristow et al., 1999; Mohrig et al., 2000; Slingerland, 2004; Jones and Hajek, 2007; Miall, 2014).

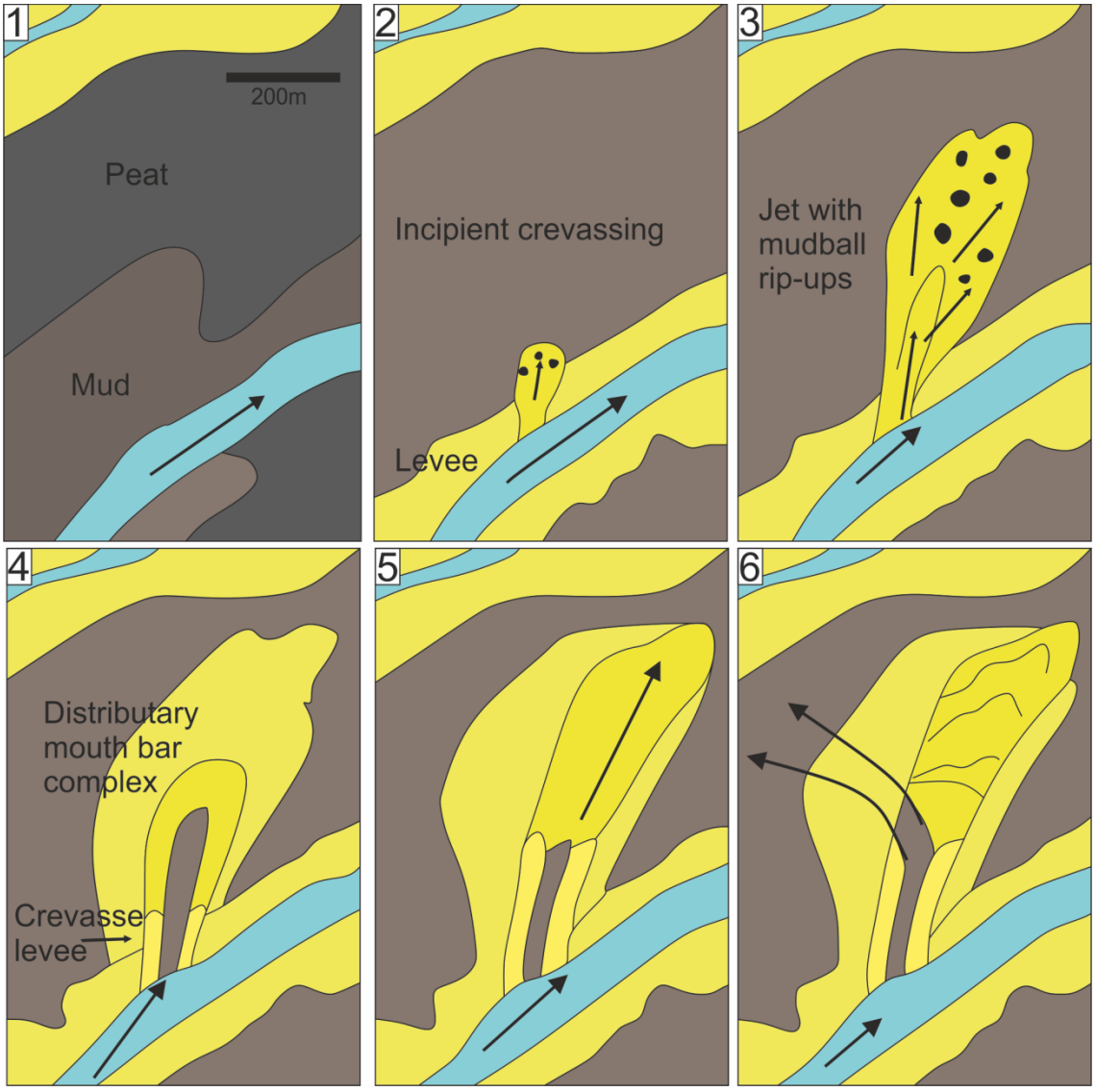

Figure 2.18: Conceptual diagram showing the development of an avulsion splay and subsequent avulsion channel after Farrell (2001).

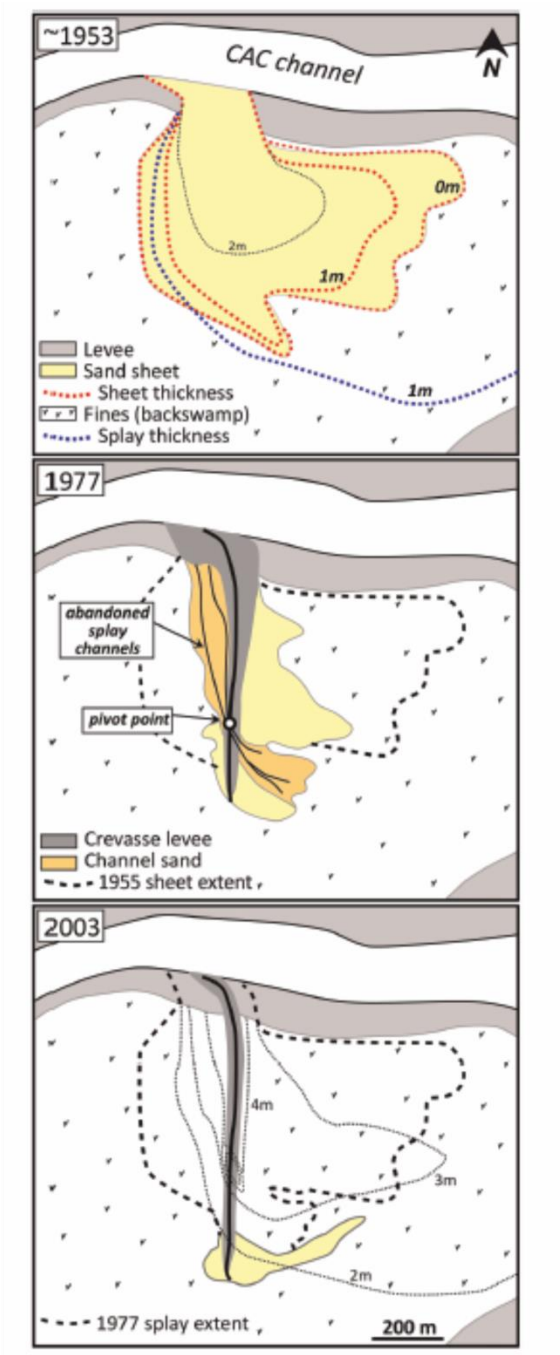

Figure 2.19: Summary diagram showing the temporal relationship of crevasse-splays and a new avulsion channel related to the CAC channel in the Cumberland Marshes, Canada from Toonen et al. (2015).

2.3.8 Controls on crevasse-splay deposition

The magnitude and duration of flooding will affect the amount and grain size of the sediment available to the floodplain. The greater the magnitude of the flood the more sediment will be deposited on the floodplain (Zwoliński, 1992) The greater the duration of the flood so coarser sediment will make it further out onto the floodplain (Smith et al., 1989).

Local accommodation also affects splay size. A crevasse splay deposit or stacked crevasse splay complex can only be as thick the available accommodation (Bristow et al., 1999). The accumulation of rheotrophic peat mires can influence the local accommodation conditions since compaction is much greater than for clastic sediments (Nadon, 1998), resulting in local accommodation generation. However, under certain conditions– for example if precipitation is greater than evaporation and extensive ombotrophic ("rain-fed") peat mires aggrade– splay development may be reduced or inhibited because the floodplain height is greater than parent channel height (McCabe and Shanley 1992).

The storage capacity of a floodbasin or its accommodation space is controlled by the elevation of the channel and bankfull level of the channel; overbank deposits cannot vertically accrete above the height of the channel water level at that time without the system becoming unstable and the deposits becoming subject to significant erosion (Wright and Mariott, 1993).

The bankfull height of the river and the local accommodation in the adjacent floodbasin has a strong control whether crevasse-splay deposition will occur. Super-elevation of a channel above the floodbasin is an unstable situation that favours development of crevasse splays and the transfer large amounts of the finer components of sediment in the flow to the floodbasin (Bryant et al., 1995; Ethridge et al., 1999). In contrast, if the floodplain level is higher than that in the channel, non-deposition of sediment on the floodplain is favoured. Sediment pedoturbation and bioturbation will then encourage the development of palaeosols in well-drained floodplains, whereas in water-saturated floodplains, coals can develop (Wright and Marriott, 1993). An increase in base-level can

result in channel super-elevation due the increased river aggradation (Etheridge et al., 1999; Bristow et al., 1999). Extreme flood discharges may also drive crevasse-splay formation by increasing the number of flooding events breaking out onto the floodplain (Törnqvist and Bridge, 2002;Fisher et al., 2008).

Changes in base level and accommodation space can also be linked to alluvial architecture; local base level controls a fluvial systems bankfull level since deposition will only be stable at a level below the channel, a rise or fall in local base level effects the amount of accommodation space (Wright and Mariott, 1993). An increase in base level can results in an increase in accommodation space which means a corresponding increase floodplain accommodation space. Depending on the balance of sediment supply, vertical accretion or retrogradational stacking of overbank elements may occur. In theory, if the rate of base-level rise and accommodation space generation is relatively high, this may permit increased confinement and vertical aggradation of the river channel (Allen, 1978; Bridge and Leeder, 1979). In contrast, relatively low rates of base level rise, accommodation creation and aggradation facilitate floodplain reworking by migrating and avulsing rivers resulting in more amalgamated channel deposits (Allen 1978; Bridge and Leeder 1979; Wright and Mariott, 1993). However, analysis of data from ancient sedimentary successions suggest that channel-body characteristics alone do not permit identification of high- and low-accommodation systems tracts (Colombera et al., 2015).

2.3.9 Sediment transport on fluvial levees

Levee formation is interpreted to occur by diffusive and advective sediment transport (Fig. 2.20) (Adams et al., 2004). Levees formed by diffusive transported are relatively steep and narrow, and the grain size of sediment rapidly fines away from the channel (Fig. 2.20A). Levees formed by advective transport have relatively gentle slopes and display a more diffuse grain size trend away from the channel (Fig. 2.20B).

Levees in different modern settings have been recognised to form by diffusive or advective sediment transport. Diffusive sediment transport was found to dominate in the Columbia River, where the interconnected nature of the system

means that floodplain water levels rise at approximately the same rate as those in the main channel during a flood (Adams et al., 2004). The equilibrium between the water levels in the channel and on the floodplain allows the unidirectional flow of the main channel to interact with the calmer flood-basin waters, resulting in formation of free-flowing turbulent eddies. These eddies entrain suspended sediment from the main channel but rapidly lose the ability to carry this sediment depositing steep narrow levees close to the main channel (Adams et al., 2004).

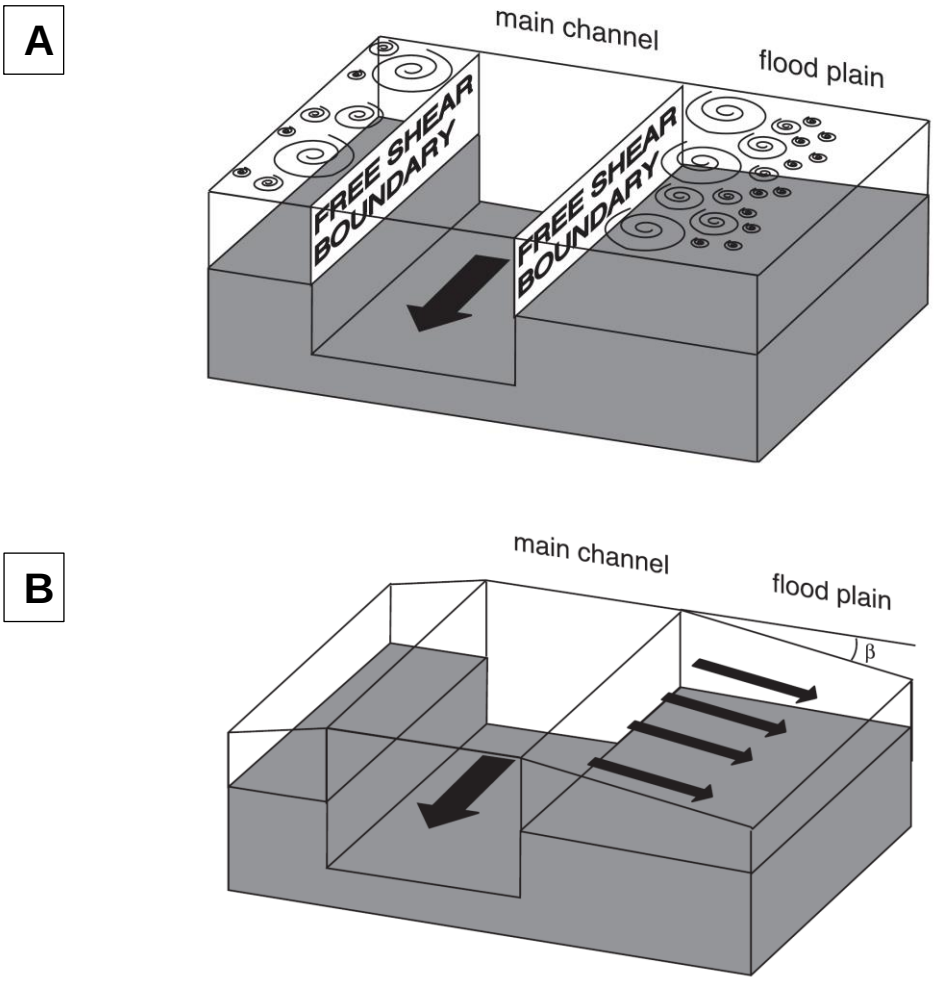

Figure 2.20: Models of levee growth by (A) turbulent diffusion and (B) advection from Adams et al. (2004).

Advective sediment transport dominates in the Cumberland marshes, where the wider more unconfined nature of the floodplain means a greater storage

capacity in the floodplains than the channel (Adams et al., 2004). This means that during a flood the water level in the adjacent floodplains lags behind the channel, which results in a water surface gradient perpendicular to the channel. Consequently, water in the main channel will be diverted onto the floodplain. As the main channel flow moves onto the floodplain, the energy and carrying capacity of the flow gradually dissipates, resulting in formation of gently sloping levees (Adams et al., 2004).

2.3.10 Fluvial hierarchical schemes

There are several classification schemes for the hierarchy of fluvial deposits (e.g. Table 2.1; Friend et al., 1979; Allen, 1983; Miall, 1985; Bridge, 1993). These schemes use a hierarchical approach to organise depositional units of different scales according to variations in facies, facies associations, geometries scales and depositional environment (Table 2.1; Miall, 1985; Bridge, 1993).

Hierarchical schemes based on numbered bounding surfaces have focussed on the identification of various contacts between rock bodies (Table 2.1; Cant and Walker,1978; Allen, 1983; Miall, 1985). First-order contacts are between individual bedsets (Allen, 1983); second order and third order contacts define architectural elements (Miall, 1985; Miall, 1988); whereas fourth-order contacts separate lithofacies assemblages, also called complexes (Allen, 1983; Miall, 1985) or storeys (Friend et al., 1979). Fifth order contacts are major erosional surfaces between groups of elements or “complexes” (Cant, 1978; Allen, 1983; Miall, 1985). Sixth order surfaces constrain a palaeovalley or succession (Table 2.1) (Miall, 1985).

Alternate schemes are based on the genetic relationships between architectural units such as similar facies types, thicknesses and palaeoflow indicators (Table 2.1). Individual beds stack to form bedsets that stack to form storeys (Willis, 1993).

<table>
<tr><th>McKee and Weir (1953)</th><th>Campbell (1967)</th><th>Jackson (1975)</th><th>Allen (1983)</th><th>Bridge and Diemer (1983)</th><th>Miall (1988, 1991)</th><th>Van Wagoner et al. (1990)</th><th>Ford and Pyles (2014)</th></tr>
<tr><td>na</td><td>lamina</td><td rowspan="2">microforms</td><td>zeroth order</td><td rowspan="3">na</td><td rowspan="3">na</td><td>lamina</td><td>lamina</td></tr>
<tr><td>na</td><td>lamina sets</td><td rowspan="2">na</td><td>lamina sets</td><td>lamina sets</td></tr>
<tr><td>set</td><td>bed</td><td rowspan="2">mesoforms</td><td>bed</td><td>bed</td></tr>
<tr><td>cosets</td><td>bedsets</td><td>first-order</td><td>bedsets or minor surfaces</td><td>first order</td><td>bedsets</td><td>bedsets</td></tr>
<tr><td>composite set</td><td rowspan="4">na</td><td>macroforms</td><td>second order or complexes*</td><td>storey or major surfaces</td><td>second-order or small architectural element</td><td rowspan="2">na</td><td>story</td></tr>
<tr><td rowspan="3">na</td><td rowspan="3">na</td><td>third-order or sheets or architectural element</td><td rowspan="3">na</td><td>third order or architectural element</td><td>element</td></tr>
<tr><td rowspan="2">na</td><td>fourth order or architectural element</td><td>parasequence</td><td>archetype</td></tr>
<tr><td>fifth order or major sand sheets or channel-fill complexes</td><td>parasequence set</td><td rowspan="2">na</td></tr>
<tr><td>sixth order or paleovalleys;</td><td>sequence</td></tr>
</table>

Table 2.1: Summary table comparing different hierarchical classification schemes of fluvial deposits from Ford and Pyles. (2014).

Chapter 3 Lithofacies

This chapter introduces the lithofacies identified in each of the formations studied and provides possible interpretations for each. Facies associations are also introduced which are specific to this study and which broadly group facies together based on sub-environments.

Study codes	FAKTS codes	Description
	G-	Gravel with undefined structure
Gm	Gmm	Matrix-supported, massive or crudely bedded gravel
Gp	Gp	Planar cross-stratified gravel
	S-	Sand deposits with undefined structure
St	St	Trough cross-stratified sand
Sp	Sp	Planar cross-stratified sand
Sr	Sr	Current ripple cross-laminated sand
Sm	Sm	Massive sand
Sd, Fd	Sd	Soft-sediment deformed sand
	F-	Fine-grained (silt/clay) deposits with undefined structure
Fl	Fl	Interlaminated very fine sand, silt and clay
Fp, Fop	Fsm	Laminated to massive silt and clay
Fm	Fm	Massive clay
Fr,Frg,Frr,Frm	Fr	Fine-grained root bed
C	C	Coal or highly carbonaceous mud

Table 3.1: Comparison table showing how the facies codes used in this study map onto those used in the FAKTS database (Colombera et al., 2012, 2013). FAKTS codes are based on that of Miall (1978).

Facies code	Morrison FM	Mesaverde Group
Gm	✕	✕
Gp	✕	
St	✕	✕
Sp	✕	✕
Sr	✕	✕
Sm	✕	✕
Sd		✕
Fd	✕	✕
Fl	✕	✕
Fp	✕	✕
Fop		✕
Fm	✕	✕
Fr		✕
Frg	✕	
Frr	✕	
Frm	✕	
C		✕

Table 3.2: Comparison table showing occurrence of different facies types in each of the studied formations.

3.1 Green structureless conglomerate (Gm)

Description

Facies Gm is composed of green-grey, poor to moderately sorted fine sandstones and conglomerate (Fig. 3.1). Bedsets are 0.8- 2.4 m (1.7 m mean) and are mostly structureless, or can reveal fining-upwards trends from conglomerate to fine sandstones. Erosive bases are common with an average 1-2 m erosion on the basal surfaces.

Interpretation

This facies records rapid deposition of sands and gravels, predominantly from bedload in a decelerating flow whereby the rate of deposition was too rapid to allow primary structures to form (Collinson et al., 2006, p. 133).

3.2 Cross stratified conglomerate (Gp)

Description

Facies Gp consists of grey-green, very-fine sandstone and conglomerate, generally poorly to moderately sorted with subangular grains. Matrix varies from very-fine to fine sandstone whereas grains vary from pebble to conglomerate size. Bedsets are 1.0 - 2.3 m (1.5 m average). Some sets exhibit uniform grain size, whereas others exhibit a fining-upward trend (Fig. 3.2). Planar cross-bedding is common with sections that are oriented parallel to palaeoflow revealing either planar foresets with angular bases or sets in which convex-up sets that exhibit an asymptotic relationship at their base.

Interpretation

This facies records the deposition from a relatively high-energy flow which was carrying a mixture of bedload gravel and suspended-load sand. Deposition was under a quasi-steady state which allowed for formation and downstream migration of gravel barforms (Bluck, 1982; Leddy et al., 1993).

3.3 Trough and planar cross-bedded sandstone (St/Sp)

Description

Facies St/Sp is composed of grey-yellow to yellow-brown, moderately to well sorted upper very-fine- to upper medium-grained sandstone that possess sub-angular to sub-rounded grains. Some sets exhibit uniform grain size, whereas others exhibit a fining-upward trend. Mudstone rip-up clasts occur (<5%) at the base of individual sets, and may also occur scattered within sets (Fig. 3.3). Less common (2-5%) are small (5 to 20 mm diameter) sub- to well-rounded pebbles of extra-formational origin. Plant fragments are common throughout the sets; bark and wood fragments (<70 mm) are confined to the basal 0.2 m of the sets.

Planar cross-stratified bedsets are 0.4 to 1.5 m thick (75% of this facies). Sections oriented parallel to palaeoflow reveal either planar foresets with angular bases or sets in which convex-up foresets pass into bottomsets that exhibit an asymptotic relationship at their base. Examples of trough cross-stratified sets (~0.5 m thick) are less common (20% of this facies), and are more difficult to identify than their planar cross-stratified counterparts. Both planar and trough cross-stratified sets can occur either as cosets (stacked sets) or as single sets. Commonly, coset boundaries are marked by mudstone pebble clasts, and sets directly beneath and above coset boundaries exhibit markedly different foreset dip azimuths. Prominent bounding surfaces, with erosional relief (up to 0.2 m), separate sets or cosets of facies St/Sp from underlying facies.

Interpretation

This facies records deposition from a relatively high-energy flow that was capable of transporting and sorting sand, and carrying mud-chip rip-up clasts (Miller et al., 1977). The inclusion and preservation of large plant and bark fragments within this facies indicates a high-energy flow. Planar and trough cross-bedded sets record the downstream migration of straight-crested (two-dimensional) and sinuous-crested (three-dimensional) dunes, respectively (Allen, 1963; Rubin, 1987; Rubin and Carter, 2006). The overall fining-upward trend within cosets indicates a waning flow. Sets and cosets that record variable

palaeocurrent azimuths indicates repeated reactivation of dunes or bars, respectively, and the occurrence of minor erosional surfaces with associated mud-clast-rich lags, are either the result of successive flood events or by a single unsteady flow (Rubin, 1987; Leeder, 2011, p. 139).

3.4 Well sorted, clean siltstones (Fm)

Description

Facies Fm is composed of light-blue or white, medium to coarse siltstone that is moderately to well sorted. Small (<2 mm thick, <50 mm long) inclined root structures of siderite and small mm-scale fragments of plant material occur within this facies; the former is generally present at the top of beds whereas the latter occurs at the base of beds. Preserved sets are 0.4 to 2.4 m thick (mean is 1.4 m) and have erosional bases (up to 2 m of local relief). The siltstones are faintly laminated or structureless (Fig. 3.4).

Interpretation

The well-sorted, weakly laminated nature of the siltstones indicates slow accumulation from sluggish flows or from a stationary water column. The erosional bedset bases indicate high-energy flows. Deposition of fine-grained sediment within an erosional feature implies either bypass of a more energetic flow and subsequent deposition from suspension of finer silts as the flow waned (cf. Toonen et al., 2012), or that fine-grained deposition took place by suspension settling when the water table was still elevated above the floodplain surface, but with no net flow.

Figure 3.1:Facies Gm: Structureless conglomerate.

Figure 3.2: Facies Gm: Cross-stratified conglomerate.

Figure 3.3: St/Sp: Trough and planar cross-bedded sandstone.

Figure 3.4: Facies Fm: Well-sorted, clean siltstone.

3.5 Structureless sandstone (Sm)

Description

Facies Sm is composed of dark grey-yellow, lower-fine to lower-very fine sandstone that is moderately to poorly sorted. It occurs in sets that vary in thickness from 0.2 to 2.2 m (mean is 1 m). Set boundaries are sharp but non-erosional bounding surfaces (Fig. 3.5). Internally, sets are structureless (Fig. 3.5).

Interpretation

This facies records rapid deposition of sand either from a hyper-concentrated flow or predominantly from suspension in a decelerating flow whereby the rate of deposition was too rapid to allow primary structures to form (Jones and Rust 1983; Collinson et al., 2006, p. 133).

3.6 Small-scale ripple cross laminated sandstone (Sr)

Description

Facies Sr is composed of grey-yellow, lower-fine to very fine sandstone that is moderately to poorly sorted. Commonly, organic detritus is present as 0.1 to 0.3 m-thick layers that notably contain small (<50 mm long) plant fragments, bark pieces and coal fragments. Cosets vary in thickness from 0.5 to 3 m (mean is 0.85 m). Bedset bases are sharp but generally non-erosional bounding surfaces, although gutter casts are present in some places. Internally, sets exhibit either a weak fining-upward or no discernible grain-size trend. Small-scale ripple cross-lamination (4 to 10 cm set thickness) is the dominant structure in this facies. Non-climbing ripple forms where the ripple sets show horizontal but erosive set boundaries are present, as are climbing forms. Most instances preserve ripple sets with boundaries that are erosional but inclined and are indicative of ripple climbing at a subcritical angle (Fig. 3.6). However, others preserve stratification with non-erosive set boundaries and so exhibit inclined set boundaries indicative of ripple climb at supercritical angles (Fig. 3.6; cf. Rubin and Carter, 2006).

Interpretation

This facies records the migration of ripple-scale bedforms (microforms). The presence of non-climbing ripple forms indicates ripple formation under relatively low sediment-supply conditions, which resulted in sets migrating laterally without vertical aggradation (Allen, 1970). The presence of climbing ripple-lamination with a subcritical angle of climb indicates a net aggradational regime, whereby some ripples formed under relatively high rates of sediment supply combined with a downstream deceleration of the flow, thereby allowing the sets to aggrade as the ripple forms migrated laterally (Allen, 1970; Collinson et al., 2006, p. 85). The layers of organic detritus are indicative of a lag deposit from an energetic flow or flows moving over a vegetated area and incorporating loose organic matter prior to its deposition farther downstream.

3.7 Soft-sediment deformed sandstone with remnant ripple forms (Sd)

Description

Facies Sd is composed of grey-yellow, lower- to upper-very fine sandstone that is poorly to moderately sorted. Fragments of cm-scale organic detritus are scattered throughout. This facies occurs as bedsets that vary in thickness from 0.4 to 2.4 m (mean is 1.1 m). Bedset bases are sharp but non-erosional and set tops are gradational into overlying facies (Fd, Fp and Fop). Soft-sediment deformation structures including convolute lamination within sets, and rare load and flame structures at basal set boundaries obscure primary sedimentary structures (Fig. 3.7). Where soft-sediment deformation structures are less prevalent, poorly preserved examples of small-scale ripple cross-lamination are present (Fig. 3.7), with both non-climbing ripple forms and subcritical angle of climbing ripple strata preserved.

Interpretation

This facies records deposition from mixed sand- and silt-laden flows onto an unstable water-saturated substrate. Soft-sediment deformation structures most commonly arise due to upward water loss through more permeable layers as

sediment aggrades and acts to load and induce compaction of underlying deposits (Allen, 1977). Convolute lamination indicates plastic deformation of water-saturated, non-consolidated sediment during or soon after deposition (Allen, 1977; Collinson et al., 2006, p. 197-198). Remnant ripple forms and poorly preserved ripple cross-lamination record a component of sluggish unidirectional flow in areas that were less prone to deformation (cf. Owen, 1996; Marconato et al., 2014).

3.8 Soft-sediment deformed chaotic sandstone and siltstones (Fd)

Description

Facies Fd is composed of dark grey-yellow, poorly sorted fine siltstone to very-fine sandstone. Bed bases tend to be sharp but non-erosional. Centimetre-scale plant fragments are present throughout. Set thicknesses are variable, from 0.1 to 3 m (0.6 m average). Within the lowermost (~1 m) parts of sets, primary sedimentary structures tend to be overprinted by soft-sediment deformation structures (Fig.3.8); overlying sand-prone parts of sets tend to load into underling silt-prone parts of sets.

Interpretation

This facies records the relatively rapid deposition of fine sand and silt from an aqueous flow onto an unstable substrate. Denser, sandier parts of a set reveal evidence of gravity driven sinking and loading into underlying silt-prone parts of a set. The silt-prone lower parts of sets were water-saturated and became over-pressured in response to loading. This lead to expulsion of fluids and the development of upward-oriented water-escape structures when the pore pressure became sufficiently high to breach the overlying sediment pile (Allen 1977; Owen 1987; Collinson et al., 2006, p. 185, p. 195).

3.9 Structureless (± organic-rich) poorly sorted siltstones (Fp/Fop)

Description

Facies Fp/Fop is composed of light-blue grey (Fp) (Fig. 3.9) or dark grey (Fop), poorly sorted very fine sandstone to fine siltstone. Bedsets of Fp (0.1 to 2.1 m thick, mean 0.6 m) and Fop (0.3 to 2.1 m thick, mean 0.8 m) are mostly structureless (Fig. 3.10), although weak fining-upwards is present locally. Small (<5mm thick) red-brown plant-root structures are preserved as siderite concretions in some places. Although these can occur throughout bedsets, they tend to be more common in the upper parts of bedsets. Sub-facies Fp and Fop are very similar: Fop has greater dispersed organic content, is dark grey in colour and contains 5% root structures; Fp is light blue-grey and contains 2% root structures.

Interpretation

This facies records relatively rapid deposition from waning-energy flows (probably sediment fallout from suspension) hence the presence of only weak normal grading (Collinson et al., 1996, p. 133-135). The occurrence of plant-root structures supports the interpretation of a non-channelized setting (Marconato et al., 2014). Sub-facies Fp represents cleaner, plant-root modified siltstones; sub-facies Fop represents a higher organic content at time of deposition. This might reflect both the organic content of the flow in the main trunk channel and entrainment of organic matter during breakout of the crevasse flow across the floodplain (Keller and Swanson 1979; Hein et al., 2003).

Figure 3.5: Facies Sm: Structureless sandstone.

Figure 3.6: Facies Sr: Small-scale ripple cross-laminated sandstone.

Figure 3.7: Facies Sd: Soft-sediment deformed sandstone with remnant ripple forms.

Figure 3.8: Soft-sediment deformed chaotic sandstone and siltstone.

Figure 3.9: Facies Fp: Structureless poorly sorted siltstone.

Figure 3.10: Structureless organic-rich poorly sorted siltstones.

3.10 Laminated organic-rich siltstones (Fl)

Description

Facies Fl comprises moderately to well sorted grey to dark-grey, fine to coarse siltstone that is rich in dispersed organic deposits. Preserved bedsets are 0.3 to 1.1 m thick (mean is 0.7 m) and ungraded. Laminations, which are common throughout bedsets, are 1 to 5 mm thick and planar but discontinuous over tens of centimetres (Fig. 3.11). Small millimetre-thick plant roots and thin anthracite coal wisps (2 to 50 mm in length) are common throughout (Fig. 3.11).

Interpretation

Well-sorted laminated siltstones record relatively slow deposition from suspension (Collinson et al., 2006, p. 70) onto a planar, near-horizontal substrate. Organic-rich sediments with preserved root traces indicate an episode of surface exposure and stabilization, which was of sufficient duration to allow plant colonisation. Coal fragments could have been incorporated as detritus derived from other areas of the overbank (Retallack 1988; Kraus 1999).

3.11 Rooted green siltstone (Frg)

Description

Facies Frg consists of green-grey fine siltstone that is moderately well sorted. Bedsets vary from 0.1- 2.7 m (0.6 m).This facies can show signs of weak lamination but is commonly structureless (Fig. 3.12). Plant root structures are common though small (<5 mm length) and tend to be concentrated at the top of sets.

Interpretation

Gradual deposition of fine sediment under low energy regime which allowed development of rooted horizons at the top of sets. The poor drainage of the floodplain and high water table produces in the green-grey colour; can be defined as a poorly drained protosol (Kraus, 1999).

3.12 Red rooted siltstones with slickenlines (Frr)

Description

Facies Frr consists of red, fine to coarse siltstone that is moderately to well sorted. Bedsets vary from 0.1- 2.7 m (0.6 m average). Facies may be weakly laminated but much of the primary sedimentary structure is typically disturbed by subsequent pedogensis (Fig. 3.13). Large plant-root structures are common, up to 10 cm long but are thin <10 mm. Roots are sideritised and taper downward towards the base. Bioturbation is present in low to moderate intensities, slickenlines are common throughout and calcium carbonate nodules are common.

Interpretation

This facies represents gradual deposition of fine sediment under a low energy regime. Sediment accumulated on a well-drained and dry floodplain with time for extensive plant colonisation (Kraus, 1999); can be classified as calcisol (Owen et al., 2015).

3.13 Purple mottled siltstones (Frm)

Description

Facies Frm consists purple-red fine to coarse siltstone which is moderaty to well sorted. Bedsets vary from 0.3- 3.6 m (1.8 m average). Sets lack physical sedimentary structures but there are small roots throughout (<5 mm length) and moderate to high intensity bioturbation (Fig. 3.14). Water marks are common throughout (Fig. 3. 14).

Interpretation

This facies represents gradual deposition of fine sediment under a low-energy regime with time for plant colonisation (Kraus, 1999).Sediment accumulated on a poorly drained floodplain with high water table (Kraus and Aslan, 1993). Conditions were favourable for life and low enough sedimentation rate for preservation (Kraus and Aslan, 1993).

Figure 3.11: Facies Fl: Laminated organic-rich siltstones.

Facies Frg- Green rooted silts

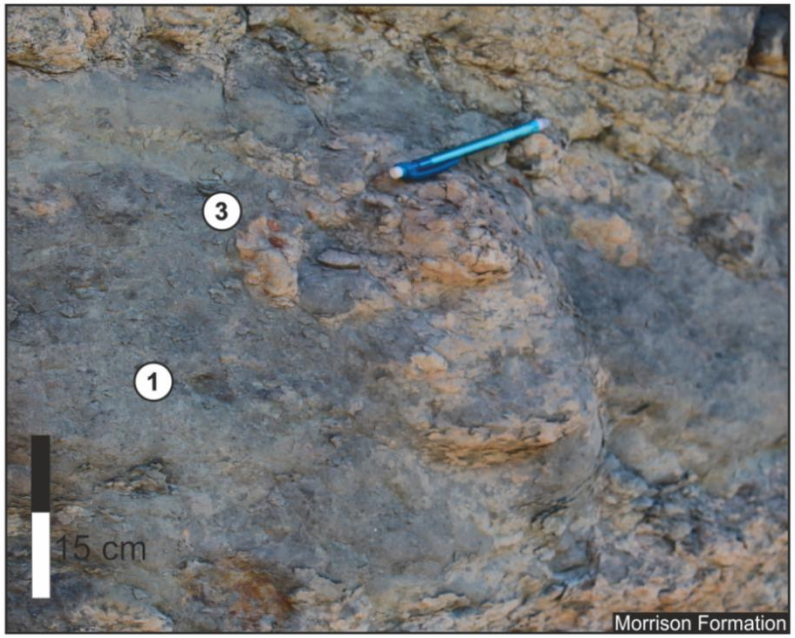

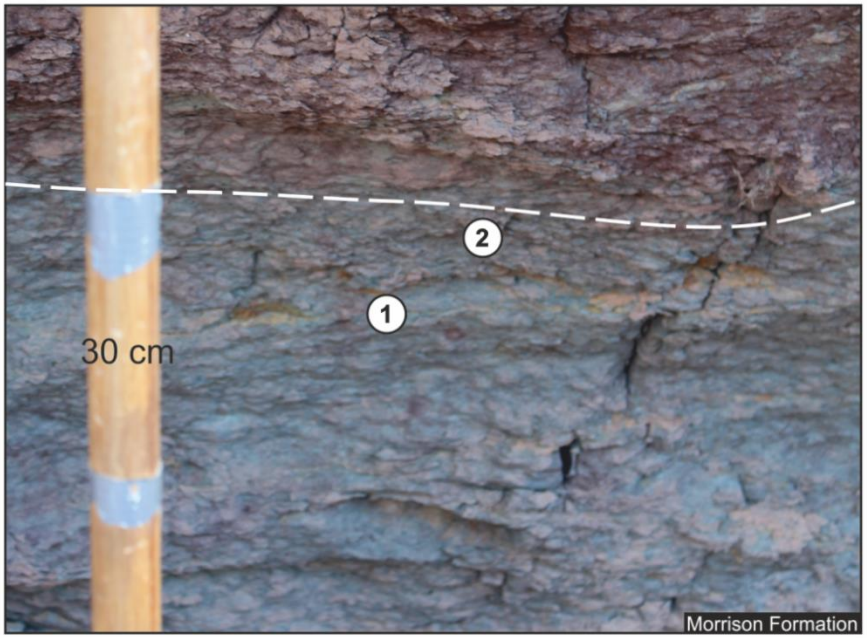

Key information

Colour	Green-grey
Grain-size	Fine siltstone
Sorting & Texture	Moderately well sorted
Thickness	0.1- 2.7 m (0.6 m average)
Facies Association	FA4
Architectural Elements	Floodplain element

Key characteristics

1. May show faint laminations or may be structureless
2. Vertical transition to facies above, burrows penetrate down through the blue siltstone.
3. Roots are very small in size

Interpretation

Gradual deposition of fine sediment under low energy regime. The poorly drained floodplain and high water table produces the green grey colour. Protosol.

Figure 3.12: Facies Frg: Rooted green siltstone.

Figure 3.13: Facies Frr: Red rooted siltstone.

Figure 3.14: Facies Frm: Purple mottled siltstone.

3.14 Laminated rooted siltstones (Fr)

Description

Facies Fr is composed of moderately well sorted blue-grey to light-grey, fine to coarse siltstone. Preserved bedsets are 0.3 to 1.4 m thick (mean is 0.7 m). This facies exhibits planar lamination, which can be either weakly or prominently developed. Plant-root structures are common throughout this facies (5% of this facies) but are notably concentrated in the uppermost parts of bedsets. Root structures narrow downwards and are composed of siderite, are 1 to 5 mm thick, and 5 to 10 cm long.

Interpretation

This facies records the development of a protosol, with at least two criteria for palaeosol development being fulfilled: organic matter present in the form of roots, and weak horizonation, with the concentration of roots at levels within the facies (cf. Mack et al., 1993). This indicates a rate of sediment aggradation that is low enough to allow pedogenesis and the absence of significant erosion. Since these palaeosols are poorly developed, pedogenesis was unlikely to have been a dominant process. Unsteady and punctuated phases of sediment influx resulted in compound and poorly developed palaeosols (cf. Retallack 1988; Kraus 1999).

3.15 Coal (C)

Description

Facies C is composed of dark-grey to black coal that has within it fragments of anthracite and bituminous coal but is mostly a poorer quality lignite or sub-bituminous coal (Fig. 3.15). Preserved coal seams vary from 0.2 to 2.1 m thick (mean is 0.7 m). In places, this facies contains preserved plant-root structures (<5 mm) and thin beds (<10 mm) of higher quality anthracite coals (Fig. 3.15).

Interpretation

Facies C records slow deposition in organic-rich floodbasin settings with only very limited clastic sediment input (McCabe, 1987; Kirschbaum and Hettinger

2004; Cole 2008). This facies accumulated in a waterlogged swamp or mire setting (Shiers et al., 2014).

Figure 3.15: Facies C: Coal.

3.16 Facies associations

Facies assocation 1: Fluvial channel-fill.

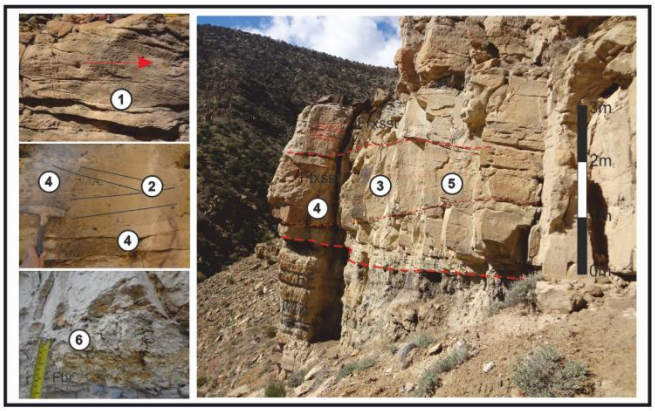

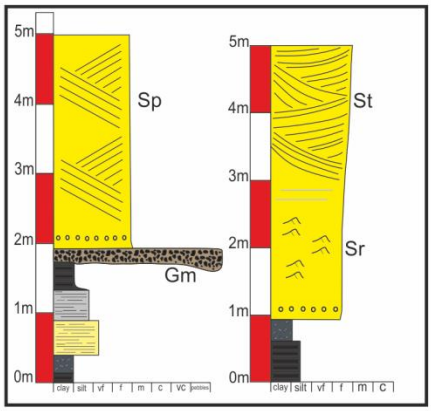

Characteristics

Constitute facies : Gp, Gm, St/p, Sm, Sr, Sd, Fm
Key attributes:

- Cross lamination at various scales prevalent throughout [1] ripple scale cross lamination, medium scale planar cross bedding, large scale trough cross-bedding
- Erosive bases with [5] rip-up clasts or pebbles lags
- Plant material and sparse poor quality coal fragments present.

Interpretation

- Major or parent channel bodies.

Facies association 2:Sand-prone overbank deposits.

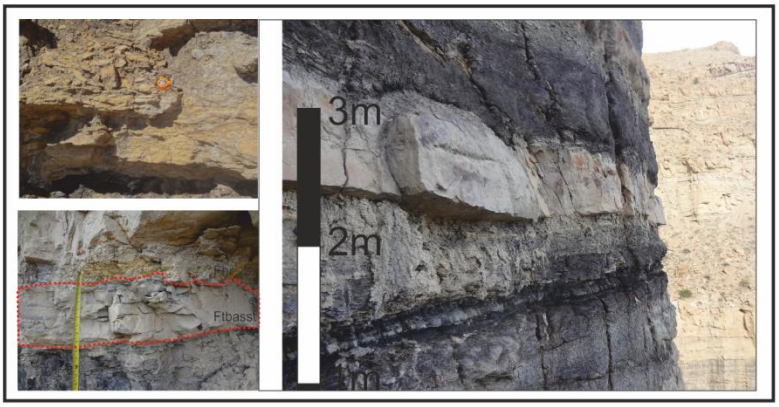

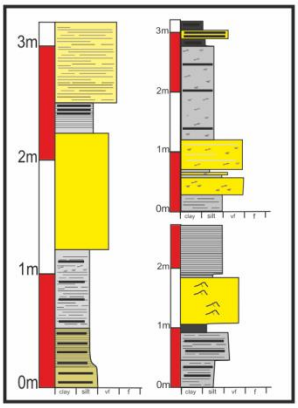

Facies Characteristics

Constituent facies: Sm, Sp, Sr, Sd, Fd, Fp
Key attributes:

- Greyish yellow fine-grained siltstones to light grey brown sandy siltstones.
- Relatively thin(<3) beds of either massive sandstones (Sm) or cross stratified sandstones (Sp) that have significant organic matter within..
- Laterally extensive thinly bedded aggradational sandstones with sharp bases.

Interpretation

Overbank sandstones proximal to the fluvial system deposits representing proximal crevasse splays and crevasse-channels

Facies assocation 3:Silt-prone overbank deposits.

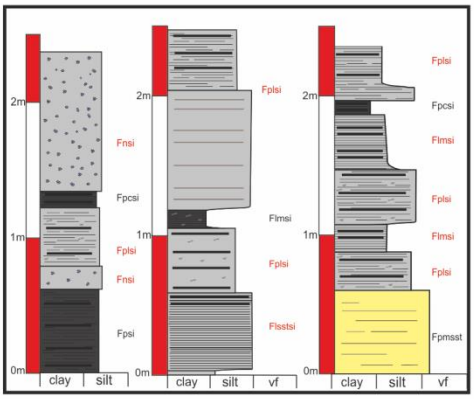

Facies Characteristics

Constituent Facies: Sd, Fd, Fp, Fop.
Key attributes:

- Light grey blue siltstones to medium blue grey siltstones.
- Strata can have varying amounts o f plant remains
- Siltstones commonly exhibit well defined lamination but can show no lamination at all, boundaries tend to be sharp or gradational

Interpretation

Distal crevasse splay deposits with varying amount of vegetation and formed under variable water table levels.

Facies association 4: Mires and soils deposits.

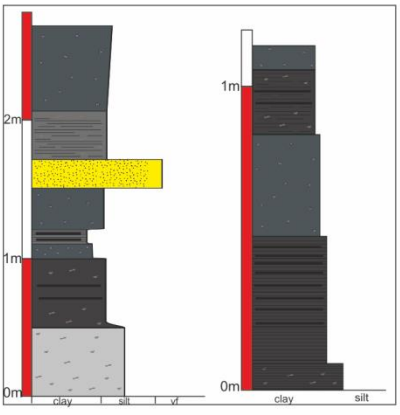

Characteristics

Constituent facies: Fr, Frg, Frr, Frm, C
Key attributes:

- Swamp and mire deposits in Neslen formation dark grey to black in colour.
- Strata dominated by well laminated coal bearing siltstones with anthracite coal bearing clays making up a smaller proportion of the volume.
- Palaesols in Morrison formation vary from red togreen to purple in colour and oftern contain well developed rooted horizons, slickenlines and bioturbaton.

Interpretation

The very fine grained deposits settled out of suspension distal from the fluvial channel system with lots of vegetation but with variable water table levels.

Chapter 4 Anatomy and dimensions of fluvial crevasse-splay deposits: examples from the Cretaceous Castlegate Sandstone and Neslen Formation, Utah, U.S.A.

This chapter quantifies lithofacies distributions and dimensions of exhumed crevasse-splay architectural elements in the Campanian Castlegate Sandstone and Neslen Formation, Mesaverde Group, Utah, USA. Lithofacies arrangements are used to establish the following: (i) recognition criteria for crevasse-splay elements; (ii) criteria for the differentiation between distal parts of crevasse-splay bodies and flood plain fines; and (iii) empirical relationships with which to establish the extent (ca. 500 m long by 1000 m wide) and overall semi-elliptical planform shape of crevasse-splay bodies. These relationships have been established by high-resolution stratigraphic correlation and palaeocurrent analysis to identify outcrop orientation with respect to splay orientation. This permits lateral changes in crevasse-splay facies architecture to be resolved. Facies models describing the sedimentology and architecture of crevasse-splay deposits preserved in floodplain successions serve as tools for determining both distance from and direction to major trunk channel sandbodies.

4.1 Introduction

Crevasse-splay deposits form a volumetrically significant part of fluvial overbank depositional elements, representing on average ~12% of all deposits in ancient preserved fluvial successions (Colombera et al., 2013). Despite this, the preserved lithofacies arrangement and stratigraphic architecture of fluvial overbank successions generally, and crevasse-splay elements in particular, have been less of a focus of analysis than in-channel deposits (e.g. Bridge, 1984, 2006; Colombera et al., 2012). Many published fluvial facies models generalize crevasse-splay deposits into a single category (e.g. Miall, 1985, 1988, 2014; Bridge, 2006; Ghazi and Mountney, 2009, 2011; Colombera et al., 2013); relatively few studies have specifically set out to undertake a detailed lithofacies characterization and architectural-element analysis of splay deposits.

O'Brien and Wells (1986), Bristow et al. (1999), Farrell (2001) and Li and Bristow (2015) examined the sedimentology of modern and recent crevasse-splay deposits, and Mjøs et al. (1993), Behrensmeyer et al. (1995), Jones and Hajek (2007), Widera (2016) and Van Toorenenburg (2016) presented examples of ancient crevasse-splay deposits. Detailed lithofacies classification schemes have been introduced for modern avulsion deposits, for example in the Cumberland Marshes, Canada (Perez-Arlucea, 1999), and for Miocene coal-prone crevasse-splay successions in Poland (Widera, 2016).

This study presents a depositional model to account for the complexity of lithofacies distribution preserved in crevasse-splay deposits that accumulated under the influence of a greenhouse climatic regime. This aim is fulfilled through an outcrop-based quantitative geometrical analysis of 35 crevasse-splay bodies present in the Cretaceous (Campanian) Castlegate Sandstone and Neslen Formation of the Mesaverde Group, eastern Utah, USA. This study seeks: (i) to establish recognition criteria of architectural elements that represent fluvial crevasse splay deposits, and to contrast these elements with overbank elements dominated by suspension settling in floodbasin settings; (ii) to demonstrate how and why these facies are arranged within an individual preserved crevasse-splay element; (iii) to quantify proportions and dimensions of crevasse-splay elements versus floodplain elements in a greenhouse overbank succession; and (iv) to develop a predictive facies model for crevasse-splay element architecture based on observations from examples identified in the Castlegate Sandstone and Neslen Formation.

4.2 Background and nomenclature

The fluvial floodplain is a geomorphic feature defined as a low-gradient area of alluvium adjacent to a channel belt and that is affected by fluvial flooding; sediment is dominantly supplied via floods that cause rivers to breach the confines of trunk channel systems (Brierley and Hickin, 1992, Nanson and Croke, 1992, Bridge, 2006, Bridge and Demicco, 2008). In the stratigraphic record, the fluvial overbank is a gross-scale composite architectural element

that comprises any part of a fluvial system that accumulates sediment outside the confines of the river channel (Miall, 1996, 2014).

The fluvial overbank is characterized by a range of smaller-scale sub-environments, including crevasse channels, crevasse splays, floodbasins, mires and lakes or ponds; these sub-environments, and their preserved expression as architectural elements in the rock record, comprise a range of sediment types of physical, chemical and biogenic origin (e.g. Brierley and Hickin, 1992; Platt and Keller, 1992; Brierley, 1997; Hornung and Aigner, 1999). Typically, the fluvial overbank comprises sediments that are finer than those associated with intra-channel deposits (Miall, 1993). Many overbank sub-environments and their preserved deposits are subject to pedogenesis, which is strongly controlled by the drainage state of the substrate at the time of accumulation (Bown and Kraus, 1987; Kraus, 1999) and the sedimentary stability of the land surface.

In fluvial sedimentary environments, a splay deposit is defined as a sheet-like progradational deposit, which is lobe-shaped in plan-view. Terminal splay deposits form at the end of a river channel whereas crevasse splay deposits, which are the focus here, form adjacent to an established channel (e.g. Nichols and Fisher, 2007; Gulliford et al. 2014). Typically, crevasse splays initiate and develop when floodwaters break through a topographically elevated levee that acts as the confining bank of a channel at times of peak flood discharge or when floodwaters overtop the levee (Coleman, 1969; Mjøs et al., 1993; Arnaud-Fassetta, 2013) (Fig. 4.1). Sediment-laden flows expand and decelerate as they pass through a distributive network of crevasse channels onto the unconfined floodplain, thereby encouraging sediment deposition (Arndorfer, 1973; Miall, 1985, 1993; Bristow et al., 1999;; Arnaud-Fassetta, 2013). Although also documented from freshwater deltaic (e.g Arndorfer, 1973; Cahoon et al., 2011), interdistributary bay-fill (e.g. Gugliotta et al., 2015), estuarine (e.g. Staub and Cohen, 1979; Cloyd et al., 1990; Baeteman et. al, 1999), and deep-marine (Morris et al., 2014) environments, crevasse splays are most widely documented from the low-relief, low-gradient parts of fluvial systems (Mjøs et al., 1993; Bristow et al., 1999; Anderson, 2005). The majority of previous research on crevasse splay deposits has focused on modern fluvial systems

(Coleman 1969; Smith et al., 1989; Farrell 2001; Smith and Perez-Arlucea, 2004; Arnaud-Fassetta, 2013).

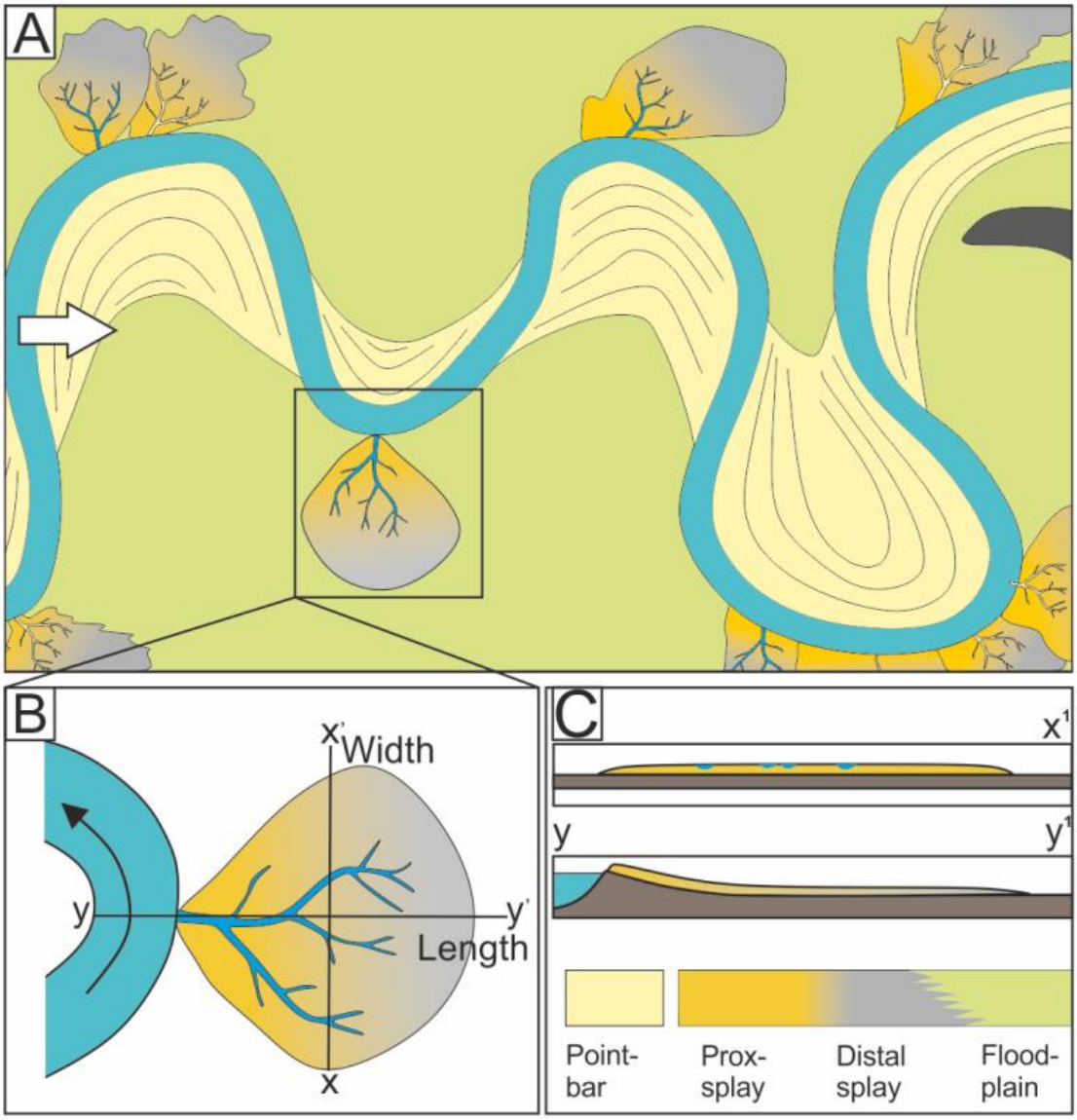

Figure 4.1: Schematic plan-view illustration of a typical crevasse-splay morphology. Thickness and grain size decrease away from the point source of the channel breach. (A) Plan-view schematic image of fluvial system with crevasse-splays. (B) Plan-view schematic image of a crevasse-splay showing length and width orientations. (C) Cross-sectional view of width and lengths of crevasse-splay.

Splay evolution in modern systems has been categorized using a three-stage model based on observations by Smith et al. (1989) from the Cumberland

Marshes, Canada, where simple lobate splays (type I) are typically succeeded by splays with a more fully developed network of distributary channels in which sediment is directed to localised areas within the developing splay (type II). Over time, growth and evolution of the splays tends to lead to the development of an anastomosing channel pattern (type III). There are two possible fates of mature splays: (i) detachment (cut-off) from the main parent fluvial channel, resulting in abandonment and stabilization by surface agents such as vegetation or chemically precipitated crusts or bio-chemical soils (Arnaud-Fassetta, 2013); or (ii) further development such that an active splay serves as the initial phase of a major avulsion of the parent channel (Smith et al., 1989; Jones and Harper, 1998; Farrell, 2001; Buehler at al., 2011). In cases where splays mark the initiation phase of a channel avulsion, they are referred to as avulsion splays (Smith et al., 1989; Slingerland and Smith, 2004; Jones and Hajek, 2007). In these instances, local erosion of the parent channel bank forms a crevasse channel through which sediment and water are diverted. As the discharge of water and sediment through a crevasse channel increases, the parent river may eventually avulse to take a new course through this new channel path (Bristow et al., 1999; Mohrig et al., 2000; Miall, 2014). In-channel accretion and levee construction leads to superelevation of the channel and channel perching above the floodplain, an unstable situation that promotes the triggering of avulsion (Mohrig et al., 2000). In the rock record, such evolution is manifest as a transitional avulsion stratigraphy (Jones and Hajek, 2007): crevasse-splay deposits underlie a new main channel and both the splay and the succeeding channel bodies exhibit similar overall palaeocurrent trends (Bristow et al., 1999; Mohrig et al., 2000; Slingerland, 2004; Jones and Hajek, 2007; Miall, 2014).

4.3 Geological setting

The Cretaceous (Campanian to Maastrichtian) Mesaverde Group, eastern Utah, USA, accumulated under the influence of a humid, subtropical, greenhouse climate. Sediment transport was eastward from the developing Sevier Orogen to the shoreline of the Western Interior Seaway that developed in the foreland

of the orogeny (Franczyk et al., 1990; Miall, 1993). This resulted in the accumulation of an eastward-prograding clastic wedge that was constructed along the western margin of the Western Interior Seaway during the Campanian (Miall, 1993; Olsen et al., 1995; Van Wagoner, 1995; Kirschbaum and Hettinger, 2004; Adams and Bhattacharya, 2005; Hampson et al., 2005; Aschoff and Steel, 2011). The Mesaverde Group comprises informal lower and upper sections, separated by the Buck Tongue of the Mancos Shale (Franczyk, 1990; Kirschbaum and Hettinger, 2004) (Fig. 4.2). Outcrops of the Upper Mesaverde Group, and specifically the Castlegate Sandstone and Neslen Formation, are the focus of this study.

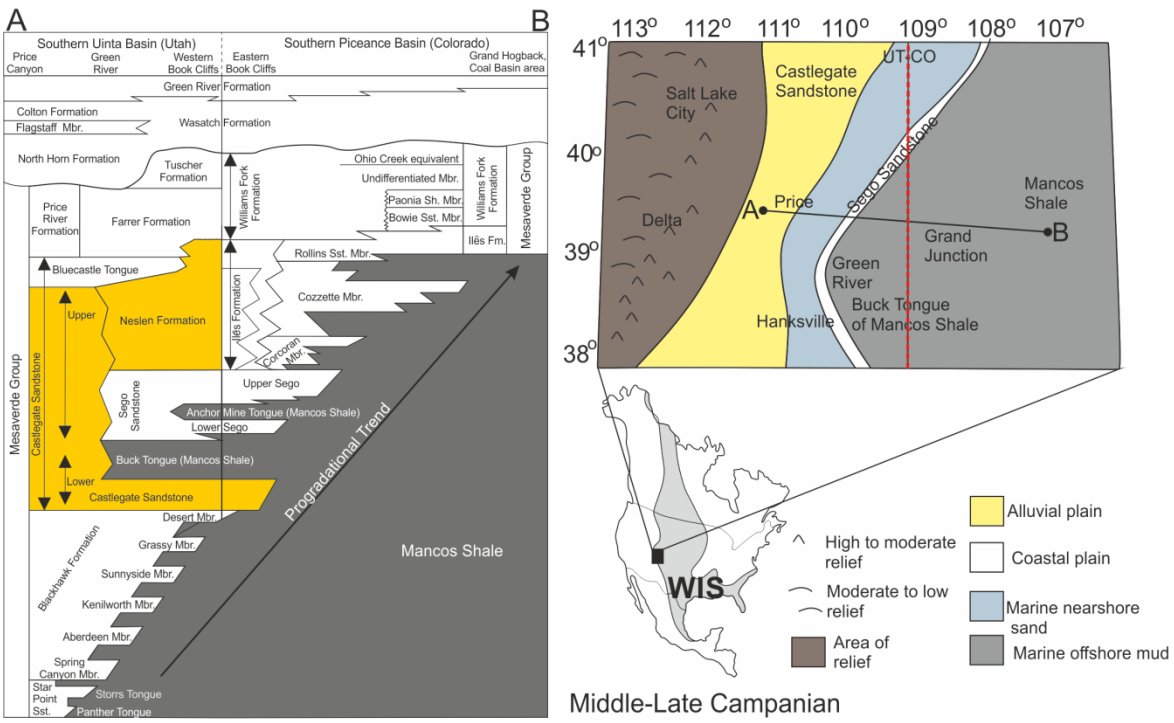

Figure 4.2: Stratigraphic scheme of the studied part of the Mesaverde Group, including the Castlegate and Neslen formations examined as part of this study. Based in part on Kirschbaum and Hettinger (2002) and Francyzk et al. (1991).

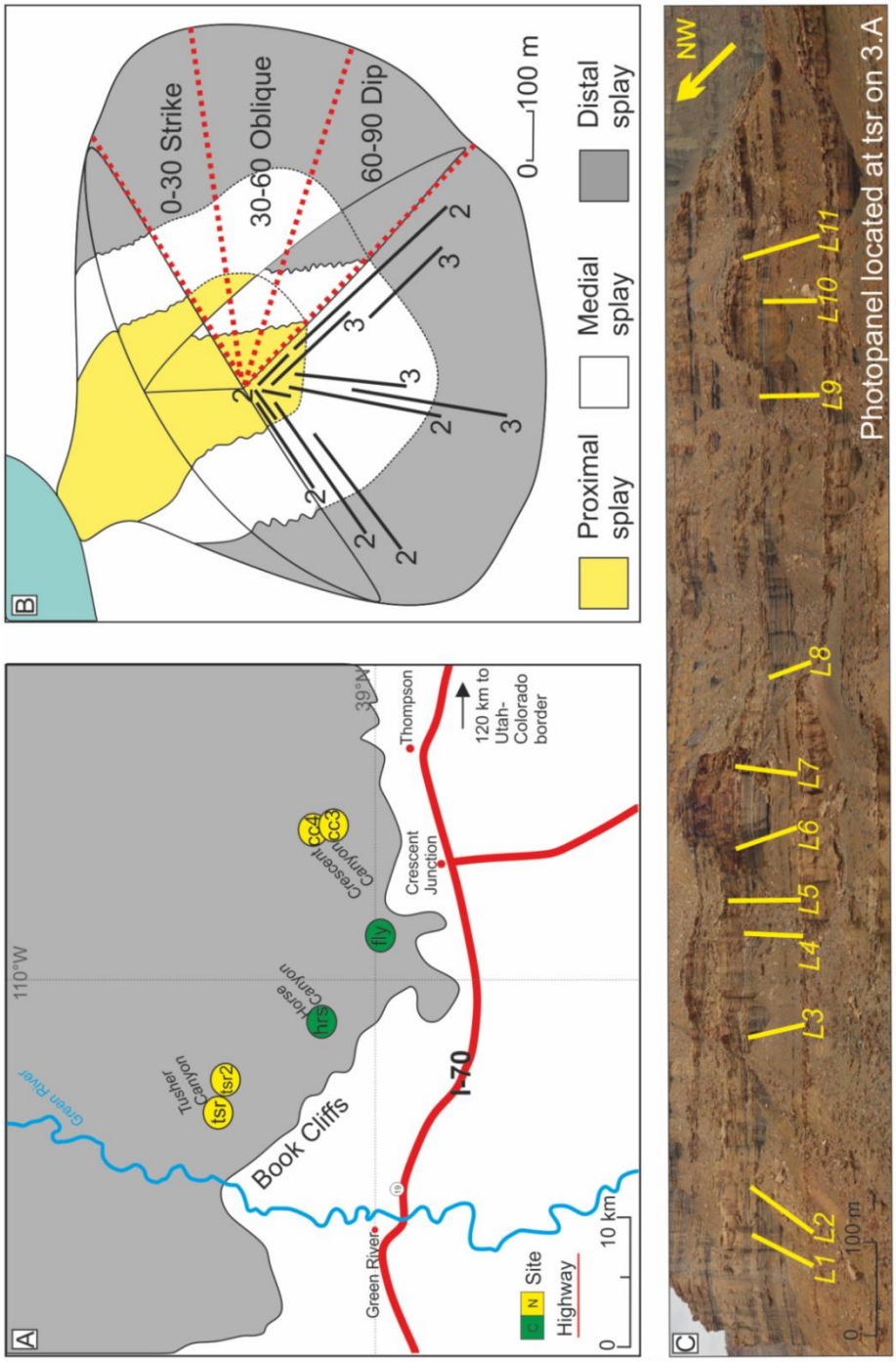

Figure 4.3: Location maps. (A) Location of Castlegate sites: Floy and Horse and Neslen sites: Tuscher, Tuscher 2, Crescent 3 and Crescent 4. (B) Representation of facies-belt regions of splays observed in the Castlegate and Neslen formations. Twenty splay elements composed of facies that yield palaeocurrent information were studied; the lines indicate the reconstructed orientations of each of the twenty studied splay bodies based on analysis of palaeocurrent data with respect to outcrop orientation; the numbers indicate how many sections of each orientation have been recorded. (C) Tuscher Canyon cliff section; the position of each measured section is indicated.

The Castlegate Sandstone is up to 160 m thick and comprises tens of metres thick amalgamated sheets of sandstones of predominantly fluvial channel origin, with few laterally extensive bodies of overbank fines (McLaurin and Steel, 2007). In contrast, the Neslen Formation, which is up to 200 m thick, comprises a succession of conglomerate, sandstone, siltstone and coal of non-marine, paralic and shallow-marine origin (Franczyk, 1990; Hettinger and Kirschbaum, 2003).

The Castlegate Sandstone and Neslen Formation merge westward near the town of Green River into a single unit of fluvial origin: the Upper Castlegate Sandstone (Franczyk et al., 1990; Willis, 2000) (Fig. 4.2). Eastward, the Castlegate Sandstone is finer grained and passes downdip into the offshore marine Mancos Shale. In Colorado, deposits equivalent to the Neslen Formation take the name of the Ilês Formation (Kirschbaum and Hettinger, 2004). The Castlegate and Neslen formations are well exposed in a series of outcrops in the Book Cliffs, Eastern Utah (Fig. 4.3A), between Green River and Thomson Springs (Fig. 4.3B). Numerous canyons yield exposures in a variety of orientations that allow for the three-dimensional geometry and internal facies arrangement of architectural elements to be constrained via lateral tracing over many hundreds of metres to kilometres.

The Castlegate Sandstone is commonly interpreted as the accumulated deposits of low- to moderate-sinuosity braided rivers (McLaurin and Steel, 2007). In contrast, the Neslen Formation represents the accumulated deposits of a series of lower-alluvial-plain, coastal-plain and near-coast fresh-to-brackish water environments that were traversed by relatively small, shallow, sinuous rivers that migrated and avulsed across extensive, low-gradient and low-relief floodplains (Franczyk, 1990; Willis, 2000; Kirschbaum and Hettinger, 2004; Cole, 2008; Aschoff and Steel, 2011b; Shiers et al., 2014; Keeton et al., 2015; Colombera et al., 2016).

Previous research has focused on the development of a robust stratigraphic framework (e.g. Franczyk, 1990; Hettinger and Kirschbaum, 2002), which is useful to place the crevasse-splay architectural elements studied here within a broader palaeoenvironmental and sequence stratigraphic context. Much

previous research has been focused on the arrangement and stacking pattern of larger-scale channel and point-bar elements within the Neslen Formation (Kirschbaum and Hettinger 2002; Shiers et al., 2014; Keeton et al., 2015). However, the sedimentology and architecture of elements of crevasse-splay origin have not been considered in detail.

4.4 Data and methods

Here, we present data from two sites from the Castlegate Sandstone and four from the Neslen Formation (Figs. 2, 3A) in eastern Utah, from the upper part of the Castlegate Sandstone and the lower and middle parts of the Neslen Formation. From the six principal study localities, sixty-two graphic logs were measured that record lithology, bed thickness, grain size, sedimentary structures, occurrence of fossils and palaeosols. Physical correlation of prominent beds and bounding surfaces between each measured graphic log was undertaken to establish geometrical relationships between individual crevasse-splay architectural elements, adjacent channel elements and other distal floodplain elements (Fig. 4.3C). Tracing beds permitted construction of 27 architectural panels and photomosaics across the studied sections. These record lateral changes of both the internal lithofacies organisation of splay elements, and the external geometry of the splay elements. In total, 1118 palaeocurrent measurements from cross-bedding foresets, ripple cross-lamination, ripple-forms on bedding surfaces and low-angle-inclined accretion surfaces are used to identify dip and strike sections of the studied crevasse-splay elements. This permits lengths, widths and thicknesses of the preserved crevasse-splay elements and their facies belts to be determined (Fig. 4.3D). Strike sections are defined as 0-30 degrees from the outcrop orientation, oblique as 30-60 degrees from outcrop orientation and dip sections as 60-90 degrees from outcrop orientation. Full lengths and widths of splays are calculated from partial exposures using thinning rates within the window of outcrop of observation.

The collation of each of these data types has allowed identification and quantification of lateral and vertical changes in facies type within 35 individual

splay bodies, of which 20 have been dip- and strike- corrected to determine original widths and lengths. For splay bodies characterised internally by facies that yield palaeocurrent information, and which were laterally more extensive than the outcrop, the predicted minimum size of the splay element was determined using element thinning rates in the known direction of growth. Thinning rates were used to extrapolate, in the direction of main palaeoflow, down to zero to produce the predicted length of the splay. This method allows quantitative analysis of the dimensions and stratigraphic changes in splay proportion in overbank successions.

A 40 m-thick interval within the Lower Neslen Formation exposed in a 1.5 km-long cliff-face in Tuscher Canyon to the east of Green River (Fig. 4.3C) has been chosen as a type succession. Here, a 20 m thick, 1.5km long, detailed architectural panel has been constructed from 11 measured graphic logs, which collectively total 315 m in measured thickness. Two marker beds that are present continuously constrain the studied stratigraphic interval: a shell bed at the boundary between the Sego Sandstone and base of the overlying Neslen Formation, and a laterally extensive coal seam (Fig. 4.5). Through high-resolution chronostratigraphic correlation the sedimentary architecture has been reconstructed to show how crevasse-splay deposits contribute to the construction of an overbank succession (Fig. 4.5).

4.5 Lithofacies

Eleven lithofacies types are recognised based on composition, grain size, sediment textural characteristics and sedimentary structures (Figs. 4.4, 4.5; Table 4.1). The facies scheme is an extended version of the schemes of Miall (1978) and Colombera et al. (2013).

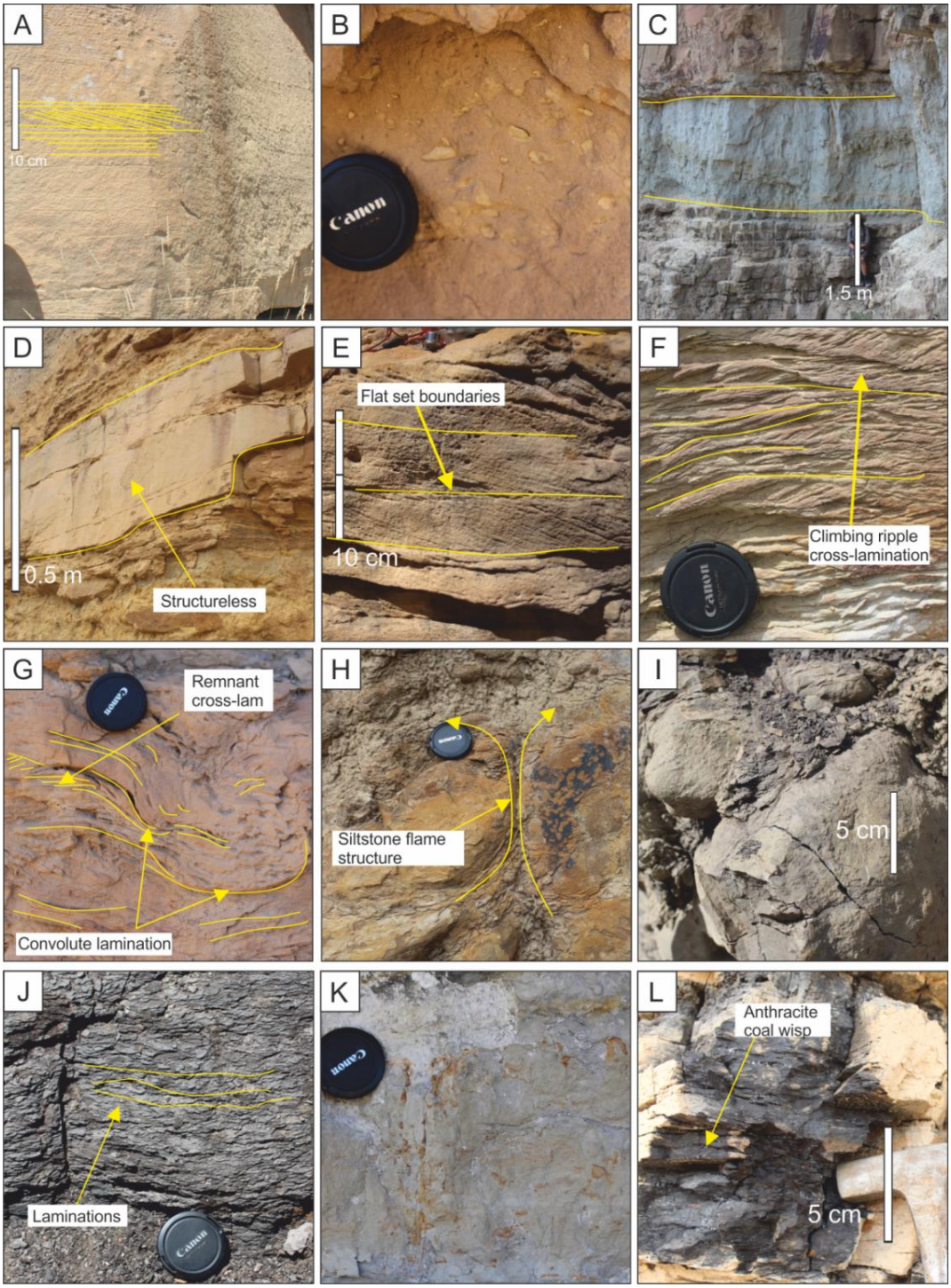
A
10 cm
B
C
1.5 m
D
0.5 m
Structureless
E
Flat set boundaries
10 cm
F
Climbing ripple
cross-lamination
G
Remnant
cross-lam
Convolute lamination
H
Siltstone flame
structure
I
5 cm
J
Laminations
K
L
Anthracite
coal wisp
5 cm

Figure 4.4: Representative photographs of lithofacies. Lens cap is 5 cm in diameter. (A) Planar cross-stratification in lower-medium sandstone (Sp); (B) Small sub-rounded to sub-angular matrix supported clasts (Gh); (C) Clean blue well sorted siltstone, not well bedded (Fm) (D) Structureless sandstone (Sm); (E) Small-scale cross-lamination flat foresets in fine grained sandstone (Sr); (F) Small-scale cross-lamination inclined foresets in fine grained sandstone (Sr); (G) Convolute lamination and inclined foresets in upper fine sandstones (Sd); (H) Soft sediment deformation, water escape structures in chaotic very sandstones and siltstones (Fd); (I) Poorly sorted cleaner siltstone, more organic-rich example not shown (Fp); (J) Laminated organic rich siltstone (Fl); (K) well to moderately sorted, rooted siltstone (Fr); (L) Coals with fragments of anthracite coals (C).

Table 1

Code	Facies	Description	Interpretation
Ftpx	Trough and planar cross-bedded sandstone	Grey-yellow upper very-fine- to upper medium-grained sandstone, moderately well sorted. Subangular to subrounded grains,Bed sets are 0.5m-0.8m thick.Mud rip-up clasts and plant fragments are common. Trough and planar cross-stratification throughout	Deposition from a relatively high-energy flow and downstream migration of sandy bar forms
Fcl	Pebbly sandstone with intraformational clasts	Brown to grey-yellow, very fine sandstone matrix with 10% rounded small to medium pebbles (up to 20 mm in diameter). Sets of this facies are <1 m thick. Pebbles poorly sorted within a overall poorly sorted sandstone matrix, No grading is present; sets are structureless	Deposition from a very high-energy environment, within which flows were capable of entraining and reworking locally derived sediment locally as incorporated rip-up clasts
Fs	Structureless sandstone	Dark grey-yellow, lower-fine to lower-very fine sandstone, moderately to poorly sorted thickness ranges 0.5m-3m. Internally beds are structureless	Records rapid deposition of sand predominantly from suspension in a decelerating flow
Frx	Small-scale ripple cross laminated sandstone	Grey-yellow, lower-fine to very fine sandstone, moderately to poorly sorted. Sets varying from 0.5m-2m. Small-scale ripple- cross lamination are common to this facies, contains small (<50 mm long) plant fragments, bark pieces and coal fragments	Down flow migration of ripple bedforms under an aggradational regime
Fdr	Soft-sediment deformed sandstone with remnant ripple forms	Grey-yellow, lower- to upper-very fine sandstone that is poorly to moderately sorted. Sets vary in thickness from 0.5 to 3 m. Convolute lamination within sets and load and flame structures at base bed boundaries, remnant ripples	Records deposition from a mixed sand and silt containing flow onto an unstable waterlogged substrate
Fss	Soft sediment deformed mixed sandstone and siltstones	Dark grey-yellow, upper-very fine sandstone and coarse siltstone that is poorly sorted. Thicknesses vary from 0.3m-3m. Within 1 m of the base of beds, primary sedimentary structures are overprinted by soft-sediment deformation structures	Records deposition from a mixed small grain size containing flow onto an unstable waterlogged substrate
Fsp/ Fop	Structureless poorly sorted rooted siltstones	Light-blue or grey, lower-very fine sandstone to fine siltstone that is poorly sorted. Bed thicknesses vary from 0.3 to 1.1 m (mean is 0.5m). Sets of this facies are structureless or show weak fining-up trend	Poorly sorted and structureless silt-prone facies was deposited rapidly from suspended load

Table 4.1: Lithofacies recorded in Castlegate Sandstone and Neslen Formation study areas. See Figure 4 for photographic examples of each lithofacies.

Table 1(Continued)

Code	Facies	Description	Interpretation
Flo	Laminated organic rich siltstones	Medium to dark grey, upper to lower silts well to moderately sorted, bed thicknesses vary from 0.1m-1.6m, 53cm average grain remains consistent throughout a bed. Planar laminations present	Steady deposition from low energy flow.
Frs	Laminated rooted siltstones	Blue grey to light grey, upper to lower silt moderately well sorted, average bed thicknesses 0.7m but bed size varies from 0.3m-1.4m. Weakly laminated	Well drained, gradual deposition under low energy regime
Fpb	Well sorted blue clean siltstones	Light blue,middle to coarse siltstone, well-moderately-well sorted, rare occurrence of roots or plant material.Bed base is erosional 1-2m. Average bed thickness 2m but can reach up to 3m thickness. Silts weakly laminated or structureless	Erosive bed bases represents erosive flow, siltstones represent deposition from low energy flow after erosive event
Fc	Coal	Dark-grey to black clay sized particles ,well sorted , sets vary from 0.4-0.9m. Plant fragments and higher quality anthracite coal fragments present	Records slow deposition, organic rich setting with limited clastic input

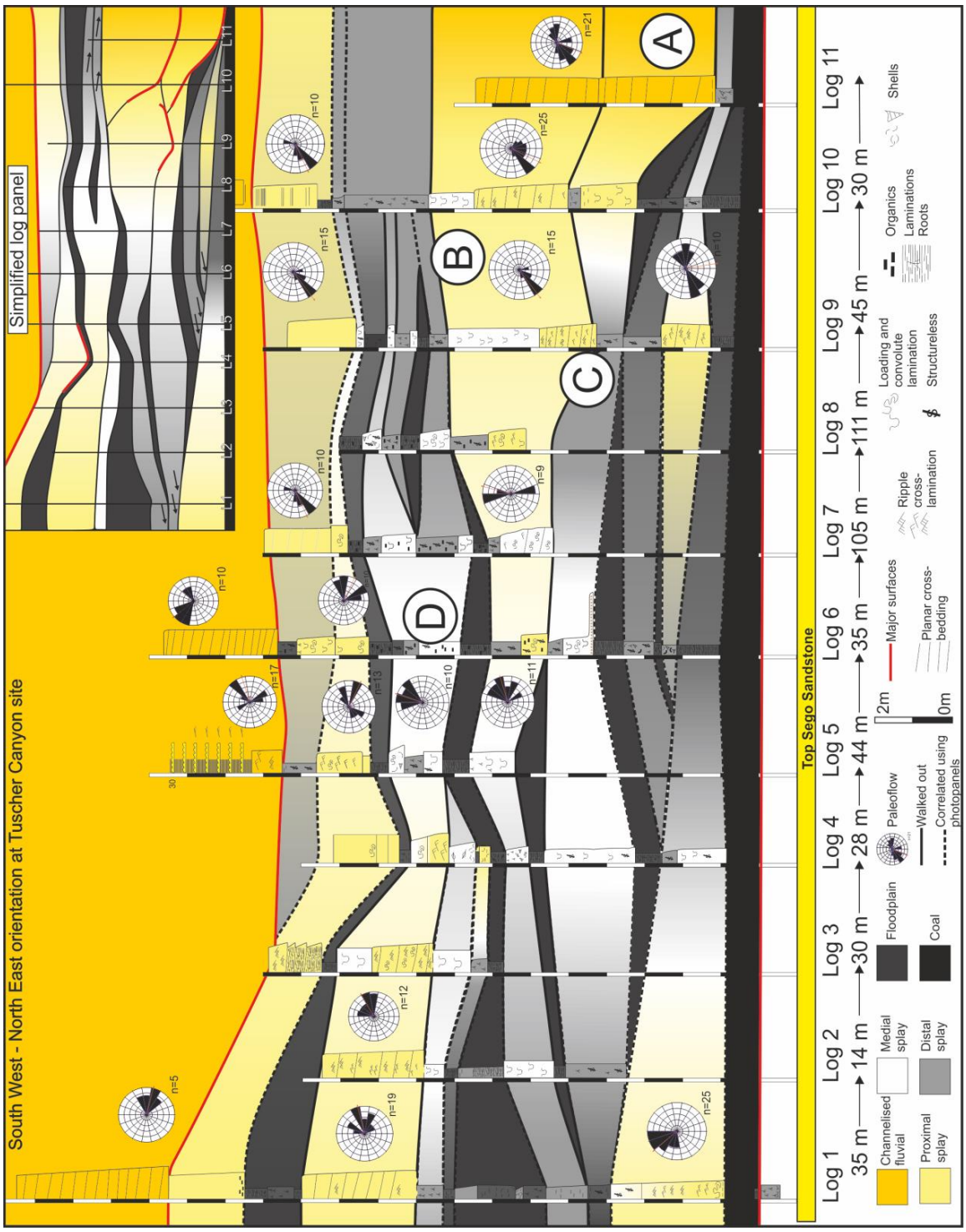

Figure 4.5: Correlation panel of 11 logged sections at Tuscher Canyon site. Surfaces and beds marked with a bold line have been walked out in field whereas dashed lines have been correlated by observation from distant vantage points in the field. This correlation panel shows the raw data collected. This outcrop "window" was used to determine a minimum extrapolated value for the dimensions of these splay elements (see methodology).

4.6 Architectural characteristics of crevasse-splay bodies

Three architectural-element types are identified: crevasse-channel, crevasse-splay and coal-prone floodplain elements. Each element type is composed internally of distinctive lithofacies associations that are vertically and laterally distributed in a repeatable pattern with distinct geometrical properties that are discernible from those of non-diagnostic overbank deposits. Relationships both within and between these elements have been traced out laterally, i.e., walked out (Fig. 4.5), to define a predictable succession of lateral facies transitions from the proximal (relative to the parent channel element to which the splay body is likely genetically linked), through medial and distal parts of splay bodies to adjoining floodplain deposits. Through establishment of empirical relationships, the length scale of facies transitions within individual splay elements can be used to predict distance to parent feeder channel (Fig. 4.6A).

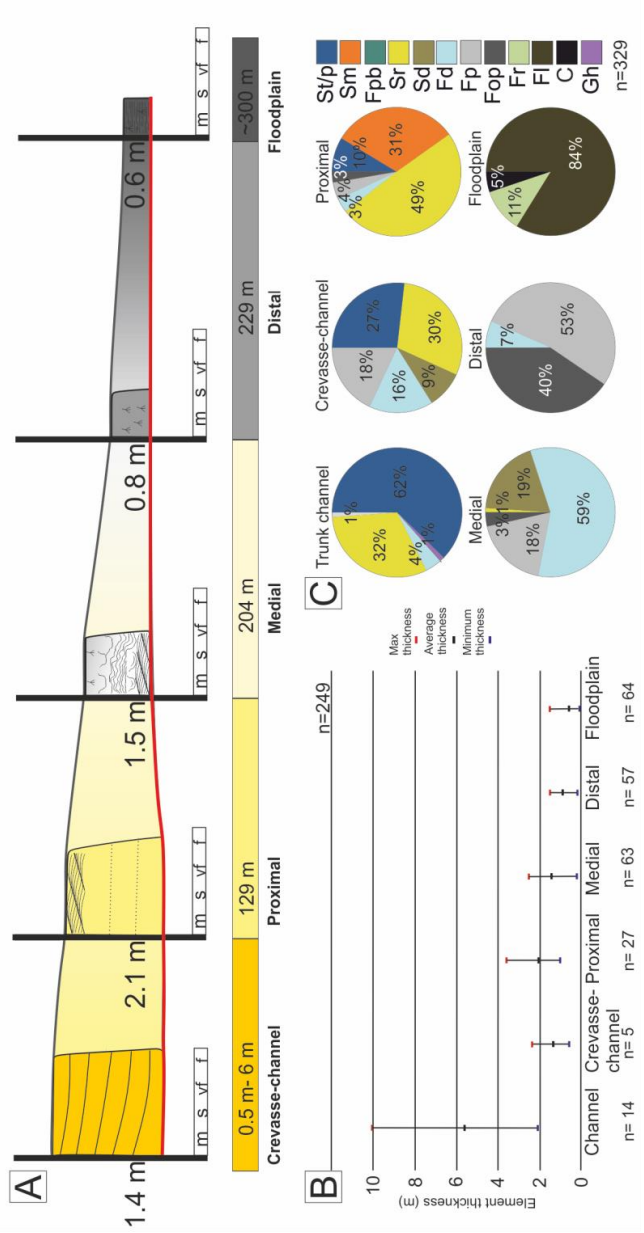

Figure 4.6: (A) Schematic graphic logs depicting the sedimentary signature of crevasse channel, proximal, medial and distal parts of crevasse-splay elements, as well as adjoining floodplain elements. The figure depicts lateral variations in facies and thickness across the dip-section of a crevasse-splay. Thickness and length scales based on analysis of 35 and 20 crevasse-splay elements respectively from the studied sites in the Castlegate and Neslen formations. (B) Average, minimum and maximum thickness of each element and facies-belt type; data based on 62 measured sections from 35 crevasse-splay bodies. (C) Pie charts depicting the proportions of facies types present in each element or facies-belt type; data are based on averaged thickness data and facies type occurrences from each of the 62 measured sections. See Table 4.1 for facies codes cited in key.

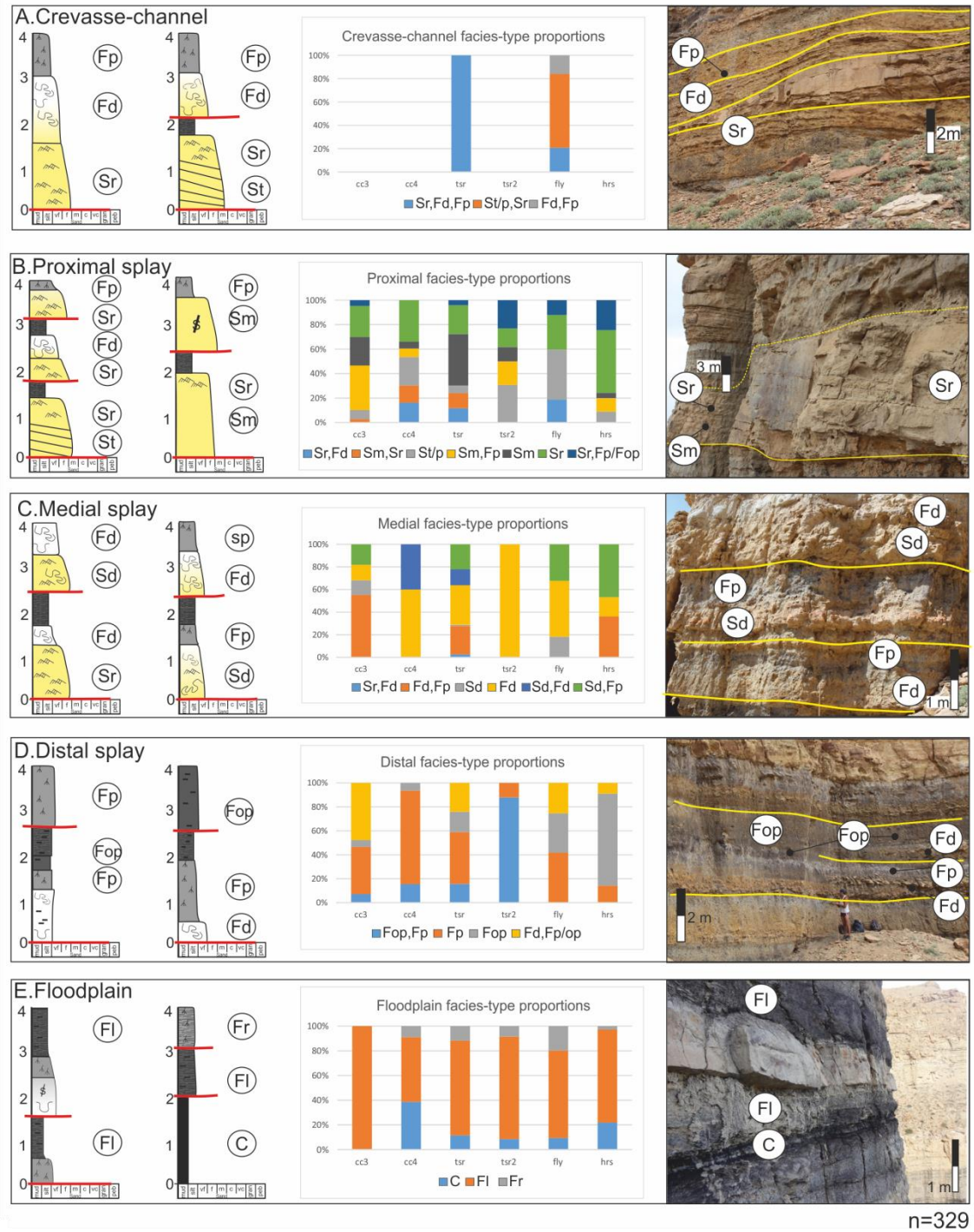

Figure 4.7: Diagram depicting typical vertical facies arrangements in each element and facies-belt type, based on average thickness occurrences. Data from 62 sections logged as part of this study. (A). Crevasse-channel. (B) Proximal splay. (C) Medial splay. (D) Distal splay. E. Floodplain. See Table 4.1 for facies codes cited in key.

4.6.1 Crevasse-channel elements

Crevasse-channel elements are channel forms with a basal surface that truncates the underlying strata, typically proximal or medial splay elements. Crevasse-channel elements are well exposed at the Tuscher Canyon and Floy Canyon sites in the Neslen Formation (Fig. 4.7A). Planar-cross bedded sandstone (St/Sp) and ripple cross-laminated sandstone (Sr) are the most dominant facies in this element (Fig. 4.6C). Crevasse-channel-fills have an average thickness of 1.4 m (0.6 m to 2.4 m, n = 5) (Fig. 4.6B) and have lenticular geometries in cross section (Fig. 4.6A). Commonly the channel-fills have sharp or erosional top surfaces but can have gradational tops where they pass into overlying fine-grained facies of non-diagnostic overbank origin.

Associations of facies are commonly arranged vertically as successions of planar cross-bedded sandstone (St/Sp) overlain by thin (<0.5 m) sets of ripple cross-laminated sandstone (Sr), ripple cross-laminated sandstones (Sr), and soft-sediment deformed chaotic sandstone and siltstone, all capped by structureless siltstones (Fp/op). Alternatively, sets of soft-sediment deformed chaotic sandstone and siltstone (Fd) may be capped by thin (<0.7 m) sets of structureless poorly sorted siltstone (Fp) (Fig. 4.7A).

Sandstone-prone crevasse-channel elements indicate a close proximity to the flood-breach; farther away from the breach, the more silt-prone facies indicate gradual deceleration and overfilling of crevasse channels with fines.

4.6.2 Splay elements

4.6.2.1 Proximal facies belt

The proximal facies belts of splay elements are composed internally of the following facies associations: trough and planar cross-bedded sandstones (St/Sp), structureless sandstone (Sm), ripple cross-laminated sandstone (Sr), soft-sediment deformed chaotic sandstone and siltstone (Fd) and poorly sorted siltstone (Fp) (Fig. 4.6A, 6C). Commonly, proximal splay elements exhibit the coarsest grain size (up to upper-fine sandstone; average fine sandstone) of the entire overbank succession (Fig. 4.6A, 4.6C), and the greatest overall thicknesses (Fig. 4.6B): up to 3.7 m. Structureless sandstone (Sm) and ripple

cross-laminated sandstones (Sr) are the dominant facies of proximal splays elements (Fig. 4.6C).

The proximal facies belts of splay elements exhibit wedge or tabular geometries (Fig. 4.6A) and have an average thickness of 2.1 m (1.0 to 3.7 m) (n = 27 measured occurrences of 35 studied splay bodies) (Fig. 4.6B). Mean lateral dip-section extent is 129 m (55 to 189 m) (n= 8); strike sections of the proximal facies belt have a mean extent of 278 m (75 to 676 m) (n= 10) (Fig. 4.9D). These bodies have sharp tops and sharp but mostly non-erosional bases, though with rare gutter casts (<0.5 m wide) (Fig. 4.5; Logs 1-3 at 23 m).

The proximal facies belts of splay elements may also exhibit different vertical arrangements of lithofacies: sets of structureless sandstone (Sm) are commonly overlain either by rippled sandstone (Sr; <0.4 m) or thin, poorly sorted siltstone (Fp; <0.4 m). Sets of rippled sandstone (Sr) can be overlain by thin (<0.4 m) structureless sandstone and siltstone (Fd), or by poorly sorted siltstone (Fp). Sets of planar cross-bedded sandstone (St/Sp) can be overlain by rippled sandstones (Sr) (Fig. 4.7B). The most common configuration is Sm and Fp, or St/Sp and Sr, and Sr alone is also common (comprising 15 to 55% of each studied vertical succession) (Fig. 4.7B).

Parts of splay elements defined as proximal show variable internal facies arrangements that suggest variations in flood energy during deposition. The facies arrangement consisting of St/Sp topped with Fp, and Sm topped with Fp, represents the preserved expression of a downstream waning flow during splay flood events. Other trends, notably Sm topped by Sr, and the lack of preserved genetically related fine-grained caps indicate (i) that the subsequent reduction in flow energy could have occurred suddenly, (ii) that fine-grained sediment fractions were bypassed to more distal parts of the system, or (iii) that subsequent flows eroded fine-grained caps. In this instance, we interpret that absence of caps indicate that the flow across the splay transported finer-grained sediment fractions farther into the floodbasin.

4.6.2.2 Medial facies belt

The proximal part of a splay element thins and fines gradationally into the medial facies belt of the splay element. Medial deposits are differentiated from more proximal deposits by their finer grain size (medium siltstone to fine sandstone; average very-fine sandstone), the overall reduction in the occurrence of sedimentary structures such as ripple strata, and the increased occurrence of soft-sediment deformation features (Fig. 4.6A,4.6C). Medial splay deposits comprise structureless sandstone (Sm), small-scale ripple cross-laminated sandstone (Sr), soft-sediment deformed sandstone with remnant ripple forms (Sr), soft-sediment deformed chaotic sandstone and siltstone (Fd), and structureless poorly-sorted siltstone (Fp/Fop). Facies Sr and Fd are the dominant facies types recorded in this element, comprising 20.3% and 43%, of medial splay elements, respectively (Fig. 4.6C).

The medial parts of splay elements have an average thickness of 1.5 m (0.2 to 2.6 m) (n = 63 measured occurrences in 35 studied splay bodies) (Fig. 4.6B) and extend laterally in dip section for an average of 204 m (124 to 281 m) (n = 4) (Fig. 4.6A) and in strike section for 423 m (112 to 848 m) (n = 10) (Fig. 4.9D); they exhibit tabular to wedge-like geometries (Fig. 4.6A). The basal surfaces of these elements are sharp; gutter casts are much less common than in proximal parts of splay elements.

Typical vertical arrangements of lithofacies in medial facies belt are thin sets of rippled sandstone (Sr) (<0.5 m) overlain by soft-sediment deformed chaotic sandstone and siltstone (Fd), and poorly sorted siltstone (Fp/op) (Fig 7C). Soft-sediment deformed sandstone with remnant ripple-forms (Sr) and soft-sediment deformed chaotic sandstone and siltstone (Fd) can both occur alone (Fig. 4.7C). At every site where medial parts of the splay are recorded facies arrangements contain Sr facies; the association of facies Sr and Fd, Sr and Fp, or Sr alone characterize 30% to 50% of facies types recorded in each medial splay element (Fig. 4.7C). Each vertical arrangement of facies tends to show either a fining-upwards trend or no discernible grain-size trend (Fig. 4.7C). Examples of medial facies belts in both the Castlegate Sandstone and the Neslen Formation are similar. However, associations of facies Sr and Fd are

not noted in the Castlegate Sandstone, whereas associations of facies Sr and Fp are abundant (Fig. 4.7C). The occurrence of deformed facies Sd and Fd within such medial splay elements implies rapid sediment accumulation on a water-saturated substrate that induced soft-sediment deformation (Rossetti and Santos, 2003; Owen and Santos, 2014). There is little discernible difference in the form of medial splay elements within the Castlegate and the Neslen formations (Fig. 4.7C).

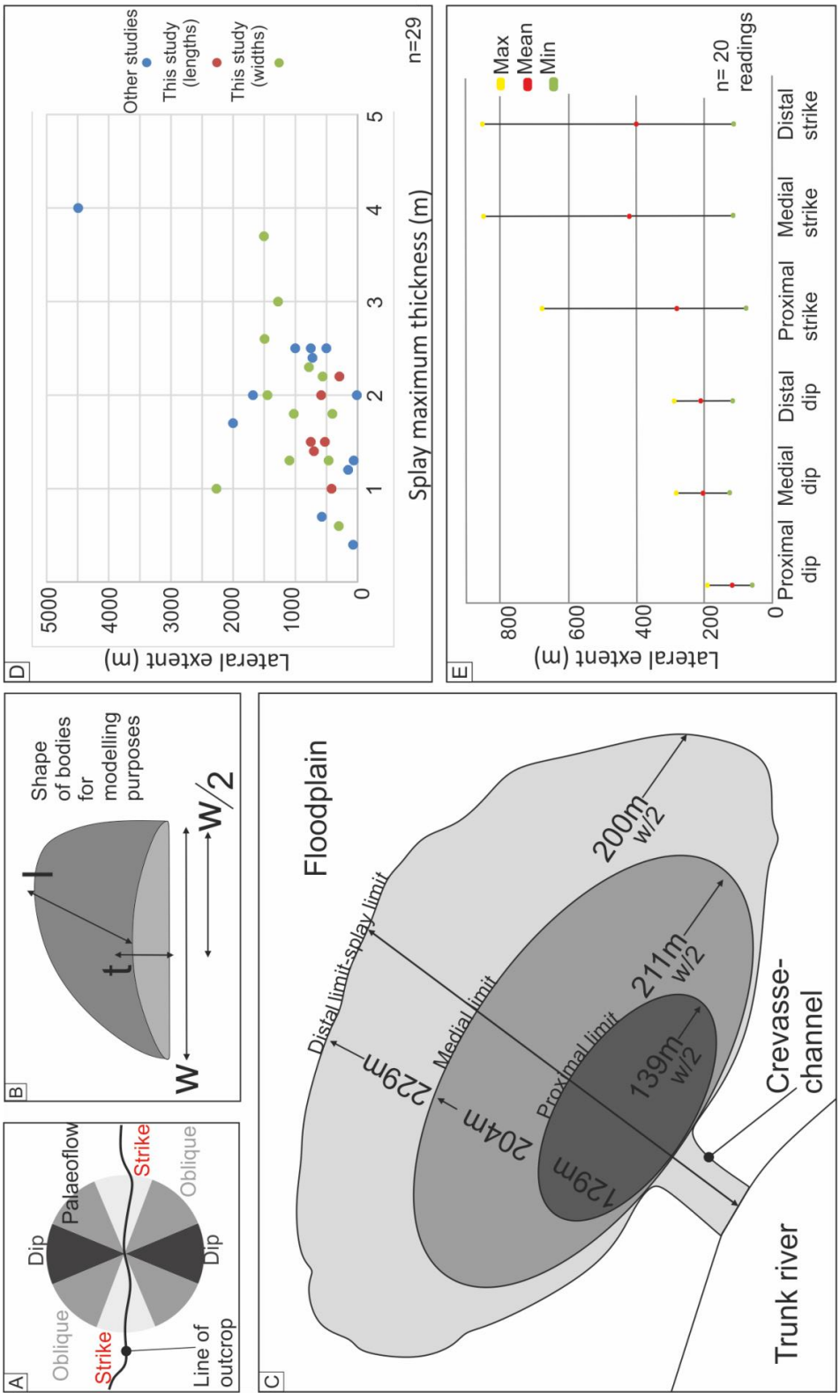

Figure 4.8: Relative abundance of different element and facies-belt types at each studied site. Castlegate Sandstone sites are the Floy and Horse canyons (Fig. 4.3B); Neslen Formation sites are Crescent Canyon sites and Tuscher Canyon sites (Fig. 4.3B).

4.6.2.3 Distal facies belt

The medial facies belt thins and fines, and laterally passes into the distal facies belt, which is itself characterized by a finer modal grain size (fine siltstone to very-fine sandstone; on average medium siltstone), a further reduction in the occurrence of primary sedimentary structures, no convolute lamination or ripples, and by draping or flat set geometries (Fig. 4.6A). Distal parts of splay elements comprise soft-sediment deformed chaotic sandstone and siltstone (Fd), structureless poorly sorted rooted siltstone (Fp) and structureless organic-rich poorly sorted siltstone (Fop) (Fig. 4.6C). Structureless poorly sorted rooted siltstone (Fp) and structureless organic-rich poorly sorted siltstone (Fop) are the most common facies, comprising 60.1% and 25.6%, of the facies types recorded distal facies belts, respectively (Fig. 4.6C). Distal parts of splay elements have an average bed thickness of 0.8 m (0.2 to 1.6 m) (n = 57 occurrences of 35 studied splay bodies), extend laterally in dip-section for an average of 229 m (118 to 286 m) (n = 2) and in strike section for 399 m (113 to 852 m) (n = 7) (Fig. 4.9D), and show tabular geometries (Fig. 4.6A). The basal surfaces of these elements are sharp but non-erosional. Distal facies belts comprise a predictable vertical succession of facies: thin (<0.5 m) soft-sediment deformed chaotic sandstone and siltstone (Fd) topped with poorly sorted siltstone (Fp/op) or, more commonly, structureless poorly sorted siltstone (Fp/op) alone (Fig. 4.7D).

Soft-sediment deformed chaotic sandstone and siltstones (Fd) topped with structureless poorly sorted siltstones are present in many studied examples of distal splay elements but are particularly common in examples from Crescent Canyon (making up 55% of the overbank succession at this locality). Generally, the Castlegate Sandstone exhibits more structureless organic-rich poorly sorted siltstones (Fop) than the Neslen Formation (Fig. 4.7D). The organic matter content could be due to local variations in floodplain vegetation type or abundance, or due to variation in the frequency of occurrence of floodwaters capable of incorporating organic matter into the flow, which itself might be due to local hydrodynamic conditions that favour accumulation of organic matter (Morozova and Smith, 2003).

4.6.3 Coal-prone floodplain element

Typically, the distal part of a splay element is laterally juxtaposed by coal-prone floodplain elements. Locally, distal splay elements merge gradationally with floodplain elements. Coal-prone floodplain elements are the finest grained elements in the overbank and comprise: laminated organic-rich siltstones (Fl), laminated rooted siltstones (Fr) and coals (C) (Fig. 4.6A). Laminated organic-rich siltstones (Fl) are the most common facies in the floodplain (84%) (Fig. 4.6C).

Coal-prone floodplain elements have an average thickness of 0.6 m (0.2 to 1.6 m) (Fig. 4.6B). Element bases can be sharp or gradational; geometries tend to be tabular and laterally extensive (Fig. 4.6B).

Coals are more common in the lower Neslen Formation. Laminated organic-rich siltstones (Fl) is dominant through all sites (Fig. 4.7E) while laminated rooted siltstones are far less abundant, making up less than 20% of the overbank succession at every site (Fig. 4.7E). Sites that have slightly more rooted siltstones (Fr) tend to have lower coal (C) proportions (Fig. 4.7E). This suggests a localised change in drainage conditions to a well-drained environment, perhaps due to fluctuating water-table levels (Bown and Kraus, 1987).

4.6.4 Overbank succession

The identified architectural elements, each of which represents the preserved expression of a depositional sub-environment, make different proportions (based on logged thicknesses) of the overbank succession at each study locality in the Castlegate and Neslen formations (Fig. 4.8). However, these proportions may be biased since the studied outcrops were selectively chosen based on the occurrence of deposits that are interpretable as crevasse-splay elements, and so might not be representative of the studied fluvial successions as a whole. Crevasse-channel fills only occur at Tuscher Canyon and Floy (Fig 8).

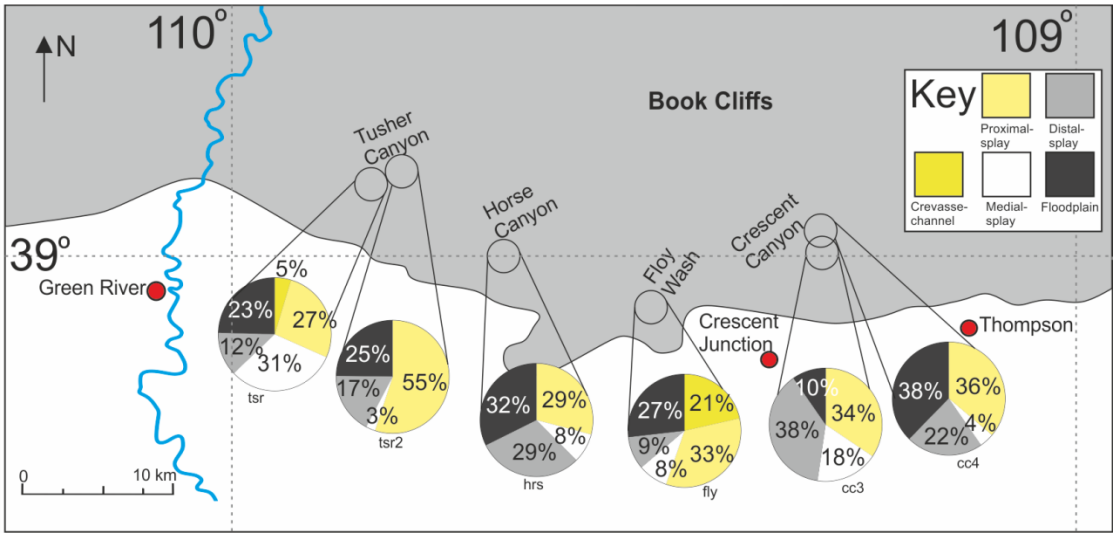

Figure 4.9: (A) Palaeoflow represented by the black (strike), grey (oblique) and white (dip) segments of the circle has been used to reconstruct the original crevasse-splay orientation. (B) Schematic rendering of shape of bodies used for volume modelling purposes. (C) Schematic rendering of different sections through a crevasse-splay element in plan view. (D) Graph plotting true, apparent and incomplete widths and lengths versus maximum thickness of each associated crevasse-splay element using from this study. This graph also plots maximum recorded lateral extents (unspecified orientation) from other works. See Table 4.2 for details of other datasets (E). Graph plotting average and range of lateral extents of each facies belt for dip and strike sections.

The high-resolution stratigraphic tracing and correlation of individual crevasse-splay elements in this study has demonstrated that a significant proportion of overbank deposits represent the distal parts of splay elements (19.8% in the Castlegate Sandstone; 22.5% in the Neslen Formation) (Fig. 4.8). Compared to the distal parts of crevasse-splay bodies, the floodplain fines comprise a similar amount of the overbank (29.6% in the Castlegate Sandstone; 24.3% in the Neslen Formation) (Figs. 8, 10).

The panel depicting the sedimentary architecture at Tuscher Canyon (Fig. 4.5) demonstrates how the various architectural elements and facies belts combine to form a succession. The splay elements commonly incise the upper part of the underlying finer-grained floodplain element (Fig. 4.5C). Medial and distal parts of the crevasse-splay bodies interfinger with laminated fines of floodplain

elements (Fig. 4.5D). Although superficially similar, the lithofacies types present in these sub-environments are distinct (Table 4.1).

4.7 Discussion

4.7.1 Quantification of splay dimensions

Lithofacies and architectural element analysis has allowed for the development of a predictive facies model for the studied successions, which are characterized by preserved remnants of crevasse-splay deposits. The architectural elements of the crevasse-splay deposits comprise a significant proportion of the overbank as a whole: average 60% of the Castlegate Sandstone overbank and 69% of the Neslen Formation overbank successions (Fig. 4.10). The documented crevasse-splay elements have an average length of 544 m (observed range is 292 to 750 m) (n = 8), an average width of 1040 m (observed range is 300 to 1503 m) (n = 12), and an average preserved thickness of 1.7 m (observed range is 0.6 to 2.6 m) (Figs. 4.6, 4.8). Length and width values include apparent and incomplete measurements for which true extents cannot be determined (cf., Greehan and Underwood, 1993). These dimensions are here used to estimate splay volume, whereby splay elements are approximated as flat-based radial bodies with a domed upper surface that approximates in shape to a quarter of a flattened ellipsoid (Fig. 4.8):

$$0.25\left(\frac{4}{3}\pi\, L\, t\frac{1}{2}W\right)$$

where L is the length, W the width and t the thickness (Fig. 4.8). Using this approximation, the average calculated volume for an individual crevasse-splay body is 5.036×10^5 m^3 (n = 20). A Pearson product-moment correlation coefficient to assess the relationship between maximum recorded thickness and splay length yields an r-value of 0.26, indicating a weak correlation and a p-value of <0.01, indicating significance of the relationship (Fig. 4.3, 4.8C). The lengths of the splay bodies recorded herein are less than the overall widths, but are comparable to the half widths (W/2) (Fig. 4.8C, 4.8D) (cf., Zwoliński, 1991; Miall, 1994). The addition of literature-derived data (Table 4.2) to splay length data from this study yields a Pearson r-value of 0.70 and a p-value of <0.001

(Fig. 4.8C), and demonstrates a strong relationship between splay thickness and splay lengths. The maximum preserved splay element thickness in a vertical section is an indicator of the overall size (length and width) of a splay body.

Mjøs et al. (1993) and van Toorenenburg et al. (2016) present ancient splay body volumes that are larger (10^8 m^3 and 10^7 m^3, respectively). These larger values could arise because the splays studied by these authors were generated by larger rivers in floodbasins with more accommodation, or were vertically or laterally amalgamated (composite). In addition, the average volume presented herein might represent an underestimation, in relation to the inclusion of apparent and incomplete measurements. Also, the definitions of splay limits used in these studies could have differed from those used here, and different calculations with different inherent biases could have been used in the other studies.

Maximum thickness (m)	Maximum lateral extent (m)	Average channel Thickness (m)	Average channel Widths (m)	Case study
0.4	70	1	5	O'Brien and Wells, 1986
0.7	575	–	–	Farrell, 2003
1.2	150	–	250	Bristow et al., 1999
1.3	60	10	–	Anderson, 2005
1.7	2000	1.7	150	Fisher et al., 2008
2	1680	6.5	135	Arnaud-Fassetta, 2013
2	10	7	–	Rhee et al., 1993
2.4	725	17	80	This study length values
2.5	500	–	650	Mjos et al., 1993
2.5	1000	–	250	Bristow et al.,1999
2.5	750	–	–	Toonen et al., 2015
4	4490	6.5	135	Arnaud-Fassetta, 2013

Table 4.2: Comparative studies from published studies on crevasse splay dimensions in ancient successions and modern settings.

4.7.2 Controls on crevasse-splay size

The dimensions of splay bodies examined in this study lie in the middle of the range of values recorded from other studies (Table 4.2). Controls that could account for variations in the size and shape of studied crevasse-splay bodies when compared to published studies include: (i) formative channel size; (ii) style of lateral and vertical amalgamation of splays; (iii) availability and shape of floodbasin accommodation; and (iv) gradient from the point of levee breach to floodbasin floor.

The formative parent-channel size partly determines the associated splay-body size; larger channels tend to experience larger floods and thereby generate larger associated crevasse splays (Table 4.2). The size of a splay body will also, in part, depend on whether it is possible to distinguish between an individual splay body versus a composite element formed from multiple amalgamated splay bodies. Lateral and vertical amalgamation of individual splay elements can result in deposits of greater thickness. Factors such as proximity to other splay bodies in a floodbasin, the repeat frequency of splay development at a particular site, and the amount of incision associated with splay emplacement over older splay deposits, will influence the amount of lateral or vertical amalgamation of splay deposits. Vertical amalgamation occurs where several crevasse-splay deposits stack together, with younger deposits potentially partly eroding older deposits (e.g. Fig. 4.5C). Such vertical amalgamation results in the generation of thicker crevasse-splay stacks that might represent composite flood events, possibly associated with sand-on-sand contacts (van Toorenenburg et al., 2016).

Lateral stacking and amalgamation occur where younger or time-equivalent crevasse-splay bodies partially overlap older or time-equivalent crevasse-splay bodies (Li et al., 2014). This can occur where the sand-prone, proximal parts of two crevasse splays merge to create a sand-on-sand contact (van Toorenenburg et al., 2016), or where the silt-prone, distal parts of two crevasse-splay bodies merge (Fig. 4.5D). The availability and spatial extent of floodbasin accommodation, and the possible presence of positive relief features in the floodbasin are important controls that influence crevasse-splay size and shape.

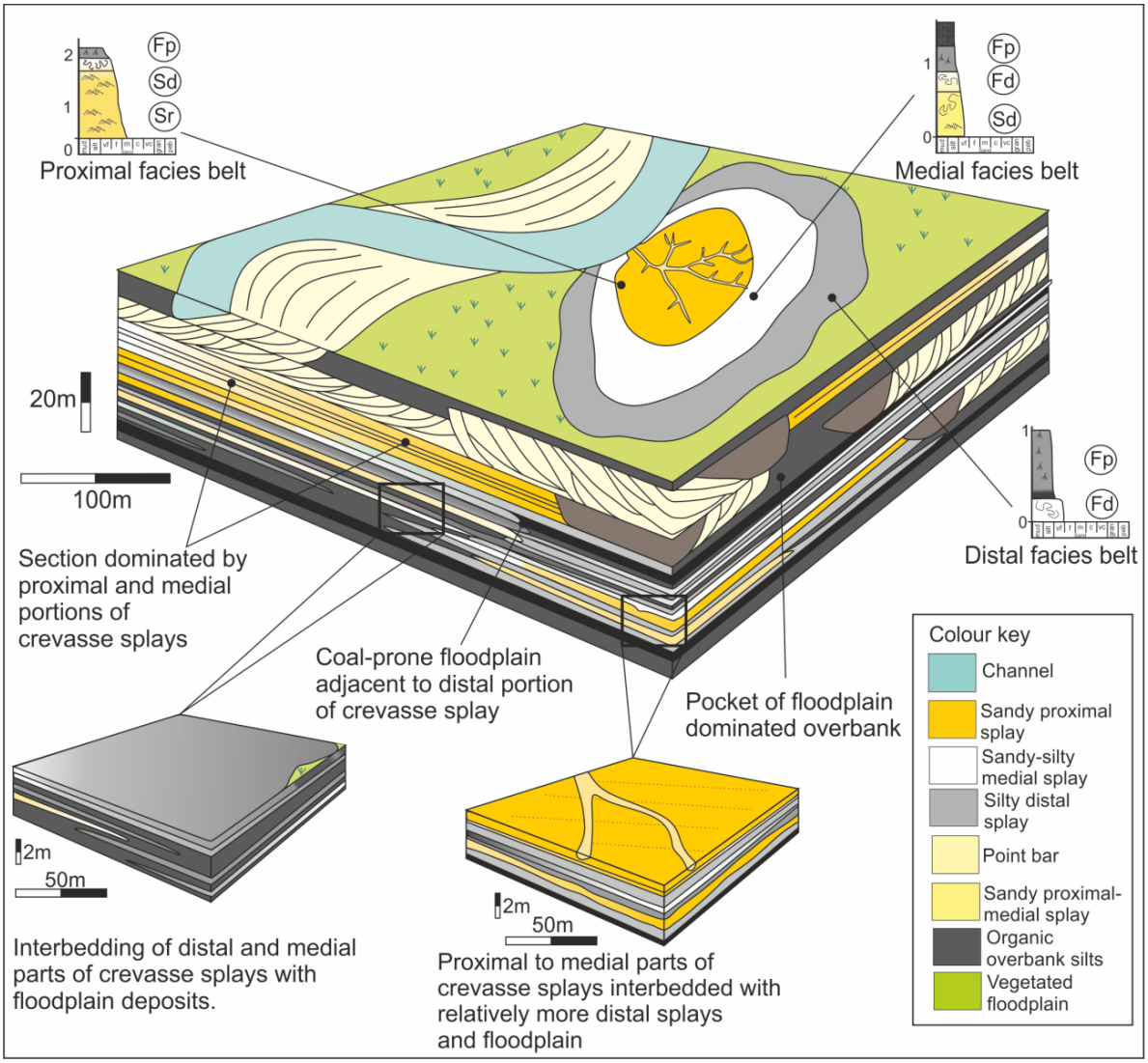

Figure 4.10: Block model depicting the typical occurrence of crevasse-splay elements within the overall succession. The model has been constructed based primarily on data from the Tuscher Canyon sections (see Fig. 4.5). Crevasse-splay facies-belt extents are shown, as is the inter-digitation of the distal parts of crevasse-splay elements with floodplain elements. See Table 4.1 for facies codes cited in key.

Features such as older splay deposits (Li et al., 2015), or raised mires on the floodplain (Perez-Arlucea and Smith, 1999) will influence splay-deposit size and shape. It might be expected that the size of splay deposits will scale directly to the amount of available accommodation (negative relief). Therefore, the thickness of the preserved splay deposit can be used as an indicator for minimum accommodation on the floodplain at the time of deposition. Specifically, in the overbank successions studied in the Castlegate Sandstone and the Neslen Formation, there is an abundance of organic-rich siltstones and coal beds (Fig. 4.8), which have greater compaction factors (Nadon, 1998) and could act as a generator for floodplain accommodation (Franczyk, 1990; Hettinger and Kirschbaum, 2003; Shiers et al., 2014; 2017). In turn, although the organic-rich siltstones and coal beds can produce additional accommodation via autocompaction, they could not have formed initially without space being available on the floodplain.

Fluctuations in floodbasin gradient can encourage crevasse-splay deposition, with deposition likely preferentially occurring in areas where the gradient decreases between proximal and distal reaches of the floodbasin (cf., Adams et al., 2004). Studied splay elements exhibit an average rate of thinning of 4.60×10^{-3} m/m in the width orientation (w/2) and 3.37×10^{-3} m/m in the length orientation.

4.7.3 Controls on the length scale of facies belts within crevasse-splay elements

The proximal to distal fining within splay bodies reflects a general down-current decrease in flow depth, velocity and sediment concentration as the flood waters expand and spread across the floodbasin (Bridge, 1984; Miall, 1993; Smith and Perez-Arlucea, 1994; Bristow, 1999; Anderson, 2005; Fisher et al., 2008) (Figs. 6A, 10). Furthermore, discharge decreases distally due to transmission losses.

The proximal sandstone-prone parts of splays are less dominant than the finer-grained, silt-prone medial and distal parts. Within the successions studied here, the proximal splay belt comprises on average 25% (15 to 47%) of the splay body volume, the medial 37% (22 to 56%) and the distal 38% (18 to 63%). Any

variations in the lateral extent of the facies transitions (Fig. 4.9B) most likely reflects facies belts in the preserved splay element that are irregular in geometry (cf. Nichols and Fisher, 2007; Fisher et al., 2008; Cain and Mountney, 2009) (Fig. 4.10).

Sediment calibre, which governs how sediment is carried in the flow (bedload or suspended load), affects both extent and shape of facies belts within splay deposits, and the sedimentary structures that develop. Each part of the splay body exhibits a different association of facies (Fig. 4.6C). The dominant facies types in the most proximal reaches is Sm 31% deposited from suspension and Sr 49% dominantly bedload tractional deposit (Fig. 4.6C). . In the more medial and distal reaches, Fd 59% (Fig 6.C medial portion) and Fp 53% (Fig. 4.6C distal portion) are deposited predominantly from suspension. During flood events, the sand-grade sediment fraction carried as bedload is deposited preferentially in the proximal part of the splay, whereas the silt and clay fraction is transported in suspension to be deposited in more distal parts of the splay where flow rates are reduced.

The overall sediment grain-size distribution of the material supplied by the parent river to the splay exerts a fundamental control on the length-scale of facies belts present in a single splay body. Flows that carry a greater proportion of sand tend to be characterised by laterally more extensive proximal facies belts. Fluvial systems with main channels that carry a significant volume of sand in suspension will favour the development of relatively more sand-prone splays.

4.7.4 The occurrence of crevasse-splay elements in overbank successions

The finer portions of crevasse-splay elements and the sediment deposited from suspension in fluvial floodbasin, i.e., finer-grained floodplain elements, can look superficially similar. However, the high-resolution stratigraphic correlation of individual crevasse-splay elements in this study demonstrate that a significant proportion of non-channelized deposits represent the distal parts of splay elements (19.8% on average in the Castlegate Sandstone; 22.5% on average in

the Neslen Formation) (Fig. 4.8). The floodplain fines comprise a similar amount of the overall overbank as the distal parts of crevasse splays (29.6% on average in the Castlegate Sandstone; 24.3% on average in the Neslen Formation), in the study areas (Figs. 8, 10).

Several possible controlling factors influence crevasse-splay occurrence and the preservation potential of accumulated splay elements: channel pattern, development of mires and base level changes. Meandering patterns as opposed to braided patterns tend to encourage splay deposition, with floodplain deposits proportionally making up very little of the overall preserved succession of braided systems (Bristow et al., 1999; Colombera et al., 2013). Rivers of the Neslen Formation have been interpreted to have been characterized by meandering channels of modest size (Franczyk et al., 1990; Kirschbaum and Hettinger, 2004; Shiers et al., 2014), which likely encouraged the occurrence of crevasse splays. Average point-bar thickness in bar deposits associated with the main channel elements of the Neslen formation are 7m thick. Average abandoned channel element widths are 80m (Shiers et al., 2017). Rivers with meandering patterns encourage flooding and crevassing due to the helical nature of the flow in sinuous rivers and the increased amount of overbank sediment flux towards the outer bank, especially during episodes of increased discharge (Ten Brinke et al., 1998), assuming that these splays are preserved and not cannibalised by the migrating channel. Conversely, raised mires can inhibit splay formation (Perez-Arlucea and Smith, 1999), through topographic relief that reduces or inverts the gradient difference between the parent channel and the floodplain or which stabilise channel banks. Both factors reduce the likelihood of splay development, or allow only laterally restricted and confined splay development. Base-level rise has been shown to play an important role in encouraging accumulation of crevasse-splay bodies with an increased rate of accommodation generation encouraging preservation of splay deposits (Zwoliński, 1991; Bristow et al., 1999). An increase in the occurrence of crevasse-splay and floodplain deposits is noted upwards through the Lower Nelsen Formation (Shiers et al., 2014), and this is likely due to the influence of

a rising base level associated with a longer term transgressive systems tract (Kirschbaum and Hettinger, 2004; Shiers et al., in press).

Differentiating a crevasse-splay element from a fine-grained floodplain element in the rock record remains problematic. Floodplain mudstones mostly comprise suspension deposits accumulated in floodbasin or floodplain lake settings (Miall, 1994); however it is difficult to determine whether the route that such sediments take to reach these sites of accumulation is via levee overtopping or via crevassing. In outcrop, the distal parts of crevasse splays from the floodplain fines can only be discriminated by walking out splay elements (Fig. 4.5, log 5 to 6). Practically, this study has shown that the distinction should be facilitated by high-resolution facies and architectural-element analyses conducted with lateral tracing of bounding surfaces.

4.8 Conclusions

This study discusses the important role crevasse-splay deposits play in building overbank successions. Splay deposits in this study make up a significant component of the overbank: up to 90% in the studied outcrops (Fig. 4.8). High-resolution facies and architectural-element analyses of crevasse-splay deposits allow overbank successions to be described in terms of depositional sub-environments: crevasse channels, and proximal, medial and distal splay deposits. Associations of lithofacies define the internal subdivisions of splay bodies. Proximal parts of splays are significantly more sandstone-prone and are characterised by cross-lamination. By contrast distal parts of splays are siltstone-prone and structureless. Lithofacies associations are arranged into vertical and lateral successions that occur in predictable orders: cross-laminated sandstone sets pass laterally to deformed finer-grained sandstone sets, which themselves pass laterally to structureless siltstone sets. These lateral transitions occur across average length and width scales of ca. 500 m and ca. 1000 m (full width), respectively, resulting in a planform shape that is approximately elliptical rather than lobate-teardrop. Crevasse-channel elements, crevasse-splay elements with proximal, medial and distal facies belts, and coal-prone floodplain elements are each defined by a subtle internal

arrangement of lithofacies. Such trends can be used to predict the occurrence and facies architecture of relatively more sand-prone or more silt-prone parts of the overbank. Within the studied overbank settings, coarser sandstone deposits occur solely in crevasse-channel and proximal splay elements; finer sandstone and siltstone deposits dominate in medial and distal splay elements; siltstone and coal-prone deposits characterize aggradational floodplain elements.

Because splay elements represent a larger proportion of the overbank succession than coal-prone floodplain elements in the studied successions, the internal complexity of splay deposits presented in this paper takes on more importance when investigating potential reservoirs in low net-to-gross fluvial settings.

Chapter 5 Stratigraphic architecture and hierarchy of fluvial overbank crevasse-splay deposits

This chapter recognizes hierarchical levels at various scale these represent the following components: (i) lithofacies; (ii) individual event beds (~1 m thick) comprising an association of lithofacies and occurring proximal to major parent channels but thinning and fining laterally, and representing the deposits of parts of individual flood events; (iii) splay elements comprising genetically related beds that stack vertically and laterally and represent the deposits of individual flood events; (iv) splay complexes comprising one or more genetically related elements that have a common breakout point and represent the deposits of multiple flood events. Recognition criteria for splay complexes are discussed; emphasis is placed on identification of bounding surfaces, thinning and fining trends of splay elements and complexes and variability of palaeoflow indicators. Stacking of bodies that comprise each tier of the hierarchy is influenced by (i) the rate of local accommodation generation, which influences whether splay elements are laterally offset due to compensational stacking; (ii) floodplain gradients; (iii) erosive force of floodwaters; and (iv) confined or unconfined nature of the floodplain. Gaining an improved understanding of the geometry and distribution of sand-prone splay bodies has applied importance because they contribute volume to fluvial reservoirs and may form significant connectors that link otherwise isolated primary channel bodies, thereby enhancing to reservoir connectivity.

5.1 Introduction

It has long been recognised that fluvial sedimentary successions can be divided into packages of strata bounded by a hierarchy of surfaces (Allen, 1983; Miall, 1985; Bridge, 1993). Although overbank successions are recognised in most fluvial hierarchical schemes (Allen, 1983; Miall, 1985; Holbrook, 2001; Colombera, et al., 2013; Ford and Pyles, 2014; Miall, 2014), relatively little work has been undertaken to evaluate how overbank sediments are organised into stratal packages that characterise ancient preserved overbank successions

(Bridge, 1984; Demko et al., 2004; Toonen, et al., 2015). This is despite extensive work undertaken to show how floodplains are constructed in modern systems (Farrell 1987; Smith et al., 1989; Nanson and Croke 1992; Morozova and Smith, 2000).

The aim of this work is to understand the mechanisms by which fluvial overbank crevasse-splay deposits accumulate and become preserved in the stratigraphic record through lateral and vertical stacking of multiple flood-related deposits at a hierarchy of different scales. Specific research objectives are as follows: (i) evaluation of outcrop data using facies and architectural-element analysis to define a hierarchical classification scheme for overbank crevasse-splay deposits; (ii) establishment of the recognition criteria used in the hierarchy scheme to aid in identification of different sediment bodies that consist fluvial overbank successions; (iii) identification of the different stacking patterns of crevasse-splay deposits; (iv) discussion of the wider applicability of the scheme for the generic classification of overbank successions; and (v) assessment of the subsurface implications of different crevasse-splay stacking styles.

5.2 Background

Fluvial floodplains are low relief, relatively flat-lying morphological features of the overbank (Nanson and Croke, 1992; Bridge, 2006) that are located adjacent to major channel belts and which act as significant sites of sediment accumulation (Brierley and Hickin, 1992; Wright and Marriott, 1993). Floodplains receive sediment via overbank flooding either by breakout through the levees and the formation of crevasse-channels and splays (Ethridge, et al., 1999; Shen et al., 2015) or by levee over-topping (Fisher et al., 2008). Levees are ribbon-like elongated features located at the interface between major fluvial channels and their floodplains (Brierley, 1996; Brierley, et al., 1997; Cazanacli and Smith, 1998). Crevasse channels erode into levees before bifurcating into distributive networks that feed sediment onto the floodplain beyond to accumulate crevasse-splay deposits (Bridge, 2006). Crevasse-splay deposits accumulate during and in the immediate aftermath of short-lived decadal flood

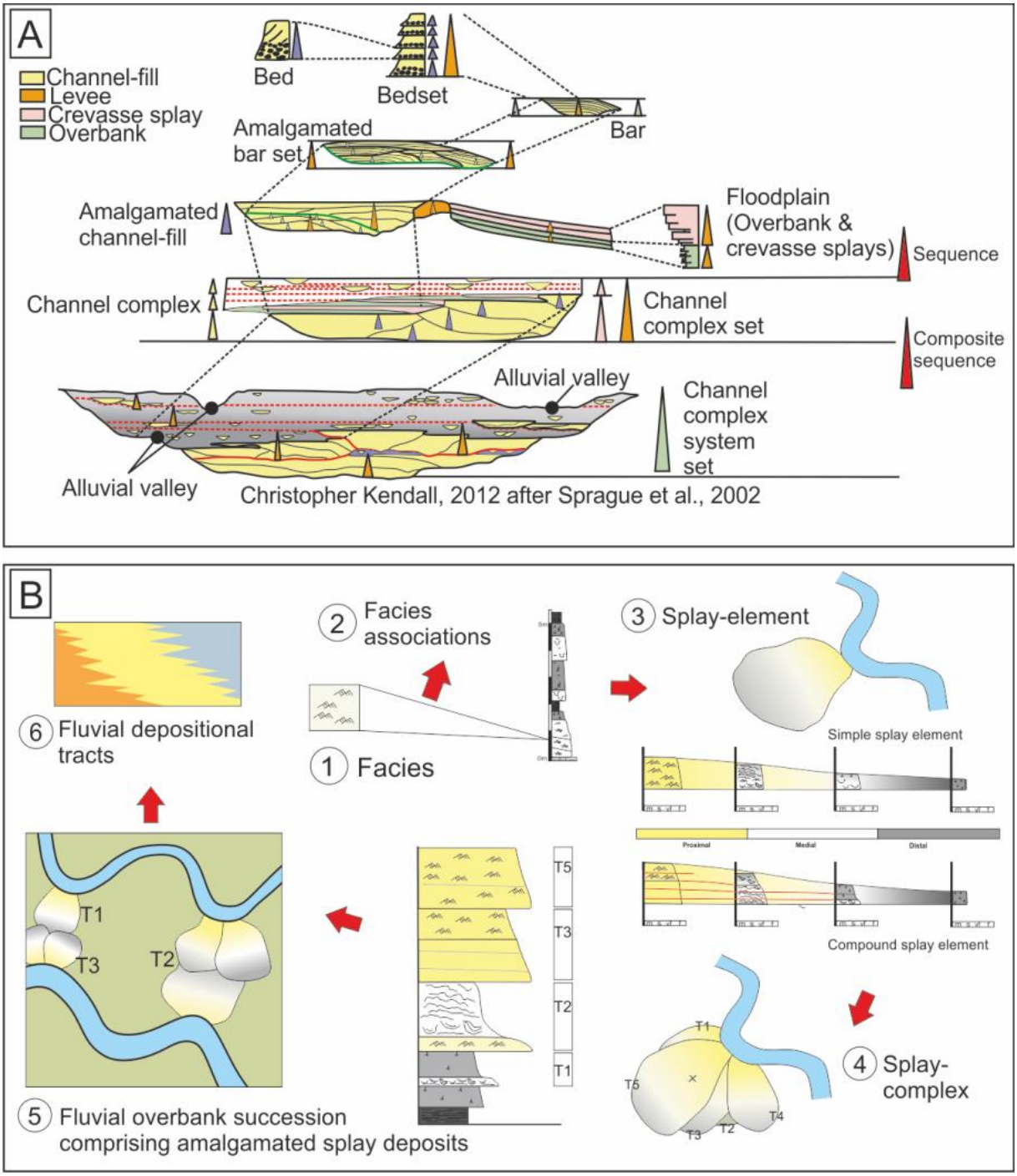

Figure 5.1: A: Example hierarchical scheme after Sprague et al. (2003) from bed-scale up to channel complex system set scale, overbank deposits are only commented on in one scale of the hierarchical scheme. B: Overview of proposed hierarchical scheme for overbank deposits and crevasse-splay deposits in this paper.

events; most splays are supplied by sediment-laden, unconfined, sheet-like flows, which themselves emanate from confined (commonly long-established) crevasse-channel networks associated with parent channels (Smith et al., 1989; Farrell, 2001). Crevasse splays commonly develop a lobate plan-form morphology, and deposits typically thin an fine away from a point source where the parent channel is breached during flooding (Miall, 1996; Mjøs et al., 1993; Burns et al.,2017).

Stratigraphic hierarchical classification schemes are employed as a method to package and divide sedimentary successions; different genetically related packages are assigned on the basis of recognition of common assemblages of one or more lithofacies that define elements with distinctive geometries and which are themselves delineated by bounding surfaces at a variety of scales from lamina-scale to basin-scale (Fig. 5.1; Allen, 1966; Allen, 1983; Miall, 1985; Miall 1988). Hierarchical schemes are used widely in sedimentology from aeolian settings (e.g. Brookfield, 1977; Kocurek, 1981) to deep-water settings (e.g. Sprague et al. 2003; Prélat, et al., 2009). Their application to fluvial settings (e.g. Allen, 1983; Friend, 1983) has provided recognisable order to larger sedimentary successions, and provides insight to palaeoenvironmental setting (Miall, 1985). Widely applied fluvial hierarchy schemes are based on the hierarchical order of bounding surfaces (e.g. Allen 1983); they have been developed in tandem with architectural-element analysis of sedimentary successions (e.g. Miall 1985). Architectural-element analysis is a method which can define deposits as elements based on the nature of upper and lower bounding surfaces of these deposits, overall external geometries of the deposit, the scale of the deposit and internal facies arrangement within that deposit (Miall, 1985). Existing fluvial hierarchy schemes do not differentiate effectively the various component parts of overbank successions which are composed of stacked splay bodies. Few outcrop studies have focused on overbank and crevasse-splay deposits (Bridge, 1984; Fielding 1986; Mjøs, 1993; Demko et al., 2004; van Toorenenburg at al., 2016; Burns et al., 2017); such deposits have received relatively little attention within general fluvial hierarchy schemes (Ford and Pyles, 2014). Outcrop studies typically define crevasse-splay

deposits as centimetre- to decimetre-thick bedsets of sandstone and siltstone interbedded with overbank mudstone (e.g., Fielding 1986; Demko et al., 2004). However, some studies have distinguished generally coarser-grained, more proximal parts of the overbank from finer-grained, more distal parts (Fielding, 1986; van Toorenenburg et al., 2016; Burns et al., 2017). Coleman (1969) in modern rivers and Mjøs et al. (1993) in outcrop examples classified crevasse-splay deposits as either single crevasse-splay lobes attached to the levees of a channel, or as larger, composite bodies composed of multiple crevasse-splay sandstone bodies.

5.3 Data and Methods

Outcrop data were collected from six sites in the Cretaceous Mesaverde Group (Castlegate and Neslen formations) of Utah, and from five sites in the Jurassic Morrison Formation of Utah and Colorado (Fig. 5.2). One-hundred-and-four graphic log sections (1241 m cumulative measured length) were measured from the eleven sites: 62 from the Mesaverde Group localities and 42 from the Morrison Formation. Logs record lithology, grain size, sedimentary structures, occurrence of fossils and palaeosols; rooting and bioturbation indices were recorded on a scale from 0 (no rooting or bioturbation) to 5 (heavily rooted throughout with large [>10 mm] rhizoliths as well as smaller root traces throughout, or intense bioturbation that masks or obliterates all original primary sedimentary structures). Localities were chosen based on lateral continuity of overbank deposits at the location,the continuity of overbank deposits vertically and the ability to place the location with pre-established stratigraphic frameworks. Logged sections were then placed at approximately even intervals, outcrop permitting.

The lithofacies of the Morrison Formation, and the Castlegate Sandstone and Neslen Formation of the Mesaverde Group have been described previously (e.g. Kirschbaum and Hettinger, 2004; Owen et al., 2015; Shiers et al., 2014).

Sixteen lithofacies types from the three studied formations are recognised based on composition, grain size, sediment textural characteristics and

sedimentary structures (Table 1). The facies scheme used is a modified and extended version of the schemes of Miall (1978) and Colombera et al. (2013).

Forty-one architectural panels and accompanying photomosaics were constructed by tracing units across each outcrop cliff section, 27 from the Mesaverde Group and 14 from the Morrison Formation.

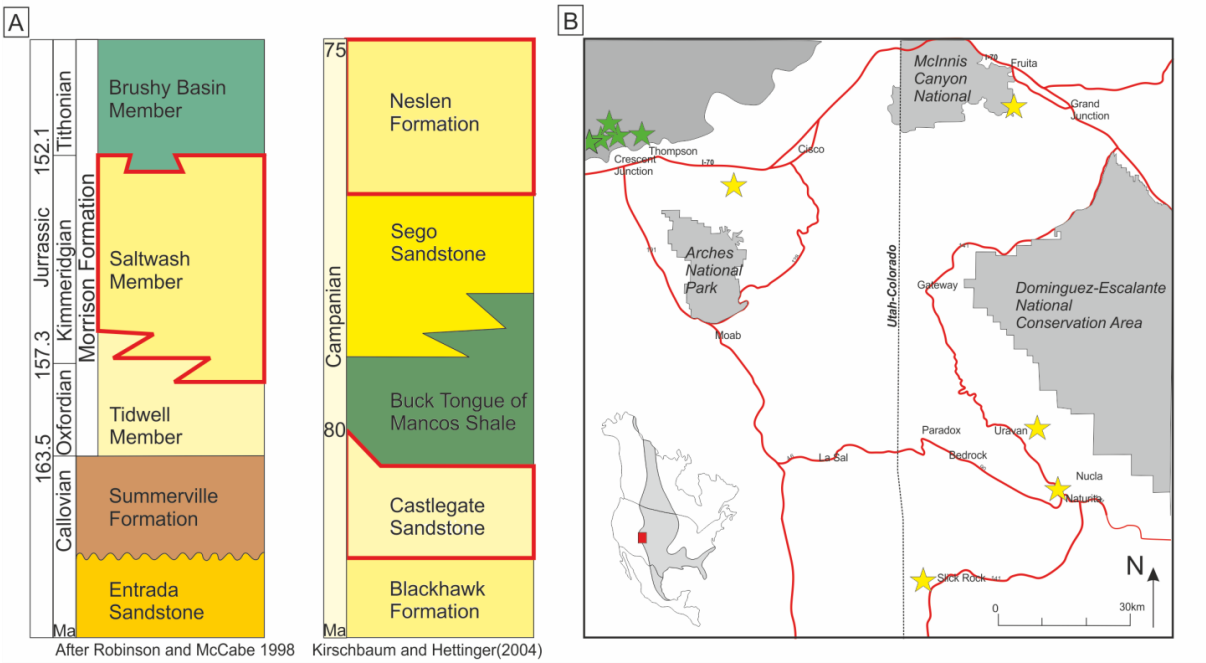

Figure 5.2: Stratigraphic columns introducing the studied formations and location map of field sites. A: The units focussed on in this study are the Saltwash Member of the Jurassic Morrison Formation, the Campanian-age Castlegate Sandstone and the Campanian-age Neslen Formation. B: The map shows the study area. There are five yellow stars marking the position of the five Morrison Field sites across Eastern Utah and Western Colorado. There are also six green stars marking the position of the Castlegate Sandstone and Neslen Formation field sites throughout the Book Cliffs in Eastern Utah.

Panels were constructed as scaled drawings using spatial measurements derived directly from outcrop; they record lithofacies arrangements and distributions. Panels and photomosaics were used to analyse the organisation and geometry of splay elements. In total, 2118 palaeocurrents were measured

from cross-bedding foresets, ripple cross-lamination, current ripple-forms on bedding surfaces and low-angle-inclined accretion surfaces, 1118 from the Mesaverde Group and 900 from the Morrison Formation.

To support the hierarchical scheme presented here, data were collected from 9 modern rivers using Google Earth imagery: the Helodrano Mahajambe, Madagascar; the Okavango River, Botswana; the Lli River, Kazakhstan; the Paraguay River, Argentina; the Saskatchewan River, Saskatchewan; the Betsiboka River, Madagascar; the Peace River, Alberta; the Mississippi River, Mississippi; the Saloum River, Russia. Recorded information is as follows: (i) lengths perpendicular to flood breakout point and trunk channel; (ii) widths parallel to flood breakout point and trunk channel; (iii) planform geometries of splays and their associated trunk channel sizes.

CODE	FACIES	DESCRIPTION	INTERPRETATION
Gm	Green structureless conglomerate	Green, subangular pebble to conglomerate, poor to moderate sorting with very-fine to fine sandstone matrix. Sets 0.8- 2.4 m (1.7 m average). Sets are structureless, or show weak fining-upwards trend.	Deposition from a relatively high-rapidly, bedload
Gp	Cross-stratified conglomerate	Green-grey, subangular pebble to conglomerate, poor to moderately sorted in a very-fine to fine sandstone matrix. Individual sets 1.0- 2.3 m (1.5 m average). Cross-bedding common (0.8 -2.4 m).	Deposition from a relatively high- energy flow and downstream migration of gravel bar forms
St/Sp	Trough and planar cross-bedded sandstone	Grey-yellow-brown very-fine- to medium-grained sandstone, moderately well sorted. Subangular to subrounded grains. Sets are 3- 12 m (4.6 m average) thick. Mud rip-up clasts and plant fragments are common. Trough and planar cross-stratification throughout sets are 0.4- 1.5 m (1.0 m).	Deposition from a relatively high-energy flow and downstream migration of sandy bar forms
Sm	Structureless sandstone	Dark grey-yellow-brown, very fine to fine sandstone, moderately to poorly sorted. Thickness ranges 0.2- 2.2 m (1 m average). Internally sets are structureless.	Records rapid deposition of sand from suspension in a decelerating flow
Sr	Small-scale ripple cross laminated sandstone	Grey-yellow-brown, very fine to fine sandstone, moderately to poorly sorted. Sets varying from 0.1m-4.1 m (1 m average). Small-scale ripple- cross lamination (0.1- 0.9 m) are common to this facies, contains small (<50 mm long) plant fragments, bark pieces and coal fragments.	Down flow migration of ripple bedforms under an aggradational regime
Sd	Soft-sediment deformed sandstone with remnant ripple forms	Grey-yellow-brown, very fine to fine sandstone, poorly to moderately sorted. Sets vary from 0.4- 2.4 m (1.1 m average). Convolute lamination within sets and remnant ripples.	Records deposition from a mixed flow onto an unstable waterlogged substrate
Fd	Soft-sediment deformed mixed sandstone and siltstones	Dark grey-yellow-brown, fine siltstone to very fine sandstone, poorly sorted. Thicknesses vary from 0.1 m- 3 m (0.6 m average). Primary sedimentary structures are overprinted by soft-sediment deformation.	Records deposition from a mixed flow onto an unstable waterlogged substrate
Fp	Structureless poorly sorted rooted siltstones	Light-blue grey or red or green, fine siltstone to very-fine sandstone, poorly sorted. Set thicknesses varies from 0.1 to 2.1 m (mean is 0.6m). Sets of this facies are mostly structureless through some show weak fining-up trends. In situ roots and some carbonised anthracite material.	Poorly sorted and structureless silt-prone facies was deposited rapidly from suspended load
Fop	Structureless organic-rich poorly sorted rooted siltstones	Dark grey, fine siltstone to very fine sandstone, poorly sorted. Set thickness vary 0.3- 2.1 m (0.8 m average). Sets structureless with weak fining upwards trend. Dispersed organic content and roots.	Deposited rapidly from suspended load
Fm	Well sorted, blue, clean siltstones	Light blue, middle to coarse siltstone, well to moderately sorted, rare occurrence of roots or plant material. Bases are erosional 1- 2 m. Set thickness 0.4- 2.4 m (1.4 m average). Structureless or weakly laminated.	Erosive bed bases represents erosive flow, siltstones represent deposition from low energy flow after erosive event
Fl	Laminated organic rich siltstones	Medium to dark grey, red, green siltstones well to moderately sorted, bed thicknesses vary from 0.3m-1.1m (0.7 m average) grain remains consistent throughout a bed. Planar laminations are common. Small plant roots (<10 mm) occur in the Morrison Fm and wisps of anthracite coals in the Neslen Fm.	Steady deposition from low energy flow.
C	Coal	Dark-grey to black clay sized particles ,well sorted, sets vary from 0.2- 2.1 m (0.7 m average). Plant fragments and higher quality anthracite coal fragments present.	Records slow deposition, organic rich setting with limited clastic input
Fr	Laminated rooted siltstones	Blue grey to light grey, upper to lower silt moderately well sorted, set thicknessness vary from 0.2m-0.9 m (0.4 m average). Can be weakly laminated.	Well drained, gradual deposition under low energy regime
Frg	Green rooted siltstones	Green-grey, fine siltstones, well-moderately sorted. Set thicknessness vary from 0.1m- 2.7 m (0.6 m average), can be weakly laminated. Plant root structures common (<5 mm width and lengths) but tend to be concentrated towards the top of sets.	Poorly drained, high water table, gradual deposition under low energy regime.
Frr	Red rooted siltstones	Red, fine siltones to coarse siltstones. Well-moderatley sorted. Set thickness varies 0.1- 2.7 m (0.6 m average).Weakly laminated, plant root structures common, sideritized, taper towards base. Roots long(up to 10 cm) and thin (<5 mm). Low to moderate intensity bioturbation and slickenlines present.	Well drained, dry, calcisols,gradual deposition under low energy regime.
Frm	Purple mottled rooted siltstones	Purple red, fine to coarse siltstones, well to moderately sorted. Sets vary from 0.3 — 3.6 m (1.8 m). Structureless. Small roots throughout (< 5 mm scale), moderate to high intensity bioturbation. Mottled pale purple colouring from watermarks.	Poorly drained, higher water table, gradual deposition.

Table 5.1: Lithofacies occurring in Morrison, Castlegate and Neslen Formations. Codes are specific to this study and are comparable to the codes used in the FAKTS database and summarised in Table 3.1.

5.4 Hierarchy

Crevasse splays and their associated deposits are defined at their simplest as lobate bodies in plan-view and wedge-shaped in cross-sectional view (O'Brien and Wells, 1986; Smith et al., 1989; Floreshein and Mount, 2002; Arnaud-Fassetta, 2013). Research on modern systems indicates that simple lobate splays can, given enough time and accommodation space, evolve into more complicated distributive splays over time and will then finally develop anastomosing channel patterns before abandonment (Smith et al., 1989; Smith and Perez-Arlucea, 1994; Bristow et al., 1999; Farrell, 2001). Additionally, individual splays deposits, regardless of internal complexity, have also been shown to build together, in both modern and ancient studies, to make larger composite splay deposits over time (Smith et al., 1989; McCabe and Shanley 1992; Mjøs et al., 1993; Florshein and Mount 2002); these units have been called 'complexes' (Smith et al., 1989). This construction of multiple, amalgamated crevasse-splay bodies, as recognised in modern systems, suggests that a hierarchical approach for the characterisation of fluvial overbank successions is appropriate. The identification of stratal packages representative of specific genetic significance requires identification and lateral tracing of elements and their bounding surfaces.

5.4.1 Lithofacies

The most fundamental building block recognised by most hierarchical schemes is the facies, a unit of sediment texture and structure (Table 1). Facies occur in genetically related associations, commonly in arrangements whereby vertical or lateral successions of facies occur in a predictable order (cf. Walker and James, 1992). Such facies associations are characteristic of a splay environment (Burns et al., 2017).

5.4.2 Defining a bed

A splay element can either comprise a single vertical accumulation of one facies type or multiple facies types stacked on top of one another (vertical

facies association), both will transition laterally to fine-grained facies (lateral facies association). Individual beds can be difficult to identify within splay elements since they tend to be amalgamated and be of similar facies types in a given location. A bed is a single depositional event (Campbell, 1967; Prélat et al., 2009) a splay bed can be defined as the product of a short-lived singular flood event; this deposit might be simple, perhaps made of only one facies vertically; in this situation the splay element is made of a single bed is the only representation of the splay element. Alternatively a splay bed can be considered again as a short-lived flood event that is part of a larger longer flood event, which produces a more complicated splay element. The beds produced in these short lived flood events will stack together to produce the splay element.

5.4.3 Overbank elements

An element has a series of defining or recognition criteria in outcrop (Allen, 1963; Miall, 1965; Colombera et al., 2013): the nature of the upper and lower bounding surfaces including the presence of fines; external geometries, including any thickness variations of the deposit; internal facies arrangements, including any sediment grain size variations and any consistent facies trends; scale of deposit including lateral extent parallel and perpendicular to flow.

Crevasse-splay element (CS)

Bounding surfaces are the most consistent criterion for splay elements particularly. The bases of splay elements are sharp or can be erosional with gutter casts (Fig. 5.3A, 5.3B, 5.3C), whereas the tops, if preserved, exhibit sharp transitions to the overlying floodplain fine units whether they are laminated organic rich rooted siltstones, coals or palaeosols (Fig. 5.3A, 5.3B, 5.3C). Organic-rich laminated floodplain fines and palaeosol deposits indicate a cessation of active splay deposition; splay elements can be bound at base and top by these fines (e.g. Fig. 5.3B) or can erode previously accumulated splay deposits (e.g. Fig. 5.3A Log 2). The preserved geometries of crevasse-splay elements consistently thin in a downstream direction (Fig. 5.3. 5.4) across all the studied formations.

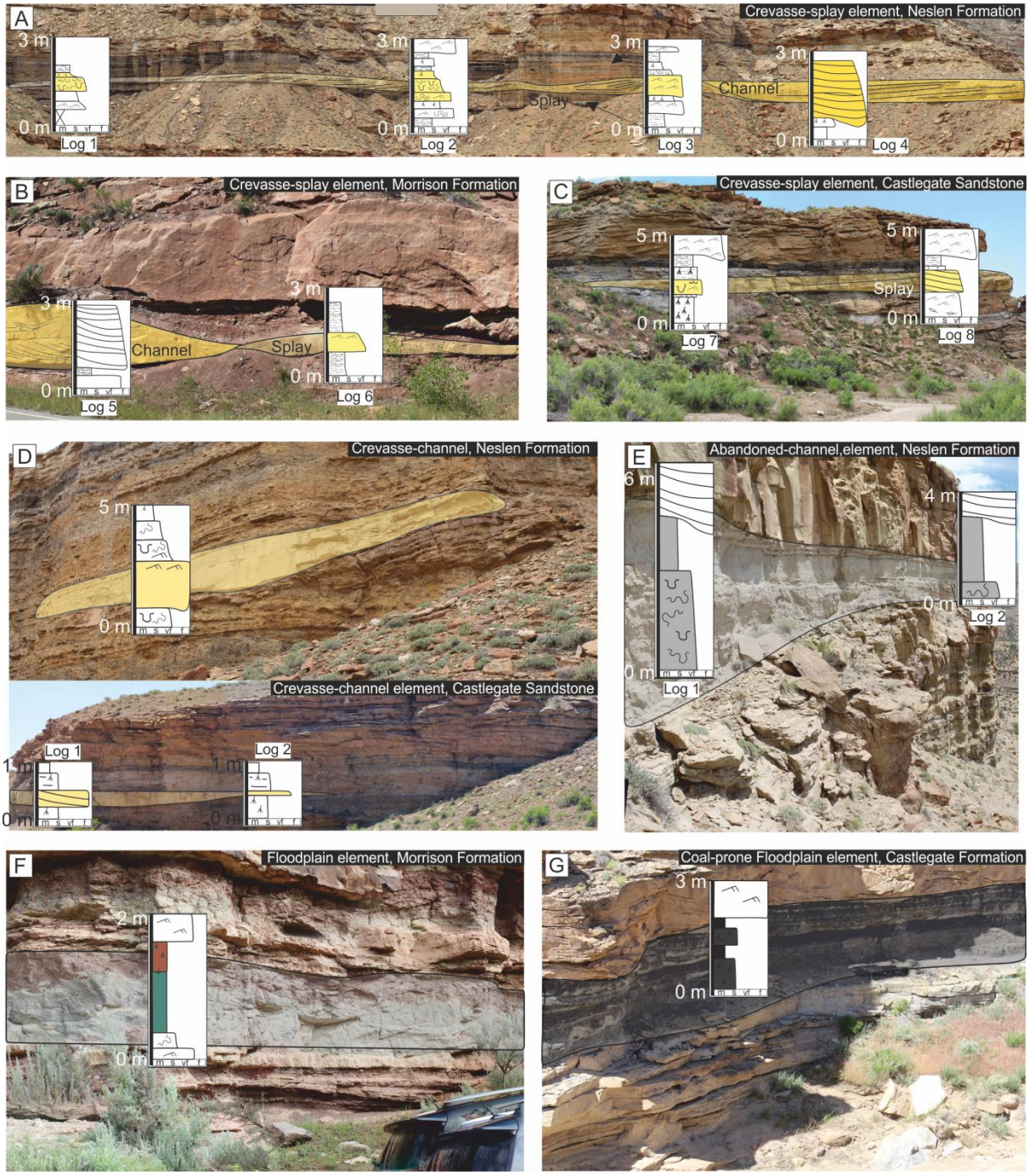
A
Crevasse-splay element, Neslen Formation
3 m
0 m
Log 1
Log 2
Log 3
Log 4
Splay
Channel
B
Crevasse-splay element, Morrison Formation
Channel
Splay
Log 5
Log 6
C
Crevasse-splay element, Castlegate Sandstone
5 m
Splay
Log 7
Log 8
D
Crevasse-channel, Neslen Formation
Crevasse-channel element, Castlegate Sandstone
Log 1
Log 2
1 m
E
Abandoned-channel,element, Neslen Formation
6 m
4 m
Log 1
Log 2
F
Floodplain element, Morrison Formation
2 m
G
Coal-prone Floodplain element, Castlegate Formation

Figure 5.3: Examples of the architectural-element types observed in the studied Formations. A: Crevasse-splay element in the Neslen Formation, exhibits thinning and fining trend away from the channel body in log 4 towards the more distal end in log 1. B: Crevasse-splay element from the Morrison Formation, which transitions laterally from a cross-bedded thicker sandstone body in log 5. The crevasse-splay element is surrounded by laminated floodplain fines. C: Crevasse-splay element from the Castlegate Sandstone with high-angle cross-stratified sandstone in log 8 and rippled deformed finer-grained sandstone in log 7. The crevasse-element in log 8 is directly on top of another crevasse-splay element while in log 7 there is a thin laminated unit between; in both logs the splay-element is tipped with rooted laminated siltstones. D: Crevasse-channel elements in the Neslen Formation and Castlegate Formation. The example from the Neslen Formation is sandstone-prone and passes gradationally to siltstones above; the example from the Castlegate Sandstone has a sharp top and is overlain by light coloured palaeosols. E: Abandoned-channel element in the Neslen Formation. F: Floodplain element in the Morrison Formation green siltstones pass gradationally to rooted red siltstones. G: Coal-prone floodplain element.

Internal facies arrangements including lateral fancies transitions within an element can be used as recognition criteria for a splay element. Laterally moving distally from the point source, a series of predicable facies transitions is common, from relatively sand-prone structureless sandstones and ripple-cross laminated sandstones, to more silt-prone facies, such as deformed sandstones and siltstones, and poorly sorted siltstones (Fig. 5. 3, 5.4). The most common facies within splay elements are structureless sandstone (22% Morrison, 16% Mesaverde), ripple-laminated sandstone (15% Morrison, 14% Mesaverde), soft-sediment deformed sandstone and siltstone (42% Morrison, 24% Mesaverde) and poorly sorted siltstones (22% Morrison, 25% Neslen) (Fig. 5.4). Splay elements can also consist of various facies types that stack in variable vertical arrangements; a splay element can be a simple accumulation of one facies type (e.g., Fig. 5.3B) or can comprise several different facies with gradational vertical transitions, typically as a fining-upward succession. The example splay element from the Neslen Formation consists of rippled-sandstone facies only in its more proximal reaches (Fig. 5.3A, Log 3). The element transitions in the palaeoflow direction to rippled sandstone beds topped with deformed sandstones beds and siltstones and poorly sorted siltstone beds (Fig. 5.3A, Log 2). The most distal reaches of individual splay elements comprise deformed sandstone and siltstone, and poorly sorted siltstone (Fig. 3A log 1).

When investigating fluvial overbank deposits, recognising a splay-element can be aided by the dimensions of splay elements and their relationships with other elements, once the aforementioned recognition criteria have been met, although not a recognition criterion, scale can act as a good indicator that a deposit is a splay element. Crevasse-splay elements across all of the studied formations have an average width across strike perpendicular to palaeoflow direction of 941 m (300 m to 1503 m), average length along dip sections parallel with palaeoflow directions of 327m (71 m to 750 m) and average thickness of 1 m (0.1 m to 2.6 m) (Fig. 5.6A).

There are limitations when defining an element using each of these recognition criteria: bounding surfaces may become amalgamated and difficult to distinguish, fines used as bounding surfaces require sufficient outcrop for

tracing laterally, associations of facies within elements can be highly variable depending on how proximal or distal the location is to the main channel (Burns et al., 2017), establishment of geometries requires outcrop of sufficient quality and lateral extent. Establishing three-dimensional geometries of an element are also problematic in outcrop, with exceptional outcrop needed to define the planform morphology of the deposit.

Modern surface expressions of crevasse splays (Fig. 5.5) demonstrate the complexity and variability of the planform shapes of elements. Common planform shapes of crevasse splays identified from modern examples include lobate, elongate(in perpendicular to oblique orientation to main channel), and irregular (Fig. 5.5A).Lengths of planform splays are taken as the longest point perpendicular to the main channel and widths are 90 degrees orientated from the lenths. Lobate splays are smooth-edged with similar widths (683 m 73 m- 2252 m), and lengths (703 m, 51 m- 2650 m) elongate splays are smooth-edged with longer lengths (1155 m, 324 m- 3574 m) than widths (599 m, 149 m- 2179 m) they tend to elongate in the direction of main river flow, irregular shaped splays have uneven edges and can have a range of width (723 m, 179 m- 2087 m) and lengths (731 m, 301 m- 1847 m) (Fig. 5.5A).

Figure 5.4: Facies types, proportions and associations within overbank elements in the Morrison Formation, Castlegate Sandstone and Neslen Formations.

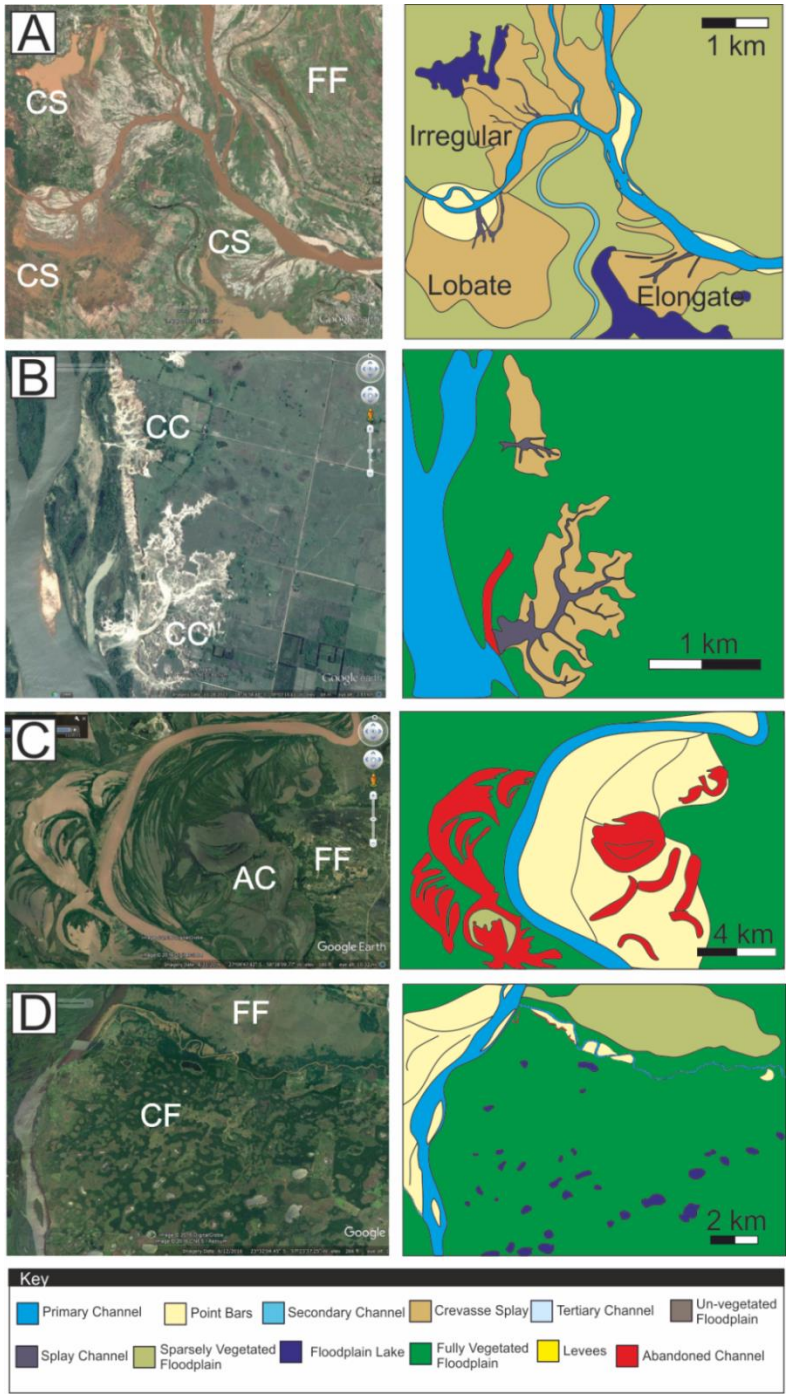

Figure 5.5: Modern illustrations of overbank elements. A: CS: Crevasse-splay example from Madagascar. This examples shows the three types of crevasse-splay plan geometry types, Lobate, elongate and irregular. B: CC: Crevasse-channel from the Paraná River, South America. C: AC: Abandoned channel and FF: Floodplain fines example from the Paraguay River, South America D: CF: Coal-prone floodplain example from the Paraguay River, South America.

Crevasse-channel-fill (CC)

Bounding surfaces of crevasse-channel fills occur as erosional bases with between 0.5 -1.5 m basal erosion. The top of a crevasse-channel element can be either abrupt, as in this example (Fig. 5.3D below) where the crevasse-channel is sandstone-prone throughout, or in other examples may be gradational, for example where the crevasse-channel elements are infilled with finer sediments (Fig. 5.3D top).

The most common facies in crevasse-channel fills differ in the Morrison Formation compared to the Mesaverde Group examples. In the Mesaverde Group, planar cross-stratified sandstones, in which the internal laminae can be at a very high angles (27%) and rippled sandstones (30%) are the most common facies, whereas in the Morrison Formation structureless sandstones (95%) dominate. Vertically crevasse-channel fill elements show different types of accumulations. Some crevasse channel-fills only comprise one or two types of facies vertically (Fig. 5.3D below), whereas others consist of sand facies such as structureless sandstones and planar cross-bedded sandstones topped with deformed sandstones and siltstones and poorly sorted siltstones (Fig. 5.3D top). Crevasse-channel fills are between 6 to 30 m wide (average 20 m) and 0.6 m to 5 m thick (2.85 m average), and can incise into floodplain elements (Fig. 5.3D below).

The modern expression of crevasse channel networks (Fig. 5.5B) shows how crevasse channels can vary in how developed the network becomes before it is finally infilled, with some crevasse channel networks far simpler than others (e.g. Fig. 5.5B), while others develop into more complicated bifurcating channel networks (e.g. Fig. 5.5A). Crevasse-channel networks are known to grow in complexity over time with associated sand-prone deposits typically becoming more isolated and encapsulated by silt-prone deposits (Smith et al., 1989).

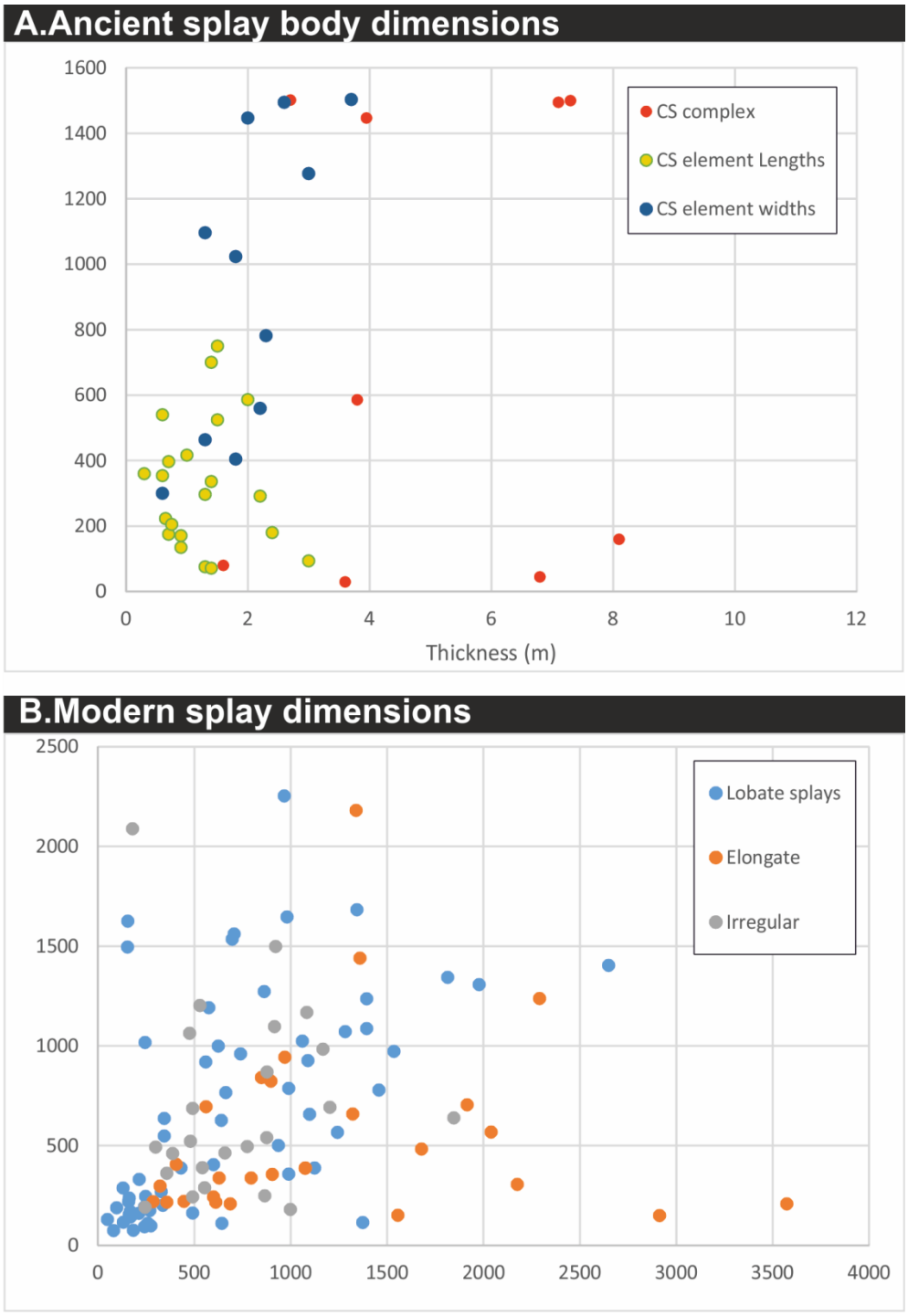

Figure 5.6: A: Lengths and widths of ancient splay elements and complexes, plotted against thickness. B: Widths vs. lengths of modern splay dimensions.

Abandoned-channel fill (AC)

The basal erosion surfaces of abandoned-channel fills cut down between 1-2 m into underlying sediments in both the Mesaverde and Morrison formation (Fig. 5.3E). In the studied examples, both Morrison and Mesaverde, top surfaces are eroded out by overlying erosional thick (>5 m thick) sandstone bodies (Fig. 5.3E). Internal facies arrangements in abandoned-channel-fill elements are simple and comprise poorly sorted siltstones (100% Morrison, 78% Mesaverde), locally with basal mixed sandstones and siltstone with soft sediment deformation (22%) (Fig.5. 4, 5.5E, 5.7). Abandoned-channel fills are wide 50 to 300 m (280 m average) and average 2 m thick.

The modern expression of abandoned-channel fills in overbank areas reveals how they can cluster as the active channel gradually migrates away, resulting in an interval dominated by fine-grained abandoned-channel deposits encapsulated by coarse-grained point- bar deposits (Fig. 5.5C). If the channel had migrated rapidly, i.e., had avulsed, the resulting interval would be dominated with only the fine-grained abandoned channel facies encapsulated by the fine-grained facies of the surrounding floodplain elements.

Floodplain element (FF)

Basal bounding surfaces in floodplain elements are flat-lying, and non-erosional; rooted horizons can be found in this element. Upper bounding surfaces with crevasse splay deposits or channel-fill deposits are sharp (Fig. 5.3F). Stratigraphic transitions between two floodplain elements are gradational where intense bioturbation or rooted horizons overprint the primary structures of the sediments. The floodplain elements of the Castlegate and Neslen formations are coal-prone, and comprise laminated organic rich siltstones (Fl 84%), less rooted siltstones (Fr 11 %) and coals (C 5 %) (Fig. 5.3). Whereas the Morrison Formation floodplain elements are rooted (Table 1; Fig. 5.3), with more rooted siltstones (Frr 24 % and Frg 6 %), mottled siltstones (Frm 28%) and laminated organic rich siltstones (Fl 42 %). In the Morrison Formation, different types of rooted siltstones (palaeosols) vertically transition from one to another (Fig. 5.3F), which reflects the drainage state of the soil at the time. In the Mesaverde Group, examples of well-laminated siltstones, sometimes with

roots, are interbedded with coals (Fig. 5.3). These units form laterally extensive sheets with thickness that is constant for tens of metres (Fig.5. 3, 5.5F,5.5 G).

Away from erosion by overlying deposits, floodplain sediments are laterally extensive for at least tens of metres across each outcrop (Fig.5. 3F, 5. 3G, 5. 7B). Floodplain elements have been recorded as being on average of 69 m in length (22-240 m) and as having average thickness of 0.73 m (0.1- 1.95 m) In the Castlegate and Neslen formations, floodplain elements are associated with coal-prone floodplain elements and distal edges of splays are seen to pass gradationally into floodplain deposits (Burns et al., 2017). In all the studied formations, the vertical stacking of floodplain elements above crevasse-splay elements record times of cessation of active splay deposition into the floodplain at that point.

The modern expression of a floodplain element (Fig. 5.5D) illustrates the variations in level of vegetation and amount of area covered by floodplain lakes. Coal-prone floodplain elements will have accumulated under a regime with a greater number of floodplain lakes and heavy vegetation as opposed to the less vegetated, better drained floodplain element.

5.4.4 Splay-complexes

Defining a splay complex

This study focuses on how genetically related splay and crevasse-channel-fill elements stack together and how they interact with other floodplain elements. A complex is a genetically related stack of splay elements. In a complex, the splay elements must originate from a similar breakout point on a river into the same geographic place on the floodplain. There are several recognition criteria for a splay complex in the field: a complex must comprise two or more splay elements (although as a complex thins there might only be a single element representing the whole complex); the complex must be bound by fines at the base and top (caveat is that they may not be well preserved and can be cut out due to erosion); a complex can also exhibit an overall thinning and fining trends in the distal direction, i.e. away from the major channel body; in the proximal reaches complexes will have similar palaeoflow directions in each of the individual splay elements (Fig. 5.7A, 5. 8). A splay complex must also be, by definition, thicker than the splay element it contains, and will be generally thicker than the average element thickness for that study succession (Fig. 5.6A). Complexes in this study are on average 6 m thick, whereas on average splay elements are 1 m thick, and on average a complex is over 3 m thick and element under 3 m thick.

Since a complex must be made up of more than one element it is important that each element within a splay complex is well-defined by its bounding surfaces and facies structure. Elements within complexes can be directly on-top of another but each of the multiple present elements must be definable with basal sharp transitions from the underling element to the following element and facies accumulations. This appears evident in proximal areas of a complex, whereas in more distal regions splay elements can intercalate with floodplain elements (Fig. 5.7A).

A. Conceptual diagram of a crevasse-complex with dimensions

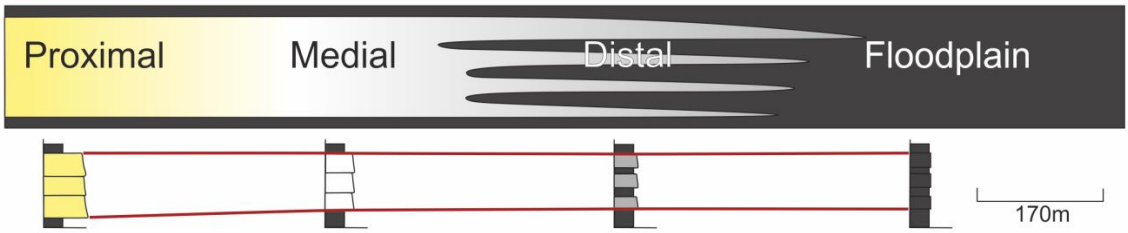

B. Proximal part of crevasse-splay complex

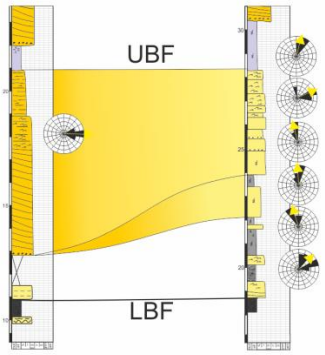

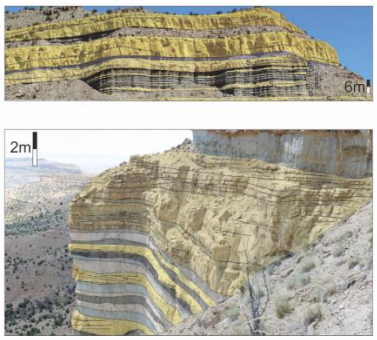

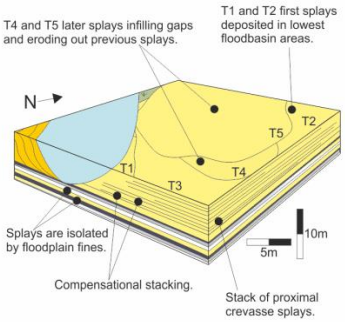

C. Medial part of crevasse-splay complex

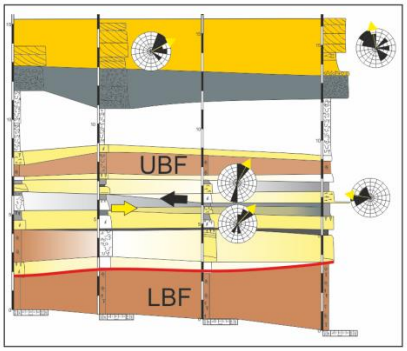

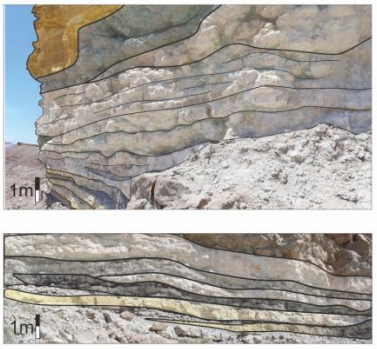

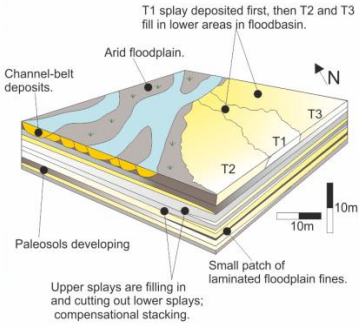

D. Distal part of crevasse-splay complex

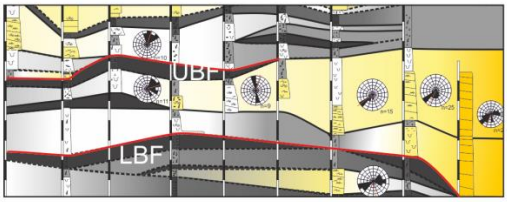

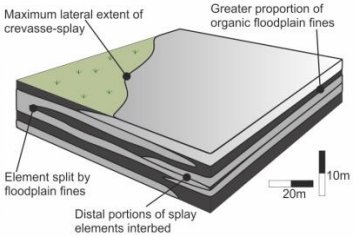

Upper bounding fines= UBF
Lower bounding fines= LBF

Figure 5.7: Crevasse complexes from proximal to distal regions. A: Simplified diagram of crevasse-complex with average lengths. B: Example of proximal crevasse-complex, coarsening upwards trend and thickening upwards trend. Logged example and images are from the upper part of Neslen Formation at Crescent Canyon C: Medial part of crevasse-complex, thickening and thinning of crevasse-splay elements. Logged example and photographs are from the Morrison Formation, medial portion of the Morrison fluvial fan at Yellow cat Canyon D: Distal part of crevasse-complex. Crevasse-splays interbed with floodplain fines. Logged example and photographs are from the lower part of the Neslen Formation at Tuscher Canyon.

A complex will be bounded at base and top by fine-grained deposits. These deposits must represent a significant period of time where splay-deposition was inactive at that point on the floodplain. Consequently bounding fines will be floodplain elements but specifically must be palaeosols, coals or laminated organic rich siltstones that contain roots rather than any or all types of floodplain fines. These floodplain elements that mark the base and tops of the splay complex tend to contain within them more rooting than floodplain elements recorded in these formations generally. All studied floodplain elements in these formations exhibit 0-4 rooting intensities, but commonly in the range 0-2, while fines that bound the base and tops of complexes have a range of 0-,4 but commonly with 1-3 intensities. The tops of the splay elements onto which bounding fines have been deposited also tend to have roots, although roots are not uncommon in splay elements. Fines marking the base of a splay-complex tend to comprise a simpler facies assemblage than in floodplain elements generally with only one or two facies generally present, but this could be due to removal of top part of fines by erosive crevasse flows. Fines denoting the top of a splay complex can have the same complexity as any other floodplain elements.

There is a consistent proximal to distal thinning and fining trend in a complex that mirrors the elements that also thin and fine away from the major channel-

fill. The elements within a complex tend to show comparable palaeoflow directions in the proximal and medial areas (Fig, 7A, 7B, 8); towards the distal end of the splay complex the facies present do not display palaeoflow indicators. Dimensions of complexes vary and scale to the dimensions of the elements that comprise the complex, i.e., the bigger the splay elements within a given complex the larger the corresponding splay complex will be. Splay complexes in the studied successions average 5.6 m thick (3.6-8.1m) and have lengths averaging 1170 m (585-1502 m) (Fig. 5.6A).

Internally, a complex will show various stacking patterns and styles. Splay elements can compensationally stack (Fig. 5.7B, 5.9). Younger splay elements within a complex can also be truncated erosionally, so that reduction in the thickness of older splays is particularly common in the proximal areas where splay elements erode and amalgamate (Fig. 5.7A). Complexes that show amalgamated sand on sand contacts seem to “split” away from one another towards the medial-distal end (Fig. 5.7D).

In modern splay complexes in plan-view, active splays can be identified by the unfilled crevasse-channel network; each individual splay element infills an area adjacent to the previously active splays, in which crevasse-channel networks are infilled with sediment (Fig 9A, 9B, 9C).

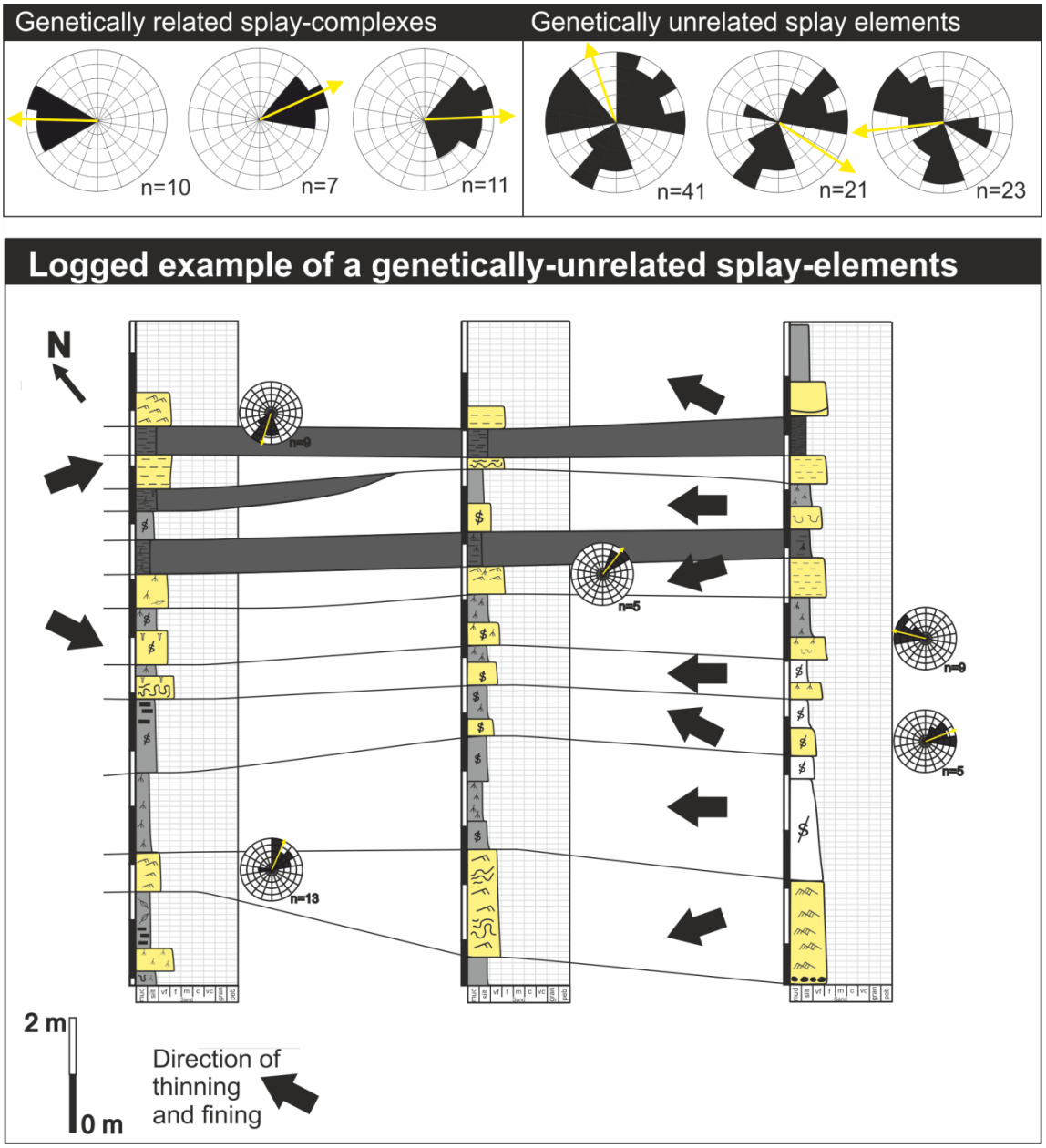

Figure 5.8: Palaeocurrent indicators from genetically related splay complexes and contrasting genetically unrelated splay stacks, examples from Morrison, Castlegate and Neslen Formations. Outcrop example from the upper part of the Neslen Formation; splay elements with different thinning and fining directions and interbedded with floodplain fines, which are therefore interpreted as genetically unrelated splay elements.

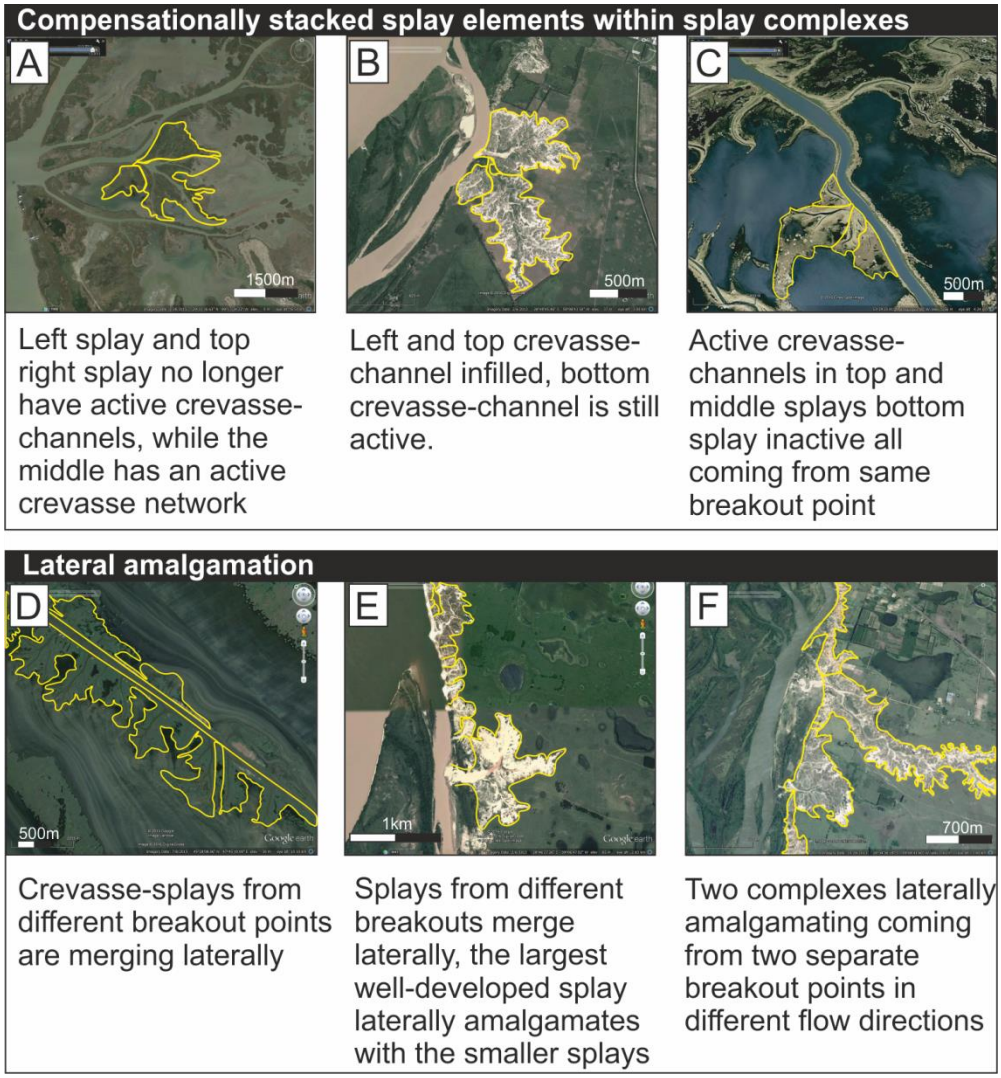

Figure 5.9: A: Genetically related splays from same breakout point, Mississippi River; B: Genetically related splays from same breakout point, Paraná River, South America; C: Genetically related splays Saskatchewan River, Canada; D: Genetically unrelated splays originating from different breakout points merging laterally, Volga River, Russia; E: Genetically unrelated splay originating from different breakout points merging laterally Paraná River, South America ; F: Genetically unrelated splay originating from different breakout points merging longitudinally Paraná River, South America.

5.5 Discussion

5.5.1 Stacking patterns of elements within splay complexes

Stacking patterns in complexes vary from compensational (cf. Donselaar et al., 2013; Li et al., 2014; van Toorenenburg et al., 2016; Gulliford et al., 2017) with minor components of lateral stacking relative to previous crevasse-spalys and/or progradation to dominantly progradational stacking styles (cf. van Toorenenburg et al., 2016). Each of these stacking styles will be expressed in vertical stratal trends. Parts of a progradational stack of splay elements could have an identical vertical profile as laterally offset splay elements (e.g. Fig. 5.10A i and iv), even though the resulting planform morphologies are very different. However, vertical profiles in the two end-members can also be very different (e.g. 10A, i, ii and iii).

Compensational stacking patterns are more likely to occur when the gradient of the floodplain is such that it encourages movement of floodwaters perpendicular or oblique to major trunk channel. The higher apparent width-to-length ratios of elements in the Castlegate and Neslen study areas indicate that this may have been the case and that compensational stacking would be the dominant stacking style these examples. Compensational stacking fundamentally is a product of local accommodation space (Mutti & Sonnino 1981): splay deposition creates topographic highs on the floodplain; subsequent splay deposits will occupy the relative lows (Donselaar et al., 2013; Donselaar et al., 2016; van Toorenenburg et al., 2016). Compensational stacking is seen in many different sedimentary environments including deep-water lobes in (Prélat et al., 2009) to delta lobes (Straub et al., 2009) and alluvial fan systems (Franke et al., 2015). Progradational stacking trends in splay complexes would require strong erosive floodwaters and/or a confined floodbasin funnelling the floodwaters and producing the thinner more elongate plan-view shape. Progradational stacking styles would also require a floodplain that consisted of compactable material which could produce increase local accommodation space into which the complex could then build into. These models of progradational and compensational stacking patterns in splay-complexes are

end-member models. It is plausible that most complexes would fall somewhere between these two end-member models (cf. van Toorenenburg et al., 2016).

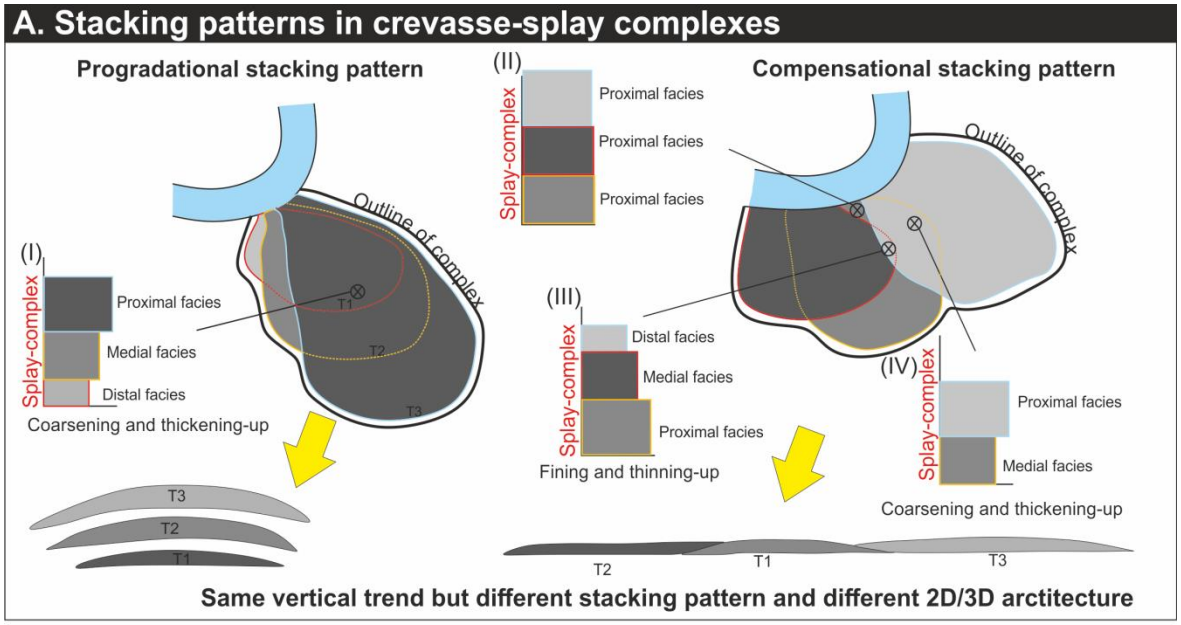

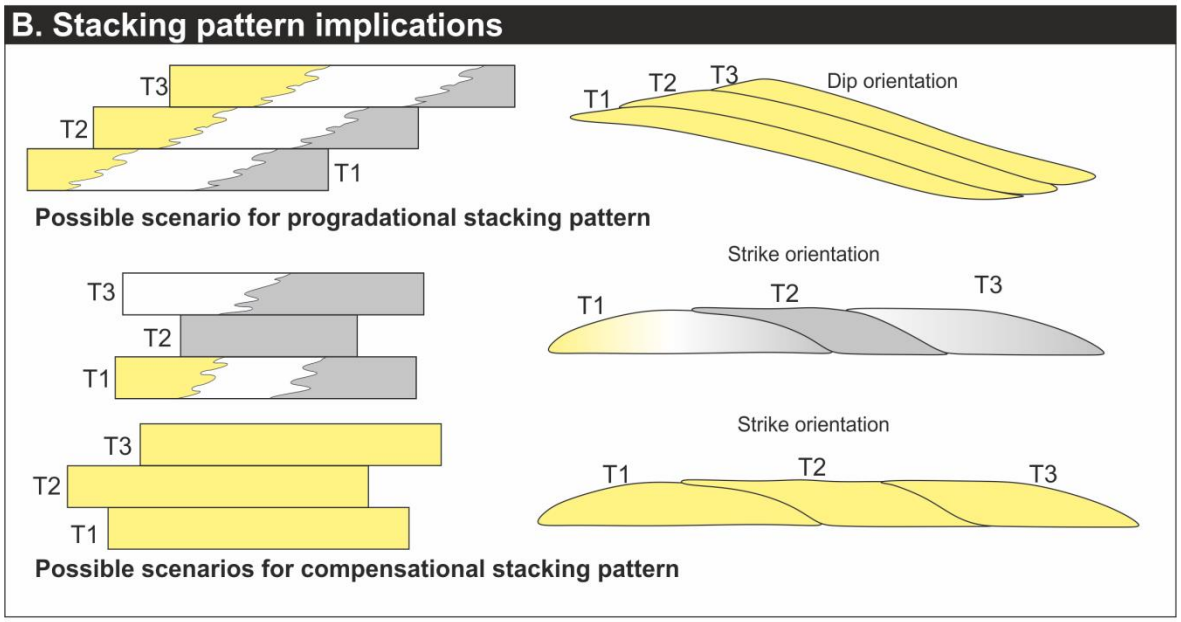

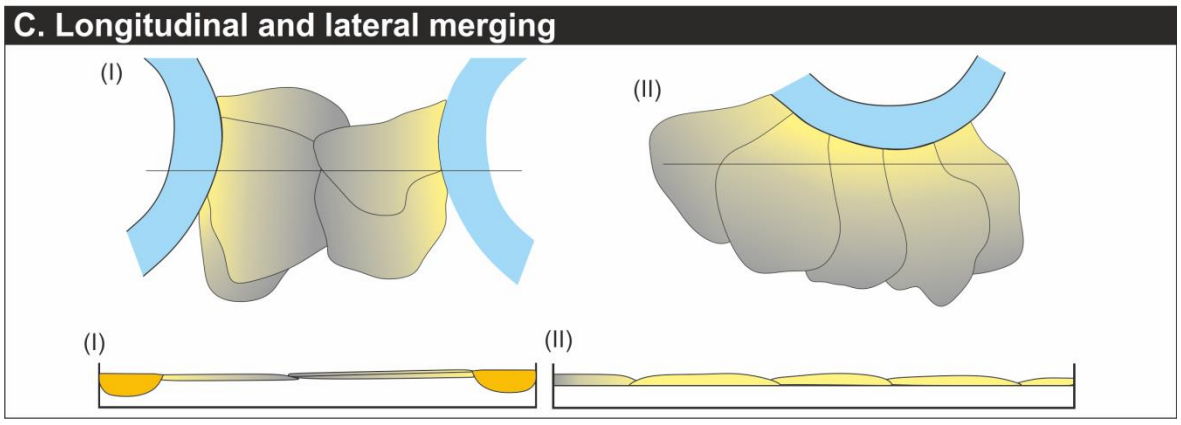

Figure 5.10: A: Stacking patterns of splay elements in complex are variable; in this figure two-end member models are presented for stacking pattern styles: progradational stacking patterns and compensational stacking patterns.(I) Progradational stacking patterns result in coarsening and thickening upwards and an elongate planform shape where the width is far less than the lengths. Compensational stacking patterns result in different vertical profiles depending on planform position of the vertical section: (II) No trend in vertical profile; (III) Fining and thinning-up trends can occur in some parts or the complex; (IV) coarsening and thickening-upwards trends in other parts of the complex (C). In some parts of the crevasse complex the complex will be represented by stacks of splays (A-C) but in others the entire complex is represented only by a single element (D). B: Stacking patterns in crevasse complexes, implications for subsurface connectivity; C: Crevasse splay deposits can interact in a number of ways. Crevasse complexes could interact at the longitudinal fringes of the complexes (G) as in Fig. 5.9F or individual splay elements could interact at their lateral margins (H) which is more likely to produce larger bodies of sand.

5.5.2 Problems with recognition of splay-complexes in the rock record

The presence of fines is a very important tool in the identification of splay complexes. The fines indicate a break in crevasse splay deposition and have previously been used for subdividing crevasse-splay deposits (Mjøs et al., 1993). In this study, the deposits used to delineate different scales of splay deposits are palaeosols and coals or laminated rooted organic-rich floodplain siltstones. In all the studied overbank successions there is laminated organic-rich rooted siltstone (Fl; Castlegate and Neslen formations: 84%; Morrison Formation: 42%). In the Neslen and Castlegate Formations well-drained palaeosol (Fr) are far less abundant (11%) (Fig. 5.6A), and there are coals (C) (5%) (Fig. 5.6A). The Morrison Formation contains well developed palaeosols that are red (Frr) (20%), green (Frg) (6%) and mottled (Frm) (28%) (Fig. 5.6A). Palaeosols of all previously listed types and organic-rich, rooted laminated siltstones (Fl) represent a break in deposition of crevasse splays, and indicate a shift of the main channel far from the deposition site (Fig. 5.11A) that determines a long, more definitive, break in splay deposition (van Toorenenburg et al., 2016).

Using both laminated siltstones and palaeosols as a primary way to delineate a splay complex is suitable where these deposits are laterally traced from proximal to distal locations, because although the internal structure of the complex may be variable these deposits at the base and tops of the complex remain continuous (Fig. 5.7). However, if the bounding fines are not traced from proximal to distal locations it can be more difficult to define a complex, particularly at its distal end, because that some bounding fines have no easily recognizable distinguishing characteristics from any present floodplain fines . Well-developed palaeosols, coals and rooted siltstones are all gaps in splay deposition; however, a palaeosol or a coal is far more easily recognised in outcrop or core, and can be directly used as a proxy for a long period of time with little sediment input to the floodplain whereas a rooted siltstone is less diagnostic. Although rooting intensities tend to be greater in bounding fines than in other floodplain deposits, this a relative measure.

A complex can be easier to recognise in the proximal reaches where the stacked elements have similar palaeoflows. In distal locations a complex is difficult to recognise as there are limited palaeocurrent indicators, and splay elements intercalate and pass laterally into floodplain elements (Fig. 5.7, 5. 10B). The intercalation of distal splay elements and floodplain fines could be the result of a complex, or a stack of non-genetically related splay-elements being deposited into the same floodbasin (Fig. 5.11B). Differentiation between the two scenarios in the distal reaches can be difficult, although increased time for colonisation of plants in the second scenario may lead to higher rooting intensities in the fines.

The next recognition criterion for a complex is that by definition it must be made by more than one element, although this too can cause problems. In some locations a complex can be represented by one element or in some locations the top of an element may be eroded away by following splay elements; this amalgamation can make identification of each individual element within the complex difficult. Since in some areas a complex may be represented only as a single element this is due to the plan-view variability that can affect the preserved stratigraphic lateral continuity within a complex; an element which is part of complex will, due to compensational stacking, not be overlain everywhere geographically with the following element in the complex leaving it isolated in that section (Fig. 5.10A). In the proximal areas the complex can be preserved in the rock record as a thick stack of splay elements, as a partial stack of elements or could be represented in part only by a single splay element (Fig. 5.11C). These multiple ways in which the complex can be represented in the rock record results in issues when trying to identify a complex and only part of it is exposed in outcrop or if only observed in 1D datasets.

Thickness is a useful guide, but not a criterion. For example, the thickest splay element recorded in Neslen Formation is 3.7 m thick but the lowest thickness of a recorded complex (with multiple definable splay elements within them and bounded by fines) in the Morrison Formation is 1.6 m (Fig. 5.6a). Although most elements are below 3 m and most complexes are above 3 m (Fig. 5.6a) these

rough guidelines of element and complex thickness depend more on the ratio of thickness of the element to the complex within the studied formation.

The identification of a splay complex must be undertaken with care, sufficient outcrop exposure and fulfilment of, realistically a majority if not all, the proposed recognition criteria.

Two splay-complexes can also accumulate in the same geographic floodplain area (e.g. Fig. 5.7D). Both complexes have different directions of palaeoflow and thinning and fining trends; both complexes thin and fine towards each other. Complexes could be consider genetically related if coming from the same parent river, contemporaneously, in such scenarios splay elements within the complex could interbed with one another. Identification of such a scenario would rely on identification of interbedding distal splay elements and associated channel deposits relating to a single parent channel; in outcrop this may be difficult.

Two non-contemporaneous, non-genetically related splay complexes can build into the same floodplain area, instead of splay elements interbedding one complex would be on top of another with fines separating the two (Fig. 5.7D).

In modern systems, these relationships between different complexes are clearer there is lateral amalgamation of separate splay elements, which tends to occur at the lateral edges of the splay elements (Fig. 5.9D, 5.9E), and of complexes which merge not only at lateral edges but also at the longitudinal edges (Fig. 5.9D). With lateral amalgamation along the lateral edges of splays many multiple splay elements can have different breakout points but can merge laterally to create an extensive sheet. Longitudinal and lateral merging of complexes could result in an interval within an overbank dominated succession that predominantly comprises of splay deposits.

Genetically unrelated splay elements

Finally not all splay elements deposited will be genetically related. Splay elements can be deposited at different time intervals and from different parent channels but still within the same reach of floodplain; but this scenario will still build part of an overbank succession. Genetically unrelated splay elements will

not meet the criteria for splay complexes: they might show different thinning and fining directions of individual elements, large differences in palaeoflow directions in each present element (Fig. 5.8), and bounding fines will not necessarily bound the bases and tops (Fig. 5.8). Instead fines such as palaeosols, coals and organic-rich rooted laminated siltstones will interbed with the splay elements.

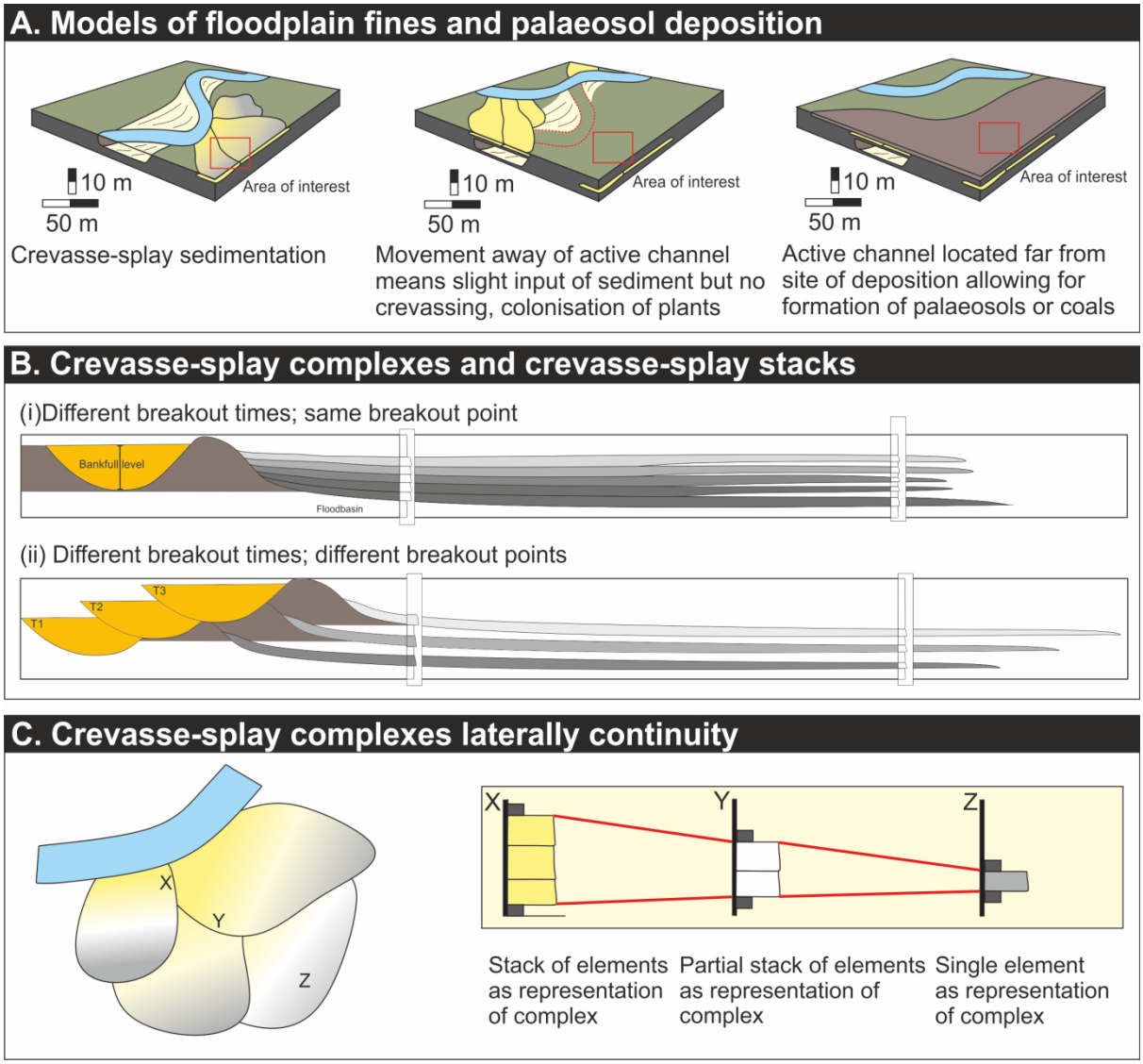

Figure 5.11: A: Cartoon of temporal evolution of a system that illustrates different types of fine deposition; as the main channel migrates away from the site of deposition and crevassing ceases, floodplain fines will start to accumulate. When the active channel has migrated away from the site of deposition for sufficient time, palaeosols will start to develop. Both types of fines with roots will indicate cessation of crevasse-splay deposition. B: Stacks of crevasse-splay elements can accumulate in the same floodbasin either as genetically related complexes (i) or as non-related elements (ii). These situations result in architectures that appear very different in the proximal reaches but may be indistinguishable in the distal reaches. C: Complex can be represented by a stack of splay elements or a single splay element.

5.5.3 Wider applicability of the hierarchy scheme

Three literature studies of crevasse-splay deposits have been chosen: two from flashy ephemeral systems, the Huesca fan, Ebro Basin, and the Beaufort Formation, Karoo Basin (cf. van Torenenburg et al., 2016; Gulliford et al., 2017), and one from deltaic crevasse splays deposits of the Ravenscar Group, Cleveland Basin a (c.f Mjøs et al., 1993). In the Huesca fan, crevasse-splay deposits are far thinner (0.5- 0.6 m thick) and stack up to 2.35 m thick (van Toorenburg et al., 2016). However, the internal facies arrangements, the prevalence of Sr and Sl and the nature of bounding surfaces (sharp lower boundaries) are similar to what described this study. In the Beaufort Formation, crevasse-splay elements are larger than those in the Huesca fan, (averaging <2 m), they are still thinner than the average splay-elements in this study (<3 m thick). While the stacked splay deposits in the Beaufort Formation are 4 m thick and have a lateral extent of 700 m, which is comparable to the splay complexes in this study (Gulliford et al., 2017). The bounding surfaces are the same as in this study and the internal facies arrangements (Sr, Sh, Sm and Sl) are similar to the proximal-splay facies recognised in this paper (Fig. 5.6a) (Gulliford et al., 2017). Geometries of the splays in both this study and the Beaufort Group are similar: tabular with lateral thinning and fining trends distally (Gulliford et al., 2017).

Splay deposits of the Ravenscar Group are the most similar to the Neslen Formation, with individual splay deposits usually less than 1 m, but up to 2.5 m, in thickness, similar facies (Sr, Sl, Sm, Sp; cf. Fig. 5.6A), sharp basal boundaries (occasionally gradational) and upper boundaries generally sharp but sometimes gradational (Mjøs et al., 1993). In the Ravenscar Group, stacks of crevasse deposits were also identified, named either crevasse-subdelta lobe deposits or composite splay bodies, which are of a very similar thickness to splay complexes of this study (2.5 to 6 m), but with far greater lateral extent (up to 20 km) (Mjøs et al., 1993).

The bounding surfaces, the internal facies arrangements and the geometries of the elements and complexes from other studies are overall similar, but the scales are different. The terminology used by other studies also differs, Gulliford

et al., (2017) record bed scale and extents up to splay sets while van Toorenenburg et al., (2016) and Mjøs et al., (1993) use architectural elements based on facies and facies assemblages. Mjøs et al., (1993) and Gulliford et al. (2017) also have defined units comparable to complexes, but with different nomenclature, as the terms ‘composite splays’ and ‘splay stack’ are used respectively by each.

5.5.4 Subsurface implications

Proximal parts of complexes could make a good reservoir sandstone, particularly if they are connected to the major channel deposits. Since most splay-dominated successions are likely to split by fines, vertical connectivity is likely to be an issue (Fig. 5.7D, 5.9).

The different stacking styles of crevasse-splay elements within complexes could have different implications for a reservoir modelling. A progradational stacking style in plan-view could lead to an elongate shaped deposit with the proximal sand-prone parts connected (Fig. 5.10A). However, compensational stacking could lead to vertically connected proximal sand-prone parts in some parts of the complex, or disconnected proximal sand-prone parts depending on the depositional architecture (Fig. 5.10B). Lateral connectivity can be promising, particularly where splay deposits merge laterally. Splays can merge at both the longitudinal and lateral margins. Merging at the longitudinal margins (Fig. 5.10C) is unlikely to produce sand-on-sand contacts. Proximal sand-prone parts of splay-elements make up proportionally far less of a splay than the distal reaches (Burns et al., 2017), which means the proximal parts of crevasse-splay bodies are less likely to overlay one another or ever merge laterally, in addition to being more likely to be cannibalized by the lateral migration of the parent river (Fig. 5.10C). Conversely, lateral and vertical merging of splay margins along the lateral edge of the major channel could result in the proximal parts of the crevasse-splays becoming a sand-prone sheet this connectivity will act as a better reservoir than the more distal parts of splay elements (Fig. 5.10C). Splays could have the potential of increasing connectivity between larger sandbodies when the proximal parts of splay elements also connect (Fig. 5.10A). However in some circumstances the non-net reservoir that is the distal

portion of splay-elements can encapsulate the proximal parts of the splays in both plan-view (Fig. 5.10C) and vertically (Fig. 5.10B) resulting in a dead-end which would render a fluvial reservoir far more difficult to produce from.

The thinning and fining trends observed in both splay complexes and splay elements, however, could be used as an indicator of the position of major channel bodies, since these transitions occur within an average length of 500 m in the ancient splay elements and 670 m in the modern studies and an average length of 835 m in ancient complexes in this study.

How splay complexes interact with one another and where within the complex a 1D section is taken will have implications for subsurface predictions and subsequent petroleum models. Since a complex can be represented at any given geographic point as one single element this laterally could be equivalent to a thicker sand-prone complex or the single element could be equivalent only to the same single isolated splay-element. Criteria for recognising complexes in core would be difficult as many of the recognition criteria used are not applicable.

5.6 Conclusions

A set of recognition criteria for defining overbank elements and complexes is proposed, based on: bounding surfaces and adjacent deposits, facies arrangements including thinning and finings trends and external geometries. Key surfaces that represent the initiation and cessation of splay deposition can be recognised in overbank successions. The former tend to be sharp bases and the latter an abrupt stratigraphic change from sandstone facies (with a variety of sedimentary structures) or structureless siltstones to laminated rooted siltstone-dominated deposits.

Two-end member models of crevasse-splay stacking types have been defined: progradational and compensational stacking, which are associated with very different architectures. Whether one type or another is dominant within the crevasse complex will be a result of available floodplain accommodation space and its spatial distribution in relation to floodplain physiography. Crevasse-splay

deposits can amalgamate laterally to form wide sand-prone bodies, representing either elements or complexes, and might stack vertically in genetically related complexes. Lateral merging of crevasse splays is more likely than merging at the longitudinal edges. Vertical connectivity depends on the stacking of the sand-prone proximal parts of deposits, whether this be at element-scale or complex-scale.

The applicability of such hierarchy scheme depends on the data, in this case the outcrop data, used to inform the hierarchy scheme. There will always be exceptions to the schemes regardless of how broad the scheme is but the key recognition criteria based on that of Miall's will always have value. Previous studies on crevasse-splay deposits in the Ravenscar Group, Huesca fan and Beaufort Formation have been chosen to illustrate the differences in such deposits under different climatic regimes and environmental settings. Although the scales of the deposits vary, each example still displays similarities with respect to bounding surfaces, facies assemblages and geometries described in the hierarchy scheme introduce here. This suggests that the recognition criteria proposed herein might be applicable to other systems. This could aid in interpretation of fluvial overbank successions in subsurface settings.

Chapter 6 Controls on fluvial overbank sedimentation in the humid Cretaceous Neslen Formation and semi-arid Jurassic Morrison Formation

This chapter looks at how allogenic controls, particularly climate, and autogenic controls, particularly floodplain conditions, influence the accumulation of sediment in fluvial overbank settings. Elements common to all the formations studied (Jurassic Morrison Formation and Cretaceous Neslen Formation) are defined and then compared. Facies type, thicknesses, lengths, widths, geometries and presence of bioturbation and rooting are all compared. The stratigraphic organisation and architecture of these elements are then demonstrated from five successions, three from the Morrison Formation and two from the Neslen Formation. These data are then compared to similar case studies from the literature using the FAKTS (Fluvial and Architectural Knowledge Transfer System) database.

Models for the overbank stratigraphy found in the different parts of the two formations are then proposed and two formation scale models to demonstrate the differences in architecture both within each formation and between the two formations.

6.1 Introduction

Allogenic and autogenic controls on fluvial sedimentary environments have important implications for how the stratigraphic architecture of fluvial successions develops, accumulates and become preserved. Many studies have considered the role of such controls on fluvial stratigraphy (e.g. Shanley and McCabe, 1994; Holbrook et al., 2006; van Dijk et al., 2009) but relatively few studies have focussed on the balance of extrinsic, particularly climate, and intrinsic controls on fluvial overbank successions generally and crevasse-splay deposits in particular (Stuart et al., 2014; van Toorenburg et al. 2016).

Studies focussed on fluvial successions have demonstrated a complex interplay of allogenic controls and autogenic processes (e.g. Shiers et al., 2014).

Allogenic controls including climate, uplift and subsidence, and changes in eustatic sea-level have been long known to influence sedimentary architectures in fluvial successions (Shanley and McCabe, 1994; Jerolmack and Paola, 2010; Abels et al., 2013). Climate is an important control in fluvial systems, particularly in upstream areas (Blum, 2000; Shanley and McCabe, 1994). For example, climate controls the discharge, for example through precipitation rates and physical and chemical weathering rates (Holbrook et al., 2006; Cecil, 2003), and consequently exerts a major influence on the sediment supply to a system (Stuart, 2015). Seasonality is also a control on sediment supply; if a system is temperate but with seasonal variations, sediment yields will be greater particuluary at high discharge seasons (Miall, 2014; Gugliotta et al., 2016). In floodplain settings variations between wetter and drier periods can influence floodplain development (Fielding, 1986; Benedetti, 2003). Mature, red palaeosols are an indicator of relatively, dry, climatically stable floodplain conditions (Abels et al., 2013), whereas coals are commonly associated with humid conditions that high amounts of vegetation (Miall, 2014).

Autogenic controls, such as avulsion and local floodplain accommodation and aggradation, have been shown to impact sedimentary successions (Stouthamer and Berendsen, 2001; Straub and Wang, 2013; Hajek et al., 2014). Avulsion is the abrupt movement of a channel from one position to another position on the floodplain (Mohrig et al., 2000; Slingerland and Smith, 2004); it is considered to be one of the major processes that supplies coarser grained deposits to the overbank (Miall, 2014). Local floodplain accommodation will determine the amount of available space for overbank sedimentation (Chapter 2) and can be in turn effected by the occurrence of peats and coal, which have a much greater compaction rate than other sediment types (Nadon, 1998; van Asselen, 2010).

This study seeks to understand how allogenic controls, in particular climate, and autogenic controls, such as local floodplain accommodation, can influence the preserved stratigraphic architecture of fluvial overbank successions. A series of specific research objectives are used to fulfil this aim: (i) definition of a series of architectural elements common to the two formations studied, the Morrison Formation and the Neslen Formation, so as to demonstrate how each of these

elements vary between the two formations. Variations in scale, lithofacies, geometries, bioturbation and rooting indices and presence and types of palaeosols are all presented; (ii) to show examples of how these different elements stack together in different intervals of the Morrison and Neslen Formations so as to develop accumulated succession. The architecture of which can be used to characterize sub-environment models for the different parts of each formation; (iii) to present data relative to other successions, from the FAKTS database (Colombera et al. 2013), which have comparable controls such as climate type, depositional settings and discharge and flow regime to the Morrison or Neslen formations and investigate variations of overbank elements in these datasets; (iv) to develop overall models of deposition for the overbank deposits present in the Morrison and Neslen Formation and (v) to use these models to discuss the range of important controls that can influence such successions.

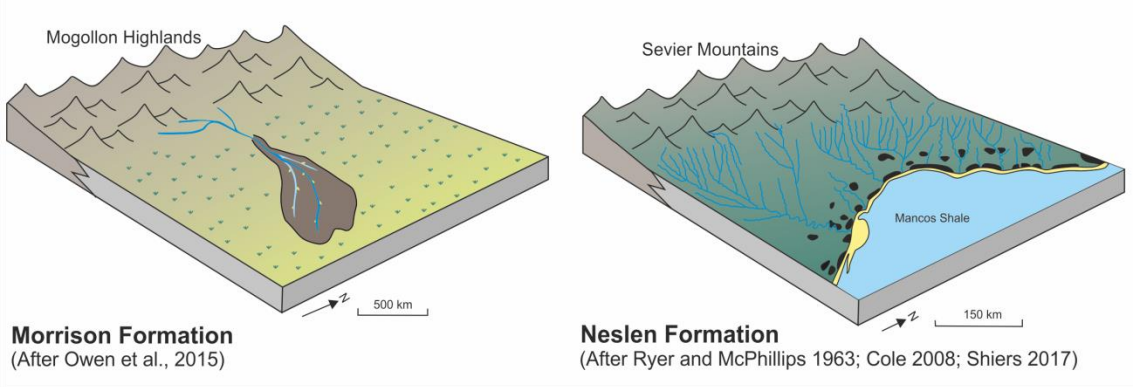

Figure 6.1: Overall palaeogeographic conceptual models of the environment of deposition of the Morrison Formation (based on Owen et al., 2015) and the Neslen Formation after Cole (2008)and Shiers (2017).

6.2 Background

In this study, the Jurassic Saltwash Member of the Morrison Formation and the Cretaceous Neslen Formation were chosen for study partially because both were deposited across the Western Interior of North America (Turner and

Peterson, 2004; Owen et al., 2015) during periods of increased tectonism (Currie, 1998). In addition, both formations have been placed within a generalized stratigraphic and palaeogeographic context by previous workers (e.g. Owen et al., 2015; Shiers et al., 2017). Although deposited within the same basin, there are many variations in the controls for each formation, each of which will be introduced in the following section (Fig. 6.2).

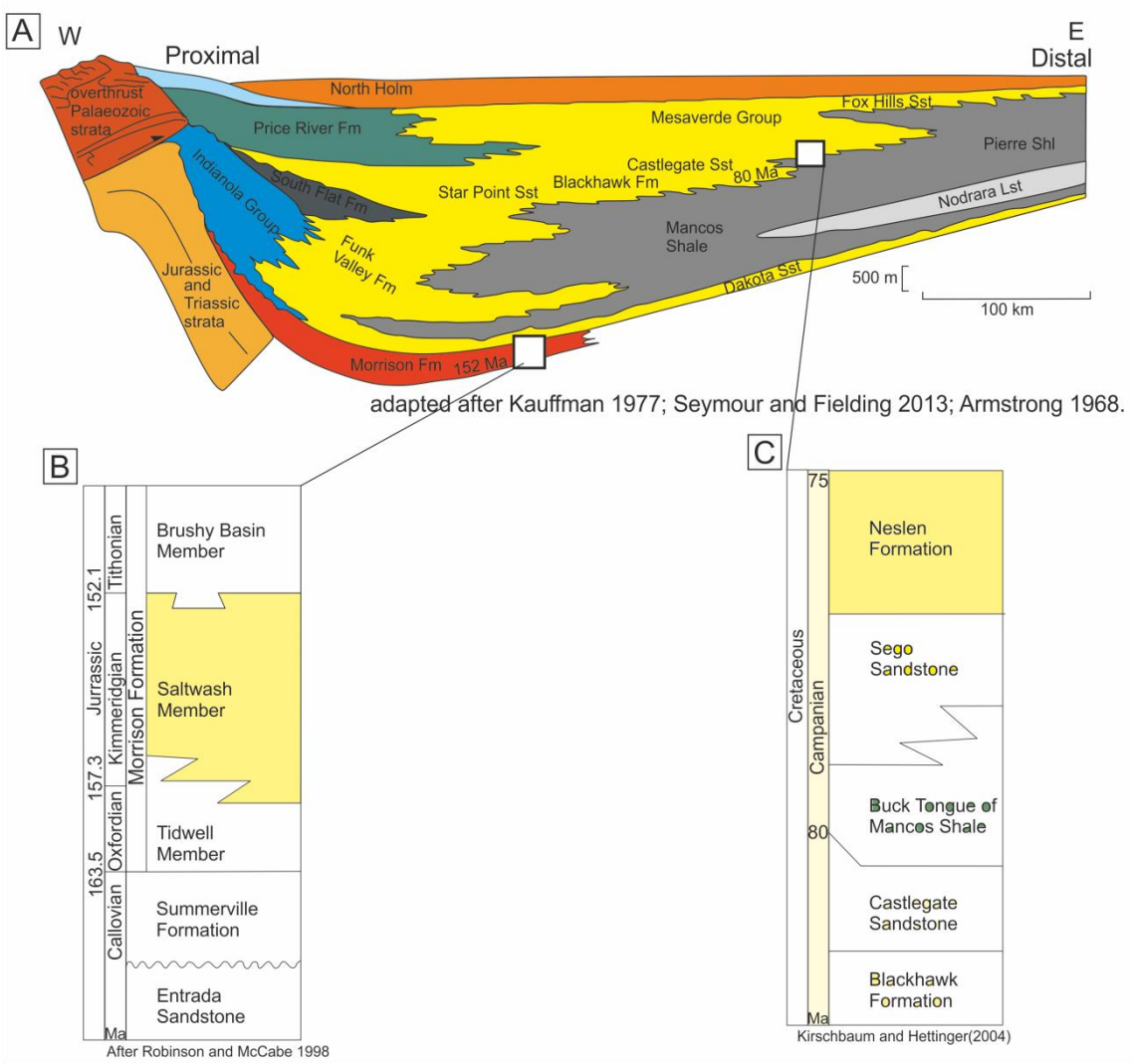

Figure 6.2: (A) Foreland basin in which Morrison and Neslen Formations were deposited within; (B) Stratigraphic column highlighting Saltwash Member of the Morrison Formation;(C)Stratigraphic column highlighting Neslen Formation.

Climate during deposition of the Morrison Formation was overall semi-arid (Demko et al., 2004; Owen et al., 2015), with some variations. Long-term intervals that were wetter (lower middle Salt Wash Member) and long-term intervals that were drier (upper Saltwash deposition) contain smaller-scale seasonal variations (Hasiotis, 2004; Owen et al., 2015). The seasonal variations in climate during deposition of the Morrison Formation likely resulted in a flashy discharge regime (Owen et al., 2015). The semi-arid climate as opposed to humid climate resulted in palaeosol deposits associated with drier settings (Demko et al., 2004).

By contrast the Neslen Formation was deposited under a long-term wet-humid climate (Huber et al., 2002). This in conjunction with the known monsoonal conditions during the Campanian (Fricke et al., 2010) resulted in larger-scale-precipitation events that had corresponding large-scale flooding events (Miller et al., 2013). The climatic regimes in the Neslen Formation favoured accumulation of extensive coals (e.g. Shiers et al., 2017).

Large-scale tectonic context for both formations was similar with deposition across the Western interior seaway either are thought to be deposited within the same foreland basin, if the North American Cordilleran foreland basin has begun to develop in earnest at during the Late Jurassic (Decelles and Burden, 1991; Decelles and Currie, 1996; Currie, 1997, 1998), or the Morrison was deposited in the precursor to that foreland basin (Heller et al., 1986; Lawton, 1994; Decelles et al., 1995). However, basin subsidence rates during deposition of the Morrison Formation were particularly low (6.2m/Myr-22m/Myr) (Hartley et al., 2015), whereas basin subsidence rates at the time of Mesaverde Group in general were far greater than in the Morrison Formation (cf. underlying Blackhawk Formation 80- 700m/Myr) (Hampson, 2016). However, accommodation space generation rate during deposition of the Neslen Formation slowed during deposition (Shiers, 2017).

Both the Morrison and Neslen formations have channel bodies that have been interpreted as being the product of meandering channel-belt styles. The Saltwash Member of the Morrison Formation has been interpreted as an amalgamated meandering channel-belt (Hartley et al., 2015). However, some

parts have been interpreted as being the product of braided channels, particularly in coarsest grain-size deposits (Craig et al., 1955). The Saltwash Member of the Morrison Formation has also been identified as forming a distributive fluvial system (Owen et al., 2015), terminating without marine influences (Anderson and Lucas, 1997; Demko et al., 2004). The different zones of the DFS will have characteristic differences in stratigraphic architectures found throughout the formation (Owen et al., 2015).

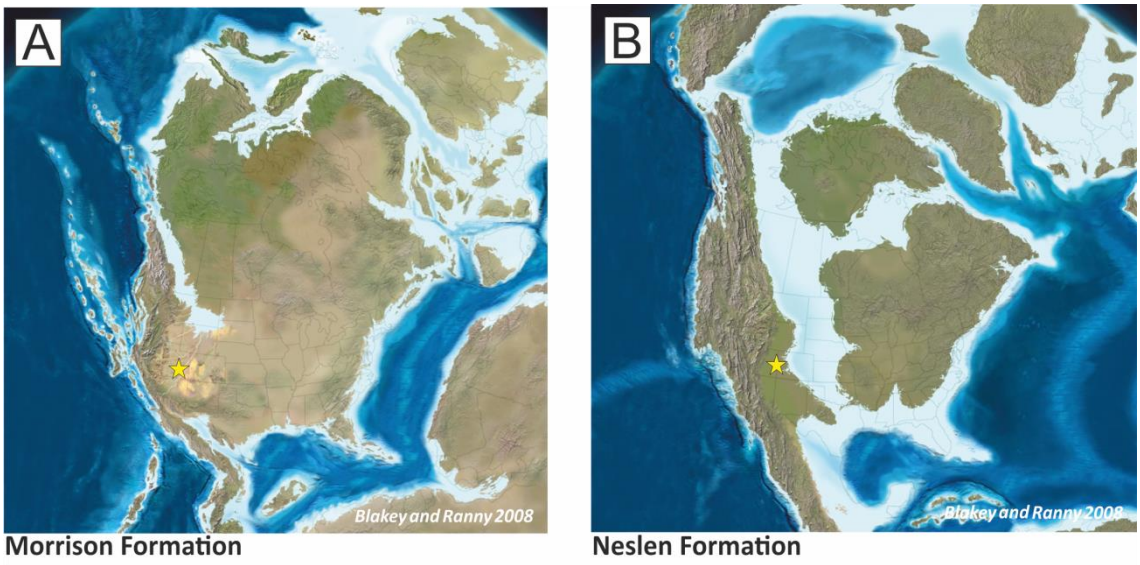

Figure 6.3: Palaeogeographic maps of Western Interior Basin at time of Morrison Formation (A) and Neslen Formation (B) deposition, after Blakey and Ranny (2008).

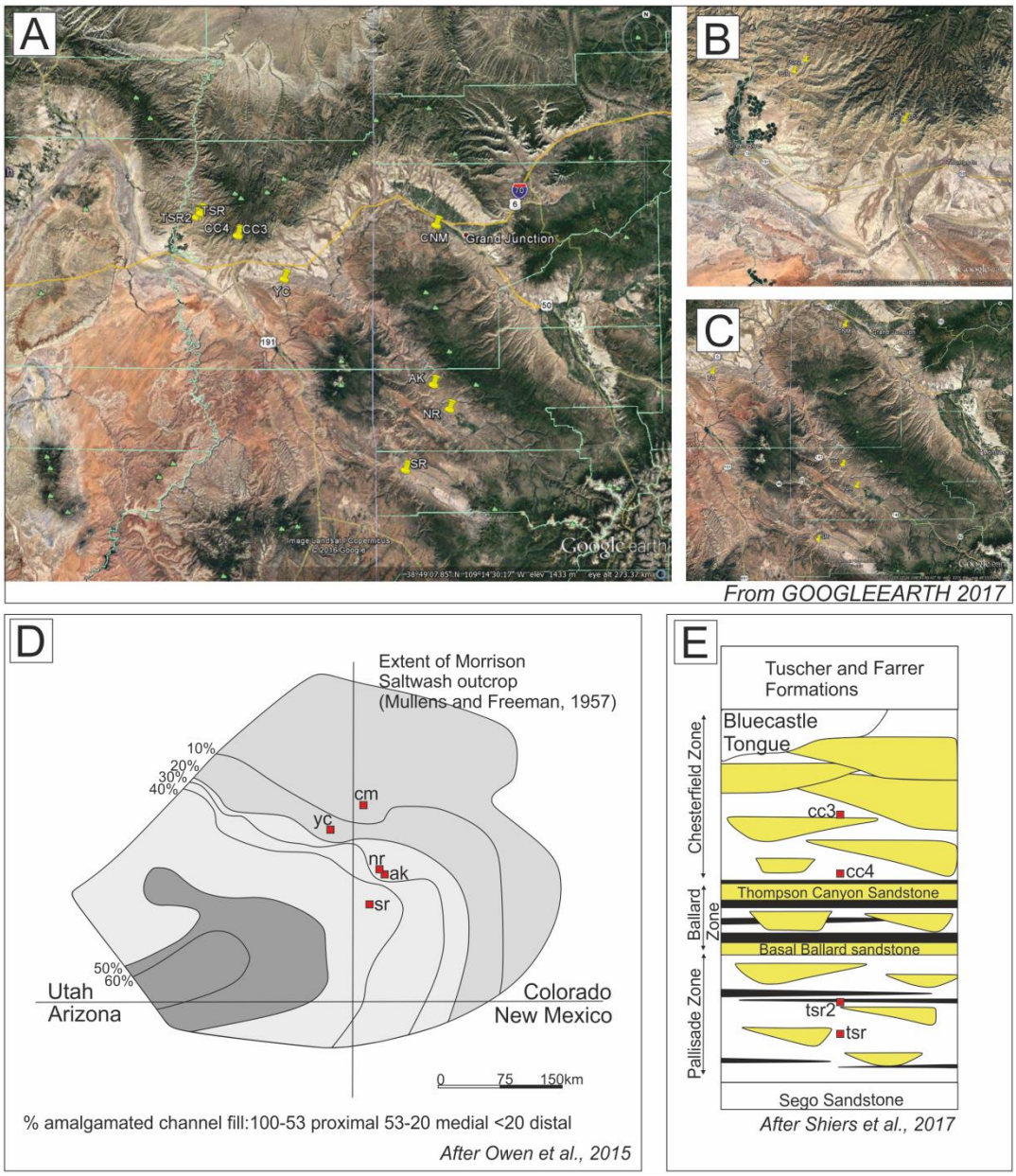

Figure 6.4: (A) Map of Western Colorado and Eastern Utah, with each site investigated marked as yellow pins, image from *GoogleEarth* ; (B) Close-up view of all sites studied in Book cliffs, image from *GoogleEarth;* (C) Close-up view of all sites studies across Western Colorado, image from *GoogleEarth; (*D)Extent of Morrison Saltwash distributive fluvial system and extent of proximal, medial and distal parts of this system, after Mullens and Freeman, 1957 and after Owen et al., 2015; (E) Stratigraphic variations in the Neslen Formation, showing differences between the Palisade, Ballard and Chesterfield zones within the Neslen, after Shiers et al., 2017.

The portion of the Neslen Formation studied is classified as being deposited in a coastal-plain setting to an alluvial-plain setting ;because of the relative position of the tide-influenced coastline, because of this unlike the Morrison Formation it is subject to various levels of tidal influence as it terminated at the Western Interior Seaway (Shiers, 2017). The level to which marine process influenced the Neslen Formation depends on stratigraphic and geographic position within the formation. In the lower part of the Neslen Formation, and the down-dip part there are more signs of tidal influence than the upper portions (Fig. 6.3) (Shiers et al., 2014).

Since the Morrison Formation, specifically the Saltwash Member, has been defined as a distributive fluvial system (Owen et al., 2015), parts of the formation have been described in published works as described as proximal (100%-53%) medial (53%-20%) or distal (<20%); depending on percentages of amalgamated fluvial channel and floodplain deposits (Owen et al., 2015). The proximal regions have less overbank deposits (0%-40%), that the medial (40%-70%) and distal (>70%) parts. Amalgamated channel deposits are not seen towards the distal parts of the DFS, where instead ribbon channel bodies dominate (Fig. 6.4D) (Owen et al., 2015).

The Neslen Formation can be broadly split into three zones: the Palisade Zone, the Ballard Zone and the Chesterfield Zone (Fig. 6.4E) (Shiers et al., 2014, 2017). The base of the Palisade Zone is defined from a marker bed that contains oysters that occurs at the top of the Sego Sandstone (Willis, 2000; Hettinger and Kirschbaum, 2003; Shiers et al., 2014). Typically, the overlying Ballard zone is dominated by coal-prone floodplain elements and is bounded at its base by the Basal Ballard Sandstone, a tabular marker sandstone, and topped by the Thompson Canyon Sandstone bed another tabular marker sandstone. Both markers are laterally extensive across the studied part of the Neslen Formation (Shiers et al., 2014, 2017). The top of the Thompson Canyon Sandstone Bed bounds the base of the Chesterfield zone the uppermost zone of the Neslen Formation. Within this zone, a lower part is dominated by channelized elements encapsulated by coal-prone floodplain elements, whereas an upper part displays less coal-prone floodplain elements and

increased abundance of splay elements and crevasse-channel elements (Shiers et al., 2014).

6.3 Data and Methods

Measured sections were collected from four Cretaceous Neslen Formation sites and five Jurassic Morrison Formation sites. In total, 40 logs from the Nelsen Formation and 42 logs from the Morrison Formation were measured. The logs record lithology, grain size, sedimentary structures, occurrence of fossils and palaeosols. Thirty-two architectural panels and accompanying photomosaics were constructed by tracing units across each section; eighteen from the Neslen Formation and fourteen from the Morrison Formation. These were used to record the organisation and geometries of splay elements. In total, 1700 palaeocurrents were measured, 800 from the Neslen Formation and 900 from the Morrison Formation (Figs. 6.11, 6.12, 6.13, 6.14, 6.15). These were recorded from cross-bedding foresets, ripple cross-lamination, ripple-forms on bedding surfaces and low-angle-inclined accretion surfaces. This permits lengths, widths and thicknesses of the preserved crevasse-splay elements and their facies belts to be determined (Fig. 6.4D). Strike sections are defined as 0-30 degrees from the outcrop orientation, oblique as 30-60 degrees from outcrop orientation and dip sections as 60-90 degrees from outcrop orientation. Full lengths and widths of splay deposits are calculated from partial exposures using thinning rates within the window of outcrop of observation.

Additional data and case studies were used to supplement the outcrop data. Data from the Fluvial Architecture and Knowledge Transfer database (FAKTS), a database with an extensive catalogue of case studies from the scientific literature and fieldwork at the University of Leeds (Colombera et al., 2012, 2013), was utilised. Datasets of element thickness, dimensions, lithofacies types and proportions were used for overbank element types defined from six system types: humid settings, semi-arid settings, ephemeral flow settings, perennial flow settings, coastal-alluvial plain settings and fluvial fan settings. The addition of these data augments field-acquired data and, importantly, also

provides an opportunity to assess the possible controls on stratigraphic architecture against a larger literature–derived dataset.

6.4 Results

Fifteen lithofacies (Fig. 6.5, table 1) are defined for both formations. Five are specific to the Morrison Formation and three to the Neslen Formation. Architectural elements are defined (Fig. 6.6) based on (Miall, 1985) and (Colombera et al., 2013). Five element types are recognised in the fluvial overbank successions in the Morrison and Neslen formations: crevasse-splay elements (CS), crevasse-channel elements (CR), abandoned channel elements (AC), floodplain elements (FF) and sub-type of this element coal-prone floodplain elements (C) (Fig. 6.6). Associated aggradational channel-fills are also described (CH). The elements identified are based on their sedimentary textures, facies associations, bounding surfaces, external geometries, palaeocurrent indicators and lateral and vertical arrangement of lithofacies (see Chapter 5).

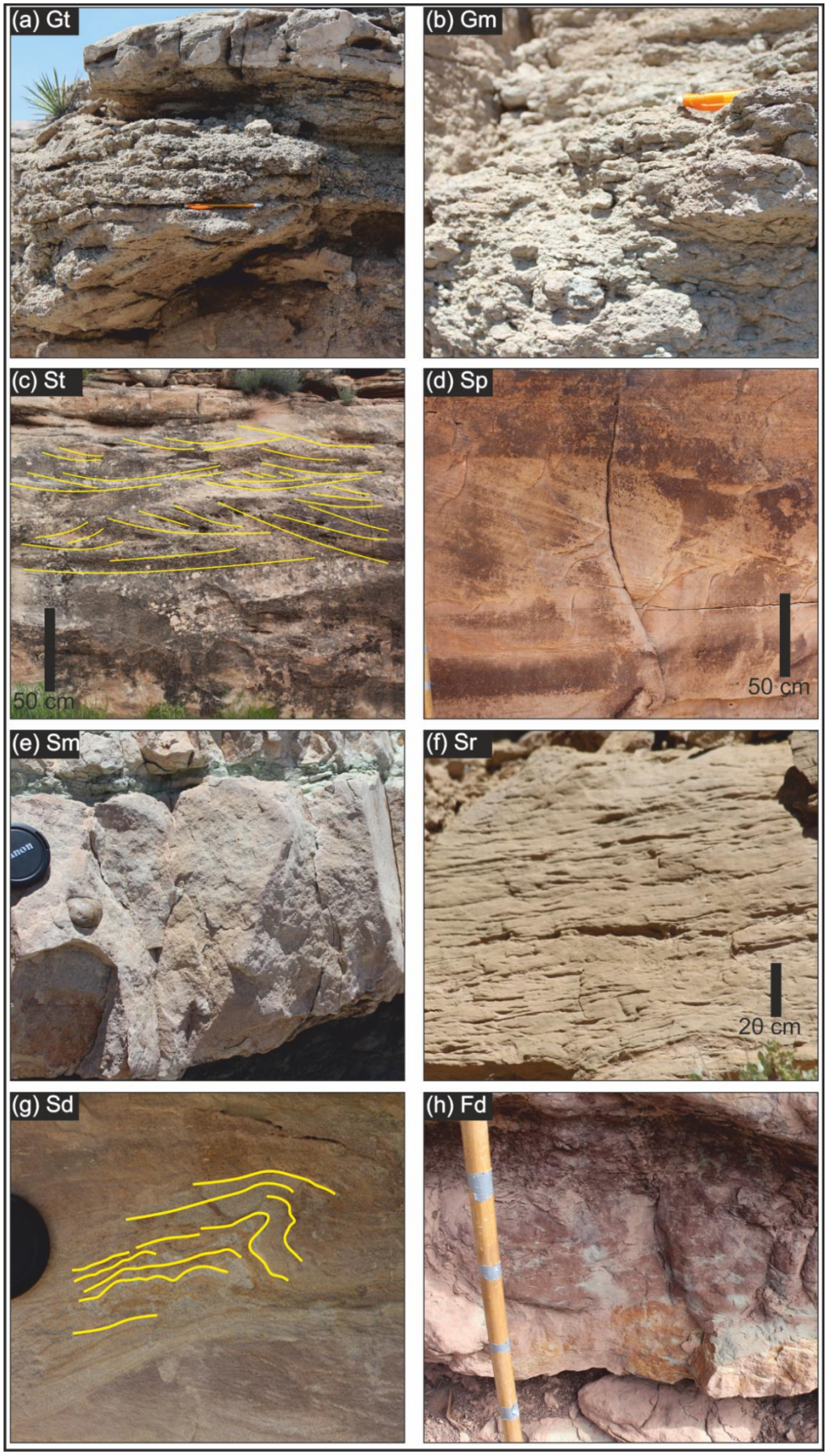
(a) Gt
(b) Gm
(c) St
50 cm
(d) Sp
50 cm
(e) Sm
(f) Sr
20 cm
(g) Sd
(h) Fd

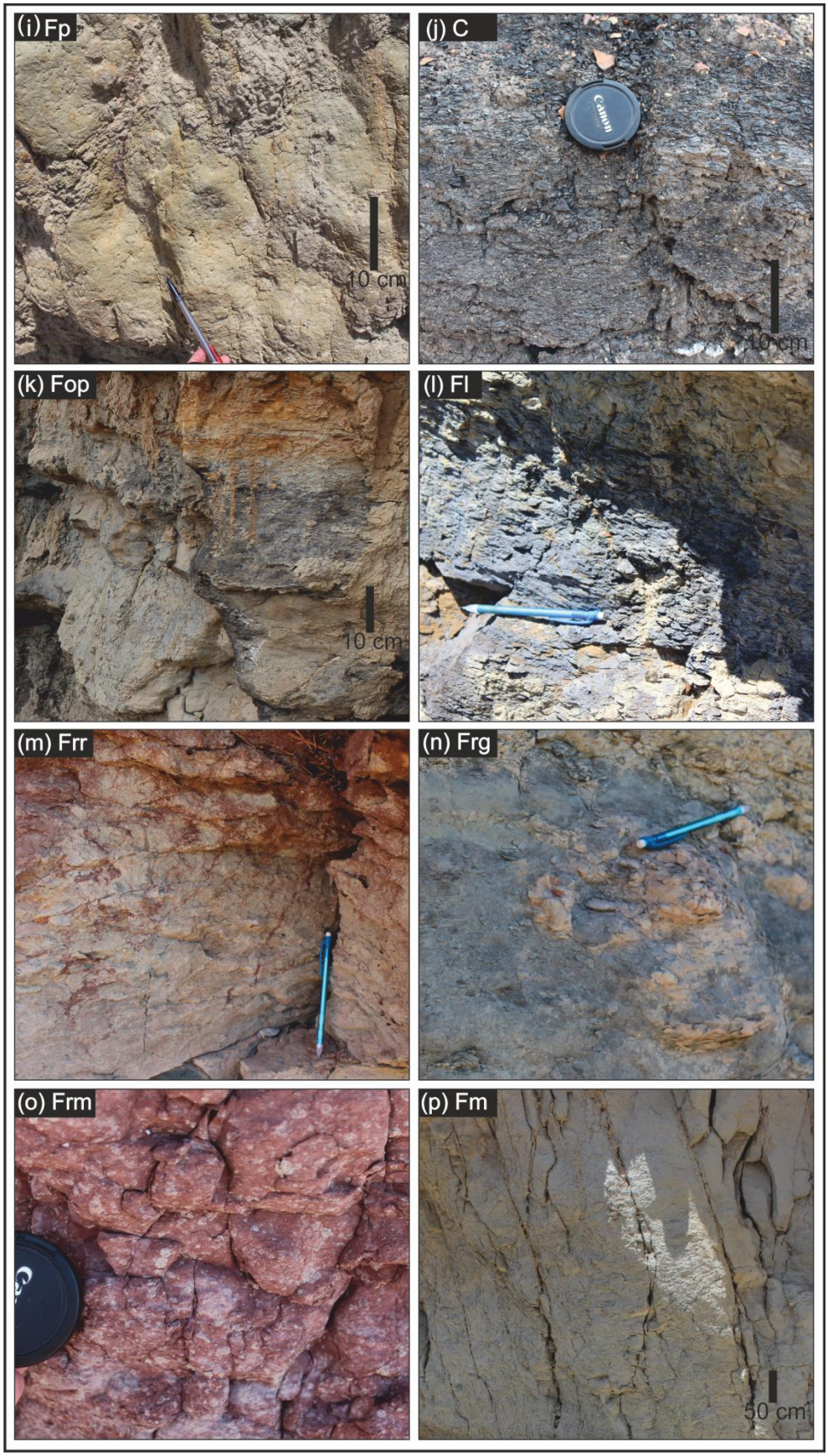
(i) Fp
10 cm
(j) C
10 cm
(k) Fop
10 cm
(l) Fl
(m) Frr
(n) Frg
(o) Frm
(p) Fm
50 cm

Figure 6.5: Representative photographs of lithofacies. Lens cap is 5 cm in diameter. (A) Cross-stratified conglomerate, Gp. (B) Green structureless conglomerate, Gm (C) Trough cross-bedded sandstone, St (D) Planar cross-bedded sandstone, Sp (E) Structureless sandstone, Sm (F) Small-scale ripple cross-laminated sandstone, Sr (G) Soft-sediment deformed sandstone with remnant ripple forms, Sd (H) Soft-sediment deformed mixed sandstone and siltstones. Fd (I) Structureless poorly sorted rooted siltstones, Fp (J) Coal, C (K) Structureless organic-rich poorly sorted rooted siltstones, Fop (L) Laminated organic –rich siltstones, Fl (M) Red rooted siltstones, Frr (N) Green rooted siltstones, Frg (O) Purple mottled rotted siltstones, Frm (P) Well-sorted structureless siltstones, Fm.

Table 1. Facies found in Morrison and Neslen Formations.

Code	Facies	Description	Interpretation
Gm	Green structureless conglomerate	Green, subangular pebble to conglomerate, poor to moderately sorted with very-fine to fine sandstone matrix. Sets 0.8- 2.4 m (1.7 m average). Sets are structureless, with occasional weak fining-upwards trend.	Deposition from a relatively high-rapidly, bedload
Gp	Cross-stratified conglomerate	Green-grey, subangular pebble to conglomerate, poor to moderately sorted in a very-fine to fine sandstone matrix. Individual sets 1.0- 2.3 m (1.5 m average).Planar cross-bedding common (0.8 -2.4 m).	Deposition from a relatively high-energy flow and downstream migration of gravel bar forms
St/Sp	Trough and planar cross-bedded sandstone	Grey-yellow-brown very-fine- to medium-grained sandstone, moderately well sorted. Subangular to subrounded grains. Sets are 3- 12 m (4.6 m average) thick. Mud rip-up clasts and plant fragments are common. Trough and planar cross-stratification throughout sets are 0.4- 1.5 m (1.0 m).	Deposition from a relatively high-energy flow and downstream migration of sandy bar forms
Sm	Structureless sandstone	Dark grey-yellow-brown, very fine to fine sandstone, moderately to poorly sorted. Thickness ranges 0.2- 2.2 m (1 m average). Internally sets are structureless.	Records rapid deposition of sand predominantly from suspension in a decelerating flow
Sr	Small-scale ripple cross laminated sandstone	Grey-yellow-brown, very fine to fine sandstone, moderately to poorly sorted. Sets varying from 0.1m- 4.1 m (1 m average). Small-scale ripple- cross lamination (0.1- 0.9 m) are common to this facies, contains small (<50 mm long) plant fragments, bark pieces and coal fragments.	Down flow migration of ripple bedforms under an aggradational regime
Sd	Soft-sediment deformed sandstone with remnant ripple forms	Grey-yellow-brown, very fine to fine sandstone, poorly to moderately sorted. Sets vary from 0.4- 2.4 m (1.1 m average). Convolute lamination within sets and load and flame structures at base bed boundaries, remnant ripples.	Records deposition from a mixed sand and silt containing flow onto an unstable waterlogged substrate

Table 1(Continued)

Code	Facies	Description	Interpretation
Fd	Soft-sediment deformed mixed sandstone and siltstones	Dark grey-yellow-brown, fine siltstone to very fine sandstone, poorly sorted. Thicknesses vary from 0.1 m- 3 m (0.6 m average). Within 1 m of the base of sets, primary sedimentary structures are overprinted by soft-sediment deformation structures such as loading and convolute lam.	Records deposition from a mixed small grain size containing flow onto an unstable waterlogged substrate
Fp	Structureless poorly sorted rooted siltstones	Light-blue grey or red or green, fine siltstone to very-fine sandstone, poorly sorted. Set thicknesses varies from 0.1 to 2.1 m (mean is 0.6m). Sets of this facies are mostly structureless through some show weak fining-up trends. In situ roots and some carbonised anthracite material.	Poorly sorted and structureless silt-prone facies was deposited rapidly from suspended load
Fop	Structureless organic-rich poorly sorted rooted siltstones	Dark grey, fine siltstone to very fine sandstone, poorly sorted. Set thickness vary 0.3- 2.1 m (0.8 m average). Sets mainly structureless with weak fining upwards trend. Dispersed organic content common as are in situ roots.	Poorly sorted and structureless silt-prone facies was deposited rapidly from suspended load
Fm	Well sorted, blue, clean siltstones	Light blue, middle to coarse siltstone, well to moderately sorted, rare occurrence of roots or plant material. Bases are erosional 1- 2 m. Set thickness 0.4- 2.4 m (1.4 m average). Structureless or weakly laminated.	Erosive bed bases represents erosive flow, siltstones represent deposition from low energy flow after erosive event
Fl	Laminated organic rich siltstones	Medium to dark grey, red, green siltstones well to moderately sorted, bed thicknesses vary from 0.3m- 1.1m (0.7 m average) grain remains consistent throughout a bed. Planar laminations are common. Small plant roots (<10 mm) occur in the Morrison Fm and thin wisps of anthracite coals in the Neslen Fm.	Steady deposition from low energy flow.
C	Coal	Dark-grey to black clay sized particles ,well sorted, sets vary from 0.2- 2.1 m (0.7 m average). Plant fragments and higher quality anthracite coal fragments present.	Records slow deposition, organic rich setting with limited clastic input

Table 1(Continued)

Code	Facies	Description	Interpretation
Fr	Laminated rooted siltstones	Blue grey to light grey, upper to lower silt moderately well sorted, set thicknessness vary from 0.2m- 0.9 m (0.4 m average). Can be weakly laminated.	Well drained, gradual deposition under low energy regime
Frg	Green rooted siltstones	Green-grey, fine siltstones, well-moderately sorted. Set thicknessness vary from 0.1m- 2.7 m (0.6 m average), can be weakly laminated. Plant root structures common (<5 mm width and lengths) but tend to be concentrated towards the top of sets.	Poorly drained, high water table, gradual deposition under low energy regime.
Frr	Red rooted siltstones	Red, fine siltones to coarse siltstones. Well-moderatley sorted. Set thickness varies 0.1- 2.7 m (0.6 m average). Can be weakly laminated, plant root structures common, sideritized, taper towards base. Roots tend to be long(up to 10 cm) and thin (<5 mm). Low to moderate intensity bioturbation and slickenlines present.	Well drained, dry, calcisols, gradual deposition under low energy regime.
Frm	Purple mottled rooted siltstones	Purple red, fine to coarse siltstones, well to moderately sorted Sets vary from 0.3 — 3.6 m (1.8 m). Structureless. Small roots throughout (< 5 mm scale), moderate to high intensity bioturbation. Mottled pale purple colouring from watermarks.	Poorly drained, higher water table, gradual deposition under low energy regime.

Table 6.1: Lithofacies present in Morrison and Neslen Formations.

6.4.1 Comparisons of elements found in Morrison and Neslen Formations

Crevasse-splay elements

Splay elements are defined as wedge-like sandstone and siltstone bodies with spatially constrained thinning and fining trends distally, sharp and occasionally erosive bed bases and sharp defined tops (Chapter 5). These can then be sub-divided into a series of three sub-elements: proximal, medial and distal parts of the crevasse-splay, which allows for the distinctive lateral facies variations of the crevasse-splay element to be taken into account when comparing different splay elements (Chapter 4).

Crevasse-splay elements in the Morrison and Neslen formations are made up of a series of different facies types some of which are common, to both formations: Sm, Sr, Fd and Fp (Fig. 6.7). Facies Sm occurs in similar amounts in the proximal parts of splay elements in both the Morrison (56%) and Neslen (55%) Formations and occurs in smaller proportions in medial portions of splay elements 1% and 7% in the Morrison and Neslen, respectively (Fig. 6.7). Facies Sr occurs in similar amounts in Morrison and Neslen proximal parts of splay-elements, 34% and 39% respectively and medial parts of splay-elements 4% and 5% respectively (Fig. 6.7). Facies Fd makes up a greater proportion of medial parts of splay elements in the Morrison Formation (80%) than in the Neslen Formation (44%); facies Fd also occurs in greater amounts in the distal parts of splay elements of the Morrison formation 25% compared to 7% in the Neslen Formation (Fig. 6.7). There are two facies types that occur only in splay elements in the Neslen Formation. Facies Sd occurs only in the medial portions of crevasse-splay elements in the Neslen Formation, and it makes up 19% of the facies found in these deposits. Facies Fop also only occurs in the Neslen Formation crevasse-splay elements, it occurs in small proportions in medial parts of splay elements (6%) but a greater proportion of distal parts of splay elements (28%) (Fig. 6.7).

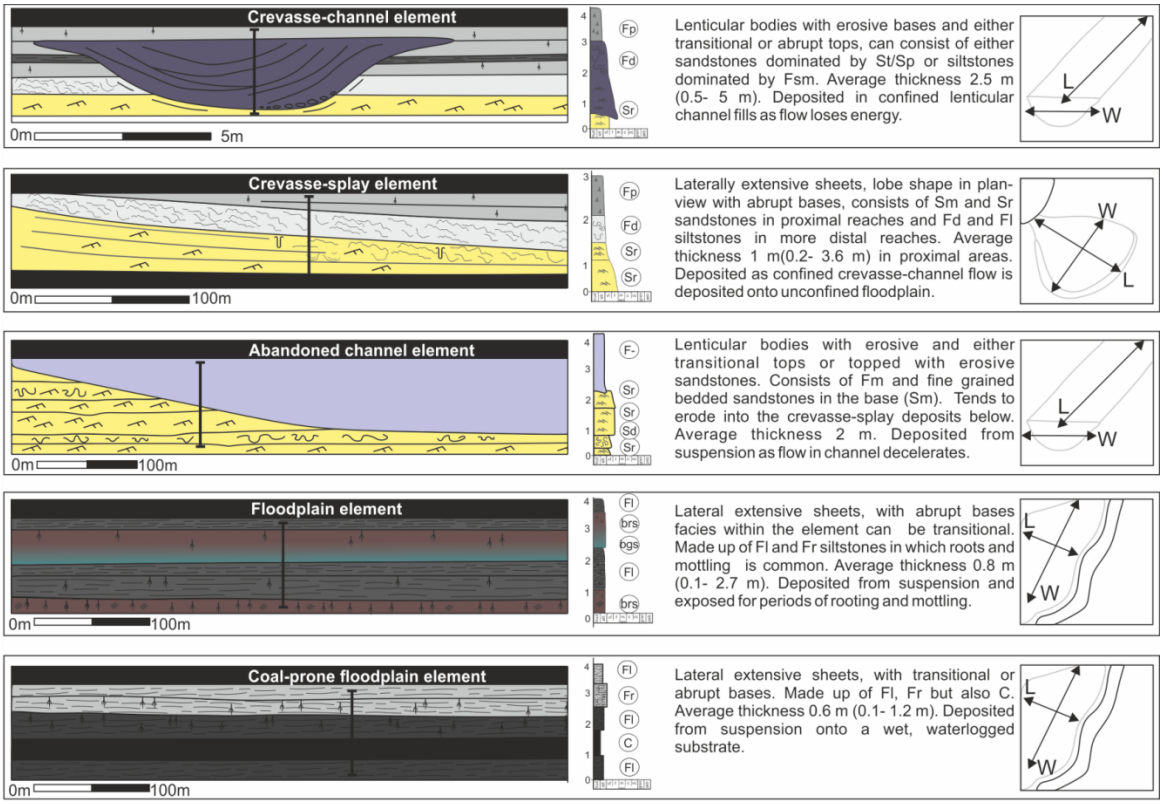

Figure 6.6: Five architectural element types are defined: crevasse-channel, crevasse-splay, abandoned channel, floodplain and coal-prone floodplain elements. The elements identified are based on their sedimentary textures, bounding surfaces, geometries, palaeocurrent indicators and lateral and vertical arrangement of lithofacies. Thicknesses displayed are based on of between the two formations, Morrison and Neslen.

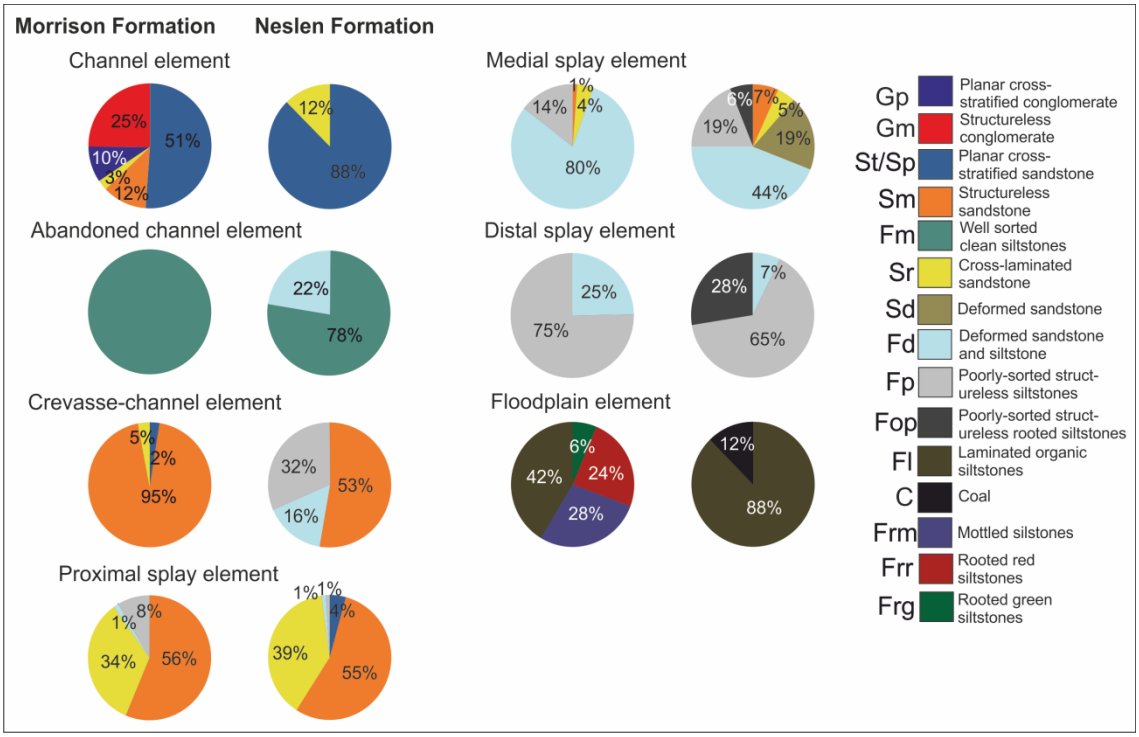

Figure 6.7: Facies types and proportions within overbank elements in the Morrison Formation and Neslen Formations.

Crevasse-splay elements in the Morrison and Neslen formations vary in thicknesses and lateral extents (widths and thicknesses) between the formations. Generally, the thickness of the proximal, medial and distal parts of crevasse-splay elements in the Neslen Formation is greater than those in the Morrison Formation (Fig. 6.8A). Splay deposits have an average of 0.9 m (0.2-2.1 m, n=47) in the proximal reaches, 0.8 m (0.2- 2.9 m, n=60) in the medial reaches and 0.7 m (0.1-1.6 m, n=34) in the distal reaches in the Morrison Formation, compared to an average of 1.4 m (0.5- 3.6 m, n=25) in the proximal reaches, 1.1 m (0.5- 2.9 m, n=32) in the medial reaches and 0.9 m (0.3-2.3 m, n=46) in the distal reaches of elements in the Neslen Formation (Fig. 6.8). Both lengths and widths of crevasse-splay elements from the Morrison Formation are lower than those measured from the Neslen

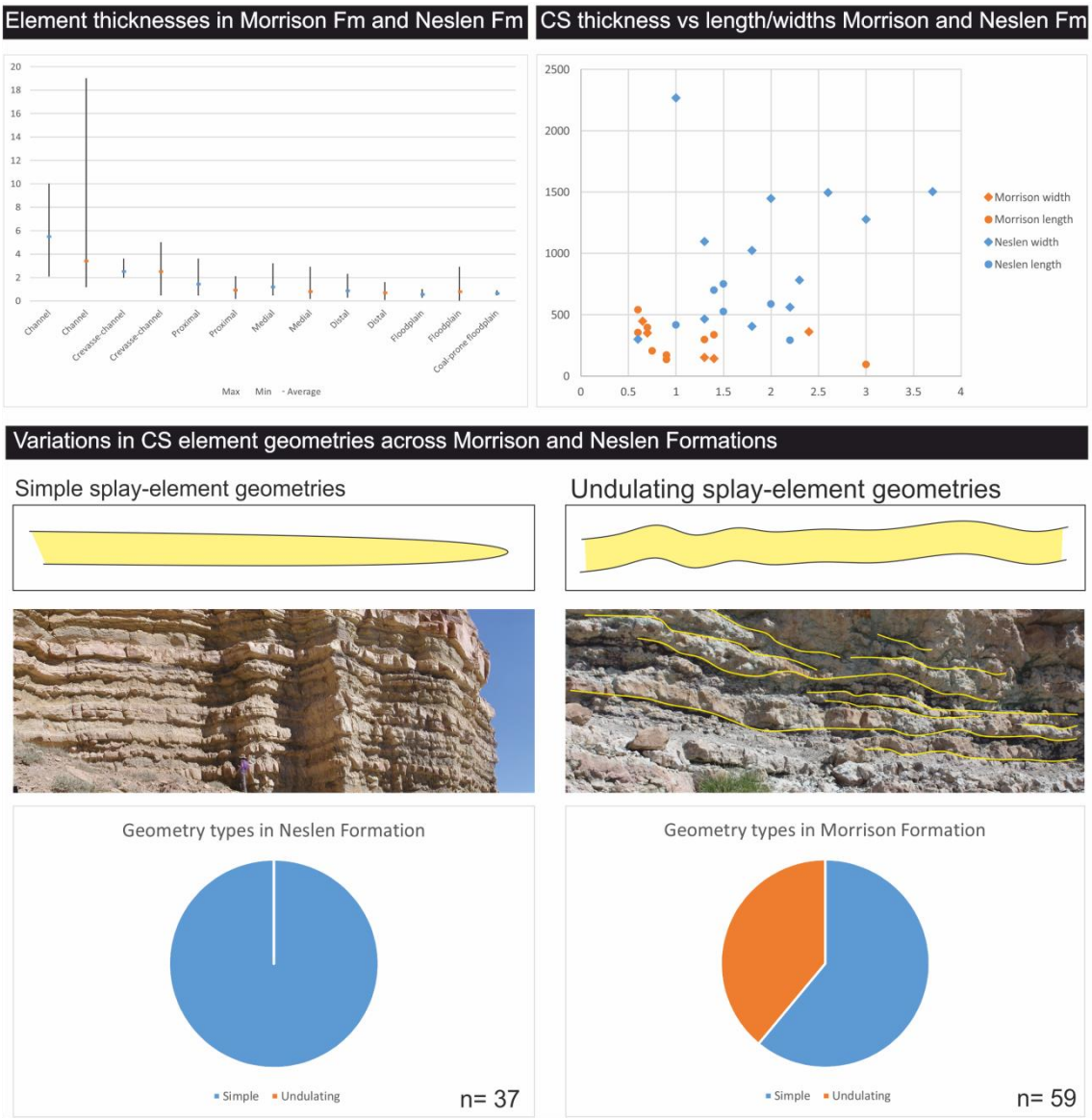

Figure 6.8: Element thickness variations in the Morrison and Neslen Formation; Crevasse-splay element thickness plotted against length and widths in Morrison and Neslen Formation; Variations in crevasse-splay element geometries across Morrison and Neslen Formations.

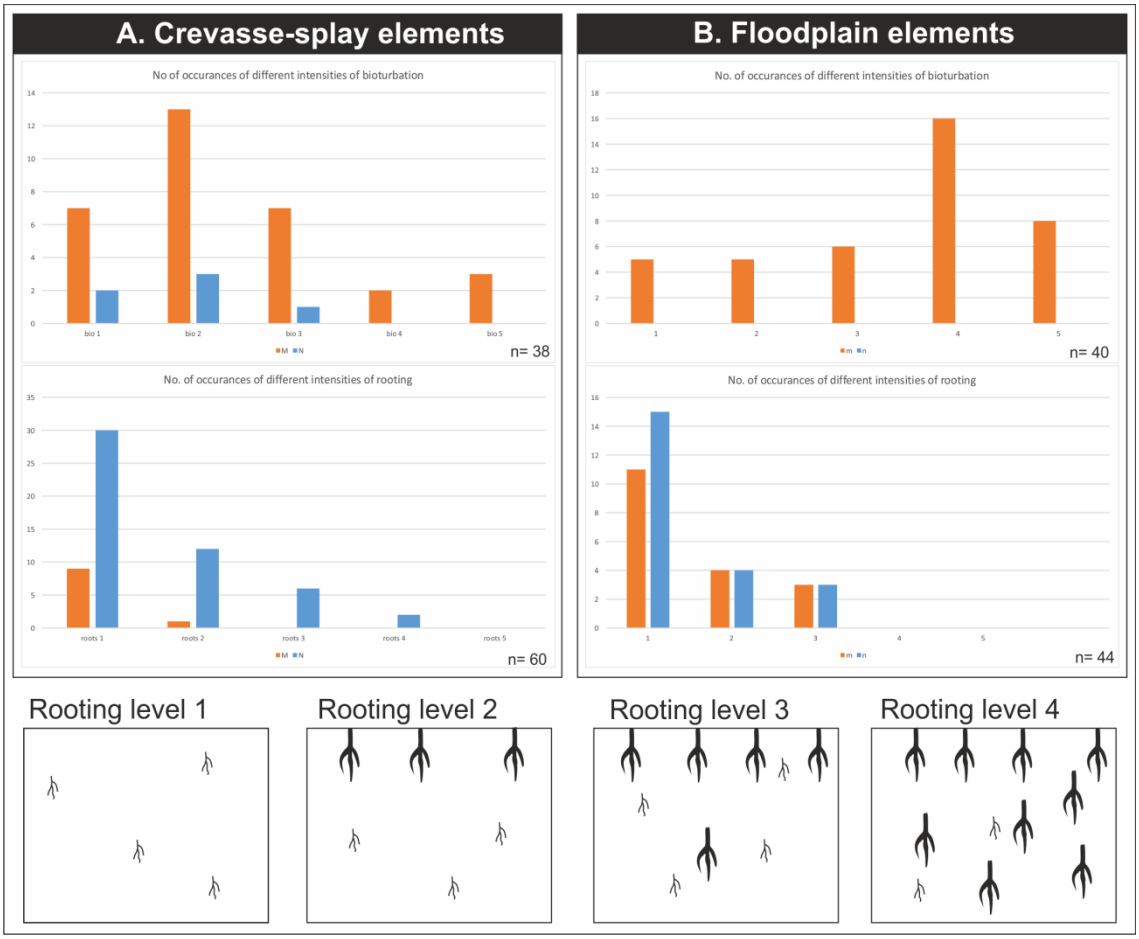

Figure 6.9: (A) Number of occurrences of different intensities of rooting and bioturbation of crevasse-splay elements (B) Number of occurrences of different intensities of rooting and bioturbation of floodplain elements.

Formation (Fig. 6.8B). Mean splay element widths in the Morrison Formation are 290 m (71- 360 m, n=5) compared to 1040 m (300- 1503 m, n=12) in the Neslen Formation. While lengths of splay elements in the Morrison Formation average 280 m (142- 446m, n=9) compared to 544 m (292- 750 m, n=6) in the Neslen Formation (Fig. 6.8B). Widths of crevasse-splay elements exceed lengths in the Neslen Formation splay elements but this is not the case in the Morrison Formation splay elements where widths are similar or are less than lengths (Fig. 6.8B). This can be expressed as a simplified length –to-width ratio:

in the Morrison Formation crevasse-splay elements have a length to width ratio of around are 1:1 while in the Neslen Formation the ratio is around 1:2.

Geometries of crevasse-splays can be classified as wedge (Miall, 1985) with some cases of undulose (Fig. 6.8). However there can be some variation in the geometries of splay elements, with some exhibiting more simple geometries and others showing a greater degree of undulation in the overall shape (Fig. 6.8). Splay-elements in the Neslen Formation conform more to the classic wedge geometries but 39% of the studied Morrison Formation splay elements were found to be more variable and undulose in overall geometry (Fig. 6.8).

Bioturbation within crevasse-splay elements is common to varying degrees of intensity; bioturbation indices have been used by many authors to define the degree of bioturbation in a deposit (Taylor and Goldring, 1993). In the Morrison Formation, the number of occurrences of splay elements with bioturbation are greater than of the Neslen Formation (Fig. 6.9A). The Morrison Formation splay elements have occurrences of bioturbation at each index level from 0- 5 but most commonly exhibit bioturbation indices from 1-3 (Fig. 6.9A). The Neslen Formation has lower occurrences of bioturbation and lower bioturbation indices 1- 3 (Fig. 6.9A). Rooting is also common within crevasse-splay elements, again to varying degrees of intensity. In this work rooting intensities have been defined from 0 -5 (Fig. 6.9). In the Neslen Formation, occurrence of splay elements exhibiting rooting are higher than the proportions of Morrison Formation splay elements with rooting (Fig. 6.9). The Neslen Formation splay elements exhibit rooting from 0-4, but most commonly in the lower intensities (1-2), whereas the Morrison Formation splay elements exhibit rooting only at lower intensities (1-2).

Crevasse-splay elements grain size and thickness are related to the range of sediment carried in the parent channel, and the dimensions of the parent channel. A proxy for this is the grain size and bankfull depth of the parent channels. There are large variations in splay element grain sizes in both the Morrison and Neslen Formations.

Splay grain sizes scale to channel-fill grain sizes (Fig. 6.10A). Splay element thicknesses and the associated channel elements in the Morrison Formation

are generally thinner than those in the Neslen Formation (Fig. 6.10B). Splay-element thickness is generally dependant on associated parent-channel element thicknesses, the preserved infill of that channel form (Fig. 6.8A).

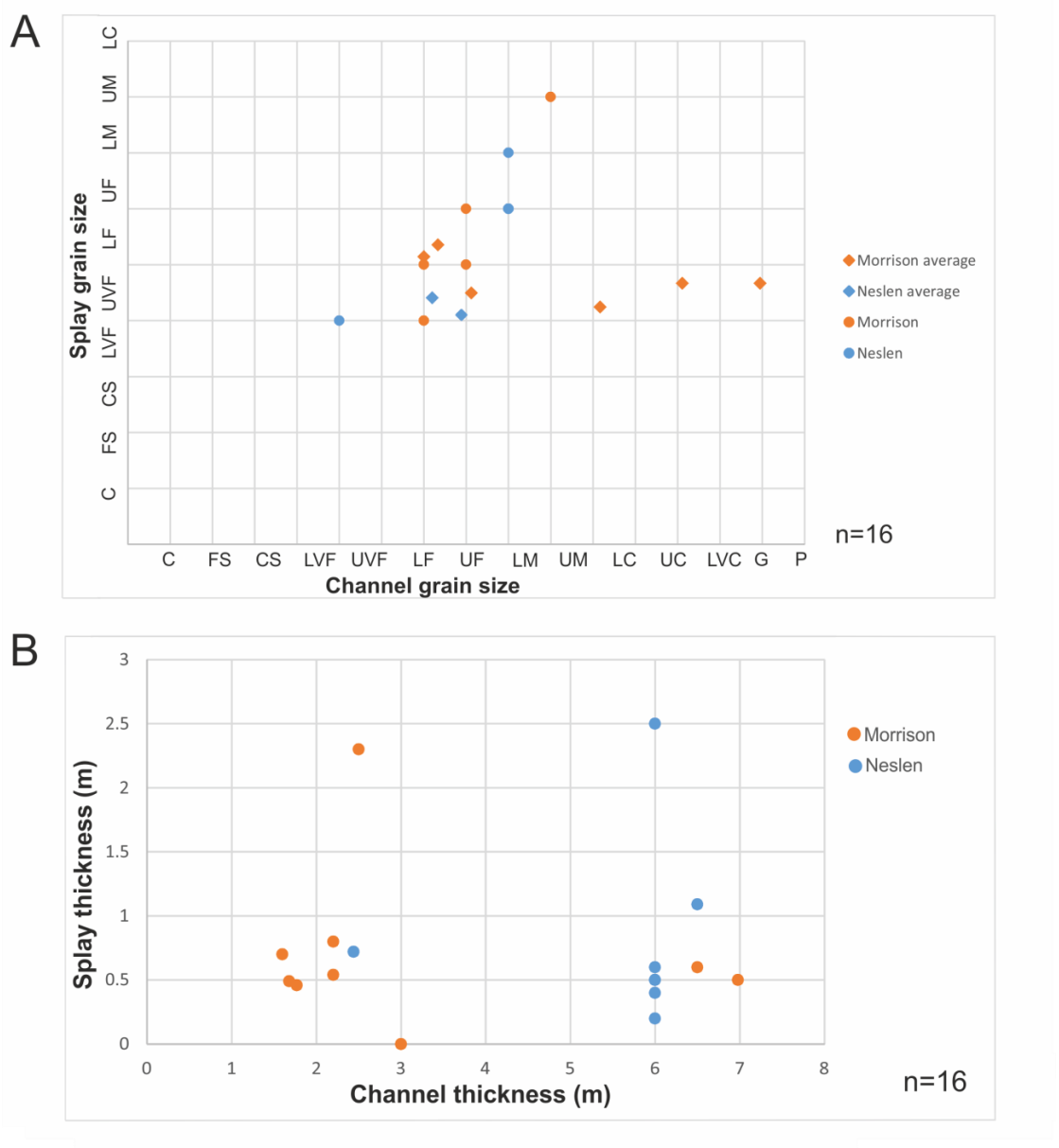

Figure 6.10: (A) Cross-plot of channel grain size and splay grain size. Averages are taken from each studied site and for individual channel and splay bodies. Pearson's R-value Morrison Formation 0.56, Neslen Formation -0.02. (B) Cross-plot of channel thickness and splay thickness of individual channel and splay bodies. Pearson's R-value Morrison Formation 0.24, Neslen Formation 0.31.

Crevasse-channel elements

Crevasse-channel elements are defined as sandstone- and/or siltstone- prone bodies with erosive bases and sharp tops; geometrically they resemble half-circles, channel shapes.

Facies types in crevasse-channel elements vary between the two formations with only one facies common to both: Facies Sm, which dominates in the Morrison crevasse-channel elements (95%) and makes up a significant proportion of Neslen Formation crevasse-channel elements (53%). The Morrison Formation crevasse-channel elements also have small amounts of facies Sr (5%) and Sp/St (2%) (Fig. 6.7). The Neslen Formation crevasse-channel elements have more diverse facies proportions and comprise facies Fd (16%) and Fp (32%). The Morrison Formation crevasse-channel elements are entirely made up of sand-prone facies but the Neslen Formation elements are made up of both sand- and silt-prone facies.

The range of thicknesses of crevasse-channel elements is much greater in the Morrison Formation crevasse-channel elements(0.5 - 5 m, n=9) compared to those in the Neslen Formation (2- 3.6 m, n=3) despite the same average thickness (2.5 m) in both formations. Crevasse-channel element widths in the Morrison Formation vary from 3 to 6 m whereas widths in the Neslen vary from 2- 3 m. (Fig. 6.6).

Geometries of crevasse channels can be broadly classified as symmetric and asymmetric. In the Neslen Formation, all crevasse-channel elements are classified as asymmetric, whereas in the Morrison Formation some can also be classified as symmetric; however an asymmetric geometry is more common. Bioturbation is not found in any of the studied crevasse-channels in either studied formation.

Channelized elements

Parent channels and channels deposited contemporaneously with the overbank deposits, although not a focus of this study, can aid in understanding the associated overbank deposits. Thus channel elements are considered here. Facies types in the studied channel elements from the Morrison Formation are

more varied than those in the studied channel elements from the Neslen Formation. Sp and Sr (%) are common to channel elements in both formations but are proportionally greater in the Neslen Formation examples than in the Morrison Formation examples (Fig. 6.7). The Morrison Formation channel elements studied contained the facies Gp and Sm, which are not observed in the Neslen Formation (Fig. 6.7). The occurrence of pebble to gravel grain sized facies in the Morrison Formation has less of a relationship with the associated splay element grain sizes. Splay elements associated with channel elements with gravel-facies are not significantly coarser than those sourced from channel elements with sandstone-facies (Fig. 6.10A).

Channel-element thickness varies greatly both in the Morrison and Neslen Formation. Neslen Formation channel elements (channel element 5.5 m thick (2.1-10 m, n=10) have a lower range of thicknesses than those from the Morrison Formation (average 3.4 m thick (1.2- 19 m, n=12) (Fig. 6.8). However, Morrison Formation elements can often reach a greater thickness than those in the Neslen Formation (Fig. 6.8).

Abandoned channel elements

Abandoned channel elements are defined as siltstone infilled convex-up bodies with a strongly erosional base. Facies types in abandoned-channel elements are homogenous and are similar in both formations: examples in the Morrison Formation are composed solely of facies Fm. In the Neslen Formation, although Fm (78%) dominates the elements, facies Fd is also present (22%).

Thicknesses are generally around 2 m in both formations. True widths and length are difficult to obtain due to the window of outcrop in which to study these elements and a lack of palaeoflow indicators in the facies types present. Therefore, minimum widths, outcrop permitting, are presented from the Neslen Formation as being 85 m and minimum lengths are 150 m (Fig. 6.6).

The geometry of abandoned channel elements is the same as most channel elements, with concave-up bases and generally flat tops. Bioturbation is not recorded in any of the studied abandoned-channel fills in either studied formation.

Floodplain and coal-prone floodplain elements

Both floodplain elements and coal-prone floodplain elements are flat tabular elements with flat non-erosive bases and tops (Fig. 6.6). Facies types in floodplain elements vary greatly between the Morrison Formation and the Neslen Formation. The only facies common to both formations is Fl, which occurs in far greater proportions in the Neslen Formation (88%) than the Morrison Formation (42%). The Morrison Formation floodplain elements are additionally composed of rooted and mottled siltstone facies, Frr (24%), Frm (28%), Frg (6%). The Neslen Formation has only one other facies: coals C (12%).

Morrison Formation floodplain elements with an average thickness of 0.6 m (0.3- 1 m, n=72) are similar in thickness to those in the Neslen Formation, 0.8 m (0.05-2.9 m,n=42), but are thicker than the coal-prone floodplain elements in the Neslen Formation, 0.6 m (0.5- 0.9 m, n=5). However, Morrison Floodplain elements have a far greater range of thicknesses than those in the Neslen Formation (Fig. 6.6).

Bioturbation in floodplain elements only occurs within the Morrison Formation elements not in the Neslen Formation floodplain elements (Fig. 6.9). Rooting is also common within floodplain elements, as many of the facies contain roots. Rooting levels within floodplain elements in both the Morrison Formation and Neslen Formation are overall very similar and most common at the lowest intensities (Fig. 6.9).

6.4.2 Examples of stratigraphic architectures from the studied formations

Five logged panels have been constructed of three sites from the Morrison Formation (Fig. 6.11; 6.12; 6.13) and two sites from the Neslen Formation (Fig. 6.14; 6.15).

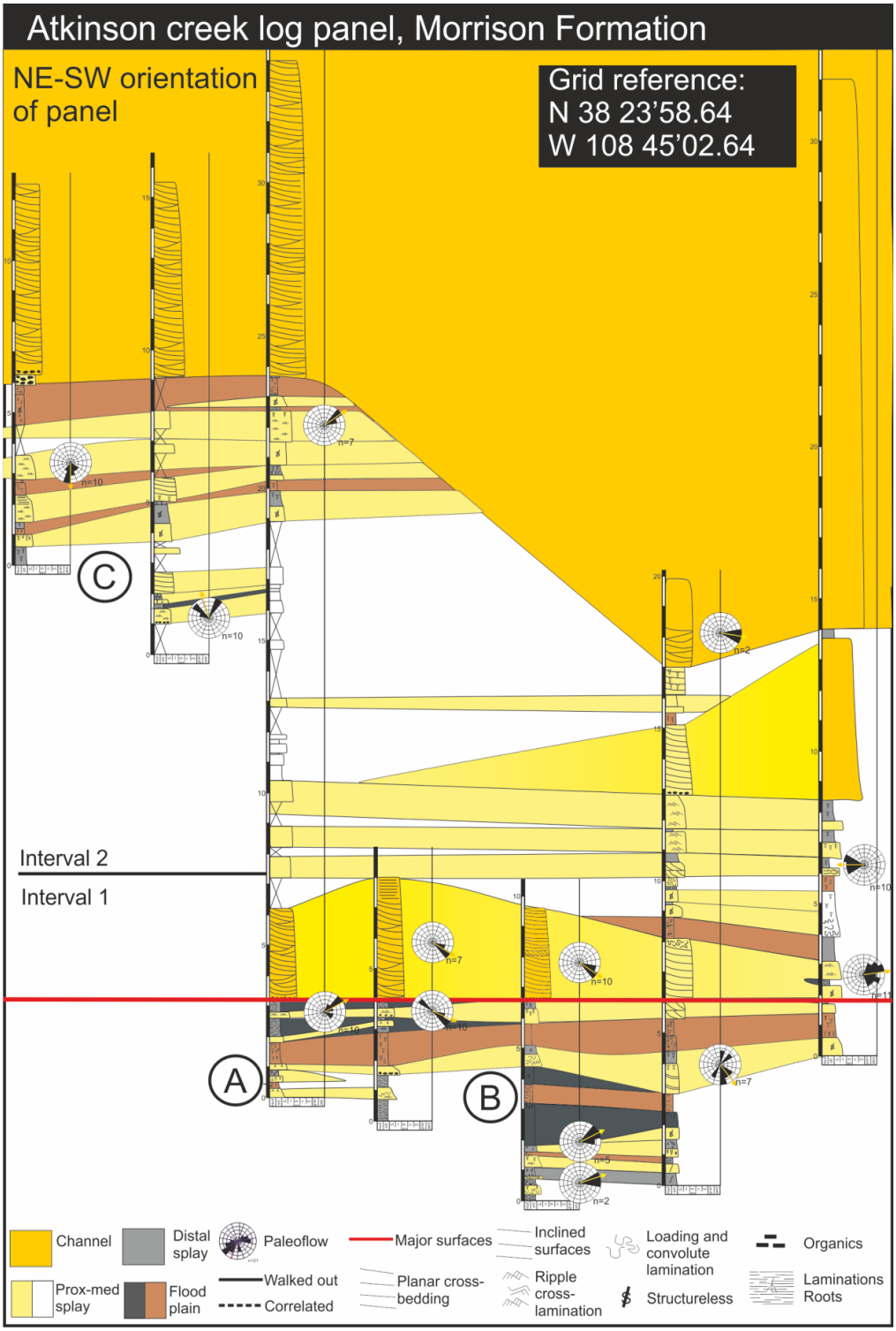

Figure 6.11: Correlation panel of 6 logged sections at Atkinson Creek Site. Surfaces and beds marked with a bold line have been walked out in field whereas dashed lines have been correlated by observation from distant vantage points in the field. This correlation panel shows the raw data collected.

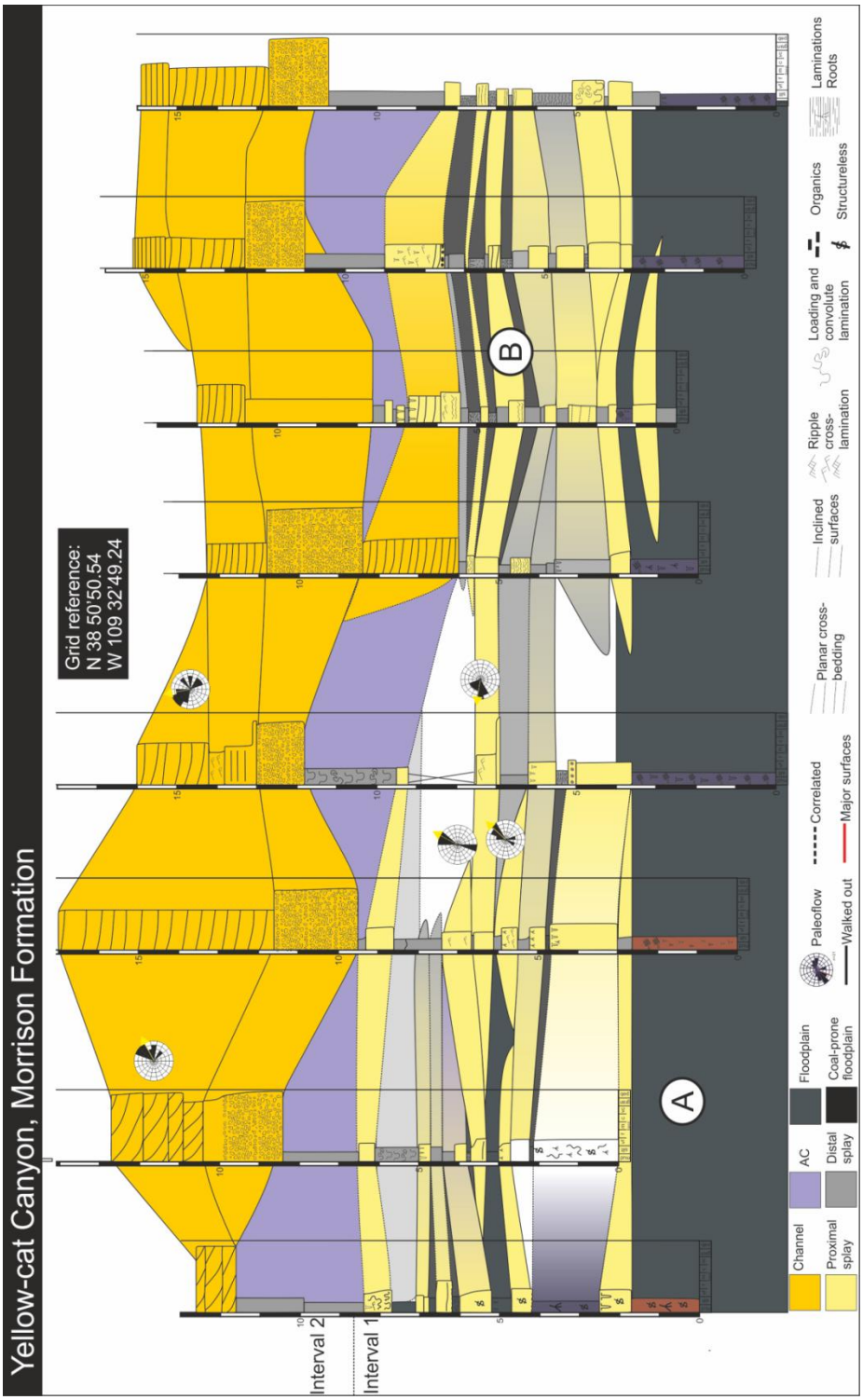

Figure 6.12: Correlation panel of 8 logged sections at Yellow Cat Canyon site. Surfaces and beds marked with a bold line have been walked out in field whereas dashed lines have been correlated by observation from distant vantage points in the field. This correlation panel shows the raw data collected.

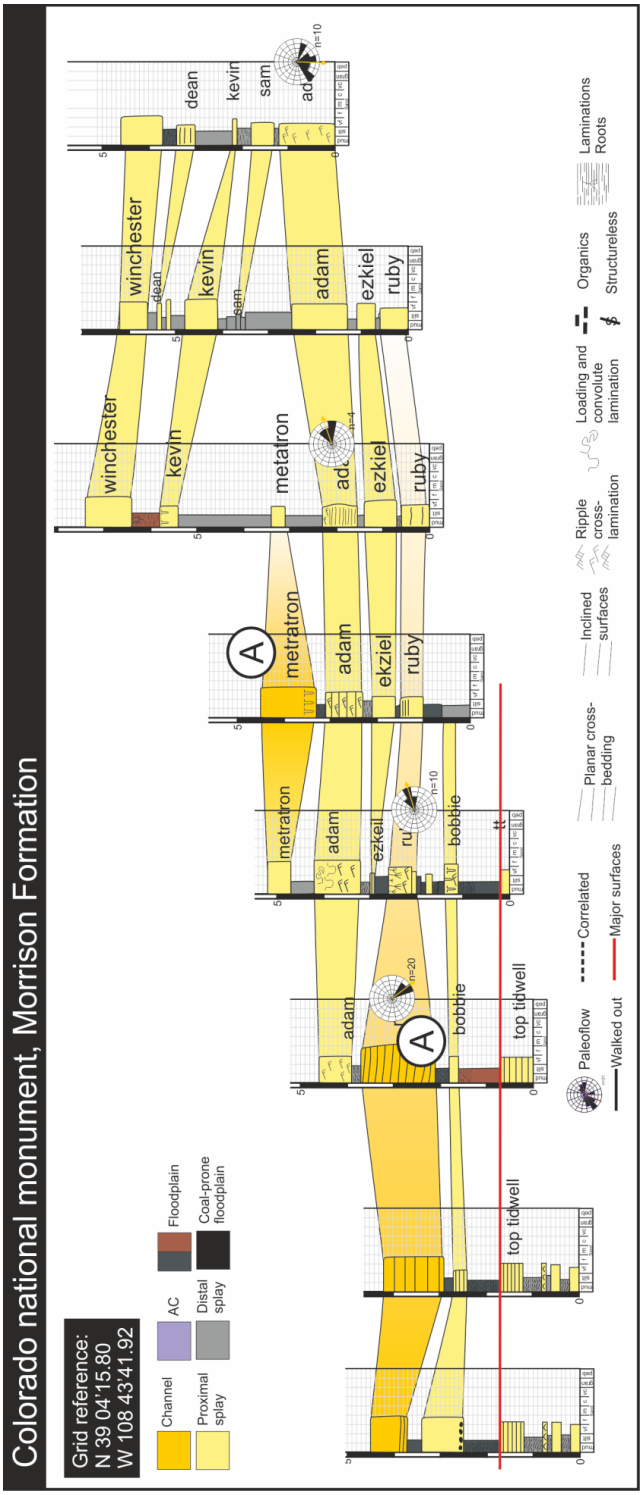

Figure 6.13: Correlation panel of 9 logged sections at Colorado National Monument site. Surfaces and beds marked with a bold line have been walked out in field whereas dashed lines have been correlated by observation from distant vantage points in the field. This correlation panel shows the raw data collected.

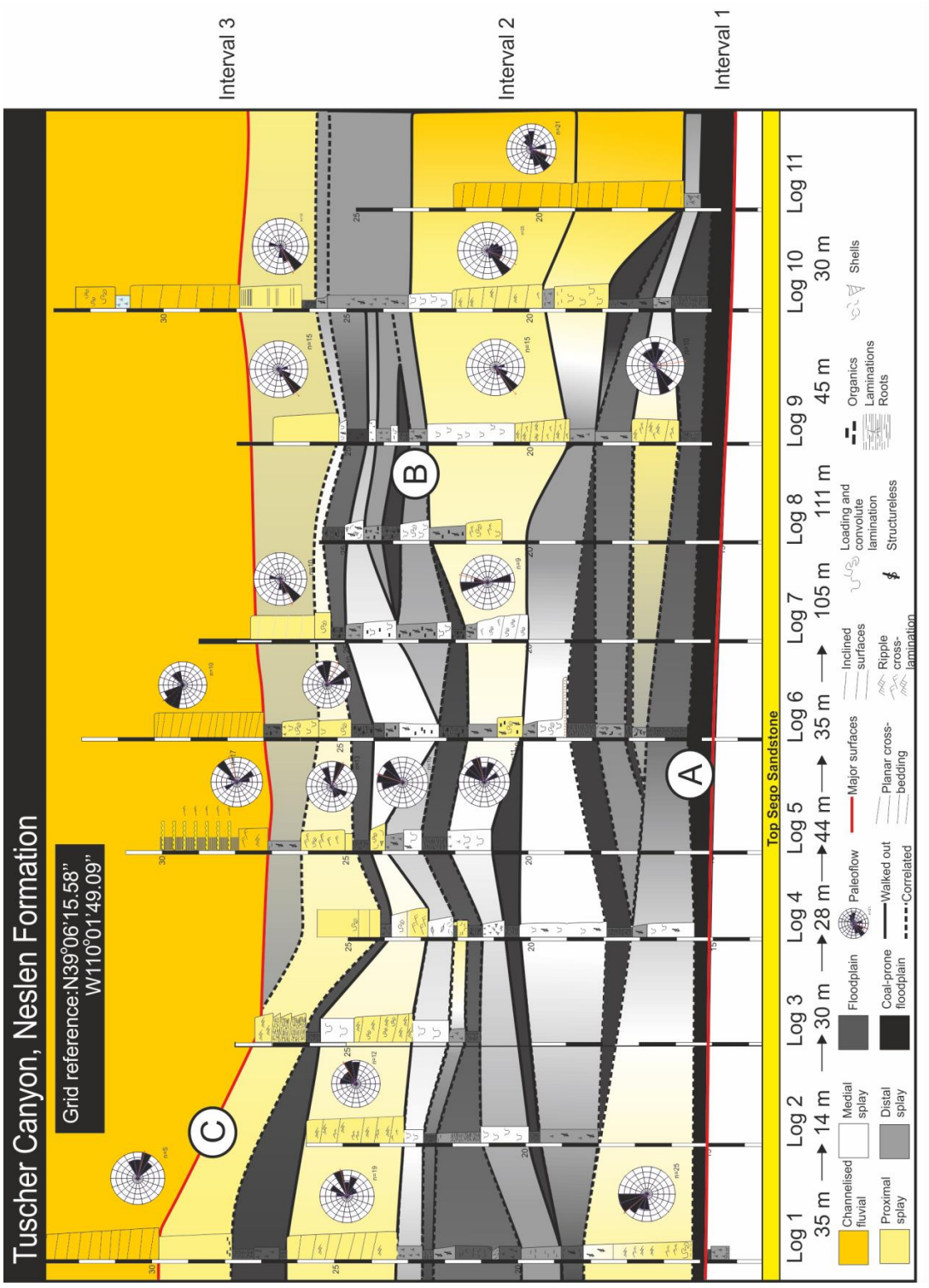

Figure 6.14: Correlation panel of 11 logged sections at Tuscher Canyon site. Surfaces and beds marked with a bold line have been walked out in field whereas dashed lines have been correlated by observation from distant vantage points in the field. This correlation panel shows the raw data collected.

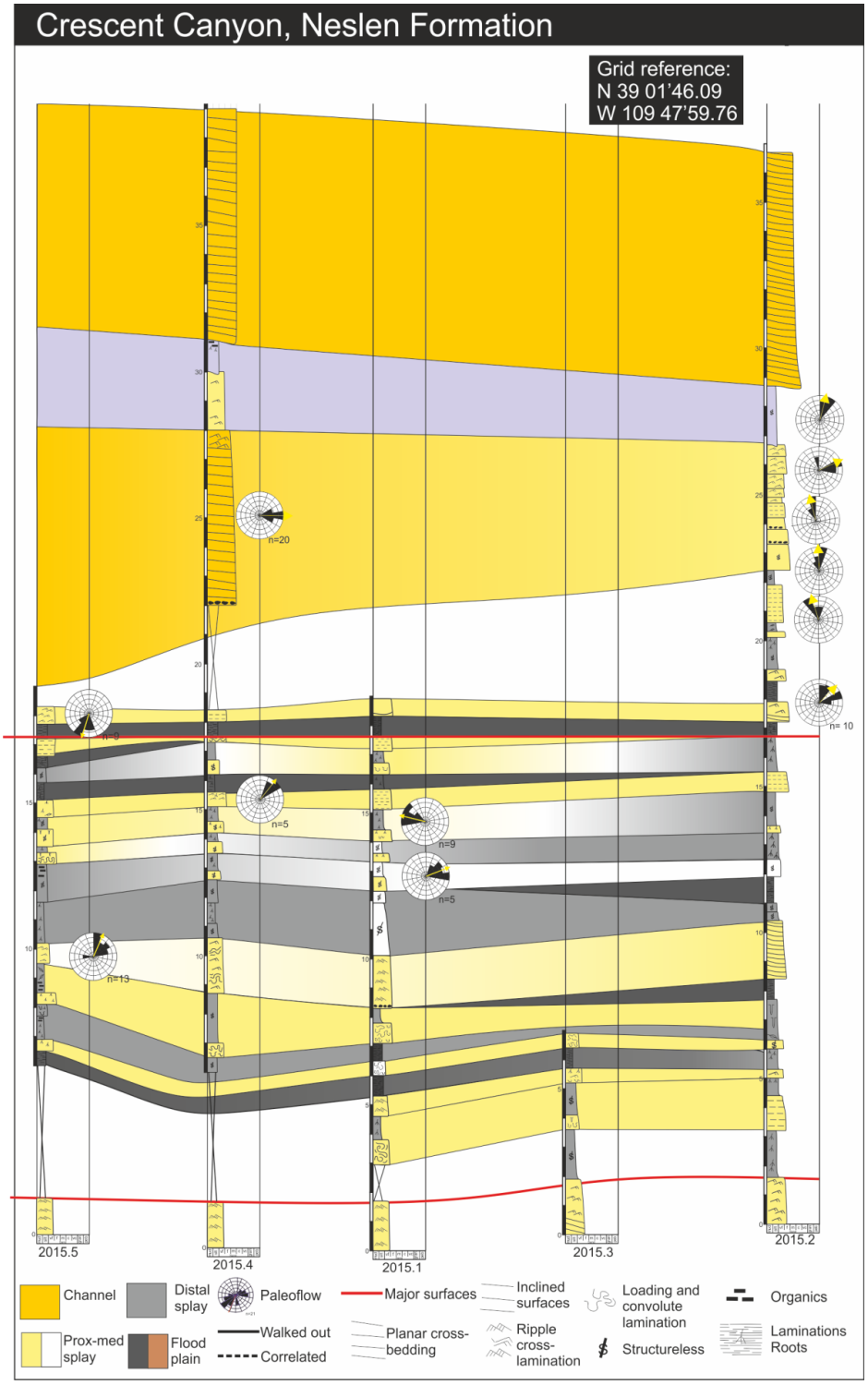

Figure 6.15: Correlation panel of 5 logged sections at Crescent Canyon site. Surfaces and beds marked with a bold line have been walked out in field whereas dashed lines have been correlated by observation from distant vantage points in the field. This correlation panel shows the raw data collected.

Atkinson Creek, Morrison Formation

The Atkinson creek site is located within the medial portion of the distributive fluvial system of the Saltwash Member of the Morrison Formation and extends for 3 km (Fig. 6.4). Consequently, the site has an abundance of overbank elements in association with amalgamated channel elements (Owen et al., 2015) (Fig. 6.11). Of the elements identified in the previous section, crevasse-splay, crevasse-channel, floodplain and fluvial channel elements are all present at this locality (Fig. 6.11).

The variations in the maximum measured thickness of each occurring individual element were recorded: crevasse-splay elements had an average maximum thickness of 0.65 m (0.3- 1.05 m, n=23); crevasse-channel elements had an average maximum thickness of 2.65 m (2.3- 3 m, n=3); floodplain elements had an average maximum thickness of 1.09 m (0.35- 2 m, n=12). Crevasse-splay lateral extents were also recorded as an average of 214 m (76- 397 m).

Proportions of each facies type in each element type also vary in each of the identified elements. In crevasse-splay elements, Sr (31%) and Fd (35%) were the most common facies types with Fp (25%) and Sm (9%) in lower proportions. In crevasse-channel elements, St/Sp (100%) was the only recorded facies type. In floodplain elements, facies Frr (60%) was the most common facies type, with facies Fl (19%), Frg (21%) comprising the remaining proportion. In channel elements, facies St/Sp (100%) was the only recorded facies type.

Grain sizes of channel elements at this site were on average lower medium sandstone (range: upper fine sandstone to upper medium sandstone), whereas splay grain size was an average of lower very-fine sandstone (range: coarse siltstone to upper fine sandstone) (Fig. 6.10).

Interval 1 consists of floodplain elements, splay deposits and channel elements. The floodplain elements are dominated by palaeosol deposits, which either occur as thin interbedded palaeosols that interbed with stacked genetically related medial-distal parts of crevasse-splay elements (Fig. 6.11A) or as stacked thick palaeosol deposits, which are substantially thicker and better developed (Fig. 6.11B). Crevasse-splay elements are adjacent to floodplain

elements, as well as being vertically topped by floodplain elements. Interval 2 is dominated by amalgamated channel elements, which cut down towards the north-eastern end of the site, leaving the overbank, floodplain elements and crevasse-splay elements, towards the south-west intact (Fig. 6.11C).

Yellow Cat Canyon, Morrison Formation

The Yellow Cat Canyon site is located within the medial-distal portion of the distributive fluvial system, and extends for 1.2 km (Fig. 6.4). It consequently has smaller channel elements and abundance of floodplain elements (Owen et al., 2015). However, the channel elements present are far coarser than those from the other studied successions. Of the elements identified in the previous section, crevasse-splay, floodplain, fluvial channel and abandoned channel elements all occur (Fig. 6.12).

The variations in the maximum measured thickness of each individual element was recorded, crevasse-splay elements had an average maximum thickness of 0.9 m (0.5- 1.4 m, n=18), floodplain elements have an average maximum thickness of 1.36 m (0.3- 3.6 m, n=9), channel elements have an average maximum thickness of 1.6 m (0.7- 2.5 m, n=5), whereas abandoned channel elements have an average maximum thickness of 2.95 m (2.9- 3 m, n=2). Crevasse-splay elements at this site had an average lateral extent of 299 m (175- 540 m).

Proportions of each facies type in each element type also vary in each of the identified elements. In crevasse-splay elements the the most common facies were Fd 49% Fp (26%). Sm (22%) with Sr (2%) Sd (2%) making up small proportions. Abandoned channel elements are made up of only one facies type, Fm (100%). Floodplain elements are dominated with the facies Frp (64%) with the facies Frr (15%) Fl (17%) Frg (4%) making up smaller proportions of the elements. Channel elements are dominated by the facies St/p (87%) with smaller occurrences of the facies Gp (13%).

Grain sizes of channel elements at this site were an average of granule-sized (lower fine sandstone- pebbles). Splay elements had an average grain size of upper very-fine sandstone (fine silt- upper fine sandstone) (Fig. 6.10).

Interval 1 (Fig. 6.12) consists of floodplain and crevasse-splay elements, a well-developed palaeosol floodplain element which is laterally extensive across the entire site bounds the base of the succession (Fig. 6.12A). Crevasse-splay elements stack together with thin floodplain elements throughout the rest of interval 1. The splay elements stack vertically with interbedded floodplain elements but in some areas splay elements thin and thicken laterally (Fig. 6.12B). Palaeocurrents recorded from crevasse-splay elements are variable with the main azimuth directions trending between 270- 45 degrees (n=30). Interval 2 (Fig. 6.12) is represented by abandoned channel deposits overlain by coarse conglomeratic channel-fills that are then overlain by a series of multiple amalgamated sand-prone channel fills. Palaeocurrents recorded from the sand-prone amalgamated channel fills trend between 350 and 050 degrees (n=20).

Colorado National Monument, Morrison Formation

Colorado National Monument is located within the distal portion of the distributive fluvial system (Fig. 6.4). There are no amalgamated channel bodies present instead there are small ribbon channels and fine-grained deposits (Owen et al., 2015) (Fig. 6.13). Of the elements identified in the previous section, crevasse-splay, crevasse-channel and floodplain elements all occur.

The variations in the maximum measured thickness of each individual element was recorded, crevasse-splay element average maximum thickness was 0.9 m (0.5- 1.6 m, n=7); while average maximum crevasse-channel element thickness was 1.4 m (1.2- 1.6 m, n=2); floodplain element average maximum recorded thickness was 0.3 m (0.05- 0.7 m, n=5).

Proportions of each facies type in each element type also vary in each of the identified elements: crevasse-splay elements have similar amount of facies Sm (27%) Sr (20%) Fd (32%) and Fp (21%). Crevasse-channel elements entirely consist of St/p (100%). Floodplain elements are dominated by Fl (81%) and have smaller proportions of Frg (17%) Frr (2%).

Grain sizes of channel elements at this site were an average of upper fine sandstone (upper fine sandstone- upper medium sandstone), while splay

element grain size was on average upper very fine sandstone (coarse silt-upper fine sandstone) (Fig. 6.10).

Thin crevasse-splay elements are linked to thicker crevasse-channel elements (Fig. 6.13A). The crevasse-splay elements are separated by floodplain elements but can exhibit minor compensational stacking in some areas (Fig. 6.13B). Palaeocurrents records from crevasse-splay elements trend from 045 to 180 degrees (n=24); palaeocurrents recorded from a crevasse-channel element trend towards 170 degrees (n=20).

Tuscher Canyon, Neslen Formation

The Tuscher Canyon site (Fig. 6.14) can be placed within the overall stratigraphic context of the Neslen Formation based on work by Shiers et al. (2017). This site is within the Palisade Zone in the Lower part of the Neslen Formation (Fig. 6.4). The Palisade Zone within the Neslen Formation has a greater amount of coals and organic-rich shales (Shiers et al., 2014). Of the elements identified in the previous section crevasse-splay, crevasse-channel, coal-prone floodplain and channel elements all occur (Fig. 6.14).

The variations in the maximum measured thickness of each occurring individual element was recorded crevasse-splay elements have an average maximum measured thickness of 2.35 m (1.3- 3.7 m, n=10), crevasse-channel elements have an average of 2.05 m (1.7- 2.4 m, n=3), channel elements have an average of 4.5 m (4- 5.5 m, n=2), while floodplain elements have an average of 0.93 m (0.5- 1.5 m, n=7). Crevasse-splay elements at this site had an average lateral extent (both width and lengths) of 961 m (292- 1502 m).

Proportions of each facies type in each element type also vary in each of the identified elements: crevasse-splay element facies Sm (18%), Sr (9%), Sd (7%), Fd (33%), Fp (20%), Fop (12%); crevasse-channel elements are made of facies Fd (33%) and Fp (97%); coal-prone floodplain element Fl (80%) and C (20%). Channel elements consist of St/p (73%), Sr (25%) and Gm (2%).

Grain sizes of channel elements at this site were an average of upper fine sandstone (lower fine sandstone- lower medium sandstone) whereas splay

element grain size was an average of lower very fine sandstone (coarse silt-upper fine sandstone).

Interval 1(Fig. 6.14) is a floodplain dominated interval with a coal-prone floodplain element that is laterally extensive across the entire site; crevasse-splay elements recorded in this interval can be classed ,mainly, as the medial and distal parts of the element and are adjacent and pass laterally to floodplain elements (Fig. 6.14A). Interval 2 is dominated by splay elements which thin and fine in opposite directions (Fig. 6.14). Several splay elements have palaeocurrents trending between 250-10 degrees, (n=99) whereas other splay elements in this interval have palaeocurrents which trend between 10 and 60 degrees, (n=54). Floodplain elements are less common in this interval, but where present the elements are interbedded with splay elements particularly at the distal reaches of the splay elements (Fig. 6.14B). Interval 3 is a channel sandstone dominated interval, with multiple amalgamated channel elements that erode, with up to 3 m of erosional relief on this surface, into the interval 2 crevasse-splay and floodplain elements (Fig. 6.14C). Palaeocurrents recorded from channel elements trend between 340 and 100 degrees, (n=32).

Crescent Canyon, Neslen Formation

The Crescent Canyon site (cc3) can be placed within the overall stratigraphic context of the Neslen Formation based on work by Shiers et al. (2017). This site is within the middle-upper portion of Neslen Formation in the Chesterfield Zone of the Upper Neslen Formation (Fig. 6.4). Of the elements identified in the previous section crevasse-splay, crevasse-channel, floodplain abandoned channel elements and channel elements all occur at this site (Fig. 6.15).

The variations in the maximum measured thickness of each element were recorded. For the crevasse-splay elements the average maximum recorded thickness was 1.3 m (0.5- 2.2 m, n=20); for crevasse-channel elements the average thickness was 2 m(n=1); for the abandoned channel element the average thickness measurements were an 2.5 m (2- 3 m, n=1); for the channel elements the average thickness was 7.5 m (7- 8 m, n=2); floodplain elements had an average thickness of 0.68 m (0.6- 0.7 m, n=7). Crevasse-splay elements

at this site had an average lateral extent (both width and lengths) of 840 m (525- 1495 m).

Proportions of each facies type in each element type also vary in each of the identified elements: crevasse-splay elements consist of the facies Sm (17%), Sr (16%), Sd (3%), Fd (16%), Fp (39%), Fop (9%); crevasse channel elements consist entirely of the facies Sm. Abandoned channel elements are made up of Fm (61%) and Fd (39%). Floodplain elements consist entirely of Fl. Channel elements consist of Gm (5%) St/p (82%) and Sr (14%).

Grain sizes of channel elements at this site were an average of lower medium sandstone (lower fine sandstone- upper medium sandstone) whereas the average splay grain size was lower fine sandstone (fine silt- upper fine sandstone).

Interval 1 consists of splay elements far from channel with floodplain interbedding, with the splay elements. Paleocurrents mainly trend between 10 and 45 degrees (n= 42) with one splay element containing palaeocurrents indicators trending towards 290 degrees (n= 9). Interval 2 is dominated by the proximal part of a series of splay elements which all contain similar paleocurrents trends between 350 and 45 degrees (n=60). These multiple splay elements pass laterally to a channel element; this channel element is trending towards 90 degrees (n= 20) (Fig. 6.15) which is perpendicular to the splay elements. This channel element and the splay elements pass vertically to an abandoned channel element that is laterally extensive across the entire site, this abandoned channel element is topped by an erosive channel element that has up to 1-2 m erosion (Fig. 6.15). This channel element at the very top of the section contains similar palaeocurrent indicators as the crevasse-splay elements below it (Fig. 6.15).

6.4.3 Literature derived data sourced from FAKTS database.

Variations in thicknesses, lengths and widths of elements present in a fluvial succession developed in semi-arid and humid climates, and subject to ephemeral and perennial flow regimes, and from fluvial fan settings and coastal plain settings have been investigated using the Fluvial Architecture and

Knowledge Transfer database (FAKTS). FAKTS is a database populated with literature-derived and in-house quantitative and qualitative data relating to architecture of ancient successions and modern rivers (Colombera et al., 2013). FAKTS can be used to generate quantitative facies models for fluvial depositional systems. The models produced provide information on proportions, geometries, spatial relations and grain sizes of genetic units at three different scales of observation: facies units, architectural elements and depositional elements (Colombera et al., 2013). To aid in comparison of data from this study to those in the FAKTS database, facies codes used in this study can be mapped onto the codes used the FAKTS database (Table 2). The raw data collected in this thesis were also added to the FAKTS database to allow for easier comparison of case studies of fluvial overbank successions and to refine future depositional models of fluvial overbank successions.

Crevasse-splay element thicknesses in each of the studied system types are between 0.1 - 12 m, with averages between 0.78 - 1.6 m , (n=856) (Fig. 6.16A). Crevasse-splay elements from humid (1. 5 m), perennial (1.5 m), coastal-plain (1.6 m) settings have the greatest average thicknesses, whereas crevasse-splay elements from semi-arid (1 m), ephemeral (0.9 m), fluvial fan (0.8 m) settings have the lowest average thicknesses. Crevasse-splay lengths and widths in all systems are between 10 and 4000 m with most falling between 50 and 1000 m (Fig. 6.16B, 6.21C). Widths of splays are smaller in ephemeral systems than in perennial systems and smaller in arid and semi-arid settings than in humid settings (Fig. 6.1, 6.6B). Although the splays in arid and semi-arid settings can be very thick they are not very wide (Fig. 6.1, 6.6B).

There are few recognisable links between settings and splay lengths (Fig. 6.1, 6.6C). Thickness instead seems to be the main predictor in splay length. However, there is a lack of a data for semi-arid and ephemeral systems (Fig. 6.1, 6.6B). Facies types that make up crevasse-splay elements vary in each of the system types. Facies Fsm commonly occurs in all settings except systems that record an ephemeral discharge regime. Facies Sr commonly occurs in all settings. Facies Sd and Sm commonly occur in all settings except in systems that are interpreted to record ephemeral discharge regimes (Fig. 6.17A). Fsm

and Sd are most dominant in all settings except in ephemeral settings where facies St and Sr are the most dominant facies; Sp only occurs in semi-arid, ephemeral and fluvial fan systems (Fig. 6.17A). Facies types in crevasse splays

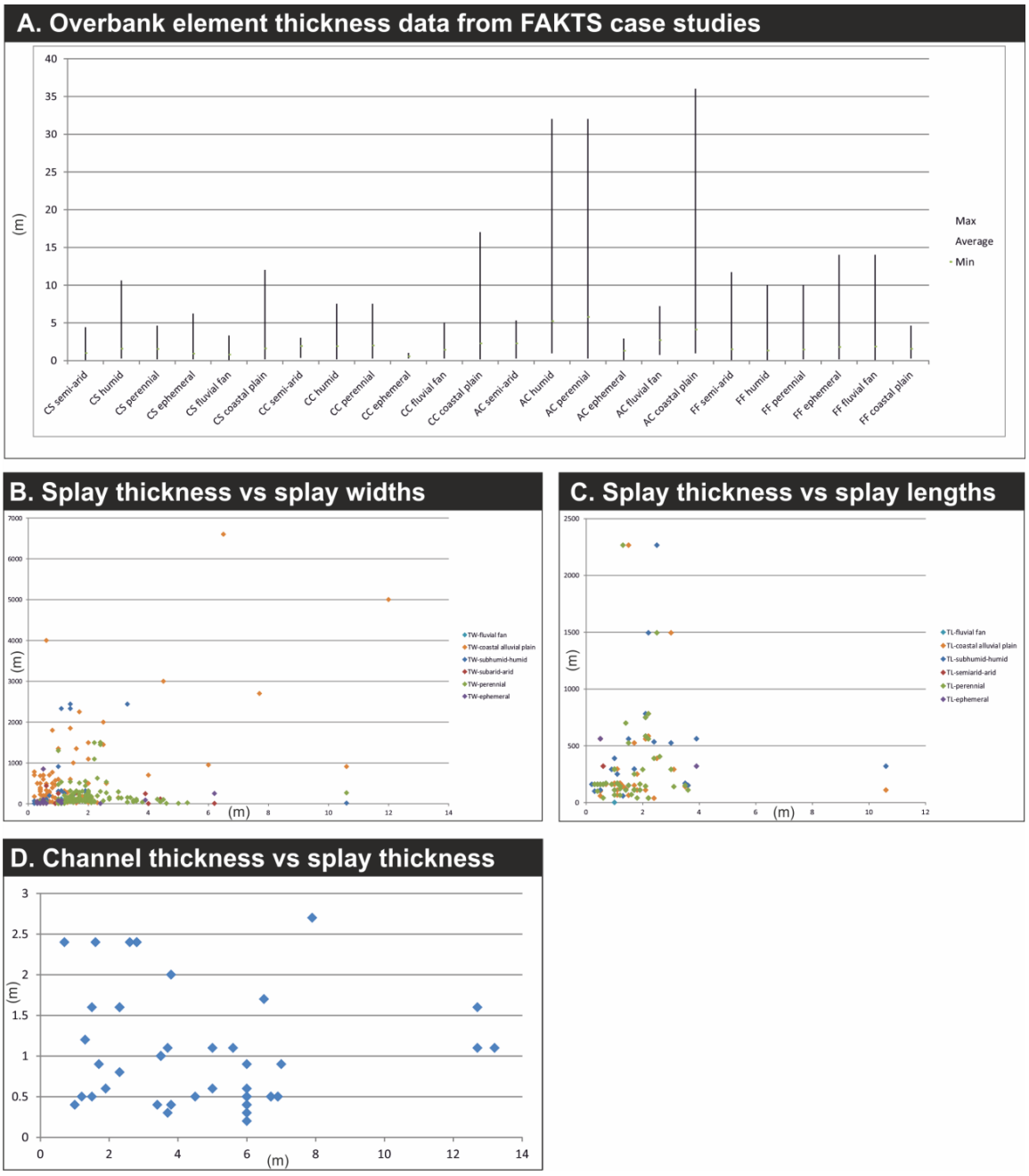

Figure 6.16: FAKTS derived overbank data. (A) Overbank element thickness from Fluvial Architecture and Knowledge Transfer database case studies (B) Splay element thicknesses plotted against splay widths (C) Splay element thicknesses plotted against splay lengths (D) Channel body thickness plotted against splay body thickness.

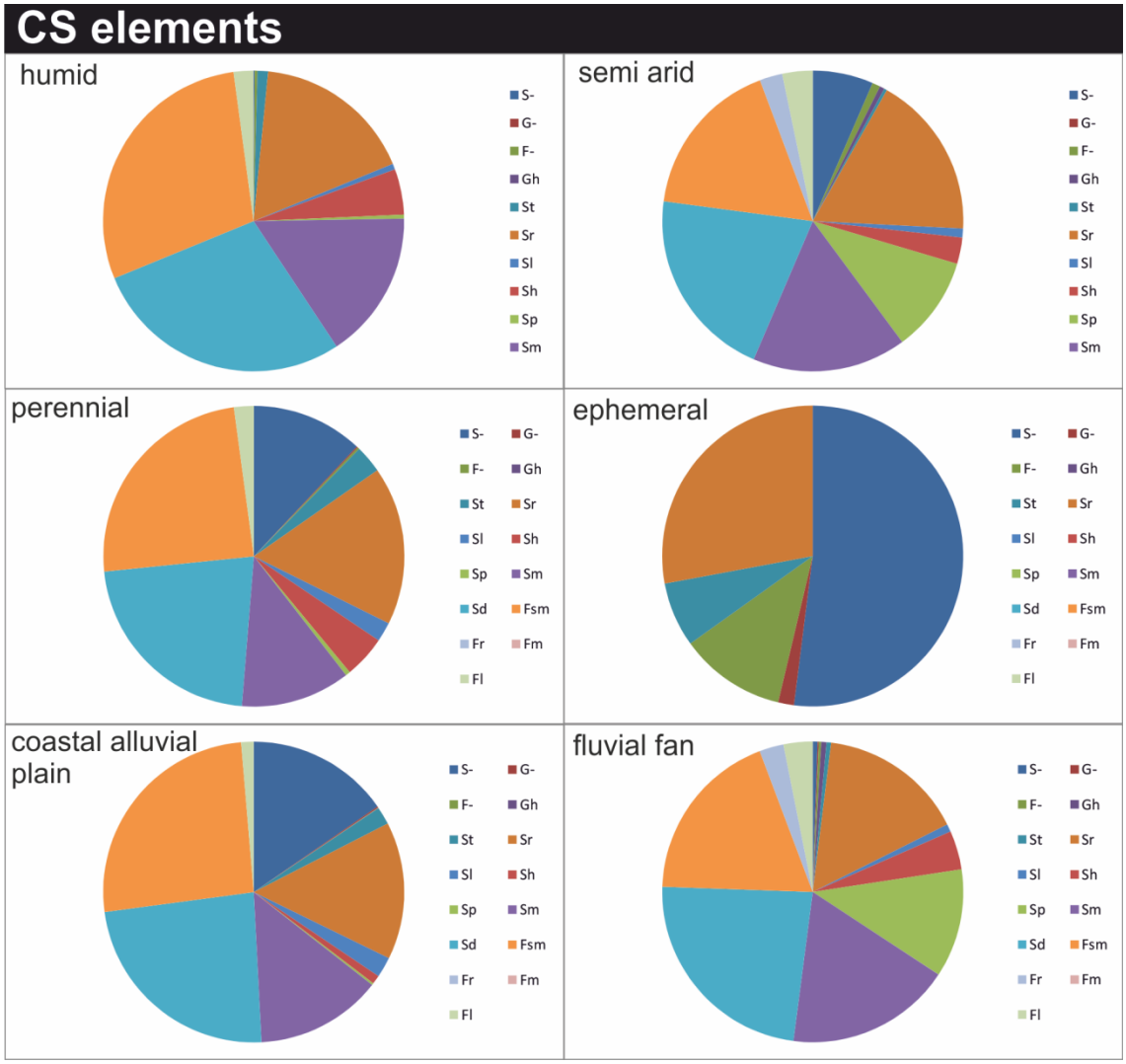

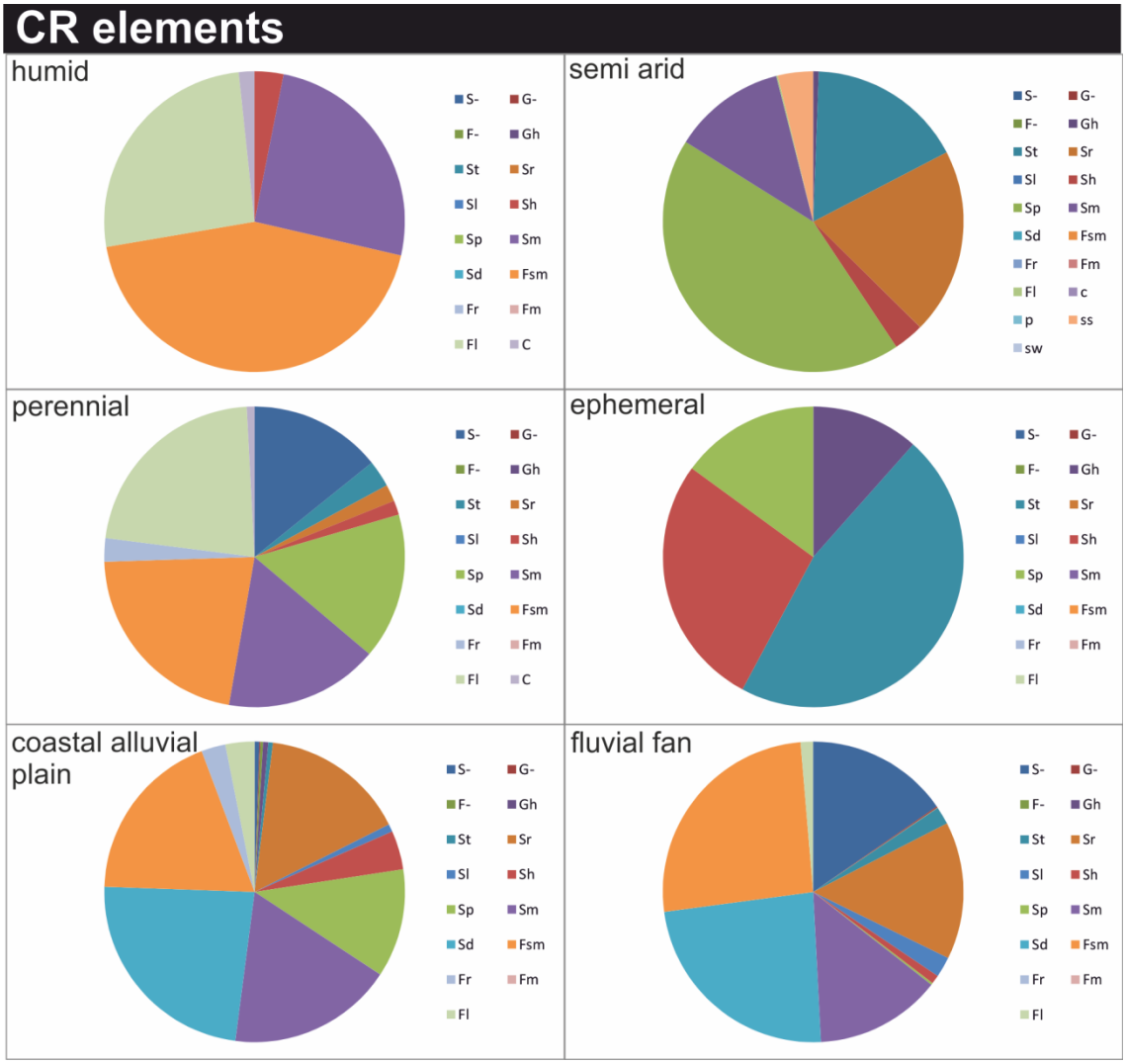
CR elements
humid
S-
G-
F-
Gh
St
Sr
Sl
Sh
Sp
Sm
Sd
Fsm
Fr
Fm
Fl
C
semi arid
S-
G-
F-
Gh
St
Sr
Sl
Sh
Sp
Sm
Sd
Fsm
Fr
Fm
Fl
c
p
ss
sw
perennial
S-
G-
F-
Gh
St
Sr
Sl
Sh
Sp
Sm
Sd
Fsm
Fr
Fm
Fl
C
ephemeral
S-
G-
F-
Gh
St
Sr
Sl
Sh
Sp
Sm
Sd
Fsm
Fr
Fm
Fl
coastal alluvial plain
S-
G-
F-
Gh
St
Sr
Sl
Sh
Sp
Sm
Sd
Fsm
Fr
Fm
Fl
fluvial fan
S-
G-
F-
Gh
St
Sr
Sl
Sh
Sp
Sm
Sd
Fsm
Fr
Fm
Fl

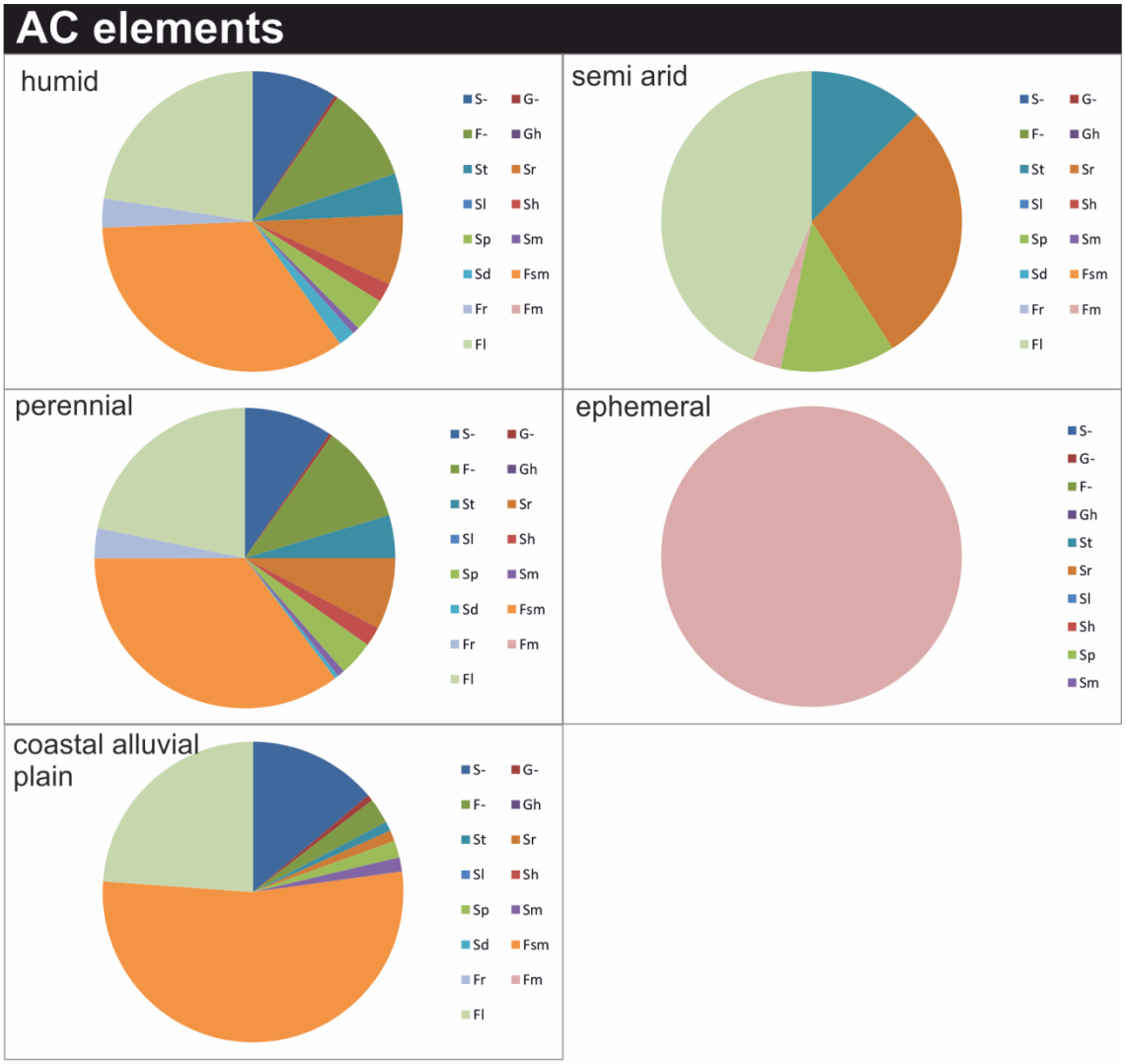
AC elements
humid
S-
G-
F-
Gh
St
Sr
Sl
Sh
Sp
Sm
Sd
Fsm
Fr
Fm
Fl
semi arid
S-
G-
F-
Gh
St
Sr
Sl
Sh
Sp
Sm
Sd
Fsm
Fr
Fm
Fl
perennial
S-
G-
F-
Gh
St
Sr
Sl
Sh
Sp
Sm
Sd
Fsm
Fr
Fm
Fl
ephemeral
S-
G-
F-
Gh
St
Sr
Sl
Sh
Sp
Sm
coastal alluvial plain
S-
G-
F-
Gh
St
Sr
Sl
Sh
Sp
Sm
Sd
Fsm
Fr
Fm
Fl

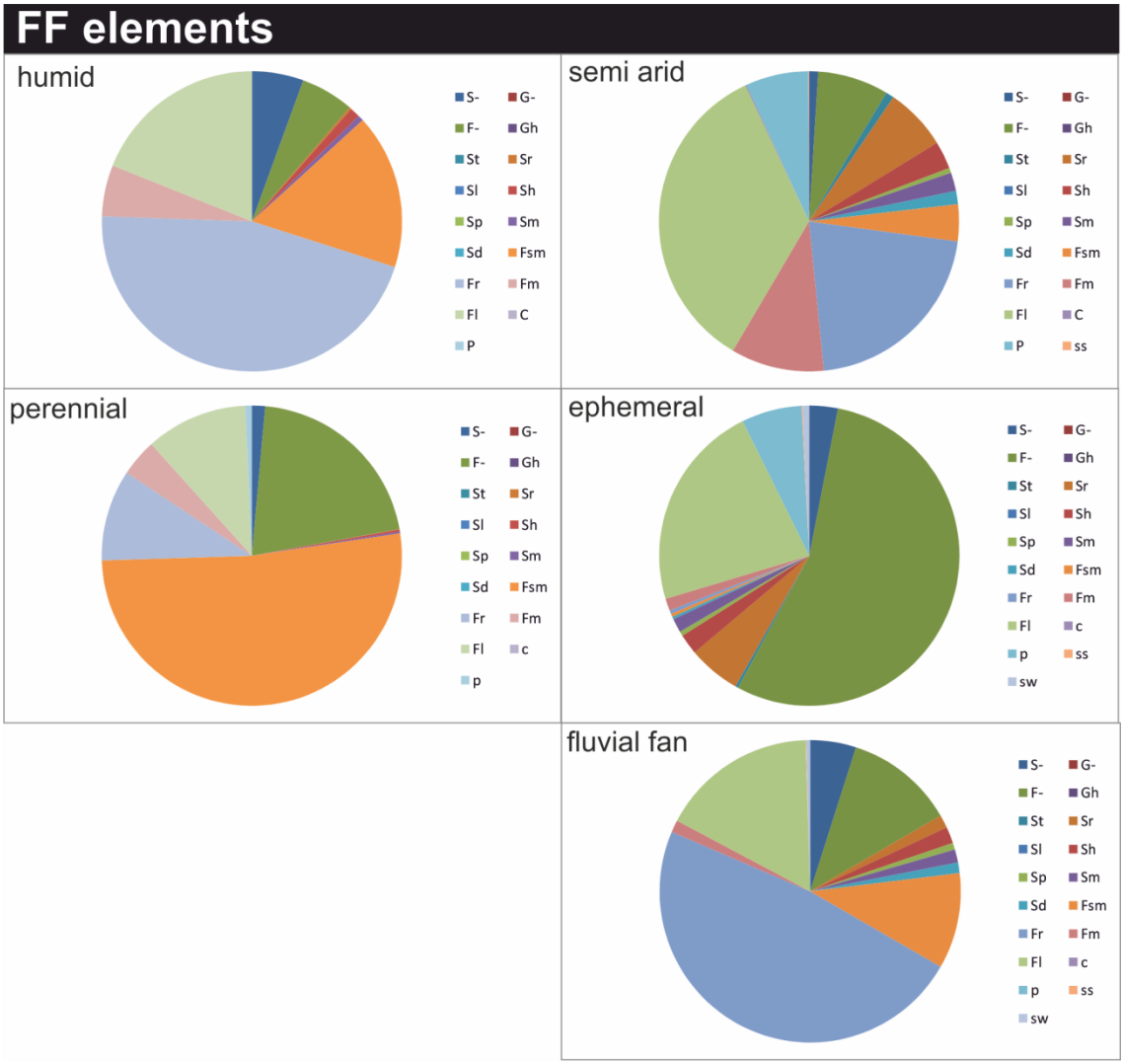

Figure 6.17: FAKTS derived overbank facies type and proportion data (A) Crevasse-splay elements (B) Crevasse-channel elements (C) Abandoned channel elements (D) Floodplain elements. Codes G-, S- and F- identify a facies as having undefined sedimentary structure instead note the grain size of that unit.

from humid settings are similar to those in semi-arid settings, with both consisting of high proportions of Fsm, Sd, Sm and Sr. Semi-arid settings have greater proportions of facies Sp than humid settings, and also have occurrences of facies St, which humid settings do not have (Fig. 6.17A).

Facies types vary more between perennial and ephemeral settings. Both perennial and ephemeral crevasse-splays have facies Sr and Sh. However,

perennial settings are dominated by Fsm and Sd facies, which do not occur in any proportion in ephemeral setting splays, ephemeral setting splays instead are dominated by Sr (Fig. 6.17A). Facies types in crevasse splays from coastal alluvial plains and fluvial fans vary but to lesser degree than in ephemeral and perennial settings. Crevasse-splays in both settings are dominated by Fsm, Sd and to a lesser degree Sm and Sr; however splays in fluvial fan settings have much greater proportions of Sp (Fig. 6.17A). Overall, crevasse-splay elements in ephemeral systems are smaller and thinner with more gravel facies than St facies. In semi-arid and fluvial fans settings the present splays are also smaller and thinner but have similar facies distributions to the humid perennial and coastal plains. Channel element thickness and associated splay element thicknesses were also investigated using the FAKTS database, with parent channel thicknesses plotted against associated splay element thicknesses (Fig. 6.16). In data from all system types, there is a positive correlation between channel thickness and splay thickness (Fig. 6.16D).

Crevasse-channel element thicknesses in all system types are between 0.2. - 17 m, with averages between 0.5- 2.3 m, (n=208) (Fig. 6.16A). Crevasse-channel elements from coastal-alluvial plain settings have the greatest average thicknesses (2.3 m); crevasse-channel element in semi-arid (1.9 m), humid (1.9 m) and perennial (2 m) settings are all of a similar thickness, whereas crevasse-channel elements in fluvial fan (1.4 m) and ephemeral (0.55 m) settings are on average thinner (Fig. 6.16A). Facies types that make up crevasse-channel elements vary in each of the system types. All crevasse-channel elements in all system types have some occurrence of Sh and all, excluding ephemeral and semi-arid settings, have occurrences of Sm, and Fsm. However, there is greater degree of variation in facies types than in crevasse-splays (Fig. 6.17A, 6.22B). All crevasse-channels in all settings except ephemeral have significant (>10%) proportions of Sm. Fl can comprise a significant proportion of crevasse-channel elements in humid and perennial settings and occurs in small proportions in coastal-alluvial plain and fluvial fan settings (Fig. 6.17B). Facies Fsm consists of a significant proportion of crevasse-channel elements from humid, perennial, coastal-alluvial plain and fluvial fan settings, whereas Sp

makes a significant proportion of crevasse-channel elements in perennial, coastal-alluvial plain settings but also semi-arid and ephemeral settings (Fig. 6.17B). Facies types in crevasse-channel elements in humid settings have little in common with those from semi-arid settings. Both have facies Sh in minor proportions (<10%), but in humid settings Fl and Fsm are the most dominant facies, whereas in semi-arid settings Sp and Sr are the most dominant facies (Fig. 6.17B). Facies types in crevasse-channel elements in perennial settings have only one facies type in common with those in ephemeral settings: facies Sp (Fig. 6.17B). All other occurring types are different. Crevasse-channel elements in perennial settings are dominated by facies Fsm (20%) and Fl (20%), whereas in ephemeral settings St (50%) and Sh (25%) are the most dominant facies types. Overall, crevasse-channel elements have very variable facies types and tend to be thinner in ephemeral and fluvial fan systems.

Abandoned channel element thicknesses in all system types are between 0.1 and 36 m, with averages between 1.3 and 5.2 m (n=334)(Fig. 6.16A). Abandoned channel elements in humid (5.2 m), perennial (5.8 m), coastal-alluvial plain (4.1 m) settings have the greatest average thickness, whereas abandoned channel elements from fluvial fan (2.7 m), semi-arid (2.3 m) and ephemeral (1.3 m) settings are far thinner (Fig. 6.16A). Facies types that make up abandoned-channel elements vary in each of the system types. In abandoned channel elements in all settings except for ephemeral settings, facies Fl occurs in significant proportions (>20%); in ephemeral settings abandoned channel elements are made up of only Fm (Fig. 6.17C). Facies types in abandoned channel elements in humid and semi-arid settings both have significant proportions of facies Fl (20-45%), as well as smaller proportions of Sp (5-15%)and Sr (10-30%); in humid settings abandoned channels have high proportions of Fsm (>30%) whereas in semi-arid setting Sr and St are present in high proportions (Fig. 6.17C). There are no common facies types in abandoned channel elements in perennial and ephemeral settings, with Fl (20%) and Fsm (30%) as the dominant facies in perennial settings whereas in ephemeral settings Fm is the only facies type (Fig. 6.17C). Facies types in coastal-alluvial plain settings are similar to those in humid and

perennial settings (Fig. 6.17C). Overall, abandoned channel elements in humid, perennial and coastal-alluvial plain settings are of similar thicknesses and facies proportions, whereas in semi-arid and ephemeral systems thicknesses are lower and the elements have markedly different facies types.

Floodplain elements in all system types are between 0.1 – 14 m thick, with averages between 1.3- 1.9 m (n=1272) (Fig. 6.16A). Floodplain elements in ephemeral (1.8 m) and fluvial fan (1.9 m) settings have greater average thicknesses than those in coastal-alluvial plain (1.5 m), perennial (1.5 m), semi-arid (1.5 m) and humid (1.3 m) settings. Facies types that make up floodplain elements vary in each of the system types with no facies common to all settings (Fig. 6.22D). Floodplain elements in humid and semi-arid settings both have significant proportions of Fl (20%) and Fr (45%) and have some proportion of facies Fsm. In humid settings, Fsm (15%), whereas in semi-arid settings Fr (20%) also makes up a significant proportion (Fig. 6.17D). Floodplain elements in both perennial and ephemeral settings both have significant proportion of Fl, but floodplain elements in perennial settings are dominated by Fsm (50%). Floodplain elements in fluvial fan settings are dominated by the facies Fr, Fl, and Fsm. Overall floodplain elements are thicker in fluvial fans and ephemeral settings, and in general are dominated by unclassified facies F-, with differing amounts of Fl and Fr.

6.5 Discussion

6.5.1 Environment of deposition

The sedimentary products in fluvial fans (Morrison Formation; Fig. 6.18) will vary from those found in coastal-alluvial plain settings (Neslen Formation; Fig. 6.19), as do the sedimentary products within the sub-environments of these depositional settings. Within these two settings the type of sedimentation varies, as is shown in the different stratigraphic architectures of the fluvial successions shown in the previous sections (Figs. 6.11, 6.12, 6.13 and 6.14, 6.15).

In coastal plain settings, particularly in humid examples such as in the Neslen Formation, the water table will be at a higher level relative to the main channel

for greater periods within the year. As a consequence, the floodplain will be wetter or even subaqueous for much of the time, which would mean that splays in the Neslen Formation could be classified as lacustrine deltas since it is likely that at least some of the splays were building into standing freshwater. This has implications for the shape of the splay deposit,and particularly the width-to-length ratios. In subaqueous deposition, the water on the floodplain is at a similar level to that in the flooding channel, which allows the sediment-laden flow coming from the channel to move more easily across the floodplain (cf. Adams et al., 2004). The configuration of the flow is more reminiscent of a radial arc, because of this the sediment is deposited equally in all directions away from the point-source that is the flood breakout; hence the higher width length ratios (Fig. 6.20A). On a subaerial less water saturated floodplain, movement of floodwater will be more likely directed by the crevasse-channel network and the slope from main fluvial channel to the distal floodplain (Fig. 6.20D).

Crevasse-splay elements in the Neslen Formation have occurrences of the facies Sd, but this is missing from the Morrison Formation, where there are still some deformed facies (Fd) but far less and only in more silt-prone units. The increased occurrence of this deformed facies could be due to the more unstable nature of the substrate on the coastal-plain depositional environment of the Neslen Formation (Fig. 6.20B). However the extended dataset of the FAKTS database deformed facies occurs in both fluvial fans and coastal plains in similar amounts, which indicates that the reduction in deformed facies in the Morrison Formation may be to do with a possible increased stability of the substrate in the Morrison Formation (Allen, 1977).

Coastal-alluvial plain settings tend to have larger channel bodies, on average, than those in fluvial fan settings. Crevasse-splay elements and all overbank elements are thicker in coastal plain settings, in both the outcrop data from this study and the FAKTS case study data, than in a fluvial fan settings. Since a link can be drawn between thicker channel deposits and corresponding thicker splay deposits (Fig. 6.10A), a reasonable assertion is that an increase in parent

channel scale in coastal plain settings determines the greater thickness of present overbank elements.

Bioturbation levels are affected by the salinity levels and sedimentation rates at time of deposition (Beynon et al., 1988; Gingras et al., 2011). An overall coastal-alluvial plain setting, such as that represented by the Neslen Formation will have reduced bioturbation due to the increased tidal-influences and corresponding salinity rise resulting in brackish stressed conditions (Shiers et al., 2014). The Saltwash Member of the Morrison Formation was deposited in a fully fluvial setting which would have been far less difficult to survive than brackish conditions; consequently the bioturbation levels (in elements that contain extensive bioturbation, crevasse-splay and floodplain elements) are far higher than in the Neslen Formation (Fig. 6.9).

Subenvironments of the Morrison Formation

The three successions in the Morrison Formation (Figs. 6.11, 6.12, 6.13) each are in different parts of the DFS fan which can have consequences for the overbank stratigraphic architectures. The Atkinson Creek succession is in the medial part of the Morrison fan (Fig. 6.4) (Owen et al., 2015). Consequently there are thick amalgamated fluvial channel belts. These cut into the present overbank deposits, and there is a reduction in the proportion of overbank deposits in the succession as a whole. Sand-prone overbank deposits, such as crevasse-splay elements, tend to be associated with the smaller ribbon channel bodies as in Interval 1 (Fig. 6.18A). This implies that overbank deposits in order to be preserved are likely to be located towards the edges of major channel belts. Floodplain elements at this site are dominated by the type of palaeosols that accumulate under drier conditions, calcisols (Frr) (Owen et al., 2015), with palaeosols that record (Facies Frg) some intermittent periods of accumulation under wetter conditions; this is likely related to local drainage conditions in the floodplain. Channel to splay grain-size ratios are similar to those in the Neslen Formation but are far lower than other parts of the Morrison Formation. This observation was unexpected considering this is the site closest to the apex of the system (Fig. 6.4), where the coarsest overbank grain sizes are generally found (Owen et al., 2015). However, there will be bypass of the coarsest

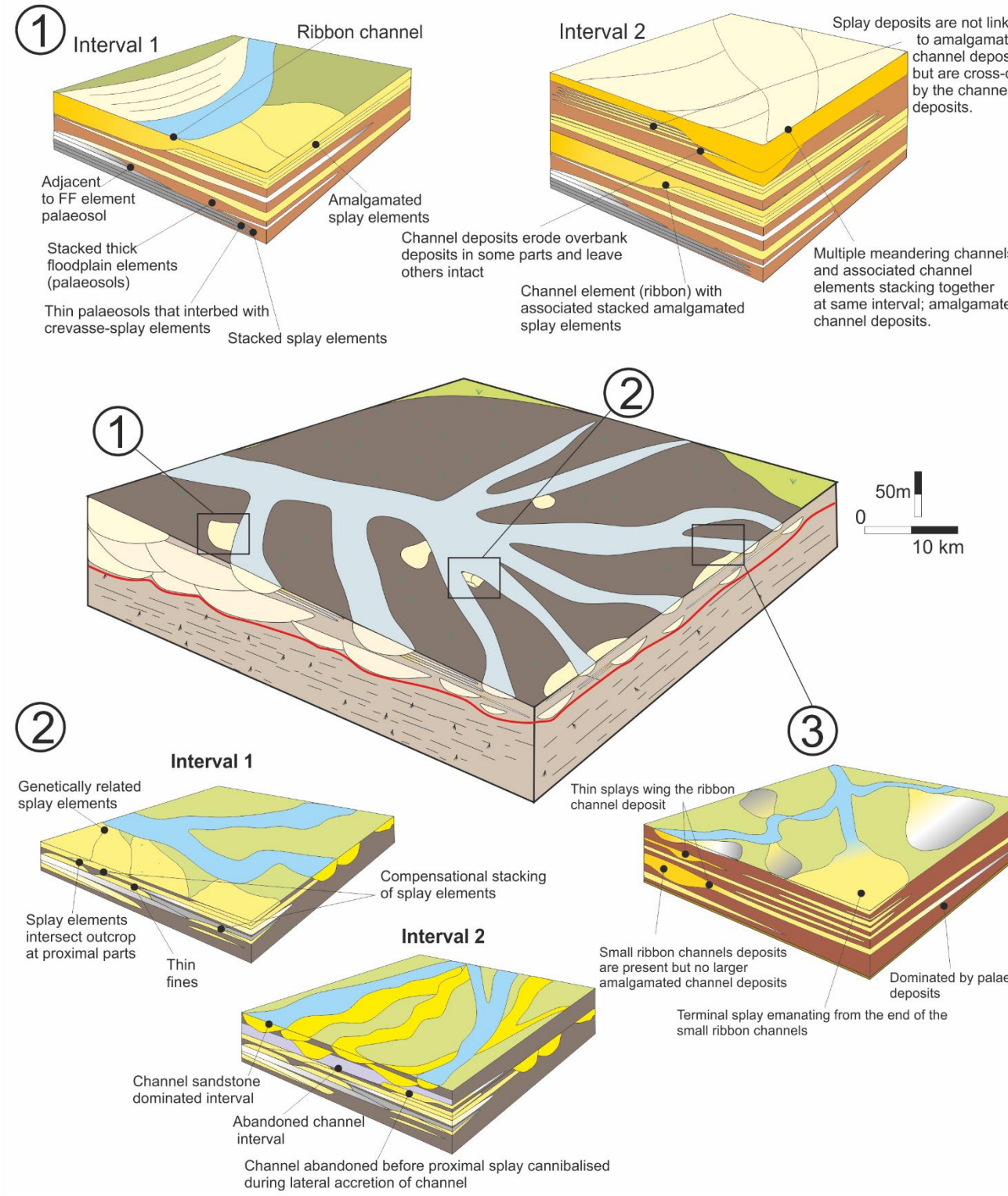

Figure 6.18: Conceptual models of evolution of successions at each presented logged panel. The models depict the intrinsic variability in architectures within each formation. (1) Models for Atkinson Creek, Morrison Fm (2) Models for Yellow Cat Canyon, Morrison Fm (3) Models for Colorado National Monument, Morrison Fm.

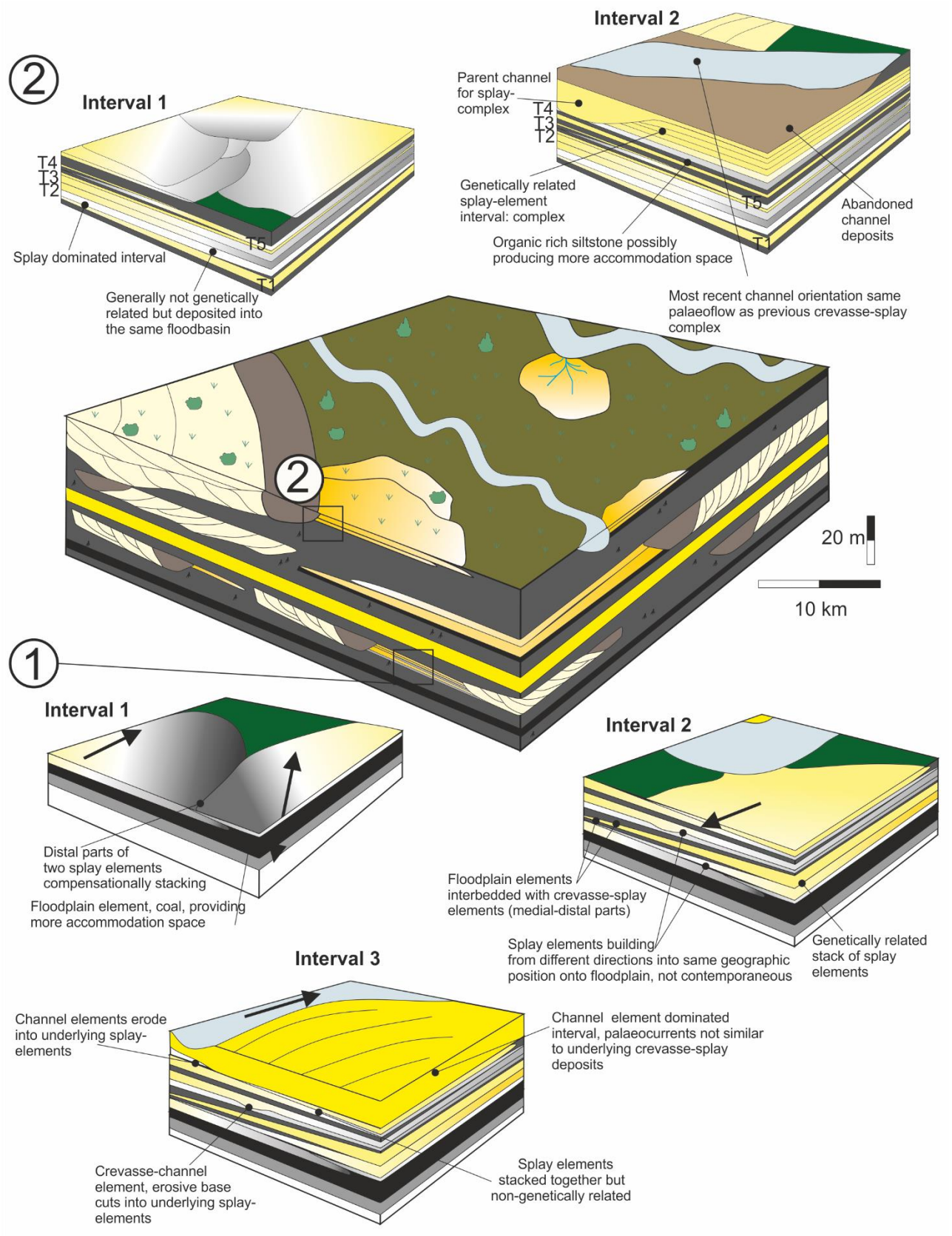

Figure 6.19: Conceptual models of evolution of successions at each presented logged panel. The models depict the intrinsic variability in architectures within each formation. (1)Models for Tuscher Canyon, Neslen Formation (2) Models for Crescent Canyon, Neslen Formation.

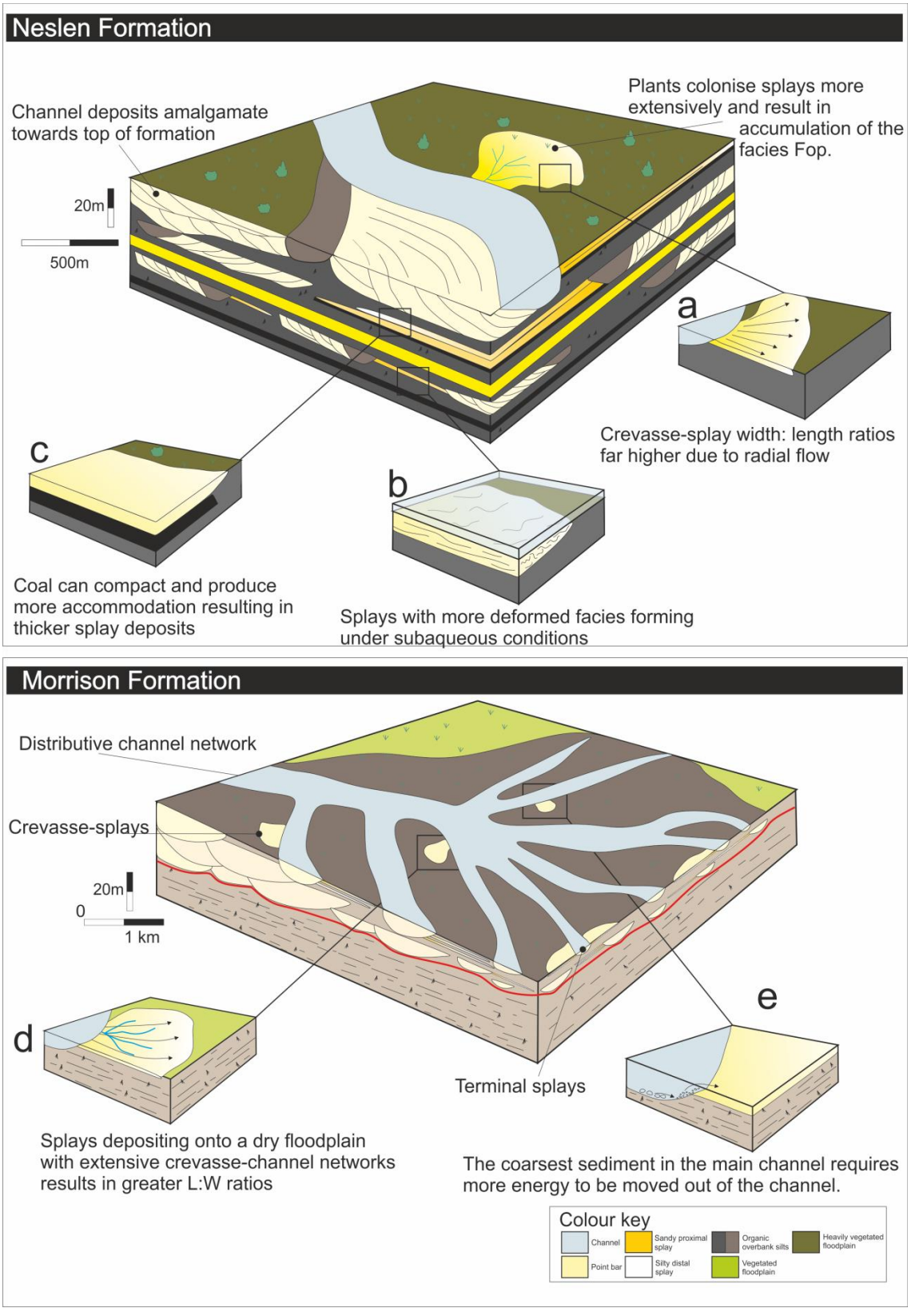

Figure 6.20: Overall models for Neslen and Morrison Formation and overbank deposits found within.

sediment within a DFS to another part of the fan, which can lead to anomalies in grain size (Weissmann et al., 2013).

The Yellow Cat succession is in the medial-distal part of the Morrison fan (Fig. 6.4) (Owen et al., 2015). Consequently, there is an increase in the proportion of overbank deposits in this succession (Fig. 6.18B). However, the channel elements are coarser than any others recorded from other studied intervals (Fig. 6.10, 6.18B) (cf. Owen et al., 2015). Crevasse-splay elements are found within an interval towards the middle of the succession. Many of these splay elements stack compensationally, which is here interpreted in terms of a reduction in accommodation space at this point of the fan. However, the occurrence of compensational stacking patterns could be linked to the greater sediment supply to this area, as indicated by the coarse extensive channel deposits in this area, overwhelming the local accommodations. There is an extensive floodplain dominated interval at the base, but most floodplain elements are thin and interbeded with splays, with insufficient time for extensive palaeosol accumulation (Kraus, 1987). Floodplain elements have less of the facies Frr more of the Frp and Frg, which are mottled by water-marks and blue-green in colour indicating a more waterlogged environment (Mack, 1993). In the crevasse-splay elements at this location, unlike other sites in the Morrison Formation, there are less well-defined sedimentary structures. This is likely due either to rapid deposition by turbulent flows that would not allow formation of sedimentary structures or due to deformation of the sediments on a more waterlogged floodplain. Splay element grain size is not particularly coarse (lower very-fine sandstone) considering how coarse the channels are; however this could because transporting the coarsest grain sizes out of the channel is difficult and would take greater floods than those that created these deposits (Fig. 6.20E).

The Colorado National Monument outcrops are located in the distal part of the Morrison fan (Fig. 6.4) (Owen et al., 2015). This part is dominated by thinner ribbon channel bodies and overbank deposits such as splay elements and floodplain elements (Fig. 6.18C). Less sediment reaches the distal reaches of the fan and a greater amount of accommodation results in less amalgamation of

deposits (Weissmann et al., 2013; Owen et al., 2015). This results in ribbon channel bodies being dominant over the amalgamated fluvial channel deposits particularly compared to the situation at Atkinson Creek. The splays are associated with these ribbon channels and are interbedded with floodplain elements. The crevasse-splay elements have similar facies to those found at the Atkinson site; the floodplain elements facies have very little palaeosol facies, and those that are present are indicative of a wetter floodplain at time of deposition (Frg), indicating that there was not enough time between splay element depositions for palaeosol accumulation (Kraus, 1987). The splay elements are quite coarse (upper very-fine sandstone) considering the feeder channel grain size (upper fine sandstone); this could be because they are not necessarily true crevasse-splay deposits as such, but instead could be classified as terminal splays (Nichols and Fisher, 2007), hence the similar grain sizes to the feeder channel deposits (Fig. 6.18C) (Donselaar et al., 2013).

Subenvironments of the Neslen Formation

The two successions in the Neslen Formation (Figs. 6.14, 6.15) are located in different zones of the Neslen Formation (Shiers et al., 2014) which can have consequences for the overbank stratigraphic architectures. The evolution of the coastal alluvial plain over time will have an important impact on the architectures found at the two successions.

The Tuscher site is part of the Palisade Zone, which has a high proportion of coal-prone elements (Figs. 6.4, 6.14) (Shiers et al., 2014). In this succession, particularly in interval 2, the coal-prone floodplain elements are topped by crevasse-splay elements (Fig. 6.19A). Splay elements in this succession are thicker than any other studied succession in both Neslen and Morrison formations. However parent channel sizes, are no thicker than channel elements at any of the other studied successions. Since the increased thickness is not due to parent channel size, instead the increased thicknesses could be due to the increased amount of coal-prone floodplain elements compacting and producing more accommodation space (Fig. 6.20C) (Nadon, 1998; Shiers et al., 2017) (Fig. 6.8; 6.10).

The Crescent Canyon site is part of the Chesterfield Zone, a younger stratigraphic part of the formation, and in terms of environment of deposition can be placed on the alluvial plain, where less marine influence is recorded. Here, channel bodies begin to amalgamate at the Crescent Canyon section and coals are absent (Fig. 6.4) (Shiers et al., 2014; 2017). The splay elements are thinner than in Tuscher Canyon even though the channel elements are thicker than in Tuscher Canyon, perhaps because of the loss of the organic-rich coals which resulted in no addition to the local accommodation space. The coals are probably absent because the palaeoenvironment changed from a waterlogged coastal-plain setting to an alluvial-plain setting (Shiers et al., 2014). Channel grain size is greater than in Tuscher example and so is the splay grain size (Fig. 6.8). This could be due to middle-upper parts of Neslen Formation having channel-deposits that are more amalgamated (Shiers et al., 2014).

6.5.2 Climate and stream discharge controls on overbank sediment accumulation

There has been a wealth of studies looking at intra-fluvial deposits such as channelized elements (Holbrook et al., 2006; van Dijk et al., 2009) and palaeosols (Retallack 1988; Kraus and Aslan, 1993; Mack et al., 1993; Kraus, 1999), where one of the major controls has been identified as climate (Shanley and McCabe, 1994; Blum, 2000; Demko et al., 2004; Dreyer, 2009; Arostegi et al.,2011). Climate has many secondary effects particularly on discharge variability (Vandenberghe, 2002), sediment supply (Stuart, 2015) and the vegetation types found in an area (Jobbágy and Jackson, 2000). Each of these will have an impact on the stratigraphic architecture of a succession.

Stable perennial environments with regular flooding events will produce larger splays (Fielding, 1986; Benedetti, 2003; Miall, 2014). The Neslen Formation is a seasonal environment subject to perennial water discharge with regular flooding events (Shiers, 2017) and the splay deposits in the Neslen Formation are larger than those in the Morrison Formation (Fig. 6.8). Similarly, in the FAKTS case studies, splay deposits and modern morphological examples are larger in humid than in semi-arid environments (Fig. 6.17).

In both the studied successions and the literature data focussed on examples from humid and semi-arid settings overbank elements are consistently larger, both in thickness and lateral extent both widths and lengths) (Fig. 6.8, 6.15). Considering that the Neslen Formation is thought to be a humid setting with seasonal or even monsoonal variations in precipitation (Fricke et al., 2010) and the Morrison Formation is considered to have been deposited under a semi-arid climate (Demko, 2004; Owen et al., 2015). There might have been an increased amount of clastic sediment transport in the Neslen Formation depending on how humid and monsoonal the climate during Neslen formation was and if the climate regime during the Morrison Formation was semi-arid. However, the difference is unlikely to have been markedly different, so perhaps there is not an easy direct link between climate and deposit scale (Fig. 6.22) (Cecil, 1990),

A humid climate results in more stable flood flows with a more steady discharge. This results in flows that gradual slow and allow for infilling of crevasse-channels with silt-sized grains not just sand-size. Crevasse-channel elements are sandstone-prone not only in the Morrison Formation, but also siltstone-prone and sandstone-prone in Neslen Formation. This trend is also seen in the FAKTS data in which the crevasse-channels are dominated by all silt-prone facies in humid systems, but less so in the semi-arid settings (Fig. 6.17B).

The climate will have also affected the plants that colonise the floodplain. In the crevasse-splay elements, roots are common but at higher intensities in the Neslen Formation (Fig. 6.9). In the floodplain elements, the amounts of roots are comparable. Splay elements in the Neslen Formation also often have in the most distal part the facies Fop, which is often rooted throughout, which is missing in the Morrison Formation. This indicates that although plants might find it easier to colonise splays under the humid greenhouse conditions of the Cretaceous (Saward, 1992) there were still plants surviving and being preserved within the floodplain elements in the Morrison. The plants growing during the time of Morrison deposition either just did not colonise the splays so extensively or perhaps were not of types that produce extensive root networks.

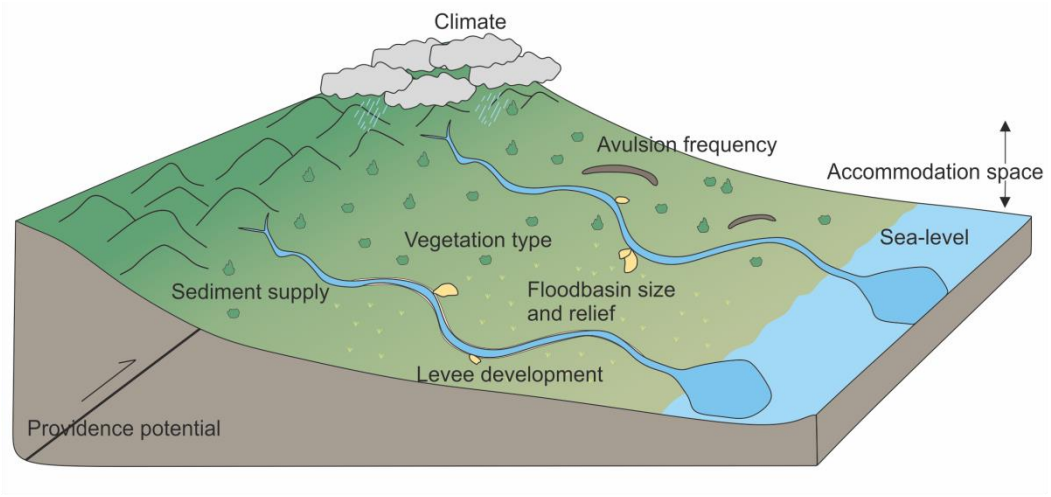

Figure 6.21: Conceptual image to illustrate the different possible interplay of controls on a system.

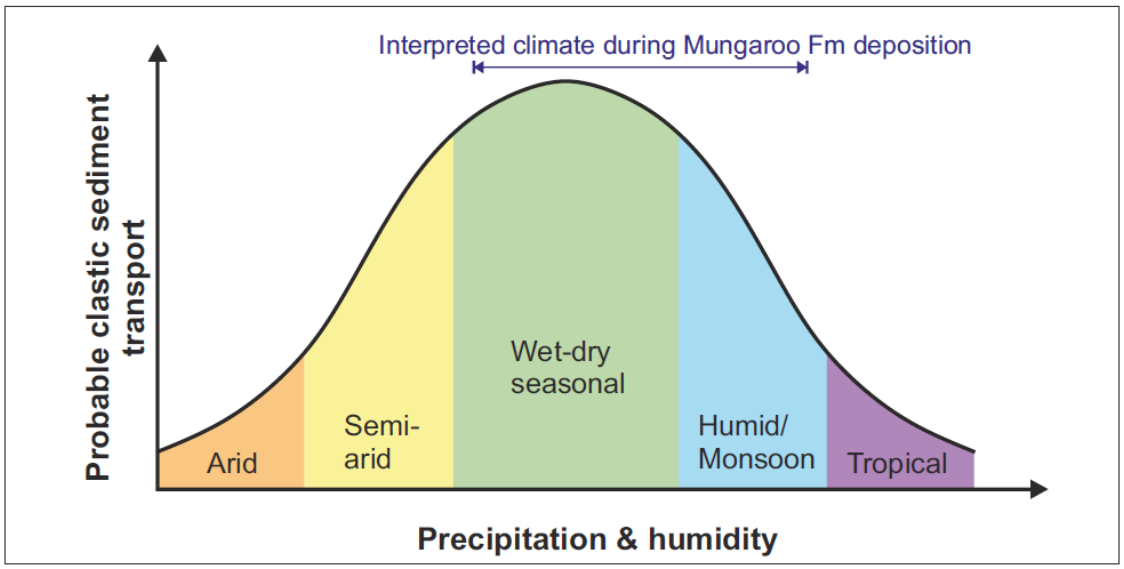

Figure 6.22: Response of sediment transport to climate change (after Cecil, 1990

6.5.3 Influences of local accommodation of floodplain; autogenic controls on overbank deposition

Local accommodation state will have a strong influence on thicknesses variations of splay elements within a formation, with areas with more local

accommodation space having the potential for thicker splay elements (Zwoliński, 1991; Bristow et al., 1999). However, local accommodation space is more likely to influence the range in thickness of the elements of a formation rather than the average thicknesses of the elements in the formation overall, i.e. the effects will be localised to where local accommodation space is greater.

Topographic variations in the floodplain will have an impact on the length-width ratios of splay elements. If depressions exist that are parallel to the main channel and parallel to the levees then the floods will be funnelled towards these lower areas resulting in splays with lower length-widths ratios.

Undulating in the floodplain surface may also impact the crevasse-splay element geometries, undulations on the floodplain will cause undulating geometries observed in the Morrison Formation splays (Fig. 6.8).

6.6 Conclusions

In general, all overbank elements are bigger in the Neslen Formation than in the Morrison Formation. Crevasse-splay elements in Neslen have widths greater than lengths, and in the Morrison widths and lengths are similar, indicating a planform difference in splay geometry. There are more occurrences of deformed facies types in the Neslen Formation than in the Morrison Formation. Floodplain elements in Morrison have palaeosols that indicate drier periods but also wetter conditions whereas the Neslen has more coal-prone and organic rich siltstones facies indicating longer periods of stable wet conditions on the floodplain.

Climate controls overbank deposition directly and indirectly. Climate directly influences the occurrence of palaeosols, which are prevalent in Morrison and directly influenced the occurrence of coals which are present in Neslen. Overbank elements are smaller in semi-arid climate this could be linked indirectly to a lower slightly sediment transport in semi-arid setting than humid setting, but the differences are not very consequential. More likely there is more complex interplay of factors related to climate, such as vegetation and

palaeosol type formation. Vegetation is also influenced by climate. Hence there are fewer roots in the Morrison than in Neslen.

In coastal plain settings, there are more deformed facies due to waterlogged sediments and less bioturbation due to salinity stresses. In the Morrison fan overbank deposits are more prevalent distally; local factors such as sediment bypass and deposition down-fan can produce areas such as at Yellow Cat Canyon where sediment is far coarser than other examples and local drainage factors can result in floodplain sediments that are dry palaeosols or wet-damp palaeosols.

Local autogenic influence are also important, with local variations in floodplain accommodation increasing or decreasing crevasse-splay element size; variations in floodplain shape affect geometries of crevasse-splay bodies in both plan-view and cross-sectional view.

Chapter 7 Discussion

This chapter integrates the results of the preceding chapters and presents a wider discussion of the stratigraphic expressions, organisation and controls on fluvial overbank and crevasse-splays with examples from modern fluvial systems and other ancient successions. The controls on the variations in crevasse-splay deposits, how to recognise levels of organisation in fluvial overbank successions, and how to classify in a meaningful way are considered. The controls on overbank deposition, accumulation and preservation of fluvial overbank successions are discussed. Reservoir implications of this study are also considered.

7.1 Research question 1: What is the detailed morphology, sedimentology and depositional architecture of overbank elements?

7.1.1 Facies belts within crevasse-splays

In this study, depositional sub-environments of individual splay elements have been sub-divided based on lithofacies types (Chapter 3.6.2) into proximal (i.e. to the fluvial sediment source), medial and distal facies belts, in a similar manner to schemes developed for larger fluvial distributive systems (e.g., Nichols and Fisher, 2007; Weissmann et al., 2010; Owen et al., 2015). This is a similar approach to other studies that distinguish sand- and silt-prone splay components (Farrell, 1987; Mjøs et al., 1993; Behrensmeyer et al., 1995; Bristow et al., 1999; Arnaud-Fassetta, 2013; van Toorenenburg et al., 2016), which are also interpreted as representing deposition in relatively proximal or distal regions in relation to channel deposits (Chapter 2.4.1).

Interpreted proximal facies belts are the most sand-prone and typically comprise an association of structureless sandstones (Sm), cross-bedded sandstones (St/p) and rippled sandstones (Sr). Subordinate facies include deformed silt- and sandstone (Fd) and poorly sorted siltstones (Fp). Interpreted medial facies belts comprise an association of deformed sandstones (Sd),

deformed silt- and sandstone (Fd), poorly sorted siltstones (Fp/Fop) and rippled sandstones (Sr). Interpreted distal parts predominantly comprise an association of deformed silt- and sandstone (Fd) and poorly sorted siltstones (Fp/Fop) (Fig. 4.6, 4.7 and 7.1).

In the splay deposits studied in this work, the proximal parts did not form the highest volume component of the preserved deposit; rather splays are fringed with extensive silt-prone distal parts (Fig. 7.1). In these deposits, the volume of the interpreted proximal component varied significantly, between 19%–47%. However, in examples from other systems, studied by other authors (e.g. Olsen, 1989), the proximal facies belt forms the dominant component by volume of the preserved splay deposit. For example, in ephemeral settings multiple case studies from the FAKTS database indicate that the splay deposits are almost entirely comprised of sand-prone facies (Fig. 6.17). Previously published examples of modern–recent splays and ancient splay deposits generally have a silt component (Chapter 2.4.1; Farrell, 1987; Smith and Perez-Arlucea, 1994; Miall, 1994; Bristow et al., 1999; Arnaud-Fassetta, 2013). However, the relative proportion of the sand-prone component in the preserved splay deposit will be markedly influenced by the type and calibre of sediment entrained by the floodwaters, which in turn is controlled by several parameters such as climate type and sediment supply from hinterland geology (discussed in Chapter 7.3).

The planform shapes of these facies belts or zones are likely to vary considerably (Fig. 7.1) due to spatial variations in flow energy, sediment calibre and flow distribution during each flood, the distribution of accommodation in the floodbasin, and temporal variations in these factors between successive floods (e.g. flow-deposit interactions in the floodbasin). The simplest architecture model depicts a series of concentric semicircles of facies belts, which assumes a radial decrease in flow energy and progressive sorting away from the splay point source (Fig. 7.1). However, this is precluded when crevasse-channel networks form, which result in the transportation of different sediment grain sizes to different parts of the splay body, which can cause significant proximal-to-distal and transverse-to-axial variability in grain size and facies proportions (Smith et al., 1989; Fig 7.1). In addition, the distribution of sediment being

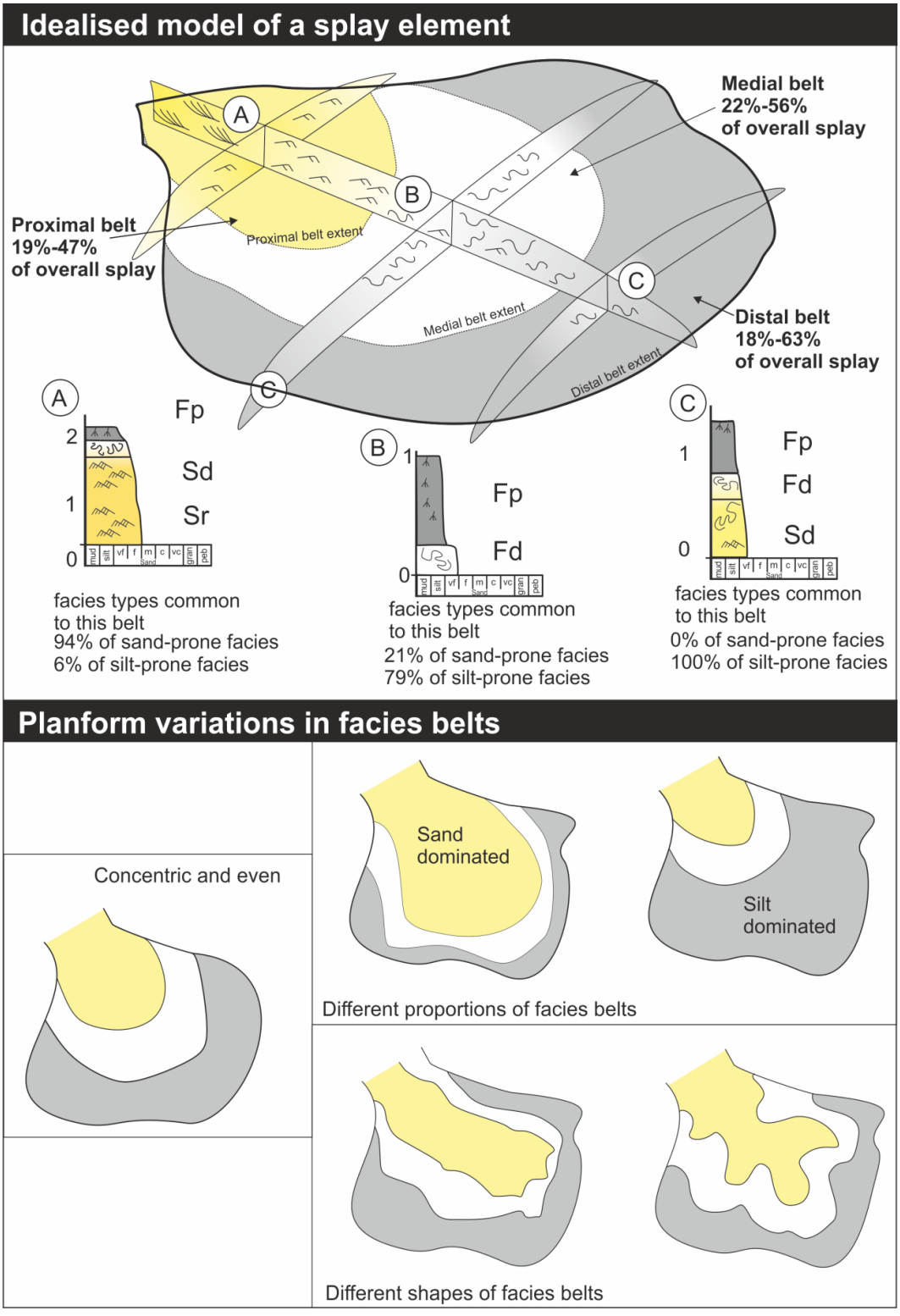

Figure 7.1: Idealised model of a splay element showing the idealised subdivision into facies belts and the vertical sedimentary profiles and variation in facies proportions for each facies belt (above). Conceptual diagram depicting how facies belts may vary in shape and proportion of overall splay (below).

transported by the flood may result in heterogeneous deposits, with potentially significant differences in the components of relatively coarse- and fine-grained sediment between different parts of the flood deposits (Moss, 1972; Abbott and Francis, 1977; Leeder, 1983).

Finally, there may be a bias in the sedimentological and stratigraphic reconstruction of ancient splay deposits due to outcrop patterns; the apparent variability in sedimentological and stratigraphic character of splay deposits can vary significantly depending on outcrop orientation (Fig. 7.2). For example, for a simple sand-dominated and lobate splay, a proximal-to-distal (sub-parallel to the long axis orientation) or axial-to-transverse (i.e. highly oblique to the long axis orientation) cross-section situated in a relatively on-axis location (B) will tend to exhibit a relatively simple, homogeneous and sand-prone architecture, whereas a proximal-to-distal (i.e. sub-parallel to the long axis orientation) cross-section in a relatively off-axis position (A) will tend to be relatively heterogeneous and will typically comprise laterally variable sand-prone to silt-prone facies transitions (Fig 7.2).

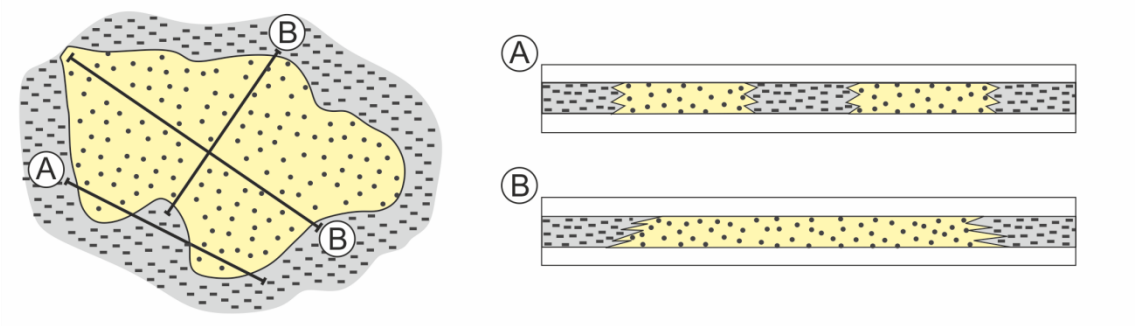

Figure 7.2: Conceptual model showing the possible outcrop bias that can difficulty in the reconstruction of ancient splay deposits.

7.1.2 Crevasse splays and terminal splays

A crevasse-splay is where the river breaks its banks during a flood and modifies or destroys the levee at a point allowing sediment-laden flows onto the floodplain (Bridge, 1984; Mjøs et al., 1993; Miall, 1996). A terminal splay is commonly defined as a lobe-shaped deposit located at the end or terminus of a

river. Commonly, such deposits are related to unconfined sheet-like flows that propagate over a normally dry floodplain (e.g., Lang et al., 2005; Fisher et al., 2008).

Despite the differences in fluvial depositional sub-environments of crevasse and terminal splays (Chapter 2.4.1), their deposits are broadly similar. Both crevasse and terminal splay deposits are thin between 0.5 m- 2 m (see Chapter 2.3.2 for more details) and generally become finer-grained in the distal and lateral (i.e. on-to off-axis relatively to the splay source) direction (Chapter 2.4.1, Chapter 4.6.2; Fisher et al., 2008). Furthermore, both types of deposits comprise associations of similar facies that are arranged into proximal-to-distal and axial-to transverse facies belts; cross-laminated sandstones and rippled sandstones to mainly structureless or laminated fine-grained facies transitions are typical (Chapter 4.6.2, Chapter 7.1.1, Fisher et al., 2007, 2008).

However, despite the sedimentological and stratigraphic similarities of crevasse-and terminal-splay deposits, their stratigraphic relationships to adjacent fluvial successions will be different (Fig. 7.3). Assuming complete preservation of a crevasse-splay deposit, it should be connected to the parent channel at the edge of that channel (Fig. 7.3A). In contrast, the proximal component of a terminal splay deposit will likely be amalgamated or cannabilised by propagating channel-fill in this proximal splay region. The grain size range of the splay deposit is likely to be similar to that preserved in the attached channel-fill. Consequently, it may be difficult to distinguish the terminal-splay deposit from the parent channel deposit other than by the architecture (Fig. 7.3). Crevasse-splays are commonly associated with well-defined crevasse networks that are active for much of the splay lifespan and produce associated deposits (Smith et al., 1989; Farrell, 2000). However, terminal splays occur at the end of distributive fluvial systems, commonly in sandy or silty systems developed in arid or semi-arid settings where flow tends to be poorly or non- channelized. Therefore, terminal-splay deposits in such settings are less likely to have a channelized architecture (Fig. 2.12; Fisher et al., 2007; Fisher et al., 2008).

The majority of the splay elements considered in this study are likely to be crevasse-splay rather than terminal-splay elements. This interpretation is based partly on an assessment of the broader sedimentological context of the studied formations. The fluvial systems of both the Castlegate and Neslen formations terminated at the coast of the Western Interior Seaway (Ryer and McPhillips, 1983; Cole, 2008), whereas terminal splays form most commonly at the termination of fluvial systems onto a dry floodplain, playa or lake bed (Fisher et al., 2007). In the DFS represented by the Morrison Formation more care must be taken given that there is an increased probability of channel termination within the interpreted DFS (Owen et al., 2015). For this succession, most the studied splay deposits were likely to have accumulated as crevasse-splay elements because the study sites are situated in the interpreted medial part of the Morrison fan (Atkinson Creek, Yellow Cat Canyon, Slick Rock and Naturita sites) and/or have architectural relationships with adjacent channel bodies consistent with a crevasse-splay interpretation (Owen et al., 2015) (Fig. 6.11). In relatively distal parts of the DFS represented by the Morrison Formation, some of the studied sites are more likely to be terminal splay deposits. For example, in the Colorado National Monument region, the preserved splay bodies exhibit architectural and sedimentological relationships with adjacent small ribbon channel bodies. These relationships are consistent with terminal splay interpretations, including amalgamation, channel and wing geometries and similar grain sizes (Fig. 6.13).

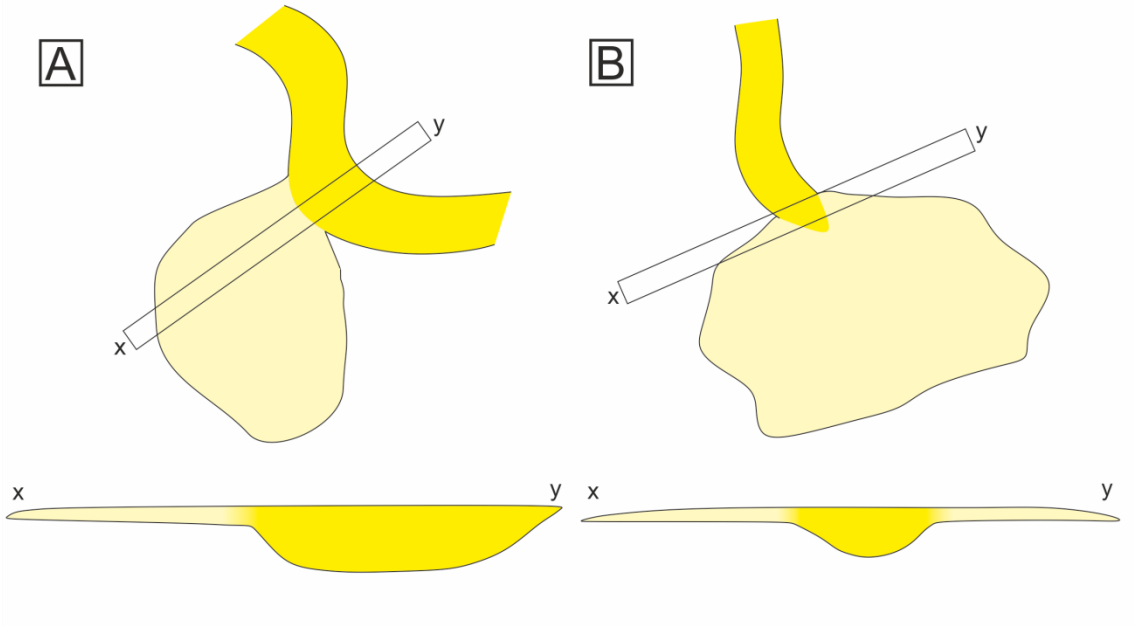

Figure 7.3: Conceptual model showing the differing relationships of crevasse-splays (A) and terminal-splays (B), and their deposits, with parent channel bodies.

7.1.3 Impacts of crevasse-channel networks on morphology of the associated crevasse-splay deposit.

The degree to which crevasse channel networks are developed will impact splay morphology. When crevasse-channel network development is absent or minimal, the flow is not channelized and deposition will be unconfined, typically resulting in development of a lobate plan-form geometry (Fig. 7.4A). The geometry of such a deposit would be relatively sheet-like (Fisher et al., 2007; Cain and Mountney, 2009; North and Davidson, 2012).

When a crevasse channel network is developed and active for the majority of a splay's lifespan, the flow is likely to be mostly confined to the crevasse channels. However, the observations that splay deposits most commonly comprise interconnected sand-bodies might suggest that flows in splays are not always confined, with the periods of unconfined flow resulting in the deposition of connecting sand (or relatively coarser grained sediment) bodies. This is similar to Stage 3 splays of Smith et al. (1989) (Fig. 2.13, 2.17, 7.4). Nonetheless, for splays with well-developed crevasse channel form, especially

given that once channel networks are developed, they are likely to be re-occupied and further developed by succeeding episodic flows (Smith et al., 1989).

The planform morphologies of crevasse-channel networks is also worthy of further consideration. Where the crevasse-splay channel network comprises a single unbranching channel, the resultant crevasse-splay deposit will tend to develop a relatively elongate planform geometry (Fig. 7.4B, 7.4C). By contrast, if the crevasse-channel network comprises distributive channels, the crevasse-splay deposit is likely to develop a lobate plan-form geometry (Fig. 7.4C, 7.4D). Consequently, the development and subsequent re-occupation and migration of intra-splay channel networks are the fundamental control on splay cross-section architecture and planform geometry.


A
Unconfined flow
Secondary channel
© 2017 Google
Image © 2017 DigitalGlobe
Google earth
Imagery Date: 2/11/2013 15°44'37.67" S 46°56'48.01" E elev 5 m eye alt 2.25 km

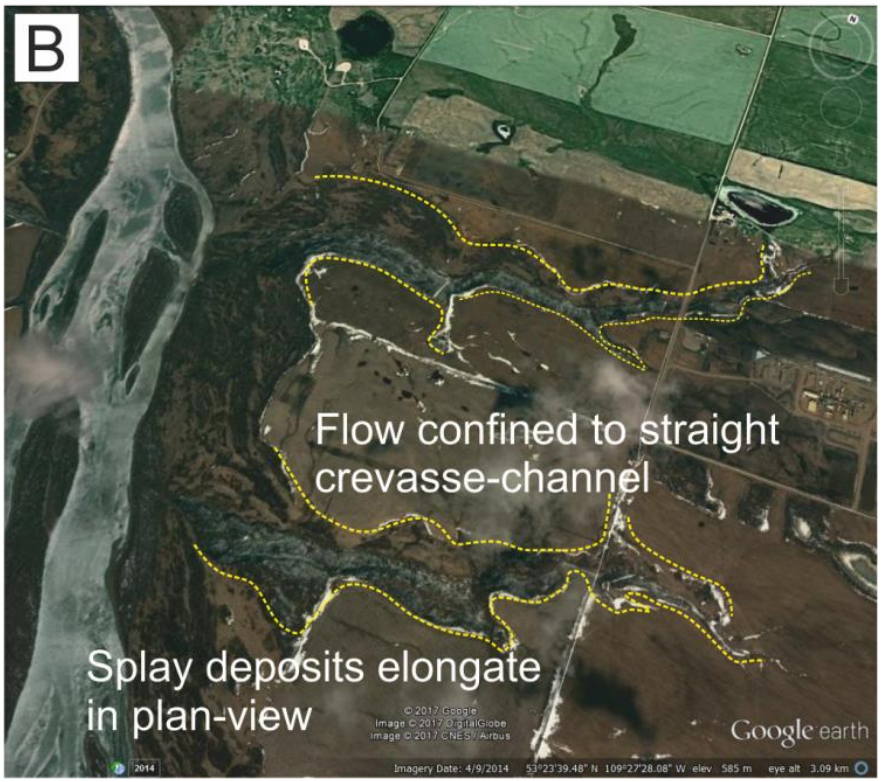
B
Flow confined to straight crevasse-channel
Splay deposits elongate in plan-view
© 2017 Google
Image © 2017 DigitalGlobe
Image © 2017 CNES / Airbus
Google earth
Imagery Date: 4/9/2014 53°23'39.48" N 109°27'28.08" W elev 585 m eye alt 3.09 km

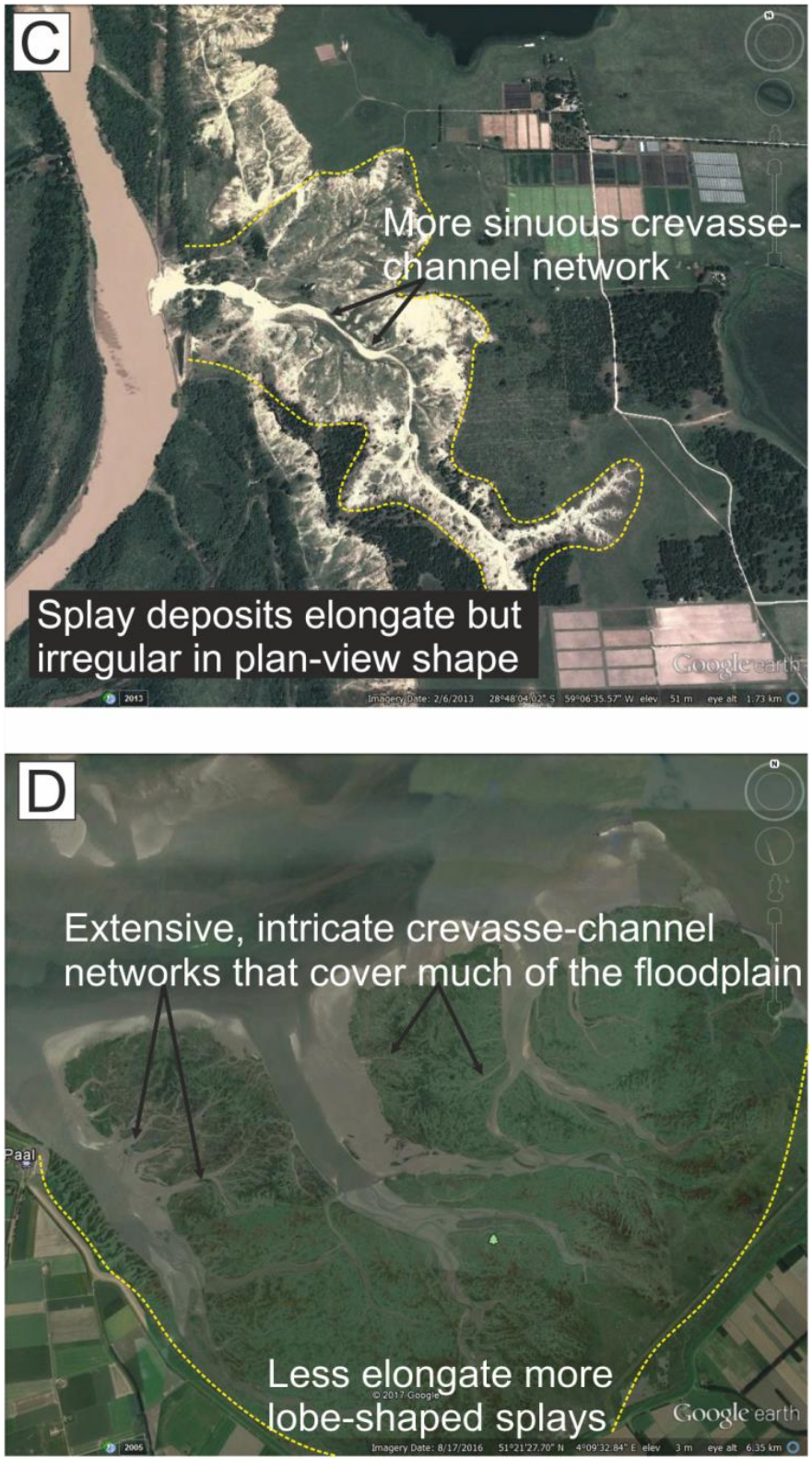

Figure 7.4: Modern crevasse-networks in Mahajamba River, Northern Madagascar; Saskatchewan River, Canada; Parana River, Argentina; Rhine River, Netherlands.

7.1.4 Summary

Splay deposits can be divided into sub elements based on the relative proportion of facies, especially the distribution of sand-prone facies. The relative proportion of sand-prone facies by volume in crevasse-splay deposits is highly variable (19 to 47%), but in the studied deposits, they do not comprise the dominant facies type. Splays may be either crevasse-splays, which result from flooding and subsequent breakout of the channel levees, or terminal-splays formed at the termination of channels on a dry floodplain or lake (more common in arid settings). Crevasse- and terminal-splay deposits may possess very similar internal facies associations. For example, proximal-to-distal thinning and fining trends. However, they are likely to have different relationships with surrounding fluvial elements. Channel networks are likely to be more developed in crevasse-splays; channel networks are likely to be less developed in terminal splays because at the end of the fluvial channel, the energy of the flow is low resulting in a decreased capacity for channel network development. Crevasse-channel planform morphology may exert an important effect on the morphology of the resultant crevasse-splay deposit. Splays with a single long-lived crevasse channel will tend to develop a relatively elongate associated deposit, whereas a crevasse-splay with a more distributive crevasse-channel network, will have a relatively lobate planform geometry.

7.2 Research question 2: What is the stratigraphic organisation of fluvial overbank successions?

7.2.1 Stacking styles of crevasse-splays

The stacking style of crevasse splay may vary between compensational, progradational, aggradational to retrogradational. Compensational stacking occurs where the topography formed by preceding splay deposits causes lateral offset of succeeding splay deposits, which exploit the adjacent topographically lower area (Fig. 7.5; Straub et al., 2009). Compensational stacking requires little to no confinement by floodplain topography and is genetically related to the sedimentary dynamics of the splay complex. Compensational stacking of splay deposits has been identified within the multiple stacked splay deposits in the formations studied here (Fig. 5.7, 6.12), and has additionally been identified in stacked splay deposits in several other studies (e.g. van Toorenenburg et al., 2016; Gulliford et al., 2017). When floodplains are extensive and unconfined, splays will inherently generate depositional topography that will influence the flow path of succeeding floods. Consequently, compensational stacking is likely to be a feature of stacked splay deposits (complexes).

Development of progradational stacking requires high rates of sediment input, well-developed crevasse-channel networks and/or powerful erosive flood events, which can erode and re-deposit preceding deposits in relatively distal and/or lateral positions (Chapter 5). This type of stacking can be identified in splay successions when relatively proximal splay-element deposits overly relatively distal splay-element deposits (Fig. 6.14, 6.15, 7.1). However, given that preceding splays will generate depositional topography, progradational stacking is likely to occur in combination with compensational stacking. Published examples of progradational stacked crevasse-splay complexes are rare. However, Mjøs et al. (1993) indicate that the “composite” splay sandstones are likely to record an initial phase of rapid progradation.

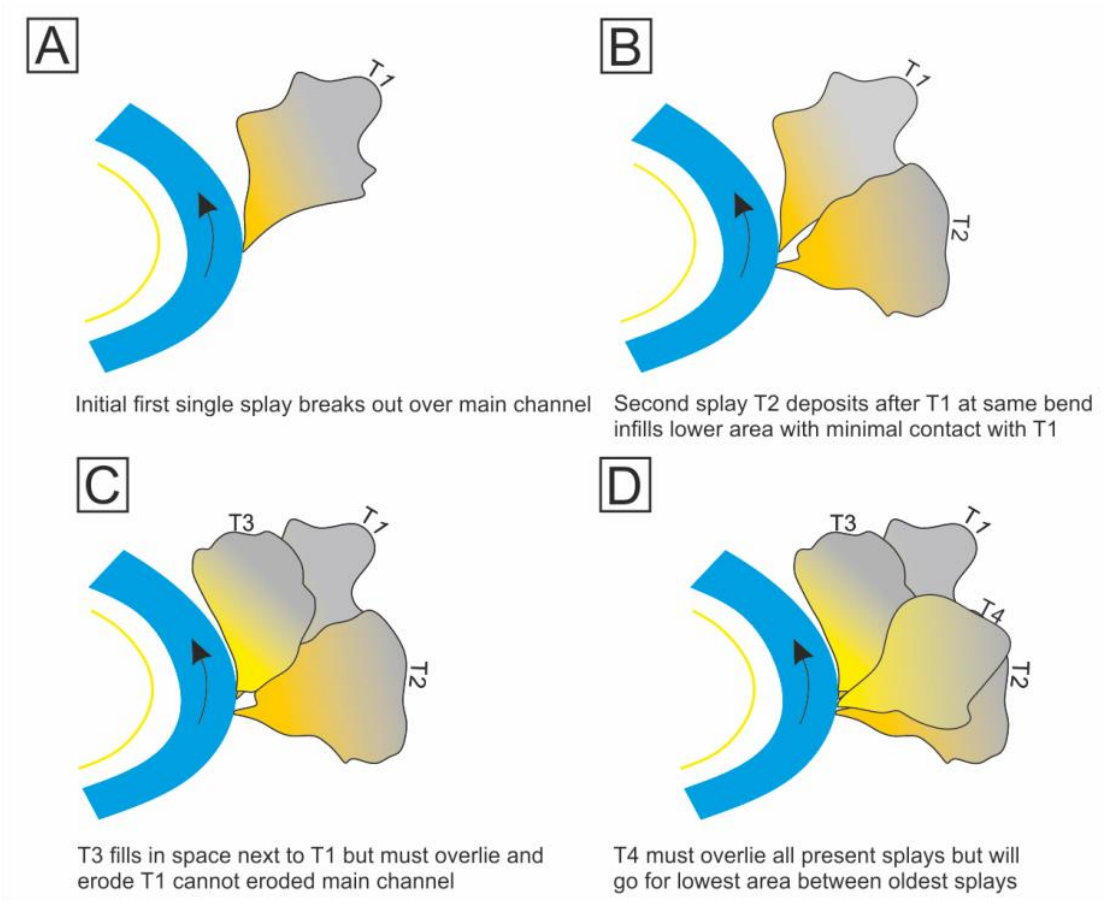

Figure 7.5: Conceptual diagram for the development of compensational stacking in a crevasse-splay complex by succeeding, laterally-offset splay development.

Aggradational stacking is likely to develop when floodplain accommodation is relatively confined, for example due to the presence of topographic lows on the floodplain. Aggradational stacking of splay elements was not observed in the studied deposits, nor are there definitive published examples of aggradationally-stacked crevasse splay complexes. However, more generally, aggradational stacking of splay- and lobe-type depositional features is possible, including, for example, delta lobes (at the parasequence to parasequence-set architectural level (Van Wagoner et al., 1990) and deep-water lobes (Burgreen and Graham, 2014; Spychala et al. 2017). However, this stacking pattern requires relatively high degrees of confinement (Burgreen and Graham, 2014), which might preclude the occurrence of this style in the types of splay deposits in fluvial floodbasin settings.

7.2.2 Possible interactions of splay complexes

Splay element stacks (complexes) may interact across the same area of floodplain. This interaction is dependent on splay geometry and orientation, which is primarily controlled by the morphology and hydrodynamics of the parent channel. Both complexes would have different directions of palaeoflow and thinning and fining trends; both complexes would thin and fine towards each other (Fig.7.6).

If deposition was contemporaneous in these scenarios, splay elements within the each of the complexes could be interstratified across the extent to which the overlap occurred (Fig.7.6A–B). Overlap of the distal splay-elements is most likely to occur and its identification in outcrop would rely heavily on sufficiently good-quality outcrop that enabled the lateral tracing out of beds from more proximal to distal positions in both splays. Identifying the relatively proximal to distal direction may also rely on sufficiently large outcrop extent (to recognise the possible gross trends in sand content) and/or the identification of the associated parent channels. For deposition to be contemporaneous it would require two simultaneously active channels to be in relatively close proximity. This is because the studied splay elements rarely exceed 2,000 m in diameter (Chapter 4) and the largest recorded is a 4,490 m-wide splay associated with the Rhone River (Arnaud-Fassetta, 2013). This relatively close proximity of active fluvial channels is a high possibility in a DFS system (Fig. 7.6). Single meandering channels, by their morphology and river type, are less likely to have closely adjacent and simultaneously active channels, but relatively tight meanders enclosing floodplain areas with a similar lateral extent to splay elements do occur (Fig. 7.6B). In the scenario where two (or more) non-contemporaneous and non-genetically related splay-complexes (i.e. developed from separate parent channels) build into the same floodplain area, complexes would be stack above or below one another, possibly with intervening floodplain elements separating the two (Fig. 7.6C). However, without the development of intervening floodplain elements, the non-genetic relationship may be difficult to distinguish from a genetic relationship but non-contemporaneous stacking relationship (i.e. same parent channel but successive depositional time

periods). Confident interpretation requires identification of the relationships of the splay elements and their parent channel bodies.

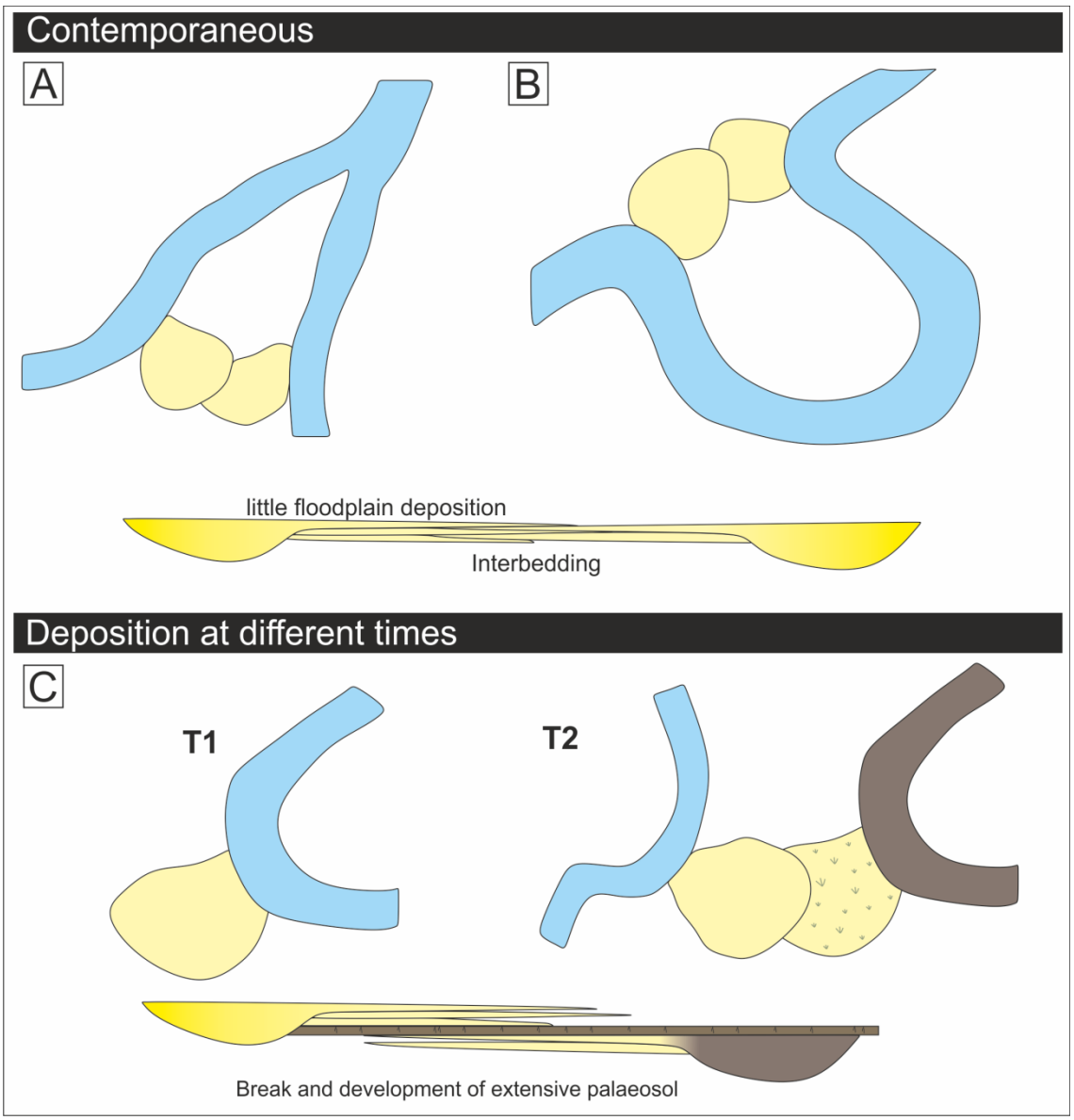

Figure 7.6: Conceptual model for the development of overlapping, genetically related, contemporaneous splay element complexes related to a distributive channel morphology (A), and sinuous meandering channel (B), and non-contemporaneous and non-genetically related element splay complexes related to successive parent channels with different positions (C).

7.2.3 Overbank elements and avulsions

Crevasse-splay deposits can act as precursors to major channel avulsions (Smith et al., 1998; Pérez-Arlucea & Smith, 1999). In planform, close spatial relationships between the position of crevasse-splay development and the subsequent position parent channel avulsion have been recognised in the present-day (Fig. 7.7). Furthermore, the stratigraphic record can have transitional avulsion stratigraphy in which channel bodies with new flow directions are preceded by crevasse-splay stratigraphy (Buehler et al., 2011; Hajek and Edmonds, 2014). The crevasse-channel network could have an impact on the subsequent new channel pathway taken by the river and, as a result, the large-scale stratigraphic architecture of the fluvial system (Donselaar et al., 2013). This includes the preceding, underlying splay stratigraphy (Fig. 2.4), principally by the removal of the pre-existing splay or splay complex. If the avulsion channel is approximately perpendicular to the original channel and situated in a relatively axial (i.e. central) position of the splay, then there is a higher potential for approximately equal amounts of splay deposits to be preserved either side of the succeeding channel infill (Fig.7.8A). In contrast, if the avulsion channel develops oblique to the original channel and the preceding splay complex, then more splay deposits will be left intact on one side of the channel deposit (Fig.7.8B). There are several scenarios in which crevasse-splay development can influence channel avulsion (Fig. 7.9). Avulsion can also occur by annexation of previously fully or partially abandoned channels, as observed in the Saskatchewan River (Smith et al., 1998; Pérez-Arlucea & Smith, 1999).

Figure 7.7: Time-series of Google Earth © images showing the initiation and growth of a splay complex (1987, 1998 and 2000) followed by development of an oblique avulsion channel in the Paraná River, Argentina.

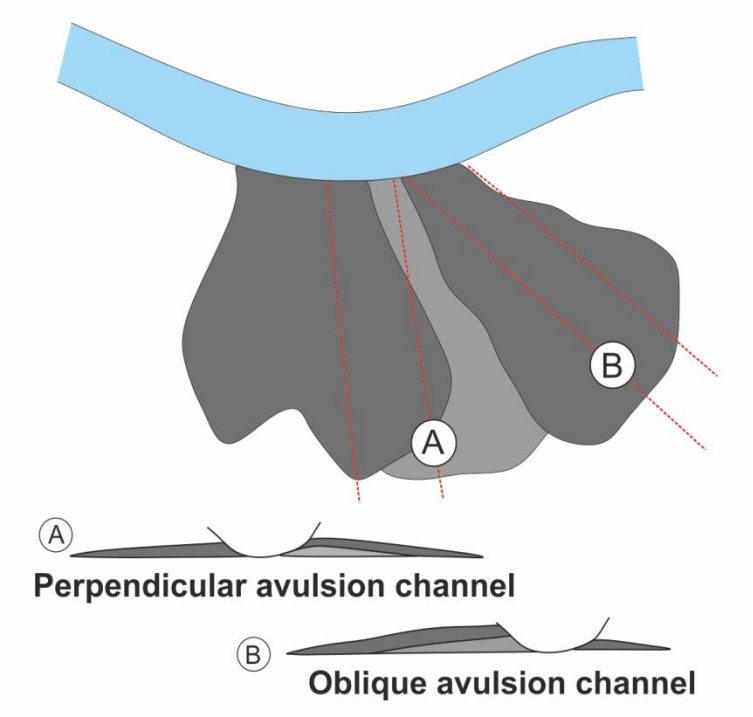

Figure 7.8: Conceptual model showing the potential degree of splay complex preservation for different avulsion channel trajectories.

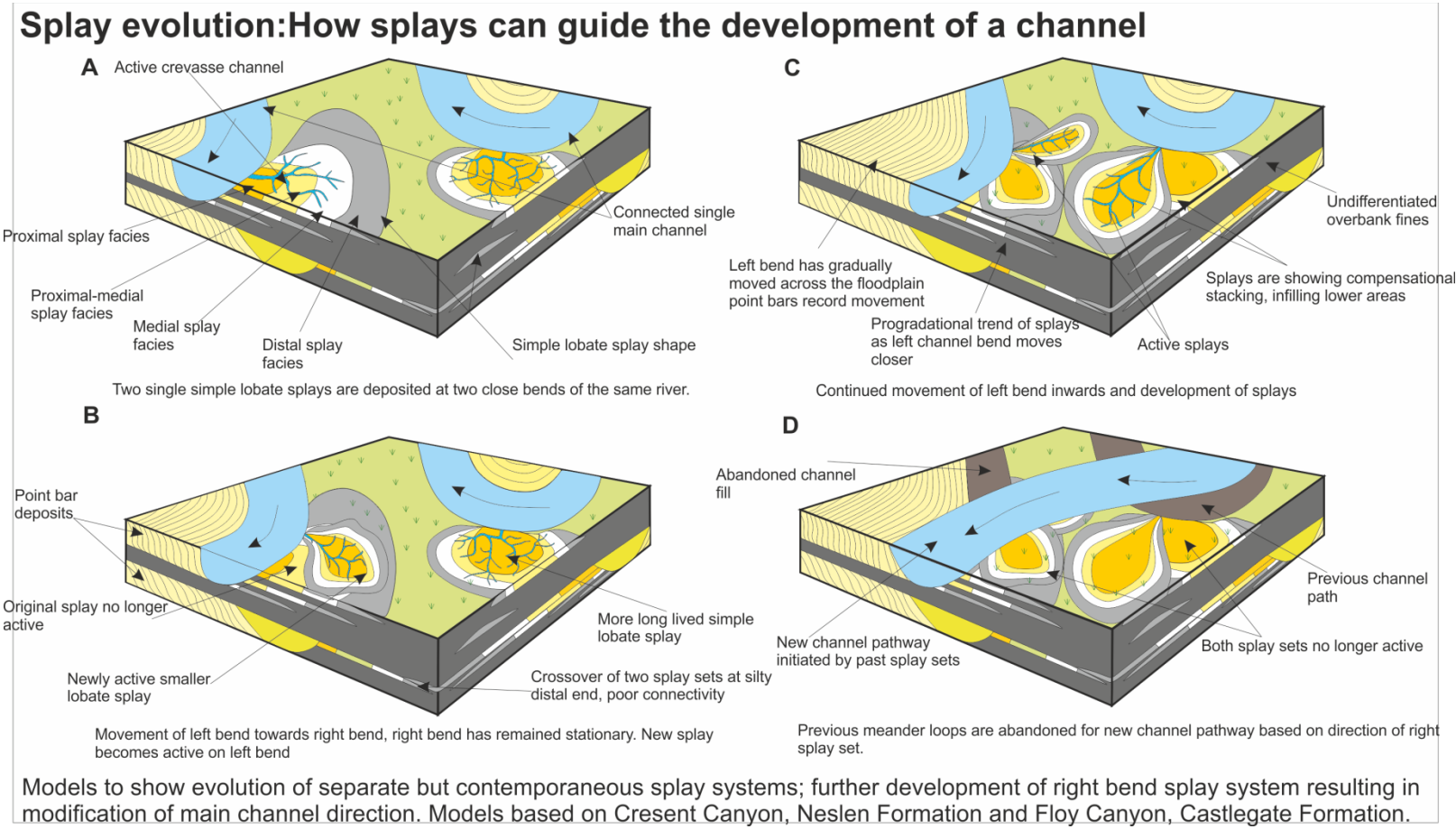

Figure 7.9: Models showing how crevasse splays and an associated crevasse channel can promote modification of the main channel direction.

7.2.4 Summary

Crevasse-splay elements can exhibit multiple styles of stratigraphic stacking. However, compensational stacking will be the most common, for the following reasons: (1) the majority of the floodplains that allow crevasse-splay deposition will be unconfined, thereby promoting compensational stacking; (2) development of depositional topography, the precursor to compensational stacking, is intrinsic to splay formation; and (3) even the minor topographic relief produced by preceding splay deposits will cause lateral offset of the succeeding flood event and splay deposition. The deposits of multiple stacked splay elements, complexes, may overlap in space and/or time, at their edges (i.e. the distal splay facies elements), resulting in potentially complex stratigraphic architectures. If deposition of splay complexes is contemporaneous, then splay elements will be interbedded, or interfinger at the edges with little or no accumulation of intervening floodplain elements (e.g. palaeosols)

However, if deposition was non-contemporaneous, then the deposits of splay complexes will not be interbedded and instead will be separated both vertically and laterally by floodplain deposits, which may represent significant periods of time that permitted the development of palaeosols or coals. Avulsion of a channel can occur for many reasons, but crevasse-splay and crevasse-channel networks can act as initiation mechanisms for an avulsion, along with partially- or fully-abandoned channels (Fig. 7.9).

7.3 Research Question 3: What are the spatial and temporal controls on the natural variability of splay deposition?

7.3.1 Allogenic controls

Climate, eustasy and tectonics are fundamental controls on the stratigraphic architecture of fluvial overbank deposits (Fig. 7.10, 7.11 and 7.12). Climate controls the amount, rate and intensity of precipitation, which impacts river discharge and sediment supply, the corresponding variations in flood intensity (Benedetti, 2003; Holbrook et al., 2006), and groundwater levels. Fluvial systems that experience seasonal fluctuations in discharge, and especially those with monsoonal climatic variations, are likely to have deposits with variations in grain size related to seasonality (Cecil, 1990; Gugliotta et al., 2016; Jablonski and Dalrymple, 2016). Climate and hinterland lithology will also affect river sinuosity through variations in weathering style, sediment supply and the grain size of supplied sediment; a river will be more sinuous when there is a greater percentage of silt–clay in the banks and the gradient is lower (Schumm, 1963). Sinuous rivers tend to have lower overall discharges than straighter channels (Bridge and Gabel, 1992), and therefore may experience relatively lower intensities of overbank flooding. Climate will also have an impact on vegetation development and soil types (Kraus, 1999). These factors are also partly controlled by weathering style and hinterland lithology, which will have a corresponding effect on the occurrence of levees and channel confinement. When there is a greater proportion of clay in the river, higher and more stable levees will tend to develop. Such accumulations will confine the channel better and result in fewer occurrences of flooding.

At a given point in the fluvial system, tectonics may potentially impact fluvial depositional processes by affecting the area of deposition, or relatively upstream or downstream. In an upstream direction, tectonics may control the hinterland geology which will impact the sediment supply to the basin (Fig. 7.10). Clastic wedges such as those studied in this work (Western Interior and associated foreland basin) form due to regional uplift of the source area (Sloss, 1962; Miall, 2014) and tectonic activity in this hinterland can be linked

to increased sedimentation in clastic wedges (Leeder, 2011; Aschoff and Steel, 2011). The sediment supply then influence the grain size of the system and the bedload type (Fig. 7.10). In a mid-stream position, at the point of deposition, tectonics will also control the subsidence and uplift, and the corresponding accommodation space available for fluvial deposition (Leeder, 1993).

Eustasy will influence the amount of accommodation generated in the basin, which is a pre-requisite for overbank preservation (Shanley and McCabe, 1994), and which impacts the degree to which the fluvial channels aggrade (Bristow et al., 1999; Ethridge et al., 1999). However, the absolute control of eustasy on fluvial architecture is debated: the relationship of fluvial channel and floodplain architecture to the aggradation rate related base-level changes is not always a main factor (Colombera et al., 2015).

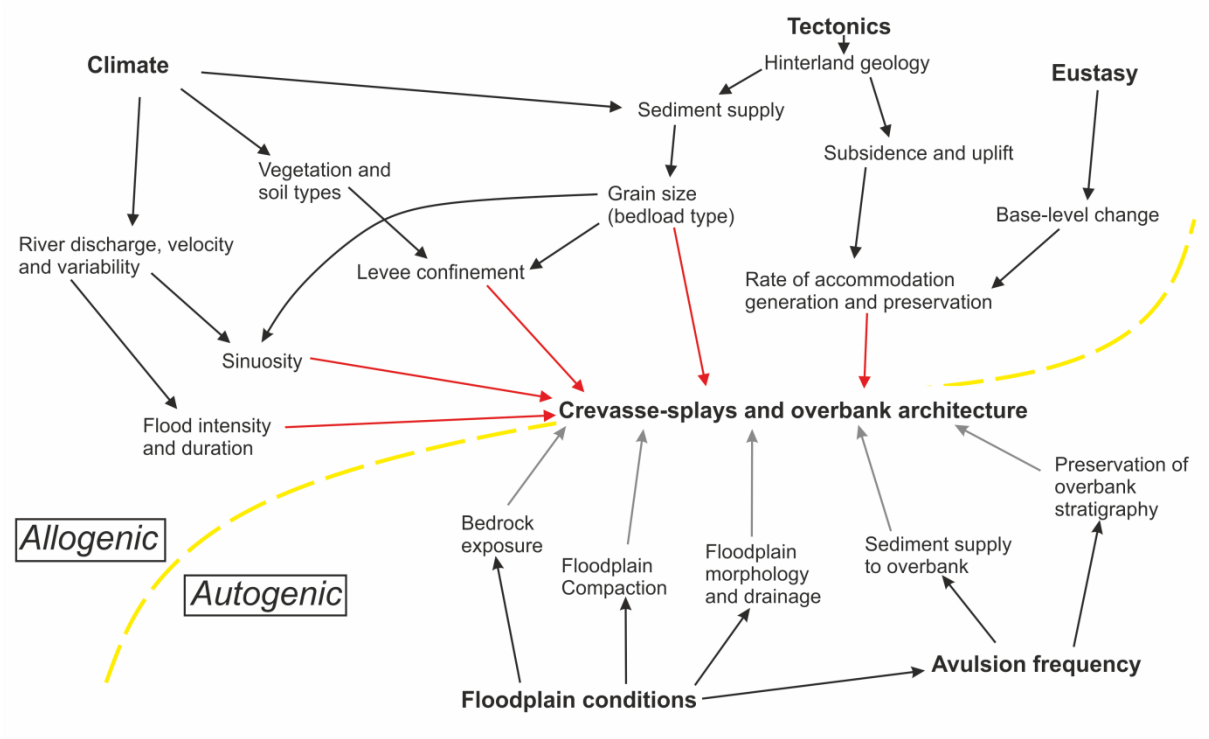

Figure 7.10: Conceptual diagram of the interpreted allogenic and autogenic controls and feedback mechanisms impacting crevasse-splay and overbank stratigraphic architecture. The red arrows indicate primary allogenic controls and the grey arrows the primary autogenic controls.

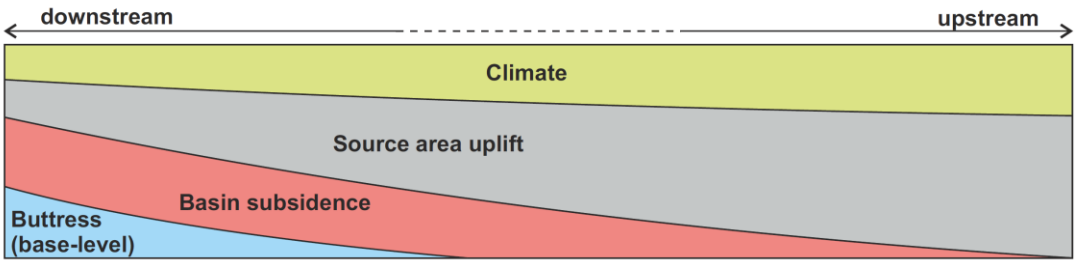

Figure 7.11: Conceptual summary diagram depicting the relative effect different allogenic controls from an upstream to downstream location. From Shanley and McCabe (1994).

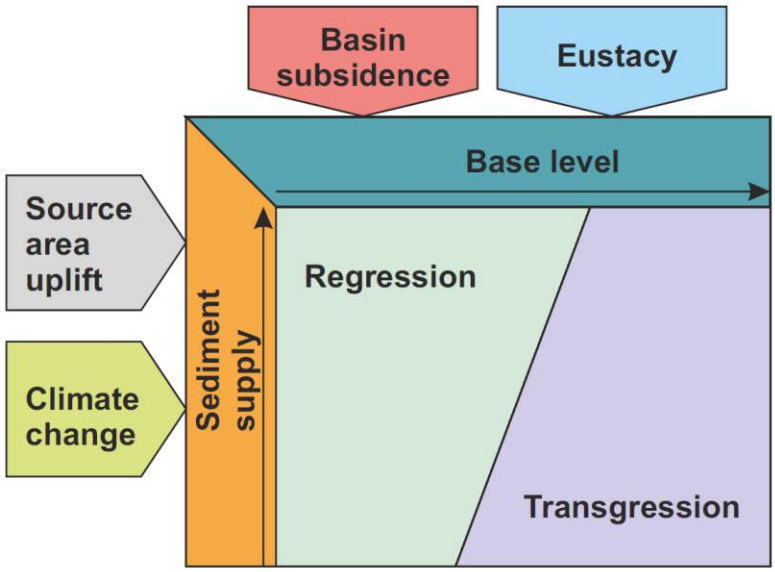

Figure 7.12: Allogenic controls on upstream and downstream conditions. From Ethridge et al. (1998).

7.3.2 Autogenic controls

Avulsion is an autogenic process but it can be influenced by allogenic processes such as variations in rates of sediment supply and discharge (Stouthamer and Berendsen, 2007). Avulsion frequency depends on the amount of preservation space available and the channel aggradation rate (Bryant et al., 1995; Postma, 2014). Floodplain gradient also impacts avulsion frequency (Törnqvist and Bridge, 2002). Avulsions are caused by a complex interplay of factors that bring a channel to the avulsion threshold (Table 7.1;

Jones and Schumm, 1999). Avulsion will occur when the slope of a potential avulsion channel course is greater than that of the present channel course (Jones and Schumm, 1999). This gradient imbalance will be due to either an increase in gradient away from the present channel course or a decrease in gradient along the present channel course, which can be created due to several factors (Table 7.1). Avulsion can also be unrelated to slope and may be triggered by a reduction in capacity of the present channel to carry the water and sediment within it (Jones and Schumm, 1999).

Processes and events that create instability and lead toward an avulsion threshold and/or act as avulsion triggers		Can act as trigger?	Ability of channel to carry sediment and discharge
Group 1. Avulsion from increase in ratio, S_a/S_e owing to decrease in S_e	a. Sinuosity increase (meandering)	No	Decrease
	b. Delta growth (lengthening of channel)	No	Decrease
	c. Base-level fall (decreased slope[a])	No	Decrease
	d. Tectonic uplift (result in decreased slope)	Yes	Decrease
Group 2. Avulsion from increase in ratio, S_a/S_e owing to increase in S_a	a. Natural levee/alluvial ridge growth	No	No change
	b. Alluvial fan and delta growth (convexity)	No	No change
	c. Tectonism (resulting in lateral tilting)	Yes	No change
Group 3. Avulsion with no change in ratio, S_a/S_e	a. Hydrological change in flood peak discharge	Yes	
	b. Sediment influx from tributaries, increased sediment load, mass failure, eolian processes	Yes	Decrease
	c. Vegetative blockage	No	Decrease
	d. Logjams	Yes	Decrease
	e. Ice jams	Yes	Decrease
Group 4. Other avulsions	a. Animal trails	No	No change
	b. Capture (diversion into adjacent drainage)	–	No change

Table 7.1: Cause of avulsion (after Jones and Schumm, 1999). S_a is the slope of the potential avulsion course. S_e is the slope of the existing channel.

Avulsion will aid in controlling the amount of sediment, particularly coarse grained sediment, supplied to overbank regions (Miall, 2014). Avulsion can also impact the preservation potential of overbank deposits, which are less likely to be cannibalised if the new avulsion pathways avoid raised areas on the floodplain (Törnqvist and Bridge, 2002). Avulsion can also affect overbank preservation potential by impacting the self-organisation and clustering of the major fluvial channels because overbank deposits have a higher preservation potential in areas beyond such clustering areas (Hajek et al., 2010).

Compaction rates of floodplain sediments will influence the amount of available local accommodation space, especially if large peat deposits are present or raised mires are formed. Compaction rate of peat may be as high as 5 mm per year, for example in the recent Mississippi deposits (Törnqvist et al., 2008), which would increase the accommodation space available for deposition and preservation of crevasse-splay and overbank sedimentation, which itself occurs at similar rates of between 1-10 mm per year (Walling et al., 1998; Kraus, 1999). However, raised peat mires (ombrotrophic mires) undergo slower compaction and this is not likely to aid in overbank sedimentation; instead, it will inhibit it by producing topographic highs (Shiers, 2017; Shiers et al., 2017). If splays are deposited, they may inhibit coal development through input of clastic material, burial of organic soils by clastic sediments and/or erosion by floodwaters and subsequent deposition terrigenous clastic sediment (Jerrett et al., 2011a, 2011b).

7.3.3 What controls the geographic and temporal occurrence of splays?

Increases in channel sinuosity will encourage flooding and crevassing because of the helical nature of flow in sinuous channels (Rozovskii, 1957; Throne et al., 1985; Bridge, 1992), which encourages flow concentration towards the outer part of meanders, particularly during episodes of elevated discharge and flooding events. This results in an increased amount of overbank sediment towards the outer-banks of river meanders which can result in increased levee breaks and crevasse splay but also higher levees accumulating on the outer bank due to spillover (Ten Brinke et al., 1998).

Consequently, crevasse splays will be associated with an area of the major channel that has increased sinuosity, which in general tends to occur further downstream on the alluvial plain.

Vegetation and soil type, which are fundamentally controlled by climate, will also influence levee confinement. For example, vegetation with extensive root systems will increase the stability of levees, allowing the height of the levee to continue to build higher (Huang and Nanson, 1998). Higher levees increase the difference in height between the channel bankfull level and the floodplain. This would increase the gravitational potential, favouring crevassing. However, this would be countered by the decreased probability of crevassing due to the stronger, higher and more stable levee (Wright and Marriott, 1993; Huang and Nanson, 1998). This could lead to a situation where crevassing is less frequent but is higher in magnitude, occurring only during larger but less frequent floods.

Levee development requires a proportion of the sediment carried by the flow to be silt, which is more cohesive and stable than coarser-grained sediment (van Dijk et al., 2013), and therefore allows levee construction. In contrast, levees will not develop much confining relief in exclusively sand systems, due to the lack of cohesion of sand grains. With little to no levees with which to confine the channel, instead sheet-like flooding will occur at times of flooding of the system (Fisher et al., 2007, 2008). Levee confinement is a fundamental pre-requisite for crevasse-splay formation. Crevassing requires the confinement of the channel by levees to cause channel aggradation sufficient to create a topographic imbalance and gravitation potential in favour of crevassing onto the topographically lower floodplain. However, to permit crevassing, the ability of the levee to confine the channel flow must be overcome, perhaps due to it becoming weaker at a certain point in space or time. Levees are only very rarely preserved in the rock record and it is almost impossible to infer the status of ancient levees that lead to crevassing (Brierley et al., 1997). Crevassing events tend to rework the levee deposits, which have a low preservation potential.

Crevassing is also more likely in areas where subsidence in overbank areas increase the relative topographic difference to the adjacent channel level. This subsidence is either due to compaction of sediments or localised subsidence in the basin. This subsidence adjacent to the channel means that the floodplain is lower than channel. When the channel has accreted vertically above the levee of the floodplain it is easier to break through the levee and deposit on the floodplain (Wright and Marriott, 1993).

Base-level variations will also impact the relative height of channel to floodplain. As base level rises, the channel belt will aggrade and groundwaters will rise, which can increase the potential and frequency of flooding and crevasse-splay deposition (Bristow et al., 1999; Ethridge et al., 1999). Several base-level fluctuations are interpreted to have occurred during formation of the Neslen Formation (Shiers et al., 2014, 2017) and could have been important for crevassing, especially since deposition occurred in a downstream area where base-level fluctuations would have had an impact (e.g. Fig. 7.11, 7.12) (Shanley and McCabe, 1994).

Finally, preservation of splay deposits in the stratigraphic record requires sufficient accommodation space in the basin for development and the rate of burial to exceed the rate of reworking (e.g. Miall, 2014). Preservation of overbank deposits can be difficult because they are commonly cannibalised by adjacent migrating fluvial channels. For example, this tends to happen in the Castlegate Sandstone, in which most overbank deposits occur as isolated pockets between amalgamated channel deposits (McLaurin and Steel, 2007). In the Morrison Formation, the amount of preserved overbank deposits is significantly lower in the proximal parts of the DFS, compared to in the medial and distal parts (Owen et al., 2015). In the Neslen Formation, accommodation space increased throughout the Campanian, and the amount of overbank deposits preserved also increased (Shiers et al., 2014).

7.3.4 What controls scale and dimensions of splays?

The key controls on the scale and dimensions of splays are as follows: river discharge; the sediment supply rate and sediment type; sediment transport capacity of the river system.

Discharge will impact the scale of the parent channel, which in turn influences the flow strength and sediment carrying capacity of the flow within the channel. Smaller channels carry lower volumes of water and sediment. However, due to their inability to accommodate increased discharge, these smaller channels may experience more frequent flooding, especially if there are fluctuations in discharge due to seasonal variations. In contrast, larger channels will carry greater volumes of water and sediment that can be transferred to the overbank during floods but they can accommodate a greater river discharge. This may result in a lower frequency of floods but a greater intensity when a flood does occur. In the Morrison Formation, the size of parent channels and splays tend to be smaller than those in the Castlegate and Neslen formations, which are associated with relatively larger splay deposits (Fig. 6.10).

The scale, intensity and duration of river floods will also impact splay dimensions (Fig. 7.10), with larger floods being associated with larger splay deposits. The Castlegate and Neslen formations were deposited under monsoonal conditions, during which large seasonal variations in river discharge would be expected (Fricke et al., 2010; Gugliotta et al. 2016). This is consistent with the formation of larger splay deposits in the Castlegate and Neslen formations (Fig. 6.8). The Morrison Formation was deposited under the influence of a semi-arid climate and the fluvial system likely experienced lower annual variations in fluvial and sediment discharge compared to the systems of the Castlegate and Neslen formations (Chapter 6; Parrish et al., 2004; Turner and Peterson, 2004). Similarly, in the literature case studies, splays and splay deposits are larger in humid climatic settings than in semi-arid environments (Fig. 6.17).

If rates of compaction are on the same order of magnitude as the rates of deposition (typically millimetres per year), floodplain sediment compaction can lead to increased accommodation space generation within the floodbasins adjacent to river channels (Zwoliński, 1991; Bristow et al., 1999). In the studied formations, compaction of floodplain sediments will be relevant in the coal-bearing Castlegate and Neslen formations. This is because compaction of coals and peats typically occur at rates and ratios that are an order of magnitude higher than for other floodplain deposits (cf. Törnqvist et al., 2008). Splay deposits in the Neslen Formation are thicker when compared to those in the Morrison Formation (Fig. 6.8). This could, in part, be due to the increased accommodation from compaction of peat deposits. Within the Neslen Formation, the thickness of splay deposits and the occurrence frequency of coals decreases upwards through the formation with no coals in the upper part of the formation (compare Fig. 6.14 and 6.15 and associated sections), which is consistent with a decrease in floodplain compaction and rate of accommodation space creation during deposition. Small variations in climate during the Campanian may have resulted in less favourable conditions for coal accumulation (Shiers et al., 2014).

Floodplain morphology will also play an important role in the dimensions of splays and splay deposits. A confined floodplain will result in splays that reflect that floodplain shape, typically with longer lengths than widths as the flow is restricted from expanding across the floodplain instead the floodwaters are funnelled into the available accommodation space. In contrast, an unconfined floodplain will allow floodwaters to spread out in all directions, most commonly in a sub-radial pattern from the channel overspill position. This would result in splays with relatively similar widths and lengths, similar to those observed in the Morrison Formation (Fig. 6.8) or even splays with higher widths than lengths, as observed in the Neslen Formation (Fig. 6.8).

7.3.5 What controls the internal complexities of splays?

Important controls on the internal complexities of splay deposits are strength and duration of the flood event, and the grain size and bedload type of the fluvial system (Chap 7.1.1, Fig. 7.1). Flood duration will impact the internal

stratigraphic complexity and expression of splay deposits by affecting the extent of crevasse-channel network development. If a flooding event is relatively strong and long in duration, there will be a higher potential for developing complicated crevasse-channel networks, which cause spatial variations in erosion and sediment transport. By contrast, lower duration floods are more likely to be associated with a less well developed crevasse-channel network, and sediment grain size may be more equally spread throughout the splay (Smith et al., 1989). In all the studied formations, there are relatively simple splay elements comprising only one or two facies types, which are more likely to represent a relatively low energy and short-lived flooding event (Fig. 4.7, 6.11, 6.15). However, other splay elements record relatively complicated vertical and lateral architectures consisting of many facies types, in different facies belts (Fig. 4.7), which most likely represent longer-lived, higher energy flooding events, or multiple superimposed events. Vegetation could also have an impact on the local floodplain topography and penetration of floodwaters on the floodplain. For example, vegetation could trap sediment, particularly coarser sediment, resulting in grain size heterogeneity.

7.3.6 Summary

Climate is the most important first-order control on fluvial overbank accumulation and preservation because it impacts river discharge and discharge fluctuations, bedrock weathering style and erosion rates, which influence sediment supply rates and grain size distribution through time. These factors influence many second-order controls on splay development, such as levee development and confinement, channel sinuosity, and the size, intensity and frequency of flooding. Sediment supply directly impacts the type of sediment available for levee development and floodplain deposition and facies variability in splay and floodplain deposits. Tectonics and eustatic sea level variations are also important first-order allogenic controls. Autogenic controls, including channel avulsion and variations in floodplain characteristics, are important second-order controls. Parent channel characteristics and the flooding intensity are very important in controlling the

scale of splay deposits, the geographic position that the flow breaks out of the parent channel.

7.4 Research question 4: How do splays and their deposits impact fluvial hydrocarbon reservoirs?

7.4.1 Baffles and connectors

The degree to which splay deposits act as baffles and connectors differs based on the type, of splay. In one scenario, splays act as blocks or baffles to connectivity due to the greater proportion of silt-prone facies and the laterally disconnected splay complex architectures. This typically means there is no direct lateral or vertical connection of sand-prone parts (Fig. 7.13) and splays/splay complexes tend to vertically and/or laterally interact across their relatively distal silt-prone parts, which dominate the splay deposits. The silt-prone parts of splay deposits in the Morrison, Castlegate and Neslen formations generally form the highest proportions of the splay element by volume (Fig. 7.1). Likewise, despite splay deposits in the Rhine-Meuse Delta containing large absolute volumes of sand, the sand deposits are generally concentrated in channels (Bos and Stouthamer, 2011) in the style of stage (III) splays of Smith et al. (1989).

In a second scenario, splays may generally act as connectors due to closer interaction of sand-prone facies (Fig. 7.13). In this scenario, crevasse splay elements and crevasse splay complexes can form important inter-channel body connectors, resulting in substantial increases in horizontal permeability. The interaction of sand-prone facies occurs when the proximal, sand-prone parts of splays form a relatively large component of the splay deposits and/or the sand-prone facies occur in relatively well-developed crevasse-channel networks that extended across part where the splays meet (Stuart et al., 2015). The former requires a relatively sand-rich fluvial system. Crevassing in relatively sand-rich systems and transfer of sand from the channel to the floodplain necessarily requires higher energy systems in which crevasse-

channel development would be higher. The interaction of splay complexes requires certain channel-floodplain geometrical configurations (Chapter 7.2.2).

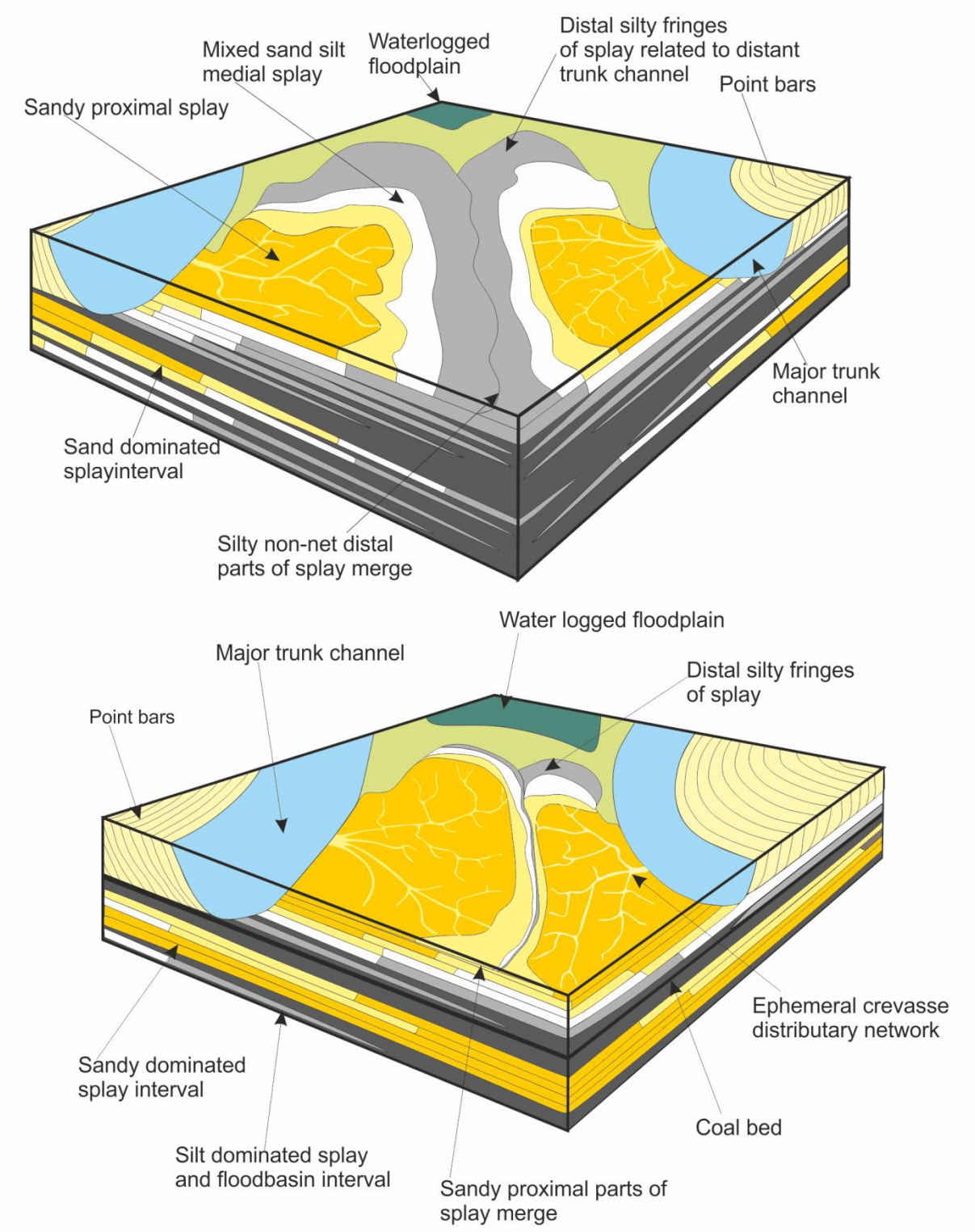

Figure 7.13: Conceptual block model diagrams for scenario 1 splays which act as baffles to connectivity (top) and scenario 2 splays which act as connectors in fluvial reservoirs (bottom), highlighting grain size, architecture variations and differences in lateral and vertical connectivity.

Several studies have recognised and interpreted the impact of intra- and inter-splay architecture. Stuart et al. (2014) observed increased levels of stratigraphic connectively at proximal positions in relatively sand-rich splays, with connectivity decreasing in distal directions. In the Blackhawk Formation, splays formed a very minor component of the overall interpreted productive reservoir (‘net’), the splays could potentially act as an important horizontal connectors between the main reservoir compartments, the fluvial channel sandstones (Sahoo et al., 2016). Similarly, splays are recognised to act as effective horizontal connectors in the Ebro Basin, despite having relatively low reservoir quality (van Toorenenburg et al., 2016).

Figure 7.14: Conceptual diagram of fluvial successions with differing levels of lateral connectivity related to the infill characteristics of the channel. Low to no net siltstone and claystones (left) or mostly high-net sandstone (right).

The connectivity of channel bodies and overbank deposits also depends on the infill characteristics of the associated channel. When the parent channel is infilled with claystones or siltstones, this will form a baffle to connectivity between the channel and overbank, and between overbank deposits on either side of the channel. However, if the channel is preserved with a sand-rich infill, this will allow lateral connectivity between the sand-prone parts of deposits and point-bar deposits (Fig. 7.14; Toonen et al., 2012).

Other deposits in the fluvial overbank and coastal or deltaic plain may act as connectors between or to relatively major sediment bodies. For example, laterally extensive sand deposits formed in organic-clastic lake fills and bay-head delta deposits can form effective connectors for channel belt deposits in fluvio-deltaic settings (Bos, 2010; Bos and Stouthamer, 2011).

7.4.2 Crevasse-splays and fluvial reservoir potential

In general, splays will comprise significantly lower volumes of sediment and sedimentary rock, and in particular those with relatively high reservoir quality, than channel bodies. In addition, splay deposits are typically lower reservoir quality than other parts of genetically-related fluvial successions. However, in low net-to-gross settings, splay deposits can contain relatively significant volumes of sand that may contribute to net reservoir (Larue and Hovadik, 2006; Bos and Stouthamer, 2011; van Toorenenburg et al., 2016). In the studied formations, the dimensions of splays can be used to work out average volumes of splay deposits. These volumes are based on a volume for an ellipsoid (Chapter 4.7.1), and the shapes of the bodies modelled are based on outcrop observations on the width to length ratios of splays. In the Morrison Formation, splays have an average volume of 2.196×10^{4} m^3 (n=17) and in the Mesaverde Group (Castlegate Sandstone and Neslen Formation) the average volume was 5.036×10^{5} m^3 (n = 20) (Burns et al., 2017). The lowest proportion of proximal sand-prone within a splay was found to be 19% and the highest was 47%, in the studied formations. This suggests that the highest amounts of possible net reservoir of splay deposits were 10.3×10^{3} m^3 in the Morrison Formation and 235×10^{3} m^3 in the Mesaverde examples. Whereas the lowest amount of possible net reservoir would be 4.17×10^{3} m^3 in the Morrison

Formation and 95.1×10^3 m^3 in the studied examples form the Mesaverde Group. Consequently, if splays stacked together and had sufficient vertical connectivity, they could form useful addition to net reservoir volume (Fig. 7.15) (cf. van Toorenenburg et al., 2016). However, the possibility and nature of vertical and/or lateral connectivity between stacks of splay elements (complexes) is dependent on the stacking style within the complex (Fig. 5.10) and the planform geometries of component splays (Fig. 7.15).

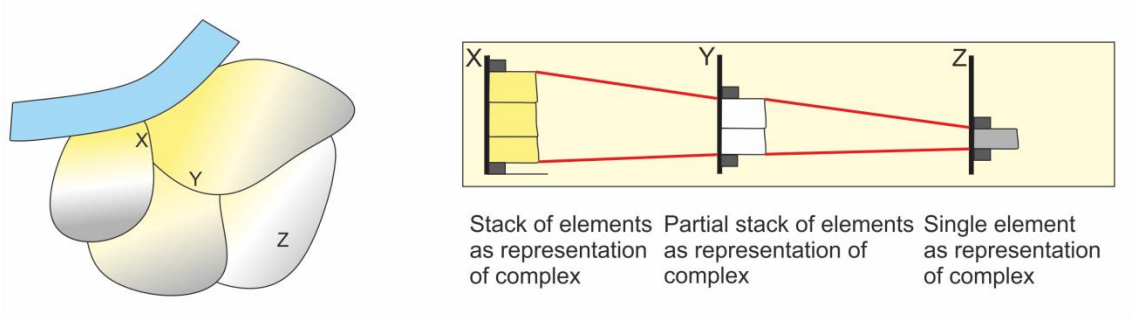

Figure 7.15: Conceptual diagram showing the lateral variability in how a splay complex can be expressed. (X) A thick stack of proximal splay deposits is then represented by one single distal splay element (Z).

For example, a vertical section through the proximal part of a splay complex will consist of several splay elements that proportionally are made up of greater amounts of sand-prone facies (Fig. 7.15X). However, a vertical profile of another part of that some complex taken distally would consist of a single splay element with silt-prone facie types (Fig. 7.15Z).

7.4.3 Summary

Crevasse-splay deposits can act as either baffles to overall reservoir connectivity or lateral connectors. Baffles occur when the splay comprises of mainly silt-prone facies types, when the arrangement of splays mean that the sand-prone parts do not interact or when the sand-prone parts of splays are intersected by non-net fine grained abandoned channel fill. Splays can act as connectors when the splay comprises of greater proportions of sand-prone facies, when the arrangement of theses splays allows for erosion and sand-

on-sand contacts and when active channels are infilled by coarse grain fill. Crevasse-splay deposits although of lower quality than coarse-grained channel fill can still add unexpected net to a fluvial reservoir particularly when multiple splays stack together with sand-prone parts adjacent.

Chapter 8 Conclusions and future work

This chapter summarises the main findings of this work and proposes possible future work that could be undertaken in light of the outcomes of this study.

8.1 Conclusions

1. Overbank elements are known to represent a significant proportion of many low net-to-gross fluvial successions. This study has shown that splays in particular can constitute a significant component of overbank successions, up 90% in some of the studied successions. Facies types in floodplain elements are superficially similar to those recorded in distal parts of splay bodies. In order to differentiate the two element types, high resolution facies and architectural analysis are required to trace out individual bodies at outcrop scale. Associations of lithofacies define the internal subdivisions of splay elements into proximal, medial and distal. These associations of lithofacies are arranged into a predictable lateral transitions that occur over average length scales of 500 m and width scales of 1000 m in the Neslen Formation and average length scales of 281 m and widths scales of 181 m in the Morrison Formation. These scales indicate a planform shape of a semi-ellipse for the Neslen Formation splays deposits and a more lobate teardrop shape for the splay deposits of the Morrison Formation.
2. Various hierarchical levels of organisation can be recognised and classified in fluvial overbank successions. Recognition criteria must be used carefully when defining different levels of the hierarchy. The recognition criteria used in this study are bounding surfaces and adjacent deposits, facies arrangements including thinning and fining trends, and external geometries. This has enabled the definition of facies and facies associations within overbank elements of different types and splay complexes. Applicability of this hierarchy has been tested on data from previous studies that have focussed on crevasse-

splay deposits. The Ravenscar Group, UK, the Huesca Fan, Spain and the Beaufort Formation, South Africa, each have different climatic regimes and accumulated in different environmental settings but each are interpreted to comprise significant amounts of crevasse-splay deposits. Although the scales of the deposits are variable, each deposit can be described by the recognition criteria proposed in this research.

3. The vertical stacking of multiple crevasse-splay elements and lateral amalgamation of multiple splay elements has been identified in this study, both in outcrop and from modern satellite imagery. Crevasse-splay elements commonly compensationally stack together since most floodplains are relatively unconfined. However, progradational stacking of splay deposits will occur when there is some local topographic confinement on the floodplain. Therefore, a combination of the two stacking styles might be expected in crevasse-splay complexes. Vertical connectivity in splay complexes depends on the proximity of the sand-prone proximal parts of the deposits, regardless of whether this is at element scale of complex scale. The planform morphology of these deposits will control the vertical connectivity of these sand-prone areas.
4. The controls on overbank deposition and preservation in the rock record are a complex interplay of allogenic and autogenic controls. Climate is one of the most important first-order controls on splay deposition since it impacts river discharge and sediment supply (i.e. amount and type); these factors in turn control levee development, channel sinuosity and size, and the intensity and duration of overbank flooding. Avulsion has long been recognised as an important autogenic control on overbank deposition; this work does not seek to question this. However, the local floodplain conditions are also important when considering splay deposition. Floodplain accommodation, for example, will impact occurrence of splay deposits, as well as their scale and planform shapes.

5. Splay deposits can act as connectors or baffles in fluvial reservoirs. Splay deposits will act as connectors where the splay deposit comprises a great enough proportion of sand-prone facies and where the lateral spatial arrangements of splay elements on the floodplain permit connectivity. Similarly, splay deposits can also act as connectors where vertical and lateral arrangements allow for erosion and sand-on-sand contacts in non-genetically related splay deposits. Conversely, splay deposits can act as baffles to permeability and flow in a reservoir when composed of mainly silt-prone facies, interbedded with non-net floodplain elements and/or intersected by silt- or clay-grain size abandoned channel-fills.
6. Crevasse-splay and crevasse-channel deposits are lower quality (i.e. more poorly sorted and finer-grained) than relatively coarser-grained fluvial channel deposits but can still add net volume to fluvial reservoirs. This is particularly important when multiple splay deposits stack together in complexes. A modest volume of the sand-prone parts of a splay, such as 10.3×10^3 m^3 in the Morrison Formation splay deposits and 235×10^3 m^3 in the Neslen Formation, can increase more than four-fold if the deposits are stacked.

8.2 Future work

The research undertaken for this study could be extended in a number of different ways to enhance our knowledge and understanding of the range of deposits associated with river flooding events.

8.2.1 Investigation into frequency of ancient-recent flood events

The temporal frequency of flooding events in the ancient is difficult to establish from ancient outcrop dating alone. Instead the use of recent deposits could be used to constrain the frequency of floods that produce overbank deposits. Age-dating of studied successions, (e.g. using OSL dating) could be used to quantify temporal frequency and preservation timescales of fluvial overbank successions. In more recent deposits an analysis of satellite data to link and

constrain annual–decadal geomorphic changes in the fluvial overbank area and ground truthing of these interpretations using core and trenching of these modern deposits. It would be iworthwhile to establish the characteristics and quantify the temporal frequency of these event beds.

8.2.2 Investigating the preservation potential of recent-modern flood deposits

Preservation potential of flood deposits observed in modern studies is relativity unknown. Many studies of active crevasse splays and flood deposits have been undertaken (e.g. Smith et al., 1989; Farrell, 2001; Buehler et al., 2011; Li and Bristow, 2015) yet how representative these are of the deposits that are actually preserved in the rock record is less well understood. Work could be undertaken to link the interpreted yearly–decadal hydrodynamic and planform geomorphic changes to the longer timescale stratigraphic record, with the aim of better understanding the preservation potential of flood events into the geological record.

Flood deposits may not be preserved in the rock record and how frequently they are preserved, could be investigated using an equivalent present-day system to compare against the ancient rock-record (e.g. how representative is the rock record in recording processes operating on a 1-1000 year timescale). Investigating these deposits in quaternary settings would provide a greater level of resolution, especially for datasets with accurate dating.

8.2.3 Detailed investigation of character of splay deposits within DFS

Other studies have noted how the amount of overbank or floodplain deposits change through DFS's system (Owen et al., 2015). Owen et al. (2015) demonstrated that splays in the Morrison Formation DFS are splays but also terminal splays towards the end of the system, that the occurrence of overbank deposits in general varies throughout a DFS's system. The internal complexities of different splays and the types of splays present in different parts of the outcrop expression of a DFS could be investigated. This also could be investigated in multiple examples of DFS under different climates and

accumulating in different basins e.g. the Permian Organ Rock Formation (Cain and Mouney, 2009), Triassic deposits of the Chinle Formation (Trendell et al., 2013), Devonian aged systems of Greenland and Ireland (Kelly and Olsen, 1993).Splay deposit types and variations and overbank deposits could aid in constraining a location proximal-distally within a DFS.

8.2.4 Three-dimensional modelling of overbank elements

Three-dimensional modelling, such as object-based reservoir modelling, could reduce uncertainty in hydrocarbon reservoir behaviour and increase recovery rates. Detailed data on facies proportions in overbank elements and the distributions of these different elements (Chapter 4, Chapter 6) could be used to populate static and dynamic reservoir models. This would allow reservoir properties such as the heterogeneities caused by overbank deposits to be quantified. Data from this thesis can also be used to contribute to quantitative fluvial facies models from databases such as FAKTS (Fluvial Architecture Knowledge Transfer System) (Colombera et al., 2013). This database approach can give insights into the modelling of overbank bodies in different climatic and environment systems.

Chapter 9 References

Abels, H.A., Kraus, M.J., and Gingerich, P.D., 2013. Precession-scale cyclicity in the fluvial lower Eocene Willwood Formation of the Bighorn Basin, Wyoming (USA). Sedimentology 60, 1467-1483.

Abbott, J.E., and Francis, J.R.D., 1977, Saltation and suspension trajectories of solid grains in a water stream: Royal Society [London], Philosophical Transactions, volume 284, 225-254.

Adams, P.N., Slingerland, R.L., and Smith, N.D., 2004. Variations in natural levee morphology in anastomosed channel flood plain complexes. Geomorphology 61, 127-142.

Adams, M., and Bhattacharya, J.P., 2005. No change in fluvial style across a sequence boundary, Cretaceous Blackhawk and Castlegate Sandstones of central Utah, USA. Journal of Sedimentary Research 75, 1038-1051.

Alexander, J., 1992. Nature and origin of a laterally extensive alluvial sandstone body in the Middle Jurassic Scalby Formation. Journal of the Geological Society, 149, 431-441.

Allen, J.R.L., 1963. The classification of cross-stratified units with notes on their origin. Sedimentology 2, 93-114.

Allen, J.R.L., 1965. A review of the origin and characteristics of recent alluvial sediments: Sedimentology 5, 89-191.

Allen, J. R. L., 1966. On bed forms and palaeocurrents. Sedimentology 6, 153-190.

Allen, J.R.L., 1970. A Quantitative Model of Climbing Ripples and their Cross-Laminated Deposits. Sedimentology, 14, 5-26.

Allen, J.R.L., 1977. The possible mechanics of convolute lamination in graded sand beds. Journal of the Geological Society 134, 19-31.

Allen, J.R.L., 1978. Studies in fluviatile sedimentation: an exploratory quantitative model for the architecture of avulsion-controlled alluvial suites. Sedimentary Geology 21, 129-147.

Allen, J.R.L., 1983. Studies in fluviatile sedimentation: Bars, bar-complexes and sandstone sheets (low-sinuosity braided streams) in the Brownstones (L. Devonian), Welsh borders. Sedimentary Geology 33, 237-293.

Allen, G.P., and Posamentier, H.W., 1993. Sequence stratigraphy and facies model of an incised valley fill: the Gironde estuary, France. Journal of Sedimentary Petrology 63, 378-391.

Allmendinger, N.E., Pizzuto, J.E., Potter, N., Johnson, T.E., and Hession, W.C., 2005. The influence of riparian vegetation on stream width, eastern Pennsylvania, USA. Geological Society of America Bulletin 117, 229-243.

Alqahtani F. A., Johnson H. D., Jackson C. A.L., and Som M. R. B., 2015. Nature, origin and evolution of a Late Pleistocene incised valley-fill, Sunda Shelf, Southeast Asia. Sedimentology 62, 1198-1232.

Ambrose, W.A., Lakshminarasimhan, S., Holtz, M.H., Nunez-Lopez, V., Hovorka, S.D., and Duncan, I., 2008. Geologic factors controlling CO2 storage capacity and permanence: case studies based on experience with heterogeneity in oil and gas reservoirs applied to CO2 storage. Environmental Geology 54, 1619-1633.

Ambrose, W.A., Hentz, T.F., Bonnaffe, F., Loucks, R.G., Brown, L.F., Wang, F.P., and Potter, E.C., 2009. Sequence-stratigraphic controls on complex reservoir architecture of highstand fluvial-dominated deltaic and lowstand valley-fill deposits in the Upper Cretaceous (Cenomanian) Woodbine Group, East Texas field: Regional and local perspectives. AAPG Bulletin 93,231-269.

Amorosi A., Pavesi M., Ricci Lucchi M., Sarti G., and Piccin A., 2008. Climatic signature of cyclic fluvial architecture from the Quaternary of the central Po Plain, Italy. Sedimentary Geology 209, 58-68.

Amy, L.A., Kneller, B.C., and McCaffrey, W.D., 2007. Facies architecture of the Grès de Peira Cava, SE France: landward stacking patterns in ponded turbiditic basins. Journal of the Geological Society London 164, 143-162.

Anderson, D.S., 2005. Architecture of Crevasse Splay and Point-Bar Bodies of the Nonmarine lles Formation north of Rangely, Colorado: Implications for Reservoir Description. The Mountain Geologist 42, 109-122.

Anderson, D.S., and Carr, M.M., 2007. Modelling crevasse splay versus point-bar bodies; relative roles in characterizing tight-gas fluvial reservoir successions. Abstracts: Annual Meeting - American Association of Petroleum Geologists 2007.

Anderson, O. J., and Lucas, S. G.,1997. The Upper Jurassic Morrison Formation in the Four Corners region. Mesozoic geology and paleontology of the Four Corners region: New Mexico Geological Society 48th Annual Field Conference, 1997. 139-155.

Arnaud-Fassetta, G., 2013. Dyke breaching and crevasse-splay sedimentary sequences of the Rhône Delta, France, caused by extreme river-flood of December 2003. Geografia Fisica e Dinamica Quaternaria 36, 7-26.

Arndorfer, D.J., 1973. Discharge patterns in two crevasses of the Mississippi River delta. Marine Geology 15, 269-287.

Arostegi, J., Baceta, J.I., Pujalte, V. and Carracedo, M., 2011. Late Cretaceous–Palaeocene mid-latitude climates: inferences from clay mineralogy of continental-coastal sequences (Tremp-Graus area, southern Pyrenees, N Spain). Clay Minerals, 46,105-126.

Aschoff, J.L., and Steel, R.J., 2011a. Anatomy and development of a low-accommodation clastic wedge, upper Cretaceous, Cordilleran Foreland Basin, USA. Sedimentary Geology 236, 1-24.

Aschoff, J., and Steel, R., 2011b. Anomalous clastic wedge development during the Sevier-Laramide transition, North American Cordilleran foreland basin, USA. Geological Society of America Bulletin 123, 1822-1835.

Beaumont, C., 1981. Foreland basins. Geophysical Journal of the Royal Astronomical Society 65,291-329.

Baeteman, C., Beets, D.J., and Van Strydonck, M., 1999. Tidal crevasse splays as the cause of rapid changes in the rate of aggradation in the Holocene tidal deposits of the Belgian Coastal Plain. Quaternary International 56, 3-13.

Behrensmeyer, A.K., Willis, B.J., and Quade, J., 1995. Floodplains and palaeosols of Pakistan Neogene and Wyoming Palaeogene deposits: a comparative study. Palaeogeography, Palaeoclimatology, Palaeoecology 115, 37-60.

Benedetti, M.M., 2003. Controls on overbank deposition in the Upper Mississippi River.Geomorphology 56 , 271-290.

Berendsen H. J. A., and Stouthamer E., 2001. Palaeogeographic Development of the Rhine–Meuse Delta, The Netherlands. Koninklijke Van Gorcum, 268 pp.

Beynon, B.M., Pemberton, S.G., Bell, D.D. and Logan, C.A., 1988. Environmental implications of ichnofossils from the Lower Cretaceous Grand Rapids Formation. Cold Lake oil sands deposits, 275- 289.

Blakey R.C., and Ranney W., 2008. Ancient Landscapes of the Colorado Plateau. Grand Canyon Association, Grand Canyon, Arizona

Bluck, B.J., 1982. Texture of gravel bars in braided streams. Gravel Bed Rivers. John Wiley and Sons, Chichester, 339-355.

Blum, M.D. And Price, D.M., 1998. Quaternary alluvial plain construction in response to glacio-eustatic and climatic controls, texas gulf coastal plain. relative role of eustasy, climate, and tectonism in continental rocks, P31.

Blum, M.D., and Törnqvist, T.E., 2000. Fluvial responses to climate and sea-level change: a review and look forward. Sedimentology 47, 2-48.

Bos, I.J., 2010. Architecture and facies distribution of organic-clastic lake fills in the fluvio-deltaic Rhine–Meuse system, the Netherlands. Journal of Sedimentary Research, 80, 339-356.

Bos, I.J., and Stouthamer, E., 2011. Spatial and temporal distribution of sand-containing basin fills in the Holocene Rhine-Meuse delta, the Netherlands. The journal of geology 119, 641-660.

Bown, T.M., and Kraus, M.J., 1987. Integration of channel and floodplain suites, I. Developmental sequence and lateral relations of alluvial palaeosols. Journal of Sedimentary Petrology 57, 587-601.

Bridge, J.S., 1984. Large-scale facies sequences in alluvial overbank environments. Journal of Sedimentary Research 54, 85-170.

Bridge, J.S., 1992. A revised model for water-flow, sediment transport, bed topography and grain-size sorting in natural river bends. Water Resource Research 28, 999–1013.

Bridge, J.S., 1993. Description and interpretation of fluvial deposits: a critical perspective. Sedimentology 40, 801-810.

Bridge, J.S., 2006. Fluvial facies models: recent developments. In: Posamentier, H.W., Walker, R.G. (Eds.), Facies Models Revisited. SEPM Special Publication 84, pp. 85–117.

Bridge, J.S., and Gabel, S.L., 1992. Flow and sediment dynamics in a low sinuosity, braided river: Calamus River, Nebraska Sandhills. Sedimentology 39, 125-142.

Bridge, J.S., Alexander, J., Collier, R.E.L., Gawthorpe, R.L., and Jarvis, J., 1995. Ground-penetrating radar and coring used to study the large-scale structure of point-bar deposits in 3 dimensions. Sedimentology 42, 839-852.

Bridge, J.S., and Demicco, R.V., 2008. Earth Surface Processes, Landforms and Sediment Deposits. Cambridge University Press, Cambridge, 815 pp.

Bridge, J.S., and Leeder, M.R., 1979. A simulation model of alluvial stratigraphy. Sedimentology 26, 617-644.

Brierley, G.J., and Hickin, E.J., 1992. Floodplain development based on selective preservation of sediments, Squamish River, British Columbia. Geomorphology 4, 381-391.

Brierley, G.J., 1996. Channel morphology and element assemblages: a constructivist approach to facies modelling. In: Carling, P.A., Dawson, M.R. (Eds.), Advances in Fluvial Dynamics and Stratigraphy. Wiley, Chichester, pp. 263-298.

Brierley, G.J., Ferguson, R.J., and Woolfe, K.J., 1997. What is a fluvial levee? Sedimentary Geology 114, 1-9.

Bristow, C., and Best, J., 1993. Braided rivers: perspectives and problems. Geological Society, London, Special Publications 75, 1-11.

Bristow, C., Skelly, R., and Ethridge, F., 1999. Crevasse splays from the rapidly aggrading, sand-bed, braided Niobrara River, Nebraska: effect of base-level rise. Sedimentology 46, 1029-1048.

Brookfield, M., 1977. The origin of bounding surfaces in ancient aeolian sandstones. Sedimentology 24, 303-332.

Bryant, M., Falk, P., and Paola, C., 1995. Experimental study of avulsion frequency and rate of deposition. Geology 23, 365-368.

Boerboom, H.T.W., Sandén, A.B., van Toorenenburg, K.A., Donselaar, M.E., and Weltje, G.J., 2016. High-resolution Reservoir Architecture Modelling of Crevasse Splay Deposits in Low-net-to-gross Fluvial Stratigraphy. In 78th EAGE Conference and Exhibition 2016.

Buehler, H.A., Weissmann, G.S., Scuderi, L.A., and Hartley, A.J., 2011. Spatial and temporal evolution of an avulsion on the Taquari River distributive fluvial system from satellite image analysis. Journal of Sedimentary Research 81, 630-640.

Burgreen, B., and Graham, S., 2014. Evolution of a deep-water lobe system in the Neogene trench-slope setting of the East Coast Basin, New Zealand: lobe stratigraphy and architecture in a weakly confined basin configuration. Marine and Petroleum Geology 54, 1-22.

Burton, D., Flaig, P.P., and Prather, T.J., 2016. Regional Controls On Depositional Trends In Tidally Modified Deltas: Insights From Sequence Stratigraphic Correlation and Mapping of the Loyd And Sego Sandstones, Uinta And Piceance Basins of Utah and Colorado, USA. Journal of Sedimentary Research 86, 763-785.

Cahoon, D.R., White, D.A., and Lynch, J.C., 2011. Sediment infilling and wetland formation dynamics in an active crevasse splay of the Mississippi River delta. Geomorphology 131, 57-68.

Cain, S.A., and Mountney, N.P., 2009. Spatial and temporal evolution of a terminal fluvial fan system: the Permian Organ Rock Formation, South-east Utah, USA. Sedimentology 56, 1774-1800.

Campbell, C.V., 1967. Lamina, laminaset, bed and bedset. Sedimentology 8, 7-26.

Cant, D.J., and Walker, R.G., 1978. Fluvial processes and facies sequences in the sandy braided South Saskatchewan River, Canada. Sedimentology 25, 625-648.

Catuneanu O., and Elango H. N., 2001a. Tectonic control on fluvial styles: the Balfour Formation of the Karoo Basin, South Africa. Sedimentary Geology 140, 291-313.

Catuneanu O., and Bowker D., 2001b. Sequence stratigraphy of the Koonap and Middleton fluvial formations in the Karoo foredeep South Africa. Journal African Earth Science 33, 579-595.

Cazanacli, D., and Smith, N.D., 1998. A study of morphology and texture of natural levees-Cumberland Marshes, Saskatchewan, Canada. Geomorphology 25, 43-55.

Cecil, C.B., 1990. Paleoclimate controls on stratigraphic repetition of chemical and siliciclastic rocks. Geology 18, 533-536

Cecil, C.B., 2003. The concept of autocyclic and allocyclic controls on sedimentation and stratigraphy, emphasizing the climatic variable, in: Blaine Cecil, C., Terence Edgar, N. (Eds.),Climate controls on stratigraphy. SEPM Special Publication 77, Tulsa, OK, USA,13-20.

Chan, M.A., and Pfaff, B.J., 1991. Fluvial sedimentology of the Upper Cretaceous Castlegate Sandstone, Book Cliffs, Utah, in: Chidset, T.C. (Ed.), Geology of east-central Utah. Utah Geological Association, pp. 95-110.

Cloyd, K.C., Demicco, R.V., and Spencer, R.J., 1990. Tidal channel, levee, and crevasse-splay deposits from a Cambrian tidal channel system: a new mechanism to produce shallowing-upward sequences. Journal of Sedimentary Petrology 60, 73-83.

Church, M., 2006. Bed material transport and the morphology of alluvial river channels. Annual Review Earth Planetary Science. 34, 325-354.

Clymo, R., 1987. Rainwater-fed peat as a precursor of coal, in: Scott, A.C. (Ed.), Coal and Coal Bearing Strata: Recent Advances. Geological Society, London, Special Publications 11, 17-23.

Cohen, A.D., Spackman, W., and Raymond, R., 1987. Interpreting the characteristics of coal seams from chemical, physical and petrographic studies of peat deposits. Geological Society, London, Special Publications 32, 107-125.

Cole, R., 2008. Characterization of fluvial sand bodies in the Neslen and lower Farrer formations (Upper Cretaceous), Lower Sego Canyon, Utah. In: Longman, M.W., Morgan, C.D. (Eds.), Hydrocarbons Systems and Production in the Uinta Basin, Utah. Rocky 14 Mountain Association of Geologists—Utah Geological Association Publication, 37, pp. 81-100.

Coleman, J.M., 1969. Brahmaputra River: Channel processes and Sedimentation Brahmaputra River: Channel processes and sedimentation. Sedimentary Geology 3, 129-239.

Collinson, J.D., Mountney, N., and Thompson, D., 2006. Sedimentary Structures, third edition. Terra Publishing, Hertfordshire, England.

Colombera, L., Felletti, F., Mountney, N.P., and McCaffrey, W.D., 2012. A database approach for constraining stochastic simulations of the sedimentary heterogeneity of fluvial reservoirs. AAPG Bulletin 96, 2143-2166.

Colombera, L., Mountney, N.P., and McCaffrey, W.D., 2013. A quantitative approach to fluvial facies models: Methods and example results. Sedimentology 60, 1526-1558.

Colombera, L., Mountney, N.P., and McCaffrey, W.D., 2015. A meta-study of relationships between fluvial channel-body stacking pattern and aggradation rate: implications for sequence stratigraphy. Geology 43, 283-286.

Colombera, L., Shiers, M.N., and Mountney, N.P., 2016. Assessment of backwater controls on the architecture of distributary-channel fills in a tide-influenced coastal-plain succession: Campanian Neslen Formation, U.S.A. Journal of Sedimentary Research 86, 1-22.

Constantine, J.A., McLean, S.R., and Dunne, T., 2010. A mechanism of chute cutoff along large meandering rivers with uniform floodplain topography. Geological Society of America Bulletin 122, 855-869.

Corbeanu, R.M., Soegaard, K., Szerbiak, R.B., Thurmond, J.B., McMechan, G.A., Wang, D., Snelgrove, S., Forster, C.B. and Menitove, A., 2001. Detailed internal architecture of a fluvial channel sandstone determined from outcrop, cores, and 3-D ground-penetrating radar: Example from the middle Cretaceous Ferron Sandstone, east-central Utah. AAPG bulletin, 85, 1583-1608.

Corbeanu R. M., Wizevich M. C., Bhattacharya J. P., Zeng X., and McMechan G. A., 2004. Three-Dimensional Architecture of Ancient Lower Delta-Plain Point Bars Using Ground-Penetrating Radar, Cretaceous Ferron Sandstone, Utah. In: Chidsey T. C. Jr., Adams R. D., Morris T. H. (eds.) Regional to Wellbore Analog for Fluvial-Deltaic Reservoir Modeling: The Ferron Sandstone of Utah, AAPG Studies in Geology 50, 427-449.

Cowan, E. J., 1992. The large-scale architecture of the fluvial Westwater Canyon Member, Morrison Formation (Upper Jurassic), San Juan Basin, New

Mexico, 80-93. Society for Sedimentary Geology (SEPM). The Three-Dimensional Facies Architecture of Terrigenous Clastic Sediments and its implications for Hydrocarbon Discovery and Recovery.

Craig, L. C., Holmes, C. N., Cadigan, R. A., Freeman, V. L., Mullens, T. E., and Wier, G. W., 1955. Stratigraphy of the Morrison and related formations Colorado Plateau Region. Geological Survey bulletin 1009.

Cross, T.A., 1988. Controls on coal distribution in transgressive-regressive cycles, Upper Cretaceous, Western Interior, U.S.A., in: Wilgus, C.K., Hastings, B.S., Posamentier, H.W., Van Wagoner, J.C., Ross, C.A., Kendall, C.G. (Eds.), Sea level changes: an integrated approach: SEPM Special Publication pp. 371-380.

Cuevas Gozalo M. C., and Martinius A. W., 1993. Outcrop data-base for the geological characterization of fluvial reservoirs: an example from distal fluvial fan deposits in the Loranca Basin, Spain. In: North C. P., Prosser D. J. (eds.) Characterization of fluvial and aeolian reservoirs. Geological Society Special Pubication 73, 79-94.

Cuevas Martínez J. L., Cabrera Perez L., Marcuello A., Arbues Cazo P., Marzo Carpio M., and Bellmunt F., 2010. Exhumed channel sandstone networks within fluvial fan deposits from the Oligo-Miocene Caspe Formation, South-east Ebro Basin (North-east Spain). Sedimentology 57, 162-189.

Currie, B.S., 1997, Sequence stratigraphy of nonmarine Jurassic–Cretaceous rocks, central Cordilleran foreland-basin system: Geological Society of America, Bulletin,v. 109, p. 1206–1222.

Currie, B. S., 1998. Upper Jurassic-Lower Cretaceous Morrison and Cedar Mountain Formations, NE Utah-NW Colordao: Relationships between Nonmarine Deposition and Early Cordilleran Foreland-Basin Development. Journal of Sedimentary Research 68 ,632-652.

Davidson, S.K., Hartley, A.J., Weissmann, G.S., Nichols, G.J., and Scuderi, L.A., 2013, Geomorphic elements on modern distributive fluvial systems: Geomorphology, v. 180-181, p. 82-95.

Davies, R., Diessel, C., Howell, J., Flint, S., and Boyd, R., 2005. Vertical and lateral variation in the petrography of the Upper Cretaceous Sunnyside coal of eastern Utah, USA—implications for the recognition of high-resolution accommodation changes in paralic coal seams. International Journal of Coal Geology 61, 13-33.

Decelles, P.G., 2004, Late Jurassic to Eocene evolution of the Cordilleran thrust belt and foreland basin system, western U.S.A.: American Journal of Science, v. 304, 105–168.

Decelles, P.G., and Burden, E.T., 1991, Non-marine sedimentation in the overfilled part of the Jurassic–Cretaceous Cordilleran foreland basin: Morrison and Cloverly formations, central Wyoming, USA: Basin Research volume 4, 291–313.

Decelles, P.G., and Currie, B.S., 1996, Long-term sediment accumulation in the Middle Jurassic–early Eocene Cordileran retroarc foreland-basin system: Geology 24, 591–594

Decelles, P.G., Lawton, T.F., and Mitra, G., 1995, Thrust timing, growth of structural culminations, and synorogenic sedimentation in the type Sevier orogenic belt, western United States: Geology 23, 699–702.

Demko, T.M., Currie, B.S., and Nicoll, K.A., 2004. Regional paleoclimatic and stratigraphic implications of paleosols and fluvial/overbank architecture in the Morrison Formation (Upper Jurassic), Western Interior, USA. Sedimentary Geology 167, 115-135.

Deptuck, M.E., Piper, D.J.W., Savoye, B., and Gervais, A., 2008. Dimensions and architecture of late Pleistocene submarine lobes off the northern margin of East Corsica. Sedimentology 55, 869-898.

Dickinson, W. R., and Lawton, T. F., 2001a. Carboniferous to Cretaceous assembly and fragmentation of Mexico. Geological Society of America Bulletin, 113,1142-1160.

Dickinson, W. R., and Lawton, T. F., 2001b. Tectonic setting and sandstone petrofacies of the Bisbee basin (USA Mexico). Journal of South American Earth Sciences 14, 475-504.

Donselaar, M.E., and Overeem, I., 2008. Connectivity of fluvial point-bar deposits: An example from the Miocene Huesca fluvial fan, Ebro Basin, Spain. AAPG Bulletin 92, 1109-1129.

Donselaar, M.E., Cuevas Gozalo, M.C., and Moyano, S., 2013. Avulsion processes at the terminus of low-gradient semi-arid fluvial systems: lessons from the Río Colorado Altiplano endorheic basin, Bolivia. Sedimentary Geology 283, 1–14.

Donselaar, M.E., Gozalo, M.C., and Wallinga, J., 2017. Avulsion History of a Holocene Semi-arid River System-Outcrop Analogue for Thin-bedded Fluvial Reservoirs in the Rotliegend Feather Edge. In 79th EAGE Conference and Exhibition 2017.

Dreyer, T., 2009. Quantified fluvial architecture in ephemeral stream deposits of the Esplugafreda Formation (Palaeocene), Tremp-Graus Basin, northern Spain. Alluvial Sedimentation (Special Publication 17 of the IAS) 66, 337.

Elliott, T., 1974. Interdistibutary bay sequences and their genesis. Sedimentology 21, 611-622.

Emery, D., and Myers, K.J., 1996. Sequence Stratigraphy. Blackwell, Oxford, 297 pp.

Erskine, W., McFadden, C., and Bishop, P., 1992. Alluvial cutoffs as indicators of former channel conditions. Earth Surface Processes and Landforms 17, 23-37.

Ethridge, F.G., Wood, L.J., and Schumm, S.A., 1998. Cyclic variables controlling fluvial sequence development: Problems and Perspectives. SEPM Special Publication 59, 17-29.

Ethridge, F.G., Skelly, R.L., and Bristow, C.S., 1999. Avulsion and Crevassing in the sandy, braided Niobrara River: complex response to base-level rise and aggradation. In: Smith, N. D., and Rogers, J., (Eds), Fluvial Sedimentology VI Special Publication 28 of the International Association of Sedimentologists, 179-191.

Fabuel-Perez I., Redfern J., and Hodgetts D., 2009. Sedimentology of an intra-montane rift-controlled fluvial dominated succession: The Upper Triassic Oukaimeden Sandstone Formation, Central High Atlas, Morocco. Sedimentary Geology 218, 103-140.

Fabuel-Perez I., Hodgetts D., and Redfern J., 2009. A new approach for outcrop characterization and geostatistical analysis of a low-sinuosity fluvial-dominated succession using digital outcrop models: Upper Triassic Oukaimeden Sandstone Formation, central High Atlas, Morocco. AAPG Bulletin 93, 795-827.

Farrell, K.M., 1987. Sedimentology and facies architecture of overbank deposits of the Mississippi River, False River region, Louisiana. In F.G. Ethridge, R.M. Flores, J.D. Harvey (Editors), Recent Developments in Fluvial Sedimentology. Special Publication Society Economics Palaeontology Minerals 39, 111-120.

Farrell, K.M., 2001. Geomorphology, facies architecture, and high-resolution, non-marine sequence stratigraphy in avulsion deposits, Cumberland Marshes, Saskatchewan. Sedimentary Geology 139, 93-150.

Feng Z. Q., 2000. An investigation of fluvial geomorphology in the Quaternary of the Gulf of Thailand, with implications for river classification. Unpublished PhD Thesis, University of Reading, Reading, UK.

Fielding, C.R., 1986. Fluvial channel and overbank deposits from the Westphalian of the Durham coalfield, NE England. Sedimentology 33, 119-140.

Fielding, C.R., 1987. Coal depositional models for deltaic and alluvial plain sequences. Geology 15, 661-664.

Fisher, D.J., 1936, The Book Cliffs coal field in Emery and Grand Counties, Utah: U.S. Geological Survey Bulletin 852, 104 pp.

Fisher, J.A., Nichols, G.J. and Waltham, D.A., 2007. Unconfined flow deposits in distal sectors of fluvial distributary systems: examples from the Miocene Luna and Huesca Systems, northern Spain. Sedimentary Geology 195, 55-73.

Fisher, J.A., Krapf, C.B.E., Lang, S.C., Nichols, G.J., and Payenberg, T.H.D., 2008, Sedimentology and architecture of the Douglas Creek terminal splay, Lake Eyre, central Australia: Sedimentology 55, 1915-1930.

Fillmore, R., 2010. Geological Evolution of the Colorado Plateau of Eastern Utah and Western Colorado, Including the San Juan River, Natural Bridges, Canyonlands, Arches, and the Book Cliffs. University of Utah Press.

Flores R. M., and Stricker G. D., 1993. Early Cenozoic depositional systems, Wishbone Hill District, Matanuska coal field, Alaska. In: Dusel-Bacon C., Till A.

B. (eds.) Geologic Studies in Alaska by the Geological Survey, 1992. USGS Bulletin 2068, 101-117.

Florsheim, J.L., and Mount, J.F., 2002. Restoration of floodplain topography by sand-complex formation in response to intentional levee breaches, Lower Cosumnes River, California. Geomorphology 44, 67-94.

Ford, G.L., and Pyles, D.R., 2014. A hierarchical approach for evaluating fluvial systems: Architectural analysis and sequential evolution of the high net-sand content, middle Wasatch Formation, Uinta Basin, Utah. AAPG Bulletin, 98, 1273-1304.

Franczyk, K.J., Pitman, J.K., and Nichols, D.J., 1990. Sedimentology, mineralogy, palynology, and depositional history of some uppermost Cretaceous and lowermost Tertiary rocks along the Utah Book and Roan Cliffs east of the Green River, US Government Printing Office. USGS Bulletin, 1-27.

Franke, D., Hornung, J., and Hinderer, M., 2015. A combined study of radar facies, lithofacies and three-dimensional architecture of an alpine alluvial fan (Illgraben fan, Switzerland). Sedimentology 62, 57-86.

Frazier, D.E., 1967. Recent deltaic deposits of the Mississippi River: their development and chronology. Transactions of the Gulf Coast Association of Geological Societies 17, 287-315.

Fricke, H.C., Foreman, B.Z. and Sewall, J.O., 2010. Integrated climate model-oxygen isotope evidence for a North American monsoon during the Late Cretaceous. Earth and Planetary Science Letters 289, 11-21.

Friend, P., Slater, M., and Williams, R., 1979. Vertical and lateral building of river sandstone bodies, Ebro Basin, Spain. Journal of the Geological Society 136, 39-46.

Friend, P.F., 1983: Towards the field classification of alluvial architecture or sequence, in J.D. Collinson and J. Lewin, (Eds), Modern and ancient fluvial systems, Internat. Assoc. Sedimentologists Special Publication 6, 345- 354.

Gates, T.A., Scheetz, R., 2015. A new saurolophine hadrosaurid (Dinosauria: Ornithopoda) from the Campanian of Utah, North America. Journal of Systematic Palaeontology 13, 711-725.

Ghazi, S., Mountney, N.P., 2009. Facies and architectural element analysis of a meandering fluvial succession: the Permian Warchha Sandstone, Salt Range, Pakistan. Sedimentary Geology 221, 99-126.

Ghazi, S., and Mountney, N.P., 2011. Petrography and provenance of the Early Permian fluvial Warchha Sandstone, Salt Range, Pakistan. Sedimentary Geology 233, 88-110.

Geehan, G., and Underwood, J., 1993. The use of length distributions in geological modelling. In: Flint, S.S., Bryant, I.D. (Eds.), The Geological Modelling of Hydrocarbon Reservoirs and Outcrop Analogues. International Association of Sedimentologists Special Publication 15, 205-212.

Gersib, G.A., and McCabe, P.J., 1981. Continental coal-bearing sediments of the Port Hood Formation (Carboniferous), Cape Linzee, Nova Scotia, Canada,

in: Flores, R.M., Ethridge, F.G. (Eds.), Recent and Ancient Non-Marine Depositional Environments: Models for Exploration. SEPM, 95-108.

Gingras, M. K., Maceachern, J. A. and Dashtgard, S. E. 2011. Process ichnology and the elucidation of physico-chemical stress. Sedimentary Geology 237, 115-134.

Ghinassi M., Billi P., Libsekal Y., Papini M., and Rook L., 2013. Inferring fluvial morphodynamics and overbank flow control from 3D outcrop sections of a Pleistocene point bar, Dandiero Basin, Eritrea. Journal Sedimentary Research 83, 1066-1084.

Goldhammer, R.K., 1978. Mixed siliciclastic and carbonate sedimentation. In Sedimentology 724-732. Springer Berlin Heidelberg.

Goldstrand, P.M., 1994. Tectonic development of Upper Cretaceous to Eocene strata of Southwestern Utah. Geological Society of America Bulletin 106, 145-154.

Goodwin, P.W. and Anderson, E.J., 1985. Punctuated aggradational cycles: a general hypothesis of episodic stratigraphic accumulation. The Journal of Geology 93, 515-533.

Grundvåg, S.A., Johannessen, E.P., Helland-Hansen, W., and Plink-Björklund, P., 2014. Depositional architecture and evolution of progradationally stacked lobe complexes in the Eocene Central Basin of Spitsbergen. Sedimentology 61, 535-569.

Gugliotta, M., Flint, S.S., Hodgson, D.M., and Veiga, G.D., 2015. Stratigraphic record of river-dominated crevasse subdeltas with tidal influence (Lajas Formation, Argentina). Journal of Sedimentary Research 85, 265-284.

Gugliotta, M., Kurcinka, C.E., Dalrymple, R.W., Flint, S.S., and Hodgson, D.M., 2016. Decoupling seasonal fluctuations in fluvial discharge from the tidal signature in ancient deltaic deposits: an example from the Neuquén Basin, Argentina. Journal of the Geological Society 173, 94-107.

Gulliford, A.R., Flint, S.S., Hodgson, D.M., 2014. Testing applicability of models of distributive fluvial systems or trunk rivers in ephemeral systems: reconstructing 3-D fluvial architecture in the Beaufort Group, South Africa. Journal of Sedimentary Research 84, 1147–1169.

Gulliford, A.R., Flint, S.S. and Hodgson, D.M., 2017. Crevasse splay processes and deposits in an ancient distributive fluvial system: The lower Beaufort Group, South Africa. Sedimentary Geology 358, 1-18.

Hajek, E.A., Heller, P.L., and Sheets, B.A., 2010. Significance of channel-belt clustering in alluvial basins. Geology, 38, 535-538.

Hajek, E.A., Edmonds, D.A., 2014. Is river avulsion style controlled by floodplain morphodynamics? Geology 42, 199-202.

Hampson, G.J., Davies, W., Davies, S.J., Howell, J.A., Adamson, and K.R., 2005. Use of spectral gamma-ray data to refine subsurface fluvial stratigraphy: late Cretaceous strata in the Book Cliffs, Utah, USA. Journal of the Geological Society 162, 603-621.

Hampson, G.J., 2016. Towards a sequence stratigraphic solution set for autogenic processes and allogenic controls: Upper Cretaceous strata, Book Cliffs, Utah, USA. Journal of the Geological Society 173, 817-836.

Hampton, B.A., and Horton, B.K., 2007. Sheetflow fluvial processes in a rapidly subsiding basin, Altiplano plateau, Bolivia. Sedimentology 54, 1121-1147.

Hancock, J.M., and Kauffman, E.G., 1979. The great transgressions of the Late Cretaceous. Journal of the Geological Society, 136, 175-186.

Harms, J., 1975. Stratification produced by migrating bed forms, in: Harms, J., Southard, J., Spearing, D., Walker, R. (Eds.), Depositional Environments as Interpreted from Primary Sedimentary Structures and Stratification Sequences. SEPM, 45-61.

Hartley, A. J., Weissmann, G. S., Nichols, G. J., & Warwick, G. L. 2010. Large Distributive Fluvial Systems: Characteristics, distribution, and controls on development. Journal of Sedimentary Research, 80, 167-183.

Hartley, A. J., Owen, A., Swan, A., Weissmann, G. S., Holzweber, B. I., Howell, J., Nichols, G. and Scuderi, L., 2015. Recognition and importance of amalgamated sandy meander belts in the continental rock record. Geology 43, 679-682.

Hasiotis, S. T., 2004. Reconnaissance of Upper Jurassic Morrison Formation ichnofossils, Rocky Mountain Region, USA: paleoenvironmental, stratigraphic, and paleoclimatic significance of terrestrial and freshwater ichnocoenoses. Sedimentary Geology 167, 177-268.

Hein, T., Baranyi, C., Herndl, G.J., Wanek, W., and Schiemer, F., 2003. Allochthonous and autochthonous particulate organic matter in floodplains of the River Danube: the importance of hydrological connectivity. Freshwater Biology 48, 220-232.

Heller, P.L., Bowdler, S.S., Chambers, H.P., Coogan, J.C., Hagen, E.S. Shuster, M.W., and Winslow, N.S., 1986, Time of initial thrusting in the Sevier orogenic belt, Idaho–Wyoming and Utah: Geology 14, 388–391

Hettinger, R.D., Kirschbaum, M.A., 2002. Stratigraphy of the Upper Cretaceous Mancos Shale (upper part) and Mesaverde Group in the southern part of the Uinta and Piceance basins, Utah and Colorado, US Geological Survey. Pamphlet to accompany geologic investigations series i–2764.

Hettinger, R.D., Kirshbaum, M.A., 2003. Stratigraphy of the Upper Cretaceous Mancos Shale (Upper Part) and Mesaverde Group in the Southern Part of the Uinta and Piceance Basins, Utah and Colorado. USGS Uinta-Piceance Assessment Team, Comp., Petroleum Systems and Geologic Assessment of Oil and Gas in the Uinta-Piceance Province, Utah and Colorado. U.S. Geological Survey Digital Data Series DDS-69-B, pp. 1–16 .

Hirst J. P. P.,1991. Variations in alluvial architecture across the Oligo-Miocene Huesca fluvial system, Ebro Basin, Spain. In: Miall A. D., Tyler N. (eds.) The three-dimensional facies architecture of terrigenous clastic sediments and its

implications for hydrocarbon discovery and recovery. SEPM Concepts in Sedimentology and Paleontology. 3, 111-121.

Hjulström, F.,1939. Transportation of Debris by Moving Water. In: Recent Marine Sediments (Ed P.D. Trask), 5-31. AAPG, Tulsa, OK.

Holbrook, J., 2001. Origin, genetic interrelationships, and stratigraphy over the continuum of fluvial channel-form bounding surfaces: an illustration from middle Cretaceous strata, Southeastern Colorado. Sedimentary Geology, 144, 179-222.

Holbrook, J., Scott, R.W. and Oboh-Ikuenobe, F.E., 2006. Base-level buffers and buttresses: a model for upstream versus downstream control on fluvial geometry and architecture within sequences. Journal of Sedimentary Research 76, 162-174.

Holzförster F., Stollhofen H., and Stanistreet I. G., 1999. Lithostratigraphy and depositional environments in the Waterberg-Erongo area, central Namibia, and correlation with the main Karoo Basin, South Africa. Journal African Earth Science 29, 105-123.

Hornung, J., and Aigner, T., 1999. Reservoir and aquifer characterization of fluvial architectural elements: Stubensandstein, Upper Triassic, southwest Germany. Sedimentary Geology 129, 215-280.

Larue, D.K., and Hovadik, J., 2006. Connectivity of channelized reservoirs: a modelling approach. Petroleum Geoscience, 12, 291-308.

Huang, H.Q., and Nanson, G.C., 1998. The influence of bank strength on channel geometry: an integrated analysis of some observations. Earth Surface Processes and Landforms 23, 865-876.

Hubbard S. M., Smith D. G., Nielsen H., Leckie D. A., Fustic M., Spencer R. J., and Bloom L., 2011. Seismic geomorphology and sedimentology of a tidally influenced river deposit, Lower Cretaceous Athabasca oil sands, Alberta, Canada. AAPG Bulletin 95, 1123-1145.

Huber, B.T., Norris, R.D., and MacLeod, K.G., 2002. Deep-sea paleotemperature record of extreme warmth during the Cretaceous. Geology 30, 123-126

Ielpi A., and Ghinassi M., 2014. Planform architecture, stratigraphic signature and morphodynamics of an exhumed Jurassic meander plain (Scalby Formation, Yorkshire, UK). Sedimentology 61, 1923-1960.

Jablonski, B.V., and Dalrymple, R.W., 2016. Recognition of strong seasonality and climatic cyclicity in an ancient, fluvially dominated, tidally influenced point bar: Middle McMurray Formation, Lower Steepbank River, north-eastern Alberta, Canada. Sedimentology 63, 552-585.

Jain, V., Fryirs, K., and Brierley, G., 2008. Where do floodplains begin? The role of total stream power and longitudinal profile form on floodplain initiation processes. Geological Society of America Bulletin 120, 127-141.

Jerolmack, D.J., Paola, C., 2010. Shredding of environmental signals by sediment transport. Geophysical Research Letters 37, 1-5.

Jerrett, R.M., Flint, S.S., Davies, R.C., and Hodgson, D.M., 2011a. Sequence stratigraphic interpretation of a Pennsylvanian (Upper Carboniferous) coal from the central Appalachian Basin, USA. Sedimentology 58, 1180-1207.

Jerrett, R.M., Davies, R.C., Hodgson, D.M., Flint, S.S., and Chiverrell, R.C., 2011b. The significance of hiatal surfaces in coal seams. Journal of the Geological Society 168, 629-632.

Jerrett, R.M., Hodgson, D.M., Flint, S.S., Davies, R.C., 2011c. Control of Relative Sea Level and Climate on Coal Character in the Westphalian C (Atokan) Four Corners Formation, Central Appalachian Basin, USA. Journal of Sedimentary Research 81, 420-445.

Jo H. R., 2003. Depositional environments, architecture, and controls of Early Cretaceous non-marine successions in the northwestern part of Kyongsang Basin, Korea. Sedimentary Geology 161, 269-294.

Jobbágy, E.G. and Jackson, R.B., 2000. The vertical distribution of soil organic carbon and its relation to climate and vegetation. Ecological applications, 10, 423-436.

Jordan, T.E., 1981. Thrust loads and foreland basin evolution, Cretaceous, western United States. AAPG bulletin, 65, 2506-2520.

Jordan D. W., and Pryor W. A., 1992. Hierarchical levels of heterogeneity in a Mississippi River meander belt and application to reservoir systems. AAPG Bulletin 76, 1601-1624.

Jones, H., and Hajek, E., 2007. Characterizing avulsion stratigraphy in ancient alluvial deposits. Sedimentary Geology 202, 124-137.

Jones, L.S., and Harper, J.T., 1998. Channel avulsions and related processes, and large-scale sedimentation patterns since 1875, Rio Grande, San Luis Valley, Colorado. Geological Society of America Bulletin 110, 411-421.

Jones, L.S., and Schumm, S.A., 1999. Causes of avulsion: an overview. In Special Publications International Association of Sedimentologists 28, 171-178,

Jones B.G., and Rust B.R., 1983. Massive sandstone facies in the Hawkesbury sandstone, a Triassic fluvial deposit near Sydney, Australia. Journal of Sedimentary Petrology 53, 1249-1259.

Jones S. J., Frostick L. E., and Astin T. R., 2001. Braided stream and flood plain architecture: the Rio Vero Formation, Spanish Pyrenees. Sedimentary Geology 139, 229-260.

Karaman, O., 2012. Shoreline Architecture and Sequence Stratigraphy of Campanian Iles Clastic Wedge, Piceance Basin, CO: Influence of Laramide Movements in Western Interior Seaway. University of Texas at Austin, Texas, p. 137.

Keeton, G.I., Pranter, M.J., Cole, R.D., and Edmund, R., 2015. Stratigraphic architecture of fluvial deposits from borehole images, spectral-gamma-ray response, and outcrop analogs, Piceance Basin, Colorado. AAPG Bulletin 99, 1929-1956.

Keighley D., Flint S., Howell J., and Moscariello A., 2003. Sequence stratigraphy in lacustrine basins: a model for part of the Green River Formation (Eocene), southwest Uinta Basin, Utah, USA. Journal Sedimentary Research 73, 987-1006.

Keller, E.A., and Swanson, F.J., 1979. Effects of large organic material on channel form and fluvial processes. Earth Surface Processes 4, 361-380.

Kelly, S. B., and Olsen, H., 1993. Terminal fans - a review with reference to Devonian examples. Sedimentary Geology, 85, 339-374.

Keogh, K.J., Martinius, A.W., and Osland, R., 2007. The development of fluvial stochastic modelling in the Norwegian oil industry: A historical review, subsurface implementation and future directions. Sedimentary Geology 202, 249-268.

Kirk M., 1983. Bar development in a fluvial sandstone (Westphalian 'A'), Scotland. Sedimentology 30, 727-742.

Kirschbaum, M.A., and Hettinger, R.D., 2004. Facies analysis and sequence stratigraphic framework of Upper Campanian Strata (Neslen and Mount Garfield Formations, Bluecastle Tongue of the Castlegate Sandstone, and Mancos Shale), Eastern Book Cliffs, Colorado and Utah. U.S. Geological Survey, U.S. Geological Survey Digital Data Report DDS-69-G

Kocurek, G., 1981. Significance of interdune deposits and bounding surfaces in aeolian dune sands. Sedimentology 28, 753-780.

Kraus, M.J., 1987. Integration of channel and floodplain suites, II. Vertical relations of alluvial paleosols. Journal of Sedimentary Research 57, 602-612.

Kraus M. J., 1996. Avulsion deposits in lower Eocene alluvial rocks, Bighorn Basin, Wyoming. Journal Sedimentary Research 66, 354-363.

Kraus, M.J., 1999. Palaeosols in clastic sedimentary rocks: their geologic applications. Earth-Science Reviews 47, 41-70.

Kraus, M. J. and Aslan, A. 1993. Eocene hydromorphic paleosols: significance for interpreting ancient floodplain processes. Journal of Sedimentary Research 63, 453-463.

Kraus M. J., Davies-Vollum K. S., 2004. Mudrock-dominated fills formed in avulsion splay channels: examples from the Willwood Formation, Wyoming. Sedimentology 51, 1127-1144.

Kraus M. J., and Middleton L. T.,1987. Contrasting architecture of two alluvial suites in different structural settings. In: Ethridge F. G., Flores R. M., Harvey M. D. (eds.) Recent Developments in Fluvial Sedimentology, SEPM Spec. Publ. 39, 253-262.

Lang, S.C., Payenberg, T.H.D., Reilly, M.R.W., Hicks, T., Benson, J. and Kassan, J., 2004. Modern analogues for dryland sandy fluvial-lacustrine deltas and terminal splay reservoirs. The APPEA Journal, 44,329-356.

Lawton, T.F., 1986. Fluvial systems of Upper Cretaceous Mesaverde Group and Paleocene North Horn formation, central Utah: A record of transition from thin-skinned deformation in foreland region, in: J.A. Peterson, ed.,

Paleotectonics and sedimentation in the Rocky Mountain region, United States: American Association of Petroleum Geologists Memoir 41, 423-442.

Lawton, T.F., 1994, Tectonic setting of Mesozoic sedimentary basins, Rocky Mountain region, United States, in Caputo, M.V., Peterson, J.A., and Franczyk, K.J., eds., Mesozoic Systems of the Rocky Mountain Region, USA: SEPM, Rocky Mountain Section, p. 1–25.

Leddy, J.O., Ashworth, P.J., and Best, J.L., 1993. Mechanisms of anabranch avulsion within gravel-bed braided rivers: observations from a scaled physical model. Geological Society, London, Special Publications, 75, 119-127.

Leeder, M.R., 1983, On the dynamics of sediment suspension by residual Reynolds stresses—confirmation of Bagnold's theory: Sedimentology, v. 30, p. 485-491.

Leeder, M.R., 1993. Tectonic controls upon drainage basin development, river channel migration and alluvial architecture: implications for hydrocarbon reservoir development and characterization. Geological Society, London, Special Publications 73, 7-22.

Leeder, M.R., and Stewart, M.D., 1996. Fluvial incision and sequence stratigraphy: alluvial responses to relative sea-level fall and their detection in the geological record. Geological Society, London, Special Publications 103, 25-39.

Leeder, M. R., 2011. Tectonic sedimentology: sediment systems deciphering global to local tectonics. Sedimentology 58, 2-56.

Leopold, L.B., Wolman, M.G., Miller J.P., 1995. Fluvial processes in geomorphology, Courier Dover Publications, 544 pp.

Li, J., Donselaar, M.E., Hosseini Aria, S.E., Koenders, R. and Oyen A.M., 2014. Landsat imagery-based visualization of the geomorphological development at the terminus of a dryland river system. Quaternary International 352, 100-110.

Li, J., and Bristow, C.S., 2015. Crevasse splay morphodynamics in a dryland river terminus: Río Colorado in Salar de Uyuni Bolivia. Quaternary International 377, 71-82.

Limarino C., Tripaldi A., Marenssi S., Net L., Re G., and Caselli A., 2001. Tectonic control on the evolution of the fluvial systems of the Vinchina Formation (Miocene), northwestern Argentina. Journal South America Earth Science 14, 751-762.

Longhitano, S.G., and Steel, R.J., 2016. Deflection of the progradational axis and asymmetry in tidal seaway and strait deltas: insights from two outcrop case studies. Geological Society, London, Special Publications 444- 448

MacDonald, H.A., Peakall, J., Wignall, P.B., and Best, J., 2011. Sedimentation in deep-sea lobe-elements: implications for the origin of the thickening-upward sequences. Journal of the Geological Society London 168, 319-331.

Mack, G.H., James, W.C., and Monger, H.C., 1993. Classification of palaeosols. Geological Society of America Bulletin 105, 129-136.

Mack, G.H. and James, W.C., 1994. Paleoclimate and the global distribution of paleosols. The Journal of Geology, 102, 360-366.

Makaske, B., Maathuis, B.H., Padovani, C.R., Stolker, C., Mosselman, E., and Jongman, R.H., 2012. Upstream and downstream controls of recent avulsions on the Taquari megafan, Pantanal, south-western Brazil. Earth Surface Processes and Landforms 37, 1313-1326.

Marconato, A., De Almeida, R.P., Turra, B.B., and Fragoso-Cesar, A.R.D.S., 2014. Pre-vegetation fluvial floodplains and channel-belts in the Late Neoproterozoic–Cambrian Santa Bárbara group (Southern Brazil). Sedimentary Geology 300, 49-61.

Maynard J. R., Feldman H. R., and Alway R., 2010. From bars to valleys: the sedimentology and seismic geomorphology of fluvial to estuarine incised-valley fills of the Grand Rapids Formation (Lower Cretaceous), Iron River Field, Alberta, Canada. Journal Sedimentary Research 80, 611-638.

McCabe, P.J., 1987. Facies studies of coal and coal-bearing strata. In: Scott, A.C. (Ed.), Coal and Coal-bearing Strata: Recent Advances. Geological Society of London, Special Publications 32, 51-66.

Mccabe, P.J, and Shanley, K.W., 1992. Organic control on shoreface stacking patterns: Bogged down in the mire. Geology 20, 741-744.

McLaurin, B.T., and Steel, R.J., 2007. Architecture and origin of an amalgamated fluvial sheet sand, lower Castlegate Sandstone, Book Cliffs, and Utah. Sedimentary Geology 197, 291-311.

McKie, T., 2011. Architecture and Behavior of Dryland Fluvial Reservoirs , Triassic Skagerrak Formation, Central North Sea. In: Davidson, S.K., Leleu, S., North, C.P. (Eds.), From River to Rock Record: the Preservation of Fluvial Sediments and their Subsequent Interpretation. SEPM Special Publication vol. 97, 189–214.

Miall, A.D., 1978. Lithofacies types and vertical profile models in braided river deposits: a summary, in: Miall A.D., (Ed.) Fluvial Sedimentology. Canadian Society of Petroleum Geology Memoir 5, 597–604.

Miall, A.D., 1985. Architectural-element analysis: a new method of facies analysis applied to fluvial deposits. Earth-Science Reviews 22, 261-308.

Miall, A.D., 1988. Facies architecture in clastic sedimentary basins. In: Kleinspehn, K., Paola, C. (Eds.), New Perspectives in Basin Analysis. Springer, Berlin-Heilderberg, New York, .67-81.

Miall, A.D., 1993. The architecture of fluvial-deltaic sequences in the upper Mesaverde Group (Upper Cretaceous), Book Cliffs, Utah. In: Best, J.L., Bristow, C. (Eds.), Braided Rivers. Geological Society of London, Special Publications 75, 305-332.

Miall, A.D., 1994. Reconstructing fluvial macroform architecture from two-dimensional outcrops: examples from the Castlegate Sandstone, Book Cliffs, Utah. Journal of Sedimentary Research 64, 146-158.

Miall, A.D., 1996. The Geology of Fluvial Deposits. Springer, Berlin.

Miall, A.D., 2014. Fluvial Depositional Systems, Springer, Berlin.

Miall, A. D., and Turner-Peterson C. E., 1989. Variations in fluvial style in the Westwater Canyon Member, Morrison Formation (Jurassic), San Juan Basin, Colorado Plateau. Sedimentary Geology 63, 21-60.

Miller, M., McCave, I., Komar, P., 1977. Threshold of sediment motion under unidirectional currents. Sedimentology 24, 507-527.

Miller, I.M., Johnson, K.R., Kline, D.E., 2013. A Late Campanian flora from the Kaiparowits, in: Titus, A.L., Loewen, M.A. (Eds.), At the Top of the Grand Staircase: The Late Cretaceous of Southern Utah. Indiana University Press, Bloomington, 107-131.

Mjøs, R., Walderhaug, O., and Prestholm, E., 1993. Crevasse splay sandstone geometries in the Middle Jurassic Ravenscar Group of Yorkshire, UK. In: Marzo, M., Puigdefabregas, C. (Eds), Alluvial Sedimentation. International Association of Sedimentologists, Special Publication 17, pp.167-184.

Mohrig, D., Heller, P.L., Paola, C., and Lyons, W.J, 2000. Interpreting avulsion process from ancient alluvial sequences: Guadalope-Matarranya system (northern Spain) and Wasatch Formation (western Colorado). Geological Society of America Bulletin 112, 1787-1803.

Morozova, G.S., and Smith, N.D., 2000. Holocene avulsion styles and sedimentation patterns of the Saskatchewan River, Cumberland Marshes, Canada. Sedimentary Geology 130, 81-105.

Morozova, G.S., and Smith, N.D., 2003. Organic matter deposition in the Saskatchewan River floodplain (Cumberland Marshes, Canada): effects of progradational avulsions. Sedimentary Geology 157, 15-29.

Morris, E.A., Hodgson, D.M., Flint, S.S., Brunt, R.L., Butterworth, P.J., and Verhaeghe, J., 2014. Sedimentology, Stratigraphic Architecture, and Depositional Context of Submarine Frontal-Lobe Complexes. Journal of Sedimentary Research 84, 763-780.

Moss, A.J., 1972, Bed-load sediments: Sedimentology, 18, p. 159-219.

Mullens, T. E., and Freeman, V . L., 1957. Lithofacies of the SaltWash Member of the Morrison Formation, Colorado Plateau. Geological Society of America Bulletin, 68, 505-526.

Mutti, E. and Sonnino, M., 1981. Compensation cycles: a diagnostic feature of turbidite sandstone lobes. International Association of Sedimentologists, 2nd European Meeting, Bologna, Abstracts 120-123.

Muto, T. and Steel, R.J., 1997. Principles of regression and transgression: the nature of the interplay between accommodation and sediment supply. Journal Sedimentary Research 67, 994-1000.

Muto, T., Steel, R.J., and Swenson, J.B., 2007. Autostratigraphy: a framework norm for genetic stratigraphy. Journal of Sedimentary Research 77,2-12.

Nadon, G.C., 1998. Magnitude and timing of peat-to-coal compaction. Geology 26, 727-730.

Nanson, G., and Croke, J., 1992. A genetic classification of floodplains. Geomorphology 4, 459-486.

Nichols, G.J., and Fisher, J.A., 2007. Processes, facies and architecture of fluvial distributary system deposits. Sedimentary Geology 195, 75-90.

North, C.P. and Davidson, S.K., 2012. Unconfined alluvial flow processes: recognition and interpretation of their deposits, and the significance for palaeogeographic reconstruction. Earth-Science Reviews, 111, 199-223.

North, C. P., and Warwick, G. L. 2007. Fluvial Fans: Myths, misconceptions, and the end of the terminal-fan model. Journal of Sedimentary Research 77, 693-701.

O'Brien, P., and Wells, A., 1986. A small, alluvial crevasse splay. Journal of Sedimentary Petrology 56, 876-879.

O'Brien, K.C., 2015. Stratigraphic architecture of a shallow-water delta deposited in a coastal-plain setting: Neslen Formation, Floy Canyon, Utah. Colorado School of Mines. Arthur Lakes Library, p. 77.

Olsen H., 1989. Sandstone-body structures and ephemeral stream processes in the Dinosaur Canyon Member, Moenave Formation (Lower Jurassic), Utah, U.S.A. Sedimentary Geology 61, 207-221.

Olsen, T., Steel, R., Hogseth, K., Skar, T., and Roe, S.L., 1995. Sequential architecture in a fluvial succession: sequence stratigraphy in the Upper Cretaceous Mesaverde Group, Price Canyon, Utah. Journal of Sedimentary Research, Section B: Stratigraphy and Global Studies 65B, 265-280.

Opluštil S., Martínek K., and Tasáryová Z., 2005. Facies and architectural analysis of fluvial deposits of the Nýrany Member and the Týnec Formation (Westphalian D – Barruelian) in the Kladno-Rakovník and Pilsen basins. Bull. Geoscience. 80, 45-66.

Owen, G., 1978. Deformation processes in unconsolidated sands. In: Jones, M.E., Preston R.M.F. (Eds), Deformation of sediments and sedimentary rocks. Geological Society of London Special Publications 29, pp.11-24.

Owen, G., 1996. Experimental soft-sediment deformation: structures formed by the liquefaction of unconsolidated sands and some ancient examples. Sedimentology 43, 279-293.

Owen, G., and Santos, M.G., 2014. Soft-sediment deformation in a pre-vegetation river system: the Neoproterozoic Torridonian of NW Scotland. Proceedings of the Geologists' Association 125, 511-523.

Owen, A., Nichols, G.J., Hartley, A.J., Weissmann, G. S., and Scuderi, L. A., 2015. Quantification of a Distributive Fluvial System: The Salt Wash DFS of the Morrison Formation, SW USA. Journal of Sedimentary Research 85, 544-561.

Parrish, J.T., Peterson, F. and Turner, C.E., 2004. Jurassic “savannah”—plant taphonomy and climate of the Morrison Formation (Upper Jurassic, Western USA). Sedimentary Geology, 167, 137-162.

Peterson, F., 1980. Sedimentology of the Uranium-bearing Salt Wash Member and Tidwell unit of the Morrison Formation in the Henry and Kaiparowits Basin, Utah. Pages 305-322 of: Utah Geological Association Publication 8, Henry Mountains Symposium.

Peterson, F., 1986. Jurassic Paleotectonics in the west-central part of the Colorado Plateau, Utah and Arizona. Pages 563-596 of: Paleotectonics and sedimentation in the Rocky Mountain Region, United States.

Peterson, F., 1988. Revisions to stratigraphic nomenclature of Jurassic and Cretaceous rocks of the Colorado Plateau: United States Geological Survey Bulletin 1633-B, 17-56.

Petersen, H.I., and Andsbjerg, J., 1996. Organic facies development within Middle Jurassic coal seams, Danish Central Graben, and evidence for relative sea-level control on peat accumulation in a coastal plain environment. Sedimentary Geology 106, 259-277.

Perez-Arlucea, M., and Smith, N.D., 1999. Depositional patterns following the 1870s avulsion of the Saskatchewan River (Cumberland marshes, Saskatchewan, Canada). Journal of Sedimentary Research 69, 62-73.

Pickering, K.T., and Clark, J.D., 1996. Architectural elements and growth patterns of submarine channels: application to hydrocarbon exploration. AAPG Bulletin 80, 194–221.

Pitman, J.K., Franczyk, K.J., and Anders, D.E., 1987. Marine and Nonmarine gas-bearing rocks in Upper Cretaceous Neslen and Blackhawk formations, Eastern Uinta Basin, Utah-Sedimentology, Diagenesis, and Source rock potential. AAPG Bulletin 70, 1052-1052.

Platt, N.H., and Keller, B., 1992. Distal alluvial deposits in a foreland basin setting—the Lower Freshwater Miocene), Switzerland: sedimentology, architecture and palaeosols. Sedimentology 39, 545-565.

Plint, A.G., Hart, B.S., and Donaldson, W.S., 1993. Lithospheric flexure as a control on stratal geometry and facies distribution in Upper Cretaceous rocks of the Alberta foreland basin. Basin Research 5, 69-77.

Postma, G., 2014. Generic autogenic behaviour in fluvial systems: lessons from experimental studies. Depositional Systems to Sedimentary Successions on the Norwegian Continental Margin (IAS SP 46) 46, 1-18.

Pranter, M.J., Vargas, M.F., and Davis, T.L., 2008. Characterization and 3D reservoir modelling of fluvial sandstones of the Williams Fork Formation, Rulison Field, Piceance Basin, Colorado, USA. Journal of Geophysics and Engineering 5, 158–172.

Pranter, M.J., Cole, R.D., Panjaitan, H., and Sommer, N.K., 2009. Sandstone-body dimensions in a lower coastal-plain depositional setting: lower Williams Fork Formation, Coal Canyon, Piceance Basin, Colorado. AAPG bulletin, 93, 1379-1401.

Prélat, A., Hodgson, D., and Flint, S., 2009. Evolution, architecture and hierarchy of distributary deep-water deposits: a high-resolution outcrop

investigation from the Permian Karoo Basin, South Africa. Sedimentology 56, 2132-2154.

Prélat, A., and Hodgson, D.M., 2013. The full range of turbidite bed thickness patterns in submarine lobes: controls and implications. Journal of Geological Society of London 170, 1-6.

Rasmussen A. M. S., 2005. Reservoir characterization of a fluvial sandstone: depositional environment and heterogeneities in modeling of the Colton Formation, Utah. Unpublished MSc Thesis, University of Oslo, Norway.

Reijenstein H.M., Posamentier H.W., and Bhattacharya J.P., 2011. Seismic geomorphology and high-resolution seismic stratigraphy of inner-shelf fluvial, estuarine, deltaic, and marine sequences, Gulf of Thailand. AAPG Bulletin. 95, 1959-1990.

Retallack, G.J., 1988. Field recognition of palaeosols. Geological Society of America Special Papers 216, 1-20.

Retallack, G.J., 2001. Soils of the Past: An Introduction to Paleopedology. John Wiley and Sons, 420 pp.

Reynolds A. D., 1999. Dimensions of paralic sandstone bodies. AAPG Bulletin 83, 211-229.

Roberts E. M., 2007. Facies architecture and depositional environments of the Upper Cretaceous Kaiparowits Formation, southern Utah. Sedimentary Geology 197, 207-233.

Roberts and L.N., Kirschbaum, M.A., 1995. Paleogeography of the Late Cretaceous of the Western Interior of Middle North America-coal distribution and Sediment accumulation. USGS Professional Paper 1561, 1-65.

Robinson, J.W., and McCabe, P. J. 1997. Sandstone-body and shale-body dimensionsin a braided fluvial system : Salt Wash Sandstone Member (Morrison Formation), Garfield County , Utah. AAPG Bulletin 8, 1267-1291.

Robinson, J. W., and McCabe, P. J. 1998. Evolution of a braided river system: The Salt Wash Member of the Morrison Formation (Jurassic) in southern Utah. Pages 93-107 of: Shanley, K. W., & McCabe, P. J. (eds), Relative Role of Eustasy, Climate, and Tectonism in Continental Rocks. SEPM Special Publication No 59. Tulsa, Oklahoma: Society of Economic Paleontologists and Mineralogists.

Rossetti, D.F., and Santos, A.E., 2003. Events of sediment deformation and mass failure in Upper Cretaceous estuarine deposits (Cametá Basin, northern Brazil) as evidence for seismic activity. Sedimentary Geology 161, 107-130.

Royse, F., 1993, Case of the phantom foredeep: Early Cretaceous in west-central Utah: Geology, v. 21, p. 133–136.

Rozovskii, I.L., 1957. Flow of Water in Bends of Open Channels. Academy of Sciences of the Ukrainian SSR (translated from Russian by the Israel Program for Scientific Translations, Jerusalem, 1961), Kiev, 233pp.

Rubin, D.M., 1987. Formation of scalloped cross-bedding without unsteady flows. Journal of Sedimentary Research 57, 39–45.

Rubin, D. M. and Carter, C. L. 2006. Bedforms and cross-bedding in animation, Sepm Society for Sedimentary.

Rygel M. C., and Gibling M. R., 2006. Natural geomorphic variability recorded in a high-accommodation setting: fluvial architecture of the Pennsylvanian Joggins Formation of Atlantic Canada. Journal Sedimentary Research 76, 1230-1251.

Ryer, T.A., and McPhillips, M., 1983. Early Late Cretaceous paleogeography of east-central Utah. Rocky Mountain Section (SEPM).

Sahoo, H., Gani, M.R., Hampson, G.J., Gani, N.D., and Ranson, A., 2016. Facies-to sandbody-scale heterogeneity in a tight-gas fluvial reservoir analog: Blackhawk Formation, Wasatch Plateau, Utah, USA. Marine and Petroleum Geology 78, 48-69.

Sánchez-Moya Y., Sopeña A., Ramos A. (1996) Infill architecture of a nonmarine half-graben Triassic basin (Central Spain). Journal Sedimentary Research 66, 1122-1136.

Saward, S.A., 1992. A global view of Cretaceous vegetation patterns. Geological Society of America Special Papers, 267, .17-36.

Schumm, S.A., 1963. Sinuosity of alluvial rivers on the Great Plains. Geological Society of America Bulletin 74, 1089-1100.

Schumm, S.A., 1972, Fluvial paleochannels: The Society of Economic Paleontologists and Mineralogists (SEPM), v. 16, p. 98-107.

Sethi, P.S., and Leithold, E.L., 1994. Climatic cyclicity and terrigenous sediment influx to the early Turonian Greenhorn Sea, southern Utah. Journal of Sedimentary Research, 64.

Shanley, K.W., Mccabe, P.J., and Hettinger, R.D., 1992. Tidal influence in Cretaceous fluvial strata from Utah, USA: a key to sequence stratigraphic interpretation. Sedimentology 39, 905-930.

Shanley, K.W., and McCabe, P.J., 1994. Perspectives on the Sequence Stratigraphy of Continental Strata. AAPG Bulletin 78, 544-568.

Shen, Z., Törnqvist, T.E., Mauz, B., Chamberlain, E.L., Nijhuis, A.G., and Sandoval, L., 2015. Episodic overbank deposition as a dominant mechanism of floodplain and delta-plain aggradation. Geology 43, 875-878.

Shiers, M.S., Mountney, N.P., Hodgson, D.M., and Cobain, S.L., 2014. Depositional controls on tidally influenced fluvial successions, Neslen Formation, Utah, USA. Sedimentary Geology 311, 1-16.

Shiers, M.S., Hodgson, D.M., Mountney, N.P., 2017. Response of a coal-bearing coastal plain succession to marine transgression: Campanian Neslen Formation, Utah, U.S.A. Journal of Sedimentary Research 87, 168-187.

Shiers, M.S., 2017. Controls on the deposition, accumulation and preservation of mixed fluvial and marginal-marine successions in coastal-plain settings. Unpublished PhD thesis, University of Leeds, Leeds.

Slingerland, R., and Smith, N.D., 2004. River avulsions and their deposits. Annual Review of Earth and Planetary Sciences 32, 257-285.

Sloss, l.L., 1962. Stratigraphic models in exploration. AAPG Bulletin 46, 1050-1057.

Smith R. M. H., 1987. Morphology and depositional history of exhumed Permian point bars in the southwestern Karoo, South Africa. Journal Sedimentary Petroleum 57, 19-29.

Smith, N.D., and Cross, T.A., Dufficy, J.P., Clough, S.R., 1989. Anatomy of an avulsion. Sedimentology 36, 1-23.

Smith, N.D., and Perez-Arlucea, M., 1994. Fine-grained splay deposition in the avulsion belt of the lower Saskatchewan River, Canada. Journal of Sedimentary Research 64, 159-168.

Smith, N.D., and Pérez-Arlucea, M., 2004. Effects of peat on the shapes of alluvial channels: examples from the Cumberland Marshes, Saskatchewan, Canada. Geomorphology 61, 323-335.

Sprague, A.R., Sullivan, M.D., Campion, K.M., Jensen, G.N., Goulding, F.J., Garfield, T.R., Sickafoose, D.K., Rossen, C., Jennette, D.C., Beaubouef, R.T., Abreu, V., Ardill, J., Porter, M.L. and Zelt, F.B., 2003. The physical stratigraphy of deepwater strata: a hierarchical approach to the analysis of genetically related stratigraphic elements for improved reservoir prediction (Abstract) AAPG Annual Meeting. AAPG Bulletin 87, 1.

Staub, J.R., and Cohen, A.D., 1979. The Snuggedy Swamp of South Carolina: a back-barrier estuarine coal-forming environment. Journal of Sedimentary Petrology 49, 133-143.

Steel R. J., and Thompson D. B., 1983. Structures and textures in Triassic braided stream conglomerates ('Bunter' Pebble Beds) in the Sherwood Sandstone Group, North Staffordshire, England. Sedimentology 30, 341-367.

Stewart D. J., 1983. Possible suspended-load channel deposits from the Wealden Group (Lower Cretaceous) of Southern England. In: Collinson J. D., Lewin J. (eds.) Modern and ancient fluvial systems. IAS Special Publication 6, 369-384.

Stouthamer, E., and Berendsen, H.J.A., 2007. Avulsion: the relative roles of autogenic and allogenic processes. Sedimentary Geology 198, 309-325.

Straub, K.M., Paola, C., Mohrig, D., Wolinsky, M.A., and George, T., 2009. Compensational stacking of channelized sedimentary deposits. Journal of Sedimentary Research 79, 673-688.

Straub, K.M., and Wang, Y., 2013. Influence of water and sediment supply on the long-term evolution of alluvial fans and deltas: Statistical characterization of basin-filling sedimentation patterns. Journal of Geophysical Research: Earth Surface 118, 1602-1616.

Stow, D.A., and Mayall, M., 2000. Deep-water sedimentary systems: new models for the 21st century. Marine and Petroleum Geology 17, 125-135.

Stuart, J.Y., Mountney, N.P., McCaffrey, W.D., Lang, S.C., and Collinson, J.D., 2014. Prediction of channel connectivity and fluvial style in the flood-basin successions of the Upper Permian Rangal coal measures (Queensland). AAPG Bulletin 98, 191-212

Stuart, J.Y., 2015. Subsurface Architecture of Fluvial-Deltaic Deposits in High- and Low-Accommodation Settings, School of Earth and Environment. University of Leeds, pp. 346.

Taylor, A.M. and Goldring, R., 1993. Description and analysis of bioturbation and ichnofabric. Journal of the Geological Society 150, 141-148.

Ten Brinke, W., Schoor, M.M., Sorber, A.M., and Berendsen, H.J., 1998. Overbank sand deposition in relation to transport volumes during large-magnitude floods in the Dutch sand-bed Rhine river system. Earth Surface Processes and Landforms 23, 809-824.

Thorne, C.R., Zevenbergen, L.W., Pitlick, J.C., Rais, S., Bradley, J.B.,and Julian, P.Y., 1988. Direct measurement of secondary currents in a meandering sand-bed river. Nature 316, 746–747.

Tooth, S., 2005. Splay formation along the lower reaches of ephemeral rivers on the Northern Plains of arid central Australia. Journal of Sedimentary Research, 75, 636-649.

Toonen, W.H., Kleinhans, M.G., and Cohen, K.M., 2012. Sedimentary architecture of abandoned channel fills. Earth Surface Processes and Landforms 37, 459-472.

Toonen, W.H., Asselen, S., Stouthamer, E., and Smith, N.D., 2015. Depositional development of the Muskeg Lake crevasse splay in the Cumberland Marshes (Canada). Earth Surface Processes and Landforms 37, 459-472.

Törnqvist, T.E., and Bridge, J.S., 2002. Spatial variation of overbank aggradation rate and its influence on avulsion frequency. Sedimentology 49, 891-905.

Törnqvist, T.E., Wallace, D.J., Storms, J.E., Wallinga, J., Van Dam, R.L., Blaauw, M., Derksen, M.S., Klerks, C.J., Meijneken, C., and Snijders, E.M., 2008. Mississippi Delta subsidence primarily caused by compaction of Holocene strata. Nature Geoscience 1, 173-176.

Trendell A. M., Atchley S. C., and Nordt L. C., 2013. Facies analysis of a probable large-fluvial-fan depositional system: the Upper Triassic Chinle Formation at Petrified Forest National Park, Arizona, USA. Journal Sedimentary Research 83, 873-895.

Trudgill, B.D., 2011. Evolution of salt structures in the northern Paradox Basin: Controls on evaporite deposition, salt wall growth and supra-salt stratigraphic architecture. Basin Research 23, 208-238.

Tunbridge I., 1984. Facies model for a sandy ephemeral stream and clay playa complex; the Middle Devonian Trentishoe Formation of North Devon, UK. Sedimentology 31, 697-715.

Turner, C. E. and Peterson, F., 2004. Reconstruction of the Upper Jurassic Morrison Formation extinct ecosystem—a synthesis. Sedimentary Geology, 167, 309-355.

Tyler, N., and Ethridge, F. G., 1983. Depositional setting of the Saltwash Member of the Morrison Formation, southwest Colorado. SEPM Journal of Sedimentary Research, 53 67-82.

Vandenberghe, J., 2002. The relation between climate and river processes, landforms and deposits during the Quaternary. Quaternary International, 91, 17-23.

van Asselen, S., Stouthamer, E., and Van Asch, T.W., 2009. Effects of peat compaction on delta evolution: a review on processes, responses, measuring and modelling. Earth-Science Reviews 92, 35-51.

van Asselen, S., Stouthammer, E., and Smith, N.D., 2010. Factors Controlling Peat Compaction in Alluvial Floodplains: A Case Study in the Cold-Temperate Cumberland Marshes, Canada. Journal of Sedimentary Research 80, 155-166.

van Dijk, M., Postma, G., and Kleinhans, M.G., 2009. Autocyclic behaviour of fan deltas: An analogue experimental study. Sedimentology 56, 1569-1589.

van Dijk, M., Lageweg, W.I., and Kleinhans, M.G., 2013. Formation of a cohesive floodplain in a dynamic experimental meandering river. Earth Surface Processes and Landforms 38, 1550-1565.

van Toorenenburg, K.A., Donselaar, M.E., Noordijk, N.A., and Weltje, G.J., 2016. On the origin of crevasse-splay amalgamation in the Huesca fluvial fan (Ebro Basin, Spain): Implications for connectivity in low net-to-gross fluvial deposits. Sedimentary Geology 343, 156-164.

van Wagoner, J.C., Mitchum, R.M., Campion, K.M. and Rahmanian, V.D., 1990. Siliciclastic sequence stratigraphy in well logs, cores, and outcrops: concepts for high-resolution correlation of time and facies. AAPG, Tulsa, Oklahoma, 55 pp.

van Wagoner, J.C., 1995. Sequence stratigraphy and marine to nonmarine facies architecture of foreland basin strata, Book Cliffs, Utah, and U.S.A. In: Van Wagoner, J.C., Bertram, G.T. (Eds.), Sequence Stratigraphy of Foreland Basin Deposits—Outcrop and Subsurface Examples from the Cretaceous of North America. AAPG Memoir 64, pp. 137–223.

Viseras C., Soria J. M., Durán J. J., Pla S., Garrido G., García-García F., and Arribas A., 2006. A large-mammal site in a meandering fluvial context (Fonelas P-1, Late Pliocene, Guadix Basin, Spain) Sedimentological keys for its paleoenvironmental reconstruction. Paleogeography Paleoclimate Paleoecology 242, 139-168.

Walker, R.G., and James, N., 1992. Facies, facies model and modern stratigraphic concepts. Facies model: response to sea level change. Geological Association of Canada, 1-14.

Walling, D., and He, Q., 1998. The spatial variability of overbank sedimentation on river floodplains. Geomorphology 24, 209-223.

Walling, D. E., Owens, P. N., and Leeks, G. J. L., 1998. The role of channel and floodplain storage in the suspended sediment budget of the River Ouse, Yorkshire, UK. Geomorphology 22, 225-242.

Weerts H. J. T., and Bierkens M. F. P., 1993. Geostatistical analysis of overbank deposits of anastomosing and meandering fluvial systems; Rhine-Meuse delta, The Netherlands. In: Fielding C. R. (ed.) Current Research in Fluvial Sedimentology. Sedimentary Geology 85, 221-232.

Weissmann, G. S., Hartley, A. J., Nichols, G. J., Scuderi, L. A., Olson, M. E., Buehler, H., and Banteah, R. 2010. Fluvial form in modern continental sedimentary basins: Distributive fluvial systems. Geology, 38, 39-42.

Weissmann, G. S., Hartley, A. J., Nichols, G. J., Scuderi, L. A., Olson, M. E., Buehler, H. A., & Massengill, L. C. 2011. Alluvial facies distributions in continental sedimentary basins - Distributive Fluvial systems. Pages 327-355 of: From River To Rock Record: The Preservation of Fluvial Sediments and Their Subsequent Interpretation. Tulsa, Oklahoma: Society of Economic Paleontologists and Mineralogists.

Weissmann, G.S., Hartley, A.J., Scuderi, L.A., Nichols, G.J., Davidson, S.K., Owen, A., Atchley, S.C., Bhattacharyya, P., Chakraborty, T., Ghosh, P., Nordt, L.C., Michel, L., And Tabor, N.J., 2013, Prograding distributive fluvial systems: geomorphic models and ancient examples, in Dreise, S.G., Nordt, L.C., and McCarthy, P.L., eds., New Frontiers in Paleopedology and Terrestrial Paleoclimatology: SEPM, Special Publication 104, 131–147.

Widera, M., 2016. Characteristics and origin of deformation structures within lignite seams–a case study from Polish opencast mines. Geological Quarterly 59, 181-19.

Willis, B., 1993. Ancient river systems in the Himalayan foredeep, Chinji Village area, northern Pakistan. Sedimentary Geology, 88, 1-76.

Willis, A., 2000. Tectonic control of nested sequence architecture in the Sego Sandstone, Neslen Formation and upper Castlegate Sandstone (Upper Cretaceous), Sevier foreland basin, Utah, USA. Sedimentary Geology 136, 277-317.

Wright, V.P., and Marriott, S.B., 1993. The sequence stratigraphy of fluvial depositional systems: the role of floodplain sediment storage. Sedimentary Geology 86, 203-210.

Zwoliński, Z., 1992. Sedimentology and geomorphology of overbank flows on meandering river floodplains. Geomorphology 4, 367-379.

Appendices

Appendix A: Logged sections

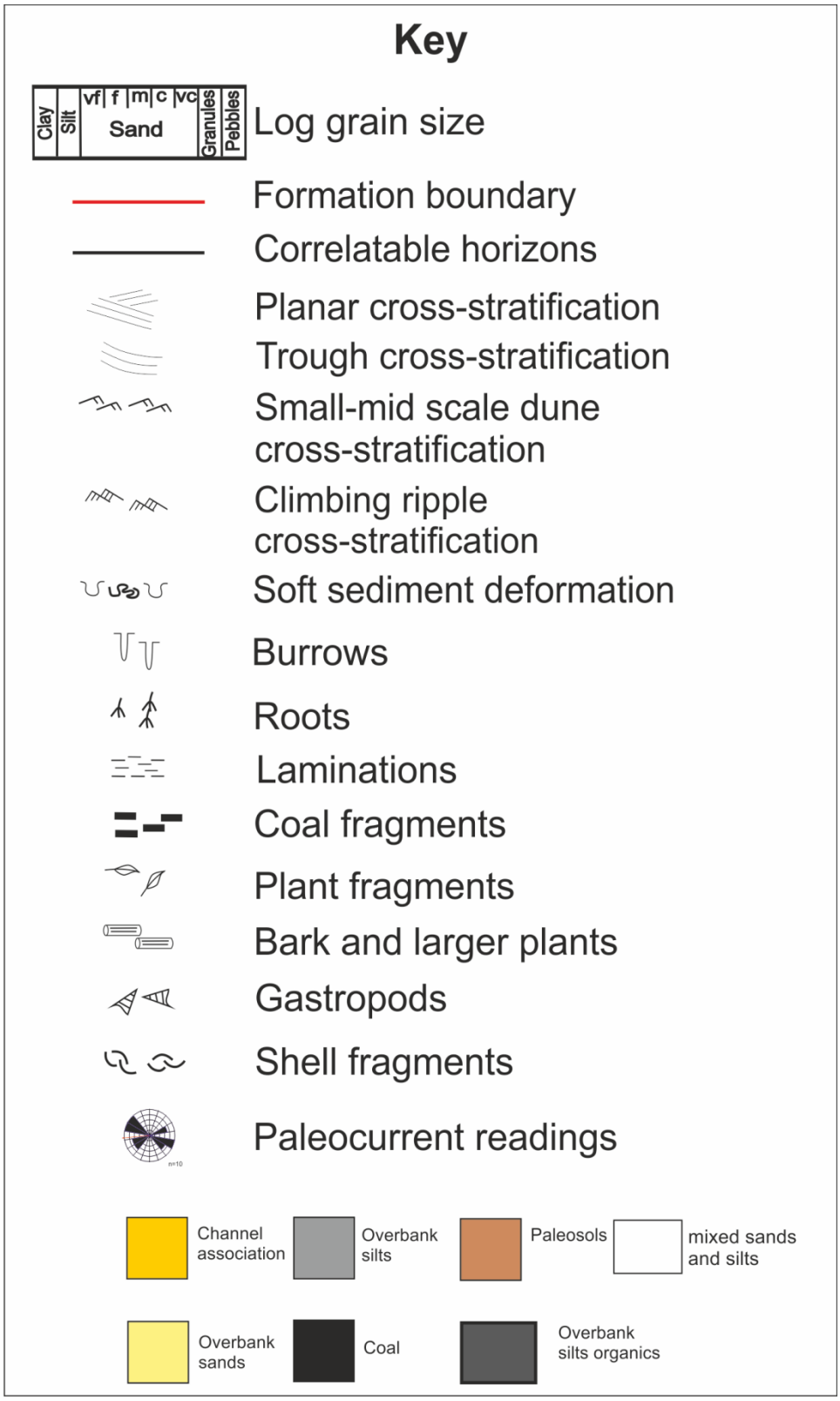

Site	No of logs drawn up
Tuscher Canyon	11/11
Crescent Canyon: including two sites	10/10
Horse Canyon	7/7
Floy Wash	11/11
Atkinson Creek	8/8
Colorado National Monument	8/8
Yellow Cat Canyon	12/12
Naturita road	11/11
Slick Rock	5/5

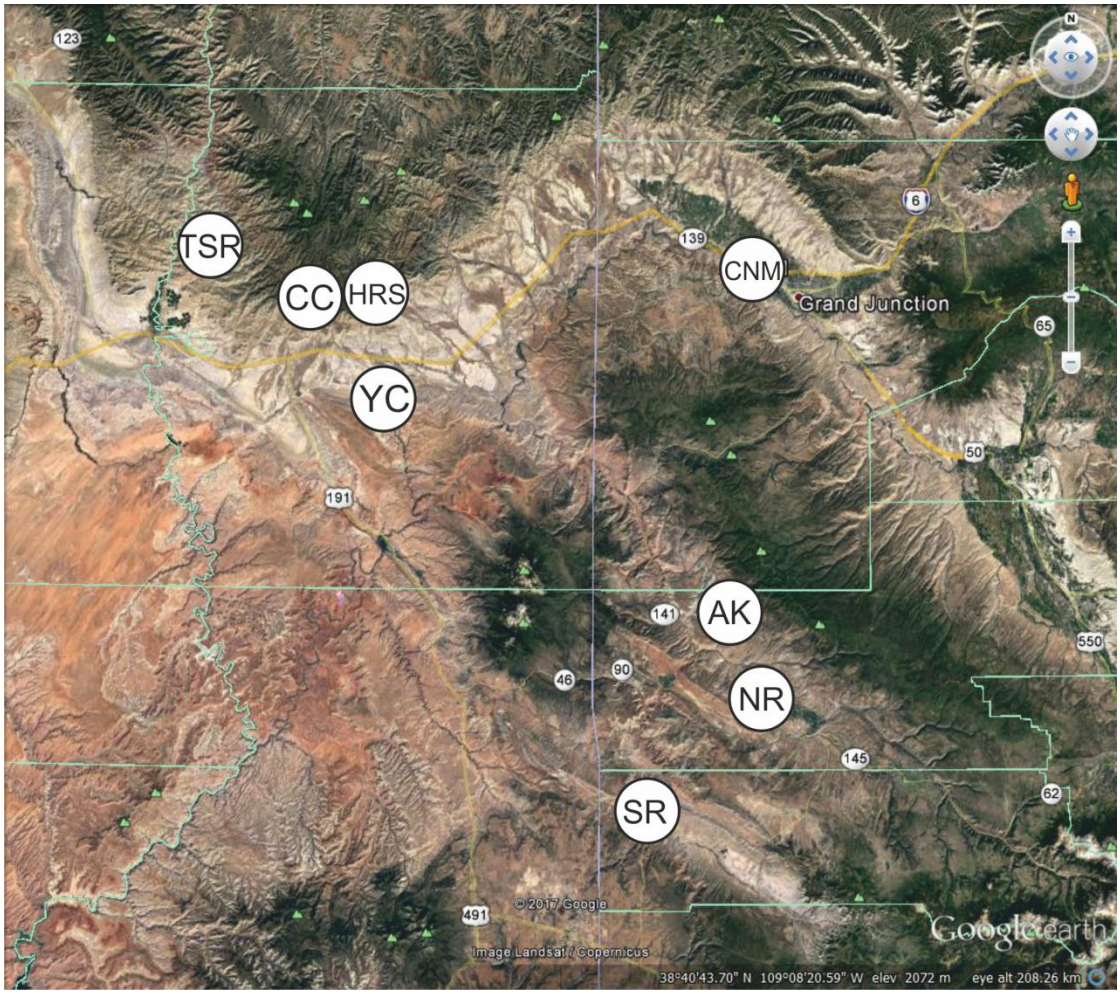

TSR: Tuscher Canyon; CC: Crescent Canyon; HRS: Horse Canyon; YC: Yellow Cat Canyon; SR: Slick Rock; AK: Atkinson Creek; CNM: Colorado National Monument; NR Naturita road site.

Tuscher Canyon Logs

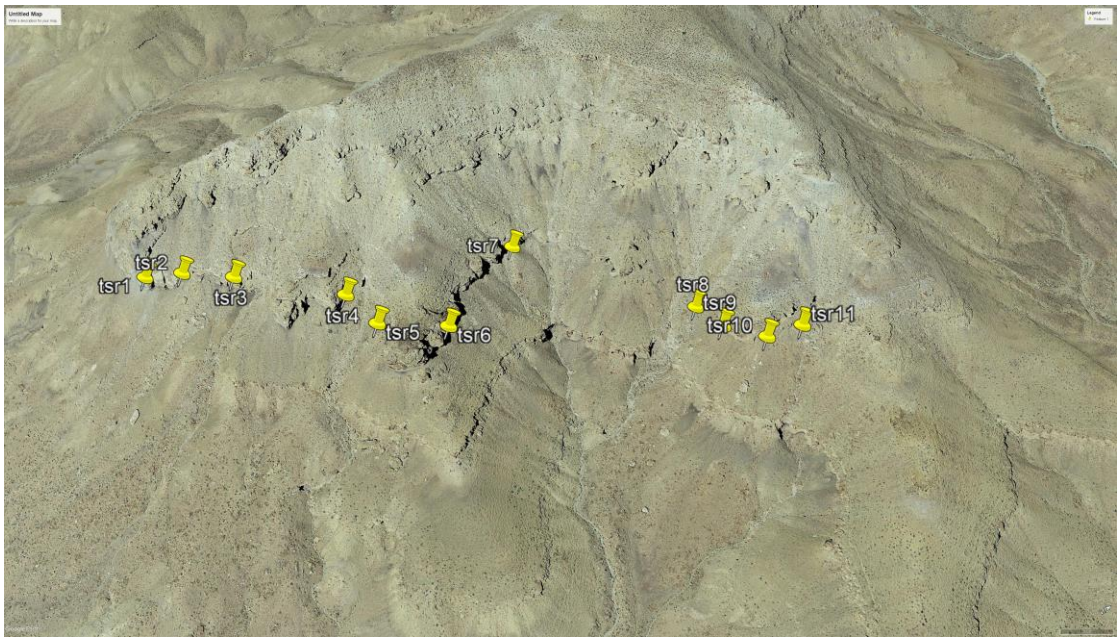

Crescent Canyon Logs

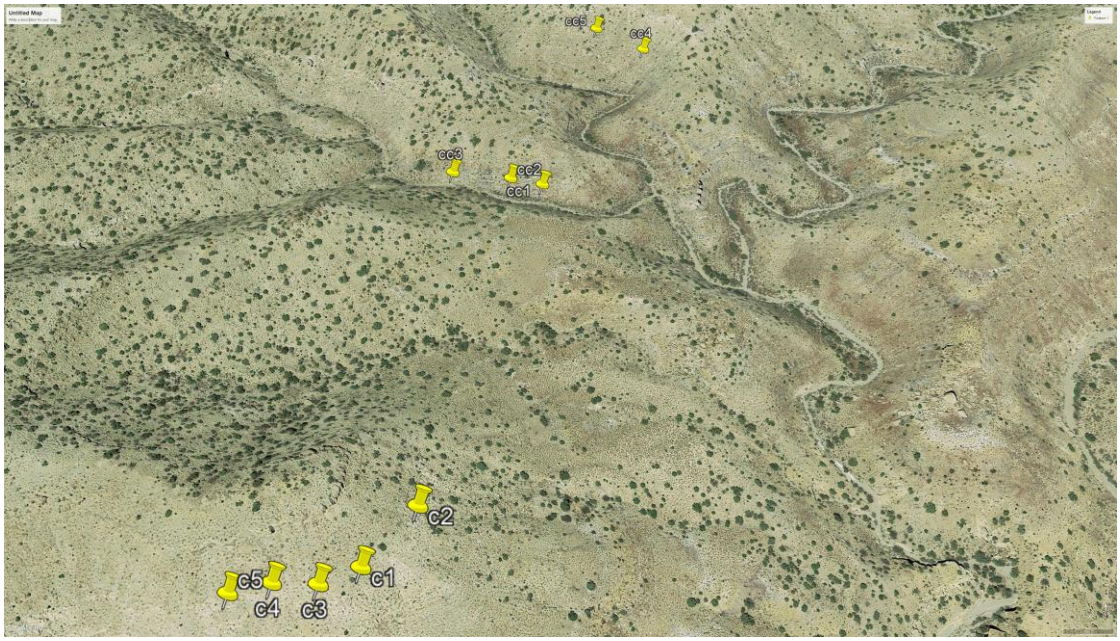

Horse Canyon Logs

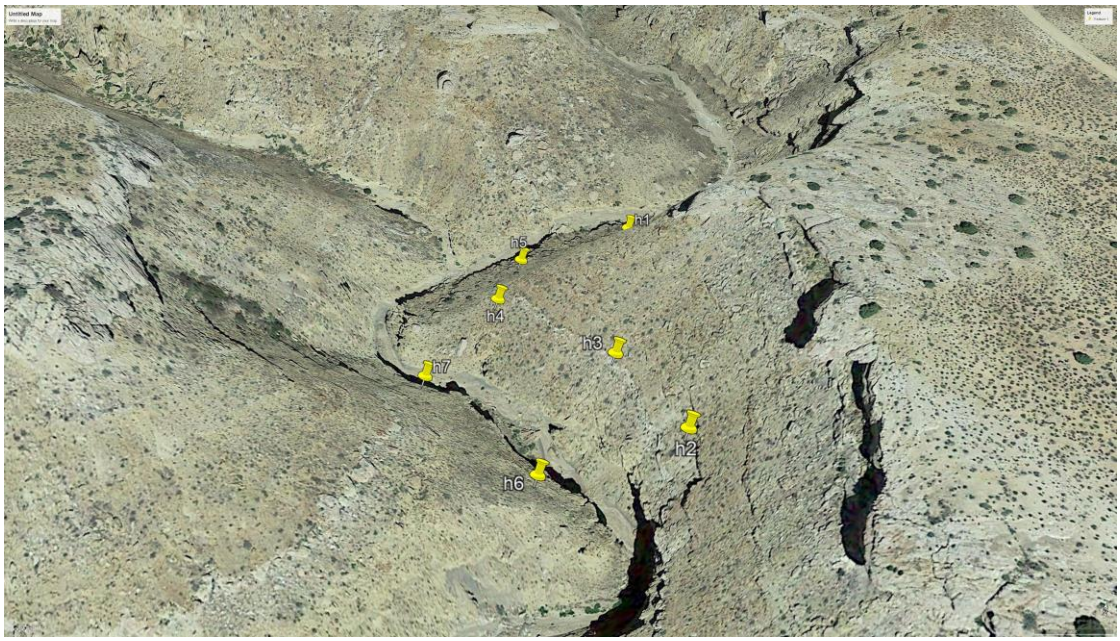

YellowCat Canyon Logs

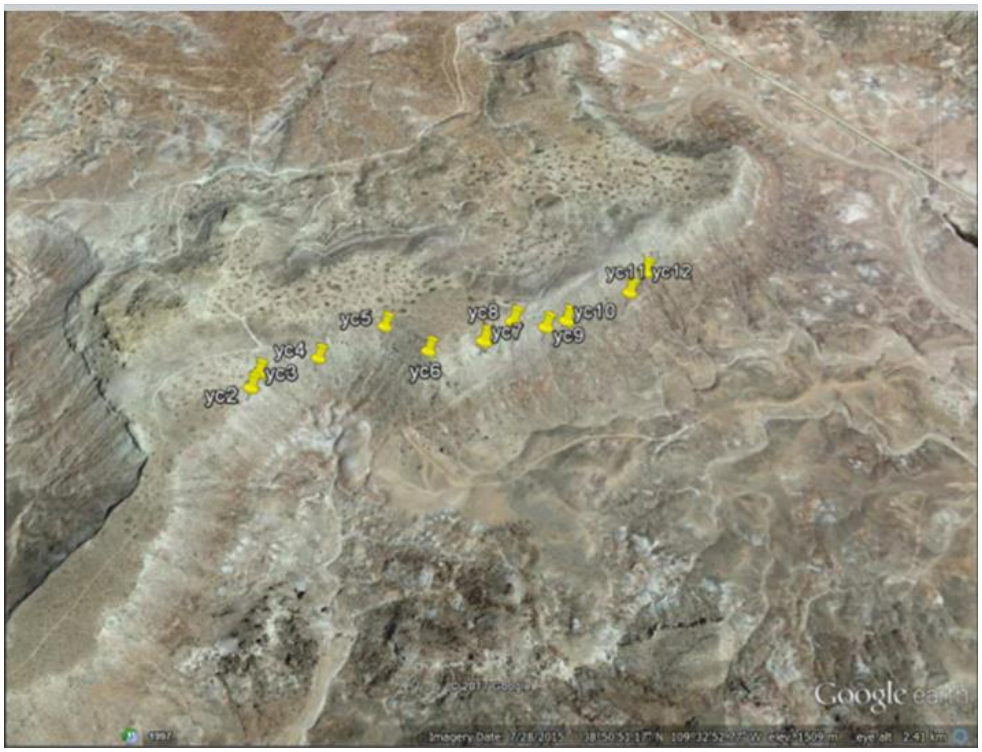

Slick Rock Logs

Atkinson Creek Logs

Colorado National Monement Logs

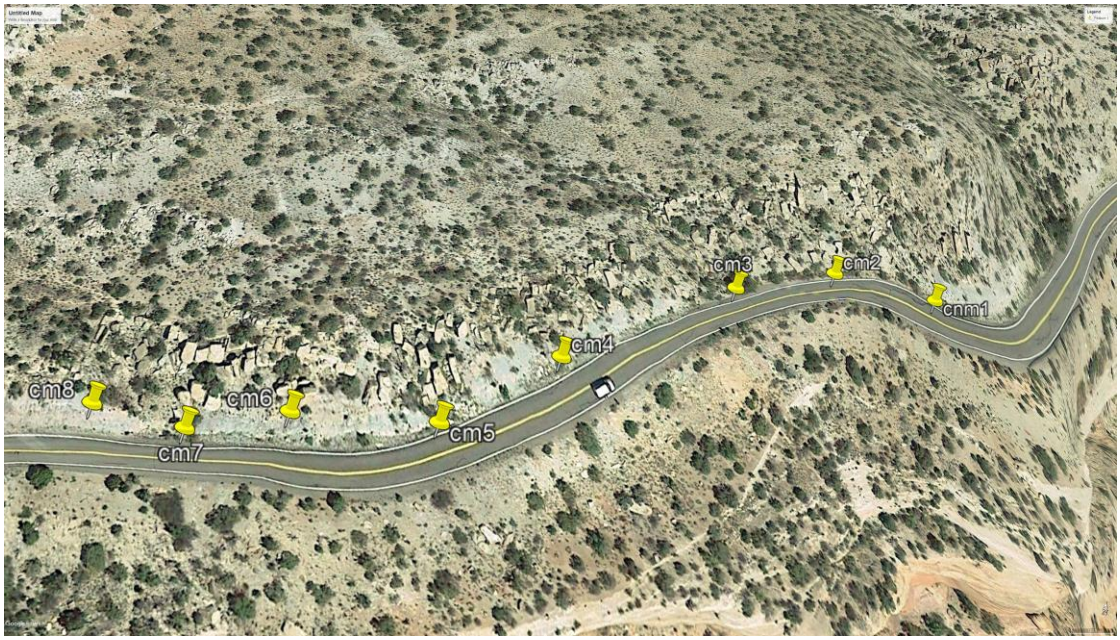

Naturita Logs

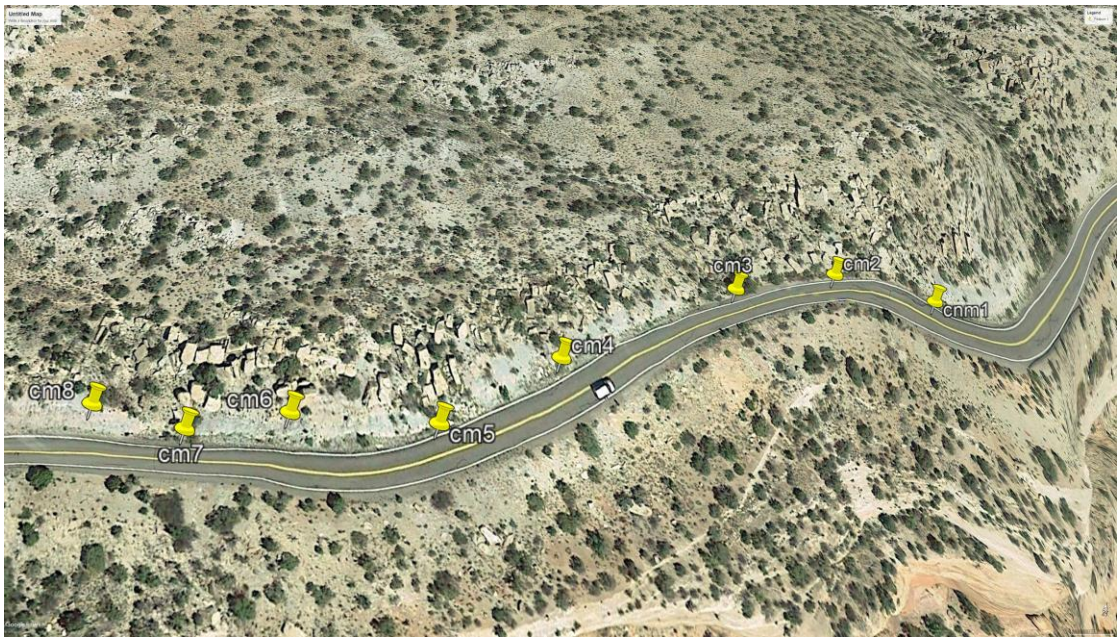

Site	Log number	GPS co-ordinates
TSR	1	N 39'10.328 W 110'03.170
TSR	2	N 39'10.349 W 110'03.133
TSR	3	N 39'103.78 W 110'031.13
TSR	4	N 39'103.83 W 110'031.09
TSR	5	N 39'103.92 W 110'030.78
TSR	6	N 39'104.29 W 110'030.19
TSR	7	N 39'105.20 W 110'031.10
TSR	8	N 39'105.57 W 110'030.58
TSR	9	N 39'105.61 W110029.70
TSR	10	N 39.105.64 W 110'029.59
TSR	11	N 39'105.82 W 110'028.90
CC3	1	N 39'01'43.66 W 109'48'01.75
CC3	2	N 39'02.805 W 109'08.537
CC3	3	N 39'01'43.33 W 109'48'02.46
CC3	4	N 39'01'43.04 W 109'48'03.33
CC3	5	N 39'01'42.64 W 109'48'04.17
CC4	1	N 39'03300 W 109'80.000
CC4	2	N 39'03368 W 109'80.016
CC4	3	N 39'03407 W 109'79.994
CC4	4	N 39'02'01.95 W 109'48'00.28
CC4	5	N 39'02'02.36 W 109'48'02.19
HRS	1	N 39'004.50 W 109'94.416
HRS	2	N 39'004.34 W 109'94.353
HRS	3	N 39'00.479 W 109'94.383
HRS	4	N 39'004.73 W 109'94.435
HRS	5	N 39'00.497 W 109'94.448
HRS	6	N 39'00.461 W 109'94.442
HRS	7	N 39'00.447 W 109'94.446
FLY	1	N 39'01.544 W 109'84.454
FLY	2	N 39'01.776 W 109'86.891
FLY	3	N 39'01.289 W 109'84.894
FLY	4	N 39'01.389 W 109'84.717
FLY	5	N 39'01.454 W 109'84.673
FLY	6	N 39'01.525 W 109'84.564
FLY	7	N 39.01.554 W 109'84.659
FLY	8	N 39'01.558 W 109'84.639
FLY	9	N 39'01.265 W 109'84.875
FLY	10	N 39'0053.92 W

		109'50'50.57
FLY	11	N 39'00'55.67 W 109'50'41.51
AK	1	N 38'39.901 W 108'74.673
AK	2	N 38'39.902 W 108'74.638
AK	3	N 38'39.941 W 108'74.628
AK	2.1	N 38'39.920 W 108'75.118
AK	2.2	N 38'39.906 W 108'75.136
AK	2.3	N 38'39.795 W 108'75.272
AK	2.4	N 38'39.813 W 108'75.323
AK	0	N 38'34.101 W 108'75.754
CNM	1	N 39'07.107 W 108'72.670
CNM	2	N 39'07.107 W 108'72.671
CNM	3	N 39'07.084 W 108'72805
CNM	4	N 39'07.039 W 108'72.849
CNM	5	N 39'07.029 W 108'72.860
CNM	6	N 39'07.022 W 108'72.071
CNM	7	N 39'07.018 W 108'72.895
CNM	8	N 39'07.006 W 108'72.946
YC	1	N 38'84.546 W 109'55.772
YC	2	N 38'84.611 W 109'55.136
YC	3	N 38'84.620 W 109'55.133
YC	4	N 38'84.662 W 109'55.058
YC	5	N 38'24.691 W 109'54.992
YC	6	N 38'84.671 W 109'54.851
YC	7	N/A
YC	8	N/A
YC	9	N/A
YC	10	N/A
YC	11	N/A
YC	12	N 38'84.925 W 109'54.376
NR	1	N 38'29.470 W 108'66.093
NR	2	N 38'29.470 W 108'66.108
NR	3	N 38'29.480 W 108'66.107
NR	4	N 38'29.496 W 108'66.124
NR	5	N 38'29.422 W 108'66.058
NR	6	N 38'29.408 W 108'66.041
NR	7	N 38'29.399 W 108'66.032
NR	8	N 38'29.393 W 108'66.029
NR	9	N/A
NR	10	N/A
NR	11	N/A
SR	1	N 38'03.903 W 108'90.157
SR	2	N 38'03.942 W 108'89.956

SR	3	N 38'03.928 W 108'49.954
SR	4	N 38'03.936 W 108'89.935
SR	5	N 38'03.935 W 108'89.932

*red text GPS are not very trustworthy.

Tuscher logs

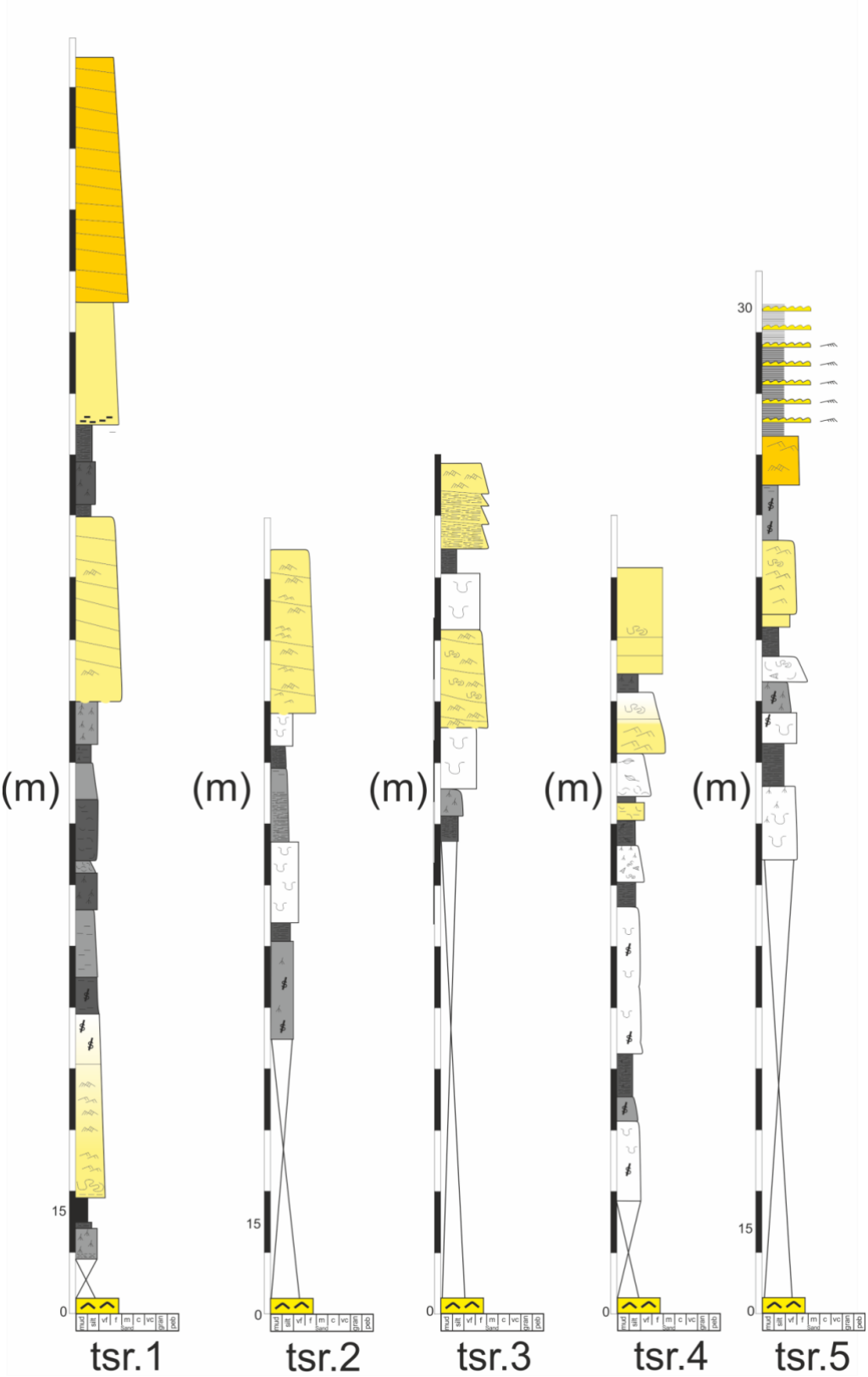

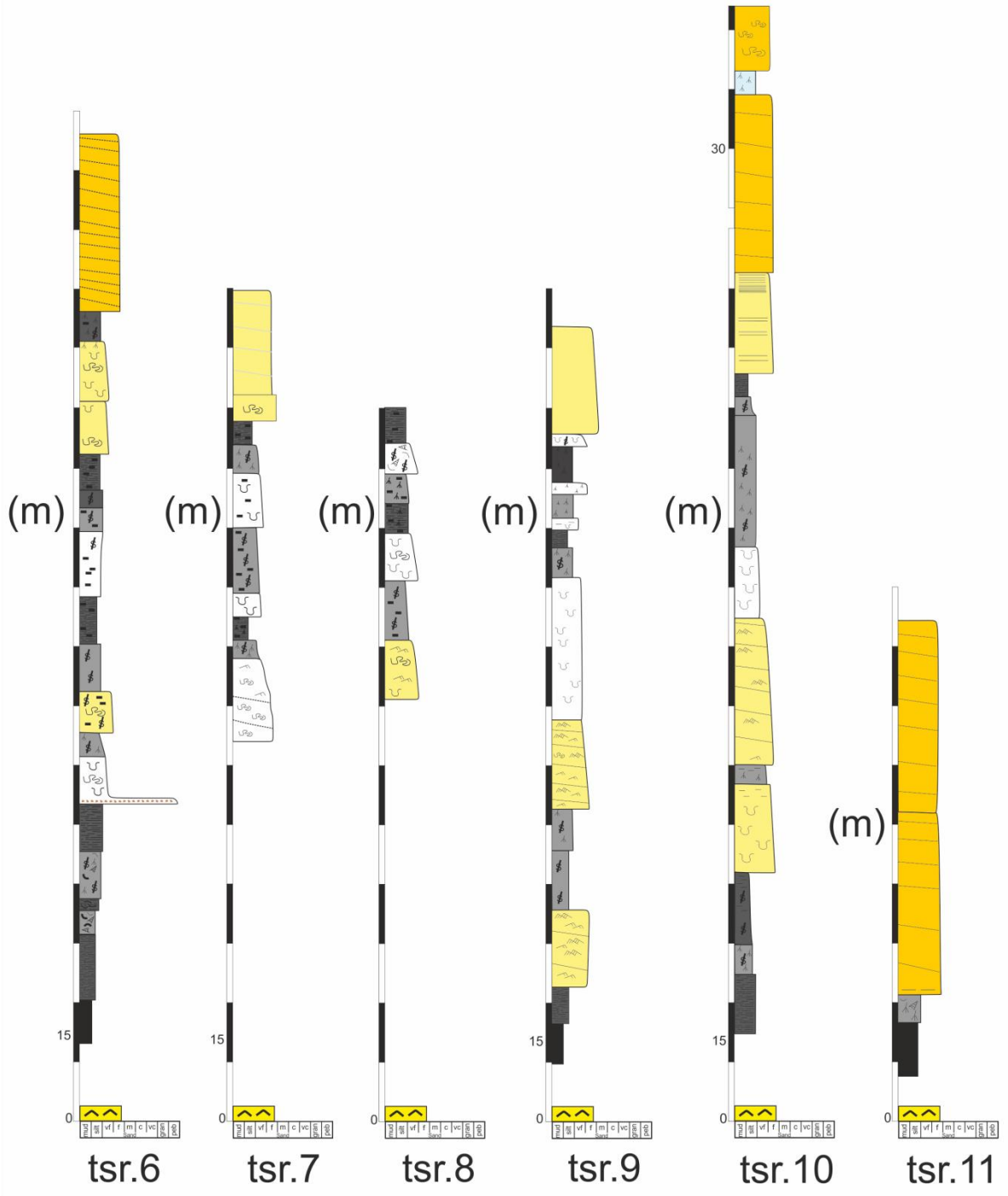
(m)
30
15
0
mud
silt
vf
f
m
c
vc
gran
peb
sand
tsr.6
tsr.7
tsr.8
tsr.9
tsr.10
tsr.11

Crescent Canyon Logs

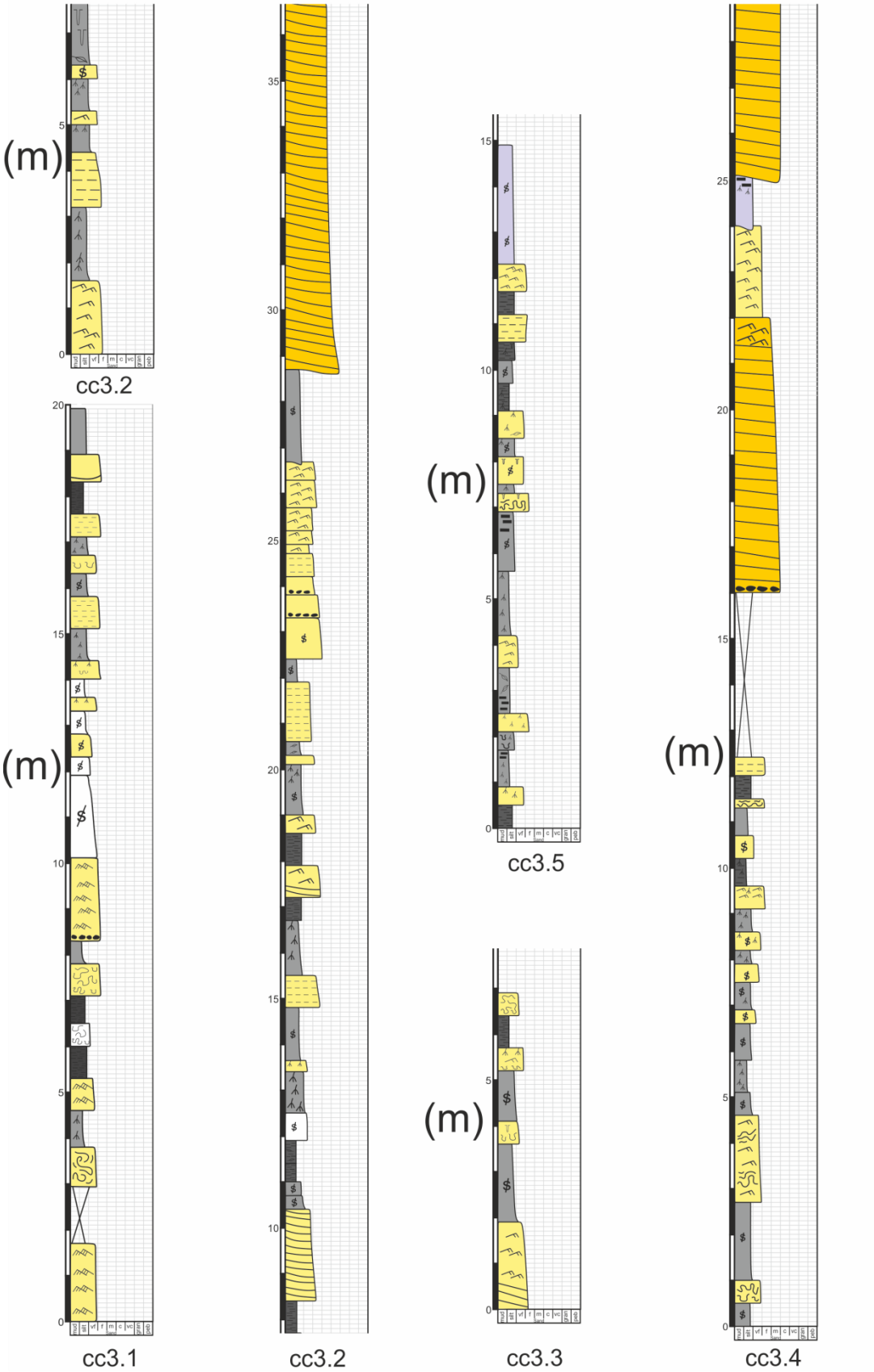

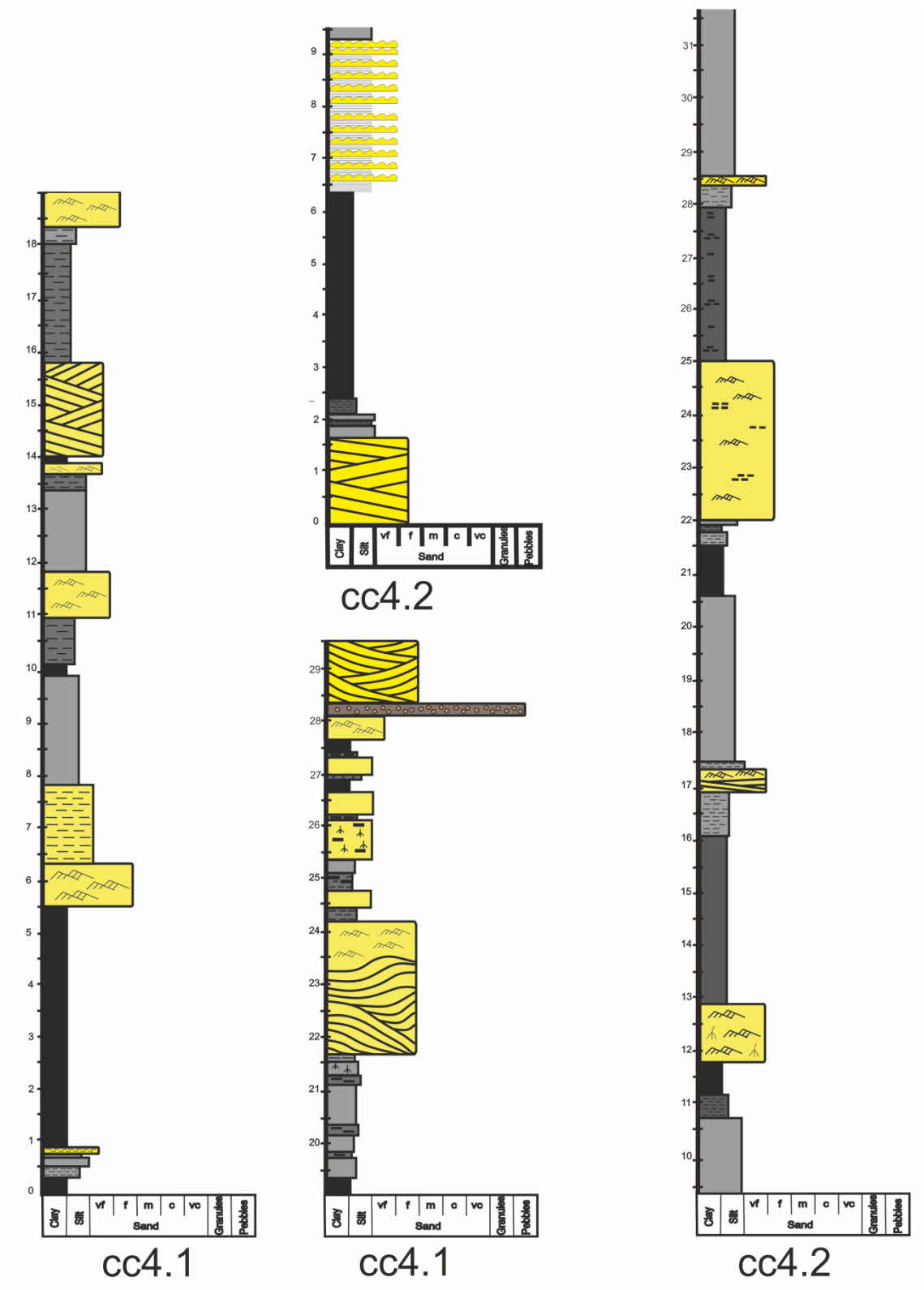
Clay
Silt
vf
f
m
c
vc
Sand
Granules
Pebbles
cc4.1
cc4.2
cc4.1
cc4.2

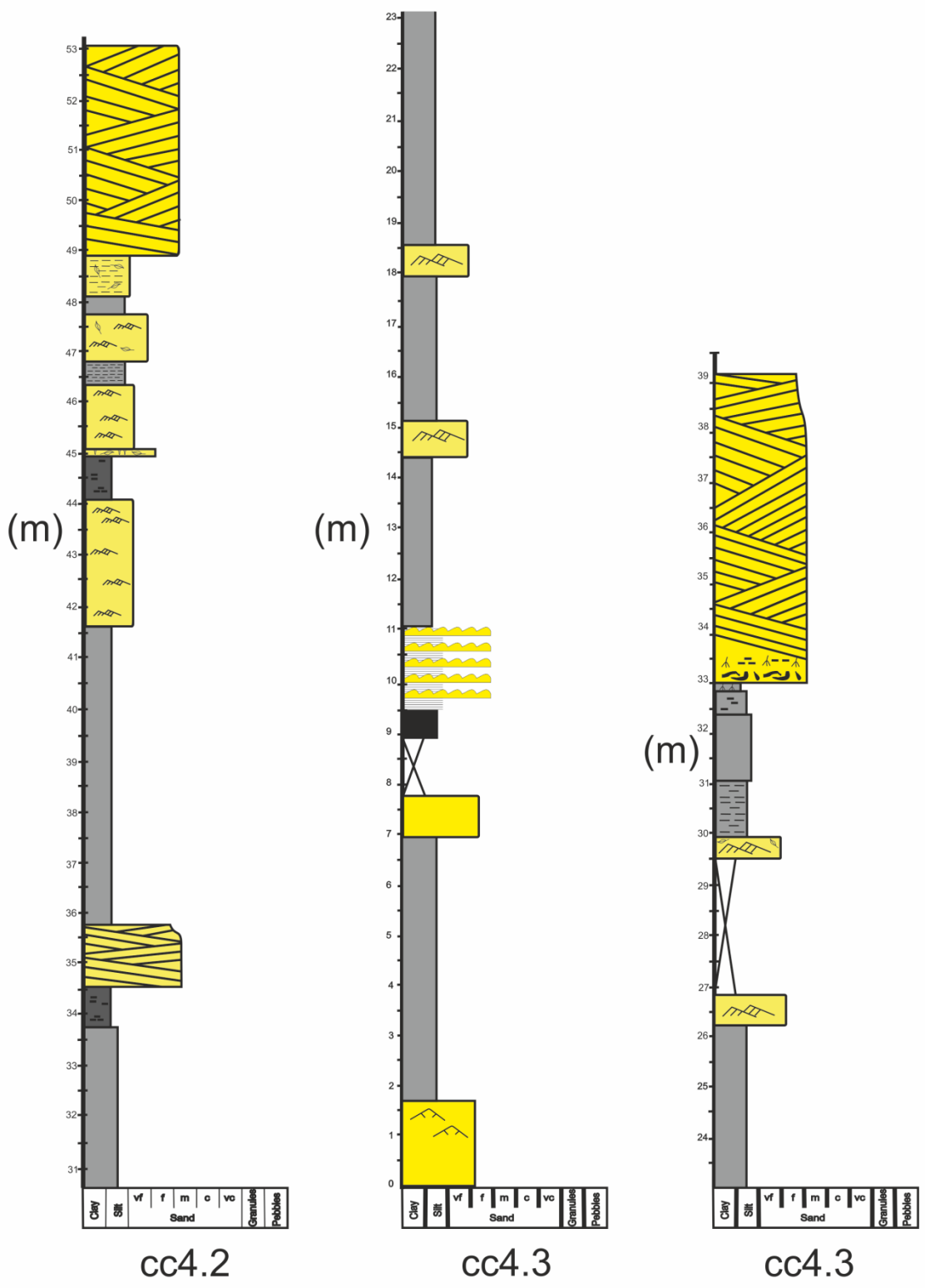
(m)
Clay
Silt
vf
f
m
c
vc
Sand
Granules
Pebbles
cc4.2
(m)
cc4.3
(m)
cc4.3

Logged sections at Floy Wash

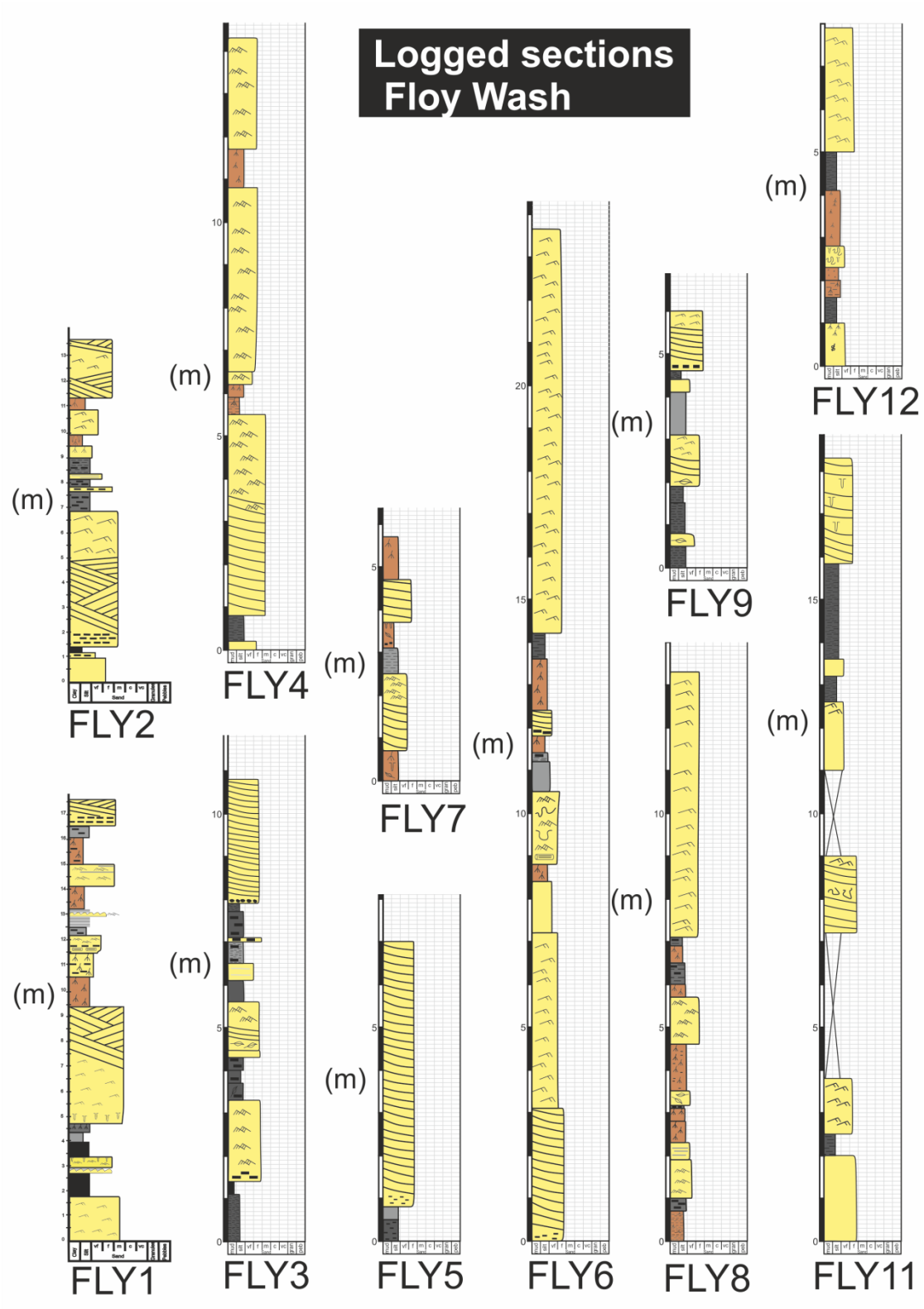

Logged sections at Horse Canyon

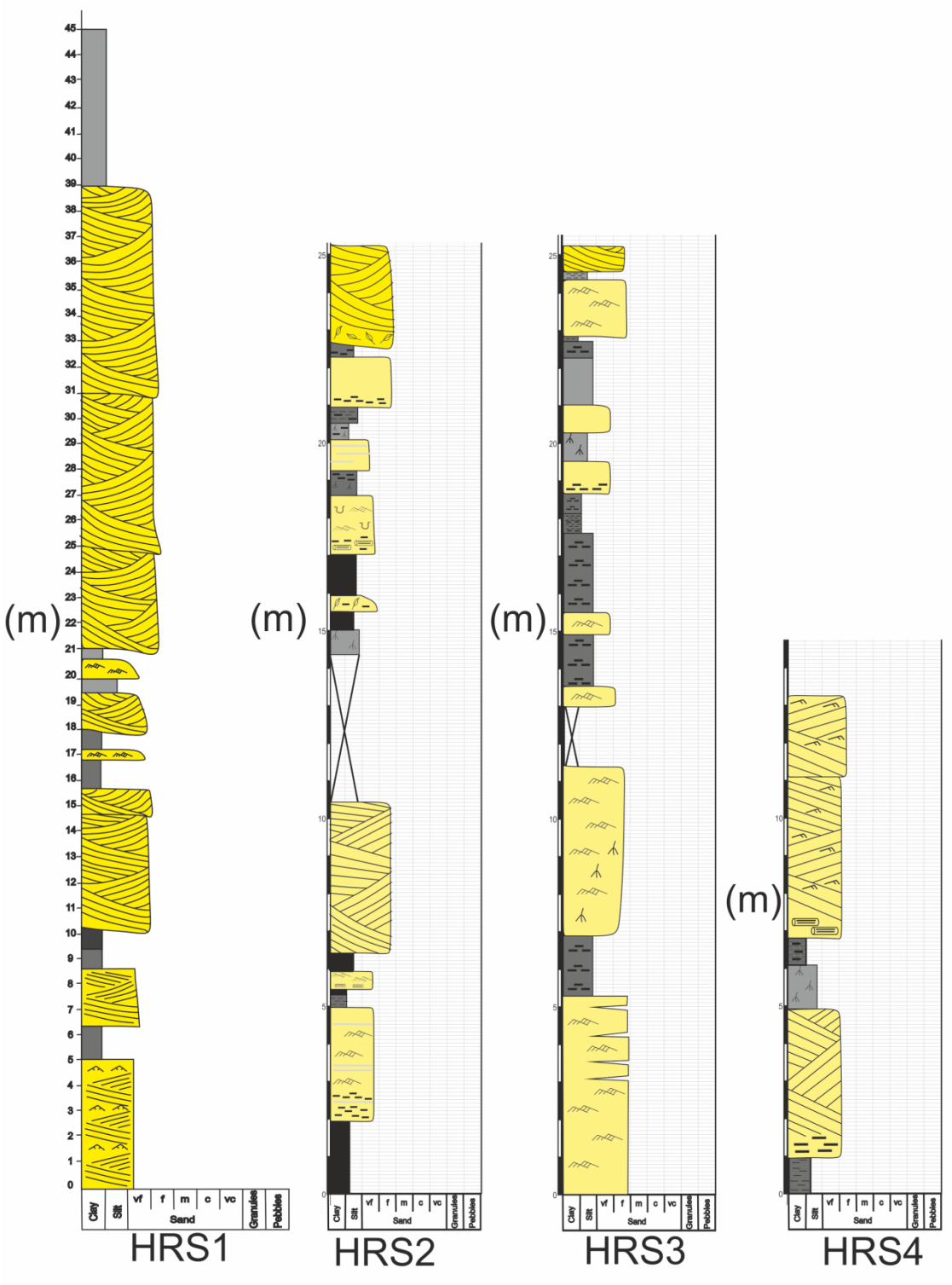

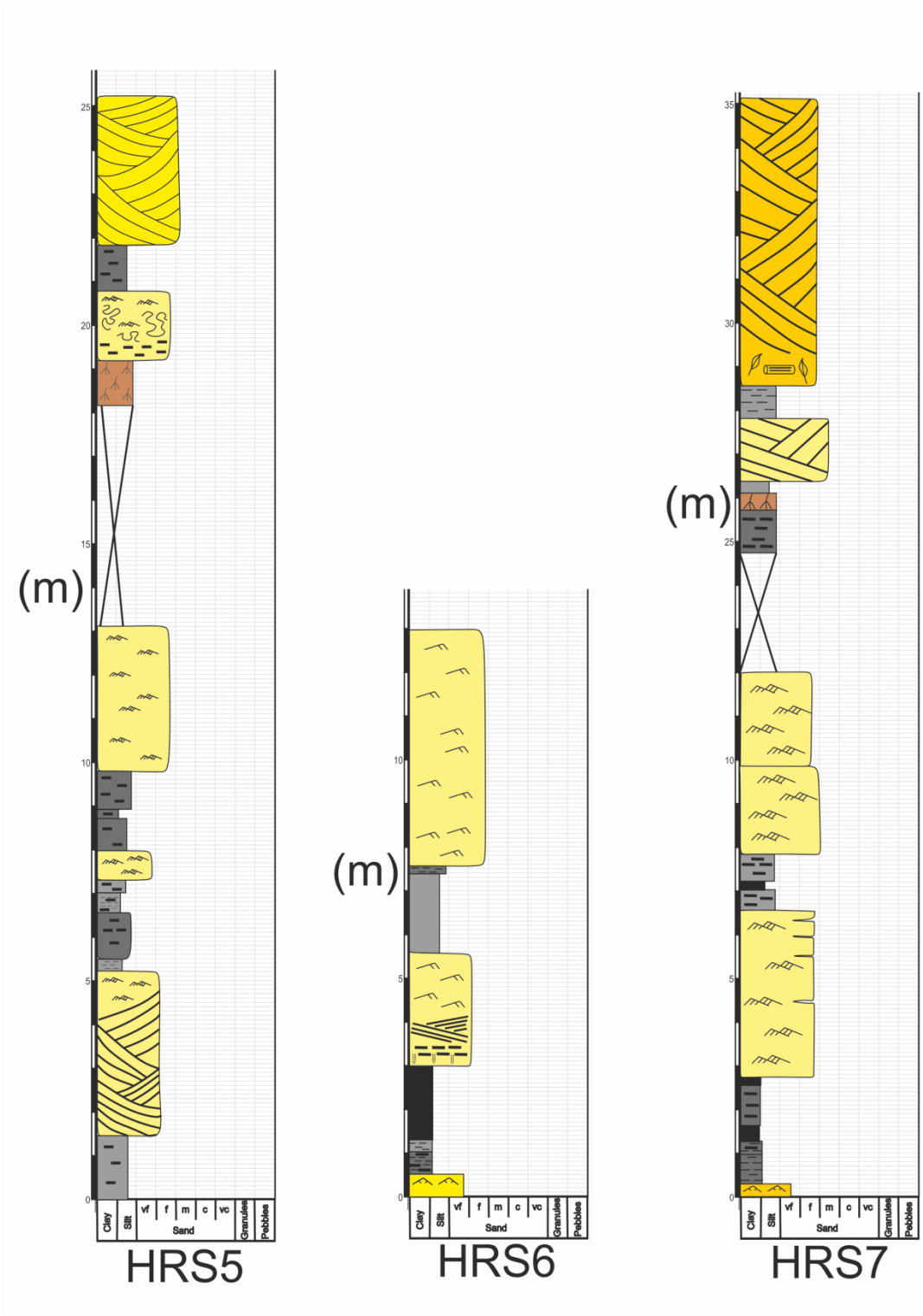
(m)
25
20
15
10
5
0
Clay
Silt
vf
f
m
c
vc
Sand
Granules
Pebbles
HRS5
(m)
10
5
0
Clay
Silt
vf
f
m
c
vc
Sand
Granules
Pebbles
HRS6
(m)
35
30
25
10
5
0
Clay
Silt
vf
f
m
c
vc
Sand
Granules
Pebbles
HRS7

Atkinson Creek Logs

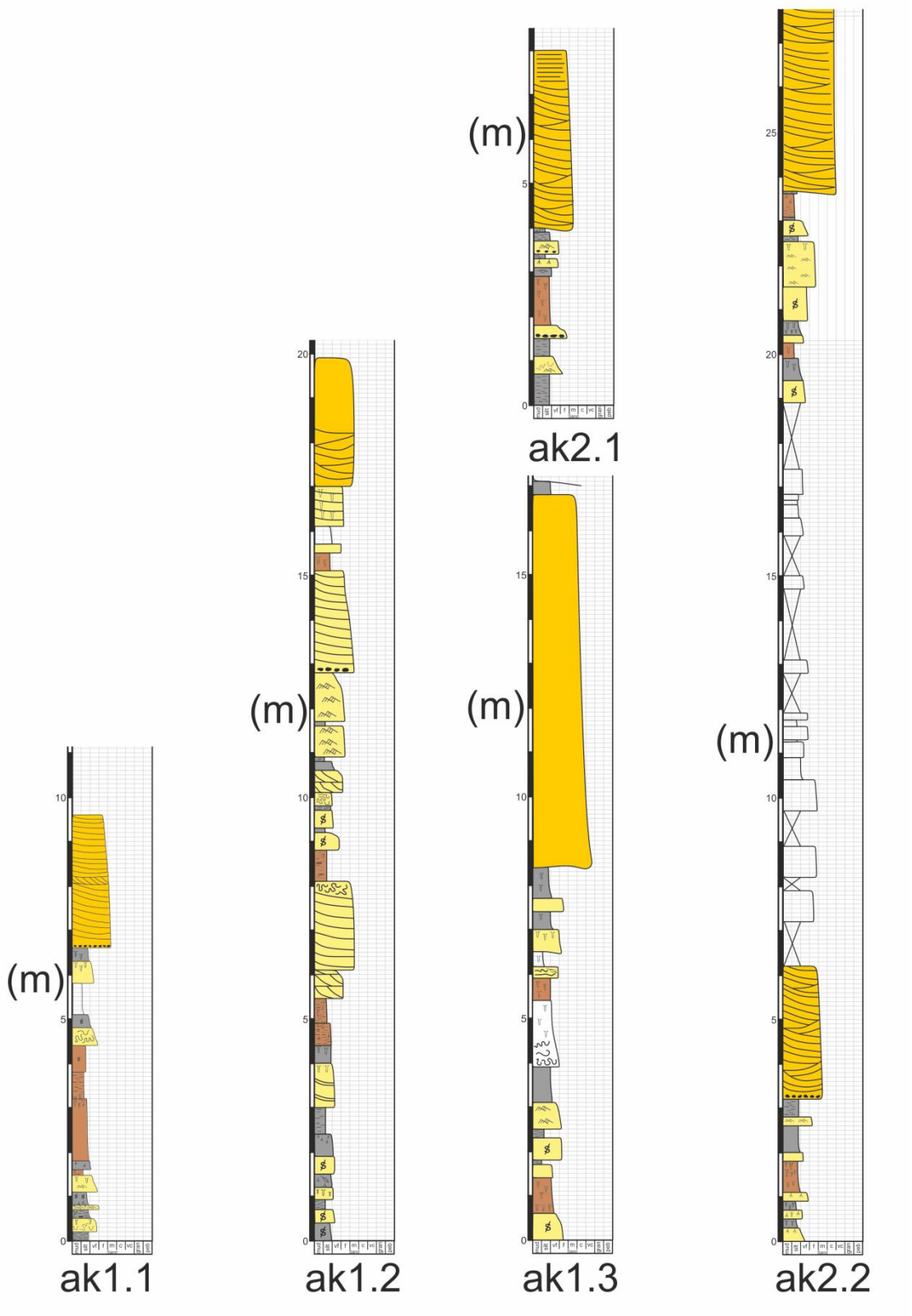

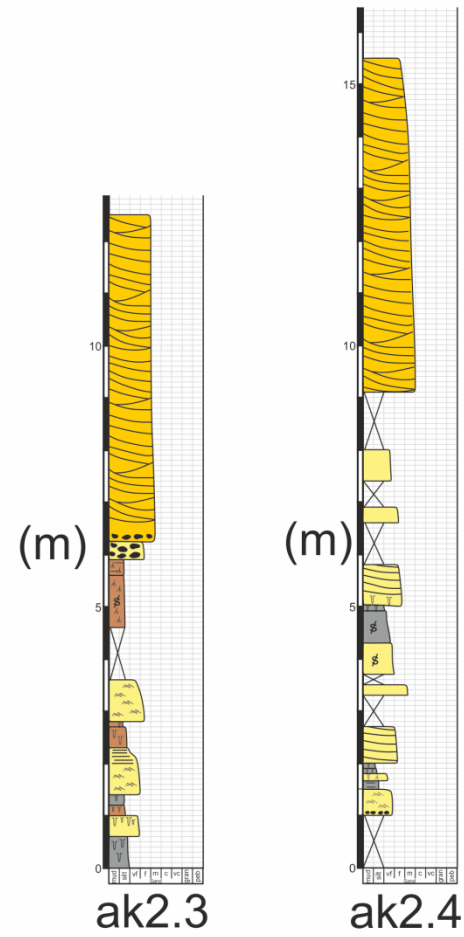
(m)
10
5
0
ak2.3
(m)
15
10
5
0
ak2.4

Yellow Cat Canyon Logs

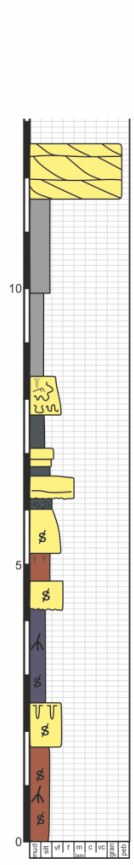

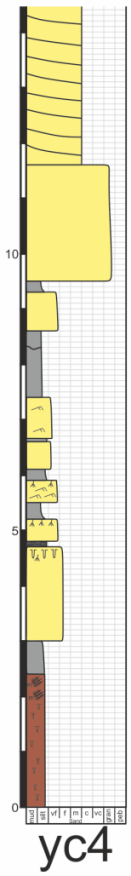

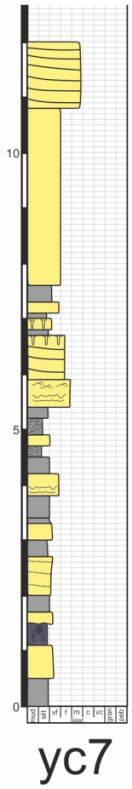

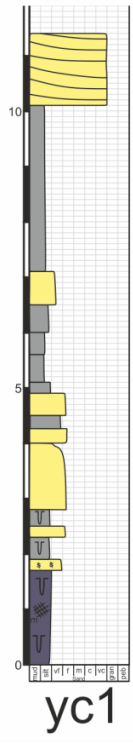

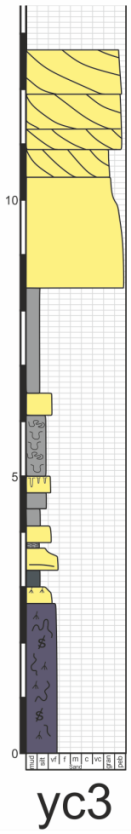

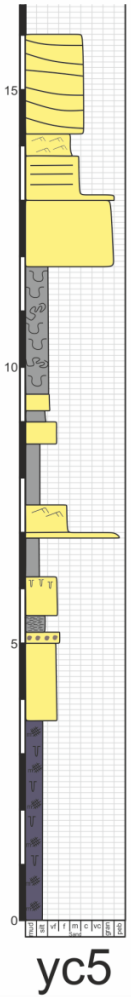

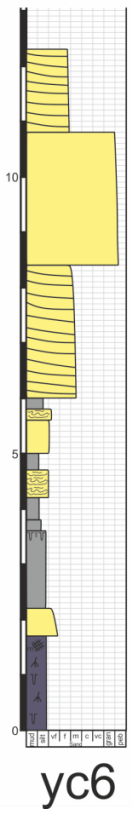

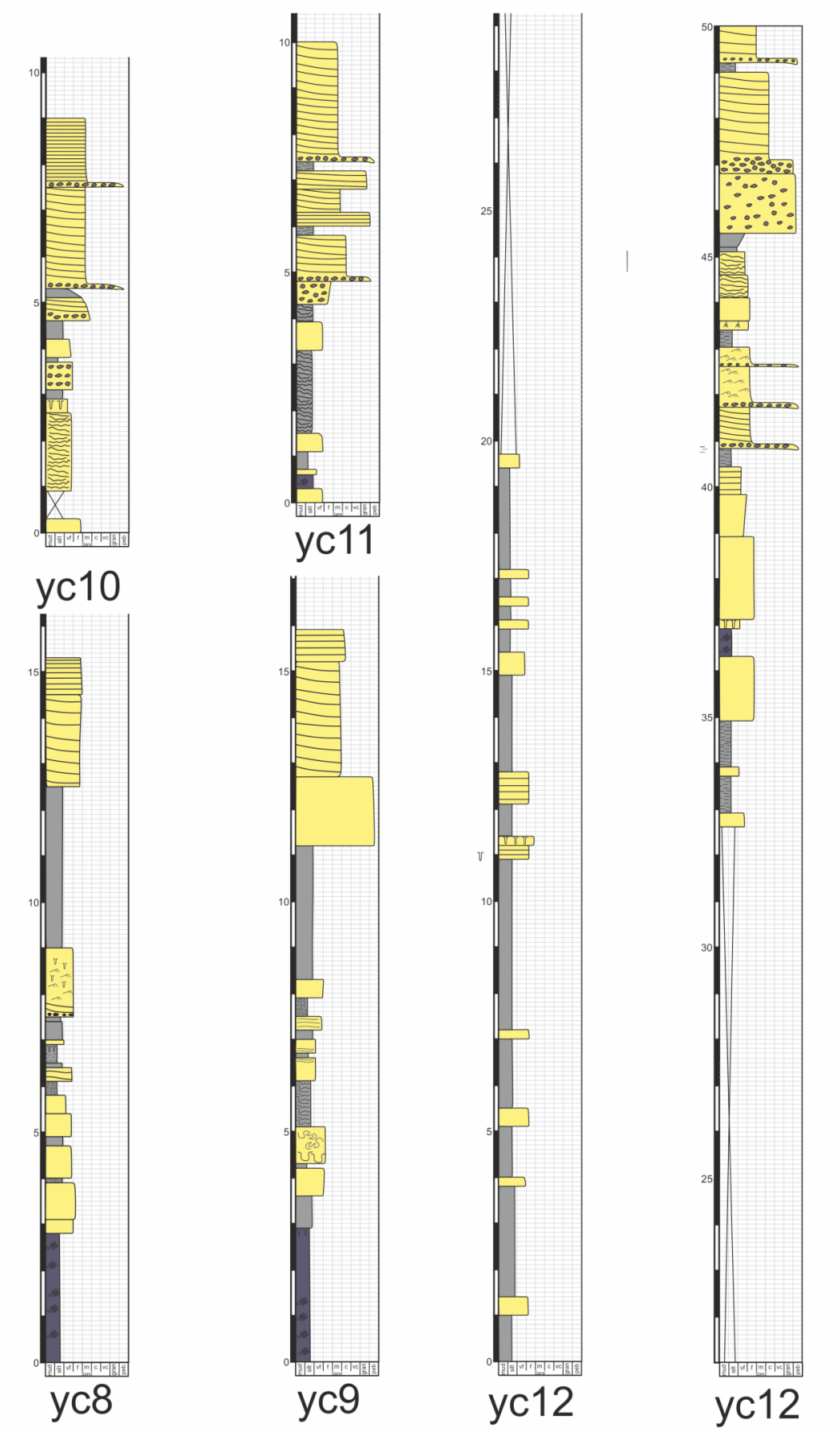
yc10
yc11
yc8
yc9
yc12
yc12

Slick rock logs

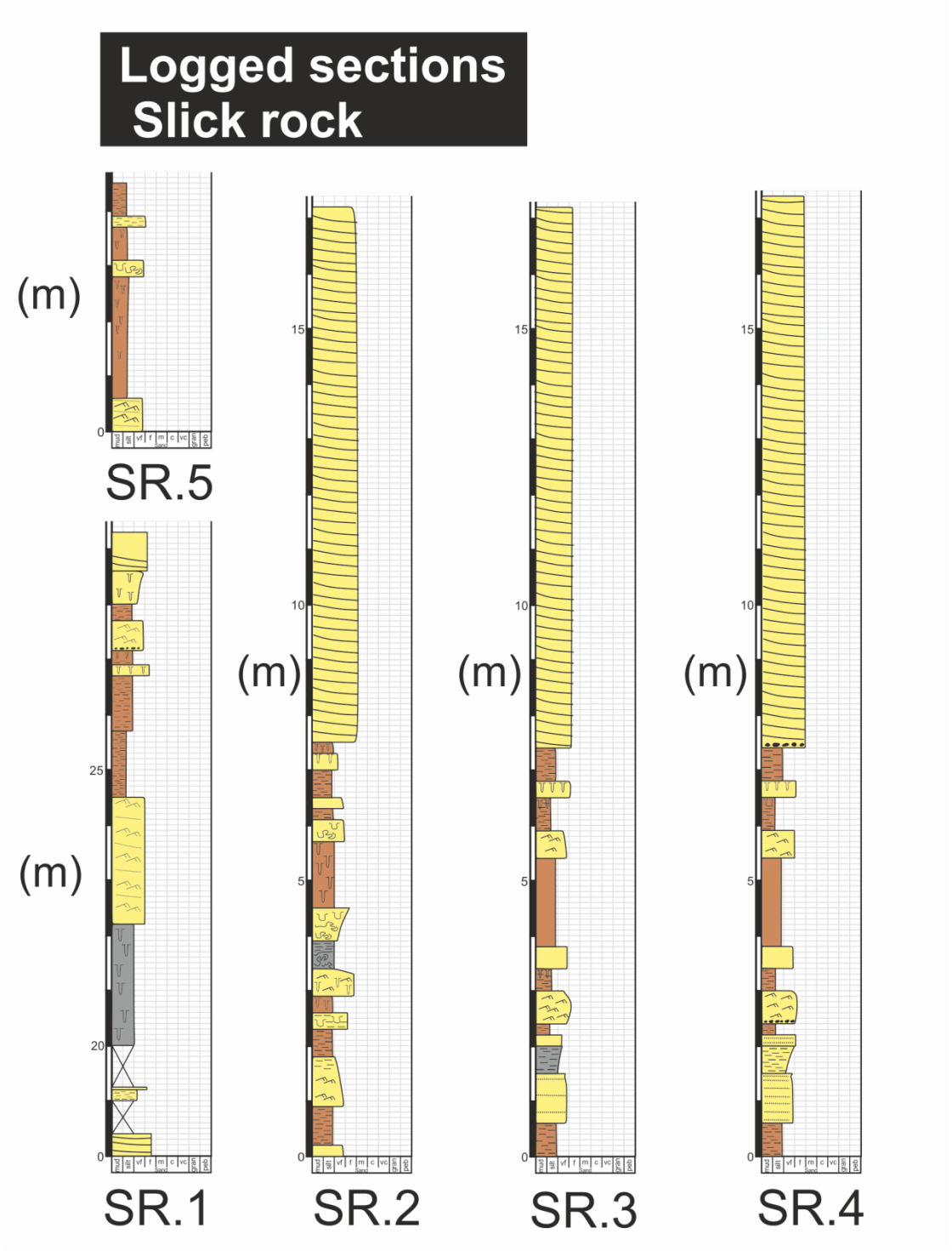

Naturita road

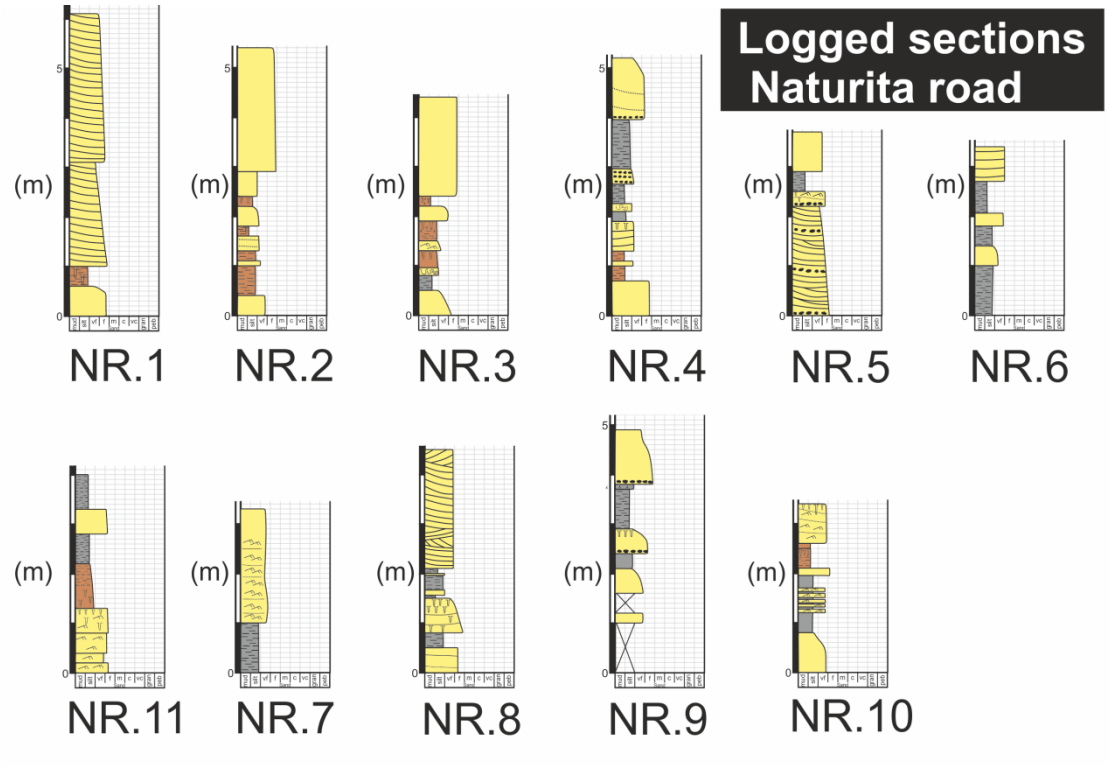

Colorado National Monument Logs

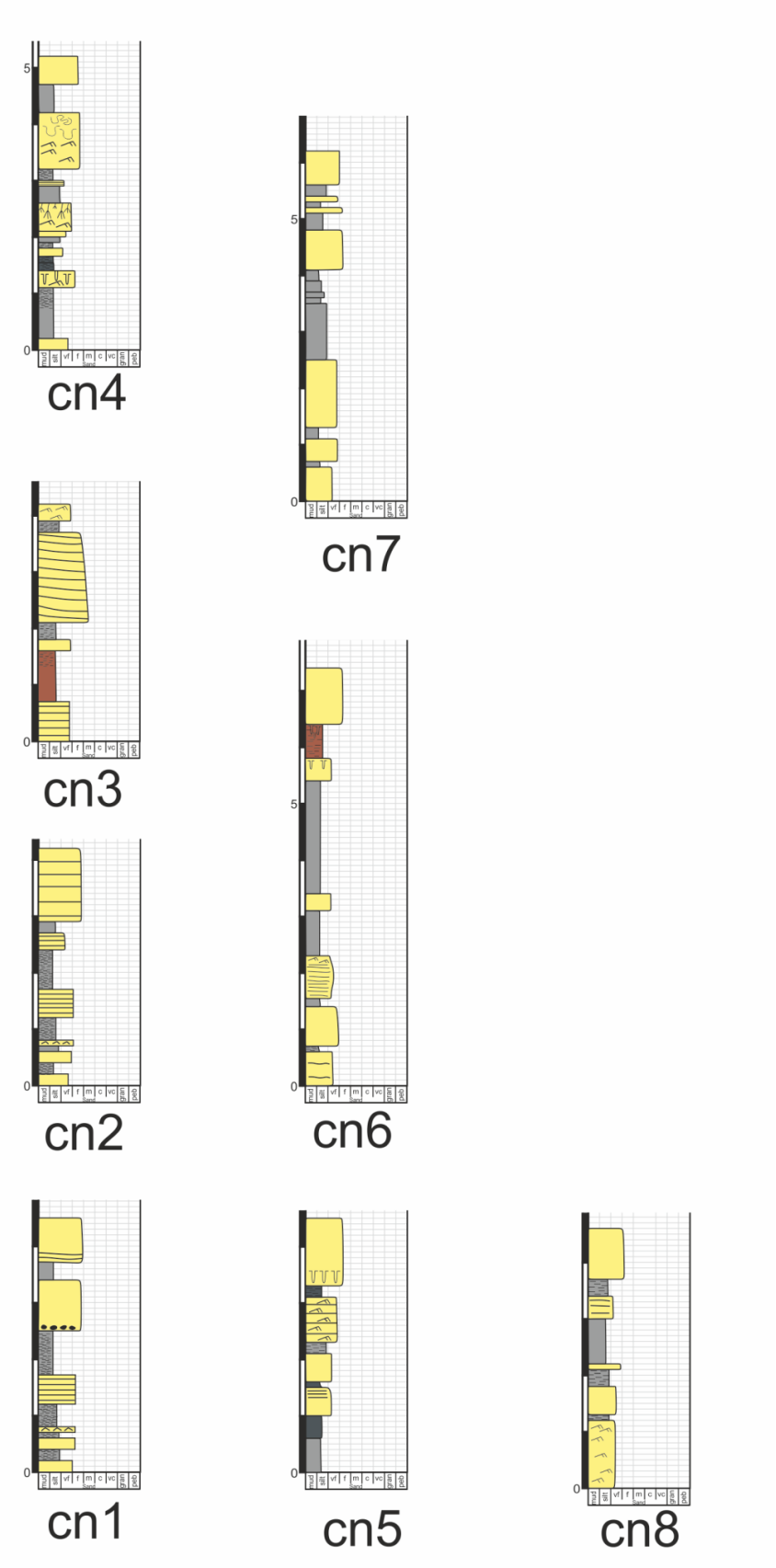

Appendix B: Photomontages of localities

Crescent Canyon: including 2 subsites	11/11
Tuscher Canyon	7/7
Floy Wash	6/6
Horse Canyon	5/5
Atkinson Creek	6/6
Slick Rock	3/3
Naturita	2/2
Yellow Cat Canyon	5/5
Colorado National Monument	2/2

Panels around Crescent Canyon

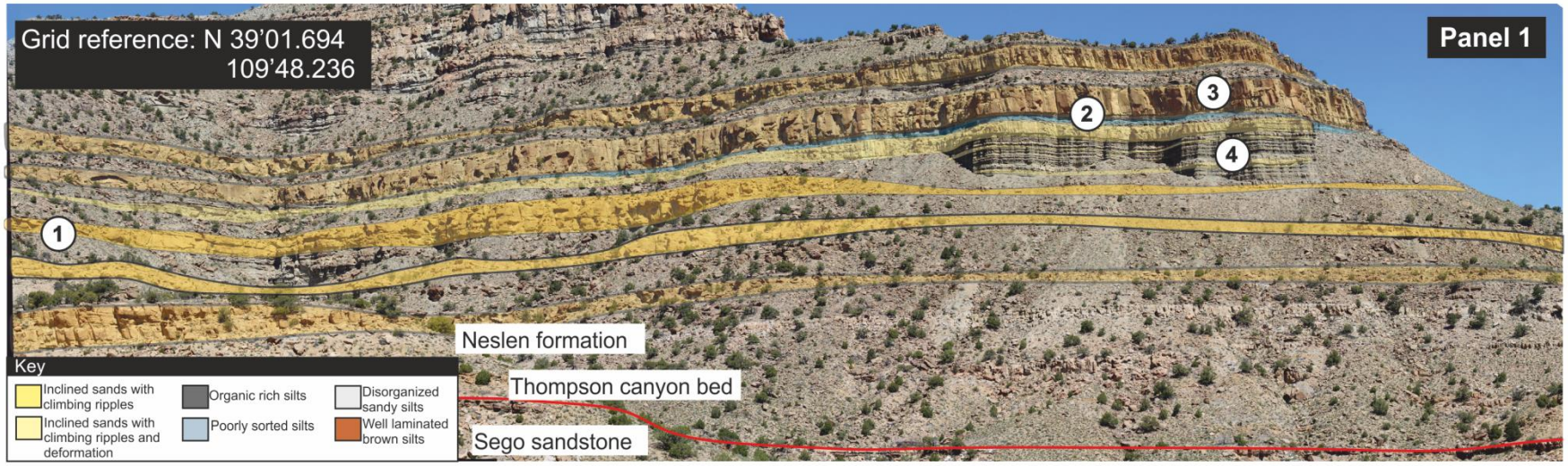

1. Succession becomes more channelised laterally
2. Abandoned channel fill
3. Succession becomes fully channelised vertically
4. Overbank deposits

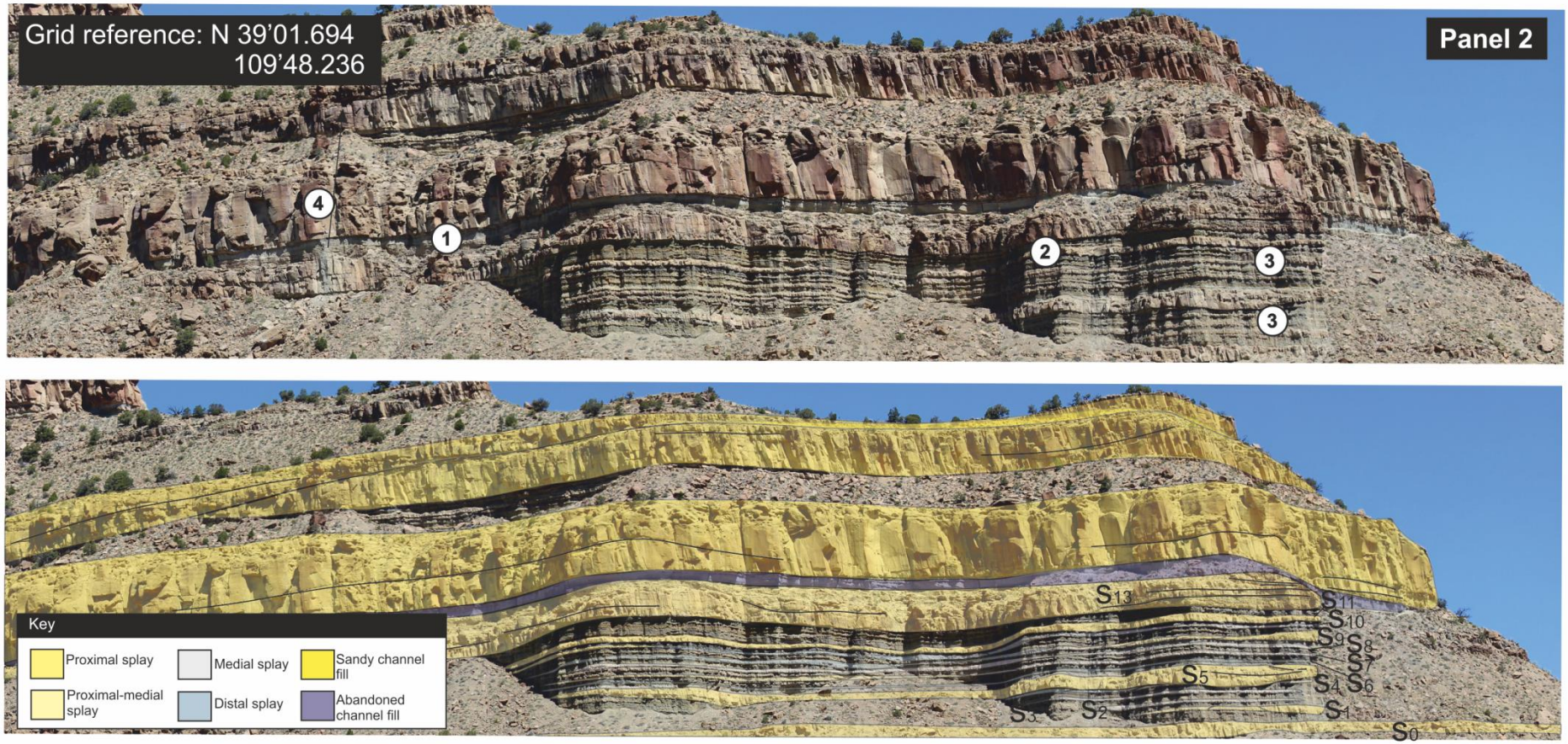

1. Extensive erosive channel filled with clean silts; abandoned channel
2. Splay that remains sandy laterally
3. Splay that laterally changes from sand to silts
4. Well defined channels


Grid reference: N 39°01.694
109°48.236
Panel 3
Builds out
inclined surfaces

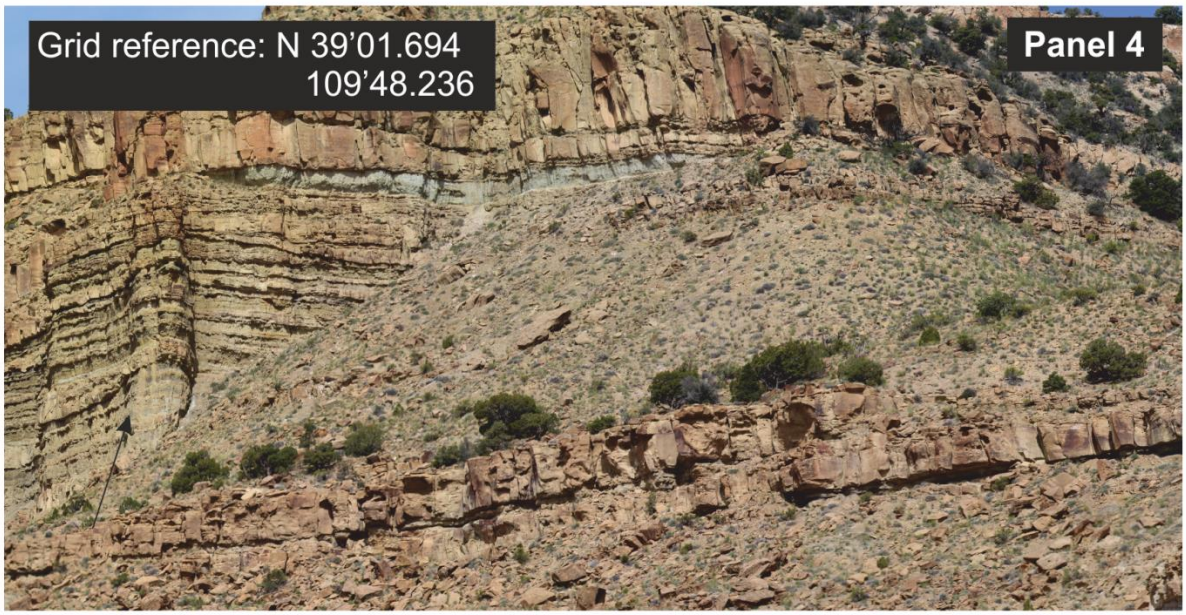

Key

- Inclined sands with climbing ripples
- Inclined sands with climbing ripples and deformation
- Organic rich silts
- Poorly sorted silts
- Disorganized sandy silts
- Well laminated brown silts

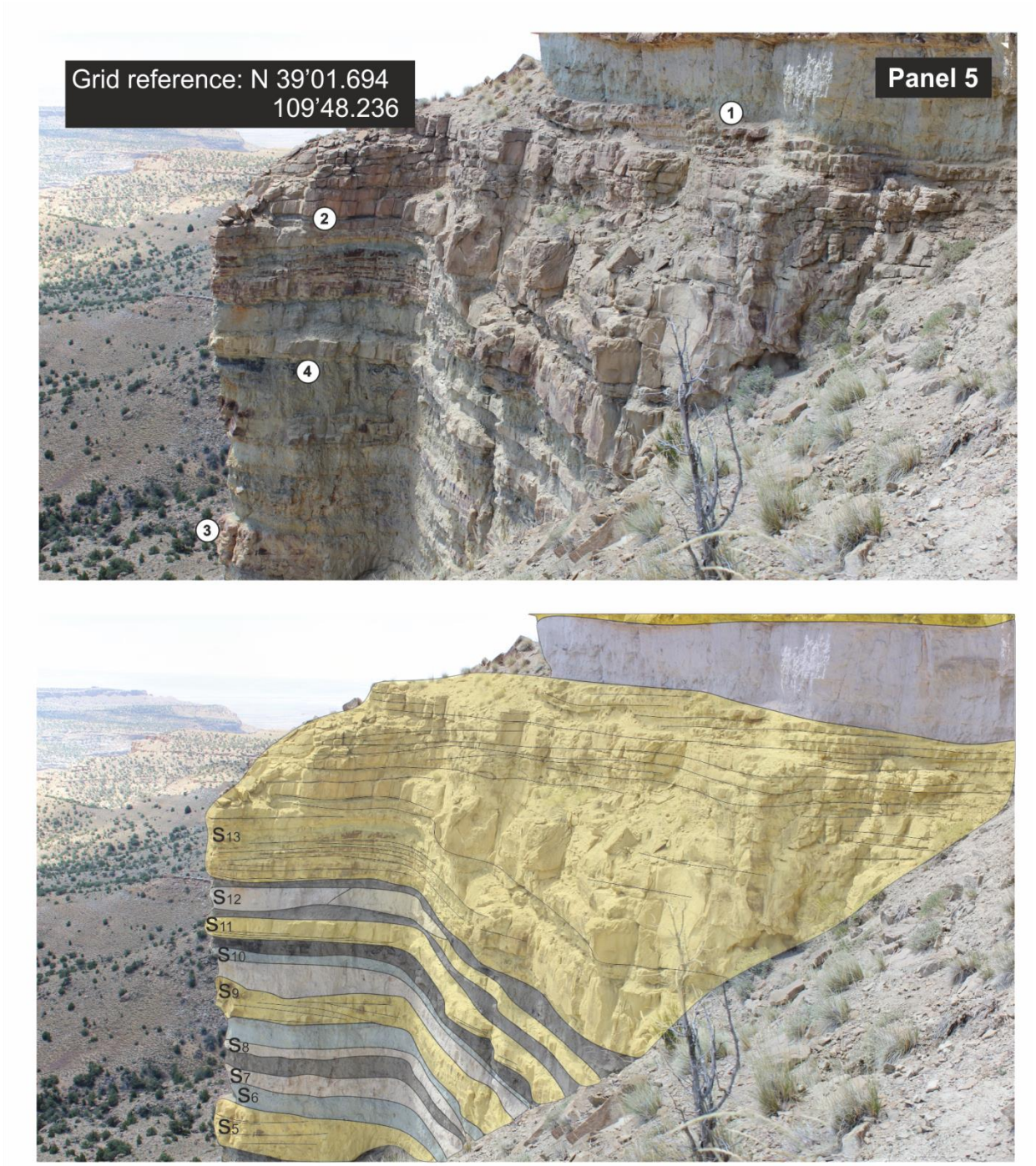
Grid reference: N 39’01.694
109’48.236
Panel 5
1
2
3
4
S13
S12
S11
S10
S9
S8
S7
S6
S5

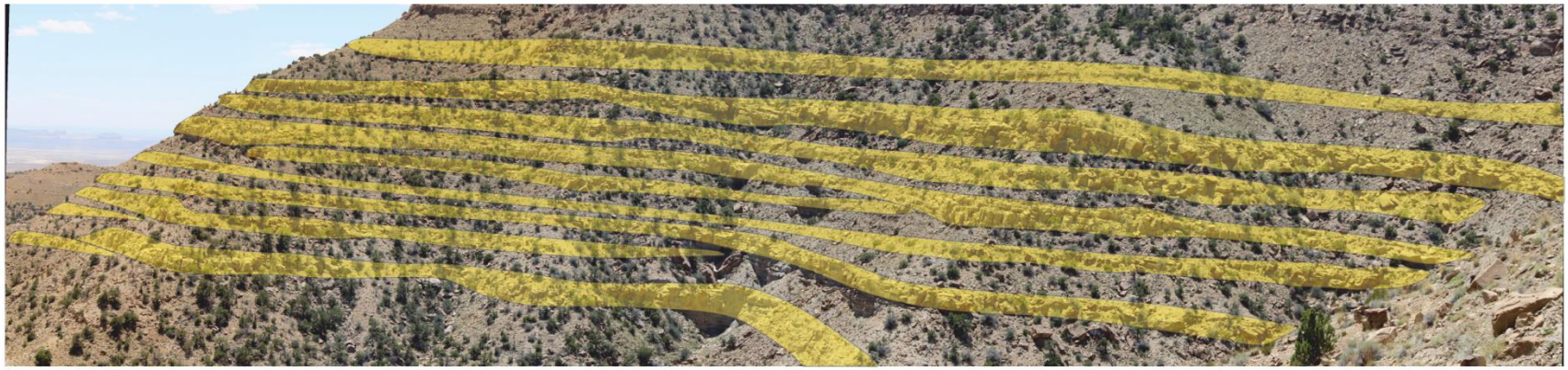

① Very laterally extensive

② Multistorey channels

③ Channel bodies opposite to cc3 site

Key

- Inclined sands with climbing ripples
- Inclined sands with climbing ripples and deformation
- Organic rich silts
- Poorly sorted silts
- Disorganized sandy silts
- Well laminated brown silts


Grid reference: N 39’03368
109’80016
Inclined sands with climbing ripples
Organic rich silts
Disorganized sandy silts
Poorly sorted silts


Grid reference: N 39’03368
109’80016
Key
Proximal splay
Medial splay
Sandy channel fill
Proimal-medial splay
Distal splay
Abandoned channel fill
Top of thompson canyon sandstone bed

Panels around Tuscher Canyon

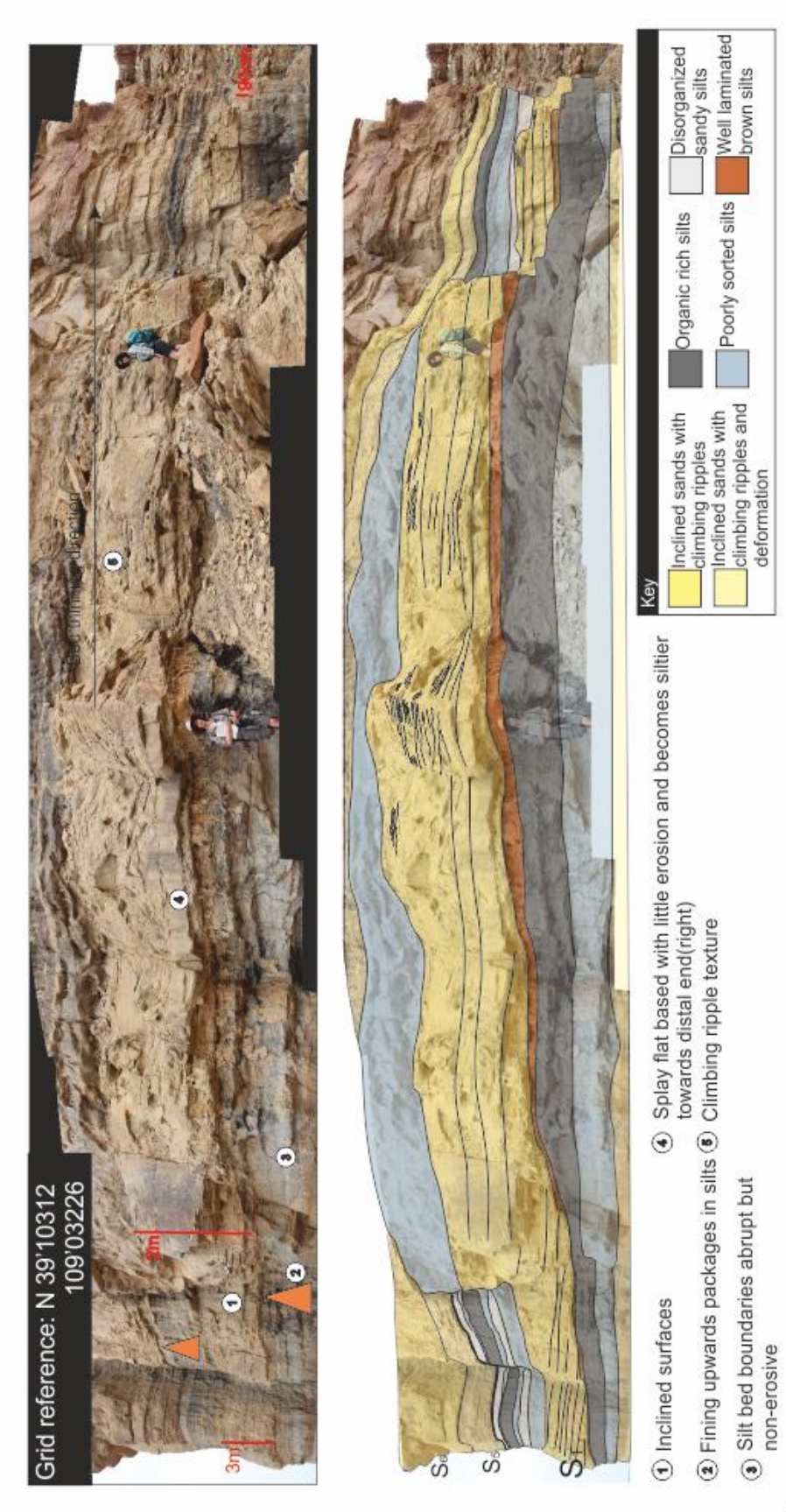

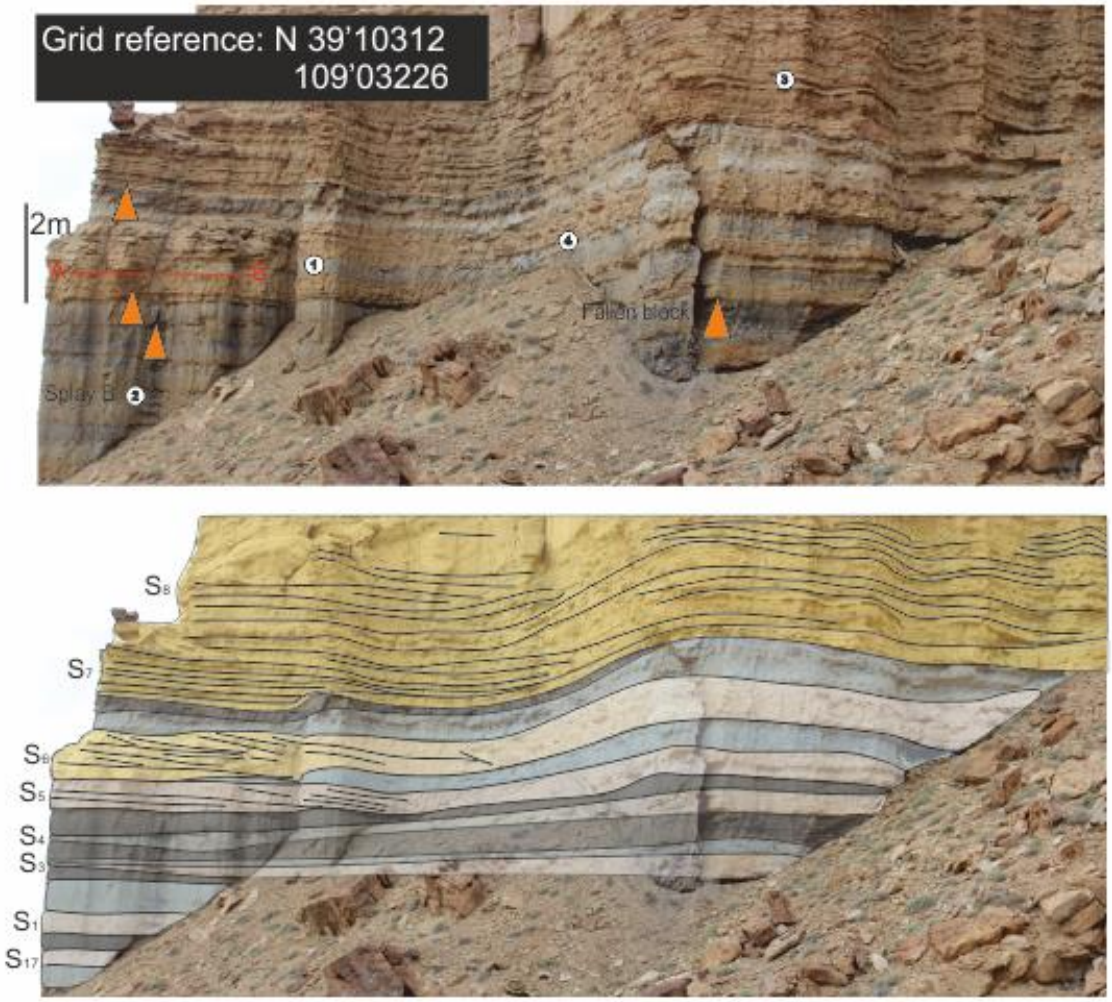

1. Upper splay cuts down into lower splay; merging together at A, at B the upper splay no longer cuts down into the lower splay.
2. S1 splay has changed laterally downdip to disorganized sandy silts
3. Crevasse splay complex
4. Much greater change proximal to distal rather than laterally across the splay

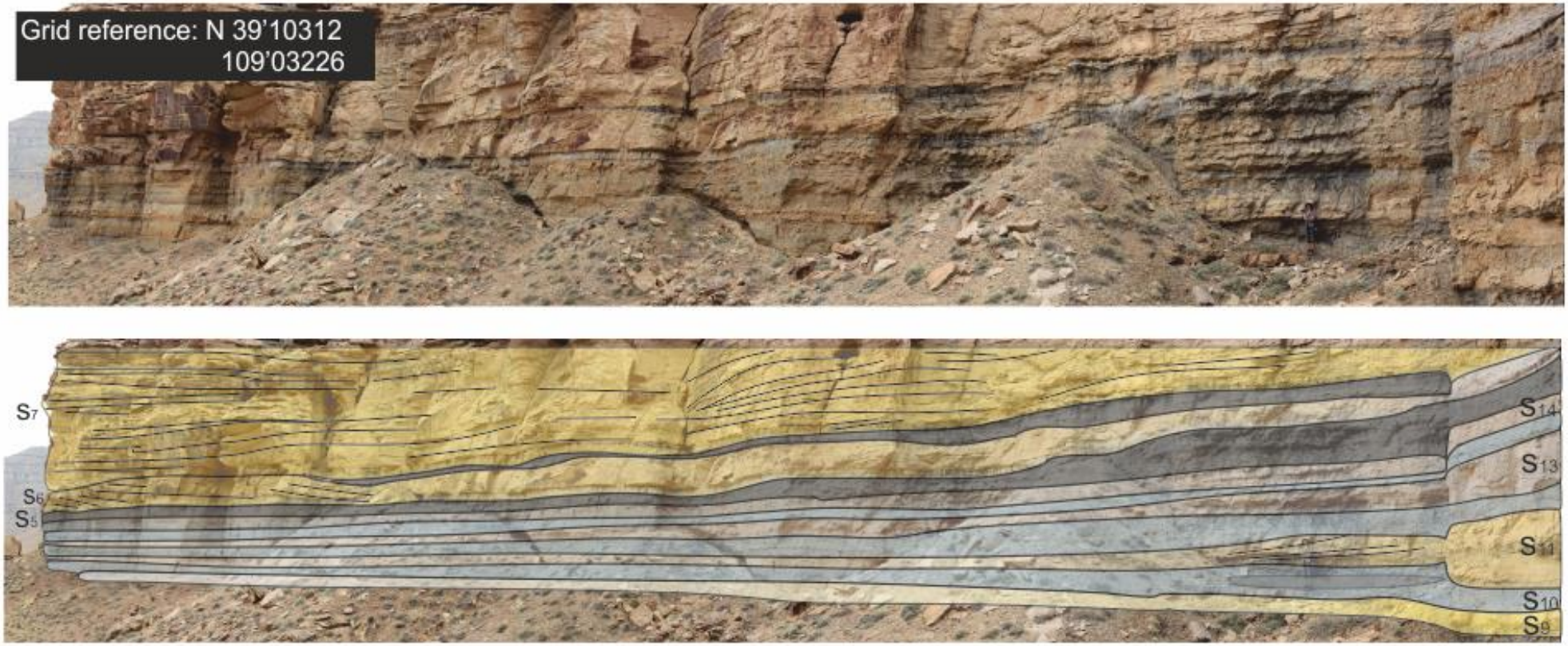
Grid reference: N 39'10312
109'03226
S7
S6
S5
S14
S13
S11
S10
S9
Key
Inclined sands with climbing ripples
Inclined sands with climbing ripples and deformation
Organic rich silts
Poorly sorted silts
Disorganized sandy silts
Well laminated brown silts

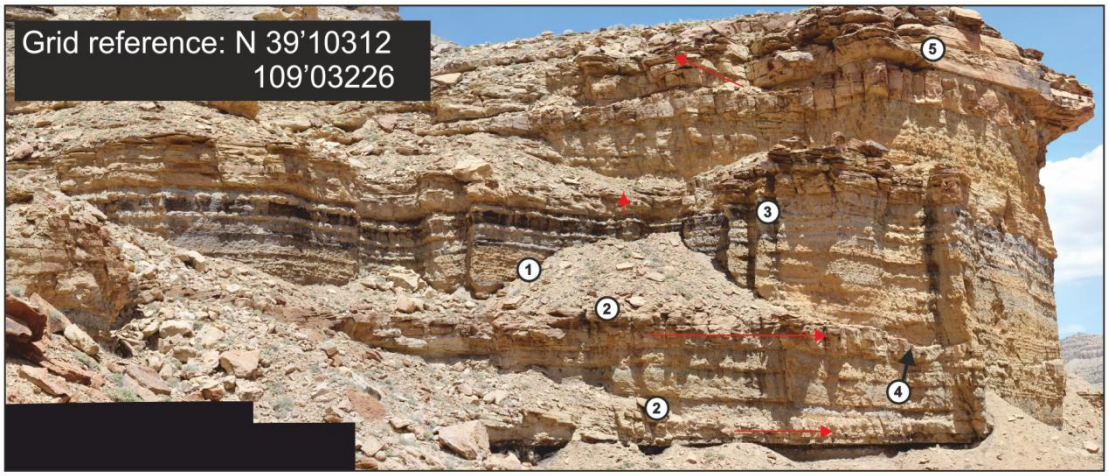

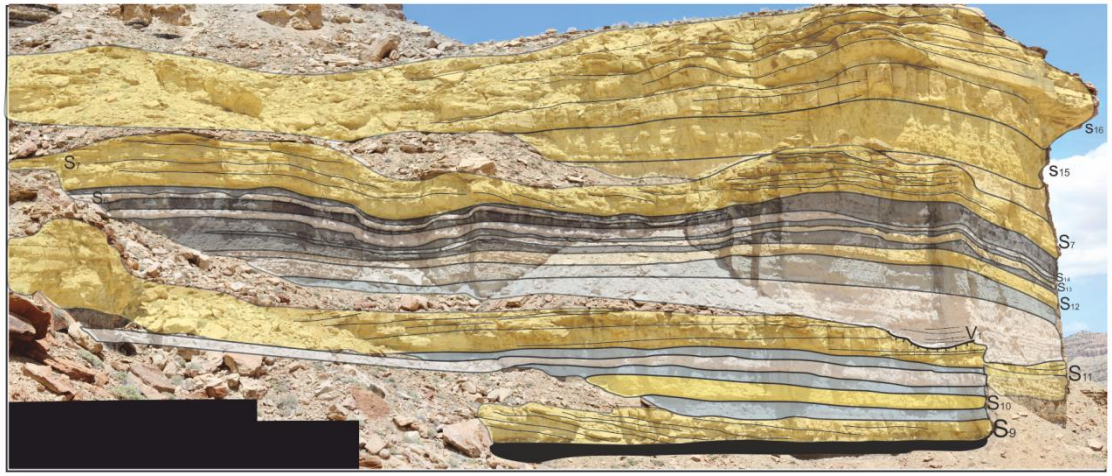

1. Facies merge laterally into one another
2. Inclined surfaces in different directions
3. Poorly sorted silt merges into organic rich silts
4. Erosional feature passive infill with sandy silts
5. Flat splays inclined into the rock face

Key

Inclined sands with climbing ripples	Organic rich silts
Inclined sands with climbing ripples and deformation	Poorly sorted silts
Disorganized sandy silts	Well laminated brown silts

1. Inclined surfaces show tendency to dip to south
2. Increasing prevalence of sand towards top of section
3. Small erosional channel infilled with silts
4. Sands have passed laterally to silty sands and poorly sorted silts

Key

- Inclined sands with climbing ripples
- Inclined sands with climbing ripples and deformation
- Disorganized sandy silts
- Organic rich silts
- Poorly sorted silts
- Well laminated brown silts

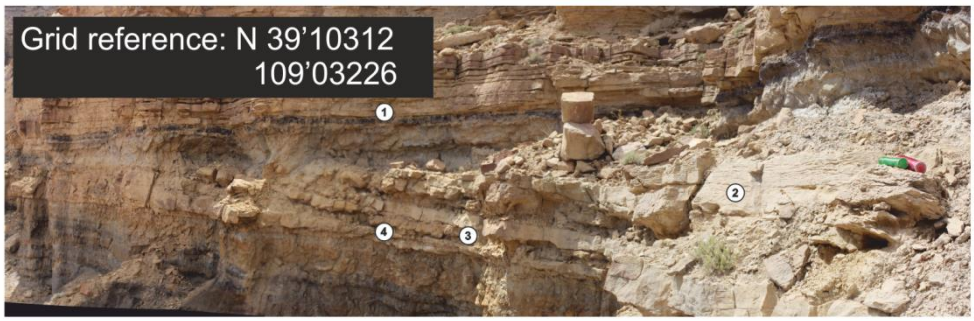

① Flat planar, very low angle surfaces non-erosive abrupt transition to sand

② Climbing ripple texture

③ Inclined surfaces terminate but at a very low angle

④ Gutter casts, erosional

Key

- Inclined sands with climbing ripples
- Inclined sands with climbing ripples and deformation
- Disorganized sandy silts
- Organic rich silts
- Poorly sorted silts
- Well laminated brown silts

Grid reference: N 39’10312
109’03226
S8
S7
S6
S5
S4
S3
S1
S17
S18

Panels around Floy Wash


Grid reference: N 39°01544
109°84454

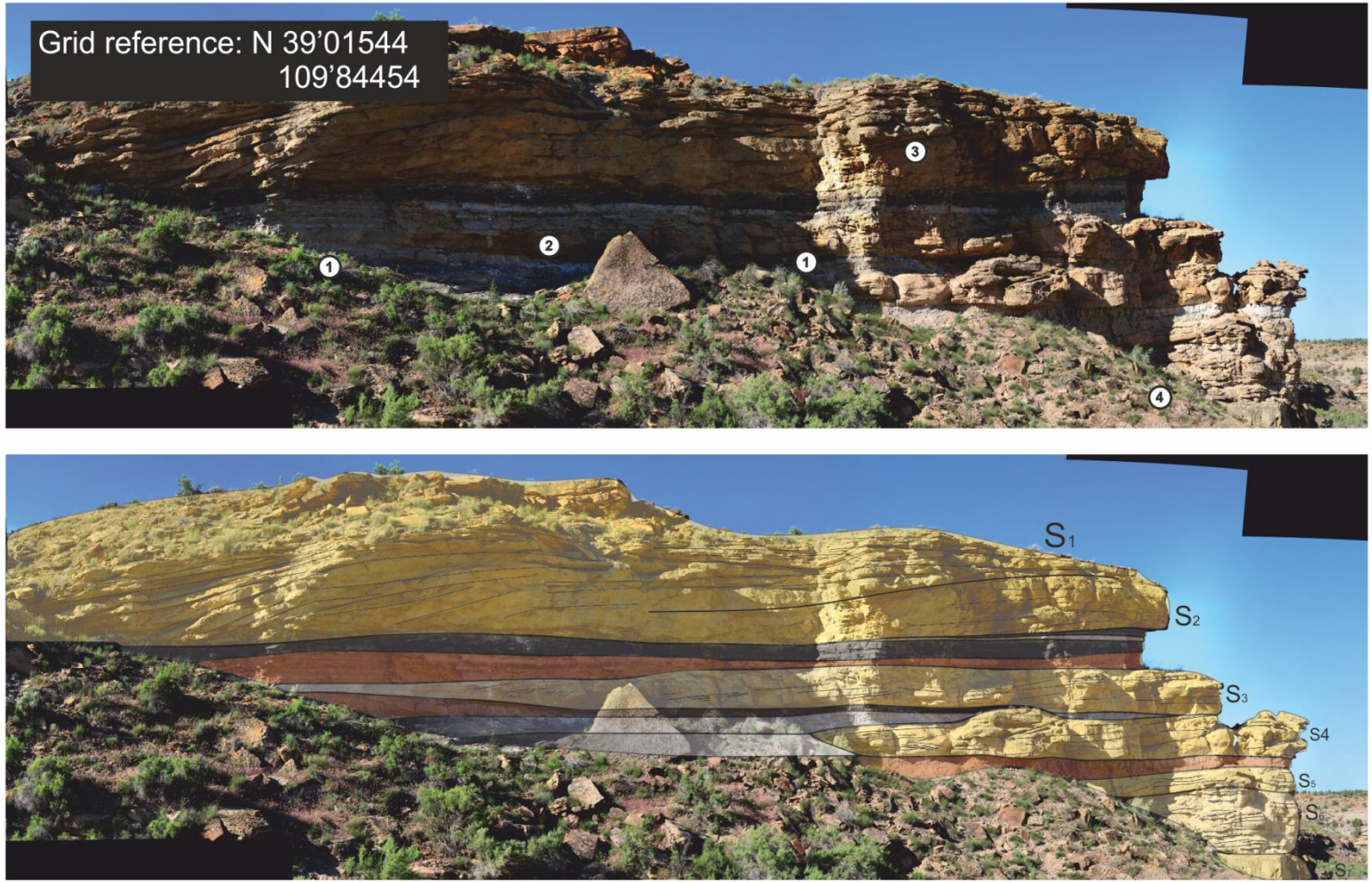

① Rapid lateral transition over less than 2m from inclined cross stratified sands to poorly sorted silts

② Very high angle cross-strata

③ Erosional surface: Multiple splays

④ Disorganised sand bed

Key

- Inclined sands with climbing ripples
- Organic rich silts
- Disorganized sandy silts
- Inclined sands with climbing ripples and deformation
- Poorly sorted silts
- Well laminated brown silts

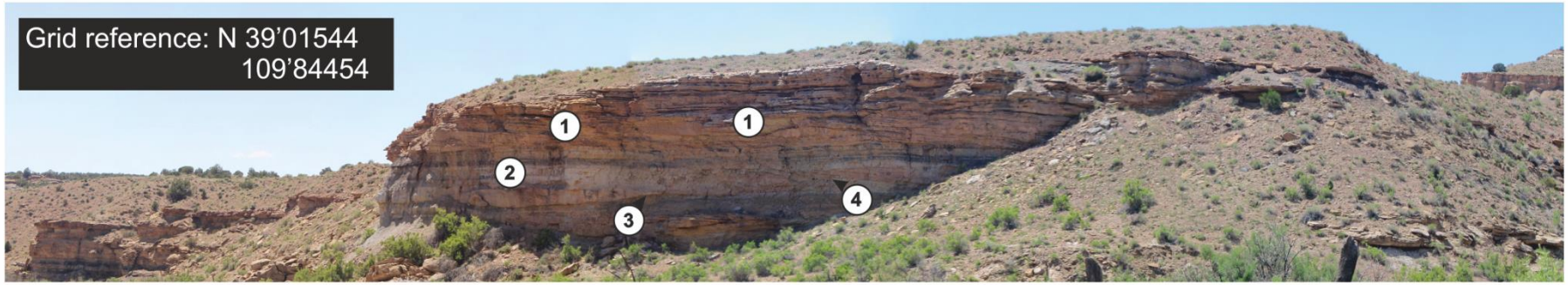

1. More significant erosional surfaces signifying new splay deposit in complex
2. Crevasse channel element: Sands with climbing ripples and high angle cross-strata; Erosional lower surface
3. Rapid bed thickness change over less than 5 metres; from 1m to 30cm
4. Inclined surfaces, edge of crevasse channel meets edge of splay

Key

- Inclined sands with climbing ripples
- Inclined sands with climbing ripples and deformation
- Organic rich silts
- Poorly sorted silts
- Disorganized sandy silts
- Well laminated brown silts

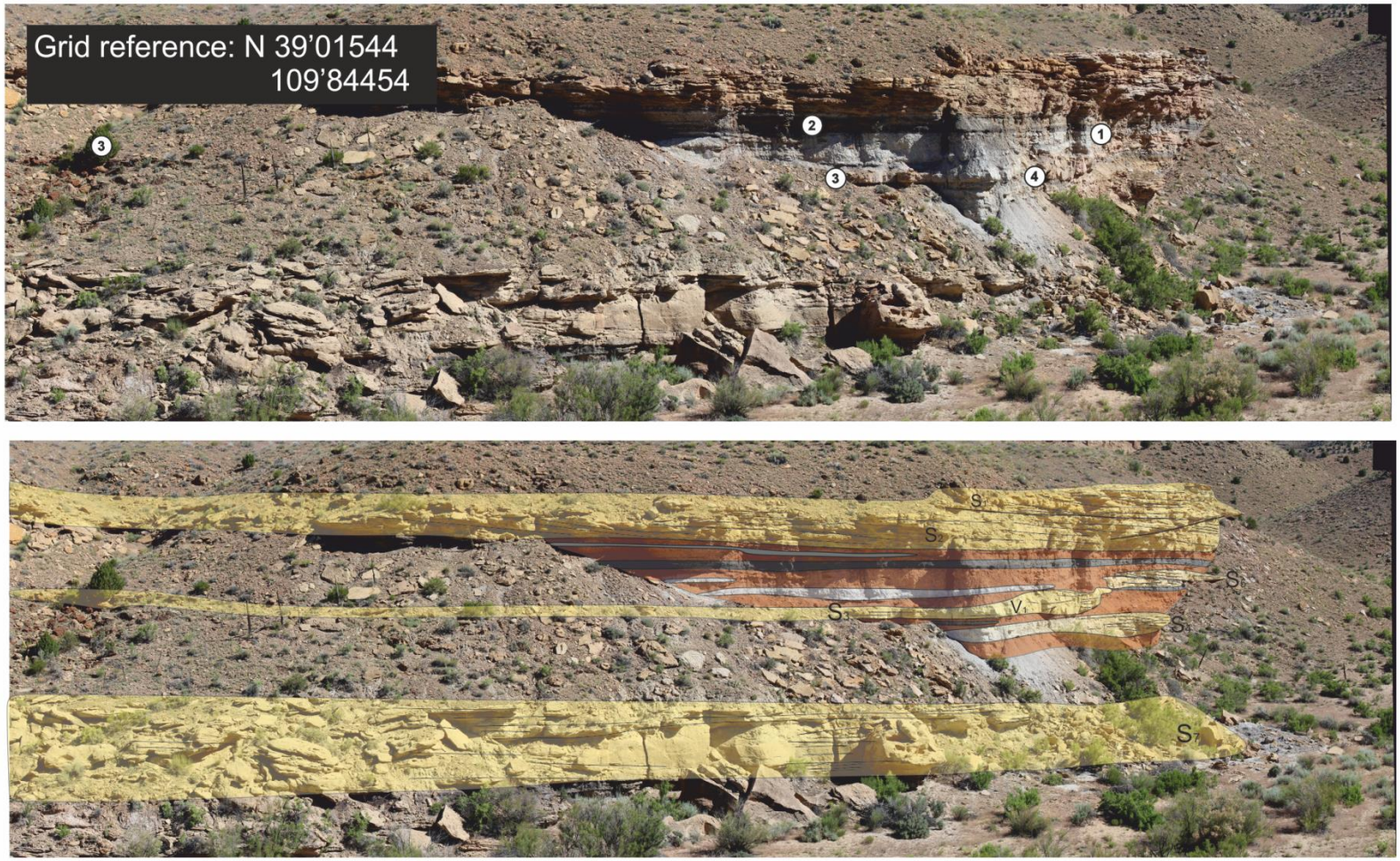

① Disorganised silty sand deposits with inclined surfaces Interfingering of paleosols and sandy silts
② Coaly marker bed
③ Crevasse channel laterally linked to more tabular splay element
④ Crevasse channel element;erosive base, lenticular shape

Key

Inclined sands with climbing ripples	Organic rich silts	Disorganized sandy silts
Inclined sands with climbing ripples and deformation	Poorly sorted silts	Well laminated brown silts

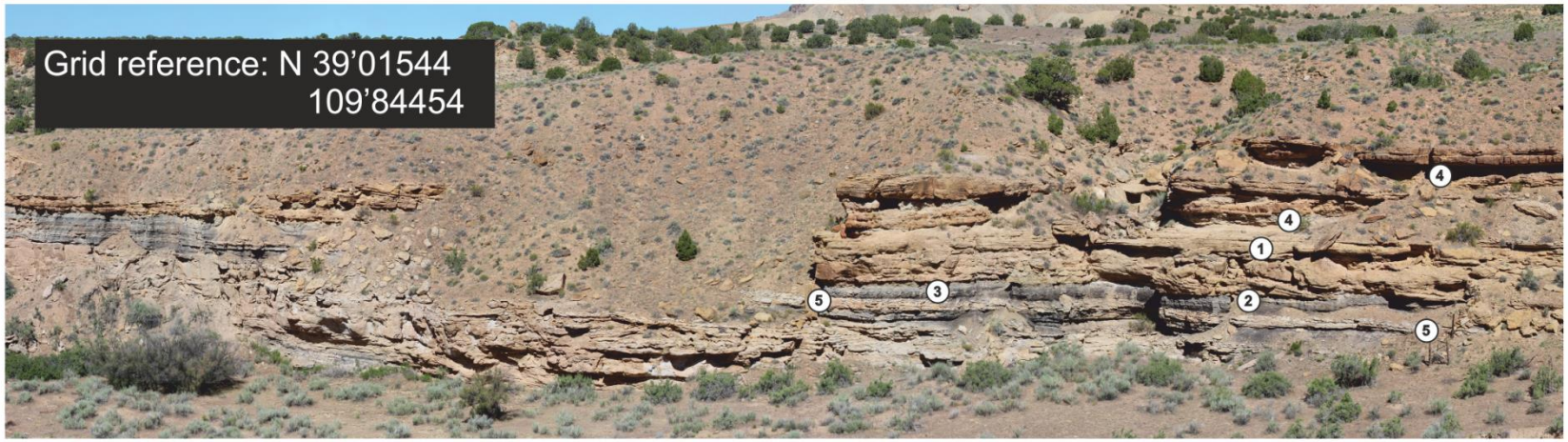

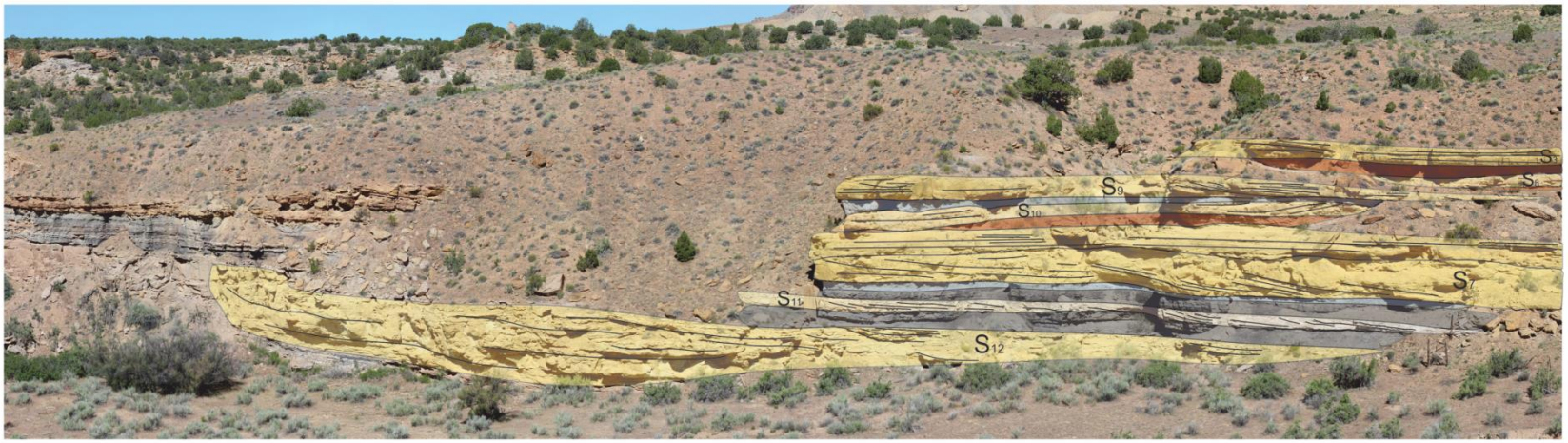

① Erosive surface

② Inclined surfaces-building out

③ Coal rich layer

④ Paleosols

⑤ S11 Becomes increasingly silty and thinner

Key

- Inclined sands with climbing ripples
- Inclined sands with climbing ripples and deformation
- Organic rich silts
- Poorly sorted silts
- Disorganized sandy silts
- Well laminated brown silts

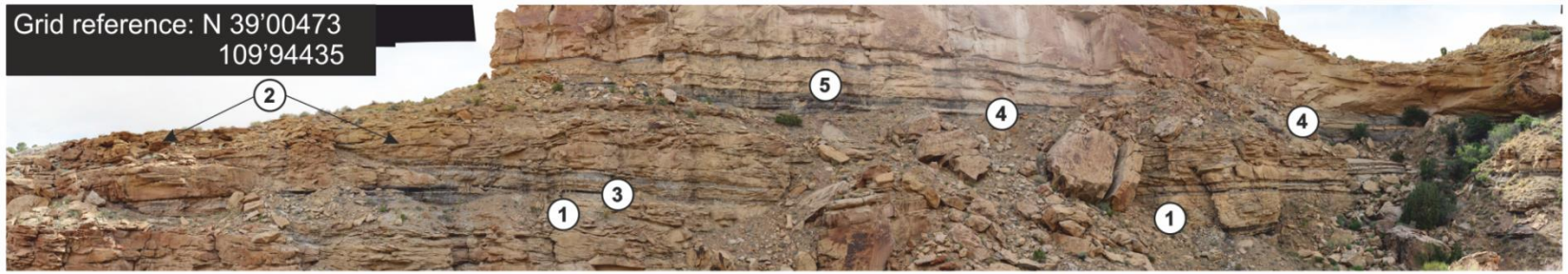

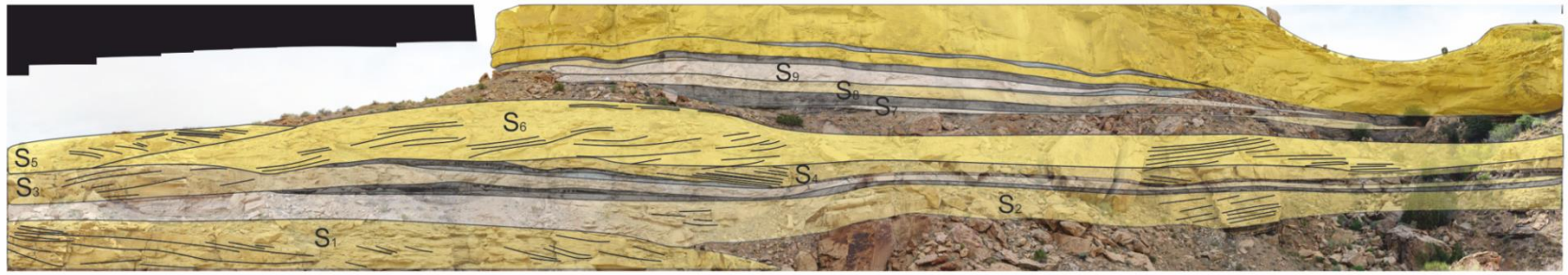

① S_2 shows transition from inclined thinning to silts towards the south before turning to thin sandy deposits

② S_5 and S_6 surfaces build out in opposite directions; merging splays

③ Coal marker bed underneath S_3 shows rapid lateral thinning and change to silt

④ Distal edge of splay S_7 with small plan view area; rapid change from sandy silt to silts

⑤ S_8 distal edge of splay

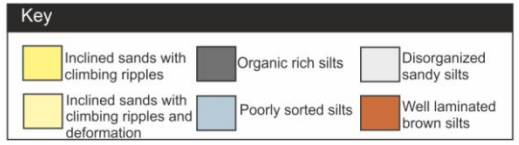

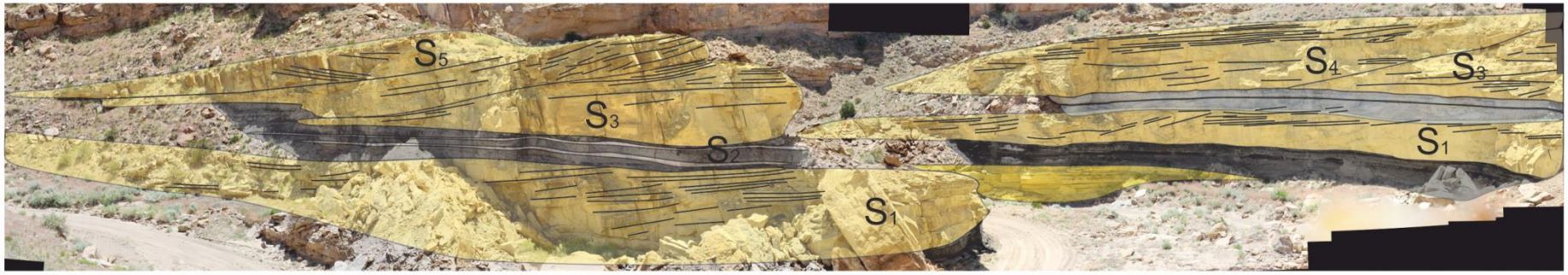

1. Blackhawk marine sandstone
2. Flat surfaces perpendicular to the build out direction
3. S4 splay cuts out S3 completely towards west side of site
4. S2 splay has changed to organic rich silts

Key

- Inclined sands with climbing ripples
- Inclined sands with climbing ripples and deformation
- Organic rich silts
- Poorly sorted silts
- Disorganized sandy silts
- Well laminated brown silts

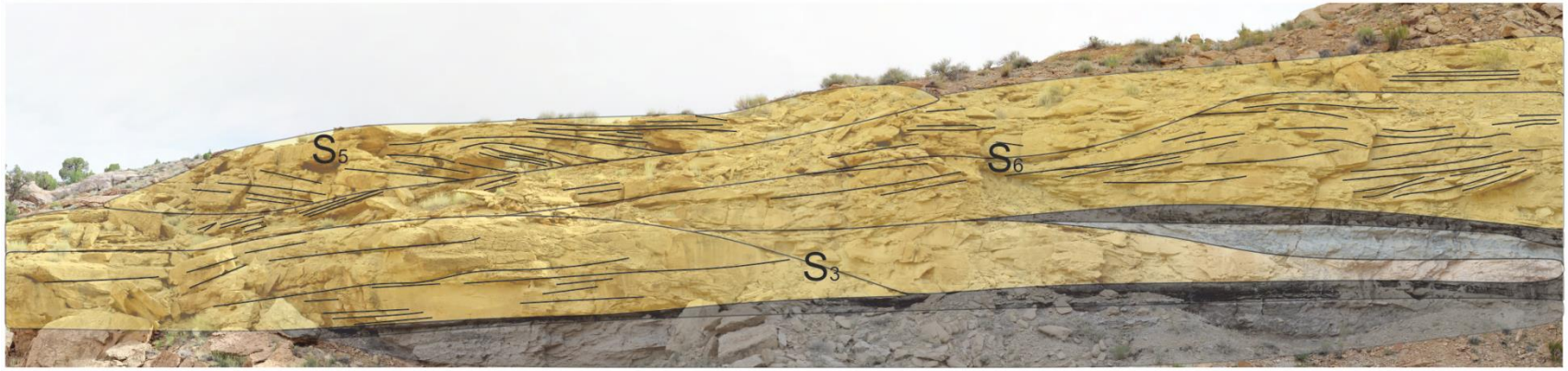

1. Shift from inclined sands to silts; rapid over space of less than a metre
2. Coal marker bed below S_6
3. Many different directions of inclined surfaces

Key

- Inclined sands with climbing ripples
- Inclined sands with climbing ripples and deformation
- Organic rich silts
- Poorly sorted silts
- Disorganized sandy silts
- Well laminated brown silts

Grid reference: N 39’00473
109’94435

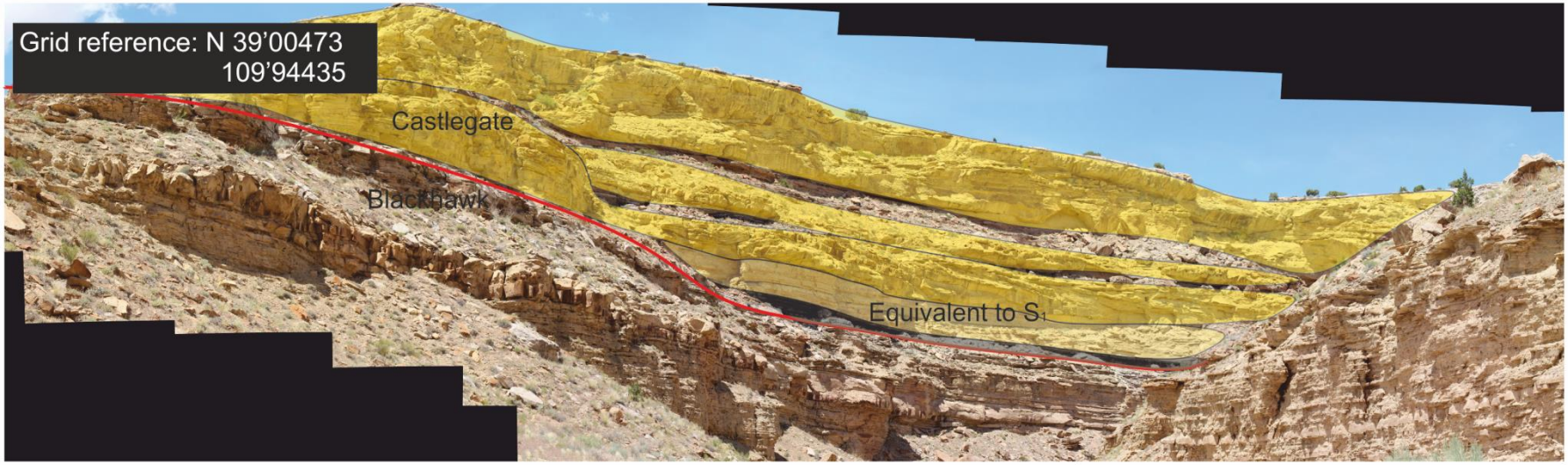

Key

- Channel bodies
- Splay deposits
- Organic rich silts
- Poorly sorted silts

C4+L

Panels around Atkinson Creek

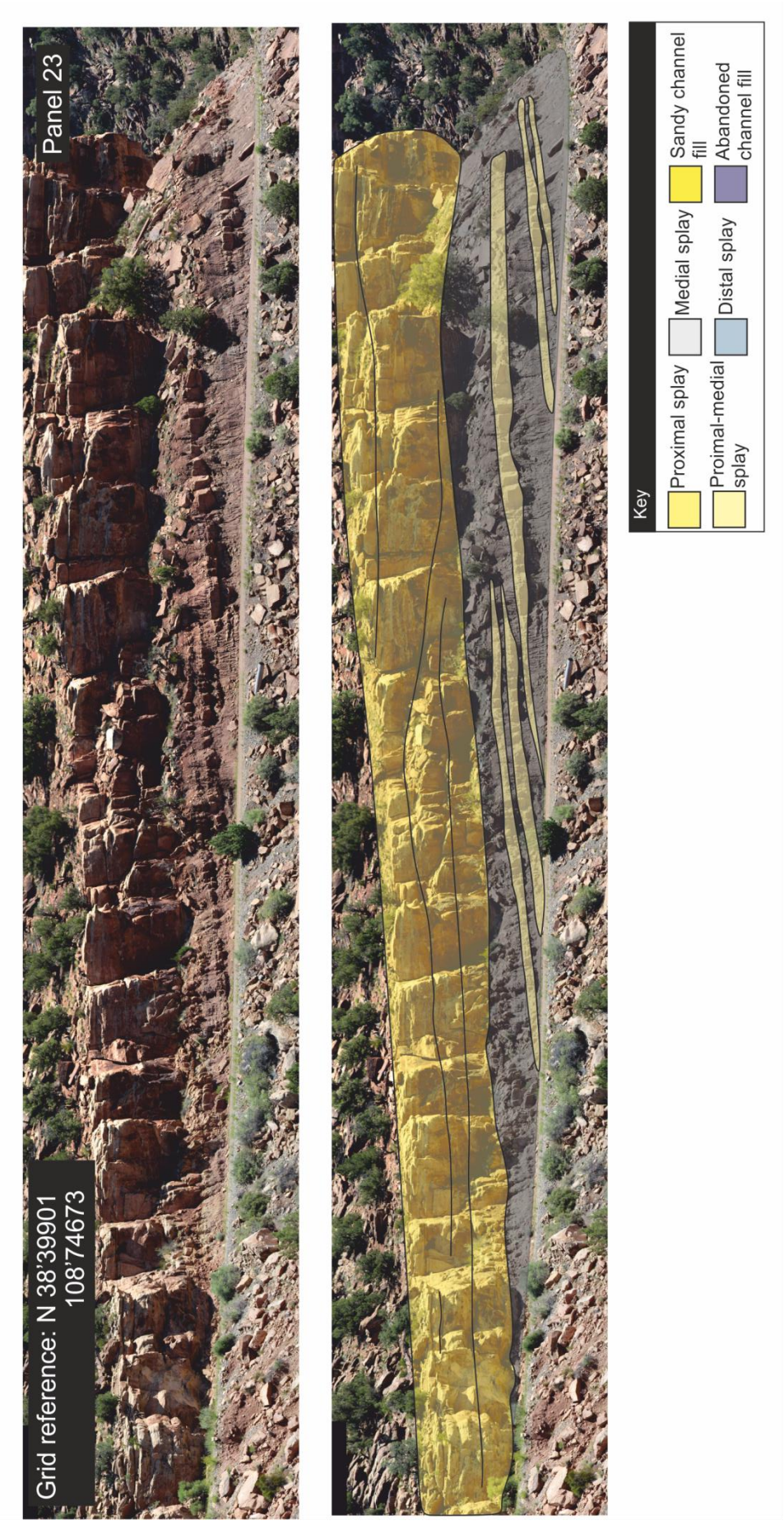

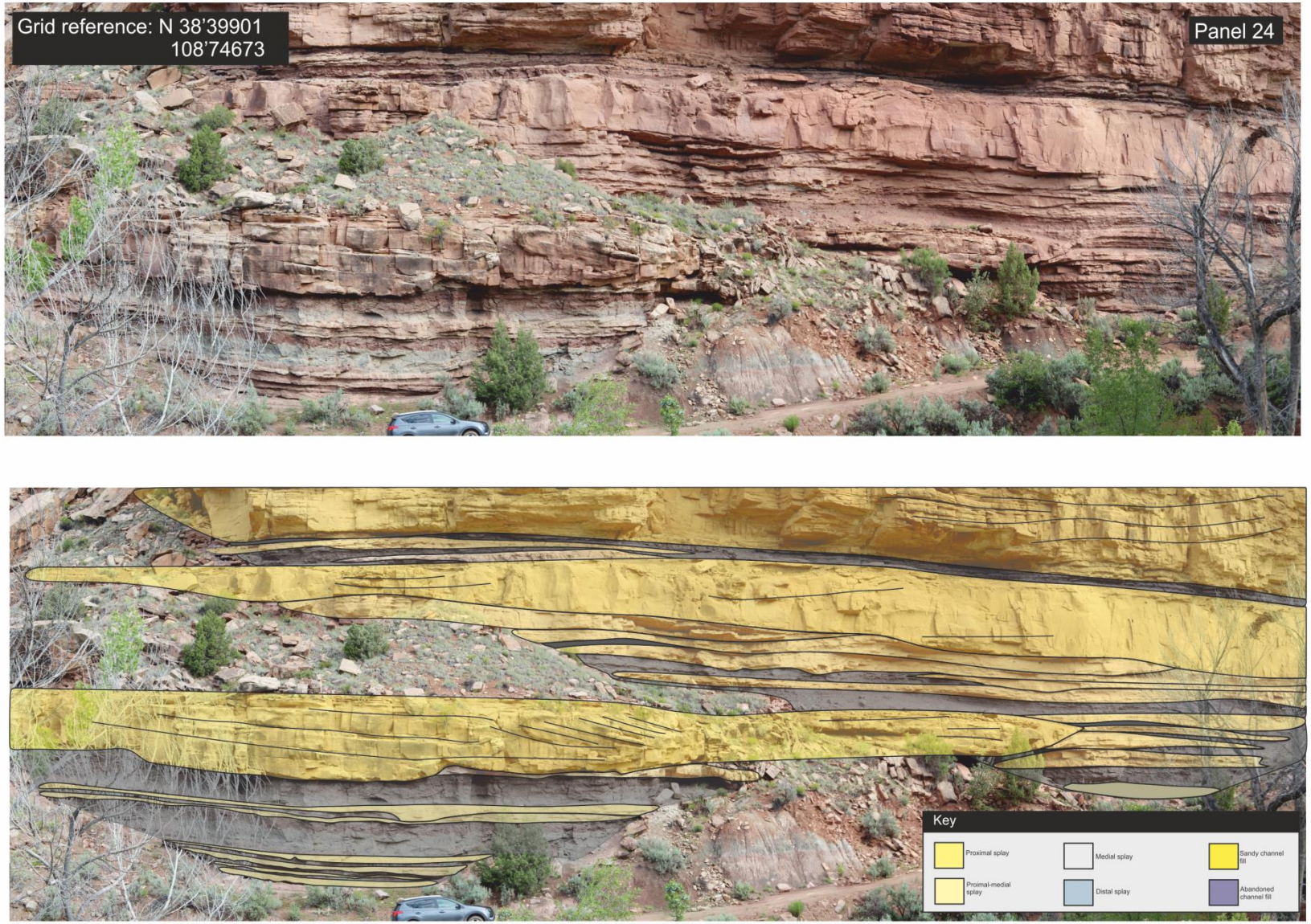
Grid reference: N 38’39901
108’74673
Panel 24
Key
Proximal splay
Medial splay
Sandy channel fill
Proximal-medial splay
Distal splay
Abandoned channel fill

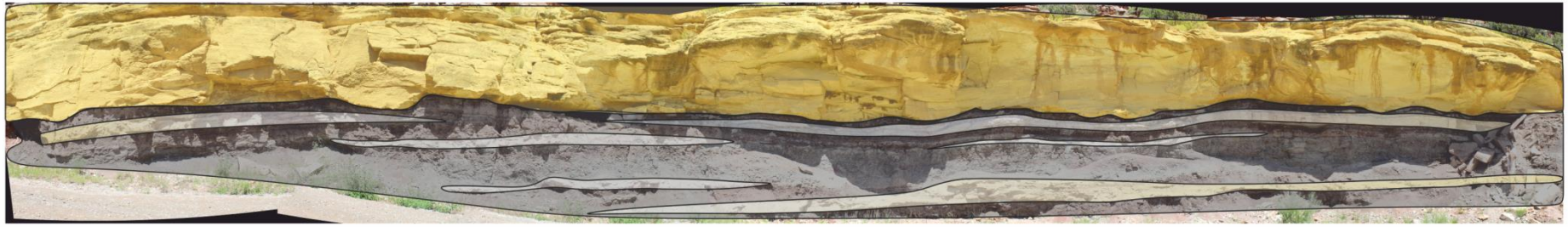

Key

- Proximal splay
- Medial splay
- Sandy channel fill
- Proimal-medial splay
- Distal splay
- Abandoned channel fill


Grid reference: N 38’39901
108’74673
Panel 26
Key
Proximal splay
Medial splay
Sandy channel fill
Proimal-medial splay
Distal splay
Abandoned channel fill

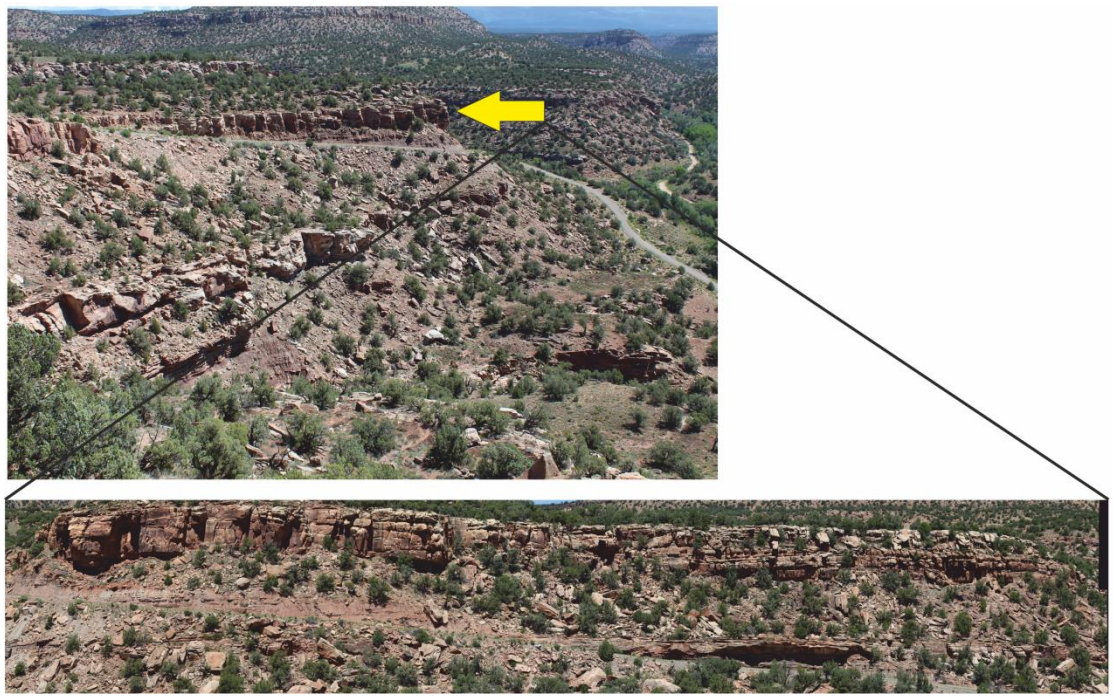

Panels around Slick Rock

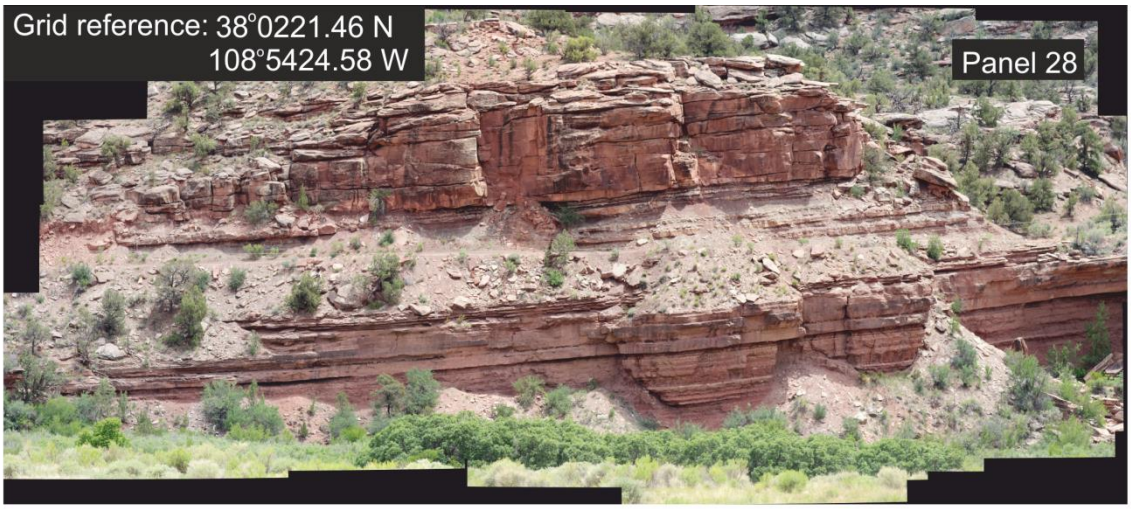

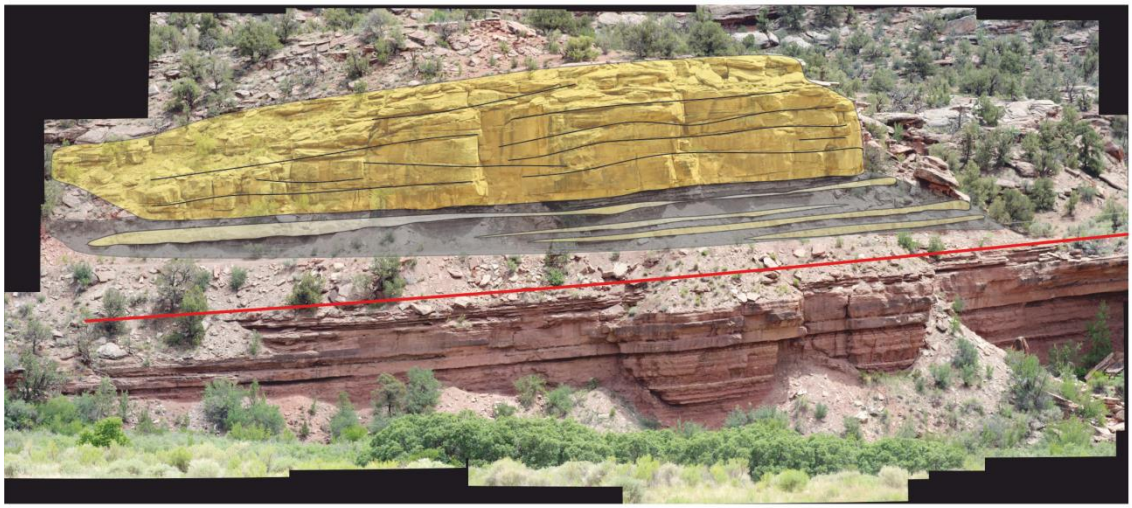

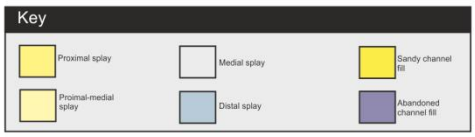

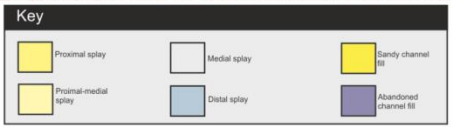
Key
Proximal splay
Medial splay
Sandy channel fill
Proimal-medial splay
Distal splay
Abandoned channel fill


1 m

Panels around Naturita

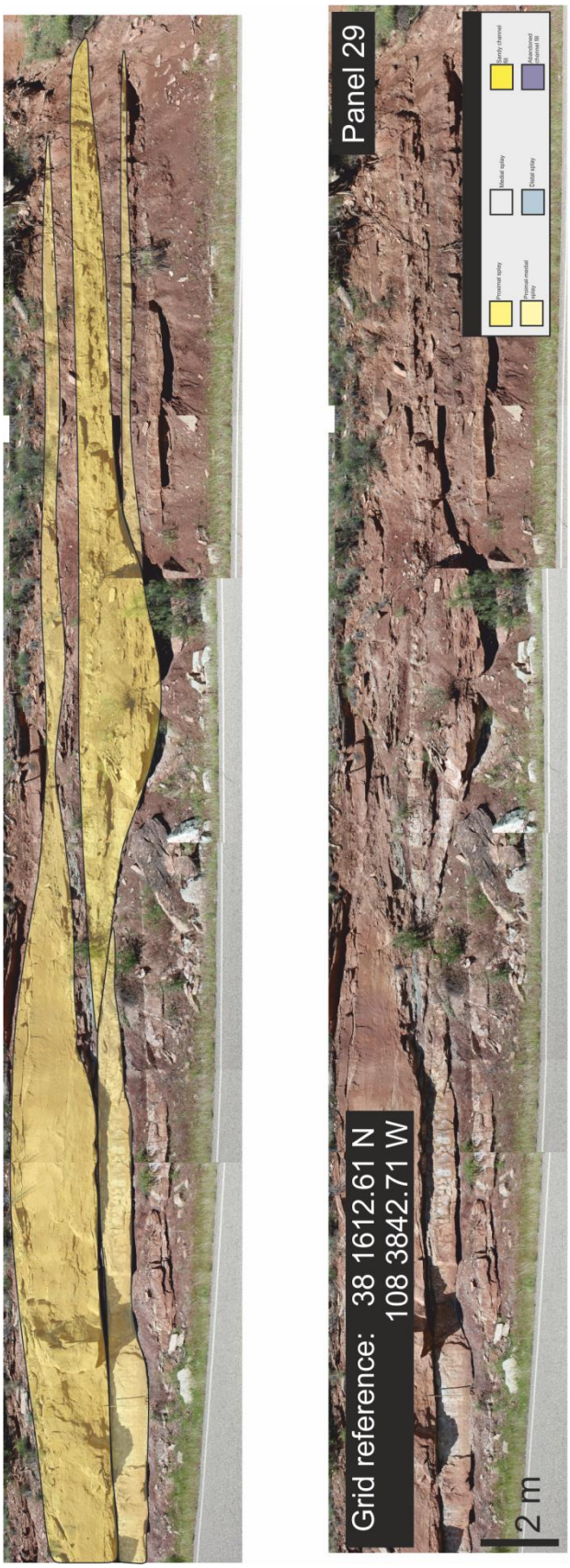

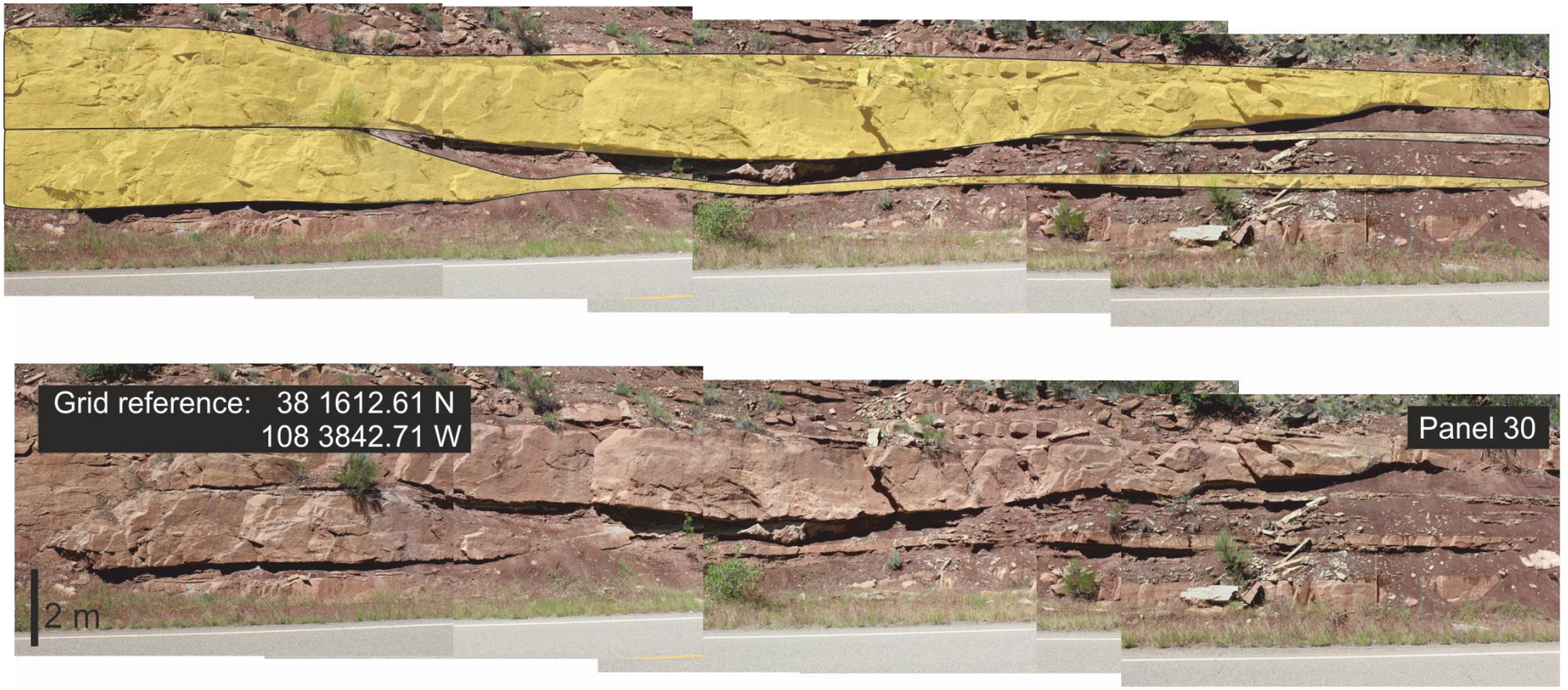
Grid reference: 38 1612.61 N
108 3842.71 W
2 m
Panel 30

Panels around Yellow Cat Canyon

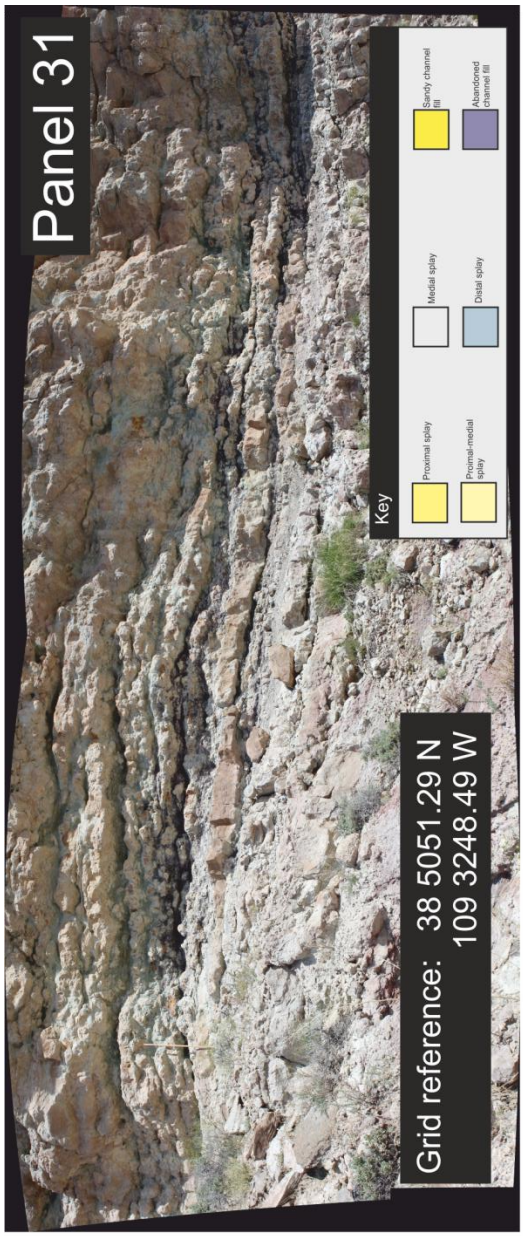

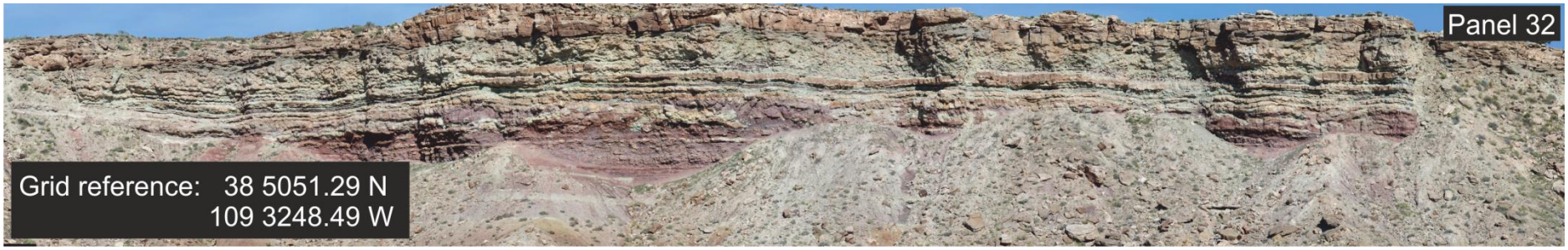
Panel 32
Grid reference: 38 5051.29 N
109 3248.49 W


Panel 33
Grid reference: 38 5051.29 N
109 3248.49 W


Panel 34
Grid reference: 38 5051.29 N
109 3248.49 W
1m

Panels around Colorado National Monument

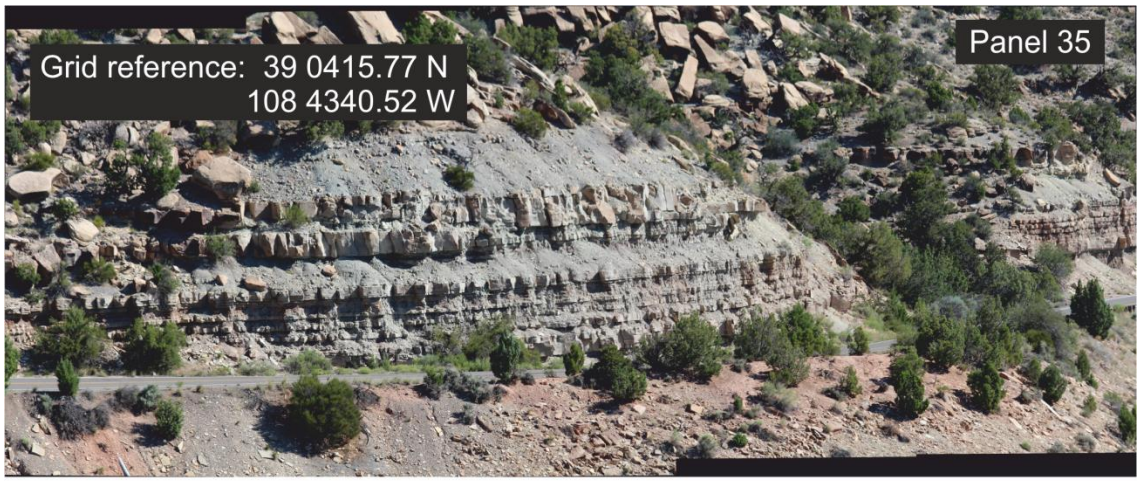

Key

Proximal splay

Medial splay

Sandy channel fill

Proimal-medial splay

Distal splay

Abandoned channel fill

Appendix C: FAKTS database

References used for FAKTS database study used in Chapter 6

FF: Floodplain elemeents

reference_citation

Hornung J., Aigner T. (1999) Reservoir and aquifer characterization of fluvial architectural elements: Stubensandstein, Upper Triassic, southwest Germany. Sed. Geol. 129, 215-280.

Amorosi A., Pavesi M., Ricci Lucchi M., Sarti G., Piccin A. (2008) Climatic signature of cyclic fluvial architecture from the Quaternary of the central Po Plain, Italy. Sed. Geol. 209, 58-68.

Jones S. J., Frostick L. E., Astin T. R. (2001) Braided stream and flood plain architecture: the Rio Vero Formation, Spanish Pyrenees. Sed. Geol. 139, 229-260.

Robinson J. W., McCabe P. J. (1997) Sandstone-body and shale-body dimensions in a braided fluvial system: Salt Wash Sandstone Member (Morrison Formation), Garfield County, Utah. AAPG Bull. 81, 1267-1291.

Jo H. R. (2003) Depositional environments, architecture, and controls of Early Cretaceous non-marine successions in the northwestern part of Kyongsang Basin, Korea. Sed. Geol. 161, 269-294.

Cain S. A. (2009) Sedimentology and stratigraphy of a terminal fluvial fan system: the Permian Organ Rock Formation, South East Utah. Unpublished PhD Thesis, Keele University, UK.

Cuevas Martínez J. L., Cabrera Perez L., Marcuello A., Arbues Cazo P., Marzo Carpio M., Bellmunt F. (2010) Exhumed channel sandstone networks within fluvial fan deposits from the Oligo-Miocene Caspe Formation, South-east Ebro Basin (North-east Spain). Sedimentology 57, 162-189.

Fabuel-Perez I., Redfern J., Hodgetts D. (2009) Sedimentology of an intra-montane rift-controlled fluvial dominated succession: The Upper Triassic Oukaimeden Sandstone Formation, Central High Atlas, Morocco. Sed. Geol. 218, 103-140.

Fabuel-Perez I., Hodgetts D., Redfern J. (2009) A new approach for outcrop characterization and geostatistical analysis of a low-sinuosity fluvial-dominated succession using digital outcrop models: Upper Triassic Oukaimeden Sandstone Formation, central High Atlas, Morocco. AAPG Bull. 93, 795-827.

Tunbridge I. (1984) Facies model for a sandy ephemeral stream and clay playa complex; the Middle Devonian Trentishoe Formation of North Devon, UK. Sedimentology 31, 697-715.

Weerts H. J. T., Bierkens M. F. P. (1993) Geostatistical analysis of overbank deposits of anastomosing and meandering fluvial systems; Rhine-Meuse delta, The Netherlands. In: Fielding C. R. (ed.) Current Research in Fluvial Sedimentology. Sed. Geol. 85, 221-232.

Steel R. J., Thompson D. B. (1983) Structures and textures in Triassic braided stream

conglomerates (‘Bunter’ Pebble Beds) in the Sherwood Sandstone Group, North Staffordshire, England. Sedimentology 30, 341-367.

Donselaar M. E., Overeem I. (2008) Connectivity of fluvial point-bar deposits: An example from the Miocene Huesca fluvial fan, Ebro Basin, Spain. AAPG Bull. 92, 1109-1129.

Hampton B. A., Horton B. K. (2007) Sheetflow fluvial processes in a rapidly subsiding basin, Altiplano plateau, Bolivia. Sedimentology 54, 1121-1147.

Holzförster F., Stollhofen H., Stanistreet I. G. (1999) Lithostratigraphy and depositional environments in the Waterberg-Erongo area, central Namibia, and correlation with the main Karoo Basin, South Africa. J. Afr. Earth. Sci. 29, 105-123.

Olsen H. (1989) Sandstone-body structures and ephemeral stream processes in the Dinosaur Canyon Member, Moenave Formation (Lower Jurassic), Utah, U.S.A. Sed. Geol. 61, 207-221.

Catuneanu O., Elango H. N. (2001) Tectonic control on fluvial styles: the Balfour Formation of the Karoo Basin, South Africa. Sed. Geol. 140, 291-313.

Catuneanu O., Bowker D. (2001) Sequence stratigraphy of the Koonap and Middleton fluvial formations in the Karoo foredeep South Africa. J. Afr. Earth. Sci. 33, 579-595.

Miall A. D., Turner-Peterson C. E. (1989) Variations in fluvial style in the Westwater Canyon Member, Morrison Formation (Jurassic), San Juan Basin, Colorado Plateau. Sed. Geol. 63, 21-60.

Stewart D. J. (1983) Possible suspended-load channel deposits from the Wealden Group (Lower Cretaceous) of Southern England. In: Collinson J. D., Lewin J. (eds.) Modern and ancient fluvial systems. IAS Spec. Publ. 6, 369-384.

Rygel M. C., Gibling M. R. (2006) Natural geomorphic variability recorded in a high-accommodation setting: fluvial architecture of the Pennsylvanian Joggins Formation of Atlantic Canada. J. Sed. Res. 76, 1230-1251.

Kirk M. (1983) Bar development in a fluvial sandstone (Westphalian 'A'), Scotland. Sedimentology 30, 727-742.

Viseras C., Soria J. M., Durán J. J., Pla S., Garrido G., García-García F., Arribas A. (2006) A large-mammal site in a meandering fluvial context (Fonelas P-1, Late Pliocene, Guadix Basin, Spain) Sedimentological keys for its paleoenvironmental reconstruction. Paleogeo. Paleoclim. Paleoecol. 242, 139-168.

Limarino C., Tripaldi A., Marenssi S., Net L., Re G., Caselli A. (2001) Tectonic control on the evolution of the fluvial systems of the Vinchina Formation (Miocene), northwestern Argentina. J. South Am. Earth Sci. 14, 751-762.

Roberts E. M. (2007) Facies architecture and depositional environments of the Upper Cretaceous Kaiparowits Formation, southern Utah. Sed. Geol. 197, 207-233.

Kraus M. J., Middleton L. T. (1987) Contrasting architecture of two alluvial suites in different structural settings. In: Ethridge F. G., Flores R. M., Harvey M. D. (eds.) Recent Developments in Fluvial Sedimentology, SEPM Spec. Publ. 39, 253-262.

Hirst J. P. P. (1991) Variations in alluvial architecture across the Oligo-Miocene Huesca

fluvial system, Ebro Basin, Spain. In: Miall A. D., Tyler N. (eds.) The three-dimensional facies architecture of terrigenous clastic sediments and its implications for hydrocarbon discovery and recovery. SEPM Concepts in Sed. and Paleo. 3, 111-121.

Trendell A. M., Atchley S. C., Nordt L. C. (2013) Facies analysis of a probable large-fluvial-fan depositional system: the Upper Triassic Chinle Formation at Petrified Forest National Park, Arizona, USA. J. Sed. Res. 83, 873-895.

Kraus M. J. (1996) Avulsion deposits in lower Eocene alluvial rocks, Bighorn Basin, Wyoming. J. Sed. Res. 66, 354-363.

Keighley D., Flint S., Howell J., Moscariello A. (2003) Sequence stratigraphy in lacustrine basins: a model for part of the Green River Formation (Eocene), southwest Uinta Basin, Utah, USA. J. Sed. Res. 73, 987-1006.

Anderson D. S. (2005) Architecture of crevasse splay and point-bar bodies of the nonmarine lles Formation north of Rangely, Colorado: implications for reservoir description. Mt. Geologist 42, 109-122.

Smith R. M. H. (1987) Morphology and depositional history of exhumed Permian point bars in the southwestern Karoo, South Africa. J. Sed. Petrol. 57, 19-29.

CS: Crevasse-splay elements

reference_citation

Hornung J., Aigner T. (1999) Reservoir and aquifer characterization of fluvial architectural elements: Stubensandstein, Upper Triassic, southwest Germany. Sed. Geol. 129, 215-280.

Amorosi A., Pavesi M., Ricci Lucchi M., Sarti G., Piccin A. (2008) Climatic signature of cyclic fluvial architecture from the Quaternary of the central Po Plain, Italy. Sed. Geol. 209, 58-68.

Jordan D. W., Pryor W. A. (1992) Hierarchical levels of heterogeneity in a Mississippi River meander belt and application to reservoir systems. AAPG Bull. 76, 1601-1624.

Cuevas Gozalo M. C., Martinius A. W. (1993) Outcrop data-base for the geological characterization of fluvial reservoirs: an example from distal fluvial fan deposits in the Loranca Basin, Spain. In: North C. P., Prosser D. J. (eds.) Characterization of fluvial and aeolian reservoirs. Geol. Soc. Spec. Publ. 73, 79-94.

Cain S. A. (2009) Sedimentology and stratigraphy of a terminal fluvial fan system: the Permian Organ Rock Formation, South East Utah. Unpublished PhD Thesis, Keele University, UK.

Weerts H. J. T., Bierkens M. F. P. (1993) Geostatistical analysis of overbank deposits of anastomosing and meandering fluvial systems; Rhine-Meuse delta, The Netherlands. In: Fielding C. R. (ed.) Current Research in Fluvial Sedimentology. Sed. Geol. 85, 221-232.

Donselaar M. E., Overeem I. (2008) Connectivity of fluvial point-bar deposits: An example from the Miocene Huesca fluvial fan, Ebro Basin, Spain. AAPG Bull. 92, 1109-1129.

Holzförster F., Stollhofen H., Stanistreet I. G. (1999) Lithostratigraphy and depositional environments in the Waterberg-Erongo area, central Namibia, and correlation with the

main Karoo Basin, South Africa. J. Afr. Earth. Sci. 29, 105-123.

Olsen H. (1989) Sandstone-body structures and ephemeral stream processes in the Dinosaur Canyon Member, Moenave Formation (Lower Jurassic), Utah, U.S.A. Sed. Geol. 61, 207-221.

Catuneanu O., Elango H. N. (2001) Tectonic control on fluvial styles: the Balfour Formation of the Karoo Basin, South Africa. Sed. Geol. 140, 291-313.

Catuneanu O., Bowker D. (2001) Sequence stratigraphy of the Koonap and Middleton fluvial formations in the Karoo foredeep South Africa. J. Afr. Earth. Sci. 33, 579-595.

Reynolds A. D. (1999) Dimensions of paralic sandstone bodies. AAPG Bull. 83, 211-229.

Stewart D. J. (1983) Possible suspended-load channel deposits from the Wealden Group (Lower Cretaceous) of Southern England. In: Collinson J. D., Lewin J. (eds.) Modern and ancient fluvial systems. IAS Spec. Publ. 6, 369-384.

Rygel M. C., Gibling M. R. (2006) Natural geomorphic variability recorded in a high-accommodation setting: fluvial architecture of the Pennsylvanian Joggins Formation of Atlantic Canada. J. Sed. Res. 76, 1230-1251.

Limarino C., Tripaldi A., Marenssi S., Net L., Re G., Caselli A. (2001) Tectonic control on the evolution of the fluvial systems of the Vinchina Formation (Miocene), northwestern Argentina. J. South Am. Earth Sci. 14, 751-762.

Roberts E. M. (2007) Facies architecture and depositional environments of the Upper Cretaceous Kaiparowits Formation, southern Utah. Sed. Geol. 197, 207-233.

Kraus M. J., Middleton L. T. (1987) Contrasting architecture of two alluvial suites in different structural settings. In: Ethridge F. G., Flores R. M., Harvey M. D. (eds.) Recent Developments in Fluvial Sedimentology, SEPM Spec. Publ. 39, 253-262.

Trendell A. M., Atchley S. C., Nordt L. C. (2013) Facies analysis of a probable large-fluvial-fan depositional system: the Upper Triassic Chinle Formation at Petrified Forest National Park, Arizona, USA. J. Sed. Res. 83, 873-895.

Rasmussen A. M. S. (2005) Reservoir characterization of a fluvial sandstone: depositional environment and heterogeneities in modeling of the Colton Formation, Utah. Unpublished MSc Thesis, University of Oslo, Norway.

Flores R. M., Stricker G. D. (1993) Early Cenozoic depositional systems, Wishbone Hill District, Matanuska coal field, Alaska. In: Dusel-Bacon C., Till A. B. (eds.) Geologic Studies in Alaska by the Geological Survey, 1992. USGS Bull. 2068, 101-117.

Ielpi A., Ghinassi M. (2014) Planform architecture, stratigraphic signature and morphodynamics of an exhumed Jurassic meander plain (Scalby Formation, Yorkshire, UK). Sedimentology 61, 1923-1960.

Anderson D. S. (2005) Architecture of crevasse splay and point-bar bodies of the nonmarine lles Formation north of Rangely, Colorado: implications for reservoir description. Mt. Geologist 42, 109-122.

Smith R. M. H. (1987) Morphology and depositional history of exhumed Permian point

bars in the southwestern Karoo, South Africa. J. Sed. Petrol. 57, 19-29.

CR: Crevasse-channel elements

reference_citation

Hornung J., Aigner T. (1999) Reservoir and aquifer characterization of fluvial architectural elements: Stubensandstein, Upper Triassic, southwest Germany. Sed. Geol. 129, 215-280.

Amorosi A., Pavesi M., Ricci Lucchi M., Sarti G., Piccin A. (2008) Climatic signature of cyclic fluvial architecture from the Quaternary of the central Po Plain, Italy. Sed. Geol. 209, 58-68.

Fabuel-Perez I., Redfern J., Hodgetts D. (2009) Sedimentology of an intra-montane rift-controlled fluvial dominated succession: The Upper Triassic Oukaimeden Sandstone Formation, Central High Atlas, Morocco. Sed. Geol. 218, 103-140.

Tunbridge I. (1984) Facies model for a sandy ephemeral stream and clay playa complex; the Middle Devonian Trentishoe Formation of North Devon, UK. Sedimentology 31, 697-715.

Weerts H. J. T., Bierkens M. F. P. (1993) Geostatistical analysis of overbank deposits of anastomosing and meandering fluvial systems; Rhine-Meuse delta, The Netherlands. In: Fielding C. R. (ed.) Current Research in Fluvial Sedimentology. Sed. Geol. 85, 221-232.

Donselaar M. E., Overeem I. (2008) Connectivity of fluvial point-bar deposits: An example from the Miocene Huesca fluvial fan, Ebro Basin, Spain. AAPG Bull. 92, 1109-1129.

Catuneanu O., Bowker D. (2001) Sequence stratigraphy of the Koonap and Middleton fluvial formations in the Karoo foredeep South Africa. J. Afr. Earth. Sci. 33, 579-595.

Fielding C. R. (1986) Fluvial channel and overbank deposits from the Westphalian of the Durham coalfield, NE England. Sedimentology 33, 119-140.

Reynolds A. D. (1999) Dimensions of paralic sandstone bodies. AAPG Bull. 83, 211-229.

Limarino C., Tripaldi A., Marenssi S., Net L., Re G., Caselli A. (2001) Tectonic control on the evolution of the fluvial systems of the Vinchina Formation (Miocene), northwestern Argentina. J. South Am. Earth Sci. 14, 751-762.

Roberts E. M. (2007) Facies architecture and depositional environments of the Upper Cretaceous Kaiparowits Formation, southern Utah. Sed. Geol. 197, 207-233.

Kraus M. J., Davies-Vollum K. S. (2004) Mudrock-dominated fills formed in avulsion splay channels: examples from the Willwood Formation, Wyoming. Sedimentology 51, 1127-1144.

Ielpi A., Ghinassi M. (2014) Planform architecture, stratigraphic signature and morphodynamics of an exhumed Jurassic meander plain (Scalby Formation, Yorkshire, UK). Sedimentology 61, 1923-1960.

AC: Abandoned channel element

reference_citation

Hornung J., Aigner T. (1999) Reservoir and aquifer characterization of fluvial architectural elements: Stubensandstein, Upper Triassic, southwest Germany. Sed. Geol. 129, 215-280.

Robinson J. W., McCabe P. J. (1997) Sandstone-body and shale-body dimensions in a braided fluvial system: Salt Wash Sandstone Member (Morrison Formation), Garfield County, Utah. AAPG Bull. 81, 1267-1291.

Jordan D. W., Pryor W. A. (1992) Hierarchical levels of heterogeneity in a Mississippi River meander belt and application to reservoir systems. AAPG Bull. 76, 1601-1624.

Jo H. R. (2003) Depositional environments, architecture, and controls of Early Cretaceous non-marine successions in the northwestern part of Kyongsang Basin, Korea. Sed. Geol. 161, 269-294.

Cain S. A. (2009) Sedimentology and stratigraphy of a terminal fluvial fan system: the Permian Organ Rock Formation, South East Utah. Unpublished PhD Thesis, Keele University, UK.

Steel R. J., Thompson D. B. (1983) Structures and textures in Triassic braided stream conglomerates ('Bunter' Pebble Beds) in the Sherwood Sandstone Group, North Staffordshire, England. Sedimentology 30, 341-367.

Donselaar M. E., Overeem I. (2008) Connectivity of fluvial point-bar deposits: An example from the Miocene Huesca fluvial fan, Ebro Basin, Spain. AAPG Bull. 92, 1109-1129.

Corbeanu R. M., Wizevich M. C., Bhattacharya J. P., Zeng X., McMechan G. A. (2004) Three-Dimensional Architecture of Ancient Lower Delta-Plain Point Bars Using Ground-Penetrating Radar, Cretaceous Ferron Sandstone, Utah. In: Chidsey T. C. Jr., Adams R. D., Morris T. H. (eds.) Regional to Wellbore Analog for Fluvial-Deltaic Reservoir Modeling: The Ferron Sandstone of Utah, AAPG Studies in Geology 50, 427-449.

Olsen H. (1989) Sandstone-body structures and ephemeral stream processes in the Dinosaur Canyon Member, Moenave Formation (Lower Jurassic), Utah, U.S.A. Sed. Geol. 61, 207-221.

Opluštil S., Martínek K., Tasáryová Z. (2005) Facies and architectural analysis of fluvial deposits of the Nýrany Member and the Týnec Formation (Westphalian D – Barruelian) in the Kladno-Rakovník and Pilsen basins. Bull. Geosci. 80, 45-66.

Stewart D. J. (1983) Possible suspended-load channel deposits from the Wealden Group (Lower Cretaceous) of Southern England. In: Collinson J. D., Lewin J. (eds.) Modern and ancient fluvial systems. IAS Spec. Publ. 6, 369-384.

Viseras C., Soria J. M., Durán J. J., Pla S., Garrido G., García-García F., Arribas A. (2006) A large-mammal site in a meandering fluvial context (Fonelas P-1, Late Pliocene, Guadix Basin, Spain) Sedimentological keys for its paleoenvironmental reconstruction. Paleogeo. Paleoclim. Paleoecol. 242, 139-168.

Sánchez-Moya Y., Sopeña A., Ramos A. (1996) Infill architecture of a nonmarine half-graben Triassic basin (Central Spain). J. Sed. Res. 66, 1122-1136.

Hirst J. P. P. (1991) Variations in alluvial architecture across the Oligo-Miocene Huesca fluvial system, Ebro Basin, Spain. In: Miall A. D., Tyler N. (eds.) The three-dimensional facies architecture of terrigenous clastic sediments and its implications for hydrocarbon

discovery and recovery. SEPM Concepts in Sed. and Paleo. 3, 111-121.

Rasmussen A. M. S. (2005) Reservoir characterization of a fluvial sandstone: depositional environment and heterogeneities in modeling of the Colton Formation, Utah. Unpublished MSc Thesis, University of Oslo, Norway.

Ghinassi M., Billi P., Libsekal Y., Papini M., Rook L. (2013) Inferring fluvial morphodynamics and overbank flow control from 3D outcrop sections of a Pleistocene point bar, Dandiero Basin, Eritrea. J. Sed. Res. 83, 1066-1084.

Hubbard S. M., Smith D. G., Nielsen H., Leckie D. A., Fustic M., Spencer R. J., Bloom L. (2011) Seismic geomorphology and sedimentology of a tidally influenced river deposit, Lower Cretaceous Athabasca oil sands, Alberta, Canada. AAPG Bull. 95, 1123-1145.

Berendsen H. J. A., Stouthamer E. (2001) Palaeogeographic Development of the Rhine–Meuse Delta, The Netherlands. Koninklijke Van Gorcum, 268 pp.

Maynard J. R., Feldman H. R., Alway R. (2010) From bars to valleys: the sedimentology and seismic geomorphology of fluvial to estuarine incised-valley fills of the Grand Rapids Formation (Lower Cretaceous), Iron River Field, Alberta, Canada. J. Sed. Res. 80, 611-638.

Alqahtani F. A., Johnson H. D., Jackson C. A.-L., Som M. R. B. (2015) Nature, origin and evolution of a Late Pleistocene incised valley-fill, Sunda Shelf, Southeast Asia. Sedimentology 62, 1198-1232.

Feng Z.-Q. (2000) An investigation of fluvial geomorphology in the Quaternary of the Gulf of Thailand, with implications for river classification. Unpublished PhD Thesis, University of Reading, Reading, UK.

Reijenstein H.M., Posamentier H.W., Bhattacharya J.P. (2011) Seismic geomorphology and high-resolution seismic stratigraphy of inner-shelf fluvial, estuarine, deltaic, and marine sequences, Gulf of Thailand. AAPG Bull. 95, 1959-1990.